Universidade de São Paulo
Instituto de Biociências
Departamento de Botânica

Fisiologia do estresse em macroalgas: efeito das condições abióticas

Fanly Fungyi Chow Ho

2021

Universidade de São Paulo
Instituto de Biociências
Departamento de Botânica

Fisiologia do estresse em macroalgas: efeito das condições abióticas

Texto apresentado para concurso público de títulos e provas, visando a obtenção do título de Livre-Docente junto ao Departamentos de Botânica do Instituto de Biociências da Universidade de São Paulo na área de conhecimento de Diversidade e Evolução de Organismos Fotossintetizantes.

Fanly Fungyi Chow Ho

2021

Agradecimentos

Ao Departamento de Botânica, ao Instituto de Biociências, à Universidade de São Paulo (USP) e a todos os seus membros pelo apoio ao longo da minha trajetória.

Às agências de fomento (FAPESP, CAPES, CNPq, STINT, BMBF, Pró-Reitorias da USP) pelo apoio financeiro nas minhas atividades de ensino, pesquisa, extensão e orientação.

Aos meus colegas ficólogos do Departamento de Botânica por todas as experiências compartilhadas. Em especial à Mariana Cabral de Oliveira por me proporcionar minha primeira experiência no IB-USP, e à Déborah Yara A.C. dos Santos, à Cláudia M. Furlan e à Gladys/Flávia A.M. de Pinna por compartilhar inspirações e insucessos nesta jornada 'centopeica' de vida acadêmica.

A todos os funcionários da ficologia que passaram pelo LAM e que de certa forma fizeram parte do meu histórico profissional e em especial ao Rosario e à Vivian.

A todos meus aluninhos atuais e passados minha grande admiração, respeito e agradecimentos por terem compartilhado e confiado parte da sua caminhada profissional comigo, com os quais tenho aprendido muito com as suas experiências. Vocês sabem que são peça fundamental da minha prática docente.

A todos os membros do LAM atuais e passados com os quais compartilhei momentos de pós-graduação, pesquisa, descontração e churras.

A todos meus colaboradores brasileiros e estrangeiros, com os quais compartilhei e continuo compartilhando excelentes experiências e projetos.

A todos os que estiveram presentes na minha jornada e que guardo com enorme aprecio, mas que por falta de espaço e naturalidade da minha memória curta podem não estar aqui explicitamente mencionados.

À minha família que torcem por mim à distância.

Sumário

Lista de Figuras

Lista de Tabelas

Lista de Anexos

Apresentação

A busca pelo entendimento da fisiologia das algas marinhas de maneira mais abrangente e dentro do cenário da fisiologia do estresse, tem reforçado a necessidade de estudos sobre fisiologia experimental que possam ampliar nosso conhecimento relacionado à sensibilidade e resiliência das macroalgas e seus mecanismos de ação, assim como aproveitar os conhecimentos gerados para sua aplicabilidade prática com enfoques de bioprospecção.

Dada a sensibilidade das áreas costeiras, a acelerada pressão de estresses abióticos, as constantes perturbações antropogênicas e o importante papel das macroalgas no ambiente marinho, a fisiologia experimental pode contribuir de forma significativa na compreensão da sua biologia, assim como fornecer enfoques relevantes para o entendimento e proteção desses ecossistemas.

Uma das vertentes das pesquisas do Laboratório da Algas Marinha 'Édison José de Paula' visa a contribuição para o amplo conhecimento e entendimento do funcionamento biológico das macroalgas marinhas sob diferentes abordagens experimentais (desenvolvimento e validação de metodologias, abordagem integrativa[1] e abordagem multifásica[2]), incluindo o estudo das respostas relacionadas à fisiologia do estresse sob fatores abióticos como irradiância, radiação UV, temperatura e nutrientes. Nesse contexto, o objetivo deste texto é apresentar um panorama resumido sobre a fisiologia do estresse em macroalgas, sobretudo daquelas que habitam na zona do mediolitoral e sob influência de fatores ambientais abióticos de estresse, e discutir as descobertas e contribuições mais relevantes do nosso grupo de pesquisa para o enriquecimento do conhecimento nessa área da ficologia[3]. Para finalizar, apresentarei uma sinopse conceitual das principais alterações detectadas nas macroalgas marinhas baseadas nas nossas pesquisas e discutirei alguns gargalos ainda presentes na fisiologia ficológica experimental.

[1] ABORDAGEM INTEGRATIVA – Estudos com foco em fisiologia, bioquímica, histologia e ultraestrutura e ciências ômicas.

[2] ABORDAGEM MULTIFÁSICA – Estudos de múltiplas etapas e dimensões que incluem pesquisa básica, pesquisa descritiva, pesquisa aplicada, subsídios para políticas públicas e para empresas e divulgação científica.

[3] Outros trabalhos produzidos pelo nosso grupo de pesquisa e colaborações que venham a contribuir com a apresentação e discussão da temática, foram incluídos como referências.

1. O ambiente marinho e as macroalgas

Dois terços da Terra é constituída por oceanos. Habitada por organismos fotoautótrofos capazes de captar e aproveitar a energia luminosa ainda que em condições extremamente limitantes, como por exemplo, em profundezas cerca de 260 m. No ecossistema marinho costeiro, especialmente nos costões de substrato consolidado, as macroalgas representam organismos de vital importância para o funcionamento do ecossistema, contribuindo para a estruturação do ambiente, fornecendo assim diversos habitats e áreas de reprodução e alimentação. As macroalgas não apenas apresentam relevância ecológica, mas também são utilizadas como alimento para consumo humano e animal, ficocoloides, aditivos e bioativos nas indústrias de alimentos, cosméticos e farmacêutica, biofertilizantes e aplicações biotecnológicas (Graham et al. 2008).

As macroalgas, além de outorgar uma paisagem encantadora, oferecem um cativante panorama de pesquisa, pois elas habitam um ecossistema em que ocorrem diversas variações ambientais em uma pequena escala temporal e espacial. Essa característica, aliada à natureza bentônica[4] das macroalgas, acentua os gradientes de flutuação às quais as macroalgas estão expostas, intensificando seus atributos ecológicos e fisiológicos de tolerância ao estresse (Israel et al. 2010; Abele et al. 2012; Hurd et al. 2014).

O ecossistema costeiro é dividido em três zonas litorâneas: supralitoral[5], mediolitoral[6] e infralitoral[7]. Cada uma com particularidades específicas relacionadas aos principais fatores ambientais de estresse: irradiância, radiação UV, temperatura, exposição ao ar (dessecamento), salinidade, nutrientes, competição e hidrodinamismo (Fig. 1) (Huovinen et al. 2007; Graham et al. 2008; Gómez & Huovinen 2011; Aguilera & Rautenberger 2012; Hurd et al. 2014). A constante flutuação do nível da água, devido à oscilação das marés, é a major responsável pelos impactos das condições abióticas, especialmente na faixa do mediolitoral, frequentemente descrito como o habitat mais rigoroso da Terra, em razão às rápidas alterações das condições ambientais. No mediolitoral, essa vulnerabilidade é mais acentuada, pois em um curto período de tempo as algas

[4] **BENTÔNICO** – Organismo que vive associados ao substrato (consolidado ou não), seja em ambientes marinhos, salobros ou dulcícolas.
[5] **SUPRALITORAL** – Região do litoral localizada acima do limite da maré alta, raramente atingida pelas ondas.
[6] **MEDIOLITORAL** ou **ENTREMARÉS** – Região do litoral localizada entre a maré-baixa e a maré-alta, diariamente exposta à variação da maré.
[7] **INFRALITORAL** – Região do litoral localizada abaixo da linha das marés, sempre coberta de água.

permanecem submersas durante a maré cheia (completamente hidratadas, com atenuação de incidência de luz e acesso a nutrientes inorgânicos) e emersas durante a maré baixa, sujeitas à exposição de condições terrestres, com alta incidência de luz, elevada temperatura e dessecamento.

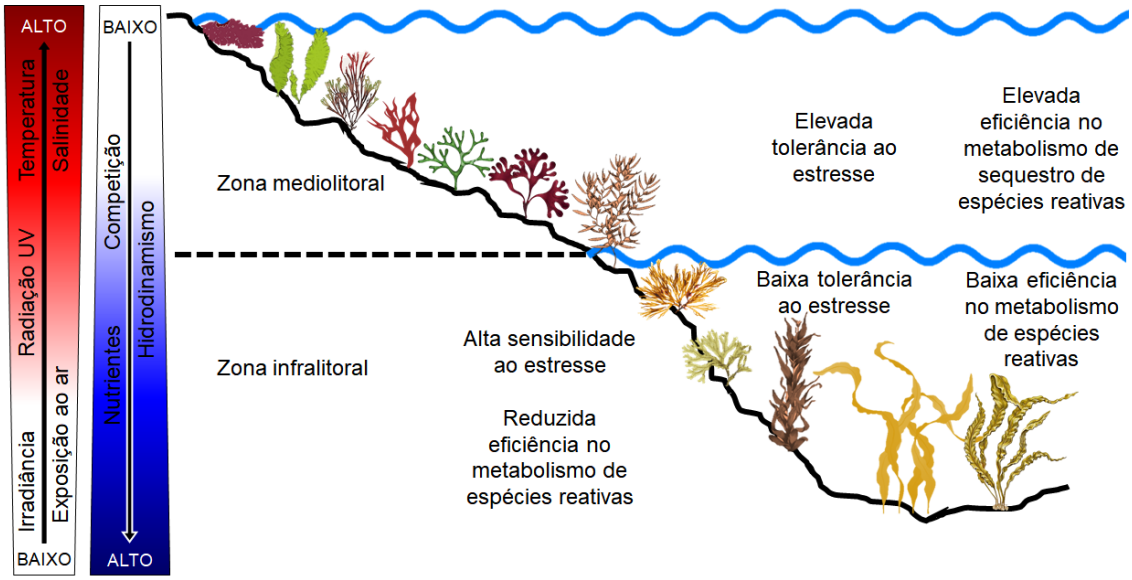

Figura 1. Representação esquemática dos principais fatores abióticos de estresse que afetam a tolerância e resiliências das macroalgas na região do mediolitoral e infralitoral [modificado de Huovinen et al. (2007), Gómez & Huovinen (2011), Marine Biological Association – https://www.mba.ac.uk/fact-sheet-rocky-shore e Aguilera & Rautenberger (2012)].

Espécies de macroalgas que ocorrem na região do mediolitoral são excelentes modelos biológicos para estudar as respostas fisiológicas[8] e metabólicas[9] frente aos efeitos dos fatores abióticos. Nessa região, as condições abióticas são as que determinam de forma decisiva a distribuição e ocorrência das espécies, diferente da região do infralitoral, na qual condições bióticas são mais influentes nas macroalgas.

As macroalgas incluem representantes filogeneticamente distintos: algas vermelhas (Rhodophyta), algas verdes (Chlorophyta) e algas pardas (Phaeophyceae, Ochrophyta), embora algas vermelhas e verdes pertencerem ao clado Archaeplastida (Fig. 2). Apesar das suas diferenças biológicas (Tabela 1), ocupam o mesmo ambiente e apresentam respostas

[8] FISIOLOGIA – Estudo do funcionamento celular.
[9] METABOLISMO – Conjunto de transformações responsáveis pelo funcionamento celular.

adaptativas semelhantes. Por serem, na sua maioria, organismos sésseis (bentônicos), estão expostas a expressivas alterações das condições ambientais, especialmente na zona entre-marés. Situação que tem levado à seleção de uma série de caracteres genotípicos e fenotípicos que são rápida e dinamicamente ativados e que propiciam uma plasticidade de respostas frente às situações de estresse. Desse modo, as macroalgas marinhas possuem diferentes níveis de respostas de sensibilidade e tolerância que circunscrevem sua resistência, aclimatação, susceptibilidade, senescência e morte, todas elas demarcadas por estratégias de sobrevivência, vulnerabilidade e resiliência (Fig. 3-4).

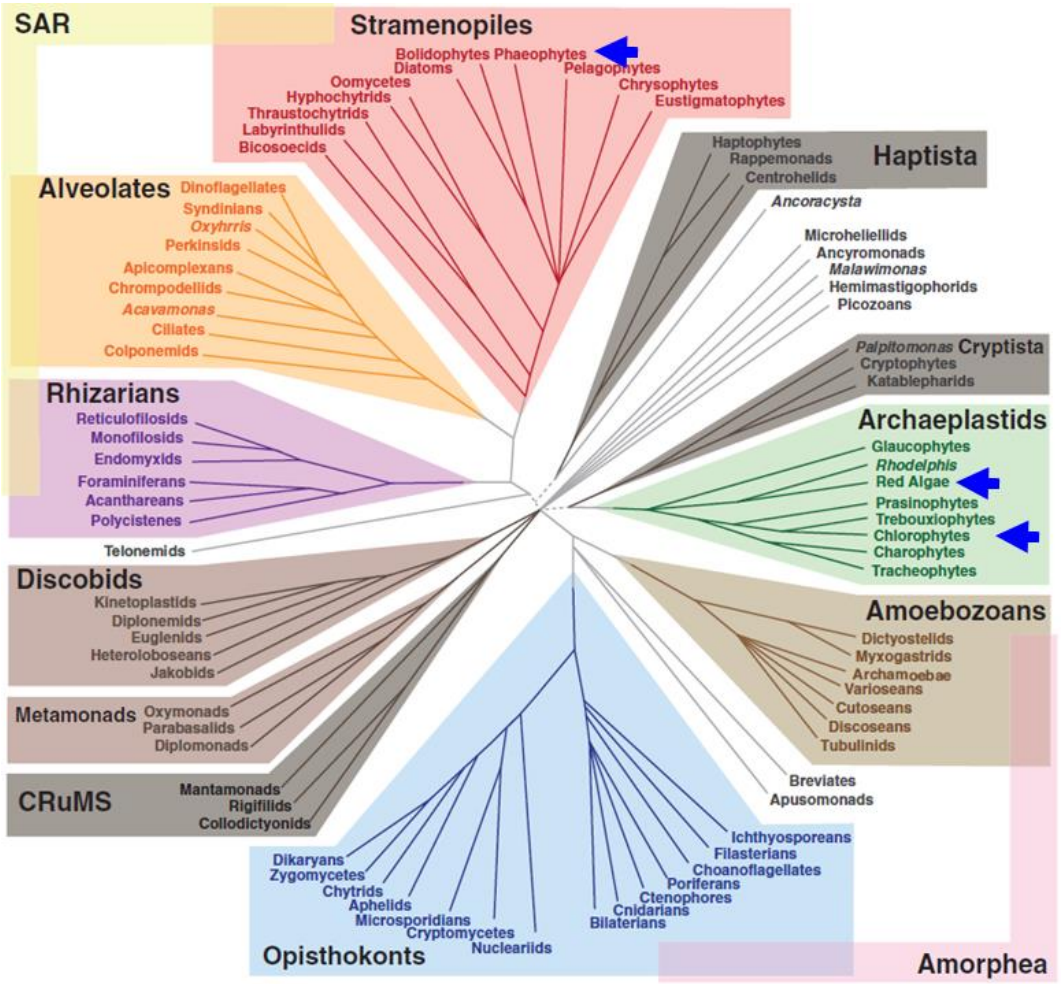

Figura 2. Representação esquemática de árvore da vida de eucariotos, baseada em estudos filogenômicos e informações morfológicas e celulares (Keeling & Burki 2019). Supergrupos melhores sustentados estão enquadrados em caixas coloridas, enquanto que grupos menos sustentados estão em caixas cinzas. As três linhagens de macroalgas estão identificadas com seta em azul. SAR: aglomerado Stramenopila, Alveolados e Rhizaria.

Tabela 1. Características distintivas de algas marinhas. Baseado em Bold & Wynne (1984), Lee (2008), Graham et al. (2008) e Evert & Eichhorn (2014).

Grupo	Chlorophyta	Phaeophyceae	Rhodophyta
Organização do corpo celular	Unicelular, colonial ou multicelular.	Multicelular. Talo morfologicamente complexo.	Unicelular ou multicelular. Talo complexo.
Pigmentos	Clorofilas a e b α, β e γ carotenos xantofilas	Clorofilas a e c β caroteno e fucoxantina xantofilas	Clorofilas a R- e C-ficocianinas, aloficocianina, R- e B-ficoeritrinas, α e β carotenos, xantofilas
Produto de armazenamento	Amido (amilose e amilopectina) Óleos em alguns representantes	Laminarina (β-1,3-glucopiranosídeo), manitol e compostos fenólicos.	Amido floridean (tipo amilopectina). Óleos em alguns representantes.
Parede celular	Celulose (β-1,4-glucopirosídeo), glicosídeos de hidroxiprolina, xilanas e mananas. Ausente em alguns. Calcificação em alguns.	Celulose, ácido algínico, mucopolissacarídeos sulfatados (fucoidano).	Celulose, xilanos, polissacarídeos sulfatados (galactanas). Calcificadas em alguns. Alginato em coralináceas.
Flagelos	Presente: dois iguais.	Presente: dois diferentes.	Ausente
Cloroplasto: invólucro e tilacoides	2 invólucros. Empilhados (2-6) ou grana.	4 invólucros. Empilhados (3).	2 invólucros. Livres.
Ciclo de vida	Haplobionte haplonte. Haplobionte diplonte. Diplobionte.	Haplobionte diplonte. Diplobionte heteromórfico.	Diplobionte bifásico heteromórfico. Diplobionte trifásico heteromórfico.

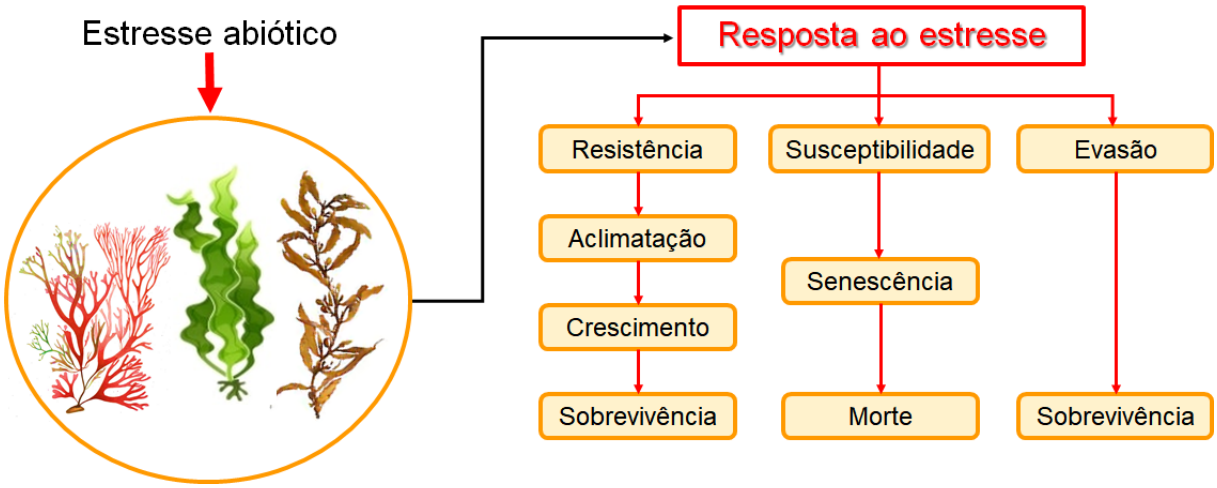

Figura 3. Panorama geral dos níveis e estratégias de resposta frente ao estresse abiótico. Mudanças ambientais promovem mecanismos de reconhecimento de sinais (percepção) que irão ativar diversos níveis de resposta para alcançar um novo estado estável ou homeostase[10].

[10] HOMEOSTASE – Condição de relativa estabilidade da qual o organismo realiza suas funções de forma adequada e em equilíbrio.

2. Fisiologia do estresse e estresse oxidativo

Fatores de estresse são um dos principais agentes que moldam as estratégias de sobrevivência dos seres vivos (aquisição de recursos, crescimento e reprodução), sendo a principal força que limita a distribuição das espécies e a estrutura da população (Gómez & Huovinen 2011; Aguilera & Rautenberger 2012; Hurd et al. 2014). O impacto do estresse nos indivíduos e nas populações ocorre em diferentes magnitudes e escalas de tempo, pelo qual o organismo possui diversos mecanismos de susceptibilidade/sensibilidade, tolerância, resiliência e recuperação.

Mas, qual seria a definição de estresse/estressor? Apesar do amplo entendimento de que o estressor basicamente é responsável por causar respostas adversas, o balanço entre a tolerância e a sensibilidade é fundamental para determinar a capacidade de resiliência do organismo e seu sucesso biológico. Dessa forma, mais do que uma dose particular do estresse ou seu impacto negativo, o estresse deve ser definido de acordo à resposta do organismo. Assim, na busca de um consenso mais apropriado para o conceito, particularmente apoio a definição de estresse como sendo uma alteração na aquisição de recursos, no crescimento e/ou na reprodução do organismo, em nível molecular, celular, metabólico ou fisiológico, propiciado pela mudança da condição externa (ex. fator abiótico ou biótico) e levando a modificações negativas ou positivas no seu desempenho, aptidão e bem-estar [ver Lichtenthaler (1996), Kranner et al. (2010) e Mosa et al. (2017)].

As respostas ao estresse abiótico incluem mecanismos de reconhecimento das alterações ambientais que desencadeiam ações categorizadas em quatro principais fases: fase de alarme, fase de resistência, fase de exaustão e fase de regeneração ou resiliência (Mosa et al., 2017) (Fig. 4).

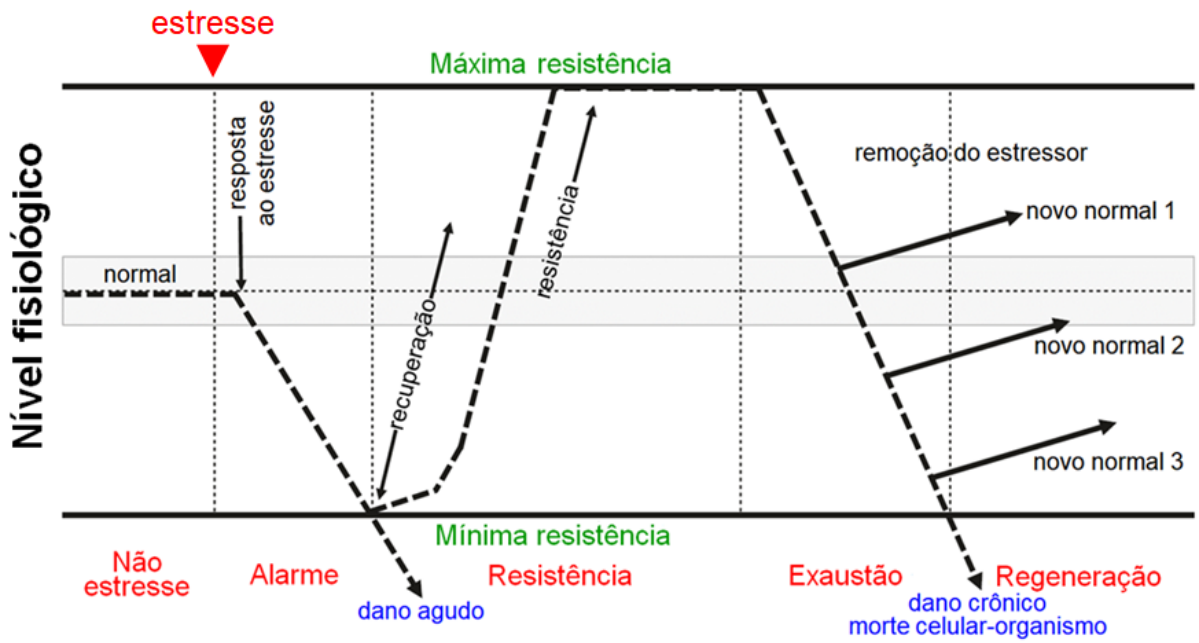

Figura 4. Fases de resposta frente ao estresse, incluindo os conceitos gerais e sequência de resposta a um estressor em nível fisiológico [modificado de Lichtenthaler (1996), Kranner et al. (2010) e Mosa et al. (2017)].

Na fase de alarme, ocorre a percepção do estresse, e quase que imediatamente são ativados diversos mecanismos de defesa (fase de resistência) que levam a desvios funcionais em relação à sua condição inicial de homeostase (dano agudo). Durante a fase de resistência, pode ser alcançado o reestabelecimento da homeostase, ocorrendo a recuperação metabólica por meio de mecanismos de tolerância definidos pela sua adaptação e aclimatação. Fisiologicamente, essa alteração funcional é percebida por nós como uma alteração na performance do organismo (ex. crescimento, fotossíntese), e inclui uma maior taxa catabólica. Dependendo da permanência do estresse, o organismo pode estabelecer um novo normal fisiológico dentro do seu limite de tolerância.

Se a condição adversa ou alterada permanece e fica próxima do limite do efeito agudo, ocorre a fase de exaustão, na qual danos crônicos começam a se manifestar. Essa exposição prolongada ou acima dos limites de tolerância leva a um desgaste ou sobrecarga dos mecanismos de defesa, acima dos limites de recuperação do metabolismo, resultando em um dano severo e, finalmente, morte do organismo.

Caso o estressor for removido antes de ocorrer processos crônicos de necrose, senescência[11] antecipada ou morte do organismo, a alga pode ainda alcançar sua recuperação (**fase de regeneração**), restabelecendo aos poucos seu estado fisiológico de forma lenta e com enorme investimento de gasto energético.

Em nível molecular, as respostas também acompanham as respostas fisiológicas (Mosa et al., 2017) (Fig. 5). A percepção de sinal leva à ativação de mecanismos de reparo e proteção para evitar consequências de dano agudo. Os mecanismos de tolerância possibilitam respostas de reparo e proteção mediante processos de aclimatação e adaptação, que enfatizam a manutenção da viabilidade e performance biológica. Quando os mecanismos de tolerância são excedidos, ocorre a manifestação de danos crônicos, danos significativos à maquinaria molecular, levando à perda da integridade celular e viabilidade do organismo, podendo finalizar em um estado crônico de morte celular e do organismo.

Considerando as respostas aos danos agudo e crônico, é possível diferenciar duas categorias de estresse fisiológico: (a) o estresse limitante, em que há uma alteração na resposta fisiológica ou metabólica, mas ocorre a resiliência, e (b) o estresse disruptivo, aquele que ultrapassa o limite de tolerância e que resulta em distúrbio prejudicial (Davison & Pearson, 1996). Tanto o estresse limitante como o estresse disruptivo levam ao dano celular ou requerimento de mecanismos metabólicos para neutralizar e reparar os danos (ex. redução dos centros de captação e reação luminosa, ativação de sistemas de defesa antioxidativo, síntese de metabólitos primários e secundários de defesa, mobilização de fontes de C e N, síntese de osmólitos[12]).

[11] **SENESCÊNCIA** – Processo metabólico ativo associado ao envelhecimento celular. Ocorre por meio de uma programação genética.

[12] **OSMÓLITOS** – Moléculas orgânicas pequenas que servem para contrabalançar estresses ambientais (ex. açúcares pequenos, polióis (glicerol, inositóis, sorbitol), aminoácidos e (glicina, prolina, taurina) e metilaminas (glicina betaina).

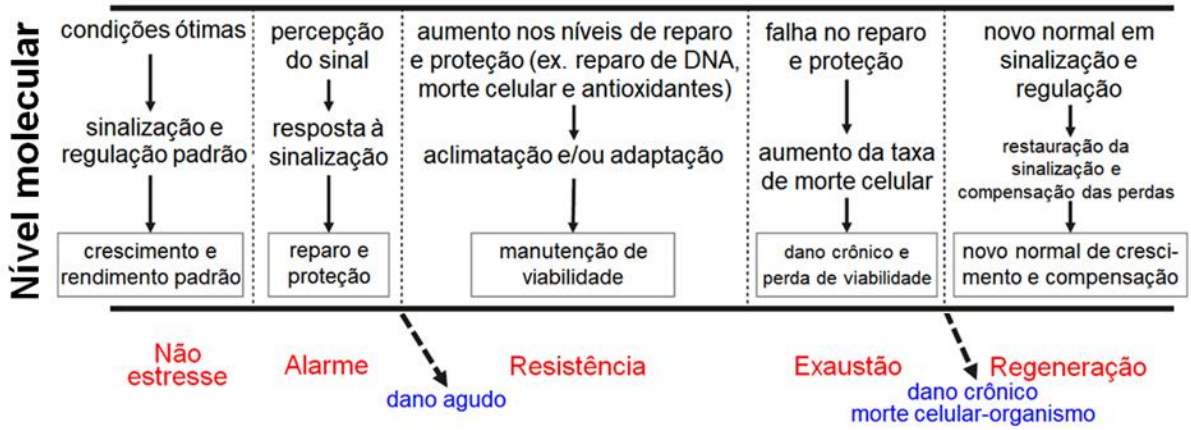

Figura 5. Fases de resposta frente ao estresse em nível molecular [modificado de Lichtenthaler (1996), Kranner et al. (2010) e Mosa et al. (2017)].

O estresse fisiológico é geralmente associado ao estresse oxidativo, ou seja, produção excessiva e acúmulo de espécies altamente reativas, como as espécies oxigenadas (ex. peróxido de hidrogênio, H_2O_2; radical superóxido, $O_2^{\bullet-}$; oxigênio singleto, $^1O_2$; radical hidroxil, $HO^{\bullet}$) e as espécies nitrogenadas (ex. óxido nítrico, $NO^{\bullet}$; peroxinitrito, $ONOO^-$) (Foog 2001; Mittler 2002; Abele et al. 2012; Aguilera & Rautenberger 2012). As espécies reativas são produzidas em diversas organelas e locais celulares sob condições não estressantes (Fig. 6), e desde que controladas, desempenham múltiplas funções metabólicas incluindo sinalização celular e oxidoredução de metais essenciais ou tóxicos, além de atuar na defesa química contra predadores e competidores. Portanto, o prejuízo das espécies reativas ocorre quando os mecanismos de defesa antioxidativos e de reparo não são suficientes para detoxificar as células e neutralizar o processo oxidativo, levando ao seu acúmulo e a uma série de reações em cascata que vão em detrimento da performance do organismo.

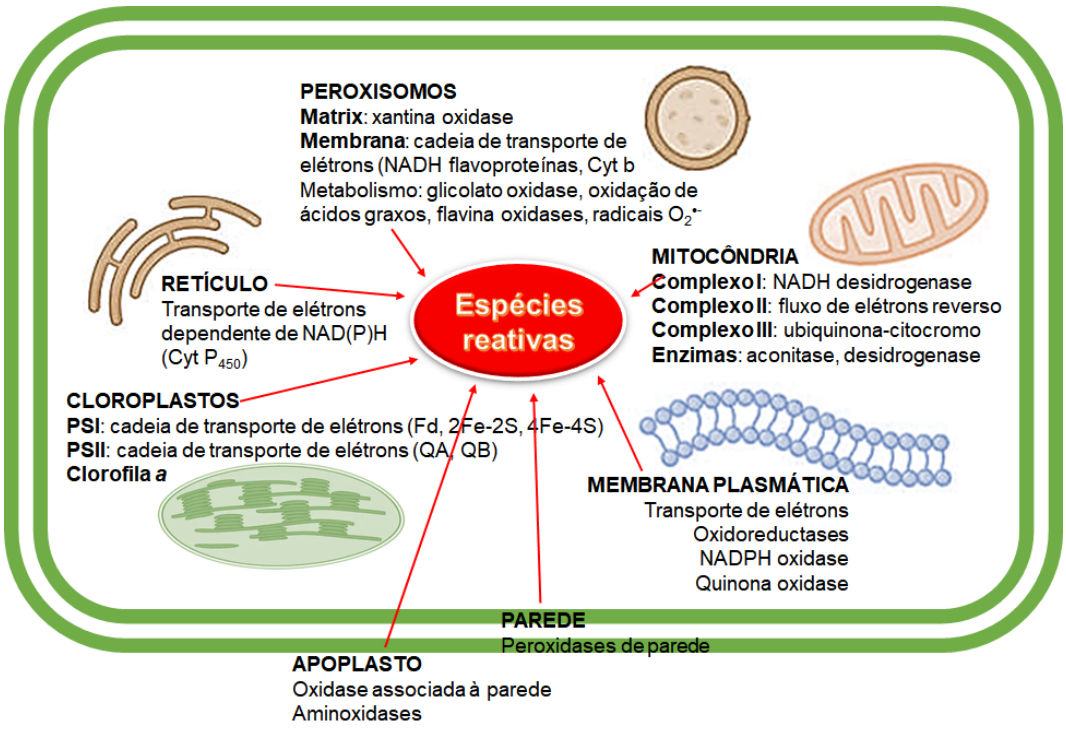

Figura 6. Representação de uma célula fotossintetizante eucarionte e os principais locais de produção de espécies reativas.

As macroalgas exibem diversas respostas frente a condições de estresse fisiológico, porém os mecanismos moleculares e bioquímicos associados ou responsáveis pela sua regulação, ainda permanecem sem definição para as macroalgas, diferente do extenso contingente de informações e descobertas realizadas em plantas terrestres ou mesmo em microalgas. A maior parte dos estudos caracteriza muito bem as alterações das macroalgas ante estressores abióticos, porém, ainda existe uma vasta lacuna de conhecimento a ser preenchida de forma mais integrada nas diversas abordagens fisiológicas, metabólicas e moleculares. Diante esse cenário, tanto o estabelecimento de metodologias analíticas como abordagens experimentais e integrativas são fundamentais para entender os mecanismos que levam à susceptibilidade, tolerância e resiliência nas macroalgas.

Assim, serão apresentadas e discutidas algumas das principais contribuições do nosso grupo de pesquisa sobre a fisiologia experimental sob condições de estresse que integram abordagens multianalíticas.

3. Fisiologia experimental: efeito dos fatores abióticos

Abordagens integradas combinando métodos clássicos e modernos são cruciais para um melhor entendimento da fisiologia e do metabolismo das macroalgas marinhas. Estudos experimentais que avaliam as respostas biológicas frente a fatores abióticos de estresse têm sua utilidade para o entendimento da performance biológica, assim como para identificar a sensibilidade, a tolerância e a resiliência das macroalgas, além de conhecer sua amplitude de aclimatação e adaptação. Porém, ainda existe uma extensa lacuna sobre a compreensão 'mecanicista' de diversos processos biológicos que definem o comportamento das macroalgas frente a condições abióticas de estresse. Não obstante, a compreensão da sua vasta complexidade requer de abordagens mais reducionistas, a fim de limitar sua multiplicidade em partes menores, estudando uma variável por vez.

Quanto mais conhecermos a biologia e o funcionamento das macroalgas, mais eficientemente poderão ser as estratégias de proteção e exploração que fundamentam a valorização de cada entidade e ecossistema, assim como o manejo e a seleção de genótipos e fenótipos mais relevantes para fins de Pesquisa, Desenvolvimento e Inovação (PD&I) do pais.

Nesse contexto, parte das investigações realizadas pelo nosso grupo de pesquisa tem focado no estabelecimento e validação de metodologias analíticas e no estudo das respostas biológicas em macroalgas marinhas com importante papel ecológico e econômico, na busca de acrescentar conhecimentos que possam auxiliar para uma compreensão mais integrada.

3.1. Irradiância

A irradiância[13] que atinge a superfície da Terra, regularmente referida como luz, é um dos principais fatores abióticos estudado nas macroalgas, fundamentado no fato das macroalgas serem organismos fotossintetizantes e, portanto, requerem de energia luminosa para sua sobrevivência. Cerca da metade da energia radiante emitida pelo Sol e que chega à superfície terrestre compreende a faixa espectral da luz visível[14] (400 nm a 700 nm; 40%), referida também como radiação fotossinteticamente ativa (PAR, do inglês *Photosynthetically Active Radiation*), enquanto que o restante corresponde ao espectro do infravermelho próximo (700 nm a 2500

[13] IRRADIÂNCIA – Fluxo de energia radiante que incide sobre uma superfície.
[14] LUZ VISÍVEL ou LUZ – Porção do espectro eletromagnético cuja radiação é percebida pelo olho humano.

mm; 55% infravermelho) e do ultravioleta (UV: 100-280 nm UVC, 280-320 nm UVB, 320-400 nm UVA; 5%) (Fig. 7).

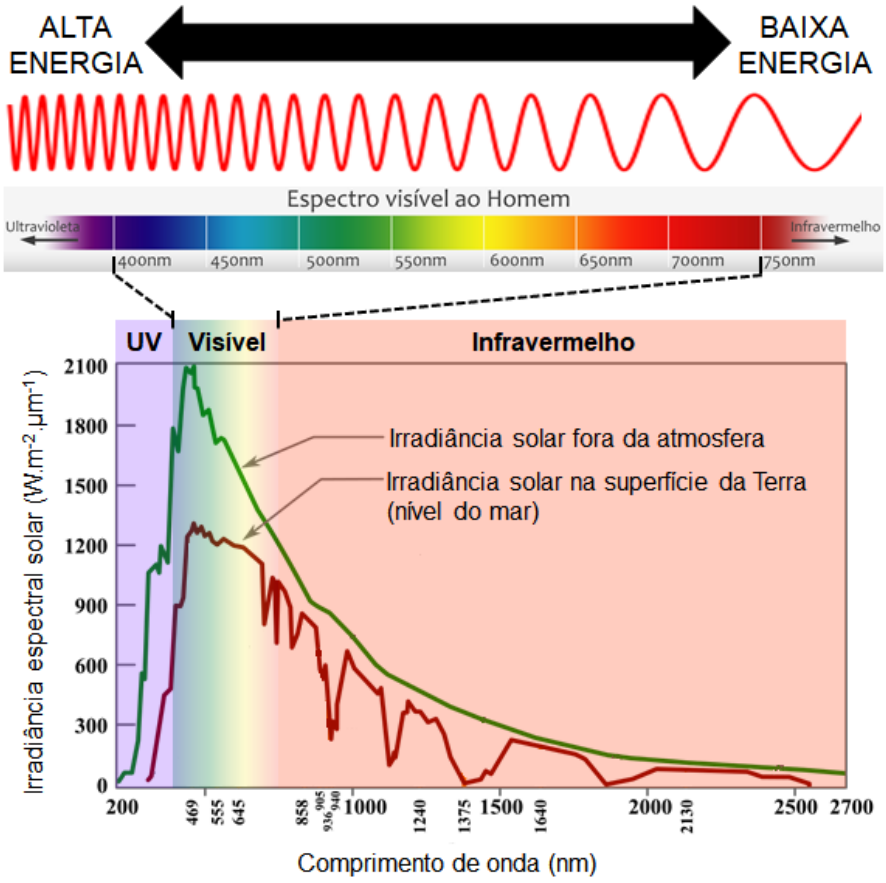

Figura 7. Espectro da radiação solar na atmosfera e aquela que alcança a superfície da Terra, indicando sua correspondência em radiações ultravioleta (UV), visível e infravermelho. Comprimentos de onda menores (radiação UV) possuem maiores níveis de energia.

A taxa fotossintetizante resulta do tamanho e da composição dos centros de captação e de reação luminosa, associados aos pigmentos acessórios e à clorofila *a*, respectivamente (Falkoswki & Raven 1997). Portanto, é lógico pensar que a concentração de pigmentos possa refletir a performance fotossintetizante, o qual justifica a ampla aferição deste parâmetro em estudos fisiológicos. Como consequência, abordagens fisiológicas mais tradicionais caracterizam respostas de crescimento, fotossíntese e conteúdo de pigmentos, fornecendo assim importantes informações para entender os mecanismos de fotoproteção, fotoresiliência e fotoinibição (Huovinen et al. 2006; Gómez et al. 2007; Rautenberger et al. 2009; Gómez & Houvinen 2011).

Devido à natureza séssil e fotossintetizante das macroalgas, estudos sobre a condição de estresse da irradiância têm sido um forte foco nas pesquisas fisiológicas. Condições extremas

podem ser desfavoráveis, levando à fotoinibição e fotodano. Por outro lado, níveis agudos subletais, podem estimular a resiliência fisiológica e a síntese de metabólitos de interesse para diversas aplicações (Salehi et al. 2019; Lourenço-Lopes et al. 2020; Sudatti et al. 2020; Gambichler et al. 2021).

Com o propósito de caracterizar algumas das respostas fisiológicas na macroalga vermelha *Gracilariopsis tenuiforns* (C.J. Bird & E.C. Oliveira) Fredericq & Hommersand frente a baixa (60 µmol fótons.m^{-2}.s^{-1}) e altas irradiâncias (600 e 1000 µmol fótons.m^{-2}.s^{-1}), alguns estudos foram realizados pelo nosso grupo de pesquisa. No estudo de Torres et al. (2015) (ANEXO 1), foi verificada uma despigmentação gradual ao longo dos dias de cultivo e em maior intensidade em doses maiores de irradiância, no entanto, não foi registrada diminuição na taxa de crescimento, o que de certa forma parece ser contraditório quando considerada a aparência visual dos talos. Tanto o conteúdo de clorofila *a* quanto o de β-caroteno (carotenoide do tipo caroteno) tiveram seus níveis diminuídos com o aumento de irradiância. Em contraposição, o conteúdo de zeaxantina (carotenoide polar do tipo xantofila) foi aumentado. Esta variação quantitativa dos centros de captação e reação fotossintetizante é conhecido como 'adaptação cromática' (mas estritamente, corresponde a um processo de aclimatação), uma das primeiras consequências visíveis em resposta a mudanças no espectro luminoso (Falkowski & .Raven 1997) e que funciona como mecanismo de defesa para reduzir a circulação de excesso energético e, por conseguinte, a fotoxidação e o fotodano. Por sua vez, a zeaxantina atua como mecanismo de fotoproteção ativo mediante o ciclo da xantofila, em um esforço para reduzir o estado excitado da clorofila *a* e, consequentemente, o estado oxidativo celular. Outros mecanismos de fotoproteção também foram identificados no estudo de Torres et al. (2016) (ANEXO 2) para a mesma espécie ao estudar a composição de aminoácidos do tipo micosporinas (MAAs[15]). A composição qualitativa dos MAAs não variou em relação à exposição de PAR (asterina-330, palitinol, paliteno, usujireno e um componente não identificado com $[M+H]^-$ equivalente a *m/z* 271 e λmax em 333 nm). Porém, a abundância de palitinol foi estimulada em irradiâncias mais elevadas. Esses estudos evidenciaram a ativação de mecanismos de fotoproteção, mediados pela redução dos centros de captação e de reação luminosa, aumento da zeaxantina e elevação de palitinol, metabólitos que podem estar associados à ação antioxidante.

[15] AMINOÁCIDOS DO TIPO MICOSPORINAS – Pequenos metabólitos secundários presentes nas macroalgas, principalmente em algas vermelhas. São metabólitos que absorvem comprimentos de ondas na faixa do UV e atuam como fotoprotetores naturais.

Diversos estudo têm focado no estímulo de biossíntese de MAAs sob efeitos da radiação UV, mas poucos trabalhos têm caracterizado as respostas em condições de PAR, tendo a pesquisa de Torres et al. (2016) (ANEXO 2) identificado quatro MAAs em *G. tenuifrons*. Estudos complementares de Serra (2013) na mesma espécie também verificaram a despigmentação de talos submetidos a 600 µmol fótons.m^{-2}.s^{-1}, com significativa redução da clorofila *a*, carotenoides totais e ficobiliproteínas, porém, não observaram redução na taxa de crescimento. A pesar de não registrar alterações na taxa de crescimento, indicativos bioquímicos foram detectados, como aumento no teor de C e redução de N, assim como aumento de compostos fenólicos totais, atividade antioxidante e óxido nítrico[16] (NO). Considerando o aumento da atividade antioxidante e concentração de NO sob condições de 600 µmol fótons.m^{-2}.s^{-1} foi possível verificar que o estresse por luminosidade desencadeou resposta de fotoproteção ao estresse oxidativo, com a intervenção de produção de NO. A partir desses estudos, é possível afirmar que a intensidade luminosa ativa diferentes mecanismos de fotoproteção e fotoresiliência em macroalgas, a fim de evitar a fotoinibição e o fotodano e manter em homeostase a resposta de taxa de crescimento.

Esses estudos, além das respostas biológicas detectadas, possibilitaram incorporar procedimentos analíticos novos no nosso laboratório (realizados em colaboração com outros grupos de pesquisa em plantas terrestres), como o estabelecimento de um protocolo padrão para a análise quantitativa e qualitativa de clorofila *a* e carotenoides mediante metodologias de espectrofotometria e cromatografia líquida de alta eficiência (CLAE) (Torres et al. 2014), o estabelecimento de biomassa mínima para análise de pigmentos (50 mg de massa fresca), a testagem de melhor solvente para extração de pigmentos (metanol, acetona, acetona 90%, acetona 80%, DMF – dimetil formamida, DMSO – dimetil sulfóxido e dietil éter), a avalição do número de extrações do material (única extração versus duas e três extrações) e a quantificação de espécies reativas de oxigênio e NO. Adicionalmente, foram propostas novas equações baseadas em métodos espectrofotométricos para o cálculo de clorofila *a* e carotenoides totais, e específicas para algas vermelhas e sob os diferentes solventes testados, modificações baseadas nas equações publicadas por Jeffrey & Humphrey (1975), Wellburn (1994) e Lichtenthaler & Buschmann (2001). Cabe ressaltar que a reformulação das equações propostas por esses autores é de extrema importância, pois as fórmulas propostas por eles se baseiam em cálculos que

[16] ÓXIDO NÍTRICO – Importante molécula sinalizadora intra e extracelular, é um gás solúvel e altamente lipofílico, envolvido na regulação do crescimento, desenvolvimento, defesa e respostas ao estresse abiótico.

consideram a presença de clorofilas *a* e *b*, do qual algas vermelhas apresentam apenas clorofila *a*.

Com base nos estudos de Serra (2013), Torres et al. (2015) (ANEXO 1) e Torres et al. (2016) (ANEXO 2), e considerando que a exposição sob 600 µmol fótons.$m^{-2}.s^{-1}$ seria uma condição de estresse agudo-crônico, podendo levar a uma situação de fotoinibição e fotodano, o estudo de Harb et al. (2018) (ANEXO 3) abordou o efeito de uma menor magnitude de alta irradiância (300 µmol fótons.$m^{-2}.s^{-1}$) na fotossíntese da alga vermelha *Pterocladiella capillacea* (S.G. Gmelin) Santelices & Hommersand. Esse estudo trouxe um avanço às pesquisas do nosso grupo, pois incorporou a aferição de diversos parâmetros fotossintetizantes mediante o uso de um flourímetro de amplitude de pulso modulado que mede a fluorescência *in vivo* da clorofila *a* do PSII, uma metodologia rápida e não destrutiva. Nessa pesquisa, *P. capillacea* se mostrou aclimatada à condição de aumento de luminosidade, tendo aumentado sua taxa de crescimento em mais de 3,5 vezes em relação à condição considerada controle (60 µmol fótons.$m^{-2}.s^{-1}$) e diminuído levemente seu rendimento de dissipação (*quenching*) fotoquímica [Y(PSII)[17]], sem nenhuma evidência de dissipação não fotoquímica regulada [Y(NPQ)][18]. Leves alterações no conteúdo de pigmentos fotossintetizantes (clorofila *a* e ficobiliproteínas) foram observadas entre ambos tratamentos luminosos, porém nenhuma mudança foi registrada em carotenoides totais, proteínas solúveis e teor de C e N, indicando a presença de outros mecanismos de fotoaclimatação. Estes resultados com *P. capillacea* podem ser interpretados como uma resposta eficiente de recuperação e resistência, sendo esta dose de irradiância como uma condição subaguda nas condições experimentais testadas.

Todas essas mudanças fisiológicas evidenciam investimento das macroalgas para equilibrar seu estado metabólico a fim de reduzir danos prejudiciais e retomar sua homeostase. Mudanças conhecidas como aclimatação, ou fotoaclimatação quando sob efeito da irradiância (Falkowski & LaRoche 1991; Hurd et al. 2014). A absorção excessiva da energia luminosa pelo aparato fotossintetizante aumenta a extensão do fotodano. Como consequência, ocorre a produção e o

[17] DISSIPAÇÃO FOTOQUÍMICA – Utilização da energia luminosa para os processos fotoquímicos da fotossíntese (doação do elétron proveniente da molécula de água para um aceptor NADP. Este processo é a base da fotossíntese e a Esta energia dissipada é usada para a formação do poder redutor e da molécula de ATP, os quais serão utilizados na fase bioquímica do processo de fotossíntese.

[18] DISSIPAÇÃO NÃO FOTOQUÍMICA REGULADA – Dissipação de energia luminosa não utilizada em processos fotoquímicos da fotossíntese e relacionado a sistemas ativos de proteção, como por exemplo, o ciclo das xantofilas. Mecanismo que ajuda a regular e proteger a fotossíntese em condições de excesso de energia, quando este excede a capacidade de utilização da luz.

acúmulo prejudicial de espécies reativas que atacam diversas moléculas-alvo, como a proteína D1 que faz parte do centro de reação do PSII, clorofilas e ácidos graxos insaturados (Bischof & Rautenberger 2012). A neutralização do dano ao fotossistema ocorre por processos de reparo que envolvem a inativação parcial do PSII, degradação proteolítica da proteína D1 fotodanificada e ciclo de reparo da proteína D1 (Barber & Andersson 1992; Aro et al. 1993). O estresse oxidativo devido a espécies reativas é contingenciado pela ação de compostos antioxidantes (ex. carotenoides, ascorbato, tocoferol, MAAs e compostos fenólicos) e de enzimas como a superóxido dismutase, peroxidase de hidrogênio e catalase.

A fotossíntese, assim como os seus processos relacionados de síntese de pigmentos e crescimento, não são os únicos metabolismos regulados por luz. O metabolismo de assimilação do nitrogênio também parece ser regulado pela irradiância. A enzima nitrato redutase (NR) é regulada principalmente pela disponibilidade de nitrogênio (concentração e formas de fontes nitrogenadas), mas também mostra ser regulada pela luz. A NR é a primeira enzima da via de assimilação de nitrogênio, portanto, é uma peça chave para a síntese de compostos orgânicos nitrogenados como aminoácidos e proteínas. A flutuação circadiana da enzima correlacionada com a atividade fotossintetizante foi evidenciada em Chow et al. (2004), Granbom et al. (2004) e Chow et al. (2007), com níveis duas vezes maiores durante a fase clara do que a fase escura. Porém, sua regulação parece não ser controlada por um relógio biológico. Além da regulação luminosa da atividade da NR devido ao fotociclo, Chow et al. (2007) mostraram a indução da atividade enzimática após estímulos de pulsos luminosos durante a fase escura.

A habilidade de utilizar e lidar com a energia luminosa, e sua associação com o metabolismo do N, constituem uma das principais adaptações das macroalgas que interliga tanto o metabolismo de C (produção de fotossintatos) como o metabolismo de N (produção de aminoácidos, proteínas e enzimas), ambos fundamentais para o funcionamento integral das macroalgas. Dessa forma, devido à sua natureza séssil e ocorrerem em um ambiente constantemente flutuante, principalmente aquelas que habitam o mediolitoral, as macroalgas devem gerenciar a captação e utilização dessa energia de forma que não crie um estado de excitação excessivo e, consequentemente, a fotoxidação de todo o aparato fotossintetizante e o estresse oxidativo (Gómez & Houvinen 2011). Os mecanismos pelos quais essa fotoaclimatação ocorre em macroalgas ainda são incertos, porém, adaptações fotobiológicas constituem uma memória evolutiva nas macroalgas e conferem diversas habilidades competitivas (Gómez & Houvinen

2011; Galviz et al. 2020), uma vez que a incidência de luminosidade no mediolitoral pode ser um dos principais fatores que limita a fisiologia e o metabolismo das macroalgas, desencadeando mecanismos de fotoproteção, respostas de fotoinibição e consequências de fotoestresse.

3.2. Radiação UV

Os estudos apresentados por Wiencke & Bischof (2012) na obra 'Seaweed Biology. Novel insights into ecophysiology, ecology and utilization' mostram que a zonação vertical[19] de espécies de macroalgas é estreitamente correlacionada com a sensibilidade da fotossíntese à radiação UV. Segundo Larkum & Wood (1993), o aumento dos níveis de radiação UV pode causar efeitos semelhantes a alta radiação PAR; entretanto, os mecanismos de resposta são provavelmente diferentes. A faixa espectral da radiação UV não contribui com o fornecimento de energia para a fotossíntese e o efeito adverso da radiação UV sobre a fotossíntese pode ser considerado como indireto, pois seu comprimento de onda menor com alto nível energético é absorvido por biomoléculas aromáticas que contêm grupos sulfidrilas (-SH) (ex. aminoácidos e proteínas), ácidos nucléicos (DNA), enzimas, componentes de membrana (ex. proteínas e lipídios), quinonas e pigmentos (Vass et al. 2005), causando sérios danos agudos e crônicos em todo o metabolismo.

Danos estruturais foram verificados nos estudos com as algas vermelhas *Porphyra acanthophora* var. *brasiliensis* E.C. Oliveira & Coll (Bouzon et al. 2012), *Gelidium floridanum* W.R. Taylor (Simioni et al. 2014) e *Acanthophora spicifera* (M. Vahl) Børgesen (Pereira et al. 2018), com diversas alterações fisiológicas, bioquímicas, histoquímicas e ultraestruturais advindas da exposição à radiação UV. Esses estudos trazem uma importante caracterização das alterações celulares e ultraestruturais sob o efeito da radiação UV, destacando alterações na organização ultraestrutural de cloroplastos (ex. disrupção dos tilacoides e aumento de plastoglóbulos) e mitocôndrias, associadas provavelmente a fotodanos nas membranas. O dano estrutural a organelas é uma evidência crônica do efeito da radiação UV em biomoléculas essenciais para a atividade celular e metabólica, como lipídios e proteínas, fundamentais para a organização das membranas, levando a uma redução em cascata da performance fisiológica (ex. fotossíntese e crescimento) e do conteúdo de pigmentos fotossintetizantes (clorofila *a* e ficobiliproteínas).

[19] ZONAÇÃO – Distribuição dos organismos em faixas, onde os organismos se dispõem horizontalmente de acordo com suas adaptações.

Adicionalmente, mudanças metabólicas de defesa foram identificadas nesses estudos, como indução na síntese de proteínas solúveis e na atividade de enzimas de defesa, mas provavelmente com ação insuficiente para evitar o dano crônico.

Nos trabalhos de Polo et al. (2014) (ANEXO 4) e Polo et al. (2015) (ANEXO 5) sobre exposição da alga parda *Sargassum cymosum* C. Agardh à radiação UV também foram verificadas variações bioquímicas e ultraestruturais. Não obstante, *S. cymosum* exibiu fotoaclimatação e ativação de mecanismos de reparo mais eficientes ao estresse por radiação UV, uma vez que, no geral, a taxa de crescimento não foi evidentemente afetada (Polo et al., 2014; ANEXO 4). Porém, foram observadas alterações no conteúdo de pigmentos (clorofilas *a* e *c* e carotenoides) e de compostos fenólicos, assim como na atividade antioxidante, mas não foi possível identificar um claro padrão de resposta relacionado ao efeito da radiação. Curiosamente, a radiação UVA propiciou aumento na concentração de clorofila *a* e na produção de substâncias fenólicas; porém houve uma redução da clorofila *c* sob qualquer radiação UV. É importante notar que na maioria dos tratamentos sob influência da radiação UV houve extrusão para o meio de cultivo de substância que absorvem na faixa do UV (*UV-absorbing compounds*[20]), situação que também tem sido reportado para outras espécies de algas pardas (ver ANEXO 4). A presença de substâncias fenólicas dentro de fisoides[21] também foi evidenciada por microscopia de luz e microscopia eletrônica de transmissão, além de serem observadas próximas à parede celular e também migração através do plasmalema. Aparentemente, a presença de níveis mais elevados de compostos fenólicos e presença de fisoides é característico em algas pardas (Schoenwaelder 2002; Imbs & Zvyagintseva 2018), e parecem desempenhar múltiplas funções como componentes estruturais, proteção em estágios precoces de desenvolvimento, evitar poliespermia e antiherbivoria, resistência a poluição por metais, fotoproteção contra UV e reguladores de atividade enzimática.

Por sua vez, Polo et al. (2015) (ANEXO 5) registraram variações nos níveis de C e N, provavelmente associado à alocação do balanço de C-N para sua disponibilização em mecanismos de defesa, e nos níveis de poliaminas[22]. Resultados semelhantes às alterações de C

[20] ***UV-absorbing compounds*** – Metabólitos secundários que atuam como agentes naturais que filtram radiação UV. Aminoácidos do tipo micosporinas e compostos fenólicos estão entre os exemplos de *UV-absorbing compounds* em macroalgas.
[21] **FISOIDES** – Inclusões vesiculares intracelulares que contém compostos fenólicos.
[22] **POLIAMINAS** – Aminas alifáticas com função de defesa frente a condições de estresse abiótico.

e N também detectados para o conteúdo de carboidratos, proteínas e compostos fenólicos quando expostas a radiação UV.

A população de *Sargassum* desses estudos habita a faixa do mediolitoral inferior e infralitoral superior, locais frequentemente sujeitas a variações de radiação UV durante a maré baixa. Portanto, é de se esperar que os mecanismos de aclimatação e de reparo ao estresse por radiação UV sejam rápidos e dinâmicos, a fim de reduzir ao máximo os efeitos danosos, evitando assim situações crônicas de exaustão fisiológica. Aparentemente, um dos mecanismos dinamicamente mais ativos em espécies de *Sargassum* frente à radiação UV é a síntese de compostos fenólicos, armazenamento em fisoides e extrusão em situações de estresse.

Estudos com macroalgas de regiões polares e subpolares, geralmente não mostram efeitos de reparo estimulado por radiação UV (Hanelt et al. 1997a, b, c; Bischof et al. 2000). Isso provavelmente devido a uma adaptação especial das macroalgas do mediolitoral que habitam ambientes com níveis permanente altos de radiação solar e radiação UV. No entanto, algas que crescem em locais mais profundos, sujeitos a menor exposição diária de radiação UV e protegidos pela coluna d'água, são mais sensíveis a radiação UV (Hanelt et al. 1997a).

Considerando o efeito deletério que doses agudas-crônicas de radiação UV pode desencadear na fisiologia das macroalgas, a continuidade das pesquisas no nosso grupo se deu com estudos sob doses moderadas não letais de radiação UV em *Sargassum filipendula* C. Agardh (Polo et al. 2020) (ANEXO 6). As respostas fisiológicas aos tratamentos de dose moderada de radiação UV mostraram pouca variação entre os tratamentos e o tempo de cultivo, sugerindo a ativação de mecanismos de aclimatação que possibilitaram resiliência para o restabelecimento da condição de homeostase celular sem apresentar danos agudos ou crônicos severos à maquinaria metabólica. A taxa de crescimento não mostrou diferença significativa entre os tratamentos e ao longo do tempo, porém algas expostas a PAR+UVB apresentaram menores valores médios. A ativação de sistemas de defesa foi observada mediante o aumento na síntese de compostos fenólicos e compostos que absorvem radiação UV/visível, assim como sua extrusão para o meio de cultivo. Uma vez que o estresse pela radiação UV estimula a produção de espécies reativas, estas poderiam atuar como sinalizadores para a ativação de mecanismos de defesa antioxidantes, a fim de manter a homeostase, delimitada inicialmente pela sua capacidade de

aclimatação e intrinsicamente associada ao seu estado de hormese[23]. Ambos processos determinam uma regulação positiva e transitória de defesas antioxidantes frente a fatores de estresse, que visam a melhoria da desintoxicação por espécies reativas, possibilitando a tolerância ao estrese oxidativo. Essa tolerância ao estresse oxidativo tem sido associado a um mecanismo conhecido como 'preparo para o estresse oxidativo' (POS, do inglês *Preparation for Oxidative Stress*), fenômeno descrito em plantas terrestres, principalmente sob estresse de hipóxia (Oliveira et al. 2019), mas muito pouco mencionado em algas.

Estudos adicionais em *S. filipendula* sustentam a hipótese de aclimatação à condição aguda-moderada de exposição à radiação UV (Polo 2019), visto que foi registrado um aumento na atividade antioxidante e no nível de formação de dímeros de pirimidina no DNA, este último gerado principalmente pela ação de radiação ionizante, sendo significativamente mais elevado sob radiação PAR+UVB. Além dos estudos fisiológicos, esse trabalho avaliou também o potencial de inibição da enzima transcriptase reversa da do vírus HIV de extratos submetidos a radiação UV e constatou que a exposição à radiação diminuiu a capacidade dos extratos de inibir a enzima quando comparado com extratos de algas sob radiação PAR, mostrando que algas expostas a doses moderadas de radiação UV poderiam ser mais susceptíveis ao ataque de microrganismos como os vírus. Apesar disso, os resultados mostraram que amostras cultivadas em radiação PAR apresentaram a maior capacidade de inibição da enzima transcriptase reversa, tornando a espécie uma fonte promissora para futuros estudos sobre *screening* de bioativos.

Visando ampliar as abordagens e a compreensão dos mecanismos de ação, as ciências ômicas (ex. transcriptômica e proteômica) podem fornecer uma perspectiva mais ampla e sem um alvo específico direcionado para a identificação global das alterações, possibilitando uma melhor compressão de certos mecanismos que levam à elaboração de novas hipóteses de comportamento e desempenho. Com esse intuito, realizamos um estudo focando a identificação do perfil diferencial de proteínas responsivas à exposição de radiação UV (Polo & Chow, em prep.) (ANEXO 7). Esse estudo, além de aprofundar nas abordagens fisiológicas, se constitui, até o nosso conhecimento atual, no primeiro estudo sobre proteômica diferencial com macroalgas no Brasil. Portanto, sua inovação não apenas trata da geração de conhecimento científico, mas se equipara à extensão do desafio no estabelecimento de protocolos adequados para esse tipo

[23] HORMESE – Fenômeno de resposta associado a doses de um estímulo, caracterizada por uma resposta bifásica sob doses baixas e doses altas.

de pesquisa, além da interpretação do vasto conjunto de dados através de bioinformática. Nesse estudo, testamos alguns dos protocolos descritos na literatura e os adaptamos para *Sargassum*, considerando cuidados para a preservação apropriada das proteínas frente a fatores como degradação e contaminação (ex. temperatura, proteases, compostos fenólicos, polissacarídeos), podendo chegar a um elevado rendimento e qualidade de proteínas. Foram realizadas análises de identidade e comparação das proteínas diferencialmente abundantes sob os tratamentos de radiação UV, sendo identificados cinco clusters metabólicos que foram afetados pela radiação UV: (I) metabolismo de carboidratos (ex. Rubisco), fotossíntese (ex. centros de reação) e sistema de defesa antioxidante (ex. peroxidase, glutamato sintase); (II) fotossíntese (ex. citocromos e centro de reação), processamento genético e metabolismo do amônio; (III) fotossíntese (ex. citocromos e complexos de captação luminosa), metabolismos de carboidratos (ex. Rubisco) e de fosfatos; (IV) proteínas de defesa antioxidante e metabolismo de síntese de aminoácidos; (V) sistema transportador e defesa antioxidante. Esses resultados são extremamente valiosos para melhor entender a regulação de certas rotas metabólicas e como eles respondem ante a exposição moderada de dose de radiação UV, possibilitando também a expansão dos horizontes das nossas pesquisas.

Aparentemente, algas que habitam entre o mediolitoral e o infralitoral superior possuem uma capacidade de recuperação mais rápida ao estresse pela radiação, seja ela radiação PAR ou radiação UV (Hanelt 1998; Hanelt & Roleda 2009), uma vez que condições extremas de exposição à radiação fazem parte do seu dia-a-dia. Os efeitos da exposição aos raios UV são múltiplos, atuando principalmente no nível molecular, mas com potencial para atingir mudanças na estrutura e função do ecossistema. Ácidos nucleicos e proteínas possuem cromóforos na faixa espectral no UV (Vass et al. 2005), resultando em danos estruturais ao DNA pela formação de dímeros de ciclobutano, quebra da dupla fita e formação de fotoprodutos de pirimidina (6-4) e pirimidona (6-4) (Lois & Buchanan 1994), e danos às proteínas pela alteração nas ligações dissulfeto, cruciais para o seu dobramento e funcionamento (Vass 1997). Esses cromóforos susceptíveis à radiação UV podem produzir espécies reativas (Mitchell & Karentz 1993) e assim desencadear um processo crônico de vulnerabilidade na qual a velocidade de reparo pode não ser suficiente para equilibrar o estado de declínio metabólico.

3.3. Temperatura

Entre os componentes do meio ambiente em constante mudança, o aumento da temperatura é considerado um dos estressores mais prejudiciais, destacando-se como um dos principais fatores abióticos que determinam a distribuição geográfica, desenvolvimento, reprodução e sobrevivência das macroalgas. O estresse térmico causa alterações multifásicas e frequentemente adversas ao crescimento, desenvolvimento, produtividade e diversos processos fisiológicos (Fig. 8). Uma das principais consequências diretas do estresse de alta temperatura é a produção excessiva de espécies reativas, que leva ao estresse oxidativo, desencadeando uma série de mecanismos de tradução de sinal de termotolerância.

O estresse oxidativo desencadeado pelo estresse térmico, altera o metabolismo das macroalgas de várias maneiras, afetando diretamente na organização das membranas (ex. membranas plasmática, dos cloroplastos e das mitocôndrias) mediante a alteração da estabilidade de proteínas e das funções catalíticas das enzimas, e como resultado da homeostase celular. Genes responsivos ao termoestresse são ativados e diversos mecanismos de defesa iniciam sua função a fim de detoxificar as espécies reativas, recuperar a estabilidade de proteínas e enzimas e reestabelecer a homeostase.

Figura 8. Representação esquemática dos efeitos biológicos (blocos), das possíveis alterações fisiológicas (em vermelho) e das principais respostas imediatas (em verde) desencadeadas pelo estresse de aumento de temperatura. Baseado em Clark et al. (2013) e Khanna-Chopra & Semwal (2020).

Além da produção excessiva de espécies reativas, outra resposta direta ao estresse térmico é a síntese e realocação de diversos solutos capazes de reorganizar proteínas, enzimas e estruturas celulares, a fim de manter o turgor celular mediante ajuste osmótico e modificar o sistema antioxidante para reestabelecer o equilíbrio redox celular e a homeostase. Algumas moléculas termoprotetoras considerados eficazes na mitigação de danos induzidos pelo estresse por calor incluem osmoprotetores (ex. prolina, betaína glicina, sacarídeos), fitormônios, moléculas de sinalização (ex. NO), poliaminas (ex. putrescina, espermidina e espermina), oligoelementos (ex. Se, Si), nutrientes (ex. N, P, K, Ca) e substâncias antioxidantes (ex. MAAs, compostos fenólicos, carotenoides).

Entretanto, estas respostas não são exclusivas para o termoestresse. Nos trabalhos descritos anteriormente foi possível identificar uma série de efeitos com o mesmo desfecho. Diante isso, será que é possível identificar alguns descritores que possam ser propostos como marcadores de estresse? Será que os mecanismos moleculares e celulares de defesa contra o estresse são semelhantes independentemente do tipo de estressor?

A pesar das macroalgas tropicais e subtropicais estarem mais adaptadas a altas temperaturas, especialmente aquelas que crescem no mediolitoral ou poças entremarés, durante a maré baixa podem sofrer mudanças bruscas de temperatura que comumente podem chegar a 10–20°C de diferença (Helmuth & Hofmann 2001), constituindo uma amplitude de variação muito elevada.

Nesse sentido, os estudos de Urrea-Victoria (2018) e Urrea-Victoria et al. (2020; ANEXO 8) foram baseados na alga parda *Sargassum stenophyllum* J. Agardh e na alga vermelha *Pyropia spiralis* (E.C. Oliveira & Coll) M.C. Oliveira, D. Milstein & E.C. Oliveira a fim de caracterizar suas respostas frente à exposição a diferentes temperaturas. Espécies de *Sargassum* são de extrema relevância ecológica em ambientes tropicais e subtropicais por serem engenheiros ecossistêmicos e estruturadores de densos bancos marinhos. Por sua vez, *Pyropia* é um dos gêneros de macroalgas mais explorados no mundo como base para a preparação do '*sushi*'. Por suas características distintivas, *Sargassum* é uma alga parda que habita entre o mediolitoral superior e o infralitoral e *Pyropia* é uma alga vermelha que habita o mediolitoral superior, é lógico pensar que tanto sua faixa de tolerância assim como seus mecanismos de resposta a termoestresse sejam diferentes.

Tanto *S. stenophyllum* como *P. spiralis* mostraram vulnerabilidade crônica quando cultivadas em 35°C, afetando negativamente fotossíntese e transporte de elétrons, concentrações de carotenoides, ficobiliproteínas em *P. spiralis*, proteínas solúveis, carboidratos solúveis e

aminoácidos totais. Sob condição de 30°C foi possível constatar resiliência e aclimatação, uma vez que não houve alteração na fotossíntese e em pigmentos fotossintetizantes (clorofilas e carotenoides), exibindo modulação na concentração de carboidratos e diversos aminoácidos.

Uma análise de agrupamento mostrou que *S. stenophyllum* apresentou três fases de respostas: uma agrupando o comportamento das algas sob 15, 20 e 25°C, um outro agrupando as respostas de algas sob 30°C e um terceiro agrupando o desempenho sob 35°C. Para *P. spiralis*, sob 35°C foi observada necrose nos talos, provavelmente devido à produção de unidades de reprodução, levando ao completo esvaziamento do seu conteúdo celular e à desintegração do talo. Característica própria do gênero devido a sua reprodução sazonal, na qual a fase macroscópica (gametofítica) ocorre nos períodos de clima mais frio e a fase microscópica em épocas mais quentes. Assim como para *Sargassum*, *Pyropia* também apresentou três agrupamentos de respostas: dois grupos isolado com 15°C e 30°C e um grupo agregando 20 e 25°C. Aparentemente, *P. spiralis* responde melhor sob temperaturas mais baixas que as toleradas por *S. stenophyllum*. A tendência de variação do conteúdo total de aminoácidos foi igual para ambas as espécies, com aumento no conteúdo total sob exposição em 30°C. Porém a abundância do perfil dos aminoácidos foi diferente, indicando que o papel metabólico dos aminoácidos pode revelar mecanismos diferentes de ação para ambas as espécies.

Aprofundando em outros descritores químicos para ambas espécies, Urrea-Victoria (2018) identificou mecanismos diferentes de resposta. Enquanto a taxa de crescimento de *P. spiralis* se agrupava com o conteúdo de carboidratos, para *S. stenophyllum* ambos parâmetros ficaram separados, sendo o crescimento agrupado com o conteúdo de proteínas. Tendências oposta também foram identificadas para o teor de C e N. *Sargassum stenophyllum* teve maior concentração de C e N em temperaturas mais baixas, enquanto que *P. spiralis* apresentou concentrações menores em baixas temperaturas. As respostas aos ensaios antioxidantes também tiveram suas diferencias entre as espécies estudadas. *Sargassum stenophyllum* se mostrou muito mais ativa do que *P. spiralis* em todos os ensaios antioxidantes avaliados e todas as temperaturas estudadas, assim como uma maior concentração de compostos antioxidantes.

A pesar de *P. spiralis* ocorrer no mediolitoral superior, o que levaria a pensar na presença de mecanismos de resiliência mais eficientes ao termoestresse do que *S. stenophyllum* que habita no mediolitoral superior, aparentemente a fase macroscópica de *P. spiralis* é bastante susceptível a altas temperaturas, o que justifica que esta fase não seja observada em épocas mais cálidas.

Além disso, em *P. spiralis* a temperatura teve um efeito significativo em diversas alterações no conteúdo de ficobiliproteínas, aminoácidos, proteínas solúveis e MAAs, o que leva a pensar que fontes orgânicas nitrogenadas seriam altamente susceptíveis à temperatura. Diferente de *S. stenophyllum*, no qual sistemas antioxidantes mais eficientes, como polifenóis característicos de algas pardas, poderiam ser extremamente relevantes para a aclimatação aguda e recuperação crônica da espécie.

3.4. Nitrogênio

A disponibilidade de nitrogênio é um fator abiótico de estresse limitante no ambiente natural, e crucial na determinação das atividades biológicas nas macroalgas, sendo fundamental para a síntese de aminoácidos, proteínas, enzimas e pigmentos (Wanderley 2009). A limitação de nitrogênio pode ser ainda mais severa em algas vermelhas, visto que as ficobiliproteínas, principais pigmentos acessórios deste grupo, constituem importantes fontes de nitrogênio e um reservatório imediato para a alocação/utilização deste elemento. No geral, sob limitação de nitrogênio, as ficobiliproteínas são rapidamente degradadas, levando à redução da capacidade de captação de energia e, indiretamente, à diminuição de condições de estresse oxidativo e à realocação de nitrogênio para mecanismos de defesa contra estresse. Estudos de Figueroa & Korbee (2010) mostram que o estado fisiológico interno de estoque de nitrogênio nas macroalgas é fundamental para salvaguardar as respostas de aclimatação frente ao estresse ambiental.

Em regiões tropicais e subtropicais, o ambiente marinho geralmente é pobre em nitrogênio devido à forte estratificação da coluna d'água que impede a mistura vertical dos nutrientes, exceto em locais costeiros próximos a escoamento terrestre e áreas agrícolas ou regiões com ressurgência[24]. Diferente das regiões temperadas em que as águas são mais nutritivas, devido a uma mistura mais homogênea na coluna d'água (Gordillo 2012; Hurd et al. 2014).

Dessa forma, os estudos baseados na disponibilidade de nitrogênio tratam de suplementar este elemento a fim de obter melhor performance das macroalgas. Como referido anteriormente, a NR é a primeira enzima da rota de assimilação do nitrogênio, portanto, fundamental para

[24] RESSURGÊNCIA – Fenômeno de afloramento oceanográfico que consiste na subida de águas subsuperficiais, muitas vezes ricas em nutrientes, para camadas de água superficiais no oceano.

regulação desse metabolismo. Além da modulação luminosa da atividade da NR, ela é fortemente regulada pela disponibilidade de nitrato, assim como a presença de outras fontes nitrogenadas (Chow & Oliveira 2008) e elementos não nitrogenados como o fósforo (Martins et al. 2009). Evidentemente, um equilíbrio nutricional é fundamental para a manutenção metabólica do organismo, de forma a preservar a boa performance fisiológica de homeostase.

Mecanismos de regulação pós-traducional da NR também foram evidenciados em macroalgas. Chow et al. (2013) (ANEXO 9) mostraram resultados que evidenciaram a modulação da cadeia fotossintetizante de transporte de elétrons e o balanço de NO na atividade da NR na alga vermelha *Gracilaria chilensis* C.J. Bird, McLachlan & E.C. Oliveira. Essa associação pode estar ligada à crucial modulação entre a assimilação do nitrogênio e o metabolismo do carbono, a fim de garantir a incorporação de fontes nitrogenadas em compostos orgânicos, evitando assim a toxicidade celular por nitrito, amônio e espécies reativas de oxigênio ou de nitrogênio. Ao que tudo indica, o NO pode ser uma importante molécula sinalizadora e reguladora da atividade da NR, no qual o cGMP poderia participar como mensageiro secundário na regulação de processos de fosforilação e desfosforilação. Um panorama geral sobre a assimilação do nitrato e o papel da NR pode ser examinado em Chow (2012) (ANEXO 10). Desde então, vários avanços sobre a atividade e regulação da NR têm sido desenvolvidos com plantas vasculares, porém, ainda permanecem limitados os estudos com macroalgas, destacando os estudos recentes de Paine et al. (2020), Shahar et al. (2020), Zhong et al. (2020), Yang et al. (2021).

Um trabalho relacionado também ao estudo de nutrientes em macroalgas é o realizado por Nardelli et al. (2019) (ANEXO 11) em sistema de cultivo '*outdoor*'[25], em condições semicontroladas. Nesse estudo, a alga verde *Ulva lactuca* Linnaeus foi cultivada em sistema '*outdoor*' com integração multitrófica de efluentes de mexilhões e peixes como fonte fornecedora de nutrientes, com o objetivo de avaliar o aproveitamento da produção de biomassa algácea aliado à capacidade de bioremediação dos efluentes de cultivo animal. O cultivo de *U. lactuca* com efluentes de peixes e efluentes de mexilhões+peixes promoveram significativamente o crescimento e a taxa de crescimento da alga, exibindo elevadas taxas de captação de fosfato, amônio, nitrito e nitrato e produção de oxigênio. Considerando que a única manipulação experimental foi o suprimento de diferentes fontes de nutrientes, providas como efluentes de cultivo de peixes ou efluentes de cultivo de mexilhões+peixes, e as demais condições abióticas

[25] **OUTDOOR** – Sistema de cultivo ao ar livre, com aproveitamento das condições ambientais naturais.

foram as oferecidas pelo ambiente, os resultados mostram que os nutrientes (tanto na sua forma e concentração) tiveram um papel importante na produção de biomassa de *U. lactuca*. Um sistema de cultivo '*outdoor*' tem a vantagem de ser um cultivo de menor custo, menor manutenção e requerimento de equipamentos especializados e melhor aproveitamento das características ambientais de forma mais natural quando comparado com um cultivo em condições controladas de laboratório ou '*indoor*'[26], sendo apropriado para a produção de biomassa e seleção de mudas. Além disso, um cultivo associado a um sistema integrado multitrófico possibilita a bioremediação de nutrientes, reduzindo o despejo de efluentes ricos em N e P que podem levar à eutrofização[27] do ambiente.

Essa prática de cultivos integrados com diversas espécies no mesmo corpo d'água são comumente chamados de policultivos ou Aquacultura MultiTrófica Integrada (AMTI), baseados na criação de um ecossistema de cultivo com espécies de diferentes níveis tróficos, na qual cada nível utiliza ou reaproveita os produtos residuais de outro nível do sistema (Chopin et al. 2008). Além dos objetivos de produção, focado principalmente na produção de proteína animal (ex. peixes, camarões ou mariscos), a incorporação de macroalgas em um sistema integrado pode suprir a demanda por certas algas marinhas para consumo humano ou ração animal ou por matéria-prima para a produção de ficocoloides (Neori et al. 2004, 2007), um mercado de mais de 22,4 bilhões de US$ registrado em 2008 (FAO 2016). Além disso, locais com águas oligotróficas, como no caso do litoral do Brasil, a aquacultura integrada parece ser uma alternativa viável para gerar uma nova fonte de produto aquícola e melhor aproveitar os recursos de diferentes fontes subutilizadas de forma sustentável (Schuenhoff et al. 2003; Neori et al. 2004; Butterworth 2010).

3.5. Estudos ecofisiológicos

Estudos ecofisiológicos relacionados à fisiologia do estresse em macroalgas têm ganhado maior atenção nos últimos 10 anos, devido principalmente às mudanças climáticas e ao aquecimento global (Israel et al. 2010; Gómez & Houvinen 2020). A pesar dos estudos controlados em

[26] INDOOR – Sistema de cultivo sob condições controladas.
[27] EUTROFIZAÇÃO ou EUTROFICAÇÃO – Quando um corpo de água recebe uma grande quantidade de efluentes com matéria orgânica enriquecida com minerais e nutrientes que induzem o crescimento excessivo de algas e plantas aquáticas.

laboratório possibilitar uma melhor compreensão sobre as respostas mecanicistas dos processos, eles geralmente contemplam variáveis isoladas ou apenas algumas variáveis, proporcionando uma visão reducionista do funcionamento e do efeito das condições abióticas de estresse nas macroalgas. Resultados de estudos em campo se revelam mais complexos na sua interpretação, uma vez que em condições naturais a interação dos fatores é inerente e muitas vezes difíceis de se estabelecer relações entre o efeito e a resposta. No entanto, certos padrões de resposta fisiológica observados sob condições laboratoriais controladas são também identificados em estudos ecofisiológicos em campo.

O ambiente natural do mediolitoral constitui-se por si só um ecossistema sujeito constantemente a estressores, governado principalmente pela flutuação diária das marés, mas também condicionado pelas variações sazonais. Tanto as variações diárias como as sazonais parecem determinar respostas de estresse oxidativo que são dinamicamente moduladas e que permitem a aclimatação das macroalgas (Bischof & Rautenberger 2012). Tudo indica que existe um mecanismo de preparo para o estresse oxidativo (POS), apesar deste conceito não ter sido utilizado para macroalgas até o meu conhecimento. A dinâmica de fotoproteção e fotoinibição em resposta à variação luminosa e radiação UV natural é amplamente discutida em Hanelt & Figueroa (2012). Respostas das macroalgas à temperatura (Eggert 2012), disponibilidade de nutrientes (Gordillo 2012) e salinidade e dessecamento (Karsten 2012) também têm sido largamente tratados sob a perspectiva de mudanças climáticas globais.

Nos estudos sobre fenologia de Tala & Chow (2014a) (ANEXO 12) e ecofisiologia de Tala & Chow (2014b) (ANEXO 13) da alga vermelha *Porphyra* spp. em um gradiente latitudinal no litoral do Chile, foram identificadas respostas ecofisiológicas que caracterizam a percepção antecipada das macroalgas às variações sazonais e latitudinais. O ajuste mais evidente entre as populações estudadas foi o aumento da abundância em relação ao aumento da latitude, variando em cobertura e biomassa reprodutiva. O gradiente sazonal dos fatores físicos, especialmente o aumento da temperatura, parece determinar a susceptibilidade de *Porphyra* ao longo do ano, exibindo alterações fenológicas, redução no seu fitness fotossintetizante e conteúdo de pigmentos e proteínas, assim como aumento na sua capacidade antioxidante. A variação em abundância, fotossíntese, pigmentos, proteínas e atividade antioxidante foi registrada gradualmente ao longo do ano, indicando a existência de sistemas endógenos sensíveis a mudanças sazonais que permitem antecipar condições desfavoráveis para o seu

desenvolvimento, provavelmente relacionado à conjunção da radiação solar, temperatura, umidade do ar e fotoperíodo. Essas respostas bioquímicas e fisiológicas têm sido identificadas como mecanismos de proteção da integridade celular a danos e perda de homeostase (Demmig-Adams & Adams 1992; Franklin & Forster 1997; Häder & Figueroa 1997; Cruces et al. 2012). Contudo, devido à falta da aferição de outros descritores bioquímicos, como por exemplo compostos antioxidantes e atividade de enzimas antioxidantes, é precoce estabelecer a relação das respostas aos mecanismos de regulação de estresse oxidativo, parâmetros necessários para esclarecer a compreensão dos mecanismos de POS imposto pelas variações sazonais.

Estudos ecofisiológicos avaliando a atividade antioxidante (Santos et al. 2019a; ANEXO 14) e o perfil de ácidos graxos (Santos et al. 2019b; ANEXO 15) nas algas parda *Sargassum vulgare* C. Agardh, vermelha *Palisada flagellifera* (J. Agardh) K.W. Nam e verde *Ulva fasciata* Delile durante as estações seca e chuvosa, mostram algumas variações. No geral, o rendimento dos extratos foi significativamente maior durante a estação chuvosa para *S. vulgar* e *P. flagellifera*, indicando uma elevada susceptibilidade destas espécies para a produção de maior quantidade de metabólitos nesse período. A atividade antioxidante dos extratos metanólicos dessas espécies seguiram a mesma tendência, apresentando maior atividade antioxidante na estação chuvosa. O oposto foi registrado para o extrato metanólico de *U. fasciata*, na qual a maior atividade foi nas amostras da estação seca. Extratos aquosos de *S. vulgare* tiveram maior atividade em amostras da estação seca, não sendo possível identificar um padrão de resposta para as outras duas espécies. Esta inversão dos resultados entre os extratos metanólicos e aquosos mostra diferenças na presença de metabólitos de defesa antioxidativo entre as espécies estudadas e entre as estações, podendo ser variações em abundância e composição. Esses resultados reforçam a existência de sistemas antioxidantes diferencialmente expressos sob condições ambientais variáveis, podendo estar orquestrados no funcionamento para os mecanismos de POS. Por sua vez, a variação nas respostas de defesa antioxidativo entre ambas estações, parece não estar acompanhadas por uma variação no conteúdo total de ácidos graxos, no qual as diferenças foram observadas apenas entre as espécies. A estabilidade no conteúdo de ácidos graxos em algas tropicais é corroborada por Khotimchenko (2003), Narayan et al (2005) e Susanto et al. (2016), diferente do que ocorre em macroalgas de ambientes polares, no qual mecanismos de regulação termo-adaptativos estão relacionados à fluidez das membranas (Nozawa 2011).

4. Considerações finais, perspectivas e desafios

Dado o panorama da fisiologia do estresse em macroalgas apresentado neste texto e considerando as descobertas realizadas pelo nosso grupo de pesquisa, identificamos um conjunto de respostas fisiológicas, bioquímicas e ultraestruturais presentes nas espécies estudadas e que podem ser categorizadas em três estágios de respostas: dano agudo, dano agudo-crônico e dano crônico (Fig. 9). Aparentemente, independente do fator abiótico de estresse, algumas das respostas são semelhantes e irá depender da dose do estressor e da capacidade de aclimatação e resiliência da espécie. Alguns metabólitos primários e secundários parecem ser mais informativos para entender as respostas e os mecanismos sob efeito de situações de estresse abiótico (Lalegerie et al. 2020).

O **estágio 1** corresponderia a uma condição de dano agudo, na qual as algas ativariam mecanismos resilientes de aclimatação, resistindo à condição de estresse, ocorrendo, portanto, poucas alterações nas respostas fisiológicas tais como crescimento, fotossíntese, pigmentos, proteínas, C:N e atividade antioxidante. Variações nas respostas seriam perceptíveis se o estresse aumentar em tempo de exposição, intensidade ou frequência, considerado como **estágio 2**, ocorrendo a diminuição dessas respostas fisiológicas e aumentando os níveis de dissipação não fotoquímica regulada, síntese e extrusão de compostos fenólicos, taxa de ação do ciclo da xantofila, desbalanço nos níveis de C;N, produção de osmólitos e variação nas concentrações de aminoácidos. No estágio 2, o dano agudo extremo e o dano agudo-crônico afetam seriamente a performance da macroalga, comprometendo o seu nível de resistência e desencadeando a exaustão do sistema de defesa. Cabe destacar que sob estresse de dano agudo devido a radiação UV, alterações na integridade do DNA já são perceptíveis. No **estágio 3**, a partir do limite superior de dano agudo-crônico e no dano crônico, a redução do crescimento e da fotossíntese são nitidamente evidentes, produto do comprometimento de uma série de rotas metabólicas e que permanecem em fase de contínua exaustão. Falhas irreversíveis nos sistemas de reparo e proteção começam a aparecer, ocorre aumento da taxa de morte e perda de viabilidade celular e diversas alterações ultraestruturais são evidenciadas, como desorganização dos cloroplastos e das mitocôndrias. Mecanismos de defesa antiestresse são ativados em taxas exacerbadas, na tentativa de restaurar o estado homeostático celular, principalmente àquelas relacionadas ao estresse oxidativo como zeaxantina, carboidratos, aminoácidos, compostos fenólicos, osmólitos, espécies reativas de oxigênio e óxido nítrico, respostas congruentes com o exposto por Aguilera

& Rautenberger (2012) e Bischof & Rautenberger (2012). Se os níveis de estresse não são diminuídos ou não ocorre um período de recuperação, o desenlace levará à morte do indivíduo.

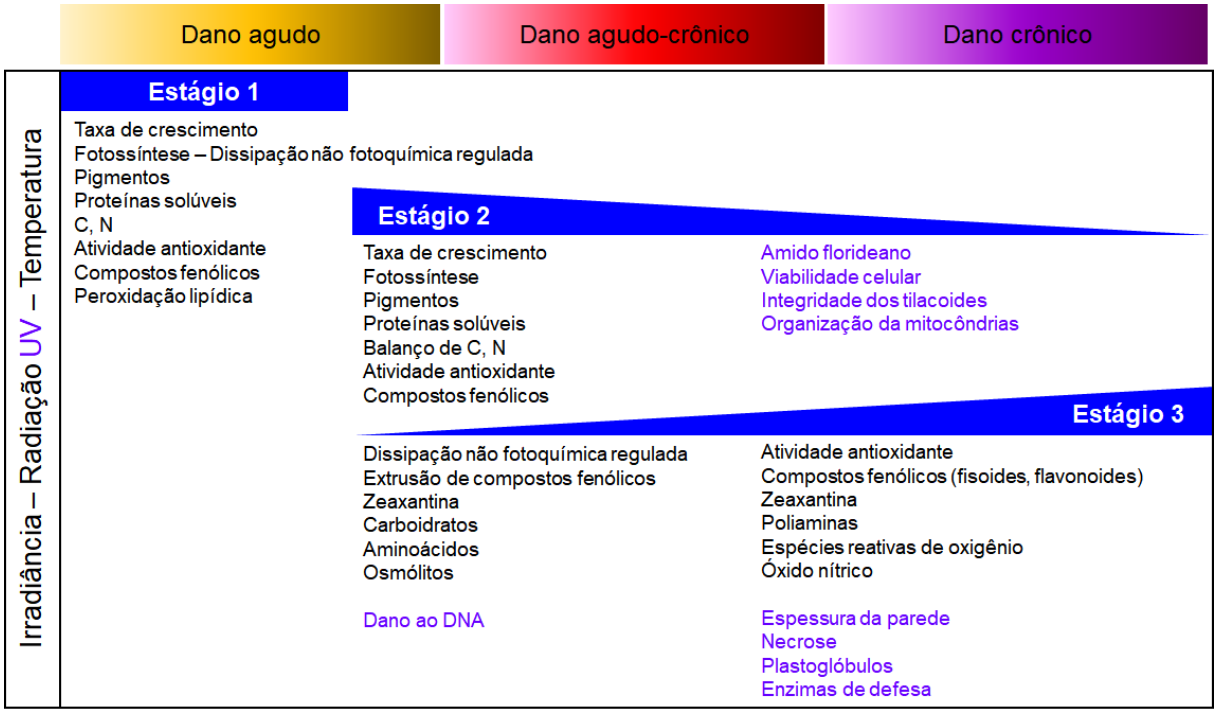

Figura 9. Sinopse das respostas fisiológicas e metabólicas de macroalgas desencadeadas por condições de estresse (dano agudo, dano agudo-crônico e dano crônico) categorizadas em três estágios de alterações. Respostas em roxo correspondem a alterações detectadas sob radiação UV.

A partir dessa sinopse, considerando apenas os descritores avaliados nos nossos estudos, é possível identificar que macrodescritores como fotossíntese e crescimento podem ser menos sensíveis a alterações sob condições de estresse. Descritores bioquímicos parecem ser mais informativos e sensíveis aos efeitos do estresse e aparentemente entre mais específico é o descritor, por exemplo, enzimas antioxidantes, osmólitos, produção de óxido nítrico, melhor é o esclarecimento dos mecanismos responsáveis pelas respostas. Essa sinopse, a pesar de ser simples e baseada na caracterização descritiva de respostas frente ao estresse, ainda está longe de elucidar os mecanismos que controlam essas respostas. Isto é um dos maiores gargalos e desafios para o avanço da fisiologia do estresse em macroalgas. Apesar de diversos estudos caracterizar muito bem as perturbações fisiológicas e bioquímicas desencadeadas nas macroalgas sob condições de estresse dos fatores abióticos, ainda existe uma grande lacuna na compreensão de como esses mecanismos se integram e são regulados nas macroalgas. Situação que se contrapõe ao número de estudos sobre fisiologia do estresse de microalgas e plantas

vasculares, e que fortemente embasam as discussões em macroalgas. Em macroalgas, um dos poucos mecanismos de ação melhor caracterizado frente a condições de estresse está relacionado às pesquisas em fotossíntese.

Portanto, temos um longo caminho a percorrer nas temáticas de fisiologia do estresse nas macroalgas, especialmente no entendimento dos mecanismos de POS. No entanto, esse desafio parece estar mais próximo de ser desvendado, visto que os grupos de pesquisa em fisiologia ficológica vêm cada vez mais investindo em procedimentos analíticos que permitem essa compreensão mais ampla, a fim de entender os mecanismos celulares que direcionam as respostas frente ao estresse. Aparentemente, as diversas respostas às condições ambientais são conduzidas pelo protagonismo do estresse oxidativo, conhecimento que já vem se consolidando na fisiologia ficológica.

Dessa forma, estudos abrangentes que englobem metodologias como *screening* fitoquímico, atividade enzimática e estudos ômicos, por exemplo, proteômica e metabolômica, podem vir a contribuir com o conhecimento e compreensão dos mecanismos que levam à regulação das respostas ao estresse. Perspectivas que fazem parte dos objetivos futuros do nosso grupo de pesquisa. Objetivamente, pretendemos incorporar procedimentos analíticos para estudos metabolômicos e de enzimas relacionadas ao estresse oxidativo, com vistas a contribuir com o entendimento de como algumas rotas metabólicas são reguladas e quais são os principais metabólitos e enzimas que respondem ao estresse oxidativo. Adicionalmente, é de nosso interesse auxiliar na compreensão dos mecanismos de preparo para o estresse oxidativo (POS) e balanço de carbono/nitrogênio em situações de dano agudo e agudo-crônico nas macroalgas, uma vez que, até nosso conhecimento, ambos processos não têm sido cogitados ou explorados na ficologia.

Para alcançar esses objetivos, parte dos desafios será iniciado com o estabelecimento e a validação de metodologias complementares em nosso grupo de pesquisa, assim como capacitação de recursos humanos que possam lidar com um grande número de informações aliadas a ferramentas de bioinformática. Para tal, colaborações de pesquisa já foram estabelecidas e temos pretensão de iniciar essas abordagens no segundo semestre de 2021.

5. Referências bibliográficas

Abele D., Vázquez-Medina J.P. Zenteno-Savín T. 2012. Introduction to oxidative stress in aquatic ecosystems. In: Oxidative stress in aquatic ecosystems. Abele D., Vázquez-Medina J.P., Zenteno-Savín T. (eds.). Blackwell Publishing Ltd. pp. 1-6.

Aguilera J., Rautenberger R. 2012. Chapter 4. Oxidative stress tolerance strategies of intertidal macroalgae. In: Oxidative stress in aquatic ecosystems. Abele D., Vázquez-Medina J.P., Zenteno-Savín T. (eds.). Blackwell Publishing Ltd. pp. 58-71.

Aro E.-M., McCaffery S., Anderson J.M. 1993. Photoinhibition and D1 protein degradation in peas acclimated to different growth irradiances. Plant Physiol.103: 835-843.

Barber J., Andersson B. 1992. Too much of a good thing: light can be bad for photosynthesis. Trends Biochem. Sci. 17(2): 61-66.

Bischof K., Hanelt D., Wiencke C. 2000. Effects of ultraviolet radiation on photosynthesis and related enzyme reactions of marine macroalgae. Planta 211: 555-562.

Bischof K., Rautenberger R. 2012. Chapter 6. Seaweed responses to environmental stress: reactive oxygen and antioxidative strategies. In: Seaweed biology. Novel insights into ecophysiology, ecology and utilization. Wiencke C., Bischof K. (eds.). Springer. pp. 109-132.

Bischof K., Steinhoff F.S. 2012. Chapter 20. Impacts of ozone stratospheric depletion and solar UVB radiation on seaweeds. In: Seaweed biology. Novel insights into ecophysiology, ecology and utilization. Wiencke C., Bischof K. (eds.). Springer. pp. 433-448.

Bold H.C., Wynne M.J. 1984. Introduction to the algae. 2nd edition. Prentice-Hall.

Bouzon Z.L., Chow F., Zitta C.S., Santos R.W., Ouriques L.C., Felix M.R.L., Osorio L.K.P., Gouveia C., Martins R.P., Latini A., Ramlov F., Maraschin M., Schmidt E.C. 2012. Effects of natural radiation, photosynthetically active radiation and artificial ultraviolet radiation-B on the chloroplast organization and metabolism of *Porphyra acanthophora* var. *brasiliensis* (Rhodophyta, Bangiales). Microsc. Microanal. 18: 1467-1479.

Chopin T., Robinson S.M.C., Troell M., Neori A., Buschmann A.H., Fang J. 2008. Multitrophic integration for sustainable marine aquaculture. In: Ecological engineering, vol. 3, Encyclopedia of ecology. Jørgensen S.E., Fath B.D. (eds.). Elsevier, Oxford. pp. 2463-2475.

Chow F., Oliveira M.C. 2008. Rapid and slow modulation of nitrate reductase activity in the red macroalga *Gracilaria chilensis* (Gracilariales, Rhodophyta): influence of different nitrogen sources. J. Appl. Phycol. 20: 775-782.

Chow F., Oliveira M.C., Pedersén M. 2004. *In vitro* assay and light regulation of nitrate reductase in red alga *Gracilaria chilensis*. Journal of Plant Physiology 161: 769-776.

Chow F., Capociama F.V., Faria R., Oliveira M.C. 2007. Characterization of nitrate reductase activity *in vitro* in *Gracilaria caudata* J. Agardh (Rhodophyta, Gracilariales). Rev. Brasil. Bot. 30(1): 123-129.

Clark J.S., Poore A.G.B., Ralph P.J. Doblin M.A. 2013. Potential for adaptation in response to thermal stress in an intertidal macroalga. Journal of Phycology 49(4): 630-639.

Cruces E., Huovinen P., Gómez I. 2012. Stress proteins and auxiliary anti-stress compounds in intertidal macroalgae. Lat. Am. J. Aquat. Res. 40(4): 822-834.

Davison I.R., Pearson G.A. 1996. Stress tolerance in intertidal seaweeds. J. Phycol. 32: 197-211.

Demmig-Adams B., Adams W.W. 1992. Photoprotection and other responses of plants to high light stress. Annu. Ver. Plant Physiol. Plant Mol. Biol. 43: 599-626.

Eggert A. 2012. Chapter 3. Seaweed responses to temperature. In: Seaweed biology. Novel insights into ecophysiology, ecology and utilization. Wiencke C., Bischof K. (eds.). Springer. pp. 47-64.

Evert R.F., Eichhorn S.E. 2014. Raven Biologia vegetal. 8ª edição. Guanabara Koogan, RJ, Brasil.

Falkowski P.G., LaRoche J. 1991. Acclimation to spectral irradiance in algae. Journal of Phycology 27(1): 8-14.

Falkowski P.G., Raven J.A. 1997. Aquatic photosynthesis. 2nd Edition. Princeton University Press, USA.

FAO. 2016. The state of world fisheries and aquaculture 2016. Contributing to food security and nutrition for all. FAO, Rome.

Figueroa F.L., Korbee N. 2010. Interactive effects of UV radiation and nutrientes on ecophysiology: vulnerability and adaptation to climate change. In: Seaweeds and their role in globally changing environment. Israel A., Einav R., Seckbach J. (eds.). Springer-Verlag Berlin Heidelberg. pp. 157-181.

Fogg G.E. 2001. Chapter 1. Algal adaptation to stress – Some general remarks. In: Algal adaptation to enviromental stresses. Physiological, biochemical and molecular mechanisms. Rai L.C., Gaur J.P. (eds.). Springer-Verlag Berlin Heidelberg. pp. 1-20.

Franklin L.A., Forster R.M. 1997. The changing irradiance environment: consequences for marine macrophyte physiology, productivity and ecology. Eur. J. Phycol. 32: 207-232.

Galviz Y.C.F., Ribeiro R.V., Souza G.M. 2020. Yes, plants do have memory. Theor. Exp. Plant Physiol. 32: 195-202.

Gambichler V., Zuccarello G.C., Karsten U. 2021. Seasonal changes in stress metabolites of native and introduced red algae in New Zealand. Journal of Applied Phycology (online first) https://doi.org/10.1007/s10811-020-02365-0

Gómez I., Houvinen P. 2011. Morpho-functional patterns and zonation of South Chilean seaweeds: the importance of photosynthetic and bio-optical traits. Mar. Eco. Prog. Ser. 422: 77-91.

Gómez I., Houvinen P. 2020. Antarctic seaweeds. Diversity, adaptations and ecosystems services. Springer.

Gómez I., Orostegui M., Huovinen P. 2007. Morpho-functional patterns of photosynthesis in the south Pacific kelp *Lessonia nigrescens*: effects of UV radiation on ^{14}C fixation and primary photochemical reactions. J. Phycol. 43: 55-64.

Gordillo F.J.L. 2012. Chapter 4. Environment and algal nutrition. In: Seaweed biology. Novel insights into ecophysiology, ecology and utilization. Wiencke C., Bischof K. (eds.). Springer. pp. 67-85.

Graham J.E., Wilcox L.W., Graham L.E. 2008. Algae. 2nd edition. Benjamin Cummings.

Granbom M., Chow F., Lopes P.F., Oliveira M.C., Colepicolo P., Paula E.J., Pedersén M. 2004. Characterisation of nitrate reductase in the marine macroalga *Kappaphycus alvarezii* (Rhodophyta). Aquat. Bot. 78: 295-305.

Häder D.P., Figueroa F.L. 1997. Photoecophysiology of marine macroalgae. Photochem. Photobiol. 66: 1-14.

Hanelt D. 1998. Capability of dynamic photoinhibition in Arctic macroalgae is related to their depth distribution. Mar. Biol. 131: 361-369.

Hanelt D., Figueroa F.L. 2012. Chapter 1: Physiological and photomorphogenic effects of light on marine macrophytes. In: Seaweed biology. Novel insights into ecophysiology, ecology and utilization. Wiencke C., Bischof K. (eds.). Springer. pp. 3-23.

Hanelt D., Roleda M.Y. 2009. UVB radiation may ameliorate photoinhibition in specific shallow-water tropical marine macrophytes. Aquat. Bot. 91: 6-12.

Hanelt D., Wiencke C., Nultsch W. 1997a. Influence of UV radiation on the photosynthesis of arctic macroalgae in the field. J. Photo. Photobiol. B: Biol. 38(1): 40-47.

Hanelt D., Melchersmann B., Wiencke C., Nultsch W. 1997b. Effects of high light stress on photosynthesis of polar macroalgae in relation to depth distribution. MEPS 149: 255-266.

Hanelt D., Wiencke C., Karsten U., Nultsch W. 1997c. Photoinhibition and recovery after high light stress in different developmental and life-history stages of *Laminaria saccharina* (Phaeophyta). J. Phycol. 33(3): 387-395.

Helmuth B.S.T., Hofmann G.E. 2001. Microhabitats, thermal heterogeneity, and patterns of physiological stress in the rocky intertidal zone. Biol. Bull. 201(3): 374-384.

Houvinen P., Gómez I., Lovengreen C. 2006. A five-year study of solar ultraviolet radiation in southern Chile (39 degrees S): potential impact on physiology of coastal marine algae? Photochem. Photobiol. 82(2):515-522.

Houvinen P., Gómez I., Orostegui M. 2007. Patterns and UV sensitivity of carbono anhydrase and nitrate reductase activities in South Pacific macroalgae. Mar. Biol. 151: 1813-1821.

Hurd, C.L., Harrison, P.J., Bischof, K., Lobban, C.S. 2014. Seaweed ecology and physiology. 2nd Ed. Cambridge University Press, UK.

Imbs T.I., Zvyagintseva T.N. 2018. Phlorotannins are polyphenolic metabolites of brown algae. Russian Journal of Marine Biology 44(4): 263-273.

Israel A., Einav R., Seckbach J. Seaweeds and their role in globally changing environments. Springer.

Jeffrey S.W., Humphrey G. 1975. New spectrophotometric equations for determining chlorophylls *a*, *b*, *c1* and *c2* in higher plants, algae and natural phytoplankton. Biochem. Physiol. Pflanz. 649(1): 105-149.

Karsten U. 2012. Chapter 5. Seaweed acclimation to salinity and dessication stress. In: Seaweed biology. Novel insights into ecophysiology, ecology and utilization. Wiencke C., Bischof K. (eds.). Springer. pp. 87-106.

Khanna-Chopra R., Kumar S.V. 2020. Ecophysiology and response of plants under high temperature stress. In: Hasanuzzaman M. (eds), Plant ecophysiology and adaptation under climate change: mechanisms and perspectives I. Springer, Singapore. pp. 295-329.

Khotimchenko S.V. 2003. Fatty acids of species in the genis *Codium*. Bot. Mar. 46: 456-460.

Kelling P., Burki F. 2019. Progress towards the tree of eukaryotes. Current Biology 29: R808-R817.

Kranner I., Minibayeva F.V., Beckett R.P., Seal C.E. 2010. What is stress? Concepts, definitions and applications in seed science. New Phytol. 188: 655–673.

Lalegerie F., Gager L., Stiger-Pouvreae V., Connan S. 2020. Chapter 8: The stressful life of red and brown seaweeds on the temperate intertidal zone: effect of abiotic and abiotic parameters on the physiology of macroalgae and contente variability of particular metabolites. In: Seaweeds around the world: state of art and perspectives. Bourgougnon N. (ed.). Advanced in Botanical Research Volume 95.

Larkum A.W., Wood W.F. 1993. The effect of UV-B radiation on photosynthesis and respiration of phytoplankton, benthic macroalgae and seagrasses. Photos. Res. 36: 17-23.

Lee R.E. 2008. Phycology. 4th edition. Cambridge University Press.

Lichtenthaler H.K. 1996. Vegetation stress: an introduction to the stress concept in plants. J. Plant Physiol. 148: 4–14.

Lichtenthaler H.K., Buschmann C. 2001. Chlorophylls and carotenoids: measurement and characterization by UV-VIS. In: Current protocols in food analytical chemistry. Wrolstad R.E., Acree T.E., Decker E.A., Penner M.H., Reid D.S., Schwartz S.J., Shoemaker C.F., Sporns P. (eds.). John Wiley, New York. pp. F4.3.1–F4.3.8.

Lois R., Buchanan B.B. 1994. Severe sensitivity to ultraviolet radiation in an *Arabidopsis* mutant deficient in flavonoid accumulation. II. Mechanisms of UV-resistance in *Arabidopsis*. Planta 194: 504-509.

Lourenço-Lopes C., Fraga-Corral M., Jimenez-Lopez C., Pereira A.G., Garcia-Oliveira P., Carpena M., Prieto M.A., esus Simal-Gandara J. 2020. Metabolites from macroalgae and its applications in the cosmetic industry: a circular economy approach. Resources 9: 101.

Martins A.P., Chow F., Yokoya N.S. 2009. Ensaio in vitro da enzima nitrato redutase e efeito da disponibilidade de nitrato e fosfato em variantes pigmentares de *Hypnea musciformis* (Wulfen) J. V. Lamour. (Gigartinales, Rhodophyta). Rev. Brasil. Bot. 32(4): 635-645.

Mitchell D.L., Karentz D. 1993. The induction and repair of DNA photodamage in the environment. In: Environmental UV photobiology. Young A.R., Bjom L.O., Moan J., Nultsch W. (eds.). Plenum Press, New York. pp. 345-377.

Mittler, R. 2002. Oxidative stress, antioxidante and stress tolerance. Trends in Plany Science 7(9): 405-410.

Mosa K.A., Ismail A., Helmy M. 2017. Plant stress tolerance. An integrated omics approach. Springer, Switzerland.

Narayan B., Miyashita K., Hosakawa M. 2005. Comparative evaluation of fatty acid composition of diferente *Sargassum* (Fucales, Phaeophyta) species harvested from temperate and tropical Waters. J. Aquat. Food Prod. Technol. 13: 53-70.

Neori A., Troell M., Chopin T., Yarish C., Critchley A., Buschmann A.H. 2007. The need for a balanced ecosystem approach to blue revolution aquaculture. Environment: Science and Policy for Sustainable Development 49(3): 36-43.

Neori A., Chopin T., Troell M., Buschmann A.H., Kraemer G.P., Halling C., Shipigel M., Yarish C. 2004. Integrated aquaculture: rationale, evolution and state of the art emphasizing seaweed biofiltration in modern mariculture. Aquaculture 231: 361-391.

Nozawa Y. 2011. Adaptative regulation of membrane lipids and fluidity during termal acclimation in *Tetrahymena*. Proc. Jpn. Acad. Ser. B Phys. Bio. Sci. 87: 450-462.

Oliveira M.F., Geihs M.A., França T.F.A., Moreira D.C., Hermes-Lima M. 2019. Is the "Preparation for Oxidative Stress" a case of physiological conditioning hormesis? Frontiers in Physiology 9: 945.

Paine E.R., Schmid M., Revill A.T., Hurd C. Light regulates inorganic nitrogen uptake and storage, but not nitrate assimilation, by the red macroalga *Hemineura frondosa* (Rhodophyta). European Journal of Phycology, DOI: 10.1080/09670262.2020.1786858.

Pereira D.T., Simioni C., Ouriques L.C., Ramlov F., Maraschin M., Steiner N., Chow F., Bouzon Z.L., Schmidt É.C. 2018. Comparative study of the effects of salinity and UV radiation on metabolism and morphology of the red macroalga *Acanthophora spicifera* (Rhodophyta, Ceramiales). Photosynthetica 56(3): 799-810.

Polo L.K. 2019. Physiological responses, bioactivity and differential analysis of protein abundance of the brown seaweed *Sargassum* (Phaeophyceae, Fucales) submitted to UV radiation. Tese de Doutorado, Instituto de Biociências, Universidade de São Paulo, Brasil.

Rautenberger R., Mansilla A., Gómez I., Wiencke C., Bischof K. 2009. Photosynthetic acclimation to UV-radiation of intertidal macroalgae from the Strait of Magellan (Chile). Rev. Chil. Hist. Nat. 82: 43-61.

Salehi B., Sharifi-Rad J., Seca A.M.L., Pinto D.C.G.A., Michalak I., Trincone A., Mishra A.P., Nigam M., Zam W., Martins N. 2019. Current trends on seaweeds: looking at chemical composition, phytopharmacology, and cosmetic applications. Molecules 24:4182.

Schoenwaelder M.E.A. 2002. The occurrence and cellular significance of physodes in brown algae. Phycologia 41(2): 125-139.

Schuenhoff A., Shpigel M., Lupatsch I., Ashkenazi A., Msuya F.E., Neori A. 2003. A semirecirculating, integrated system for the culture of fish and seaweed. Aquaculture 221: 167-181.

Serra D.R. 2013. Respostas de *Gracilariopsis tenuifrons* (Gracilariales – Rhodophyta) a estímulos de irradiância *in vitro*. Dissertação de Mestrado, Instituto de Biociências, Universidade de São Paulo, Brasil. 97 pp.

Shahar B., Shpigel M., Barkan R., Masasa M., Neori A., Chernov H., Salomon E., Kiflawi M., Guttman L. 2020. Changes in metabolism, growth and nutrient uptake of *Ulva fasciata* (Chlorophyta) in response to nitrogen source. Algal Res. 46: 101781.

Simioni C., Schmidt É.C., Felix M.R.L., Polo L.K., Rover T., Kreusch M., Pereira D.T., Chow F., Ramlov F., Maraschin M., Bouzon Z.L. 2014. Effects of ultraviolet radiation (UVA+UVB) on young gametophytes of *Gelidium floridanum*: growth rate, photosynthetic pigments, carotenoids, photosynthetic performance, and ultrastructure. Photochemistry and Photobiology 90: 1050-1060.

Sudatti D.B., Duarte H.M., Soares A.S., Salgado L.T., Pereia R.C. 2020. New ecological role of seaweed secondary metabolites as autotoxic ans allelopathic. Frontiers in Plant Science 11: 347.

Susanto E., Suhaeli A., Abe M. 2016. Lipids, fatty acids, and fucoxanthin contente from temperate and tropical brown seaweeds. Aquat. Proce. 7: 66-75.

Torres P.B., Chow F., Furlan C.M., Mandelli F., Mercadante A., Santos D.Y.A.C. 2014. Standardization of a protocol to extract and analyze chlorophyll *a* and carotenoids in *Gracilaria tenuistipitata* var. *liui* Zhang & Xia (Rhodophyta). Braz. J. Oceanogr. 62(1): 57-63.

Urrea-Victoria V. 2018. Efeito do estresse térmico sobre respostas fisiológicas, composição química e potencial antioxidante de *Sargassum stenophyllum* (Fucales, Ochrophyta) e *Pyropia spiralis* (Bangiales, Rhodophyta). Tese de Doutorado, Instituto de Biociências, Universidade de São Paulo.

Vass I., Szilárd A., Sicora C. 2005. Chapter 43 – Adverse effects of UV-B light on the structure and function of the photosynthetic apparatus. In: Handbook of photosynthesis. Pessarakli M. (ed.). 2nd Ed. Taylor & Francis Group, LLC.

Vass I. 1996. Adverse effects of UV-B light on the structure and function of the photosynthetic apparatus. In: Pessarakli M. (ed.). Handbook of photosynthesis, Marcel Dekker, New York. pp. 931-950.

Wanderley, A. 2009. Influência da disponibilidade de nitrato sobre crescimento, atividade da nitrato redutase, composição química e captação de nitrato e fosfato em *Gracilariopsis tenuifrons* (Gracilariales, Rhodophyta). Dissertação de Mestrado, Instituto de Biociências, Universidade de São Paulo.

Wellburn A.R. 1994. The spectral determination of chlorophylls a and b, as well as total carotenoids, using various solvents with spectrophotometers of different resolution. J. Plant Physiol. 144(3): 307-313.

Wiencke, C., Bischof K. 2012. Seaweed biology. Novel insight into ecophysiology, ecology and utilization Springer.

Yang J., Yin Y., Yu D., He L., Shen S. 2021. Activation of MAPK signaling in response to nitrogen deficiency in *Ulva prolifera* (Chlorophyta). Algal Res. 53: 102153.

Zhong Z., Liu Z., Zhuang L., Song W., Chen W. 2020. Effects of temperature on photosynthetic performance and nitrate reductase activity in vivo assay in *Gracilariopsis lemaneiformis* (Rhodophyta). Journal of Oceanology and Limnology, DOI: 10.1007/s00343-020-9256-9.

ANEXO 1

J Appl Phycol (2015) 27:1243–1251
DOI 10.1007/s10811-014-0418-z

Growth and photosynthetic pigments of *Gracilariopsis tenuifrons* (Rhodophyta, Gracilariaceae) under high light in vitro culture

Priscila B. Torres · Fungyi Chow · Déborah Y. A. C. Santos

Received: 17 February 2014 / Revised and accepted: 17 September 2014 / Published online: 25 September 2014
© Springer Science+Business Media Dordrecht 2014

Abstract High levels of irradiance may affect the growth and development of photosynthetic organisms, changing concentrations of carotenoids and chlorophylls. These changes may indicate different photoprotection strategies. In this study, gametophytic apical portions of *Gracilariopsis tenuifrons* were cultivated under controlled laboratory conditions for 1 week, at different light irradiances: 60 (control), 600, and 1,000 μmol photons m^{-2} s^{-1}. Growth rate, amount, and composition of pigments were analyzed daily. Color of seaweeds exposed to 600 and 1000 μmol photons m^{-2} s^{-1} varied along the days, from red to yellowish, suggesting a decrease in vital processes as photosynthesis and growth. However, no decrease in biomass was observed. Actually, there was an increase at growth rates for the algae kept under higher light intensities. The main registered pigments were chlorophyll *a*, β-carotene, and zeaxanthin. β-carotene and chlorophyll *a* levels were lower in algae exposed to high light intensity. In treatment exposed to 600 μmol photons m^{-2} s^{-1}, this reduction was 42 and 35 %, respectively, while in those exposed to 1000 μmol photons m^{-2} s^{-1} the values were 55 and 50 % lower than the control. The lower levels of these pigments may be associated with the reduction in energy harvesting by the photosynthetic complexes-antennae, in an effort to dissipate the high excitation impinged over the photosynthesis system as a whole. For zeaxanthin levels, a 20 % increase was observed in the beginning of the experiment, which was followed by a drop to the initial levels, suggesting the role of this pigment in this alga's photoprotection process.

P. B. Torres · F. Chow · D. Y. A. C. Santos (✉)
Departamento de Botânica, Instituto de Biociências, Universidade de São Paulo, Rua do Matão, 277, São Paulo, SP 05508-090, Brazil
e-mail: dyacsan@ib.usp.br

Keywords *Gracilariopsis tenuifrons* · Red algae · Photosynthetic pigments · Growth rate · Light stress · Carotenoids

Introduction

In aquatic environments, high irradiance is common throughout the day, seasons of the year, cycles of sea, and sudden changes in weather (Schubert et al. 2001). In this sense, like any other photosynthetic organism, red seaweeds may be exposed to light incidence rates above the values required by the photochemical processes involved in photosynthesis, leading to light stress, photoinhibition, and photoprotection. In this scenario, the antenna complexes may absorb excess energy, which increase the production of highly unstable molecule known as reactive oxygen species (ROS) (Müller et al. 2001). These unstable molecules may affect the photosynthesis apparatus. In more extreme cases, damage caused by light overexposure may cause cell death or even kill the organism (Osmond 1994). Therefore, high levels of irradiance may considerably affect growth and development of photosynthetic organisms (Taiz and Zeiger 2009; Murchie and Niyogi 2011). These organisms, red seaweeds included, have developed photoprotection mechanisms against light overexposure. Several photoprotection responses regulate photosynthetic light harvesting in order to balance absorption and use of light energy so as to minimize photooxidant damage (Müller et al. 2001). Under intense irradiance, photosynthetic pigments undergo quantitative and compositional changes that are directly associated with distinct photoprotection strategies.

Carotenoids and chlorophyll *a* are present in all organisms that carry out oxygenic photosynthesis, including red algae (Archibald and Keeling 2002; Mimuro and Akimoto 2003). Chlorophyll *a* is present in the photosynthetic reaction center, where it acts in the conversion of solar energy into chemical

©Fungyi Chow / 2021

energy, and in antennae, in which the energy is absorbed and transferred to the photosynthetic reaction center. This pigment plays an essential role in ROS formation. High irradiances increase the probability that chlorophyll *a* molecules reach the triplet state (Müller et al. 2001), which in turn may react with free oxygen, forming singlet oxygen, which is one of the main ROS responsible for severe damage to lipids, proteins, and pigments (Krieger-Liszkay 2005). On the other hand, under high irradiances, some carotenoids seem to be involved in several photoprotection mechanisms, such as direct ROS deactivation, or as scavengers of triplet chlorophyll, which avoid the formation of singlet oxygen (Dall'Osto et al. 2007). Studies using land plants and green algae have shown that carotenoids are important accessory pigments (Sholes et al. 2011). Nevertheless, in red algae the exact role of these compounds remains to be elucidated.

Since light stress is directly correlated with productivity and nutritional quality of commercial cultivations, light responses of photosynthetic organisms have considerable economic and scientific interest. Additionally, light responses represent a source of essential information to better understand the biology and distribution of natural populations, broadening the panorama of the effects of climate change at global level, and the ecophysiology of species, favoring the sustainable, rational management and use of natural resources (Hanelt 1996; Taiz and Zeiger 2009).

In this scenario, the present study evaluates how the increase of photosynthetically active radiation (PAR) affects photosynthetic pigments (carotenoids and chlorophyll *a*) and growth rates of the red seaweed *Gracilariopsis tenuifrons* (C.J. and E.C Oliveira) Fredericq and Hommersand under laboratory conditions. The results obtained should help better understand the biology of this species and to evaluate the behavior of these pigments under light stress.

Materials and methods

Materials and general growth conditions

Apical tips of *Gracilariopsis tenuifrons* female gametophytic phase (haploid) (BG0039, Germplasm Bank) were acclimatized for 1 month under controlled conditions (25±1 °C; photosynthetic photon flux density (PPFD) of 60±5 μmol photons m^{-2} s^{-1}; 14-h light/10-h dark photocycle, intermittent aeration at 30-min intervals) using sterilized seawater (32 psu) enriched with von Stosch solution 50 % (Ursi and Plastino 2001 based on Edwards 1970). The light was provided by fluorescent lamps (model day light, 40 W), and the irradiance was determined using a PPFD spherical sensor (LI-COR Model LI-1935B) connected to a recorder (LI-COR Model LI-250). The unialgal culture was done in the Laboratory of Marine Algae Edison José de Paula, Institute of Biosciences, University of São Paulo.

Experimental design and growth

Acclimatized apical portions of 3 cm in length were submitted to three treatments of PPFD: 60 μmol (control), 600 μmol, and 1000 μmol photons m^{-2} s^{-1} in Erlenmeyer flasks. All other cultivation conditions were the same described above. The algae biomass and seawater inside each Erlenmeyer flask was 1 g L^{-1}. Seven sets of three (replications) Erlenmeyer flasks, with known initial mass (M_i), were prepared for each PPFD treatment. Daily, during the 1-week experimental period, three flasks (replication) from each light treatment were analyzed. These flasks were sampled, and final algal biomass (M_f) was recorded to calculate the growth rate (GR) as GR (% day^{-1})=$[(M_f/M_i)^{1/t}-1]\times100$ in which M_f=final biomass (g), M_i=initial biomass (g), t=day of sampling (Lignell and Pedersen 1989; Yong et al. 2013). After weight, samples of 50 mg (fresh weight-FW) of apical portions of each flask were retrieved, frozen in liquid nitrogen and stored at -80 °C for subsequent pigment analyses.

Extraction, analyses, and quantification of carotenoids and chlorophyll *a* by HPLC

Extraction of carotenoids and chlorophyll *a* was carried out using the frozen samples of 50 mg FW described above. The material was triturated in liquid nitrogen. Next, 1.5 mL methanol was added, the mixture was homogenized and centrifuged (28,800×*g*, 4 °C, 5 min) (Torres et al. 2014). Aliquots of the supernatant were then immediately analyzed by high performance liquid chromatography (HPLC) in a chromatograph (HP1200) equipped with a reverse-phase C_{30} column (Ultracarb ODS, 250×4.6 mm i.d., 5 μm). The chromatograms obtained were processed at λ=450 nm. The mobile phase was a gradient of methyl-terc-butyl ether (MTBE) in methanol following the program: 5 % MTBE (0 min), 70 % MTBE (30 min), and 50 % MTBE (50 min). The mobile phase flux was kept constant at 0.9 mL min^{-1} and the column temperature was adjusted to 29 °C (Faria et al. 2009).

The pigments were quantified by HPLC using external calibration curves constructed for chlorophyll *a* and zeaxanthin. The curves were constructed using standard solutions of known concentrations and analyzed under the same conditions as the samples.

Characterization of the photosynthetic pigments

Carotenoids and chlorophyll *a* were characterized using HPLC coupled to a mass spectrometer (HPLC-MS/MS) with an ion trap analyzer and atmospheric pressure chemical ionization (APCI) ionization source (Shimadzu, LC-20 AD; Bruker Daltonics, Esquire 4000, Germany). The UV/visible spectra were obtained

©Fungyi Chow / 2021

at between 200 and 800 nm, and chromatograms were processed at λ 450 nm. The parameters of the mass spectrometer were adjusted following Rosso and Mercadante (2007): APCI positive mode, corona current 4,000 nA, source temperature 450 °C, N_2 as dissecating gas at 350 °C and 5 mL min^{-1} and as nebulizing gas at 414 kPa, and MS/MS fragmentation energy 1.4 V. Mass spectra were acquired at a 100–1000 *m/z* interval. Separation of carotenoids was carried out in a C_{30} YMC column (250×4.6 mm i.d., 5 μm) (Waters, USA) using the same mobile phase as described above.

Carotenoids and chlorophylls were identified in HPLC-MS/MS according to retention times in the C_{30} column, based on the UV/visible (λ_{max}, fine structure, *cis* peak structure) and mass spectra, comparison with literature data (Gauthier-Jaques et al. 2001; Breemen et al. 2011), and comparison of retention times with those of standards (chlorophyll *a* and β-carotene were purchased from Sigma-Aldrich; other carotenoids were supplied by CaroteNature).

Statistical analyses

The one-factor analysis of variance (ANOVA) was used to determine the significant differences between means of each variable on a daily basis, between treatments. Existing differences were analyzed using the post-hoc Tukey test. Additionally, variations in pigment concentrations in apices exposed to the light regimens with time were analyzed by single linkage hierarchical clustering with Pearson correlation (1-r) distance index. All analyses were carried out considering $\alpha = 5$ % using Minitab 16.1.0, except the multivariate analyses, which was conducted using Statistica 10. The treatments were carried out in triplicate.

Results

Effects of irradiance on the general aspect of growth

In the control group (60 μmol photons m^{-2} s^{-1}), apices did not present variation in color throughout the experiment. Control apices analyzed on day 7 presented similar color to that of apices analyzed on day 0. However, exposure to the other two experimental light levels (600 and 1000 μmol photons m^{-2} s^{-1}) led to phenotypic changes manifested as variation in color, from reddish to yellowish. This variation was more intense in the apices exposed to the highest irradiance, and seemed to build up throughout the experimental period. Apices exposed to 1000 μmol photons m^{-2} s^{-1} for 7 days were the most affected, becoming totally yellow (Fig. 1).

As a rule, the increase in irradiance raised growth rates of exposed apices from day 1. The growth rates were of 11.7 % day^{-1} for apices exposed to 600 μmol photons m^{-2} s^{-1} (Fig. 2b) and 12.6 % day^{-1} for apices exposed to 1000 μmol photons.m^{-2} s^{-1} (Fig. 2c), in comparison with control (6.4 %.day^{-1}) (Fig. 2a). For the control group, a significant increase between growth rates measured on day 1 (6.4±0.08 % day^{-1}) and those measured on day 3 (9.8±1.37 % day^{-1}) was observed, which remained constant throughout the rest of the experiment. Similar results were observed for apices exposed to 1000 photons m^{-2} s^{-1} at the beginning of the experiment, whose growth rates increased between day 1 (12.6±1.75 % day^{-1}) and day 3 (15.9±0.91 % day^{-1}). However, from day 4 on (13.7±0.84 % day^{-1}), a significant decrease in growth rates was recorded until day 6 (12.7±1.16 % day^{-1}) and day 7 (13.5±0.65 % day^{-1}), when they became identical to the measurements carried out on day 1. Growth rates of apices exposed to 600 μmol photons m^{-2} s^{-1} did not vary significantly, remaining essentially constant during the experiment. These results indicate that apices exposed to the three irradiance values grew along the experimental period. However, even though the apices exposed to 1000 μmol photons m^{-2} s^{-1} experienced a slowing down of growth rate at the end of the experiment, these apices did not stop growing. They only grew at a slower pace.

Effects of irradiance on pigment composition

β-carotene (all-*trans*-β-carotene), β-cryptoxanthin (all-*trans*-β-cryptoxanthin), zeaxanthin (all-*trans*-zeaxanthin), and chlorophyll *a* were identified in the extracts of the macroalga studied (Fig. 3). The main pigments present in the extract were chlorophyll *a* and zeaxanthin, which was the main carotenoid detected in apices exposed to all experimental light irradiance values. The carotenoid β-cryptoxanthin was highly variable among replicates; when present, it was at low concentrations (under 1 % of the total area). No changes in pigment composition were observed across the apices exposed to the three light levels. Yet, quantitative changes in response to higher irradiance values were significant.

No significant changes were observed for photosynthetic pigments in apical portions cultivated as control group. β-carotene, zeaxanthin, and chlorophyll *a* remained constant throughout the seven day-experiment (means 52.5±3.1 μg g^{-1}, Fig. 4a; 77.1±3.8 μg g^{-1}, Fig. 4b; and 495.4±27.8 μg g^{-1}, Fig. 4c, respectively). Concentration of zeaxanthin was 1.5 times as high as that of β-carotene, while levels of chlorophyll *a* were roughly 3.8 times higher than total carotenoid concentrations (zeaxanthin+β-carotene).

On the other hand, higher irradiances led to a large reduction in chlorophyll *a* and β-carotene levels. Chlorophyll *a* levels in apices exposed to 600 μmol photons m^{-2} s^{-1} remained constant until day 3. From then on, significant

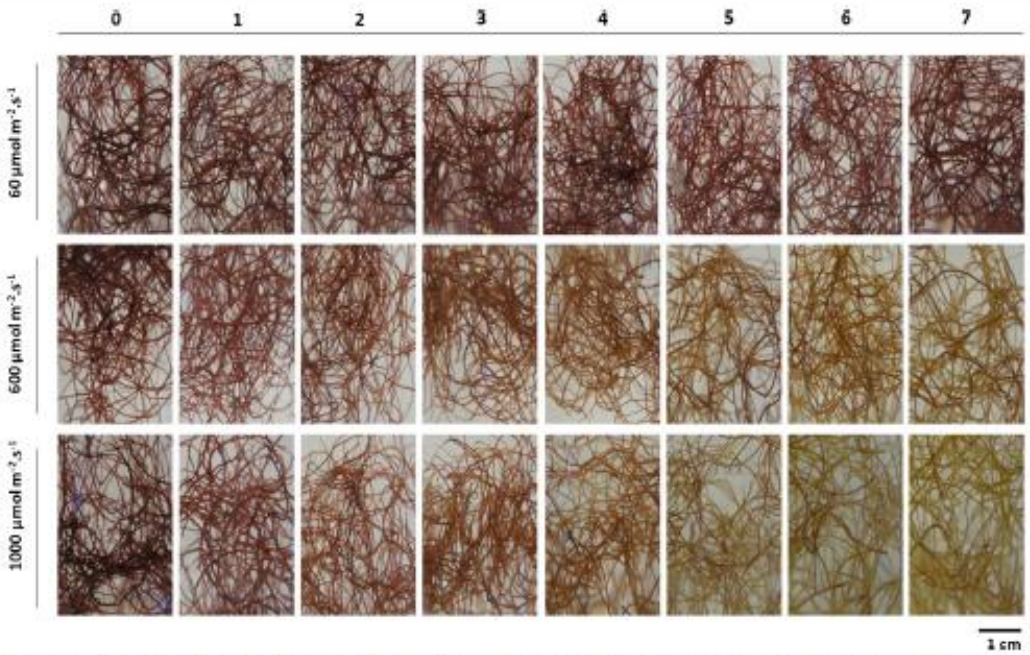

Fig. 1 Apices of *Gracilariopsis tenuifrons* after exposure to 60, 600, and 1000 µmol photons $m^{-2} s^{-1}$ throughout the growth period. The numbers above columns indicate the time, in days, of the experiment (day 0–7)

decreases were recorded, until day 7, when chlorophyll *a* levels in these apices were 35 % lower, compared to the beginning of the experiment (day 0) (Fig. 4f). The same was observed for apices exposed to 1000 µmol photons $m^{-2} s^{-1}$, with a significant linear reduction (R^2=0.998, simple linear regression) during the experiment, accounting for over 50 % on day 7, compared to day 0 (Fig. 4i). Regarding β-carotene levels in apices exposed to 600 µmol photons $m^{-2} s^{-1}$, significant decreases were observed as early as on day 2. The largest drop, of around 42.9 %, was recorded on day 7, compared to day 0 (Fig. 4d). As for apices exposed to 1000 µmol photons $m^{-2} s^{-1}$, a significant linear decrease (R^2=0.989, simple linear regression) was noticed during the experiment, which summed up to more than 55 % (Fig. 4g). Therefore, increased irradiances decrease β-carotene levels in a steep fashion.

Zeaxanthin levels in apices exposed to 600 µmol photons $m^{-2} s^{-1}$ showed a large increase, of around 20%, between day 0 (68.9±2.1 µg g^{-1}) and day 2 (82.1±3.7 µg g^{-1}). From day 3 on, zeaxanthin levels began to drop, reaching values similar to day 0 on day 7 (Fig. 4e). At the beginning of the 1000 µmol photons $m^{-2} s^{-1}$ regime, zeaxanthin levels presented the same pattern observed in apices exposed to 600 µmol photons $m^{-2} s^{-1}$, though they increased significantly (by 20 %) between day 0 (76.6±2.0 µg g^{-1}) and day 3 (92.5±3.1 µg g^{-1}). However, the reduction in concentrations of this carotenoid was more evident in apices exposed to the highest irradiance (1,000 µmol photons $m^{-2} s^{-1}$), and fell from day 4 on, reaching the lowest value on day 7, (7.9 % lower than on day 0; Fig. 4h).

In spite of the significant decrease in zeaxanthin levels after exposure to high irradiances, the zeaxanthin/β-carotene and

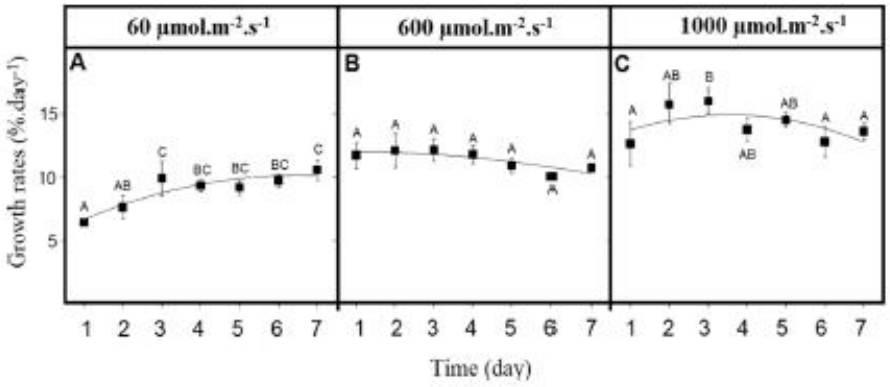

Fig. 2 In vitro growth rates (% day^{-1}) (means±SD) of apices of *Gracilariopsis tenuifrons*, on a daily basis, exposed to different irradiances (60, 600, and 1000 µmol photons $m^{-2} s^{-1}$). Identical letters on one same curve indicate that values did not differ in the one-factor ANOVA and in the Tukey test, (p<0.05)

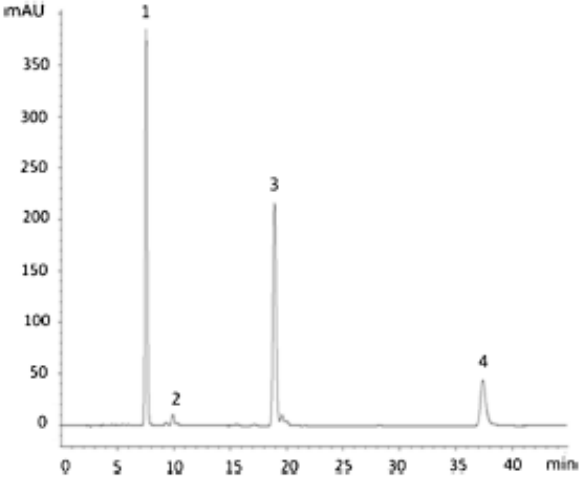

Fig. 3 HPLC chromatogram of methanol extract of *Gracilariopsis tenuifrons*. The numbers above each peak represent Zeaxanthin (*1*), β-Cryptoxanthin (*2*), Chlorophyll *a* (*3*), and β-carotene (*4*)

zeaxanthin/chlorophyll *a* ratios increased throughout the experimental period (Table 1). Concerning the zeaxanthin/β-carotene ratio, exposure to 600 μmol photons m^{-2} s^{-1} led to a 74 % increase as measured on day 7, compared to day 0, while 1000 μmol photons m^{-2} s^{-1} caused an increase of 114 % for the same period. As for the zeaxanthin/chlorophyll *a* ratio, exposure to 600 μmol photons m^{-2} s^{-1} caused a 57 % increase, while exposure to 1000 increased this by 87 %. A trend towards decrease was observed in the β-carotene/chlorophyll *a* ratio in apices exposed to the highest irradiance (Table 1). When compared to day 0, a 9 % decrease was observed in this ratio for apices exposed to 600 μmol photons m^{-2} s^{-1}, while for apices exposed to 1000 μmol photons m^{-2} s^{-1} this decrease was 8 %, on day 7. These results indicate that zeaxanthin levels decrease at a lower rate, when compared to β-carotene and chlorophyll *a* over the experimental period.

For the control group, zeaxanthin/β-carotene, zeaxanthin/chlorophyll *a*, and β-carotene/chlorophyll *a* ratios remained essentially constant throughout the experimental period (means 1.40±0.03, 0.15±0.00, and 0.11±0.00, respectively).

Analyses of hierarchical clustering

In order to facilitate the global comprehension of the behavior of pigments with exposure to different irradiances, a hierarchical cluster analysis was carried out (Fig. 5). The parameters

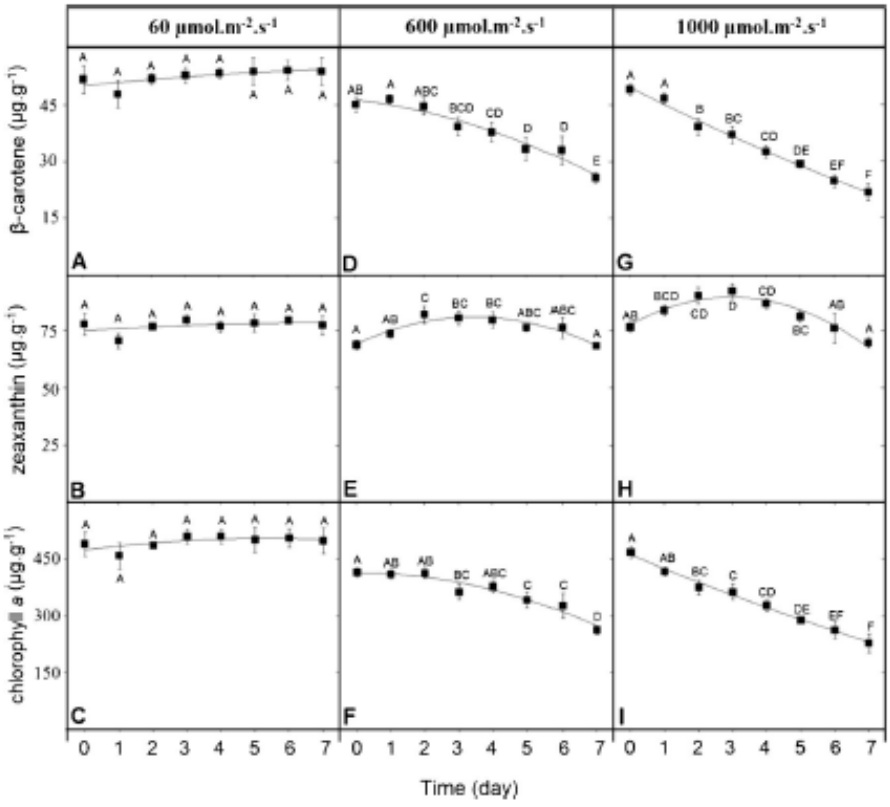

Fig. 4 Effect of the different irradiances (60, 600, and 1000 μmol photons m^{-2} s^{-1}) on β-carotene, zeaxanthin, and chlorophyll *a* concentrations (μg g^{-1}) (means±SD, $n=3$) in apices of *Gracilariopsis tenuifrons*. Identical letters on one same curve indicate that values did not differ in the one-factor ANOVA and in the Tukey test ($p<0.05$)

Table 1 Effect of the different irradiances (600 and 1000 μmol photons m^{-2} s^{-1}) on the zeaxanthin/β-carotene (z/β), zeaxanthin/chlorophyll *a* (z/Chl), and β-carotene/chlorophyll *a* (β/Chl) ratios (means±SD) in apices of *Gracilariopsis tenuifrons* over the experimental period

	600 μmol photons m^{-2} s^{-1}			1000 μmol photons m^{-2} s^{-1}		
Time (day)	z/β	z/Chl	β/Chl	z/β	z/Chl	β/Chl
0	1.53 ± 0.04^{a}	0.16 ± 0.00^{a}	0.11 ± 0.00^{a}	1.56 ± 0.01^{a}	0.16 ± 0.00^{a}	0.10 ± 0.00^{a}
1	1.58 ± 0.01^{a}	0.18 ± 0.00^{ab}	0.11 ± 0.00^{a}	1.79 ± 0.07^{a}	0.20 ± 0.00^{b}	0.11 ± 0.00^{d}
2	1.84 ± 0.03^{ab}	0.20 ± 0.00^{bc}	0.11 ± 0.00^{a}	2.30 ± 0.04^{b}	0.24 ± 0.00^{c}	0.10 ± 0.00^{a}
3	2.06 ± 0.13^{bc}	0.22 ± 0.01^{cd}	0.11 ± 0.00^{a}	2.50 ± 0.08^{bc}	0.25 ± 0.00^{cd}	0.10 ± 0.00^{a}
4	2.12 ± 0.23^{bc}	0.21 ± 0.01^{cd}	0.10 ± 0.01^{b}	2.66 ± 0.06^{c}	0.26 ± 0.00^{cde}	0.10 ± 0.00^{ab}
5	2.30 ± 0.16^{cd}	0.22 ± 0.01^{d}	0.10 ± 0.01^{b}	2.77 ± 0.01^{cd}	0.28 ± 0.00^{def}	0.10 ± 0.00^{ab}
6	2.33 ± 0.16^{cd}	0.23 ± 0.01^{d}	0.10 ± 0.00^{b}	3.06 ± 0.09^{de}	0.29 ± 0.00^{ef}	0.09 ± 0.00^{c}
7	2.68 ± 0.13^{d}	0.26 ± 0.01^{e}	0.10 ± 0.00^{b}	3.20 ± 0.27^{e}	0.31 ± 0.02^{f}	0.10 ± 0.00^{bc}

Identical letters on one same column indicate that values did not differ in the one-factor ANOVA and in the Tukey test, ($p<0.05$)

included daily means of each pigment's concentrations after treatments.

Algae grown in the control group (60 μmol photons m^{-2} s^{-1}) (group 1) separated from those exposed to light stress (600 μmol and 1000 μmol photons m^{-2} s^{-1}) (group 2) (Fig. 4). In the cluster formed by algae exposed to light stress, subclusters formed with high correlation ($r\geq0.95$) between chlorophyll *a* and β-carotene, independently of the treatment (group 4), which indicates that these pigments exhibited similar behavior during the experiment.

In turn, the response pattern exhibited by zeaxanthin was quite different from those observed for chlorophyll *a* and β-carotene at each treatment of light stress. However, the similar responses observed for zeaxanthin in both high irradiance treatments, that is, an initial increase followed by a drop in concentration, led to the formation of group 3.

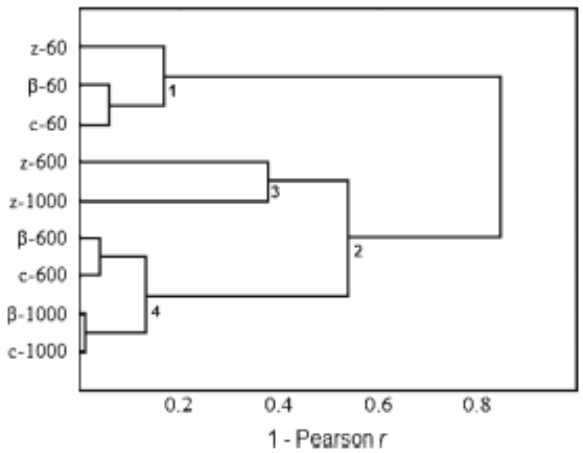

Fig. 5 Hierarchical clustering dendrogram constructed using the different pigment compositions over the experimental period (day 0–7) for the different irradiations used. *Z* zeaxanthin, *β* β-carotene, *c* chlorophyll a. *The numbers associated with each pigment* refer to the irradiances 60, 600, and 1000 μmol photons m^{-2} s^{-1}, while the numbers *1–4* describe the clusters formed. Distances were estimated as 1-Pearson *r*

Discussion

The growth rate of control treatment from this study was higher than that observed in experimental field cultures of *G. tenuifrons* in Venezuela (3.63±0.50 % day^{-1}; Gómez and Millán 1997) and in Colombia (0.59±0.39 % day^{-1}; Rincones and Moreno 2011). Additionally, the growth rate was almost twice than the growth rates observed in laboratory conditions for *Gracilariopsis lemaneiformis* (4±0, 5 % day^{-1}; Zou and Gao 2014) and *Gracilariopsis longissima* (3.03±0.11 % day^{-1}; Qing et al. 2014), indicating a superior physiological performance than reported for the same and similar species.

Zeaxanthin was the main carotenoid in apices of *Gracilariopsis tenuifrons* exposed to control treatment and to high irradiance treatments. This observation is distinct from what has been reported for leaves of land plants and for most red algae, which have lutein as the main carotenoid (Young 1993; Marquardt and Hanelt 2004; Schubert et al. 2006). Other studies with different species of *Gracilariopsis* also detected zeaxanthin as the main carotenoid. However, distinctly from the results observed here, violaxanthin and anteraxanthin were also detected in *G. lemaneiformis* (Schubert et al. 2006) and, for two other species, components of α-carotene biosynthetic pathway were also present (Andersson et al. 2006). Thus, based on our results and previous data for different red algal species, there is a considerable difference between carotenoid profiles in these organisms. These findings contrast with what has been reported for leaves of land plants, in which carotenoid compositions are consistently similar between the different species analyzed, with lutein being predominant (Young 1993; Britton 2008).

It is known that carotenoids exhibit different photoprotection responses (Britton 2008). In this sense, this diversity in pigment composition observed for red algae may indicate behavioral differences in response to high irradiances across different species with distinctive pigment composition.

Under the conditions of light exposure studied here, variations in pigment concentrations in *G. tenuifrons* were observed, but compositional differences were not detected. The concentrations of the pigments chlorophyll *a* and β-carotene were reduced, and were inversely correlated with irradiance. Similar results have been obtained for other red algae species, such as *Gracilaria tenuistipitata* var. *liui* (Carnicas et al. 1999) and *Chondrus crispus* (Yakovleva and Titlyanov 2001).

The responses of these pigments were highly correlated ($r \geq 0.95$), suggesting that these compounds were affected, in a similar way, by the increase in irradiance. Reductions in the area of thylakoids, in the number of photosystems or in the size of antennae may be considered as different photoprotection strategies that affect both chlorophyll *a* and β-carotene in a similar way. These strategies have been described for the red microalga *Porphyridium cruentum* (Cunningham et al. 1989).

In land plants and green algae, it is well known that chlorophyll *a* and β-carotene are involved in harvesting light in antennae (Ritz et al. 2000). Therefore, in a scenario of high light intensity, it is possible to suppose that a decrease in these pigments reduces energy absorption in the antennae, lessening the excitement effect on the photosynthetic system as a whole. The real role of chlorophyll *a*, and more precisely, of β-carotene in photosynthetic process for red seaweeds is not totally known, even less so at stress conditions. However, since we observed a marked decrease of these pigments under high light intensity culture, it is not impossible to suggest that they could be involved in harvesting light in antennae. The decrease observed could be a way to avoid the over excitement of the photosynthetic system.

The behavior of the carotenoid zeaxanthin differed from that exhibited by chlorophyll *a* and β-carotene. Under high irradiance, zeaxanthin concentrations rose in the beginning of the experiment, followed by a slight decrease towards the end. In spite of this falling trend, the zeaxanthin/chlorophyll *a* and zeaxanthin/β-carotene ratios increased consistently throughout the experiment, indicating that zeaxanthin production was higher, as compared to other pigments, during acclimation. Under this perspective, it is possible to suppose that zeaxanthin plays an important protective role in this algal species. These results can be corroborated by analyzing the ratios of zeaxanthin and β-carotene or chlorophyll *a* under 600 and 1000 μmol photons m^{-2} s^{-1}, in which a significant increase of z/ β and z/Chl ratios indicate the increase of zeaxanthin concentration probably due to the photoprotection function of this antenna pigment as a thermal dissipator of excess absorbed light energy under high irradiance, a process identified as the xanthophyll cycle, a process which is little known and still uncertain in red macroalgae.

In the literature, several studies have assessed the photoprotective role of zeaxanthin, indicating that this pigment is efficient in eliminating chlorophyll triplet, oxygen singlet, and other ROS (Havaux and Niyogi 1999; Betterle et al. 2010; Dall'Osto et al. 2010). Several studies also suggested that the antioxidant capacity of zeaxanthin is higher than that of other xanthophylls (Havaux et al. 2007). Schubert and Garcia-Mendoza (2008) studied different red algae with distinct carotenoid compositions and concluded that the species richer in zeaxanthin exhibit less light sensitivity. Other studies on red algae, such as *G. tenuistipitata* (Carnicas et al. 1999) and *Corallina elongata* (Esteban et al. 2009) also have reported an increase in zeaxanthin levels at higher irradiances in long-term experiments. Additionally, in land plants and green algae, experiments using mutants that accumulate zeaxanthin have demonstrated that this pigment is an efficient antioxidant, and that it plays a role in the protection of lipoprotein membranes against peroxidation (Havaux et al. 2007).

In land plants and green algae, the photoprotective role of zeaxanthin is associated mainly with its presence in the outer antennae of PSII and, more specifically, with the xanthophyll cycle, as shown by Niyogi et al. (1998), Holt et al. (2004), and Dall'Osto et al. (2005), among others. Nevertheless, it is known that the outer antennae of red algae are quite different, since these are formed by a protein-pigment complex extrinsic to thylakoid membranes, which are known as phycobilisomes, and which do not contain zeaxanthin (Grossman et al. 1993). This difference supports the uncertainty surrounding the functional presence of a typical xanthophyll cycle in red algae, or the role of this pigment in immediate thermal dissipation, for instance.

Phycobiliproteins, the characteristic reddish pigment of red macroalgae, are the most sensitive antenna pigment, localized externally to the reaction center and the first photosynthetic pigment to decrease in concentration under light stress (Bouzon et al. 2012, Gouveia et al. 2013, Santos et al. 2014). Under the most extreme condition of this experiment (day 7, 1000 μmol photons m^{-2} s^{-1}), the apical portions of *G. tenuifrons* were completely yellowish (Fig. 1). Decreases in pigment concentration associated with dramatic loss of color under high irradiances have been described, mainly for land plants, as a sign of chronic photoinhibition (Powles 1984; Osmond 1994). At this stage, the photosynthesizing capacity and consequently the biomass are reduced, indicating the occurrence of severe damage to metabolism. In the present study, however, the growth rates observed show that this alga continues to grow, even when exposed to higher light intensities. Therefore, it is possible to suggest that the loss of pigmentation by *G. tenuifrons*, at least in the experimental design adopted here, is not necessarily associated with severe damage to the photosynthetic apparatus; on the contrary, the

©Fungyi Chow / 2021

loss of color may reflect photoacclimation and photoprotection strategies.

Quintano et al. (2013), in a field study with *Gelidium corneum*, suggested that pigment lost could be associated with nitrogen deficiency, resulting in more fragile individuals. In our study, nitrogen supply was tentatively kept the same during the week and, at least for the treatment of 600 μmol photons m^{-2} s^{-1}, more rigid individuals were observed. Morphological similarities between our results and Quintano et al. (2013) were verified only by the end of the 1000 μmol photons m^{-2} s^{-1} culture treatment, associated with a reduction on the growth rate. It suggests that, above a critical point, light intensity turns prejudicial to algae development.

The loss of the reddish color in red algae may be common in scenarios of high irradiance. In the field, for instance, red algae may appear yellowish or brownish in summer, as opposed to the deep red color observed in winter (Jones and Williams 1966; Waaland et al. 1974). The increased number of soft-pigmented algae in the field has been pointed out as consequence of climatic changes (Díez et al. 2012). Thus, understanding the mechanisms of photoprotection of these organisms is an important subject from an ecological and economical point of view.

Acknowledgments The authors thank FAPESP (Fundação de Amparo à Pesquisa do Estado de São Paulo) for financial support (2010/02948-3), CNPq (Conselho Nacional de Desenvolvimento Científico e Tecnológico) for PBT fellowship, Dr Adriana Mercadante and Fernanda Mandelli from Department of Food Science, Faculty of Food Engineering, University of Campinas (UNICAMP) for HPLC-MS/MS support.

References

Andersson M, Schubert H, Pedersén M, Snoeijs P (2006) Different patterns of carotenoid composition and photosynthesis acclimation in two tropical red algae. Mar Biol 149:653–665

Archibald JM, Keeling PJ (2002) Recycled plastids: a "green movement" in eukaryotic evolution. Trends Gen 18:577–584

Betterle N, Ballottari M, Hienerwadel R, Dall'Osto L, Bassi R (2010) Dynamics of zeaxanthin binding to the photosystem II monomeric antenna protein *Lhcb6* (CP24) and modulation of its photoprotection properties. Arch Biochem Biophys 504:67–77

Bouzon ZL, Chow F, Zitta CS, Santos RW, Ouriques LC, Felix MR, Osorio LKP, Gouveia C, Martins RP, Latini A, Ramlov F, Maraschin M, Schmidt ÉC (2012) Effects of natural radiation, photosynthetically active radiation and artificial ultraviolet radiation-B on the chloroplast organization and metabolism of *Porphyra acanthophora* var. *brasiliensis* (Rhodophyta, Bangiales). Micros Microanal 18: 1467–1479

Breemen RB, van Dong L, Pajkovic ND (2011) Atmospheric pressure chemical ionization tandem mass spectrometry of carotenoids. Int J Mass Spectrom 312:163–172

Britton G (2008) Functions of intact carotenoids. In: Britton G, Liaaen-Jensen S, Pfander H (eds) Carotenoids, Volume 4: Natural Functions. Birkhäuser Verlag, pp 189–212

Carnicas E, Jiménez C, Niell FX (1999) Effects of changes of irradiance on the pigment composition of *Gracilaria tenuistipitata* var *liui* Zhang et Xia. J Photochem Photobiol B: Biol 50:149–158

Cunningham FX, Dennenberg RJ, Mustardy L, Jursinic PA, Gantt E (1989) Stoichiometry of Photosystem I Photosystem II and phycobilisomes in the red alga *Porphyridium cruentum* as a function of growth irradiance. Plant Physiol 91:1179–1187

Dall'Osto L, Caffarri S, Bassi R (2005) A mechanism of nonphotochemical energy dissipation independent from PsbS revealed by a conformational change in the antenna protein CP26. Plant Cell 17:1217–1232

Dall'Osto L, Fiore A, Cazzaniga S, Giuliano G, Bassi R (2007) Different roles of alpha- and beta-branch xanthophylls in photosystem assembly and photoprotection. J Biol Chem 282:35056–35068

Dall'Osto L, Cazzaniga S, Havaux M, Bassi R (2010) Enhanced photoprotection by protein-bound vs free xanthophyll pools: a comparative analysis of chlorophyll *b* and xanthophyll biosynthesis mutants. Mol Plant 3:576–593

Díez I, Muguerza N, Santolaria S, Ganzedo U, Gorostiaga JM (2012) Seaweed assemblage changes in the eastern Cantabrian Sea and their potential relationship to climate change. Estuar Coast Shelf Sci 99:108–120

Edwards P (1970) Illustrated guide to the seaweeds and sea grasses in the vicinity of Porto Aransas Texas. Contrib Mar Sci 15:1–228

Esteban R, Martínez B, Fernández-Marín B, Becerril JM, García-Plazaola JI (2009) Carotenoid composition in Rhodophyta: insights into xanthophyll regulation in *Corallina elongata*. Eur J Phycol 44: 221–230

Faria AF, De Hasegawa PN, Chagas EA, Pio R, Purgatto E, Mercadante AZ (2009) Cultivar influence on carotenoid composition of loquats from Brazil. J Food Compos Anal 22:196–203

Gauthier-Jaques A, Bortlik K, Hau J, Fay LB (2001) Improved method to track chlorophyll degradation. J Agric Food Chem 49:1117–1122

Gómez A, Millán J (1997) Cultivo experimental de *Gracilaria dentata* Agardh y de *Gracilariopsis tenuifrons* (Bird et Oliveira) (Rhodophyta: Gigartinales) en la isla de Margarita, Venezuela. Rev Biol Mar Ocean 32:137–144

Gouveia C, Kreusch M, Schmidt ÉC, Felix MRL, Osorio LKP, Pereira DT, Santos R, Ouriques LC, Martins RP, Latini A, Ramlov F, Carvalho TJG, Chow F, Maraschin M, Bouzon ZL (2013) The effects of lead and copper on the cellular architecture and metabolism of the red alga *Gracilaria domingensis*. Microsc Microanal 19: 513–524

Grossman AR, Schaeffer MR, Chiang GG, Collier JL (1993) The phycobilisome a light-harvesting complex responsive to environmental conditions. Microbiol Rev 57:725–749

Hanelt D (1996) Photoinhibition of photosynthesis in marine macroalgae. In: Figueroa FL, Jiménez C, Pérez-Lloréns JL, Niell FX (eds) Underwater Light and Algal Photobiology Sci Mar 60 (Suppl1), Barcelona, pp 243–248

Havaux M, Niyogi KK (1999) The violaxanthin cycle protects plants from photooxidative damage by more than one mechanism. Proc Natl Acad Sci USA 96:8762–8767

Havaux M, Dall'osto L, Bassi R (2007) Zeaxanthin has enhanced antioxidant capacity with respect to all other xanthophylls in *Arabidopsis* leaves and functions independent of binding to PSII antennae. Plant Physiol 145:1506–1520

Holt NE, Fleming GR, Niyogi KK (2004) Toward an understanding of the mechanism of nonphotochemical quenching in green plants. Biochem 43:8281–8289

Jones WE, Williams R (1966) The seaweeds of Dale. Field Stud 2:303–330

Krieger-Liszkay A (2005) Singlet oxygen production in photosynthesis. J Exp Bot 56:337–346

Lignell A, Pedersen M (1989) Agar composition as a function of morphology and growth rate studies on some morphological strains of

Gracilaria secundula and *Gracilaria verrucosa* (Rhodophyta). Bot Mar 32:219–227
Marquardt J, Hanelt D (2004) Carotenoid composition of *Delesseria lancifolia* and other marine red algae from polar and temperate habitats. Eur J Phycol 39:285–292
Mimuro M, Akimoto S (2003) Energy transfer processes from fucoxanthin and peridinin to chlorophyll. In: Larkum AWD, Douglas S, Raven JA (eds) Photosynthesis in algae. Kluwer Academic Publishers, Dordrecht, pp 335–349
Müller P, Li X-P, Niyogi KK (2001) Non-photochemical quenching: a response to excess light energy. Plant Physiol 125:1558–1566
Murchie EH, Niyogi KK (2011) Manipulation of photoprotection to improve plant photosynthesis. Plant Physiol 155:86–92
Niyogi KK, Grossman AR, Björkman O (1998) *Arabidopsis* mutants define a central role for the xanthophyll cycle in the regulation of photosynthetic energy conversion. Plant Cell 10:1121–1134
Osmond CB (1994) What is photoinhibition? Some insights from comparison of shade and sun plants. In: Baker RR, Bowyer JR (eds) Photoinhibition of photosynthesis: from molecular mechanisms to the field. Bios Scientific Publications, Oxford, pp 1–24
Powles SB (1984) Photoinhibition of photosynthesis induced by visible light. Annu Rev Plant Physiol 35:15–44
Qing H, Zhang YJ, Chai Z, Wu H, Wen S, He P (2014) *Gracilariopsis longissima* as biofilter for an Integrated Multi-Trophic Aquaculture (IMTA) system with *Sciaenops ocellatus*: bioremediation efficiency and production in a recirculating system. Ind J Geo-Mar Sc 43:528–537
Quintano E, Ganzedo U, Díez I, Figueroa FL, Gorostiaga JM (2013) Solar radiation (PAR and UVA) and water temperature in relation to biochemical performance of *Gelidium corneum* (Gelidiales, Rhodophyta) in subtidal bottoms off the Basque coast. J Sea Res 83:47–55
Rincones ER, Moreno DA (2011) Technical and economical aspects for the commercial establishment of seaweed mariculture in Colombia: experiences in the Guajira Peninsula. Amb Desarr 15:123–144
Ritz T, Damjanović A, Schulten K, Zhang J (2000) Efficient light harvesting through carotenoids. Photosynth Res 66:125–144
Rosso VDE, Mercadante AZ (2007) Identification and quantification of carotenoids by HPLC-PDA-MS/MS from Amazonian fruits. J Agric Food Sci 55:5062–5072
Santos WS, Schmidt ÉC, Felix MR, Polo LK, Kreusch M, Pereira DT, Costa GB, Simioni C, Chow F, Ramlov F, Maraschini M, Bouzon Z (2014) Bioabsorption of cadmium, copper and lead by the red macroalga *Gelidium floridanum*: physiological responses and ultrastructure features. Ecotox Envir Safe 105:80–89
Scholes GD, Fleming GR, Olaya-castro A, Grondelle R, Van Grondelle RV (2011) Lessons from nature about solar light harvesting. Nat Chem 3:763–774
Schubert N, García-Mendoza E (2008) Photoinhibition in red algal species with different carotenoid profiles. J Phycol 44:1437–1446
Schubert H, Sagert S, Forster RM (2001) Evaluation of the different levels of variability in the underwater light field of a shallow estuary. Helgol Mar Res 55:12–22
Schubert N, García-Mendoza E, Pacheco-Ruiz I (2006) Carotenoid composition of marine red algae. J Phycol 42:1208–1216
Taiz L, Zeiger E (2009) Fisiologia Vegetal, 4th edn. Artmed Editora, Porto Alegre
Torres PB, Chow F, Furlan CM, Mandelli F, Mercadante A, Santos DYAC (2014) Standardization of a protocol to extract and analyze chlorophyll *a* and carotenoids in *Gracilaria tenuistipitata* var. *liui* Zang and Xia (Rhodophyta). Braz J Oceanogr 62:57–63
Ursi S, Plastino M (2001) Crescimento *in vitro* de linhagens de coloração vermelha e verde clara de *Gracilaria birdiae* (Gracilariales, Rhodophyta) em dois meios de cultura: análise de diferentes estádios reprodutivos. Rev Bras Bot 4:587–594
Waaland JR, Waaland SD, Bates G (1974) Chloroplast structure and pigment composition in the red alga *Griffithsia pacifica*: regulation by light intensity. J Phycol 10:193–199
Yakovleva IM, Titlyanov EA (2001) Effect of high visible and UV irradiance on subtidal *Chondrus crispus*: stress photoinhibition and protective mechanisms. Aquat Bot 71:47–61
Yong YS, Yong WTL, Anton A (2013) Analysis of formulae for determination of seaweed growth rate. J Appl Phycol 25:1831–1834
Young AJ (1993) Occurrence and distribution of carotenoids in photosynthetic systems. In: Young AJ, Britton G (eds) Carotenoids in photosynthesis. Chapman & Hall, London, pp 16–71
Zou D, Kunshan G (2014) Temperature of photosynthetic light- and carbon-use characteristics in the red seaweed *Gracilariopsis lemaneiformis* (Gracilariales, Rhodophyta). J Phycol 50:366–375

ANEXO 2

J Appl Phycol (2016) 28:2035–2040
DOI 10.1007/s10811-015-0708-0

Mycosporine-like amino acids from *Gracilariopsis tenuifrons* (Gracilariales, Rhodophyta) and its variation under high light

Priscila B. Torres[1] · Fungyi Chow[1] · Marcelo J. P. Ferreira[1] · Déborah Y. A. C. dos Santos[1]

Received: 28 April 2015 / Revised and accepted: 31 August 2015 / Published online: 10 September 2015
© Springer Science+Business Media Dordrecht 2015

Abstract Mycosporine-like amino acids (MAAs) have been identified as photoprotective agents for photosynthetic organisms, mainly against ultraviolet radiation. However, the role of these compounds associated with high intensity of photosynthetically active radiation (PAR) is not completely understood. In the present study, the MAA profile of laboratory-cultivated *Gracilariopsis tenuifrons* was investigated at three PAR levels. Ethanolic extract afforded a mixture of five components. Four of them were identified as asterina-330, palythinol, palythene, and usujirene. This is the first report of usujirene for Gracilariaceae. Despite the fact that the PAR increase did not alter the qualitative composition of MAAs, a clear correlation between palythinol amount and irradiance during the 7-day experiment was detected. This increase of palythinol correlated to high PAR supports the hypothesis of photoprotection related to these compounds.

Keywords *Gracilariopsis tenuifrons* · Rhodophyta · Mycosporine-like amino acids · Light stress · Photosynthetic active radiation · Photoprotection

Introduction

Photosynthetic organisms are often exposed to ultraviolet (UV) radiation, which is common in natural conditions, but highly deleterious when in excess and may lead the organism to death (Asada and Takahashi 1987). However, these organisms present defensive strategies to mitigate or avoid the harmful effects of UV radiation. An effective strategy previously reported for red algae is the accumulation of photoprotective compounds such as mycosporine-like amino acids (MAAs) (see, e.g., Sinha et al. 2000).

MAAs are characterized by low molecular weight (usually less than 400 Da), water solubility, high peak absorption at wavelength of UV, particularly between 310 and 360 nm, and high molar extinction coefficient which corroborates the action as photoprotective compounds. These compounds have an amino-cyclohexenone or amino-cyclohexenimine ring linked to one or two amino acids (Cardozo et al. 2007). Some studies have suggested that 4-deoxigadusol, the precursor of MAAs, is biosynthesized by the shikimate pathway (Barre et al. 2014).

There are about 21 MAAs described in the literature, most of them found in marine organisms such cyanobacteria, algae, and vertebrate and invertebrate animals. For animals, MAAs are obtained by feeding on MAA-producing organisms. Besides UV-photoprotective activity, these compounds act as antioxidants, osmoprotectants, and, probably, anti-desiccation (Oren and Gunde-Cimerman 2007). Due to high UV absorption, MAAs have been used in cosmetic products by the pharmaceutical industry, as in the sunblock Helioguard 365® (Carreto and Carignan 2011). As laboratory synthesis of MAAs is not yet available, these compounds are obtained only from natural sources. Cardozo et al. (2011) suggest that MAA extraction could be carried out on commercial agarophytes, improving the commercial value of these species.

Quantitative and qualitative variations in MAAs have been observed in many algal species in high irradiance conditions. Post and Larkum (2006) verified an increase in the content of these compounds in *Palmaria decipiens* (Palmariales, Rhodophyta) and *Prasiola crispa* (Prasiolales, Chlorophyta)

✉ Déborah Y. A. C. dos Santos
dyacsan@ib.usp.br

[1] Departamento de Botânica, Instituto de Biociências, Universidade de São Paulo, Rua do Matão, 277, 05508-090 São Paulo, SP, Brazil

©Fungyi Chow / 2021

during the summer, while a decrease was observed during the winter. Aguilera et al. (2002) observed the same pattern for *Palmaria palmata* (Palmariales, Rhodophyta) and *Devaleraea ramentacea* (Palmariales, Rhodophyta). Karsten et al. (1998a) determined that tropical species of red algae have twice MAA content than those species from temperate zones. Photoprotective function of MAAs against UV radiation is well documented. However, studies such as Sinha et al. (2000) have not observed an increase in MAA content in high UV radiation. Actually, they showed a decrease in MAA content indicating that these substances do not necessarily act only in UV stress.

Photosynthetically active radiation (PAR) is the essential spectral range of solar radiation for photosynthetic organisms, since it is crucial for vital processes such as primary and secondary metabolism. However, high levels of irradiance can be deleterious to the organisms, affecting photosynthesis, growth, primary production, development, and reproduction. High levels of PAR lead to MAA accumulation (see, e.g., Karsten et al. 1998b, Krabs et al. 2004, and Roleda et al. 2012), and the real role of these compounds for visible light photoprotection needs further investigation.

In this scenario, the main goal of the present study was to identify the MAAs present in *Gracilariopsis tenuifrons* (C. J. Bird & E. C. Oliveira) Fredericq & Hommersand and verify the variation under distinct levels of PAR. This red seaweed is a native species from Brazil, distributed along the coast and has been used as model for several physiological studies at Laboratory of Marine Algae Edison José de Paula (University of São Paulo) (Rossa et al. 2002; Torres et al. 2015).

Materials and methods

General growth conditions Acclimatization of *Gracilariopsis tenuifrons* (BG0039, Germplasm Bank) (Costa et al. 2012) was carried out in the Laboratory of Marine Algae Edison José de Paula (Institute of Biosciences—University of São Paulo) as described before (Torres et al. 2015). Briefly, apical portions of female gametophytic phase were kept at 25±1 °C, photosynthetic photon flux density (PPFD) of 60±5 μmol photons m^{-2} s^{-1}, 14-h light/10-h dark photocycle, intermittent aeration at 30-min intervals, using sterilized 32 psu seawater enriched with von Stosch solution 50 % (Ursi and Plastino 2001). The light was provided by fluorescent lamps (model day light, Philips, 40 W), and the photon flux density was determined by PPFD spherical sensor (LI-COR Model LI-1935B) connected to a recorder (LI-COR Model LI-250). The amount of UV in lamps used in this study is considered negligible.

Experimental design Acclimatized apical portions of 3 cm in length, kept at the same conditions described above, were submitted to three treatments of PPFD: 60 (control), 600, and 1000 μmol photons m^{-2} s^{-1} in Erlenmeyer flasks for 1 week. Each PPFD treatment consisted of 21 Erlenmeyer flasks arranged in seven sets of three replications. Daily, during the 1-week experimental period, three flasks (replication) of 400 mg of fresh biomass from each light treatment were sampled, frozen in liquid nitrogen, and stored at −80 °C (Torres et al. 2015) until analysis.

Extraction and mycosporine-like amino acids analyses Samples were powdered with liquid nitrogen and extracted with 5 mL of 70 % ethanol at 50 °C during 1 h, and centrifuged for 10 min at 12,000×*g*. Aliquots of 40 μL from the supernatants were analyzed by high-performance liquid chromatography (HPLC) using a HP 1260 chromatograph equipped with Zorbax C18 (4.6×250 mm) column. Isocratic mixture of 0.1 % acetic acid and acetonitrile (9:1 *v*/*v*) was used as mobile phase at constant flux of 0.3 mL min^{-1} for 15 min. Column temperature was adjusted to 45 °C. The chromatograms were processed at λ=270 and 330 nm, and the UV/visible spectra were obtained between 220 and 600 nm. Mycosporine-like amino acid (MAA) identification was carried out using HPLC coupled to a mass spectrometer with electrospray ionization (HPLC-ESI-MS) (Shimadzu M10AVP—Esquire 3000 Plus—Bruker Daltonics). The parameters of the mass spectrometer were adjusted as follow: capillary volts = 4000 V, mobile phase flux 90 μL min^{-1}, skimmer 40 V, N_2 as desiccating gas at 320 °C and 7 L h^{-1} and as nebulizing gas at 1861 hPa, and source temperature 450 °C. Mass spectra were acquired at a 100–1200 *m*/*z* interval.

Statistical analyses One-factor analysis of variance (ANOVA) was used to determine the significant differences between means of each variable on a daily basis, between treatments. When differences were detected, the post hoc Tukey test was applied. All analyses were performed in triplicate and carried out considering α=5 % using Minitab 16.1.0 software.

Results and discussion

Ethanolic extract from *G. tenuifrons* yielded a mixture of five components with wavelength of the absorption maximum range from λmax=325 nm to λmax=360 nm suggesting the presence of MAAs. These compounds were identified through their mass spectral fragmentation patterns, UV-spectrum profiles (Table 1), and comparison with literature data (Cardozo et al. 2006).

Table 1 Mycosporine-like amino acids obtained from *Gracilariopsis tenuifrons*

Peak	Retention time (min)[a]	Compound	λmax (nm)	$[M+H]^+$	Mass fragments
1	8.8	Asterina-330	330	289	274, 230, 212, 186
2	9.4	Palythinol	332	303	288, 244, 186
3	9.8	n.i.	333	271	256, 241, 212, 197
4	11.6	Palythene	358	285	270, 241, 226, 197
5	12.9	Usujirene	356	285	270, 226, 197

n.i. not identified

[a] Based on HPLC-ESI-MS method

Compound 1 eluted at retention time of 8.8 min and had maximum absorption at 330 nm suggesting the presence of a substituted imine group in the structure. MAAs containing a chromophore with one unsubstituted imine functionality have a typical absorption around 320 nm (Carreto and Carignan 2011). ESI-MS in the positive mode of compound showed an intense molecular ion $[M+H]^+$ at *m/z* 289. MS^n spectrum furnished a fragment at *m/z* 274 corresponding to the loss of 15 Da which suggests a methyl radical elimination. The resultant ion lost one CO_2 molecule (44 Da), generating a fragment at *m/z* 230. This ion showed two fragmentation routes: (1) the formation of a fragment at *m/z* 212 through the subsequent neutral loss of water from the hydroxyl group bonded at C-5 or from lateral chain at C-1; and (2) the ion at *m/z* 186 formed by the loss of the lateral chain at C-1. Therefore, from this fragmentation pattern, the compound 1 was identified as asterina-330.

Compound 2 as well as compound 1 had an absorption maximum at 332 nm, suggesting the presence of a substituted imine group in the structure, with retention time at 9.6 min. ESI-MS in the positive mode of compound showed an intense molecular ion $[M+H]^+$ at *m/z* 303 and its MS^n spectrum furnished two fragments at *m/z* 288 $[(M+H)-15]^+$ and 244 $[(M+H)-59]^+$ corresponding, respectively, to methyl radical elimination and subsequently CO_2 molecule. The loss of the lateral chain bonded in the imine group resulted in the fragment at *m/z* 186. From this fragmentation pattern and by comparison with literature data, compound 2 was assigned as palythinol.

Compounds 4 and 5 exhibited maximum absorption at 358 and 356 nm and retention times at 11.6 and 12.9 min, respectively. Both compounds displayed a molecular ion $[M+H]^+$ at *m/z* 285 suggesting that the structures are stereoisomers. In general, the *cis*- and *Z*-isomers showed a hypsochromic displacement of 2–3 nm with respect to their *trans*- and *E*-analogues, as verified in literature for the isomeric pairs palythene/usujirene and *E/Z* palythenic acid (Carreto and Carignan 2011). The same fragmentation pattern proposed for compounds 1 and 2 was followed by these compounds, showing fragments at *m/z* 270, *m/z* 226, and *m/z* 197 corresponding to the methyl radical elimination followed by a decarboxylation, ubiquitous fragmentations in most of MAAs studied. Furthermore, compound 4 showed an additional fragment at *m/z* 241 enabling its characterization as palythene. Thus, compound 5 was identified as usujirene, the respective *Z*-isomer of palythene.

Compound 3 remains unidentified (Table 1). However, the UV-spectrum with maximum peak between 310 and 360 nm suggests another MAA (Cardozo et al. 2007). Moreover, molecular ion $[M+H]^+$ at *m/z* 271 and maximum absorption at 330 nm suggests another compound with a substituted imine group.

There are few reports for MAAs in species of Gracilariaceae (Table 2), most of them comprise the genus *Gracilaria* (seven species), followed by *Hydropuntia* (two species), and *Curdiea* (one species). The present study is the first report of MAAs in a species of *Gracilariopsis*.

Although, shinorine, porphyra-334, palythine, and asterina-330 are the most common MAAs described in Gracilariaceae, only the latter was found in *G. tenuifrons*. Palythinol and palythene, both present in *G. tenuifrons*, are less frequent in the family, and have been previously described for *Curdiea racovitzae*, *Gracilaria changii*, and *G. tenuistipitata*. These two compounds are absent in *Hydropuntia*. The presence of usujirene in *G. tenuifrons* is the first report of this compound for Gracilariaceae. Karsten et al. (1998a) described the "non-identified" compound found in *G. changii* as MAA-357, due to the maximum peak of UV-spectrum. The authors suggested the possibility that MAA-357 could be usujirene; however, it could not be confirmed. Almost all MAAs found in Gracilariaceae have the amino-cyclohexenimine ring. Only the mycosporine-glycine described for *C. racovitzae* is characterized by amino-cyclohexenone ring (Table 2).

Despite the fact that PAR increase did not alter the qualitative composition of MAAs of all extracts of *G. tenuifrons*, some quantitative variation was observed (Fig. 1a). A slight decrease on total MAA amounts from day 1 to day 7 was detected for control samples (60 μmol photons m^{-2} s^{-1}), while for treatments of 600 and 1000 μmol photons m^{-2} s^{-1} an increase of around 20 % was detected. Notwithstanding, among all MAAs, the palythinol amount presented a clear correlation with PAR intensity (Fig. 1b). For control samples, a slight but significant decrease was

Table 2 Summary of mycosporine-like amino acids identified in species of Gracilariaceae (Rhodophyta)

Species	Mycosporine-like amino acids									References
	S	Po	Pn	A	Pl	P	Mg	U	n.i.	
Curdiea racovitzae	X		X	X	X	X	X			Karentz et al. (1991)
Curdiea racovitzae	X	X	X	X			X		X	Hoyer et al. (2001)
Gracilaria birdiae	X	X	X							Cardozo et al. (2011)
Gracilaria changii	X	X	X	X		X			X	Karsten et al. (1998a)
Gracilaria chilensis	X	X	X	X						Gomez et al. (2005)
Gracilaria conferta	X	X								Figueroa et al. (2010)
Gracilaria domingensis	X	X	X							Cardozo et al. (2011)
Gracilaria salicornia	X	X	X	X						Karsten et al. (1998a)
Gracilaria tenuistipitata	X	X	X	X	X					Cardozo et al. (2011)
Gracilaria tenuistipitata	X	X								Barufi et al. (2011)
Gracilariopsis tenuifrons				X	X	X		X	X	Present study
Hydropuntia cornea[a]	X	X								Sinha et al. (2000)
Hydropuntia cornea	X	X	X							Figueroa et al. (2012)
Hydropuntia eucheumatoides[b]	X	X	X	X						Karsten et al. (1998a)

S Shinorine, *Po* Porphyra-334, *Pn* Palythine, *A* Asterina-330, *Pl* Palythinol, *P* Palythene, *Mg* Mycosporine-glycine, *U* Usujirene, *n.i.* not identified, *X* presence

[a] In original paper—*Gracilaria cornea*

[b] In original paper—*Gracilaria eucheumatoides*

observed from day 1 to day 7. In contrast, for treatments of 600 and 1000 µmol photons m^{-2} s^{-1}, the palythinol amount increased three- to four- fold. All other MAAs found in *G. tenuifrons* did not present stable behavior, making it impossible to correlate them with PAR treatments.

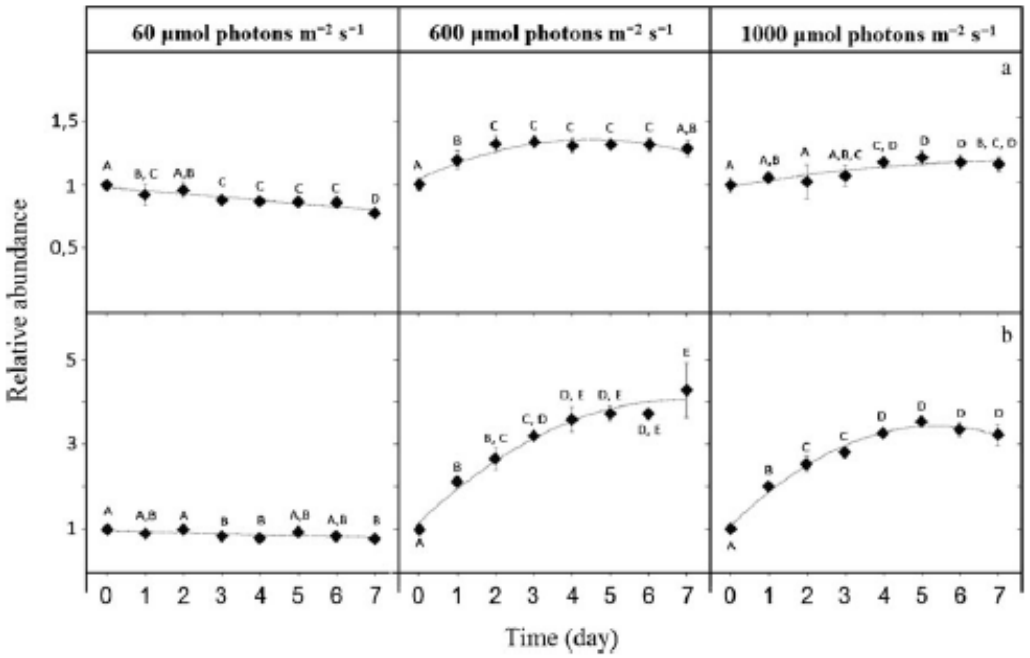

Fig. 1 Total mycosporine-like amino acids (**a**) and palythinol (**b**) from apical portions of *Gracilariopsis tenuifrons* over seven experimental days with different levels of photosynthetically active radiation (PAR): 60, 600, and 1000 µmol photons m^{-2} s^{-1}. Values are means±SD (n=3). *Distinct letters* in each box mean statistically difference (p<0.05)

©Fungyi Chow / 2021

Studies with the increase of PAR and MAA variation have been conducted mainly in *Chondrus crispus* (Gigartinales, Rhodophyta) and have shown that this radiation has influence on the synthesis of MAAs. Krabs et al. (2002) have verified an increase in total MAA content with PAR elevation. However, this raise was associated mainly to palythine. Similar results have been found by Franklin et al. (2001). Karsten et al. (1998b) verified that besides of palythine content, shinorine, palythinol, and palythene content have also increased with elevated PAR. Korbee et al. (2005) studied *Porphyra leucosticta* (Bangiales, Rhodophyta) and also verified an accumulation of asterina-330, porphyra 334, shinorine, and palythine when exposed to high PAR. All these examples show that high PAR acts distinctly on different MAAs, reinforcing our data which show that PAR acts on the synthesis of MAAs mainly in palythinol. These differences may be inherent to each species or can be related to the distinct conditions in the experiments, such as acclimatization period, quality and intensity of the light and temperature (Oren and Gunde-Cimerman 2007).

The synthesis of MAAs via PAR can possibly be a sign that there will be an increase in UV in the environment, and the synthesis of photoprotection substances against UV before the stress caused by this increase is an ecological advantage. Franklin et al. (2001) found that the synthesis of shinorine reached the higher amount when *C. crispus* was first exposed to blue light followed by UVA exposure. Based on the results, they suggested that the perception of increase of blue light could work as signaling of future high incidence of UV.

In land plants, MAAs have not been found and the photoprotective function against UV radiation is played by phenolic compounds, such as flavonoids and phenolic acids. PAR increase also promotes the accumulation of these substances which are well known by their antioxidant function through oxidative stress (Agati et al. 2013). Antioxidant activity via scavenging of reactive oxygen species, protecting cell from oxidative damage, has already been suggested as possible roles for MAAs. Dunlap and Yamamoto (1995) suggested that imino-MAAs, such as palythinol, present a low-moderate antioxidant activity, while Carreto and Carignan (2011) described high activity for oxocarbonyl-MAAs (with ketone group), mainly due to easier oxidation. In contrast, de la Coba et al. (2009) verified high in vitro antioxidant activity for imino-MAAs using β-carotene/linoleic acid assay. However, based on all these finds, the antioxidant activity of imino-MAAs like palythinol are still inconclusive, but does not exclude the possibility of these substances act to prevent oxidative stress under high PAR.

In conclusion, *G. tenuifrons* presents a particular profile of MAAs among the Gracilariaceae reported in the literature with the unusual compounds usujirene and palythene. Moreover, the increase of palythinol correlated to high PAR supports the idea of photoprotection related to these compounds.

Acknowledgments The authors thank FAPESP (Fundação de Amparo à Pesquisa do Estado de São Paulo) for financial support (2010/02948-3, Biota/Fapesp 2013/50731-1), and CNPq (Conselho Nacional de Desenvolvimento Científico eTecnológico) for PBT fellowship. DYACS and MJPF are supported by a CNPq research fellowship.

References

Agati G, Brunetti C, Di FM, Ferrini F, Pollastri S, Tattini M (2013) Functional roles of flavonoids in photoprotection: new evidence, lessons from the past. Plant Physiol Biochem 72:35–45

Aguilera J, Bischof K, Karsten U, Hanelt D, Wiencke C (2002) Seasonal variation in ecophysiological patterns in macroalgae from an Arctic fjord. II. Pigment accumulation and biochemical defence systems against high light stress. Mar Biol 140:1087–1095

Asada K, Takahashi M (1987) Production and scavenging of active oxygen in chloroplasts. In: Kyle DJ, Osmond CB, Arntzen CJ (eds) Photoinhibition. Elsevier, Amsterdam, pp 227–287

Barre SL, Roullier C, Boustie J (2014) Mycosporine-Like Amino Acids (MAAs) in Biological Photosystems. In: Barre S L, Komprobst J (eds) Outstanding Marine Molecules: Chemistry, Biology, Analysis. Wiley-Blackwell, pp 333–360

Barufi JB, Korbee N, Oliveira MC, Figueroa FL (2011) Effects of N supply on the accumulation of photosynthetic pigments and photoprotectors in *Gracilaria tenuistipitata* (Rhodophyta) cultured under UV radiation. J Appl Phycol 23:457–466

Cardozo KHM, Carvalho VM, Pinto E, Colepicolo P (2006) Fragmentation of mycosporine-like amino acids by hydrogen/deuterium exchange and electrospray ionisation tandem mass spectrometry. Rapid Commun Mass Spectrom 20:253–258

Cardozo KHM, Guaratini T, Barros MP, Falcão VR, Tonon AP, Lopes NP, Campos S, Torres MA, Souza AO, Colepicolo P, Pinto E (2007) Metabolites from algae with economical impact. Comp Biochem Physiol C Pharmacol Toxicol 146:60–78

Cardozo KHM, Marques LG, Carvalho VM, Carignan MO, Pinto E, Marinho-Soriano E, Colepicolo P (2011) Analyses of photoprotective compounds in red algae from the Brazilian coast. Rev Bras Farmacogn 21:202–208

Carreto JI, Carignan MO (2011) Mycosporine-like amino acids: relevant secondary metabolites. Chemical and ecological aspects. Mar Drugs 9:387–446

Costa ES, Plastino EM, Petti R, Oliveira EC, Oliveira MC (2012) The Gracilariaceae Germplasm Bank of the University of São Paulo, Brazil-a DNA barcoding approach. J Appl Phycol 24:1643–1653

De la Coba F, Aguilera J, de Gálvez MV, Alvarez M, Gallego E, Figueroa FL, Herrera E (2009) Prevention of the ultraviolet effects on clinical and histopathological changes, as well as the heat shock protein-70 expression in mouse skin by topical application of algal UV-absorbing compounds. J Dermatol Sci 55:161–169

Dunlap W, Yamamoto Y (1995) Small-molecule antioxidants in marine organisms: antioxidant activity of mycosporine-glycine. Comp Biochem Physiol 112:105–114

Franklin LA, Krăbs G, Kuhlenkamp R (2001) Blue light and UV-A radiation control the synthesis of mycosproine-like amino Acids in *Chondrus crispus* (Florideophyceae). J Phycol 37:257–270

Figueroa FL, Israel A, Neori A, Martínez B, Malta EJ, Put A, Inken S, Marquardt R, Abdala R, Korbee N (2010) Effect of nutrient supply on photosynthesis and pigmentation to short-term stress (UV radiation) in *Gracilaria conferta* (Rhodophyta). Mar Pollut Bull 60:1768–1778

Figueroa FL, Korbee N, Abdala R, Jerez CG, López-de la Torre M, Güenaga L, Larrubia MA, Gómez-Pinchetti JL (2012) Biofiltration of fishpond effluents and accumulation of N-compounds

(phycobiliproteins and mycosporine-like amino acids) versus C-compounds (polysaccharides) in *Hydropuntia cornea* (Rhodophyta). Mar Pollut Bull 64:310–318

Gomez I, Figueroa F, Huovinen P, Ulloa N, Morales V (2005) Photosynthesis of the red alga under natural solar radiation in an estuary in southern Chile. Aquaculture 244:369–382

Hoyer K, Karsten U, Sawall T, Wiencke C (2001) Photoprotective substances in Antarctic macroalgae and their variation with respect to depth distribution, different tissues and developmental stages. Mar Ecol Prog Ser 211:117–129

Karentz D, McEuen F, Land M, Dunlap W (1991) Survey of mycosporine-like amino acid compounds in Antarctic marine organisms: potential protection from ultraviolet exposure. Mar Biol 108: 157–166

Karsten U, Sawall T, Wiencke C (1998a) A survey of the distribution of UV-absorbing substances in tropical macroalgae. Phycol Res 46: 271–279

Karsten U, Franklin L, Lüning K, Wiencke C (1998b) Natural ultraviolet radiation and photosynthetically active radiation induce formation of mycosporine-like amino acids in the marine macroalga *Chondrus crispus* (Rhodophyta). Planta 205:257–262

Korbee N, Figueroa FL, Aguilera J (2005) Effect of light quality on the accumulation of photosynthetic pigments, proteins and mycosporine-like amino acids in the red alga *Porphyra leucosticta* (Bangiales, Rhodophyta). J Photochem Photobiol B 80:71–78

Krabs G, Bischof K, Hanelt D, Karsten U, Wiencke C (2002) Wavelength-dependent induction of UV absorbing mycosporine-like amino acids in the red alga *Chondrus crispus* under natural solar radiation. J Exp Mar Biol Ecol 268:69–82

Krabs G, Watanabe M, Wiencke C (2004) A monochromatic action spectrum for the photoinduction of the UV-absorbing mycosporine-like amino acid shinorine in the red alga *Chondrus crispus* 7. 79:5–9

Oren A, Gunde-Cimerman N (2007) Mycosporines and mycosporine-like amino acids: UV protectants or multipurpose secondary metabolites? FEMS Microbiol Lett 269:1–10

Post A, Larkum AWD (2006) UV-absorbing pigments, photosynthesis and UV exposure in Antarctica: comparison of terrestrial and marine algae. Aquat Bot 45:231–243

Roleda MY, Nyberg CD, Wulff A (2012) UVR defense mechanisms in eurytopic and invasive *Gracilaria vermiculophylla* (Gracilariales, Rhodophyta). Physiol Plant 146:205–216

Rossa MM, Oliveira MC, Okamoto OK, Lopes PF, Colepicolo P (2002) Effect of visible light on superoxide dismutase (SOD) activity in the red alga *Gracilariopsis tenuifrons* (Gracilariales, Rhodophyta). J Appl Phycol 14:151–157

Sinha RP, Klisch M, Gröniger A, Häder D-P (2000) Mycosporine-like amino acids in the marine red alga *Gracilaria cornea*—effects of UV and heat. Environ Exp Bot 43:33–43

Torres PB, Chow F, Santos DYAC (2015) Growth and photosynthetic pigments of *Gracilariopsis tenuifrons* (Rhodophyta, Gracilariaceae) under high light *in vitro* culture. J Appl Phycol 27:1243–1251

Ursi S, Plastino EM (2001) Crescimento *in vitro* de linhagens de coloração vermelha e verde clara de *Gracilaria* sp. (Gracilariales, Rhodophyta) em dois meios de cultura: análise de diferentes estádios reprodutivos. Revta Brasil Bot 24:587–594

ANEXO 3

DOI: 10.1007/s11099-018-0805-9 PHOTOSYNTHETICA 56 (4): 1093-1106, 2018

Physiological responses of *Pterocladiella capillacea* (Rhodophyta, Gelidiales) under two light intensities

T.B. HARB+, A. NARDELLI, and F. CHOW

Institute of Bioscience, University of São Paulo, São Paulo, SP, CEP 05508-090, Brazil

Abstract

Macroalgae must be able to survive in conditions of different light intensities with no damage to their physiological performance or vital processes. Irradiance can stimulate the biosynthesis of certain photoprotective compounds of biotechnological interest, such as pigments and proteins. *Pterocladiella capillacea* is a shade-grown alga, which play a role key in the balance of marine ecosystems. In addition, it is considered one of the best sources of bacteriological agar and agarose with a wide pharmacological potential. In order to evaluate the photosensitivity in *P. capillacea* under 60 (control) and moderate light intensity of 300 μmol(photon) m^{-2} s^{-1}, photosynthetic performance and chemical composition were assessed. *P. capillacea* showed photosensitivity without evidence of photodamage. The results indicate the possibility to increase a growth rate and probably infer productivity in long-term cultivation by stimulation at moderate light intensity. Increasing photosynthetic pigment and protein contents were also observed under medium light, an interesting result for functional ingredient approaches.

Additional key words: algae; chlorophyll fluorescence; growth rate; pigments; productivity; radiation.

Introduction

The energy associated with ultraviolet (UV) radiation and photosynthetically active radiation (PAR) determines the photosynthetic capacity of macroalgae and is frequently associated with photosensitivity, phototolerance, photoinhibition, and photodamage processes when it exceeds the photochemical demand or energy dissipation capacity of organisms (Hanelt and Figueroa 2012). Photosynthetic photoinhibition occurs under excessive light availability where the irradiance is greater than the acclimation capacity, causing a reduction of photosynthetic activity (Asada 1994, Takahashi and Murata 2008, Hou and Hou 2013). High intensities of solar radiation can cause photoinhibition or even cellular death due to the inability of certain algae to adjust their composition or concentration of pigments at high irradiances (Hanelt *et al.* 2006, Gómez and Huovinen 2011, Figueroa *et al.* 2014a). Photodamage is usually associated with oxidative stress through the overproduction of reactive oxygen species, reactive nitrogen species and their derivatives (Hideg *et al.* 1994, Hanelt *et al.* 2006, Takahashi and Badger 2011). Oxidative stress has also been associated with specific cleavage of the D1 protein, a component of PSII, activating certain defense mechanisms, such as the production of antioxidant compounds (Nishiyama *et al.* 2004) and the activity of specific antioxidant enzymes (Lee and Shiu 2009, dos Santos *et al.* 2012).

In seaweeds, oxidative stress can cause DNA mutation, protein denaturation, lipid peroxidation, loss of pigments, and alterations in membrane integrity, the latter photochemically affecting photosystems (Cherry and Nielsen 2004). Changes in physiological responses have also been identified and variations in photosynthetic parameters for macroalgae, such as the maximal quantum yield of PSII (F_V/F_M), have already been reported (Liu and Pang 2010).

Received 21 February 2017, *accepted* 18 August 2017, *published as online-first* 12 April 2018.
+Corresponding author; phone: +55+11+30918068, fax: +55+11+30917546, e-mail: talissaharb@ib.usp.br
Abbreviations: A – absorptance; Ab – absorbance; APC – allophycocyanin; DM – dry mass; Car – carotenoids; Chl – chlorophyll; CL – control irradiance of 60 μmol(photon) m^{-2} s^{-1}; ETR – electron transport rate; ETR_{MAX} – maximal electron transport rate; FM – fresh mass; F_V/F_M – maximal quantum yield of PSII photochemistry; GR – growth rate; I_K – saturation irradiance; ML – irradiance of 300 μmol(photon) m^{-2} s^{-1}; PC – phycocyanin; PE – phycoerythrin; P_{MAX} – maximum photosynthesis; TSP – total soluble proteins; UV – ultraviolet; VSES – von Stosch enrichment solution; Φ_{PSII} – effective quantum yield of PSII photochemistry; $Y_{(PSII)}$ – photochemical quenching; $Y_{(NO)}$ – nonregulated nonphotochemical quenching; $Y_{(NPQ)}$ – regulated nonphotochemical quenching; α – photosynthetic efficiency.
Acknowledgements: The authors thank FAPESP (São Paulo Research Foundation; 2014/09380-3 and Biota/Fapesp 2013/50731-1) and CNPq (National Counsel of Technological and Scientific Development) for financial support and scholarships. F. Chow thanks CNPq for CNPq Research Productivity Scholarship (303937/2015-7).

Seaweeds are known to contain a range of antioxidant molecules and secondary metabolites, which protect them from oxidative stress (Balboa *et al.* 2013). Algal species living in the intertidal zone are subjected to diverse solar radiation regimes, depending on their habitat environment, which can result in differences in oxidative stress and antioxidant responses between algal species (Park *et al.* 2016). Marine algae have the ability to acclimate when exposed to variable light intensities. Under long periods of high light intensity, an accumulation of excess excitation energy usually occurs, consequently inducing photostress conditions. Under this circumstance, phycobiliproteins are the most sensitive pigments, being the first to be degraded, followed by carotenoids (Car) and chlorophyll *a* (Chl) (Donkor and Häder 1996, Beach *et al.* 2000). Algae adapted to high light intensity, denoted as sun algae, usually inhabit the supra- and mid-intertidal of the coastal zone on the rocky shore littoral, commonly exposed to elevated levels of solar radiation (Falkowski 1980). These high light-adapted macroalgae show high rates of maximum photosynthesis (P_{MAX}), low photosynthetic efficiency (α), high values of saturation irradiance (I_K), low Chl content, and high short-term increase of accessory pigments such as Car and phycobiliproteins (Gómez and Huovinen 2011). When exposed to high irradiance, sun algae may increase at a short term the concentration of photosynthetic pigments as a defense mechanism to avoid photosynthetic photosaturation and quench the high incident energy. At the long term or under stronger light stress, the tendency is to degrade pigments as consequence of photodamage and then depigmentation of the thallus occurs (Martone *et al.* 2010, Betancor *et al.* 2014.)

On the other hand, algae adapted to low light intensity, denoted as shade algae, commonly inhabit the lower intertidal and upper infralittoral zones or sun-protected shadow areas like crevices, frequently exposed to low light irradiances. Physiologically, shade algae are characterized by low rates of P_{MAX}, high α, low values of I_K, and higher concentrations of photosynthetic pigments (Falkowski 1980, Grobbelaar and Kurano 2003, Copertino *et al.* 2006, Betancor *et al.* 2014).

Under natural conditions, there is a wide variation of light intensity throughout the day, especially in intertidal environments; therefore, many algae seem to acclimate their light-harvesting complex to distribute the excess of excitation energy among the photosystems in order to avoid photodamage (Falkowski 1980, Franklin *et al.* 2003). In general, the capacity to use light energy serves as a sensor to regulate the appropriate concentration of pigments to maintain the balance between excitation energy, photochemical ability, and demand for growth (MacIntyre *et al.* 2000, Necchi 2005). Therefore, marine macroalgae need to be able to absorb light in low- and high-irradiance situations without compromising the photosynthetic process (Franklin and Larkum 1997, Necchi 2005, Sampath-Wiley *et al.* 2008).

High irradiance can cause nutritional deficiency in macroalgae by an indirect effect on carbon/nitrogen metabolism through cellular organic component reallocation. At excessive light, the photosynthetic machinery is forced beyond the carbon and nitrogen availability, creating a carbon/nitrogen imbalance (Polo *et al.* 2014). In response to high light, algae can degrade carbon stocks, such as starch and polysaccharides (He *et al.* 2002, Nyvall-Cóllen *et al.* 2004), and photosynthetic pigments as a reallocation strategy for providing organic and inorganic components (nitrogen and carbon skeletons, for example) which can be transferred to synthesize other compounds for cell maintenance and defense (MacIntyre *et al.* 2000).

Nishihara *et al.* (2005) observed an improvement in nitrate and ammonium uptakes by *Laurencia brongniartii* J. Agardh with increasing irradiance. The authors attributed this result to the consumption of internal nitrogen reserves due to the rise of photosynthetic activity. The placement of macroalgae in the rocky shore also influences the algal metabolism. Martínez and Rico (2008) observed that algae acclimated to local high irradiances usually have a higher carbon and lower nitrogen contents when compared to acclimated algae from areas with low irradiances.

For this study, *Pterocladiella capillacea* (S.G. Gmelin) Santelices & Hommersand (Rhodophyta, Gelidiales) was chosen as a biological model because it is a species ecologically relevant and abundant in shadow intertidal rocky shores (Oliveira *et al.* 1996). The *Pterocladiella* beds are natural nurseries for many marine species, mainly marine invertebrates, such as crustaceans, amphipods, polychaetes, among others; they also serve as refuge for several organisms (Nascimento and Rosso 2007). Additionally, *P. capillacea* is one of the most studied species of Gelidiales in Brazil, due to the great ecological and economic importance for human consumption and extraction of good quality agar (Oliveira *et al.* 1996). This species is characterized as a shade alga, commonly in lower intertidal and shallow subtidal, inhabits crevices and wave-beaten locals, attached to consolidate substrate, generally in the rocky shore (Gal-Or and Israel 2004). It is widely found in the Brazilian coast, from the state of Espírito Santo to the coast of Rio Grande do Sul (Guimarães 2006).

As an ecologically and economically important species, the elucidation of acclimation, sensitivity, tolerance, and defense mechanisms of *P. capillacea* under moderate light conditions are valuable physio-chemical informations. The aim of this study was to evaluate the photosensitivity and tolerance mechanisms of *P. capillacea* under two light intensities (a control treatment and at moderate irradiance) to assess the possibility to improve a growth rate and chemical composition for further biotechnological applications. The results of the present study can complement previous ecological and physiological studies and the knowledge regarding the life strategy of *P. capillacea* under increasing irradiance. The understanding of these processes can enable the management and sustainable exploitation of the species.

Materials and methods

Alga material, culture conditions and growth rate (GR): *Pterocladiella capillacea* was collected in September 2014 at Praia da Cruz (21°02'01.68"S; 40°48'44.43"W), Espírito Santo State, in the southeastern region of Brazil. Distal segments of 10 cm in length of *P. capillacea* were maintained in sterile seawater (32 psu) and von Stosch enrichment solution (VSES) 100% [Ursi and Plastino (2001) modified from Edwards (1970)]. The algae were acclimated for one week in a temperature-controlled room at 25 ± 1°C with a photoperiod of 14 h, irradiance of 60 μmol(photon) m^{-2} s^{-1}, and intermittent aeration for 30 min, at the culture proportion of 3 g of biomass for 1 L of culture medium. Eight specimens were deposited in the SPF Herbarium of the University of São Paulo (voucher SPF-57890).

After acclimation, distal algal portions (7 cm) were submitted to two light treatments, provided as PAR of 60 (CL) and 300 μmol(photon) m^{-2} s^{-1} (ML) (n = 5) for eight experimental days, in total of 80 Erlenmeyer flasks, and the same culture acclimation conditions described below. With the aim of studying a moderate light intensity, 300 μmol(photon) m^{-2} s^{-1} was chosen as moderate irradiance, since 10-times higher irradiation is considered a high stressing light (Torres *et al.* 2014). Biological independent replicates for each treatment and experimental period were cultivated in separated Erlenmeyer flasks. Experimental measurements were carried out at 0, 1, 3, 5, 7, and 8 (t0, t1, t3, t5, t7. and t8) d by the analysis of growth rate (GR), photosynthetic performance, cellular carbon-hydrogen-nitrogen (CHN) content, pigments, and total soluble proteins (TSP). Time t0 represents the treatment before starting the experimental condition and t8 represents the treatment after a 24-h supplementation with VSES 100%. The objective of this last time (t8) was to evaluate the recovery of *P. capillacea*.

GR was estimated by the equation: GR (% per day) = $[(M_f/M_i)^{1/t} - 1] \times 100\%$ (Penniman *et al.* 1986), where M_f is the final fresh mass (FM) at final experimental time (t), M_i is the initial fresh mass, and the results were represented as daily average GR.

***In vivo* Chl *a* fluorescence**: Photosynthetic performance was estimated as *in vivo* fluorescence of Chl *a* of PSII by using a portable fluorometer *PAM-2500 (Walz,* Germany). The measurements were made between 4 and 7 h after switching on the photoperiod light. F_V/F_M was measured in 15-min dark-adapted sample and calculated following Schreiber *et al.* (1986). Effective quantum yield of PSII (Φ_{PSII}), or photochemical quenching [$Y_{(PSII)}$], was measured in light-adapted sample and calculated following Schreiber and Neubaer (1990). Photosynthesis–irradiance curves were estimated on light-adapted samples from electron transport rate (ETR)–irradiance curves at eight increasing actinic irradiances [PAR: 0, 24, 61, 108, 186, 456, 752, and 1,024 μmol(photon) m^{-2} s^{-1}]. ETR was calculated as $ETR = \Phi_{PSII} \times PAR \times A \times 0.15$; where A is the absorptance (Ramus and Rosenberg 1980, Mercado *et al.* 1996) and 0.15 is the fraction of Chl *a* associated with PSII for red algae. The Chl *a* fraction is different from that of green algae or vascular plants (0.5) and brown algae (0.8), since lower Chl *a* is associated to the PSII in red algae (Grzymski *et al.* 1997). From the ETR–irradiance curves, the maximum ETR (ETR_{MAX}), α, and I_K were determined (Maxwell and Johnson 2000) by fitting the curves to a hyperbolic tangent model of Jassby and Platt (1976). Photochemical quenching [$Y_{(PSII)}$], nonregulated nonphotochemical quenching [$Y_{(NO)}$], and regulated non-photochemical quenching [$Y_{(NPQ)}$] were also determined using the method of Roháček (2002).

Photosynthetic pigments and total soluble proteins (TSP): Frozen samples of 70 mg(FM) were ground in liquid nitrogen and extracted into 1.5 mL of ice-cold 0.05 M phosphate buffer (pH 5.5). The homogenate was centrifuged at 12,000 rpm and 4°C for 15 min and the supernatant analyzed in a UV-visible spectrophotometer (*Epoch Biotek,* USA) for phycobiliprotein determination [μg g^{-1}(FM)] according to the formulas (Kursar *et al.* 1983): PE (phycoerythrin) = $(155.8 \times Ab_{498}) - (40 \times Ab_{614}) - (10.5 \times Ab_{652})$, PC (phycocyanin) = $(151.1 \times Ab_{614}) - (99.1 \times Ab_{652})$, and APC (allophycocyanin) = $(181.3 \times Ab_{652}) - (22.3 \times Ab_{614})$; where Ab represents the absorbance at the respective wavelength. The concentration of TSP was estimated from the same supernatant following Bradford (1976) by using *Bio-Rad®* protein assay reagent *(Bio-Rad,* USA) and bovine serum albumin as standard. Chl *a* and Car analyses were performed using the resulting pellet of phycobiliproteins and protein extraction by resuspending the sedimented material in 1 mL of methanol extracted for 3 h at 4°C and protected from light (Wanderley 2009). The homogenate was centrifuged at 12,000 rpm at 4°C for 15 min and the supernatant was analyzed in a UV-visible spectrophotometer (*Epoch Biotek,* USA). Concentrations of Chl *a* and Car were calculated from their absorbances based on the formulas: Chl *a* [μg g^{-1}(FM)] = $(12.61 \times 153\ Ab_{664})$ and Car [μg g^{-1}(FM)] = $(1000 \times Ab_{470} - 1.63 \times$ Chl *a*$)/221$ as modified from Lichtenthaler and Buschmann (2001).

Carbon-hydrogen-nitrogen (CHN) contents: The quantification of cellular CHN was performed at the Analytical Center of the Chemistry Institute of USP using a *Perkin-Elmer 2400* elemental composition analyser *(Perkin-Elmer,* USA). Dry samples (60°C) of 500 mg were ground to a fine powder and aliquots of 1 mg were ashed at 925°C under pure oxygen, causing complete oxidation of the material. All C was converted to CO_2. N was changed into several oxides (N_xO_x) and then to N_2 by reduction. Individual components were separated from the resultant mixture in a chromatographic column (640°C) and

detected through thermal conductivity changes of the products. The total CHN content was calculated as a percentage, in which each element was standardized to the dry mass (DM) of seaweed and expressed as mg g^{-1}(DM).

Data analysis: All parameters were studied with five replicates for each treatment and each experimental time. Data were statistically analyzed with the *Statistica 12* software by previously testing normality (*Kolmogorov–Smirnov's* test) and homoscedasticity (*Bartlett's* test) ($p<0.05$) and then analyzed by a repeated measures analysis of variance (*ANOVA*) and *Newman-Keul's* multiple-comparison *post-hoc* test ($p<0.05$).

Results

GR and *in vivo* Chl *a* fluorescence: The GR of *P. capillacea* at the end of the experimental period increased more than two fold at 300 µmol(photon) m^{-2} s^{-1} (ML) (2.68 ± 0.07 % d^{-1}) regarding to control (CL) at 60 µmol(photon) m^{-2} s^{-1} (0.71 ± 0.19 % d^{-1}). On the other hand, photosynthetic performance showed a moderate variation between both treatments over experimental time. At control irradiance, the F_V/F_M were constant over time (data not shown). In contrast, there was a decrease in F_V/F_M and variable Φ_{PSII} over the days under ML (data not shown). The A was also constant at both irradiances over time (data not shown).

$Y_{(PSII)}$ showed no variation over the days at CL irradiance (Fig. 1), in contrast, at ML, the $Y_{(PSII)}$ declined starting from t3 with the lowest value at t7 (Fig. 1). Comparing the $Y_{(PSII)}$ between irradiance treatments, the yield was reduced at ML. The $Y_{(NO)}$, which is the heat dissipation without energy expenditure, was greater at ML than that at CL (Fig. 1). The $Y_{(NPQ)}$, which is the energy dissipation with energy expenditure (*e.g.*, xanthophyll cycle), was also estimated, but no values were registered at any irradiance (Fig. 1).

The ETR_{MAX} showed not differences over the experimental time for the irradiances, except for t7 at CL (Fig. 2*A*). The α did not vary over time for the two irradiance treatments (Fig. 2*B*). I_K under CL showed increasing difference only at t5 and t7 (Fig. 2*C*), whereas at ML, the greatest I_K was observed at t7.

ETR–irradiance curves over time for CL and ML are shown in Fig. 3*A* and 3*C*, respectively. Different dynamic plots were observed when compared the two light intensities, however, no clear pattern was noted. For CL, an increasing curve was observed at t7 (Fig. 3*A*), with a significant area under the curve of 2,803 ± 288 (Fig. 3*B*). For other experimental times at the same irradiance, the curve plots were similar and no differences were observed for the area under the curves (Fig. 3*A,B*). At ML, the ETR–PAR curve plots (Fig. 3*C*) and the areas under the curves (Fig. 3*D*) remained constant until the end of the experiment without statistical differences.

Table 1 shows the photosynthetic parameters of *P. capillacea* under the effect of increasing PAR. In the present study, none of the irradiations tested activated $Y_{(NPQ)}$ and *P. capillacea* did not dissipate heat with energy expenditure.

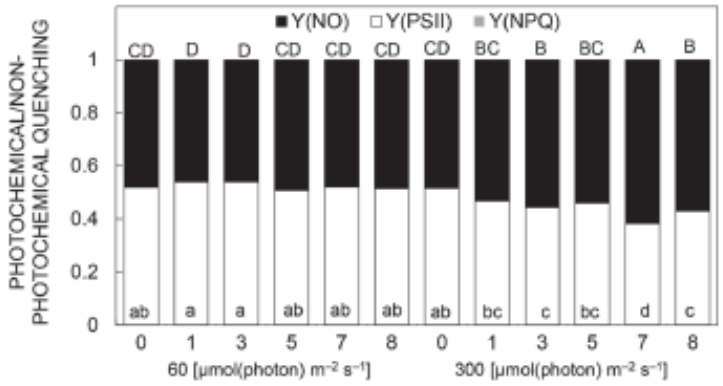

Fig. 1. Photosynthetic performance (mean ± SD, $n = 5$) of *Pterocladiella capillacea* under 60 and 300 µmol(photon) m^{-2} s^{-1} over the experimental time, measured as $Y_{(NO)}$ – nonregulated nonphotochemical quenching, $Y_{(PSII)}$ – photochemical quenching, and $Y_{(NPQ)}$ – regulated nonphotochemical quenching. *Different letters* represent statistically differences by repeated-measure *ANOVA* and *post hoc Newman-Keuls* test ($p<0.05$).

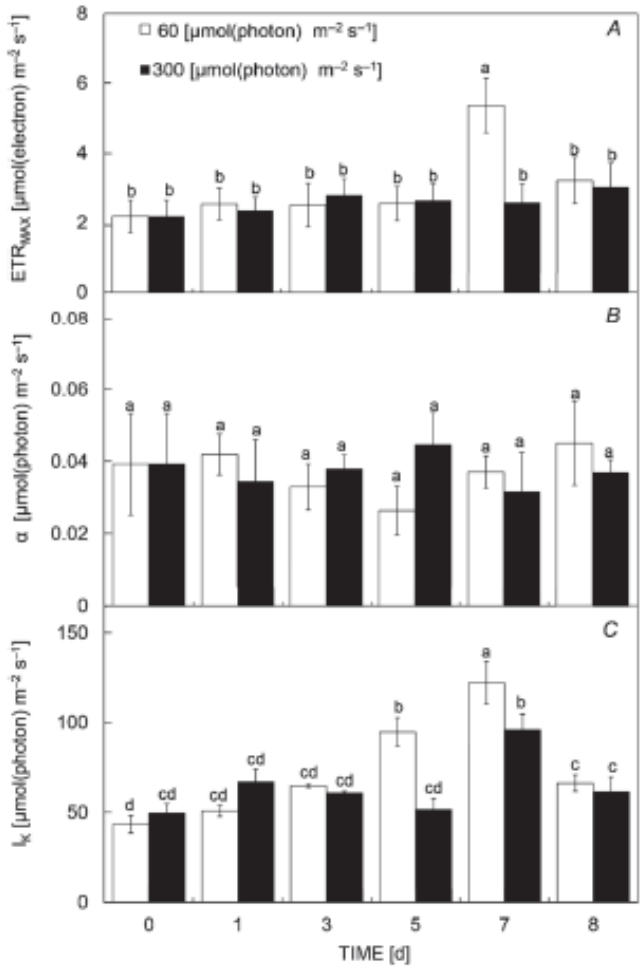

Fig. 2. Photosynthetic performance (mean ± SD, $n = 5$) of *Pterocladiella capillacea* under 60 (*white bars*) and 300 µmol(photon) m^{-2} s^{-1} (*black bars*) over the experimental time, measured as (*A*) ETR_{MAX} – maximum electron transport rate, (*B*) α – photosynthetic efficiency, and (*C*) I_K – saturation irradiance. *Different letters* represent statistically differences by repeated-measure *ANOVA* and *post hoc Newman-Keuls* test ($p<0.05$).

Photosynthetic pigments, TSP and CHN contents: For phycobiliproteins, a gradual increase over time in samples under CL was observed, with a greater pigment content at t8 (Fig. 4*A–C*). For ML, however, PE and PC decreased over the days when compared with t0 (Fig. 4*A–C*). Different responses were observed for Chl *a*, where for both irradiances, Chl *a* decreased over the days (Fig. 4*D*). No differences were observed in the total Car contents when the experimental times were compared with the respective t0 (Fig. 4*E*).

TSP results (Fig. 4*F*) showed that, for both irradiances, there was an increase from the t3 when compared to t0. For the two light treatments, the same contents of proteins were observed.

For the cellular CHN content, no variations between the days and irradiance treatments were observed in C (Fig. 5*A*), H (Fig. 5*B*) or N (Fig. 5*C*).

The results of repeated-measured *ANOVA* for all studied parameters is shown in Table 1S (*supplement available online*).

Discussion

The knowledge of the chemical composition (CHN, pigment, and TSP contents) and physiological parameters (GR and photosynthetic performance) under increasing irradiance presented here provides an important basis for understanding the photosensitivity of the species. *P. capillacea* showed the photosensitivity to the treatment of moderate light intensity, however, no photodamage was observed. Our results indicate that the species turn on defense mechanisms of efficient phototolerance, especially nonphotochemical nonregulated quenching of excess of energy and regulatory synthesis/degradation of the photosynthetic antenna complex. Thus, *P. capillacea*

showed high efficiency in photoacclimation under the laboratory conditions tested in this study and request low light intensity to maintain their life processes.

The increase in irradiance positively affected the GR of *P. capillacea*, however, a reduction in photosynthetic parameter ($Y_{(PSII)}$, ETR_{MAX}, ETR curves) at moderate light intensity were observed. The decrease in photosynthesis was coupled with energy dissipation by $Y_{(NO)}$, indicating passive heat energy dissipation. This quenching mechanism is an efficient process when there is a reduction of photosynthetic expenditure without a GR reduction (Klughammer and Schreiber 2008). These results indicate that 300 µmol(photon) m^{-2} s^{-1} under the experimental conditions studied here did not represent a severe stress conditions that could negatively affect the photodynamics of the photosynthetic apparatus.

As a shade alga, moderate or higher irradiances of *P. capillacea* would be expected to negatively affect GR and photosynthesis, since it inhabits shaded sites, preferably crevices protected from the direct incidence of light, often found in the lower intertidal zone, where it is constantly in contact with seawater. Similar results were obtained by Gómez *et al.* (2004) for some species from a different intertidal localizations. Photosynthetic parameters are valuable descriptors for analyzing the sensitivity and recovery of macroalgae under variable abiotic conditions, making possible to assess acclimation and stress responses. Gal-Or and Israel (2004) showed that irradiances during winter time, 100–500 µmol(photon) m^{-2} s^{-1}, stimulated GR of *P. capillacea*; on the other hand, higher summer irradiances [400–800 µmol(photon) m^{-2} s^{-1}] decreased the GR of the species. In Espírito Santo, the place of origin of our material, the monthly mean irradiance during the summer is around 1,012 µmol(photon) m^{-2} s^{-1} and in the winter it is 512 µmol(photon) m^{-2} s^{-1} (data provided by the Center for Weather Forecasting and Climate Studies in Brazil), similar values to those reported by Gal-Or and Israel (2004). In this sense and considering the results of this study, we can assume that levels above 500–600 µmol(photon) m^{-2} s^{-1} should be adverse conditions for *P. capillacea*. At low irradiances, 120 and 190 µmol(photon) m^{-2} s^{-1}, Sudatti *et al.* (2011) also verified growth rate increase for *Laurencia dendroidea* J. Agardh; results were interpreted by the authors as nonphotoinhibitory conditions. A ten-fold elevated irradiance [600 µmol(photon) m^{-2} s^{-1}] compared to the experimental

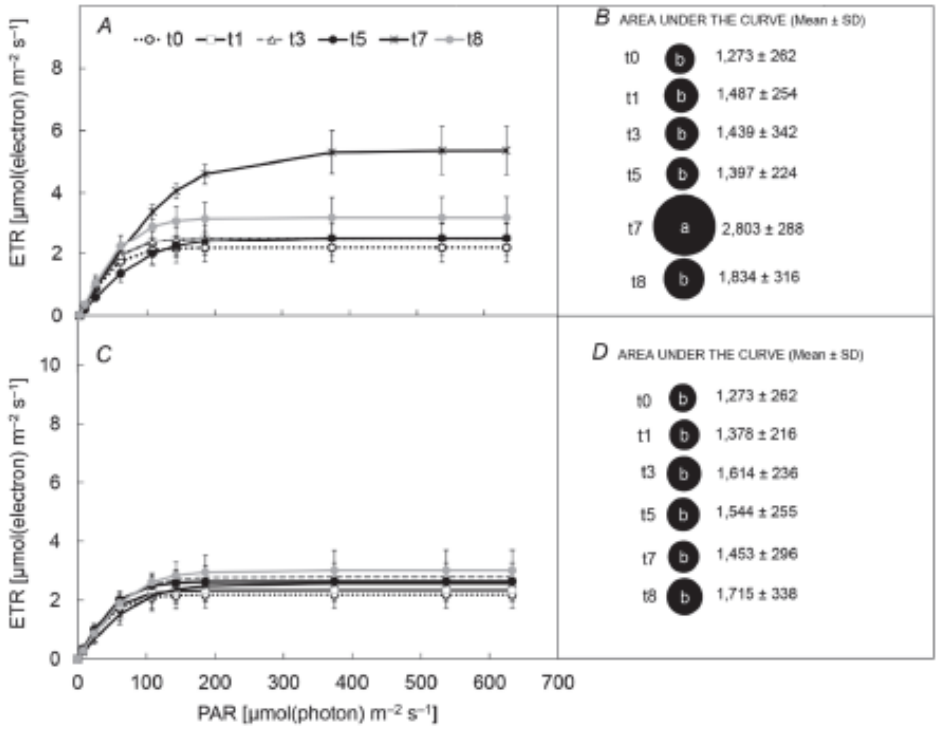

Fig. 3. Electron transport rate (ETR)–PAR curves and the respective area under the curve (mean ± SD, $n = 5$) of *Pterocladiella capillacea* over the experimental time for (*A–B*) 60 µmol(photon) m^{-2} s^{-1} and (*C–D*) 300 µmol(photon) m^{-2} s^{-1}. *Different letters* for values of area under the curve represent statistically differences by repeated-measure *ANOVA* and *post hoc Newman-Keuls* test ($p<0.05$).

Table 1. Summary of some studies on the effect of irradiance on photosynthetic performance in red macroalgae. PAR – photosynthetically active radiation, Y(NPQ) – regulated non-photochemical quenching, I_K – saturation irradiance, ETR_{MAX} – maximum electron transport rate, α – photosynthetic efficiency.

Species	PAR [μmol(photon) m^{-2} s^{-1}]	Y(NPQ) [μmol(photon) m^{-2} s^{-1}]	I_K [μmol(photon) m^{-2} s^{-1}]	ETR_{MAX} [μmol(electron) m^{-2} s^{-1}]	α [μmol(photon) m^{-2} s^{-1}]	Reference
Porphyra leucosticta	50	0.06 ± 0.00	--	2.30 ± 0.00	--	Figueroa *et al.* (2003a)
	100	0.11 ± 0.01	--	4.10 ± 0.21	--	
	500	0.22 ± 0.01	--	13.20 ± 1.10	--	
	1000	0.36 ± 0.03	--	13.90 ± 1.30	--	
	2000	0.58 ± 0.04	--	20.70 ± 2.10	--	
Ahnfeltiopsis durvillaei	2000	--	138.60 ± 8.70	31.30 ± 3.70	0.22 ± 0.02	Gómez *et al.* (2004)
Callophyllis variegata	2000	--	81.90 ± 20.10	11.20 ± 2.30	0.14 ± 0.02	
Gelidium lingulatum	2000	--	335.60 ± 21.20	80.90 ± 10.40	0.34 ± 0.03	
Gracilaria chilensis	2000	--	182.80 ± 34.10	28.20 ± 4.60	0.15 ± 0.00	
Gracilaria dictyophora	2000	--	104.00 ± 35.50	21.20 ± 2.70	0.21 ± 0.04	
Gymnogongrus furcellatus	2000	--	117.70 ± 47.10	20.70 ± 11.30	0.16 ± 0.04	
Lebingia hookeri	2000	--	256.10 ± 25.60	33.80 ± 5.60	0.13 ± 0.03	
Mazzaella laminarioides	2000	--	237.20 ± 73.80	14.10 ± 2.30	0.06 ± 0.01	
Polysiphonia sp.	2000	--	237.40 ± 69.60	33.80 ± 8.70	0.14 ± 0.01	
Porphyra columbina (sun)	2000	--	136.50 ± 116.10	20.50 ± 7.60	0.20 ± 0.09	
Porphyra columbina (shade)	2000	--	179.90 ± 25.10	25.60 ± 2.60	0.14 ± 0.01	
Sarcothalia crispata	2000	--	181.70 ± 40.20	24.80 ± 5.60	0.13 ± 0.00	
Porphyra sp.	Spring (north – Chile)	0.60 ± 0.13	54.20 ± 18.10	1.70 ± 0.40	0.03 ± 0.01	Tala and Chow (2014)
	Spring (center – Chile)	0.58 ± 0.21	151.90 ± 54.50	5.70 ± 1.70	0.04 ± 0.01	
	Spring (south – Chile)	0.66 ± 0.22	151.00 ± 22.00	5.30 ± 0.80	0.04 ± 0.00	
Pterocladiella capillacea	60	0	122.17 ± 11.92	4.86 ± 0.28	0.04 ± 0.01	*Present study*
	300	0	95.90 ± 8.78	2.96 ± 0.07	0.03 ± 0.00	

control conditions [60 µmol(photon) m^{-2} s^{-1}] represented photostress conditions for *Gracilariopsis tenuifrons* (C.J. Bird & E.C. Oliveira) Fredericq & Hommersand (Serra 2013, Torres *et al.* 2014), since photoinhibition of photosynthesis and photodamage of photosynthetic pigments were registered.

Low values of F_V/F_M indicate that the algae are less tolerant to high radiation. Red algae usually have a lower F_V/F_M than that of green and brown macroalgae (Chaloub *et al.* 2010), as observed for *P. capillacea*. Low ETR curves at 300 µmol(photon) m^{-2} s^{-1} could be expected for a shade-adapted alga, then the capacity for transfer and transport electrons through the electron transport chain of the photosystem is adapted for reducing the transport rate to avoid photoxidative excessive energy and oxidative stress (Bautista and Necchi 2008).

Comparing the photosynthetic parameters of *P. capillacea* with published results for other rhodophytes on the effect of increasing PAR (Table 1), variable responses can be noted. In this compilation data, it is worth highlighting the results of $Y_{(NPQ)}$. In the present study, none of the irradiances used activated $Y_{(NPQ)}$, thus *P. capillacea* did not dissipate heat with energy expenditure. In contrast, Table 1 shows that *Porphyra* species under four increasing irradiances activated this defense mechanism.

Changes in accessory pigments are among the first evidence observed under excessive irradiance, in the case of red algae, these are phycobiliproteins and carotenoids (Schmidt *et al.* 2012). At high irradiance, these pigments regulate photosynthetic activity by efficiently dissipating excess energy through fluorescence (Del Campo *et al.* 2007, Heldt and Piechulla 2011). The antenna complexes

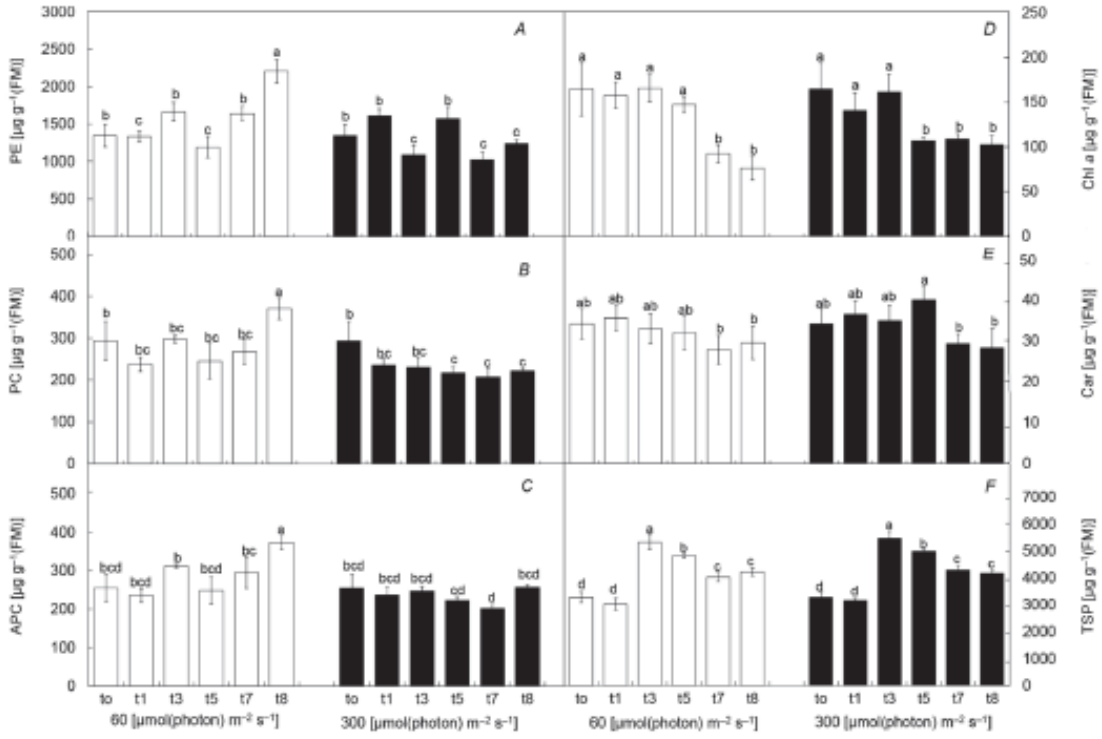

Fig. 4. Effect of 60 (*white bars*) and 300 (*black bars*) µmol(photon) m^{-2} s^{-1} on (*A*) PE – phycoerythrin, (*B*) PC – phycocyanin, (*C*) APC – allophycocyanin, (*D*) Chl *a* – chlorophyll *a*, (*E*) Car – carotenoids, and (*F*) TSP – total soluble proteins of *Pterocladiella capillacea* over the experimental time (mean ± SD, $n = 5$). *Different letters* represent statistically differences by repeated-measure *ANOVA* and *post hoc Newman-Keuls* test ($p<0.05$).

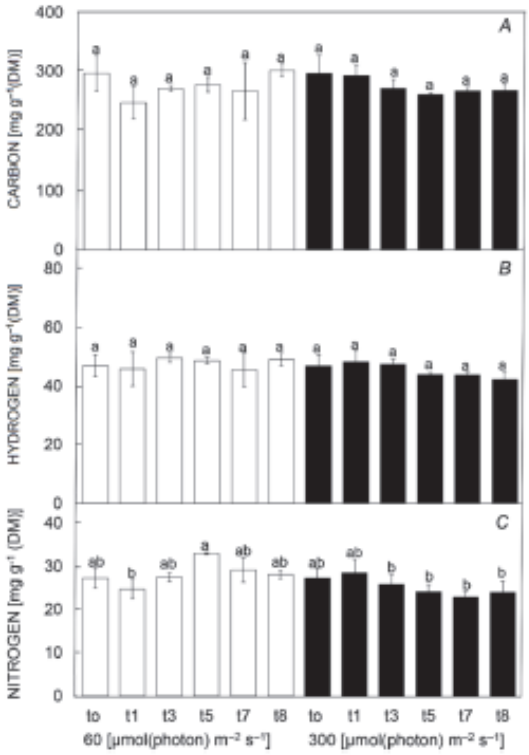

Fig. 5. Effect of 60 (*white bars*) and 300 (*black bars*) µmol(photon) m^{-2} s^{-1} on the cellular contents of (*A*) carbon, (*B*) hydrogen, and (*C*) nitrogen of *Pterocladiella capillacea* over the experimental time (mean ± SD, n = 5). *Different letters* represent statistically differences by repeated-measure *ANOVA* and *post hoc Newman-Keuls* test ($p<0.05$).

of PSI in red algae are composed of protein–pigment complexes intrinsic to the membranes. The pigments, which form this antenna complexes, are Chl *a* and Car, such as zeaxanthin and β-carotene (Gantt 1990).

Ursi *et al.* (2003) reported the existence of violaxanthin cycle in *Gracilaria birdiae* E.M. Plastino & E.C. Oliveira, but the existence of the xanthophyll cycles in Rhodophyta is still uncertain although several species show high concentrations of zeaxanthin (Goss and Jacob 2010). The diversity of mechanisms for photoaclimation and photoprotection in red algae are related to the types of Car present and acting as antioxidants and in the deactivation of reactive oxygen species, protecting the photosynthetic apparatus (Sampath-Wiley *et al.* 2008, Schubert *et al.* 2011).

Additionally, the arrangement of phycobiliproteins in the external membrane of the thylakoids facilitates the neutralization of reactive species that could damage the photosynthetic apparatus (Schubert and Mendoza-García 2008). When high irradiance exposure becomes potentially harmful, these pigments usually decline as a photoprotection mechanism, in order to reduce excessive harvesting of energy and to avoid the photoxidation of the D1 proteins in the photosystems (Adir *et al.* 2003). Photoacclimation processes by $Y_{(NO)}$ at moderate light seem to be adequate and efficient for *P. capillacea*, whereas minimal variations were observed in pigment concentrations. These results reinforce the hypothesis that the irradiance of 300 µmol(photon) m^{-2} s^{-1} was not a condition that caused photodamage to *P. capillacea*. Discoloration of the apical segments is a strong evidence for the pigment loss. However, this situation was not observed in *P. capillacea*. Under higher irradiances, 600 and 1,000 µmol(photon) m^{-2} s^{-1}, Torres *et al.* (2014) observed an acute and chronical effect on a pigment content for *G. tenuifrons*. The authors suggested that the decrease in the antenna complex is a strategy to reduce light absorption by the alga and thus avoid excessive photo-oxidation. Similar results at high irradiance were also registered for other red algae, *e.g.*, Levy and Gantt (1988) for *Porphyridium purpureum* (Bory de Saint-Vincent) K.M. Drew & R. Ross, Carnicas *et al.* (1999) for *Gracilaria tenuistipitata* C.F. Chang & B.M. Xia, Sudatti *et al.* (2011) for *L. dendroidea*, and Serra (2013) for *G. tenuifrons*.

Table 2. Summary of some studies under elevated photosynthetically active radiation (PAR) in red macroalgae showing GR – growth rate, PE – phycoerythrin, PC – phycocyanin, APC – allophycocyanin, Chl *a* – chlorophyll *a*, Car – carotenoids and TSP – total soluble proteins.

Species/PAR [μmol(photon) m^{-2} s^{-1}]	GR [% day^{-1}]	PE [μg g^{-1} (FM)]	PC [μg g^{-1} (FM)]	APC [μg g^{-1} (FM)]	Chl *a* [μg g^{-1} (FM)]	Car [μg g^{-1} (FM)]	TSP [μg g^{-1} (FM)]	Reference
Chondrus crispus								Yakovleva and Titlyanov (2001)
900 to 1800	--	--	--	--	Increased	Increased	--	
900 to 3600	--	--	--	--	Decreased	Increased	--	
Gracilariopsis tenuifrons							--	Torres *et al.* (2014)
60 to 600	Increased	--	--	--	Decreased	Decreased	--	
60 to 1000	Increased	--	--	--	Decreased	Decreased		
Gracilariopsis tenuifrons								Serra (2013)
60 to 600	Increased	Decreased	Decreased	Decreased	Decreased	Decreased	Decreased	
Gracilariopsis tenuifrons								Zubia *et al.* (2014)
100 to 1000	--	Constant	Constant	--	Constant	Increased	--	
Gracilaria temuistipitata								Carmeas *et al.* (1999)
40 to 500	--	Decreased	Decreased	Decreased	Decreased	--	--	
500 to 40	--	Increased	Increased	Increased	Increased	--	--	
Porphyra leucostica								Figueroa *et al.* (2003b)
50 to 100	Increased	--	--	--	Increased	--	--	
50 to 500	Increased	--	--	--	Decreased	--	--	
50 to 1000	Increased	--	--	--	Decreased	--	--	
50 to 2000	Increased	--	--	--	Decreased	--	--	
Pterocladiella capillacea								*Present study*
60 to 300	Increased	Decreased	Decreased	Constant	Decreased	Constant	Increased	

©Fungyi Chow / 2021

The differences observed for Chl *a* and TPS over time (a tendency of inverse relationship with decreasing Chl *a* from the third day and increasing TSP from the second day) may be also related to the imbalance in carbon/nitrogen metabolism. The nutritional and photosynthetic demands could be explained by the degradation and synthesis of these components, as an acclimation mechanism for dealing with variations of light intensity (Figueroa *et al.* 2009).

The reduction of the Chl *a* content can be interpreted as a defense mechanism to avoid overloading the photosynthetic system, which could result in the formation of reactive oxygen species. Then the carbon/nitrogen demand can require differential metabolic energy for photosynthetical performance and accumulation of carbon and nitrogen into organic molecules (Gordillo *et al.* 2001, Figueroa *et al.* 2014b). According to Huertas *et al.* (2000), in addition to irradiance, the availability of intracellular C and N is a key factor for growth, since these elements can contribute to processes of organic matter accumulation and increased productivity. For some photosynthetic organisms, an increasing demand for nutrients causes a starving-induced response, which induces a transient improvement of the metabolic response (Smit 2002, Figueroa *et al.* 2009).

The increase in TSP over time could be stimulated under moderate light intensity to improve the protein content, strengthen the GR, and improve the nutritional composition for a longer period of cultivation. In macroalgae, the TSP content seems to be directly related to nutrient availability and not necessarily to irradiance. Andria *et al.* (1999) observed that the content of TSP in *Gracilaria* sp. decreased when the species was cultivated at low N availability, while Collén *et al.* (2004) observed similar results with *G. tenuistipitata*. In contrast, the light green and brown lineages of the red macroalgae *Hypnea musciformis* (Wulfen) J.V. Lamouroux accumulated proteins under increased nitrate concentration (Martins *et al.* 2009). Thus, *P. capillacea* could be used as a target species for the accumulation of proteins, aiming to use these compounds as functional ingredients.

The results of GR, photosynthetic pigments, and TSP of *P. capillacea* were compared to those reported for other red algae under increasing PAR (Table 2). It is noted that red algae responses vary by light intensity or species. All the summarized studies showed increased GR under elevated irradiance, similar to that observed in this study for *P. capillacea* under moderate increasing light intensity, despite exhibiting different responses for photosynthetic pigments. All studies showed the decrease in PE, PC, and APC, when comparing a higher irradiance relative to lower light intensity, except for *G. tenuifrons* (Zubia *et al.* 2014) where PE, PC, and APC remained constant, similarly to that observed for *P. capillacea*. Data for Chl *a* and Car showed variable responses including decreasing, constant, and increasing contents. Opposite responses were also observed for TSP.

Summarizing all the analyzed descriptors and treatments over time, the results clearly showed the physiological sensitivity of *P. capillacea*, where the increase of irradiance at moderate level activated the acclimation responses without compromising or subchronical effect on photosynthetic performance, antenna complex, GR, and protein content. Oxidative stress and photodamage was not observed in *P. capillacea*, indicating efficient tolerance through $Y_{(NO)}$ energy dissipation. Additionally, the results presented here indicate the possibility of stimulating the GR and protein content of *P. capillacea* under moderately increasing light conditions. This response is interesting because it can represent an improved productivity of a cultivation system and the management in natural banks for functional natural products. However, higher light intensity for a shade alga can implicate unfavorable responses that may compromise GR, promoting photosynthetic photoinhibition and oxidative deleterious effects. *P. capillacea* has a phenology of major biomass production in colder seasons rather than in the summer. The photodamage and low photosynthesis recorded at high irradiance indicate that *P. capillacea* is an alga adapted to the shade conditions (Coutinho and Yoneshigue 1988, Lee and Shiu 2009).

Studies on acclimation, tolerance, and recovery responses are an important tool for basic knowledge of the biology of the species, as well as the implications on ecophysiological aspects as management, monitoring, environmental pollution, and global climate changes and considerations for biotechnological applications. Additionally, the understanding of the physiology and ecological responses of macroalgae to light energy is of fundamental importance to explain *in situ* physiological behavior and to predict ecological consequences in coastal ecosystems as a result of the increase in irradiance and UV radiation due to the reduction of the ozone layer. Finally, given the ability of *P. capillacea* to acclimate its photosynthetic performance to moderate irradiance, we suggest further studies on the physiology of the species with another abiotic factors, such as temperature and nutrient availability. This integration could contribute to complementary knowledge for a better understanding of important ecophysiological implications for the cultivation, sustainable exploitation, and management of *P. capillacea*, given the great economic and ecological importance of the species.

References

Adir N., Zer H., Shochat S. *et al.*: Photoinhibition: a historical perspective. – Photosynth. Res. **76**: 343-370, 2003.

Andria J.R., Vergara J.J., Perez-Llorens J.L.: Biochemical responses and photosynthetic performance of *Gracilaria* sp. (Rhodophyta) from Cádiz, Spain, cultured under different inorganic carbon and nitrogen levels. – Eur. J. Phycol. **34**: 497-504, 1999.

Asada K.: Mechanisms for scavenging reactive molecules generated in chloroplasts under light stress. – In: Baker N.R., Bowyer J.R. (ed.): Photoinhibition of Photosynthesis: From Molecular Mechanisms to the Field. Pp. 129-142. Bios. Sci. Publ., Oxford 1994.

Balboa E.M., Conde E., Moure A., *et al.*: *In vitro* antioxidant properties of crude extracts and compounds from brown algae. – Food Chem. **138**: 1764-1785, 2013.

Baurista A.I.N., Necchi O. Jr.: Photoacclimation in a tropical population of *Cladophora glomerata* (L.) Kützing 1843 (Chlorophyta) from southeastern. – Braz. J. Biol. **68**: 129-36, *2008*.

Beach K.S., Smith C.M., Okano R.: Experimental analysis of rhodophyte photoacclimation to PAR and UV-radiation using *in vivo* absorbance spectroscopy. – Bot. Mar. **43**: 525-536, 2000.

Betancor S., Tuya F., Gil-Díaz T. *et al.*: Effects of a submarine eruption on the performance of two brown seaweeds. – J. Sea Res. **87**: 68-78, 2014.

Bradford M.: A rapid sensitive method for the quantification of microgram quantities of protein utilizing the principle of protein-dye binding. – Anal. Biochem. **72**: 248-254, 1976.

Carnicas E., Jiménez C., Niell F.X.: Effects of changes of irradiance on the pigment composition of *Gracilaria tenuistipitata* var. *liui* Zhang et Xia. – J. Photoch. Photobio. B **50**: 149-158, 1999.

Chaloub R.M, Reinert F., Nassar C.A.G. *et al.*: Photosynthetic properties of three Brazilian seaweeds. – Rev. Bras. Bot. **33**: 371-374, 2010.

Cherry J.H., Nielsen B.L.: Metabolic engineering of chloroplasts for abiotic stress tolerance. – In: Daniell H., Chase C.D. (ed.): Molecular Biology and Biotechnology of Plant Organelles. Pp. 513-525. Springer, Dordrecht 2004.

Collén P.N., Camitz A., Hancock R.D. *et al.*: Effect of nutrient deprivation and resupply on metabolites and enzymes related to carbon allocation in *Gracilaria tenuistipitata* (Rhodophyta). – J. Phycol. **40**: 305-314, 2004.

Copertino M.S., Cheshire A., Watling J.: Photoinhibition and photoacclimation of turf algal communities on a temperate reef, after *in situ* transplantation experiments. – J. Phycol. **42**: 580-592, 2006.

Coutinho R., Yoneshigue Y.: Diurnal variation in photosynthesis vs. irradiance curves from "sun" and "shade" plants of *Pterocladia capillacea* (Gmelin) Bornet et Thuret (Gelidiaciaceae: Rhodophyta) from Cabo Frio, Rio De Janeiro, Brazil. – J. Exp. Mar. Biol. Ecol. **118**: 217-228, 1988.

Del Campo J.A., García-Gonzáles M., Guerrero M.G.: Outdoor cultivation of microalgae for carotenoid production: current states and perspectives. – Appl. Microbiol. Biotechnol. **74**: 1763-1774, 2007.

Donkor V.A., Häder D.P.: Effects of ultraviolet irradiation on photosynthetic pigments in some filamentous cyanobacteria. – Aquat. Microb. Ecol. **11**: 143-149, 1996.

dos Santos R.W., Schmidt É.C., Martins R.P. *et al.*: Effects of cadmium on growth, photosynthetic pigments, photosynthetic performance, biochemical parameters and structure of chloroplasts in the agarophyte *Gracilaria domingensis* (Rhodophyta, Gracilariales). – Am. J. Plant Sci. **3**: 1077-1084, 2012.

Edwards P.: Illustrated guide to the seaweeds and sea grasses in the vicinity of Porto Aransas, Texas. – In: Edwards P. (ed.): Seaweeds and Sea Grasses: Contributions in Marine Science, vol. 15. Pp. 132. B. J. Copeland, Texas 1970.

Falkowski P.G.: Light-shade adaptation in marine phytoplankton. – In: Falkowski P.G. (ed.): Primary Production in the Sea. Pp. 531. Plenum Press, New York 1980.

Figueroa F.L., Conde-Álvarez R., Gómez I.: Relations between electron transport rates determined by pulse amplitude modulated chlorophyll fluorescence and oxygen evolution in macroalgae under different light conditions. – Photosynth. Res. **75**: 259-275, 2003a.

Figueroa F.L., Escassi L., Perez-Rodríguez E. *et al.*: Effects of short-term irradiation on photoinhibition and accumulation of mycosporine-like amino acids in sun and shade species of the red algal genus *Porphyra*. – J. Photoch. Photobio. B. **69**: 21-30, 2003b.

Figueroa F.L., Martínez B., Israel A. *et al.*: Acclimation of red sea macroalgae to solar radiation: photosynthesis and thallus absorptance. – Aquat. Biol. **7**: 159-172, 2009.

Figueroa F.L., Domínguez-González B., Korbee N.: Vulnerability and acclimation to increased UVB radiation in three intertidal macroalgae of different morpho-functional groups. – Mar. Environ. Res. **97**: 30-38, 2014a.

Figueroa F.L, Barufi B.J., Malta E.J. *et al.*: Short-term effects of increased CO_2, nitrate and temperature on three Mediterranean macroalgae: photosynthesis and biochemical composition. – Aquat. Biol. **22**: 177-193, 2014b.

Franklin L.A., Larkum A.W.D.: Multiple strategies for a high light existence in a tropical marine macroalga. – Photosynth. Res. **53**: 149-159, 1997.

Franklin L.A., Osmond C.B., Larkym A.W.D.: Photoinhibition, UV-B and Algal Photosynthesis. Pp. 352-375. Kluwer Academic Publishers, Berlin 2003.

Gal-Or S., Israel A.: Growth responses of *Pterocladiella capillacea* (Rhodophyta) in laboratory and outdoor cultivation. – J. Appl. Phycol. **16**: 195-202, 2004.

Gantt E.: Pigmentation and photoacclimation. – In: Cole K.M., Sheath R.G. (ed.): Biology of the Red Algae. Pp. 203-219. Cambridge University Press, Cambridge 1990.

Gómez I., Huovinen P.: Morpho-functional patterns and zonation of South Chilean seaweeds: the importance of photosynthetic and bio-optical traits. – Mar. Ecol. Prog. Ser. **422**: 77-91, 2011.

Gómez I., López-Figueroa F., Ulloa N. *et al.*: Patterns of photosynthesis in 18 species of intertidal macroalgae from southern Chile. – Mar. Ecol. Prog. Ser. **270**: 103-116, 2004.

Gordillo F.J.L, Jiménez C., Goutx M. *et al.*: Effects of CO_2 and nitrogen supply on the biochemical composition of *Ulva rigida* with especial emphasis on lipid class analysis. – J. Plant Physiol. **158**: 367-373, 2001.

Goss R., Jacob T.: Regulation and function of xanthophyll cycle-dependent photoprotection in algae. – Photosynth. Res. **106**: 103-122, 2010.

Grobbelaar J.U., Kurano N.: Use of photoacclimation in the design of a novel photobioreactor to achieve high yields in algal mass cultivation. – J. Appl. Phycol. **15**: 121-126, 2003.

Grzymski J., Johnsen G., Sakshaug E.: The significance of intra-

cellular self-shading on the bio-optical properties of brown, red and green macroalgae. – J. Appl. Phycol. **33**: 408-414, 1997.
Guimarães S.M.P.B.: A revised checklist of benthic marine Rhodophyta from the state of Espírito Santo, Brazil. – Bol. Inst. Bot. **17**: 143-194, 2006.
Hanelt D., Figueroa F.L.: Physiological and photomorphogenic effects of light on marine macrophytes. – In: Wiencke C., Bischof K. (ed.): Seaweed Biology: Novel Insights into Ecophysiology, Ecology and Utilization, Vol. 219. Pp. 3-23. Springer, Heidelberg 2012.
Hanelt D., Hawes I., Rae R.: Reduction of UV-B radiation causes an enhancement of photoinhibition in high light stressed aquatic plants from New Zealand lakes. – J. Photoch. Photobio. B **84**: 89-102, 2006.
He L.H., Wu M., Qian P.Y. *et al.*: Effects of co-culture and salinity on the growth and agar yield of *Gracilaria tenuistipitata* var. *liui* Zhang et Xia. – Chin. J. Oceanol. Limnol. **20**: 365-370, 2002.
Heldt H-W., Piechulla B.: Plant Biochemistry, 4th ed. Pp. 618. Elsevier, Burlington 2011.
Hideg E., Spetea C., Vass I.: Singlet oxygen and free-radical production during acceptor-induced and donor-side-induced photoinhibition: studies with spin-trapping EPR spectroscopy. – BBA-Bioenergenetics **1186**: 143-152, 1994.
Hou X., Hou H.J.: Roles of manganese in photosystem II dynamics to irradiations and temperatures. – Front Biol. **8**: 312-322, 2013.
Huertas E., Montero O., Lubián L.M.: Effects of dissolved inorganic carbon availability on growth, nutrient uptake and chlorophyll fluorescence of two species of marine microalgae. – Aquacult. Eng. **22**: 181-197, 2000.
Jassby A.D., Platt T.: Mathematical formulation of the relationship between photosynthesis and light for phytoplankton. – Limnol. Oceanogr. **21**: 540-547, 1976.
Klughammer C., Schreiber U.: Complementary PSII quantum yields calculated from simple fluorescence parameters measured by PAM fluorometry and the saturation pulse method. – PAM Appl. Notes. **1**: 27-35, 2008.
Kursar T.A., van der Meer J., Alberte R.S.: Light-harvesting system of the red alga *Gracilaria tikvahiae*. I. Biochemical analyses of pigments mutation. – Plant Physiol. **73**: 353-360, 1983.
Lee T.M., Shiu C.T.: Implications of mycosporine-like amino acid and antioxidant defences in UV-B radiation tolerance for the algae species *Pterocladiella capillacea* and *Gelidium amansii*. – Mar. Environ. Res. **67**: 8-16, 2009.
Levy I., Gantt E.: Light acclimation in *Porphyridium purpureum* (Rhodophyta): growth, photosynthesis, and phycobilisomes. – J. Appl. Phycol. **24**: 452-458, 1988.
Lichtenthaler H.K., Buschmann C.: Chlorophylls and carotenoids: measurement and characterization by UV-VIS spectroscopy. – In: Wrolstad R.E., Acree T.E., An H. *et al.* (ed.): Current Protocols in Food Analytical Chemistry. Pp. F4.3.1-F4.3.8. John Wiley & Sons, New York 2001.
Liu F., Pang S.J.: Stress tolerance and antioxidant enzymatic activities in the metabolisms of the reactive oxygen species in two intertidal red algae *Grateloupia turuturu* and *Palmaria palmata*. – J. Exp. Mar. Biol. Ecol. **382**: 82-87, 2010.
MacIntyre H.L., Kana T.M., Geider R.J.: The effect of water motion on short-term rates of photosynthesis by marine phytoplankton. – Trends Plant Sci. **5**: 12-17, 2000.
Martínez B., Rico J.: Changes in nutrient content of *Palmaria palmata* in response to changes in nutrient to variable light and upwelling in northern Spain. – J. Phycol. **44**: 50-59, 2008.
Martins A.P., Chow F., Yokoya N.S.: [*In vitro* assay of nitrate reductase enzyme and effect of nitrate and phosphate availability in colour strains of *Hypnea musciformis* (Wulfen) J. V. Lamour. E. (Gigartinales, Rhodophyta)]. – Rev. Bras. Bot. **32**: 635-645, 2009. [In Portuguese]
Martone P. T., Alyono M., Stites S.: Bleaching of an intertidal coralline alga: untangling the effects of light, temperature and desiccation. – Mar. Ecol. Prog. Ser. **416**: 57-67, 2010.
Maxwell K., Johnson G.N.: Chlorophyll fluorescence: a practical guide. – J. Exp. Bot. **51**: 659-668, 2000.
Mercado J.M., Jiménez C., Niell F.X. *et al.*: Comparison of methods for measuring light absorption by algae and their application to the estimation of package effect. – Sci. Mar. **60**: 39-45, 1996.
Nascimento E.F.I., Rosso S.: [Fauna associated with benthic marine macroalgae (Rhodophyta and Phaeophyta) from São Sebastião, São Paulo]. – Rev. Bras. Ecol. **11**: 38-52, 2007. [In Portuguese]
Necchi O. Jr.: Light-related photosynthetic characteristic of freshwater Rhodophyta. – Aquat. Bot. **82**: 193-20, 2005.
Nishihara G.N., Terada R., Noro T.: Effect of temperature and irradiance on the uptake of ammonium and nitrate by *Laurencia brongniartii* (Rhodophyta, Ceramiales). – J. Appl. Phycol. **17**: 371-377, 2005.
Nishiyama Y., Allakhverdiev S., Yamamoto H. *et al.*: Singlet oxygen inhibits the repair of photosystem II by suppressing translation elongation of the D1 protein in *Synechocystis* sp. – Biochemistry **43**: 11321-11330, 2004.
Nyvall-Cóllen P., Camitz A., Hancock R.D. *et al.*: Effect of nutrient deprivation and resupply on metabolites and enzymes related to carbon allocation in *Gracilaria tenuistipitata* (Rhodophyta). – J. Appl. Phycol. **40**: 305-314, 2004.
Oliveira E.C., Saito R.M., Neto J.F.S. *et al.*: Temporal and spatial variation in agar from a population of *Pterocladia capillacea* (Gelidiales, Rhodophyta) from Brazil. – Hydrobiologia **326**: 501-504, 1996.
Park J.J., Han T., Choi E.M.: Differences in the oxidative stress and antioxidant responses of three marine macroalgal species upon UV exposure. – Toxicol. Environ. Health Sci. **8**: 101-107, 2016.
Penniman C.A., Mathieson A.C., Penniman C.E.: Reproductive phenology and growth of *Gracilaria tikvahiae* McLachlan (Gigartinales, Rhodophyta) in the Great Bay Estuary, New Hampshire. – Bot. Mar. **29**: 147-154, 1986.
Polo L.K., Felix M.R.L., Kreusch M. *et al.*: Metabolic profile of the brown macroalga *Sargassum cymosum* (Phaeophyceae, Fucales) under laboratory UV radiation and salinity conditions. – J. Appl. Phycol. **90**: 560-571, 2014.
Ramus J., Rosenberg G.: Diurnal photosynthetic performance of seaweeds measured under natural conditions. – Mar. Biol. **56**: 21-28, 1980.
Roháček K.: Chlorophyll fluorescence parameters: the definitions, photosynthetic meaning, and mutual relationships. – Photosynth. Res. **40**: 13-29, 2002.
Sampath-Wiley P., Neefus C., Jahnke L.: Seasonal effects of sun exposure and emersion on intertidal seaweed physiology: fluctuations in antioxidant contents, photosynthetic pigments and photosynthetic efficiency in the red alga *Porphyra umbilicalis* Kützing (Rhodophyta, Bangiales). – J. Exp. Mar. Biol. Ecol. **361**: 83-91, 2008.
Schmidt E.C., Pereira B., Pontes C.L.: Alterations in architecture and metabolism induced by ultraviolet radiation-B in the

carragenophyte *Chondracanthus teedei* Rhodophyta, Gigartinales. – Protoplasma **249**: 353-367, 2012.
Schreiber U., Schliwa U., Bilger W.: Continuous recording of photochemical and non-photochemical chlorophyll fluorescence quenching with a new type of modulation fluorometer. – Photosynth. Res. **10**: 51-62, 1986.
Schreiber U., Neubauer C.: O_2-dependent electron flow, membrane energization and the mechanism of non-photochemical quenching of chlorophyll fluorescence. – Photosynth. Res. **25**: 279-293, 1990.
Schubert N., García-Mendoza E.: Photoinhibition in red algal species with different carotenoid profiles. – J. Phycol. **44**: 1437-1446, 2008.
Schubert N., García-Mendoza E., Enríquez S.: Is the photoacclimation response of Rhodophyta conditioned by the species carotenoid profile? – Limnol. Oceanogr. **56**: 2347-2361, 2011.
Serra D.R.: [*Gracilariopsis temuifrons* (Gracilariales – Rhodophyta) Response to Irradiance Stimuli *in vitro*]. – Masters Dissertation. Pp. 97. Institute of Bioscience, University of São Paulo, São Paulo 2013. [In Portuguese]
Sudatti D.B., Fujii M.T., Rodrigues S.V.: Effects of abiotic factors on growth and chemical defenses in cultivated clones of *Laurencia dendroidea* J. Agardh (Ceramiales, Rhodophyta). – Mar. Biol. **158**: 1439-1446, 2011.
Smit A.J.: Nitrogen uptake by *Gracilaria gracilis* (Rhodophyta): adaptations to a temporally variable nitrogen environment. – Bot. Mar. **45**: 196-209, 2002.
Takahashi S., Badger M.R.: Photoprotection in plants: a new light on photosystem II damage. – Trends Plant Sci. **16**: 53-60, 2011.
Takahashi S., Murata N.: How do environmental stress accelerate photoinhibition? – Trends Plant Sci. **3**: 178-182, 2008.
Tala F., Chow F.: Phenology and photosynthetic performance of *Porphyra* spp. (Bangiophyceae, Rhodophyta): seasonal and latitudinal variation in Chile. – Aquat. Bot. **113**: 107-116, 2014.
Torres P.B., Chow F., Santos D.Y.A.C.: Growth and photosynthetic pigments of *Gracilariopsis temuifrons* (Rhodophyta, Gracilariaceae) under high light *in vitro* culture. – J. Appl. Phycol. **27**: 1243-1251, 2014.
Ursi S., Plastino E.M.: [Growth of reddish and light green strains of *Gracilaria* sp. (Gracilariales, Rhodophyta) in two culture media: analysis of different reproductive phases]. – Rev. Bras. Bot. **24**: 587-594, 2001. [In Portuguese]
Ursi S., Pedersén M., Plastino E. *et al.*: Intraspecific variation of photosynthesis, respiration and photoprotective carotenoids in *Gracilaria birdiae* (Gracilariales: Rhodophyta). – Mar. Biol. **142**: 997-1007, 2003.
Wanderley A.: [Effect of Nitrate Availability on Growth, Nitrate Reductase Activity, Chemical Composition and Nitrate and Phosphate Uptake in *Gracilariopsis temuifrons* (Gracilariales, Rhodophyta)]. – Masters Dissertation. Pp. 140. Institute of Bioscience, University of São Paulo, São Paulo, 2009. [In Portuguese]
Yakovleva I.M., Titlyanov E.A.: Effect of high visible and UV irradiance on subtidal *Chondrus crispus*: stress photoinhibition and protective mechanisms. – Aquat. Bot. **71**: 47-61, 2001.
Zubia M., Freile-Pelegrín Y., Robledo D.: Photosynthesis, pigment composition and antioxidant defences in the red alga *Gracilariopsis temuifrons* (Gracilariales, Rhodophyta) under environmental stress. – J. Phycol. **26**: 2001-2010, 2014.

ANEXO 4

Photochemistry and Photobiology, 2014, 90: 560–573

Photoacclimation Responses of the Brown Macroalga *Sargassum Cymosum* to the Combined Influence of UV Radiation and Salinity: Cytochemical and Ultrastructural Organization and Photosynthetic Performance

Luz K. Polo[1], Marthiellen R. de L. Felix[1], Marianne Kreusch[2], Debora T. Pereira[2], Giulia B. Costa[2], Carmen Simioni[1], Luciane C. Ouriques[1], Fungyi Chow[3], Fernanda Ramlov[4], Marcelo Maraschin[4], Zenilda L. Bouzon[5] and Éder C. Schmidt*[6]

[1]Plant Cell Biology Laboratory, Department of Cell Biology, Embryology and Genetics, Federal University of Santa Catarina, Florianópolis, SC, Brazil
[2]Scientific Initiation-PIBIC-CNPq, Department of Cell Biology, Embryology and Genetics, Federal University of Santa Catarina, Florianópolis, SC, Brazil
[3]Institute of Bioscience, Department of Botany, University of São Paulo, São Paulo, SP, Brazil
[4]Plant Morphogenesis and Biochemistry Laboratory, Federal University of Santa Catarina, Florianópolis, SC, Brazil
[5]Central Laboratory of Electron Microscopy, Federal University of Santa Catarina, Florianópolis, SC, Brazil
[6]Postdoctoral Research of Postgraduate Program in Cell Biology and Development, Department of Cell Biology, Embryology and Genetics, Federal University of Santa Catarina, Florianópolis, SC, Brazil

Received 18 September 2013, accepted 3 December 2013, DOI: 10.1111/php.12224

ABSTRACT

The photoacclimation responses of the brown macroalga *Sargassum cymosum* were studied to determine its cytochemical and ultrastructural organization, as well as photosynthetic pigments and performance. *S. cymosum* was cultivated in three salinities (30, 35 and 40 psu) under four irradiation treatments: PAR-only, PAR + UVA, PAR + UVB and PAR + UVA + UVB. Plants were exposed to PAR at 70 µmol photons m^{-2} s^{-1}, PAR + UVB at 0.35 W m^{-2} and PAR + UVA at 0.70 W m^{-2} for 3 h per day during 7 days *in vitro*. Growth rate was not significantly affected by any type of radiation or salinity. The amount of pigments in *S. cymosum* was significantly influenced by the interaction of salinity and radiation treatments. Compared with PAR-only, UVR treatments modified the kinetics patterns of the photosynthesis/irradiance curve. After exposure to UVR, *S. cymosum* increased cell wall thickness and the presence of phenolic compounds. The number of mitochondria increased, whereas the number of chloroplasts showed few changes. Although *S. cymosum* showed insensitivity to changes in salinity, it can be concluded that samples treated under four irradiation regimes showed structural changes, which were more evident, but not severe, under PAR + UVB treatment.

INTRODUCTION

Solar radiation that reaches the Earth's surface mainly consists of ultraviolet radiation (UVR), photosynthetically active radiation (PAR) and infrared radiation (IR) (1) UVR includes a group of electromagnetic irradiation spectra with wave lengths shorter (150–400 nm) than the visible spectrum (400–700 nm). This radiation is subdivided into three different spectral regions: UVA (400–315 nm), UVB (315–280 nm) and UVC (280–100 nm). UVA radiation (UVAR) is closest to the visible spectrum, and it is not absorbed by ozone (O_3). UVB radiation (UVBR) is not completely absorbed by O_3, and it is harmful to living organisms and can lead to DNA damage. UVC radiation (UVCR) is extremely harmful, but it is completely absorbed by O_3 (2). Because UVR penetrates to ecologically significant depths in aquatic systems, it can negatively influence aquatic organisms from major primary producers to all consumers in the food chain (3).

The harmful effects of UV radiation in organisms, would be caused mainly by UVB rays and the UVA radiation that reaches earth's surface in higher quantity than UVB would contribute in the repair process of harmful effects caused by UVB (4) and many of these are caused when the rays are absorbed by the nucleic acids and proteins causing photooxidation and changes in these molecules that could lead to changes in essential metabolic process like transcription, duplication and translation of DNA (5,6). Moreover, the cellular biology and physiology (16), process like photosynthesis and growth in plants (7), nitrate absorption in diatoms (8), protists locomotion (3) and growth in macroalgae (9).

The fluctuation in salinity in marine environments is another factor that can have a deleterious effect on aquatic organisms. The Intergovernmental Panel on Climate Change (IPCC), reports have demonstrated that changes in precipitation have occurred (10). In South America, these changes include an increase in rainfall in southeast Brazil, Paraguay, Uruguay, the Argentinean Pampas and some parts of Bolivia (10). Such rainfall increases in coastal areas and drainage basins can lead to higher freshwater volumes seaward, and decreasing salinity can appear along the coast (11). Changes in salinity can drive ecological alterations in seaweed communities as different levels of salinity determine richness and distribution (12–14). Many physiological process of

*Corresponding author email: edcash@ccb.ufsc.br (É.C. Schmidt)
© 2013 The American Society of Photobiology

brown seaweeds can be affected by salinity variation, in *Sargassum muticum* was reported changes in reproduction patterns (15–17), in *Laminaria digitata, Fucus vesiculosus, Fucus serratus* were observed alterations on growth rates (18). Other aspects such as contents of phenolic compounds of *Fucus ceranoids* (19) and mannitol content of *F. serratus* and *F. vesiculosus* (20,21) were reported.

Macroalgae are major biomass producers on rocky shores and continental shelves. Macroalgal canopies form habitats for many species of larval fish, crustaceans and other marine organisms. In macroalgae, photobiological studies indicate diverse physiological alterations in response to UVR that include pigment degradation, dynamic or chronic photoinhibition of photosynthesis and DNA damage (reviews in 22,23). Alterations in the cellular organization and ultrastructure of macroalgae exposed to UVBR have also been reported (24–35). These changes mainly occur in the chloroplasts, modifying the quantity, size, organization, as well as the number of thylakoids (29). Studies evidence that macroalgae utilize photoprotection mechanisms against excessive radiation. One possible mechanism for reducing UV damage is the production of compounds capable of absorbing UVR. For example, in red algae, the presence of mycosporine-like amino acids (MAAs) was confirmed, whereas in brown algae, a UV-absorbing property has been related to phenolic compounds like phlorotatins as the most cited compound. (28,36–38).

Until now, much less has been known about the effect of UVR and salinity on brown macroalgae (39–41), and this kind of studies in Brazil is rare. The genus *Sargassum* is a brown macroalga widely distributed along the Brazilian coast, and it has ecological importance for the coastal ecosystem, particularly in communities of rocky shores that provide habitat and refuge for a large number of marine invertebrate juveniles. Some species are considered economically important because they produce chemical compounds with potential biotechnological applications. *Sargassum* is mostly found along rocky shores, partially exposed during low tides but there is some degree of self-shading that brings protection against high UVR flux. Some studies have reported on the effects of UV on macroalgal photosynthetic performance, but only a few data exist on other physiological processes (42) Therefore, this study aimed to expand the knowledge of the possible biological effects of UVR (PAR + UVA, PAR + UVB, PAR + UVA + UVB) and salinity (30, 35 and 40 psu) on the cellular organization and physiological responses of *Sargassum cymosum* by examining photoacclimation performance and photoprotection.

MATERIALS AND METHODS

Algal material and culture conditions. Several individuals of *Sargassum cymosum* were collected at Armação Beach, Ponta das Campanhas (27°44′ 42″S and 48°30′27″W), Florianopolis-SC, Brazil, in November, December, January and February 2012 during the southern summer season. The algal samples were collected from the rocky shores and transported at ambient temperature in dark containers to LABCEV-UFSC (Plant Cell Laboratory, Federal University of Santa Catarina, Florianopolis, Santa Catarina, Brazil). Macroepiphytes were meticulously eliminated by cleaning with a brush and washed with filtered seawater. Apical portions of approximately 6 cm were acclimated for 7 days in culture medium with filtered seawater plus von Stosch (VSES) enrichment solution at half strength (VSES/2; (43) and laboratory controlled conditions of 24 ± 2°C, continuous aeration, illumination from above with fluorescent lamps (Philips C-5 Super 84 16W/840, Brazil), PAR at 70 ± 10 μmol photons m^{-2} s^{-1} (Li-cor light meter 250, USA) and 12 h photocycle (starting at 8 am).

For experiments, apical thallus portions (±2.0 g) from the acclimated *S. cymosum* samples were selected and cultivated for 7 days in beakers containing 500 mL of natural sterilized seawater and VSES/2 at salinities of 30, 35 (control) and 40 psu under four different conditions of radiation: PAR-only (control), PAR + UVA, PAR + UVB and PAR + UVA + UVB. Total dose of PAR, UVA and UVB irradiance was 657.40, 7.56, 3.78 kJ^{-2}, respectively. Then, 12 treatments were performed and four replicates were made for each experimental group. Culture conditions were the same as those described for the acclimation period. Low salinities were obtained with the addition of distilled water, whereas high salinities were obtained through gradual freezing and thawing seawater until the final concentration was reached.

Ultraviolet radiation was provided through a Vilber Lourmat lamp (VL-6LM, Marne La Vallée, France) with peak output at 312 nm for UVBR and peak output at 365 nm for UVAR. The intensity was 0.35 W m^{-2} for UVBR and 0.70 W m^{-2} for UVAR (Radiometer Model IL 1400A, International Light, Newburyport, MA, USA). To avoid exposure to UVCR, a cellulose diacetate foil 0.075 mm thick was used.

Growth rates (GRs). Growth rates were calculated using the following equation: GR [% day^{-1}] = $[(W_f/W_i) - 1] \times 100/t$, where W_i = initial wet mass, W_f = wet mass after 7 days and t = time in days (44).

Pigment analysis. Photosynthetic pigments (chlorophylls *a* and *c*; Chl *a* and Chl *c*) of *S. cymosum* were analyzed from fresh frozen samples ($n = 4$) kept at −40°C until ready for use. Chlorophylls were extracted from approximately 225 mg fresh weight (FW) in 3 mL of pure acetone P.A. (Sigma-Aldrich, St. Louis, MO, USA) for 10 min in ice and light protected. Then, the extracts were centrifuged for 5 min at 1990 *g*, and the pigments were quantified spectrophotometrically (Hitachi, Model 100-20; (Hitachi Co., Japan). Pigment concentrations were calculated according to (45).

Carotenoids were extracted by exhaustive extraction from 1.0 g FW samples ($n = 4$) in 10 mL of pure methanol (Sigma-Aldrich, St. Louis, MO, USA). The methanolic crude extracts were evaporated to concentrate the extracts. The specific absorbance was determined with a Tecan microplate spectrophotometer (Infinite® M200 PRO, Männedorf, Switzerland) at 450 nm. Total carotenoid concentrations were calculated based on β-carotene standard curve (1–300 μg mL^{-1}; $y = 0.00365\times$; $r^2 = 0.999$).

Phenolic compounds. The analysis of phenolic compounds was made using the spectrophotometric method of Folin-Ciocalteau based on (46). This method allows to identify different phenolic compounds like total phenols and hydrolyzable tannins in Phaeophyceae. Phenolic compounds were extracted from 400 mg FW samples ($n = 4$) using 4 mL 80% aqueous methanol. The extracts were centrifuged for 10 min at 750 *g*. Aliquots of 50 mL of supernatant crude extracts were added to 180 mL of distilled water, 10 mL of Folin and 30 mL of sodium carbonate 20% *w/v* concentrated solution and incubated at room temperature for 1 h. The reaction mixture absorbance was measured at 750 nm using a microplate spectrophotometer (Tp Reader; Thermoplate, Nanshan District, Shenzhen, China). Fluoroglucinol was used as standard at concentrations from 5 to 35 μg mL^{-1} ($y = 0.0575\times$; $r^2 = 0.999$). All measurements were performed in triplicate. Phenolic compounds extruded by the algae to the seawater culture medium were also evaluated by measuring the spectrum of absorbance (300–700 nm) of filtered seawater culture medium of each treatment.

DPPH radical-scavenging capacity. To determine radical-scavenging ability, the method reported by (47) was used. Briefly, 2.9 mL of 0.1 mM 2,2-diphenyl-1-picrylhydrazyl (DPPH) solution in 80% aqueous methanol (Sigma-Aldrich, St. Louis, MO, USA) was added to an aliquot of phenolic compounds extracts (0.1 mL) and incubated for 30 min. The absorbance of the antioxidant reaction was measured at 517 nm using a microplate spectrophotometer (TP Reader NM, Thermoplate). The inhibition percentage (%) was determined using the following formula: Inhibition (%) = (Abs Control − Abs Sample)/Abs Control) × 100%, where Abs Control is the absorbance of DPPH control and Abs Sample is the absorbance with treated samples. The synthetic antioxidant *tert*-butyl hydroxytoluene was used as positive control. All determinations were performed in triplicate.

Light microscopy (LM). Samples approximately 5 mm in length were fixed in 2.5% paraformaldehyde in 0.1 M (pH 7.2) phosphate buffer overnight following the description in (29). Subsequently, the samples were dehydrated in increasing series of aqueous ethanol solutions and infiltrated with Historesin (Leica Historesin, Heidelberg, Germany). Then, sections of 5 μm in length were stained with 0.5% Toluidine Blue

(TB-O), pH 3.0 (Merck Darmstadt, Germany), as described in (30), and investigated with an Epifluorescent microscope (Olympus BX 41) equipped with Image Q Capture Pro 5.1 Software (Qimaging Corporation, Austin, TX, USA). Similarities based on the comparison of individual treatments with replicates suggested that the LM analyses were reliable.

Transmission electron microscopy (TEM). Samples approximately 5 mm in length were fixed with 2.5% glutaraldehyde, 2.0% paraformaldehyde, and 5 mM $CaCl_2$ in 0.075 M sodium cacodylate buffer (pH 7.2) plus 0.2 M sucrose and caffeine 1% overnight (48). The material was postfixed with 1% osmium tetroxide for 4 h, dehydrated in a graded acetone series and embedded in Spurr's resin. Thin sections were stained with aqueous uranyl acetate followed by lead citrate. Four replicates were made for each experimental group; two samples per replication were then examined under TEM JEM 1011 (JEOL Ltd., Tokyo, Japan, at 80 kV). Similarities based on the comparison of individual treatments with replicates suggested that the ultrastructural analyses were reliable.

In vivo fluorescence of chlorophyll *a*. Photosynthetic performance was estimated as *in vivo* fluorescence of chlorophyll *a* of photosystem II (PSII) using a portable pulse modulation fluorometer (PAM-2500, Walz, Germany). Maximum quantum yield (F_v/F_m) was measured adapting the seaweeds to 10 min darkness and calculated following (49). Effective quantum yield (Y[II]) was measured from light-adapted seaweeds and calculated following (50). Electron transport rate (ETR) was estimated through photosynthesis–irradiance (*P–I*) curves, irradiating thalli with seven increasing actinic irradiance intensities of PAR (E; 0, 24, 61, 108, 236, 456 and 752 µmol photon m^{-2} s^{-1}) provided by the PAM device and calculated as ETR = Y(II) × *E* × *A* × 0.8, where *A* is thallus absorbance and 0.8 is the fraction of chlorophyll *a* associated with PSII (51,52). Absorbance was determined by placing the algae on a PAR sensor (LI-COR Quantum LI-1000, USA) and then measuring with a light PAR meter (LI-COR LI-250, USA). Light transmission was calculated as $A = 1 - (E_t/E_o)$, where E_t is the irradiance below the alga (transmitted light) and E_o is the initial irradiance. The following parameters were determined from *P–I* curves: (1) photosynthetic ETR as maximum electron transport rate (ETRmax, maximal ETR at saturating irradiance), (2) photosynthetic efficiency (α, initial slope of *P–I* curve that indicates the efficiency of the electron transport), (3) light saturation (Ik, light intensity approximating onset of photosynthetic saturation) and (4) photoinhibition (*β*, initial slope of *P–I* curve at the end of the saturation phase) by fitting the *P–I* curves to a hyperbolic tangent model with photoinhibition parameter of (53). Four sample replicates were used to estimate each parameter. This process was also made after recovery treatment, where samples were incubated in culture medium with filtered seawater plus von Stosch (VSES) enrichment solution at half strength (VSES/2; and laboratory controlled conditions of 24 ± 2°C, continuous aeration, illumination from above with fluorescent lamps (Philips C-5 Super 84 16W/840, Brazil), PAR at 70 ± 10 µmol photons m^{-2} s^{-1} (Li-cor light meter 250, USA) and 12 h photocycle after 7 days of exposure to UVR and different salinities.

Data analysis. Data were analyzed by bifactorial Analysis of Variance (ANOVA), considering radiation exposure and salinity level as independent variables, and the Tukey's a posteriori test. Individual one-way ANOVAs were also performed to evaluate the isolated effects of salinity or radiation and then compared by Tukey's a posteriori test. All statistical analyses were performed using the Statistica software package (Release 10.0), considering $P \leq 0.05$.

RESULTS

Growth rates (GRs)

After 7 days of cultivation with different radiation and salinity treatments, *S. cymosum*, as analyzed by bifactorial ANOVA, showed statistical differences between GRs (Fig. 1) with notable increase in GRs under all UVR treatments at 30 psu relative to PAR-only control. Furthermore, plants treated at 30 psu and PAR-only showed lower GR than any UVR treatment. *Sargassum cymosum* analyzed by one-way ANOVA for radiation or salinity level separately showed statistical differences between GRs. Table 1 shows differences between plants treated at different radiations under the same salinity (lowercase letters) and between different salinities under the same radiation (uppercase letters). When the isolated effect of radiation treatments on *S. cymosum* was analyzed at 30 psu, the plants showed significant increase in GRs under PAR + UVB and PAR + UVA + UVB (lowercase letters). No radiation effects were observed at 35 and 40 psu. When the isolated effect of salinity treatments on *S. cymosum* was analyzed, plants under PAR-only or PAR + UVA showed significant decrease in GRs at 30 psu (Fig. 1).

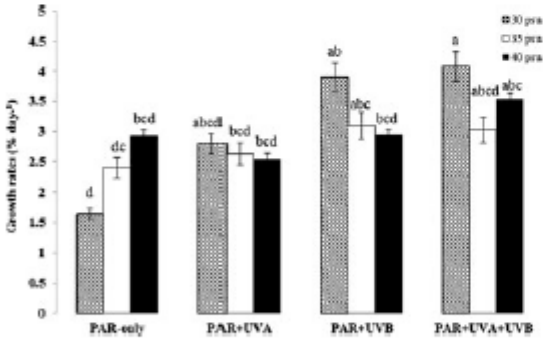

Figure 1. Growth rates (GRs) of *S. cymosum* plants after 7 days of exposure to radiation and salinity treatments ($n = 4$, mean ± SD). Letters indicate significant differences according to bifactorial ANOVA and Tukey's test ($P \leq 0.05$).

Pigments and total phenolic compounds

The amount of photosynthetic pigments in *S. cymosum* was significantly influenced by the interaction of salinity and radiation treatments (Fig. 2A–C). Although chlorophyll *a* showed the largest reduction in plants treated at 30 psu (Fig. 2A), it was significantly increased in plants at 35 or 40 psu when compared with

Table 1. Growth rates (GRs;% day^{-1}) of *S. cymosum* plants after 7 days of exposure to radiation and salinity treatments ($n = 4$, mean ± SD).

	Treatments			
	PAR-only	PAR + UVA	PAR + UVB	PAR + UVA + UVB
30 psu	1.65 ± 0.97**bA**	2.10 ± 0.88**bA**	3.90 ± 1.15**aA**	4.10 ± 1.00**aA**
35 psu	2.40 ± 0.74**aA**	2.65 ± 0.76**aA**	3.10 ± 0.97**aA**	3.05 ± 0.97**aA**
40 psu	2.90 ± 0.89**aA**	2.55 ± 0.92**aA**	2.95 ± 0.88**aB**	3.55 ± 0.87**aA**

Lowercase letters indicate significant differences between radiation treatments at individual salinity treatment according to one-way ANOVA and Tukey's test ($P \leq 0.05$). Uppercase letters indicate significant differences between salinity levels at individual radiation treatment according to one-way ANOVA and Tukey's test ($P \leq 0.05$).

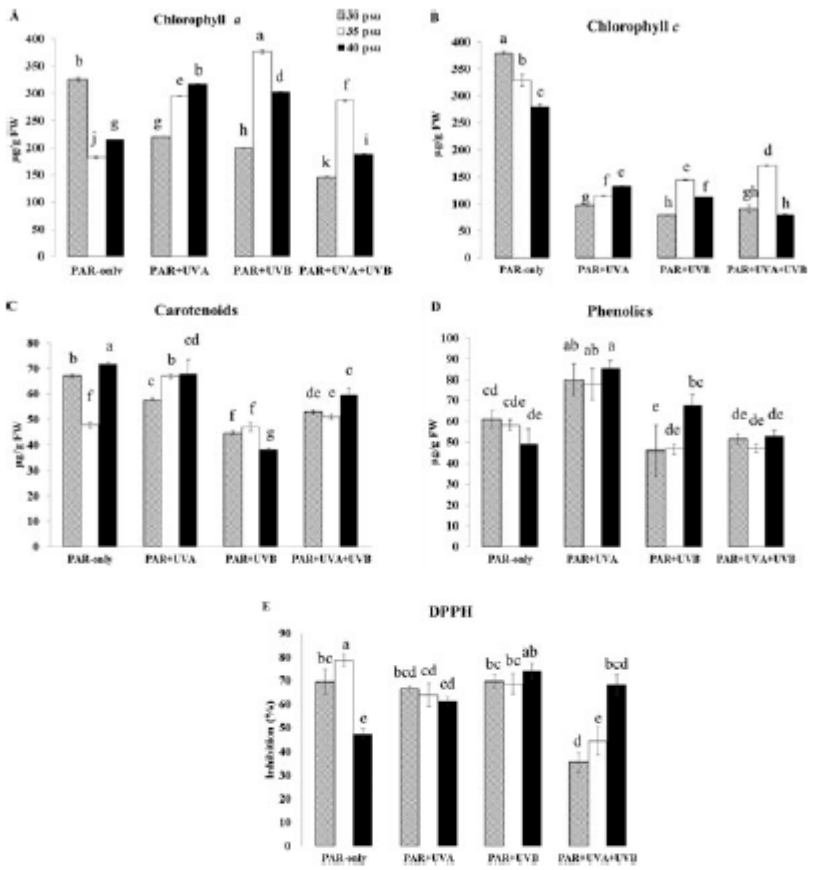

Figure 2. Photosynthetic pigments (A. Chlorophyll *a*; B. Chlorophyll *c*; C. Total carotenoids) D. Phenolic compounds and E. DPPH scavenging capacity of *S. cymosum* plants after 7 days of exposure to radiation and salinity treatments ($n = 4$, mean ± SD). Letters indicate significant differences according to bifactorial ANOVA and Tukey's test ($P \leq 0.05$).

PAR-only. Chlorophyll *c* was reduced by approximately half after exposure to PAR + UVA, PAR + UVB and PAR + UVA + UVB in all three salinities when compared with PAR-only (Fig. 2B). The amount of total carotenoids varied significantly among the treatments (Fig. 2C). Notably, PAR-only treatments at 30 and 40 psu increased carotenoid content compared with 35 psu. At 35 psu with PAR + UVA, a significant increase was also observed compared with PAR-only.

The significant influence of UVR on photosynthetic pigments can be statistically corroborated using one-way ANOVA showing the differences in isolated effect of radiation treatments on *S. cymosum* (lowercase letters) (Table 2). Although significant differences were observed under isolated effect of salinity, it seems to be less drastic than UVR.

The bifactorial ANOVA analysis of phenolic compounds showed significant variation within the salinities and radiation treatments (Fig. 2D). These compounds increased in plants treated with PAR + UVA. The isolated one-way ANOVA for radiation effect showed increases at 30 and 40 psu (Table 2), but less effect for salinity.

The analysis of seawater showed an increase in absorbance in treated samples when compared with the control. The seawater of plants treated with PAR + UVA showed the highest increase in absorbance between 300 and 400 nm in all salinities compared with PAR-only. An increased absorbance was also verified in seawater of PAR + UVB at 30 and 35 psu and PAR + UVA + UVB at 30 and 40 psu when compared with control. (Fig. 3)

DPPH radical-scavenging capacity was significantly affected by salinity and UVR treatments when compared with PAR-only (Fig. 2E) with lower scavenger activity at PAR-only at 40 psu and PAR + UVA + UVB at 30 and 35 psu. One-way analyses of DPPH scavenging capacity showed significant radiation effect at 35 or 40 psu (Table 2), but no effect of salinity when considered as an isolated variable.

LM observations and cytochemistry

The PAR-only samples (30, 35 and 40 psu) of *S. cymosum* stained with Toluidine Blue (TB-O) showed a metachromatic reaction in the cell wall, indicating the presence of acidic polysaccharides sulfated (Fig. 4A–C). When stained with TB-O, the treated samples (PAR + UVA, PAR + UVB and PAR + UVA + UVB) of *S. cymosum* showed a reaction in the cell wall

Table 2. Photosynthetic pigments (chlorophylls and total carotenoids), contents of phenolic compounds and DPPH scavenging capacity of *S. cymosum* plants after 7 days of exposure to radiation and salinity treatments ($n = 4$, mean ± SD).

	Treatments			
	PAR-only	PAR + UVA	PAR + UVB	PAR + UVA + UVB
Chlorophyll *a*				
30 psu	326.84 ± 3.43**aA**	220.04 ± 0 .38**bC**	198.78 ± 0.73**cC**	145.95 ± 0.48**dC**
35 psu	181.77 ± 2.33**cC**	294.23 ± 0.88**bB**	377.47 ± 3.14**aA**	286.48 ± 2.02**bA**
40 psu	215.37 ± 0.52**cB**	317.59 ± 0.82**aA**	302.97 ± 0.38**bB**	187.74 ± 0.55 **dB**
Chlorophyll *c*				
30 psu	379.85 ± 3.22**aA**	97.30 ± 0.51**cC**	78.75 ± 0.58**cC**	90.24 ± 7.23**bB**
35 psu	329.67 ± 0.76**aB**	115.75 ± 0.45 **dB**	144.96 ± 0.54**cA**	171.44 ± 0.92**bA**
40 psu	279.98 ± 0.23**aC**	132.47 ± 0.53**bA**	112.41 ± 0.20**cB**	79.67 ± 0.30**dC**
Carotenoids				
30 psu	67.11 ± 0.60**aB**	57.73 ± 0.72**bB**	44.47 ± 0.82**dA**	53.02 ± 0.88**cAB**
35 psu	47.83 ± 1.11**cC**	66.91 ± 0.81**aA**	46.85 ± 1.67**cA**	50.98 ± 0.87**bB**
40 psu	71.70 ± 0.77**aA**	67.83 ± 5.67**bB**	38.06 ± 0.54**cB**	59.61 ± 3.09**bA**
Phenolics				
30 psu	28.04 ± 1.88**bA**	36.80 ± 3.43**aA**	21.26 ± 5.53**bB**	23.75 ± 1.11**bAB**
35 psu	26.78 ± 1.18**cAB**	35.78 ± 3.43**aA**	21.51 ± 1.08**bB**	21.68 ± 0.90**cB**
40 psu	22.57 ± 3.67**cB**	39.21 ± 1.79**aA**	30.93 ± 2.62**bA**	24.17 ± 1.54**cA**
DPPH				
30 psu	69.54 ± 5.29**aA**	66.60 ± 1.23**abA**	69.75 ± 2.83**aA**	35.46 ± 4.13**bA**
35 psu	78.55 ± 2.52**aA**	64.01 ± 5.10**bA**	68.71 ± 4.31**bA**	44.41 ± 5.85**cA**
40 psu	47.44 ± 2.16**cA**	61.21 ± 1.65**bA**	73.99 ± 3.30**aA**	68.34 ± 4.54**aA**

Lowercase letters indicate significant differences among radiation treatments based on individual salinity treatment according to one-way ANOVA and Tukey's test ($P \leq 0.05$). Uppercase letters indicate significant differences between salinity levels at individual radiation treatment according to one-way ANOVA and Tukey's test ($P \leq 0.05$).

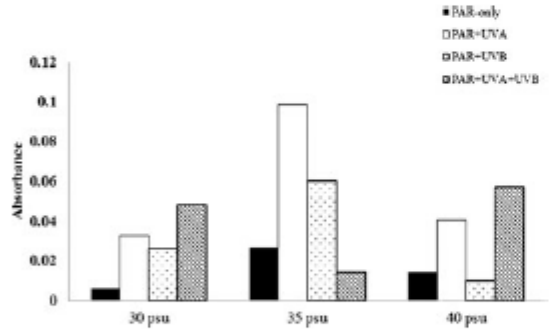

Figure 3. Phenolic compounds extruded by *S. cymosum* to the seawater culture medium (absorbance 300–400 nm) ($n = 4$).

similar to that observed in the PAR-only samples (Fig. 4D–L). In the cytoplasm of cortical cells of PAR-only samples, a large quantity of dark blue and yellow physodes was observed (Fig. 4A–C, arrows). The cytoplasm of treated samples (Fig. 4D–L, arrows) of the cortical cells was denser compared with the PAR-only samples, and an increasing quantity of physodes was observed (Fig. 4D–L, arrows). The physodes were migrating to the surface of cortical cells of treated samples.

TEM observations

When observed by transmission electron microscopy (Fig. 5A–F), *S. cymosum* control cells (PAR-only) at 30, 35 and 40 psu showed no differences in structural organization. These cells were surrounded by a thick cell wall (Fig. 5A), and the cytoplasm was filled with chloroplasts, mitochondria and a large quantity of physodes (Fig. 5A). This cell wall was formed by concentric microfibrils embedded in an amorphous matrix which consisted of sulfated polysaccharides (Fig. 5B–D), confirming the findings of samples stained with TB-O and observed under LM. Deposition of phenolic compounds in the cell wall was observed (Fig. 5C). These cells, which presented many chloroplasts (Fig. 5D), were large and exhibited the typical structure of brown algae with aggregated thylakoids in bands three to three (Fig. 5E–F). Mitochondria were present in association with the chloroplasts (Fig. 5E).

After exposure to PAR + UVA for 3 h per day during a 7-day period, *S. cymosum* showed cell wall thickness of the cortical cells (Fig. 6A–C) with a concomitant increase in the number of concentric microfibrils (Fig. 6B–C, arrows). The number of mitochondria was increased (Fig. 6A). The physodes appeared in an irregular shape near the cell wall (Fig. 6B–C). Some physodes were localized near the plasmodesmata (Fig. 6D) and were being degraded (Fig. 6E). Chloroplasts showed no changes in organization, and the number of plastoglobuli was increased (Fig. 6F).

After exposure to PAR + UVB for 3 h per day during a 7-day period, *S. cymosum* showed similar cell wall thickness of the cortical cells (Fig. 7A–B) with a concomitant increase in the number of concentric microfibrils (Fig. 7B, arrows). The cortical cytoplasm of treated samples (Fig. 7A) was denser compared with the PAR-only samples, and the physodes appeared to migrate toward the cortical cell surface (Fig. 7A). Chloroplasts showed no changes in organization (Fig. 7C–F). The number of mitochondria associated with chloroplasts was increased (Fig. 7E). Physodes with irregular shape appeared near the plasmodesmata and were being degraded (Fig. 7G–H). In the cytoplasm, crystallized structures were observed (Fig. 7I).

The plants of *S. cymosum* exposed to PAR + UVA + UVB showed similar cell wall thickness (Fig. 8A, arrows) and degraded physodes near the cell wall (Fig. 8B). A large quantity

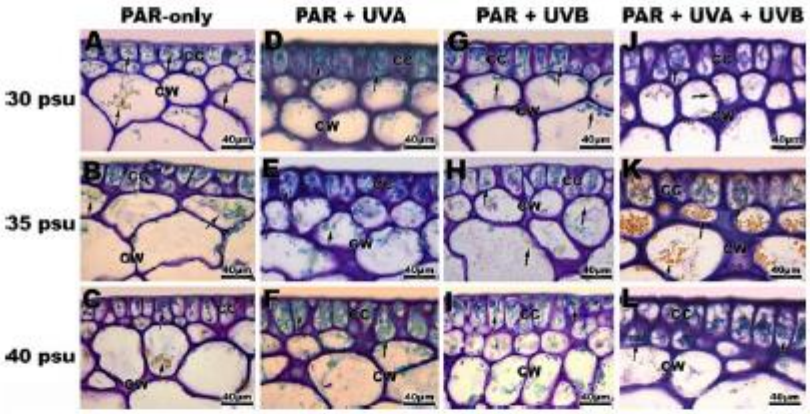

Figure 4. Light microscopy of *S. cymosum* plants after exposure to ultraviolet radiation and salinity treatments during 3 h per day over a period of 7 days, stained with TB-O. **A-C.** Control samples. Detail of cortical cells (CC) showing metachromatic reaction in the cell walls (CW), indicating the presence of acidic polysaccharides. Note the presence of physodes (arrows). **D-L:** Observe the increase in physodes in treated plants after exposure to UVR (arrows).

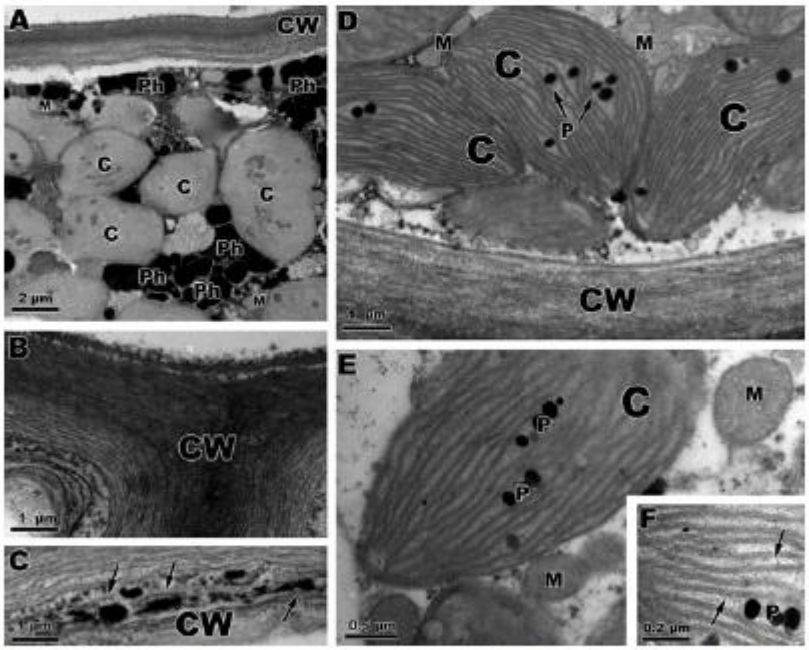

Figure 5. Transmission electron microscopy (TEM) micrographic images of *S. cymosum* control plants. **A** and **C**, plants cultivated at 30 psu. **B** and **D**, plants cultivated at 35 psu. **E** and **F**, plants cultivated at 40 psu. **A.** Note the cortical cell showing a large quantity of chloroplasts (C), mitochondria (M), physodes (Ph). **B.** Detail of thick cell wall (CW). **C.** Note the presence of phenolic compounds (arrows) in cell wall. **D–E.** Note the chloroplast with plastoglobuli (P, arrows) and associated mitochondria (M). **F.** Magnification showing internal organization of thylakoids in three bands into the chloroplasts (arrows).

of phenolic compound deposits in the cell wall was observed (Fig. 7C). In the cytoplasm, crystallized structures were observed (Fig. 8D, arrows). Chloroplasts showed an organization similar to that found in PAR-only and other treated plants (Fig. 8E). The number of plastoglobuli was increased in the chloroplasts (Fig. 8F). The number of mitochondria was increased (Fig. 8G) in association with Golgi bodies (Fig. 8G).

In vivo fluorescence of chlorophyll *a*

All UVR treatments modified the kinetics pattern of the Photosynthesis/Irradiance (PI) curve (Fig. 9) independent of the level of salinity when compared with PAR-only. UVB radiation showed the highest photoinhibitory slope at either salinity (Fig. 9A, C and E). After 24 h at PAR-only recovery treatment,

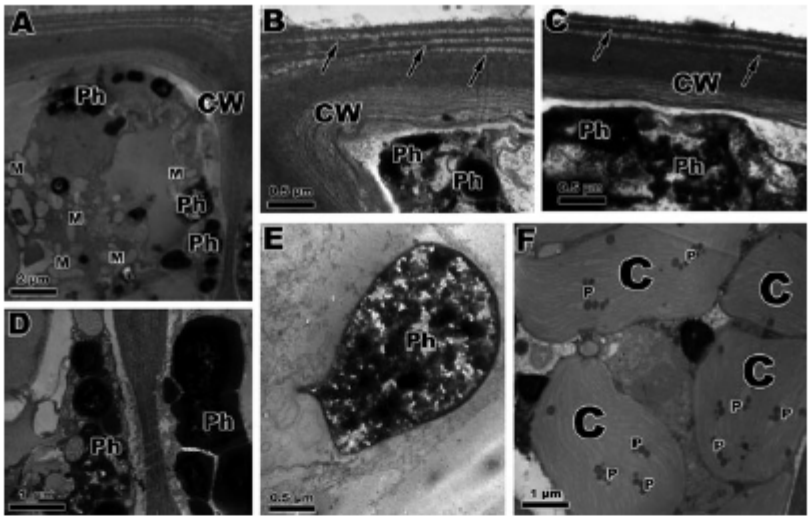

Figure 6. Transmission electron microscopy (TEM) micrographic images of *S. cymosum* plants after 7 days of exposure to PAR + UVA. **A** and **D**, plants cultivated at 30 psu. **B** and **C**, plants cultivated at 35 psu. **E** and **F**, plants cultivated at 40 psu. **A**. Note the physodes (Ph) near the cell wall (CW) and a large quantity of mitochondria (M). **B**. Detail of thick cell wall (CW) and physodes (Ph). **C**. Note the presence of phenolic compounds (arrows) near the cell wall. **D**. Phenolic compounds migrating through the plasmodesmata. **E**. Detail of physode (Ph) being degraded. **F**. Note the chloroplast (C) with plastoglobuli (P).

recuperation of ETR kinetics showed a trend similar to the ETR kinetics in plants treated with PAR-only, PAR + UVA and PAR + UVA + UVB at 35 and 40 psu.

On the other hand, plants treated with PAR + UVB showed lower ETR kinetics and no signs of recovery. Neither F_v/F_m (Fig. 10A, C) nor Y(II) (Fig. 10B, D) was affected by UVR or salinity, although the lowest quantum yields were observed in plants treated with PAR + UVB.

Salinity was not represented as a factor that significantly affected photosynthetic parameters, including ETRmax, alpha, beta and Ik, as demonstrated by one-way ANOVA (Table 3). Even though saturating irradiance shows no significant differences, these values were higher in plants exposed to PAR + UVA and PAR + UVB (Table 3). Photosynthetic parameters after recovery (Table 4) corroborate the kinetics patterns shown by the *P–I* curve, in which low variation in photosynthetic performance was observed.

Based on bifactorial ANOVA, no significant differences were observed in ETRmax, alpha, beta and Ik values for plants exposed to all types of radiation in all salinities (Fig. 11). However, the mean values for each parameter fluctuated in all treatments. It was possible to observe that ETRmax and alpha values in recovery condition showed significant differences within them (Fig. 11B, D, respectively). Exposure to any kind of radiation and salinity promoted photoinhibition with higher beta values for PAR + UVA and PAR + UVB (Fig. 11E, F).

DISCUSSION

When exposed to PAR + UVA, PAR + UVB and PAR + UVA + UVB, this study showed that *Sargassum cymosum* presents a variety of physical and photoprotective response mechanisms. Although salinity could be a factor affecting *S. cymosum* metabolism in different ways, a clear trend was not observed in this study. Exposure of *S. cymosum* to UVR showed no decrease in GRs, indicating that treatment was not stressful for this parameter, and, in fact, biomass gain occurred in treated samples was verified. Plants cultivated at 30 psu and exposed to PAR + UVB or PAR + UVA + UVB showed an increase in approximately 148% in GRs when compared with PAR-only samples. This increase in GRs in treated samples of *S. cymosum* could probably be possible because: (1) an increase in the amount of mitochondria could support the metabolic energy demands to evidence an enhancement of biomass, whereas the intact chloroplast thylakoids corroborate the viability of sustaining photosynthate production; (2) Similar to the findings of other authors, UVA radiation can activate photoprotective mechanisms to counteract the negative effect of UVB radiation, resulting in a decreasing impact of UVR on growth rates (54) and (3) as the PAR level is low, UVA levels are moderate and UVB has a longer wavelength, this would play a role in stimulating growth and photosynthesis (55). The total net balance among the effects of an environmental stress on the biochemical and physiological processes within the cell can be reflected by the changes in growth rate (56). Negative effects on growth and development by UVB radiation have been well studied, and GRs are normally related to UV damage to the photosynthetic machinery, photosynthetic pigments, antioxidant enzymes and lipid peroxidation caused by increasing UV radiation (54). However, our results do diverge from those of other studies with brown algae, such (57) who reported a decrease in GR for seven species within this group, including *Laminaria saccharina*, *Alaria esculenta*, *Saccorhiza dermatodea*, *Fucus distichus*, *Fucus serratus* and *Fucus vesiculosus*. The bilateral effects of UV-A: positive when is in a low level and negative when is in high level, could magnify the discrepancy in UV-related inhibition between the integrated photosynthetic production and growth according to the weather conditions (56).

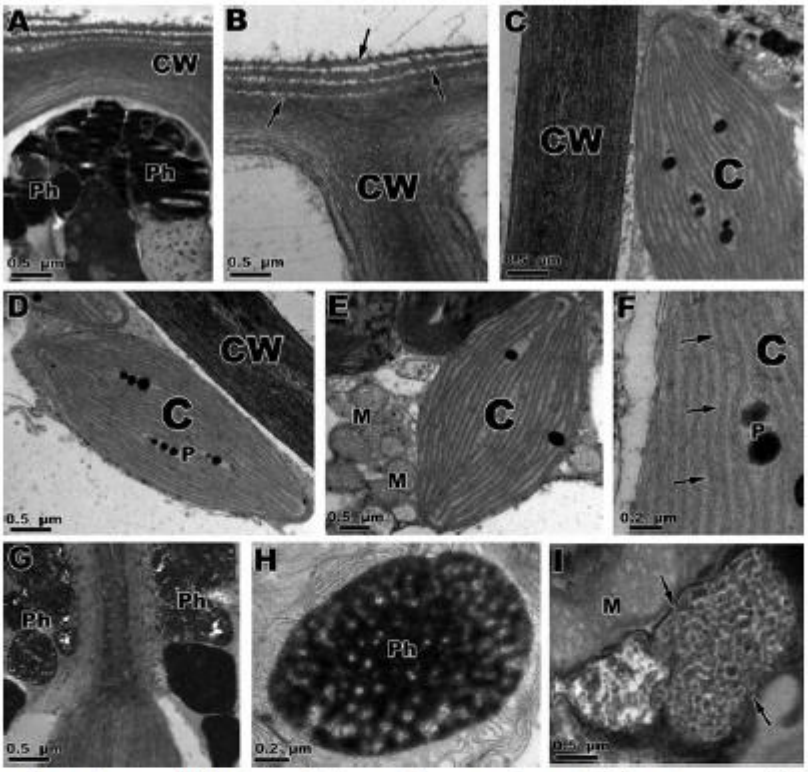

Figure 7. Transmission electron microscopy (TEM) micrographic images of *S. cymosum* plants after 7 days of exposure to PAR + UVB radiation. **C** and **I**, plants cultivated at 30 psu. **A**, **D** and **I**, plants cultivated at 35 psu. **B**, **E**, **F** and **H**, plants cultivated at 40 psu. **A**. Note the migration of phenolic compounds as physodes (P) near the cell wall (CW). **B**. Detail of cell wall (CW) thickness (arrows). **C**–**D**. Note intact chloroplast (C) with presence of plastoglobuli (P). **E**. Observe increase in the number of mitochondria (M) in association with chloroplast. **F**. Note the internal organization of thylakoids in three bands into the chloroplasts (arrows) and plastoglobuli. **G**. Note the physode (Ph) with irregular shape near the plasmodesmata. **H**. Observe the physode being degraded. **I**. Note the crystallized structures (arrows) near the mitochondria.

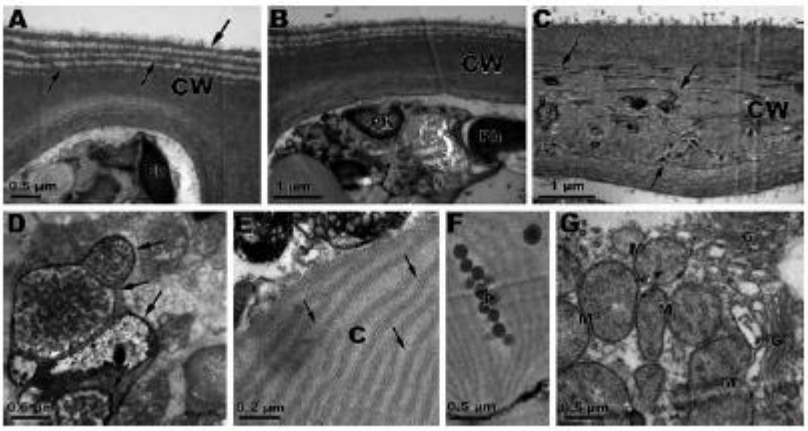

Figure 8. Transmission electron microscopy (TEM) micrographic images of *S. cymosum* plants after 7 days of exposure to PAR + UVA + UVB radiation. **A** and **F**, plants cultivated at 30 psu. **B**, **C** and **G**, plants cultivated at 35 psu. **D** and **E**, plants cultivated at 40 psu. **A**. Detail of cell wall (CW) showing thickness (arrows). **B**. Note the physodes (Ph) with phenolic compounds near the cell wall. **C**. Observe the presence of phenolic compounds in the cell wall (arrows). D. Note the crystallized structures (arrows) in the cytoplasm. **E**. Detail of chloroplasts (C) showing internal organization of thylakoids in three bands into the chloroplast (arrows). **F**. Observe the increase in plastoglobuli (P). **G**. Note the large quantity of mitochondria (M) with associated Golgi bodies (G).

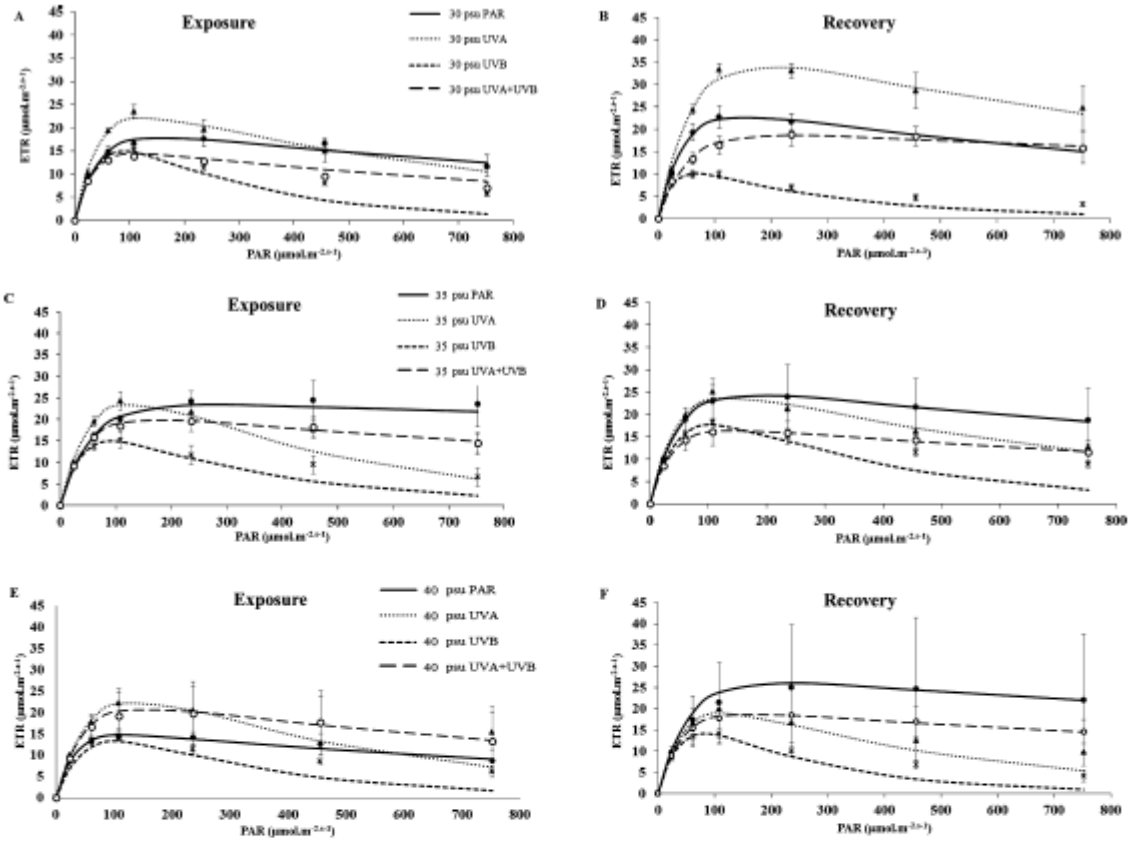

Figure 9. Electron transport rate (ETR) photosynthetic light curves (*P–I*) of *S. cymosum* plants after 7 days of exposure to radiation and salinity treatments and 24 h at PAR-only recovery treatment. **A.** Exposure treatment at 30 psu. **B.** Recovery treatment at 30 psu. **C.** Exposure treatment at 35 psu. **D.** Recovery treatment at 35 psu. **E.** Exposure treatment at 40 psu. **F.** Recovery treatment at 40 psu. PAR: photosynthetically active radiation.

In this study, chlorophyll *a* (Chl *a*) of *S. cymosum* showed different responses in the three salinities and UVR treatments. Chlorophyll *a* content decreased in *S. cymosum* plants cultivated in 30 psu salinity upon exposure to PAR + UVA, PAR + UVB and PAR + UVA + UVB. However, plants treated with 35 and 40 psu showed an increase in Chl *a*, except 40 psu salinity under PAR + UVA + UVB treatment. These treatments showed that Chl *a* is more resistant than chlorophyll *c* and that biosynthesis was stimulated in *S. cymosum* samples when compared with control plants. On the other hand, all treated samples showed a decrease in chlorophyll *c* (Chl c) content. These results agree with those of (58) who found that the contents of Chl *c* were mainly reduced by UVA and UVB. This reduction in Chl *c* could be related to a photoprotective mechanism in which the accessory pigment level is diminished to alleviate the excess of energy driven to the reaction center of photosynthesis, thus preventing oxidative damage of the photosynthetic apparatus in the treated samples.

It has been reported that exposure to UVR induces the production and accumulation of reactive oxygen species (ROS), an oxidative stress condition, indicating a key element of UVR toxicology (59) and resulting in oxidative damage to biomolecules, including membrane lipids, proteins, enzymes and DNA (60). If accumulation of ROS exceeds the capacity of enzymatic and nonenzymatic antioxidant systems, the photosynthetic apparatus is damaged by the destruction of lipids, proteins and nucleic acids, leading to apoptosis (61,62). *Sargassum cymosum* plants cultivated with 35 psu in PAR + UVA showed an increase in carotenoids content, suggesting that the treatment induced antioxidant cell defense by carotenoids when compared with control and other treatments.

As a strategy to prevent the effects of ROS, *S. cymosum* plants exposed to PAR + UVA increased the content of phenolic compounds, most likely as a photoprotective mechanism against UV damage, when compared with the control, PAR + UVB and PAR + UVA + UVB treatments. An increase in phenolic compounds was expected in all treatments as a defense to prevent damage caused by UVR. Nevertheless, the decrease in phenolic compounds presented in the treatments could be related to a change in metabolic pathway. Polyphenolics are commonly concentrated in the cortical and meristematic cells of adult brown algae; thus, they may protect cells from excess UVR (62). By microscopy analyses, it was possible to detect the presence of phenolic compounds migrating through the cell wall and being degraded. Furthermore, the absorbance screening of the seawater from each treatment showed an increase in compounds absorbing

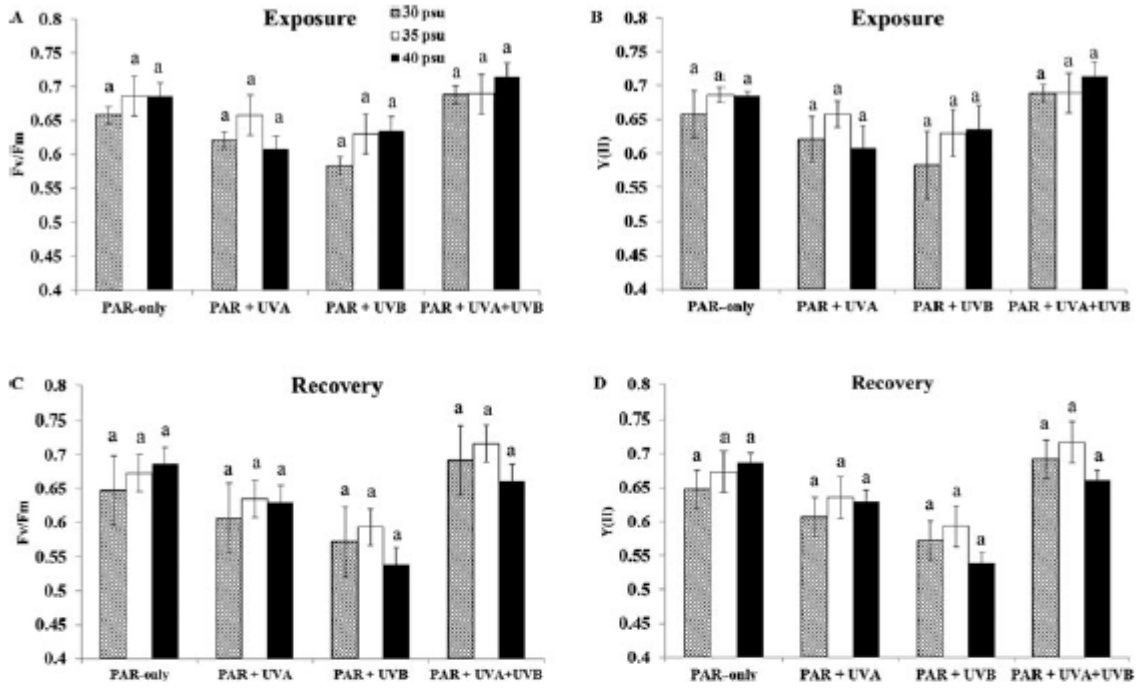

Figure 10. Photosynthetic quantum yields of *S. cymosum* plants after 7 days of exposure to radiation and salinity treatments and 24 h at PAR-only recovery treatment ($n = 4$, mean ± SD). **A.** Fv/Fm exposure treatment. **B.** Y(II) exposure treatment. **C.** F_v/F_m recovery treatment. **D.** Y(II) recovery treatment. Letters indicate significant differences according to bifactorial ANOVA and Tukey's test ($P \leq 0.05$). F_v/F_m: optimal quantum yield; Y(II): effective quantum yield.

Table 3. Electron transport rate (ETR) photosynthetic light curve (P-I) parameters of *S. cymosum* plants after 7 days of exposure to radiation and salinity treatments ($n = 4$, mean ± SD).

	Treatments			
Exposure	PAR-only	PAR + UVA	PAR + UVB	PAR + UVA + UVB
ETRmax				
30 psu	20.48 ± 1.52abA	27.81 ± 1.50aA	25.75 ± 5.88bA	16.45 ± 0.51bA
35 psu	22.00 ± 3.82bA	38.25 ± 2.14aA	22.68 ± 1.92bA	22.51 ± 2.00bA
40 psu	16.69 ± 0.28aA	34.49 ± 7.86a A	23.37 ± 3.86aA	24.48 ± 8.77aA
Alpha				
30 psu	0.47 ± 0.02aA	0.62 ± 0.03aB	0.49 ± 0.02aA	0.51 ± 0.04aA
35 psu	0.46 ± 0.03aA	0.56 ± 0.01aAB	0.51 ± 0.05aA	0.49 ± 0.06aA
40 psu	0.53 ± 0.03aA	0.52 ± 0.03aA	0.38 ± 0.20aA	0.53 ± 0.03aA
Beta				
30 psu	0.010 ± 0.003bA	0.036 ± 0.054abB	0.100 ± 0.030aA	0.010 ± 0.009bA
35 psu	0.008 ± 0.006cA	0.093 ± 0.064aA	0.070 ± 0.007bA	0.010 ± 0.001cA
40 psu	0.010 ± 0.050bA	0.072 ± 0.014aA	0.080 ± 0.020aA	0.019 ± 0.003bA
Ik				
30 psu	43.39 ± 1.48aA	44.76 ± 4.84aA	44.76 ± 4.84aA	32.45 ± 2.92aA
35 psu	48.65 ± 11.34aA	68.25 ± 2.41aA	68.25 ± 2.41aA	47.32 ± 9.47aA
40 psu	31.69 ± 1.43aA	66.38 ± 19.22aA	66.38 ± 19.22aA	47.57 ± 21.76aA

Lowercase letters indicate significant differences between radiation treatments (PAR-only, PAR + UVA, PAR + UVB, PAR + UVA + UVB) at individual salinity treatment according to one-way ANOVA and Tukey's test ($P \leq 0.05$). Uppercase letters indicate significant differences between salinity levels (30, 35, 40 psu) at individual radiation treatment according to one-way ANOVA and Tukey's test ($P \leq 0.05$). ETRmax: maximum electron transport rate; alpha (α): photosynthetic efficiency; beta (β): photoinhibition; Ik: saturating irradiance.

between 300 and 400 nm, probably related to the extrusion of phenolic compounds and other UV-absorbing compounds. According to (63), the increased concentrations of phenolic compounds in response to elevated radiation have two different functions: (1) to act as a sunscreen against potential damage of UVB and (2) to ameliorate damage caused by increased ROS. According to (64), phenolic compounds could act as a photoprotective mechanism against higher irradiance in the ecosystems by

Table 4. Electron transport rate (ETR) photosynthetic light curve (*P–I*) parameters of *S. cymosum* plants after 24 h of recovery from radiation and salinity treatments ($n = 4$, mean ± SD).

	Treatments			
Recovery	PAR-only	PAR + UVA	PAR + UVB	PAR + UVA + UVB
ETRmax				
30 psu	26.51 ± 2.68**bA**	41.34 ± 1.79**aA**	13.94 ± 1.23 **dB**	20.21 ± 1.59**cA**
35 psu	27.68 ± 5.80**abA**	30.33 ± 2.94**aB**	28.54 ± 0.61**abA**	18.10 ± 2.42**bA**
40 psu	28.67 ± 17.06**aA**	27.16 ± 15.38**aB**	24.36 ± 4.71**aA**	20.60 ± 8.59**aA**
Alpha				
30 psu	0.59 ± 0.03**abA**	0.65 ± 0.05**aA**	0.51 ± 0.01**bA**	0.38 ± 0.01**cA**
35 psu	0.56 ± 0.02**abAB**	0.61 ± 0.04**aAB**	0.50 ± 0.03**bA**	0.50 ± 0.03**bA**
40 psu	0.52 ± 0.03**aB**	0.53 ± 0.01**aB**	0.51 ± 0.03**aA**	0.51 ± 0.51**aA**
Beta				
30 psu	0.020 ± 0.006**bcA**	0.031 ± 0.016**abA**	0.050 ± 0.002**aA**	0.006 ± 0.001**cA**
35 psu	0.010 ± 0.002**cA**	0.038 ± 0.012**bA**	0.084 ± 0.007**aA**	0.010 ± 0.002**cA**
40 psu	0.010 ± 0.001**bA**	0.058 ± 0.040**abA**	0.100 ± 0.043**aA**	0.010 ± 0.011**bA**
Ik				
30 psu	44.59 ± 2.10**cA**	63.01 ± 3.96**aA**	27.23 ± 1.76 **dB**	51.87 ± 1.81**bA**
35 psu	49.81 ± 10.47**aA**	49.39 ± 1.74**aA**	56.75 ± 3.31**aA**	18.10 ± 2.42**aA**
40 psu	55.80 ± 37.75**aA**	27.16 ± 15.38**aA**	47.17 ± 7.57**aA**	39.75 ± 12.86**aA**

Lowercase letters indicate significant differences between radiation treatments (PAR-only, PAR + UVA, PAR + UVB, PAR + UVA + UVB) at individual salinity treatment according to one-way ANOVA and Tukey's test ($P \leq 0.05$). Uppercase letters indicate significant differences between salinity levels (30, 35, 40 psu) at individual radiation treatment according to one-way ANOVA and Tukey's test ($P \leq 0.05$). ETRmax: maximum electron transport rate; alpha (α): photosynthetic efficiency; beta (β): photoinhibition; Ik: saturating irradiance.

absorbing incident photons or indirectly as a result of their antioxidant activity. In addition, the distribution of these compounds in Phaeophyceae, close to the cortical cells and cell walls, is a strong indication of their significance, suggesting an important feature responsible for the evolutionary success of the group (64).

Another defense mechanism in response to high antioxidant activity, following exposure to UVR treatments, was detected by DPPH scavenging capacity in *S. cymosum* cultivated at 40 psu, when compared with plants cultivated in control conditions. These results agree with those of (65), who demonstrated that UVBR exposure stimulates the generation of ROS, and those of (66), who showed that ROS-induced toxicity can lead to an increase in antioxidant enzymatic response (35). In addition, the ability of brown macroalgae to acclimate to increasing UVR has been attributed to phenolic secondary metabolites known as phlorotannins (36,67). On the other hand, this activity decreased in treated plants of *S. cymosum* cultivated with 30 and 35 psu.

The chloroplasts of control plants of *S. cymosum* showed a typical structure of brown algae, with thylakoids aggregated in three to three bands, and after exposure to UVR these structures were not altered, confirming that this alga has a strong photoprotective mechanism against UVR. This result differs from (68) who found that chloroplasts of the vegetative tissue of the brown alga *Saccharina latissima* exposed to PAR + UVA + UVB showed changes in morphology, such as wrinkling and dilation. However, other organelles of *S. cymosum*, such as mitochondria, showed no alterations, their numbers did increase in association with chloroplasts. This could have resulted from elevated physiological activity. These results agree with (69) who reported that different organelles, such as mitochondria, Golgi bodies and the nucleus, in the green alga *Zygnema* did not present signs of alterations when exposed to PAR + UVA + UVB radiation, demonstrating good adaptation to ambient solar radiation. The same was observed in (70), who reported no ultrastructural damage after exposure to UVR in the green alga *Urospora penicilliformis*.

On the other hand, some studies reporting on red macroalgae exposed to UVR showed ultrastructural changes in chloroplasts manifested as a dilation and disorganization of thylakoids and the formation of translucent vesicles between thylakoids. These species include *Kappaphycus alvarezii* (29–31), *Gelidium floridanum* (32), *Chondracnthus teedei* (33), *Hypnea musciformis* (34) and *Porphyra acanthophora* var. *brasiliensis* (35).

Results based on the physiological and cellular features of *S. cymosum* exposed to UVR evidence high photoprotective acclimation to this stressful condition, at least when compared with red macroalgae. This acclimation plasticity of *S. cymosum* could represent an adaptation characteristic that allows it to support the constant stressful condition of radiation exposure along the lower infralittoral and upper subtidal areas of rock shore, both common habitats of this species.

The cell wall of control and treated plants of *S. cymosum* reacted positively to TB-O. This occurred because the cell wall contains polysaccharides as alginic acid and sulfated fucan. The higher intensity of reaction to TB-O in treated plants of *S. cymosum* could be related to cell wall thickness. When analyzed under TEM, the cell walls of control of *S. cymosum* showed a microfibrillar texture, with microfibrils structured in concentric layers. In contrast, the cell wall of plants exposed to UVR appeared to be enlarged, leading to changes in cell morphology, as detected by TEM and LM. The increase in cell wall thickness of *S. cymosum* exposed to UVR treatments can be interpreted as a physical defense mechanism against exposure to UVR because a denser amorphous mucilaginous composition would most likely prevent UVR penetration into the cell. An increase in phenolic compounds was also verified in the cell walls of treated plants. According to (36), compounds such as phlorotannins are normally accumulated in cell walls of brown algae.

It has been reported that the physiological processes of photosynthesis are principal targets of UV radiation; thus, it can have several effects on seaweeds (28). (71) reported, for the first time, the potential of UV to inhibit photosynthesis. The treated plants of *S. cymosum* showed low patterns of photoinhibition in all

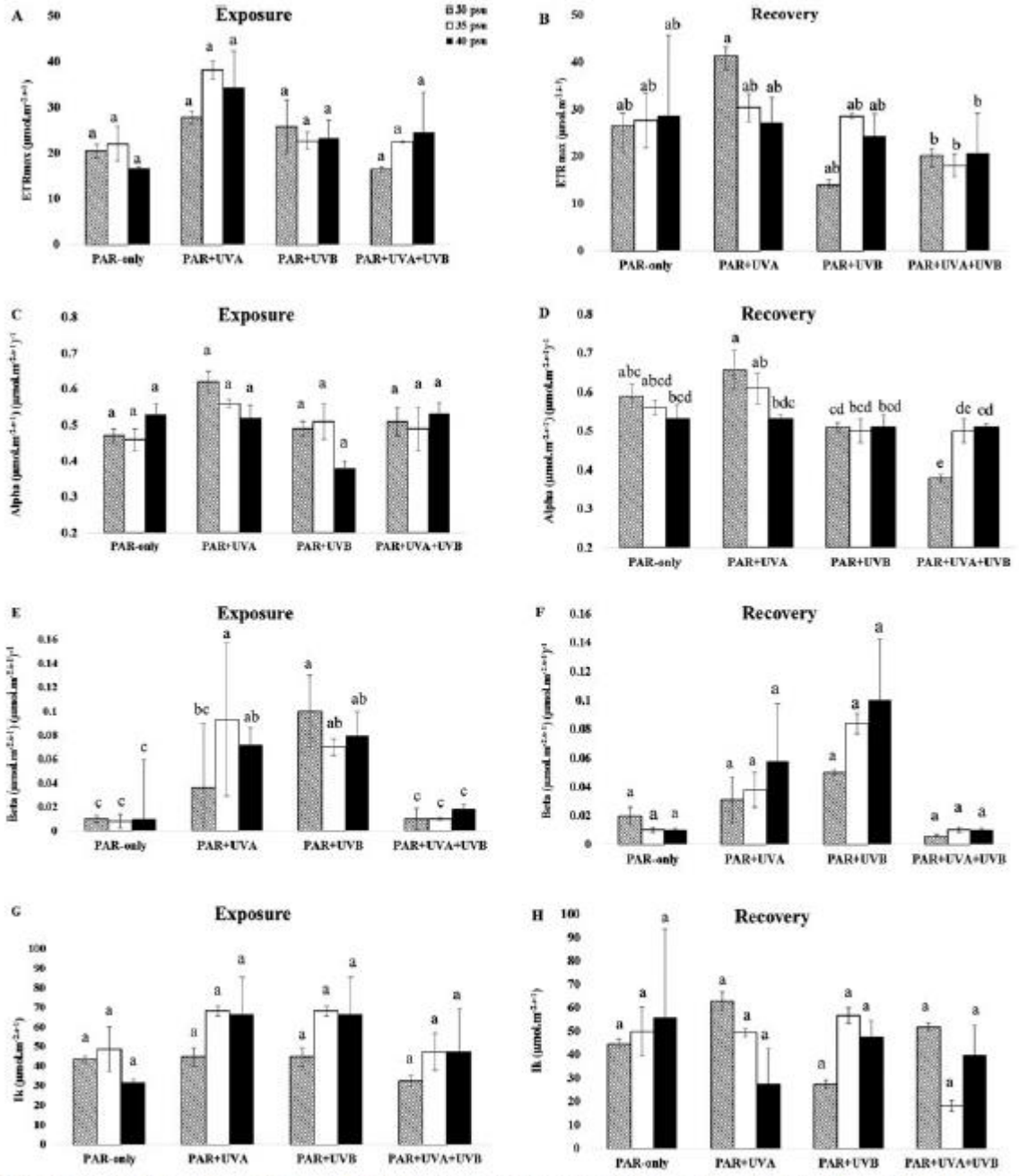

Figure 11. Photosynthetic parameters of *S. cymosum* plants after 7 days of exposure to radiation and salinity treatments and 24 h at PAR-only recovery treatment ($n = 4$, mean ± SD). **A–B.** ETRmax: maximum electron transport rate, exposure and recovery, respectively. **C–D.** Alpha (α) photosynthetic efficiency, exposure and recovery, respectively. **E–F.** Beta (β): Photoinhibition, exposure and recovery, respectively. **G–H.** Ik: Saturing irradiance, exposure and recovery, respectively. Letters indicate significant differences according to bifactorial ANOVA and Tukey's test ($P \leq 0.05$).

salinities, although this situation was more evident in plants treated with PAR + UVB. According to (72), PSII is a primary UVB target and damage involving PSII could be related to the D1 protein that is one of the main proteins involved in the PSII repair cycle. Plants treated with PAR + UVA showed no signs of photoinhibition of the optimum quantum yield of (F_v/F_m) and

presented sufficient levels of photoprotection. This response could be related to the increase in phlorotannin-containing physodes that have a protective function against UVR. After 24 h of recovery treatment, plants treated with PAR + UVA and PAR + UVA + UVB were observed to recuperate, confirming that *S. cymosum* is capable of counteracting the negative effects caused by UV radiation through different adaptive responses. Another factor that can be related to the photoprotective mechanism of *S. cymosum* involves its thickness, presenting such characteristics as multiple cell layers that help protect against the negative effects of UV (73). On the other hand, plants treated with PAR + UVB showed no signs of recuperation after 24 h in recovery condition, suggesting that the effective recovery of photosynthetic electron transport requires more time to be realized. This response can be a symptom of more chronic photoinhibition or/and photodamage to long-term UVR exposure.

It can be concluded in this study that the combined effect of salinity and UVR was not a stress factor for *S. cymosum* plants and that salinity itself is not a predominant factor affecting the analyzed parameters. Different aspects of *S. cymosum* plants, such as growth rate, pigment contents and antioxidant activity, were not drastically altered by UVR, although all the treated plants presented increasing quantity of physodes, probably as a photoprotective mechanism. This was more evident in the treatment with PAR + UVA, and the negative effect of UVR was more pronounced in plants treated with PAR + UVB. Nevertheless, all treated plants showed cell wall thickening as a barrier against the harmful effects of UVR. This protective mechanism could complement photoprotection against oxidative stress, making defense against UVR more efficient. The PSII quantum yields showed no significant reductions, and all treated plants presented signs of recuperation, except those treated with PAR + UVB. Finally, it was possible to observe the strong mechanism that *S. cymosum* plants have against stressors like UVR, allowing it to persist under highly stressful conditions.

Acknowledgements—The authors would like to acknowledge the staff of the Central Laboratory of Electron Microscopy (LCME), Federal University of Santa Catarina, Florianopolis, Santa Catarina, Brazil, for the use of their transmission electron microscope. Éder C. Schmidt holds a postdoctoral fellowship from CAPES. Zenilda L. Bouzon is a CNPq fellow. Fungyi Chow is a FAPESP fellow. This study is part of the MSc dissertation of the first author.

REFERENCES

1. Diffey, B. (2002) Sources and measurement of ultraviolet radiation. *Methods* **28**, 4–13.
2. Madronich, S., R. L. Mc Kenzie, L. O. Björn and M. M. Caldwell (1998) Changes in biologically active ultraviolet radiation reaching the Earth's surface. *J. Photochem. Bio.* **46**, 5–19.
3. Häder, D. P., H. D. Kumar, R. C. Smith and R. C. Worrest (2007) Effects of solar UV radiation on aquatic ecosystems and interactions with climate change. *J. Photochem. Photobiol.* **46**, 53–68.
4. Britt, A. B. (1995) DNA damage and repair in plants. *Plant Mol. Biol.* **47**, 75–100.
5. Lão, K. and A. N. Glaser (1996) Ultraviolet-B photodestruction of light-harvesting complex. *Proceedings of the National Academy of Science of the United States of America* **93**, 5258–5263.
6. Buma, A. G. J., W. H. Van Oijen, M. J. W. Van De Poll (2000) On the high sensitivity of the marine prymnesiophyte *Emiliania huxleyi* to ultraviolet-B. *J. Appl. Phycol.* **131**, 296–303.
7. Tevini, M. and A. H. Teramura (1989) UV-B effects on terrestrial plants. *J. Photochemix. Photobiol.* **50**, 479–487.
8. Döhler, G. and I. Biermann (1987) Effect of UV-B irradiance on the response of ^{15}N-nitrate uptake of *Lauderia annulata* and *Synedra planctonica*. *J. Plankton Res.* **9**, 881–890.
9. Wood, W. (1987) Effect of solar ultraviolet radiation on the kelp *Ecklonia radiata*. *Mar. Biol.* **96**, 143–150.
10. IPCC (2007) *Intergovernmental Panel on Climate Change. Climate Change 2007: The Physical Science Basis*, Contribution of Working Group I to the fourth assessment, pp. 996. Cambridge University Press, Cambridge.
11. Schemer, F., R. Ventura, J. Barufi and P. Horta (2012) Salinity critical threshold values for photosynthesis of two cosmopolitan seaweed species: Providing baselines for potential shifts on seaweed assemblages. *Mar. Envir. Res.* **79**, 1–12.
12. Wilkinson, M. (1981) Survival strategies of attached algae in estuaries. In *Feeding and Survival Strategies of Estuarine Organisms*, (Edited by N. V. Jones and W. J. Wolff). pp. 29–38. Plenum Publishing Company, New York.
13. Martins, I., J. Oliveira, M. Flindt and J. MArques (1999) The effect of salinity on the growth rate of the macroalgae *Enteromorpha intestinalis* (Chlorophyta) in the Mondego estuary (west Portugal). *Acta Oecol.* **20**, 259–265.
14. Wilkinson, M., P. Wood, E. Well and C. Scanlan (2007) Using attached macroalgae to assess ecological status of British estuaries for the European Water Framework Directive. *Mar. Pollut. Bull.* **55**, 136–150.
15. Norton, T., M. Melkonian and R. Andersen (1996) Algal biodiversity. *J. Appl. Phycol.* **35**, 308–326.
16. Hales, J. and R. Fletcher (1990) Studies on the recently introduced brown alga *Sargassum muticum* (Yendo) Fensholt. V. Receptacle initiation and growth, and gamete release in laboratory culture. *Bot. Mar.* **33**, 241–249.
17. Steen, H. (2004) Effects of reduced salinity on reproduction and germling development in *Sargassum muticum* (Phaeophyceae, Fucales). *Eur. J. Phycol.* **39**, 293–299.
18. Gordillo, F., M. Dring and G. Savidge (2002) Nitrate and phosphate uptake characteristics of three species of brown algae cultured at low salinity. *Mar. Ecol. Prog. Ser.* **234**(11), 1–118.
19. Munda, I. (1964) Observations on variations in form and chemical composition of *Fucus ceranoids* L. *Nova Hedwigia* **8**, 403–414.
20. Munda, I. and B. Kremer (1977) Chemical composition and physiological properties of fucoids under conditions of reduced salinity. *Mar. Bio.* **42**, 9–15.
21. Gylle, A., C. Nygard and N. Ekelund (2009) Desiccation and salinity effects on marine and brackish Fucus vesiculosus L. *(Phaeophyceae). Phycol.* **48**(15), 6–164.
22. Franklin, L. and R. Forster (1997) The changing irradiance environment: Consequences for marine macrophyte physiology, productivity and ecology. *Eur. J. Phycol.* **323**, 207–232.
23. Häder, D. and F. Figueroa (1997) Photophysiology of marine macroalgae. *Photochem. Photobiol.* **66**, 1–14.
24. Poppe, F., D. Hanelt and C. Wiencke (2002) Changes in ultrastructure, photosynthetic activity and pigments in the Antarctic Red Alga *Palmaria decipiens* during acclimation to UV radiation. *Bot. Mar.* **45**(25), 3–61.
25. Poppe, F., R. Schmidt, D. Hanelt and C. Wiencke (2003) Effects of UV radiation on the ultrastructure of several red algae. *Phycol. Res.* **51**(1), 1–19.
26. Holzinger, A. and C. Lütz (2004) The effect of ultraviolet radiation on ultrasctruture and photosynthesis in the red macroalgae *Palmaria palmata* and *Odonthalia dentata* from Artic waters. *Plant Bio.* **6**(56), 8–577.
27. Holzinger, A., U. Karsten, C. Lütz and C. Wiencke (2006) Ultrastructure and photosynthesis in the supralitoral green macroalga *Prasiola crispa* from Spitsbergen (Norway) under UV exposure. *Phycol.* **45**(16), 8–177.
28. Holzinger, A. and C. Lütz (2006) Algae and UV irradiation: Effects on ultrastructure and related metabolic functions. *Micron.* **37**, 190–207.
29. Schmidt, E., L. Scariot, T. Rover and Z. Bouzon (2009) Changes in ultrastructure and histochemistry of two red macroalgae strains of *Kappaphycus alvarezii* (Rhodophyta, Gigartinales), as a consequence of ultraviolet B radiation exposure. *Micron.* **40**(86), 0–869.
30. Schmidt, E., R. Dos Santos and P. Horta (2010) Effects of UVB radiation on the agarophyte *Gracilaria domingensis* (Rhodophyta,

Gracilariales): Changes in cell organization, growth and photosynthetic performance. *Micron* **41**(91), 9–930.
31. Schmidt, E., M. Maraschin and Z. Bouzon (2010) Effects of UVB radiation on the carragenophyte *Kappaphycus alvarezii* (Rhodophyta, Gigartinales): Changes in ultrastructure, growth, and photosynthetic pigments. *Hydrobiol.* **649**, 171–182.
32. Schmidt, E., B. Pereira, R. Santos, C. Gouveia, G. Costa, G. Faria, F. Scherner, P. Horta, M. Paula, A. Latini, F. Ramlov, M. Maraschin and Z. Bouzon (2012) Responses of the macroalgae Hypnea musciformis after in vitro exposure to UV-B. *Aquatic. Bot.* **100**, 8–17.
33. Schmidt, E., B. Pereira, C. Pontes, R. Santos, F. Scherner, P. Horta, M. Paula, A. Latini, M. Maraschin and Z. Bouzon (2012) Alterations in architecture and metabolism induced by ultraviolet radiation-B in the carragenophyte *Chondracanthus teedei* (Rhodophyta, Gigartinales). *Protoplasma* **249**, 353–367.
34. Schmidt, E., R. Santos, C. Faveri, P. Horta, M. Paula, A. Latini, F. Ramlov, M. Maraschin and Z. Bouzon (2012) Response of the agarophyte *Gelidium floridanum* after in vitro exposure to ultraviolet radiation B: Changes in ultrastructure, pigments, and antioxidant systems. *J. Appl. Phycol.* **24**(134), 1–1352.
35. Bouzon, Z., F. Chow, C. Zitta, R. Santos, L. Ouriques, M. Felix, L. K. Polo, C. Gouveia, R. Martins, A. Latini, F. Ramlov, M. Maraschin and E. Schmidt (2012) Comparative analysis of the chloroplast organization and metabolism in the red algae *Porphyra acanthophora var. Brasiliensis* under UVB radiation plus par, par-only and natural radiation. *Microsc. Microana.* **18**(146), 7–1479.
36. Shoenwaekler, M. (2002) The occurrence and cellular significance of physodes in the brown algae. *Phycol* **41**, 125–139.
37. Arroniz-Crespo, M., R. Sinha, J. Martinez-Abaigar, E. Nuñez-Olivera and D. Hader (2005) Ultraviolet radiation-induced changes in mycosporine-like amino acids and physiological variables in the red alga *Lemanea fluviatilis*. *J. Freshwat. Ecol.* **20**(67), 7–687.
38. Korbee, N., F. Figueroa and J. Aguilera (2005) Effect of light quality on the accumulation of photosynthetic pigments, proteins and mycosporine-like amino acids in the red alga *Porphyra leucosticta* (Bangiales, Rhodophyta). *J. Photochem. Photobiol.* **80**(7), 1–78.
39. Bischof, K., D. Hanelt, C. Wiencke and P. Brouwer (1998) Acclimation of brown algal photosynthesis to ultraviolet radiation in Arctic coastal waters (Spitsbergen, Norway). *Polar Biol.* **20**(38), 8–395.
40. Bischof, K., D. Hanelt and C. Wiencke (1998) UV-radiation can affect depth-zonation of Antarctic macroalgae. *Mar. Biol.* **131**(59), 7–605.
41. Bischof, K., D. Hanelt and C. Wiencke (1999) Acclimation of maximal quantum yield of photosynthesis in the brown alga *Alaria esculenta* under high light and UV radiation. *Plant Biol.* **1**(43), 5–444.
42. Aguilera, J., U. Karsten, H. Lippert, B. Vögele, E. Philipp, D. Hanelt and C. Wiencke (1999) Effects of solar radiation on growth, photosynthesis and respiration of marine macroalgae from the Arctic. *Mar. Ecol. Prog. Ser.* **191**(10), 9–119.
43. Edwards, P. (1970) Illustrated guide to the seaweeds and sea grasses in the vicinity of Port Aransas. *Texas. Contr. Mar. Sci.* **15**, 1–228.
44. Penniman, C., A. Mathieson and C. Penniman (1986) Reproductive phenology and growth of *gracilaria tikvahiae* Mclachlan (gigartinales, rhodophyta) in the Great Bay Estuary, New Hampshire. *Bot. Mari.* **29**(14), 7–154.
45. Jeffrey, S. and G. Humphrey (1975) New spectrophotometric equations for determining chlorophylls a, b. c 1 and c 2 in higher plants, algae and natural phytoplankton. *Biochem. Physiol. Pflanzen.* **167** (19), 1–194.
46. Waterman, P. and S. Mole (1994) *Analysis of Phenolic Plant Metabolites*. Blackwell Scientific Publications, Oxford, Great Britain.
47. Kim, J., J. Noh, S. Lee, J. Choi, H. Suh, H. Chung, Y. Song and W. Choi (2002) The first total synthesis of 2,3,6-tribromo-4,5- dihydroxybenzyl methyl ether (TDB) and its antioxidant activity, Bull. *Korean Chem. Soc.* **23**(66), 1–662.
48. Ouriques, L. and Z. Bouzon (2000) Stellate chloroplast organization in *Asteronema breviarticulatum* comb. nov. *(Ectocarpales, Phaeophyta). Phycol.* **39**(26), 7–271.
49. Schreiber, U., U. Schliwa and W. Bilger (1986) Continuous recordings of photochemical and non-photochemical chlorophyll fluorescence quenching with a new type of modulation fluorometry. *Photosyn. Res.* **10**(5), 1–62.
50. Schreiber, U. and C. Neubauer (1990) O_2-dependent electron flow, membrane energization and the mechanism of non-photochemical quenching of chlorophyll fluorescence. *Photosynth. Res.* **25**(27), 9–293.
51. Grymskl, J., G. Johnsen and E. Sakshaug (1997) The significance of intracellular selfshading on the bicoptical properties of brown, red and green macroalgae. *J. Phycol.* **33**(40), 8–414.
52. Figueroa, F., C. Nygard, N. Ekelund and I. Gómez (2003) Photobiological characteristics and photosynthetic UV responses in two *Ulva* species (Chlorophyta) from southern Spain. *J. Photochem. Photobiol.* **72**(3), 5–44.
53. Platt, T., C. Gallegos and W. Harrison (1980) Photoinhibition of photosynthesis in natural assemblages of marine phytoplankton. *J. Mar. Res.* **38**(68), 7–701.
54. Pessoa, F. (2012) Harmful effects of UV radiation in Algae and aquatic macrophytes. A review. *Emirates Journal of Food and Agriculture.*
55. Gao, K. and J. Xu (2008) Effects of solar UV radiation on diurnal photosynthetic performance and growth of *Gracilaria lemaneiformis* (Rhodophyta). *Euro. J. of Phycol.* **43**, 297–307.
56. Xu, J. and K. Gao (2010) UV-A enhanced growth and UV-B induced positive effects in the recovery of photochemical yield in *Gracilaria lemaneiformis* (Rhodophyta). *J. Photochem. Photobiol B Biol* **100**, 117–122.
57. Makarov, M. (2009) Influence of ultraviolet radiation on the growth of the dominant macroalgae of the Barents Sea. *Chem. Glob; Chan. Sci.* **1**, 461–469.
58. Shelton, R., M. Lebert and D. Häder (1998) Differential behaviour of two cyanobacterium species to UV radiation Artificial UV radiation induces phycoerythrin synthesis. *J. Photochem. Photobiol* **44** (17), 5–183.
59. Vincent, W. and P. Neale (2000) Mechanisms of UV damage to aquatic organisms. In *The Effects of UV Radiation in the Marine Environment*, (Edited byS. J. De Mora, S. Demers, and M. Vernet), pp. 149–176. Cambridge University Press, Cambridge.
60. Fogal, C., M. Buyarski and M. Kma (2007) Solar ultraviolet-B radiation increases phenolic content and ferric reducing antioxidant power in *Avena sativa*. *Molecules* **12**, 1220–123.
61. Malanga, M. and S. Puntarulo (2001) Iron-dependent oxidative stress in *Chlorella vulgaris*. *Plant Sci.* **161**, 9–17.
62. Dummermuth, A., U. Fish, K. Könning and C. Wiencke (2003) Responses of marine macroalgae to hydrogen-peroxide stress. *J. Exp. Mar. Biol. Ecol.* **289**(10), 3–121.
63. Schönwälder, M. (2008) The biology of phenolic containing vesicles. *Algae* **23**(16), 3–75.
64. Abdala-Díaz, R., A. Cabello-PasinI, E. Pérez-Rodríguez and F. Figueroa (2006) Daily and seasonal variations of optimum quantum yield and PC in *Cystoseira tamariscifolia* (Phaeophyta). *Mar. Biol.* **148**(45), 9–465.
65. Gallego, H. and M. Tomaro (2002) Effect of UV-B radiation on antioxidant defense system in sunflower cotyledons. *Plant Sci.* **162**(93), 9–945.
66. Shiu, C. and T. Lee (2005) Ultraviolet-B-induced oxidative stress and responses of the ascorbate-glutathione cycle in a marine macroalga *Ulva fasciata*. *J. Exp. Bot.* **56**(285), 1–65.
67. Kawaguchi, T., S. Ham, Y. Inagaki, M. Yamaguchi and T. Nakamura (2004) Local and chemical distribution of phlorotannins in brown algae. *J. Appl. Phycol.* **16**(29), 1–6.
68. Di Piazza, A., L. Lütz and M. Roleda (2011) Sporogenic and vegetative tissues of *Saccharina latissima* (Laminariales, Phaeophyceae) exhibit distinctive sensitivity to experimentally enhanced ultraviolet radiation:Photosynthetically active radiation ratio. *Phycol. Res.* **59**, 221–235.
69. Roleda, A. and C. Lütz (2009) The vegetative arctic freshwater green alga *Zygnema* is insensitive to experimental UV exposure. *Micron* **40**(83), 1–838.
70. Roleda, M., U. Lütz-Meindl, C. Wiencke and C. Lütz (2010) Physiological, biochemical, and ultrastructural responses of the green macroalga *Urospora penicilliformis* from Arctic Spitsbergen to UV radiation. *Protoplasma* **243**(10), 5–116.
71. Jones, L. and B. Kok (1966) Photoinhibition of chloroplast reaction. *Part I. Kinetics and action spectrum. Plant Physiol.* **41**(103), 4–1037.
72. Aro, E., I. Virgen and B. Andersson (1993) Photoinhibition of Photosystem II. Inactivation, protein damage and turnover. *Biochim Biophy Acta.* **1143**(11), 3–134.
73. Gómez, I. and P. Huovinen (2011) Morpho-functional patterns and zonation of South Chilean seaweeds: The importance of photosynthetic and bio-optical traits. *Mar. Ecol. Prog. Ser.* **422**(7), 7–91.

ANEXO 5

J Appl Phycol (2015) 27:887–899
DOI 10.1007/s10811-014-0381-8

Metabolic profile of the brown macroalga *Sargassum cymosum* (Phaeophyceae, Fucales) under laboratory UV radiation and salinity conditions

Luz K. Polo · Marthiellen R. L. Felix · Marianne Kreusch · Debora T. Pereira · Giulia B. Costa · Carmen Simioni · Roberta de Paula Martins · Alexandra Latini · Eny S. I. Floh · Fungyi Chow · Fernanda Ramlov · Marcelo Maraschin · Zenilda L. Bouzon · Éder C. Schmidt

Received: 10 January 2014 / Revised and accepted: 21 July 2014 / Published online: 21 September 2014
© Springer Science+Business Media Dordrecht 2014

Abstract The metabolic profile of the brown macroalga *Sargassum cymosum* was analyzed after 7 days of laboratory cultivation in three salinities (30, 35, and 40 psu) and four irradiation treatments for 3 h per day: PAR-only (control; 70 μmol photons m^{-2} s^{-1}), PAR+UVA (0.70 W m^{-2}), PAR+UVB (0.35 W m^{-2}), and PAR+UVA+UVB. Carbon (C) and nitrogen (N) levels, protein content, free polyamines (PAs), carbohydrates, phenolics, and enzymatic activities of NADH dehydrogenase and complex II were analyzed. Treatments showed variations in CN levels, with a significant reduction of C, but no evident trend for N, probably as a result of C-N balance allocation for basic biological maintenance and stress defense metabolism. Three different PAs were detected, including putrescine (PUT), spermidine (SPD), and spermine (SPM), and their variation could be explained by a defense mechanism in which PAs bound to phenolic compounds migrate through the cell wall and then degrade, concurrent with the photoprotective degradation of chlorophyll. Metabolic profiles detected through attenuated total reflection Fourier transform infrared spectroscopy/principal component analysis (ATR-FTIR/PCA) mostly showed differences in the metabolism of proteins and phenolics. It can be concluded that *S. cymosum* is less affected by salinity than exposure to ultraviolet radiation (UVR). Further studies are required to better understand the variation in PAs under resistance to stress. In addition to its exploitation as a complementary compound in fertilizer, it is suggested that *S. cymosum* could also be studied as a natural product for its antioxidant properties and high presence of phenolics and PAs, in addition to its use in nutraceutical products, human food, and animal feed.

L. K. Polo · M. R. L. Felix · C. Simioni
Plant Cell Biology Laboratory, Department of Cell Biology, Embryology and Genetics, Federal University of Santa Catarina, CP 476, Florianópolis, SC 88049-900, Brazil

M. Kreusch · D. T. Pereira · G. B. Costa
Scientific Initiation-PIBIC-CNPq, Department of Cell Biology, Embryology and Genetics, Federal University of Santa Catarina, CP 476, Florianópolis, SC 88049-900, Brazil

R. d. P. Martins · A. Latini
Laboratory of Bioenergetics and Oxidative Stress, Department of Biochemistry, Federal University of Santa Catarina, CP 476, Florianópolis, SC 88049-900, Brazil

E. S. I. Floh
Plant Cell Biology Laboratory, Department of Botany, Institute of Biosciences, University of São Paulo, São Paulo, SP 05508-090, Brazil

F. Chow
Laboratory of Marine Algae, Department of Botany, Institute of Bioscience, University of São Paulo, São Paulo, SP 05508-090, Brazil

F. Ramlov · M. Maraschin
Plant Morphogenesis and Biochemistry Laboratory, Federal University of Santa Catarina, CP 476, Florianópolis, SC 88049-900, Brazil

Z. L. Bouzon
Central Laboratory of Electron Microscopy, Federal University of Santa Catarina, CP 476, Florianópolis, SC 88049-900, Brazil

É. C. Schmidt (✉)
Postdoctoral Research of Postgraduate Program in Cell Biology and Development, Department of Cell Biology, Embryology and Genetics, Federal University of Santa Catarina, CP 476, Florianópolis, SC 88049-900, Brazil
e-mail: edcash@ccb.ufsc.br

Keywords Antioxidant activity · Carbon and nitrogen balance · Polyamines · Photoprotection · *Sargassum cymosum* · Ultraviolet radiation

Introduction

Solar radiation that reaches the Earth's surface mainly consists of ultraviolet radiation (UVR), photosynthetically active radiation (PAR), and infrared radiation (IR) (Diffey 2002). UVR penetrates to ecologically significant depths in aquatic systems that can negatively influence aquatic organisms from major primary producers to all consumers in the food chain (Häder et al. 2007). However, for aquatic macrophytes acclimated to high solar radiation and growing at the upper shoreline, UVB may facilitate or induce recovery processes (Hanelt and Roleda 2009). Also, moderate levels of UVA may stimulate photosynthesis and growth in both microalgae and macroalgae (Gao and Xu 2008; Xu and Gao 2009).

Salinity fluctuation in marine environments is another abiotic factor that can have a deleterious effect on aquatic organisms. During past decades, reports of the Intergovernmental Panel on Climate Change (IPCC) have shown that changes in precipitation have occurred (Parry et al. 2007). In South America, these changes include an increase in rainfall in southeast Brazil, Paraguay, Uruguay, the Argentinean Pampas, and some parts of Bolivia (Parry et al. 2007). Such rainfall increases in coastal areas, and drainage basins can lead to higher freshwater volumes seaward, and decreasing salinity can occur along the coast (Schemer et al. 2012). Changes in salinity can drive ecological alterations in seaweed communities since different levels of salinity determine richness and distribution of species in general (Wilkinson 1981; Martins et al. 1999; Wilkinson et al. 2007). Many physiological aspects of brown seaweeds can be affected by salinity variation, such as reproduction patterns of *Sargassum muticum* (Yendo) Fesholt (Norton 1977; Hales and Fletcher 1990; Steen 2004) and *Alaria esculenta* (Linnaeus) Greville (Fredersdorf et al. 2009); growth rates of *Laminaria digitata* (Hudson) J.V. Lamouroux, *Fucus vesiculosus* Linnaeus, *Fucus serratus* Linnaeus (Gordillo et al. 2002), and *S. muticum* (Steen 2004); and pigment loss and high mortality in *A. esculenta*, *Saccharina latissima* (Linneus), Lane, Mayes, Druehl & Saunders and *Laminaria solidungula* J. Agardh (Karsten 2007).

Macroalgae are major biomass producers on rocky shores and continental shelves. Macroalgal canopies form habitats for many species of larval fish, crustaceans, and other marine organisms. In macroalgae, photobiological studies indicate diverse physiological alterations in response to UVR that include pigment degradation, dynamic or chronic photoinhibition of photosynthesis, and DNA damage (Häder and Figueroa 1997; Pakker et al. 2000a, b; Pescheck et al. 2014, 2014).

Additionally, polyamines (PAs), including putrescine (PUT), spermidine (SPD), and spermine (SPM), are small flexible organic polycations found in almost all cells (Santa-Catarina et al. 2007; Fuell et al. 2012). Because of their biochemical properties, PAs are involved in several processes, including cell growth, plant development, and responses against multiple stress events. Studies have demonstrated that plants use PAs as structural platforms for building a wide range of specialized chemical defenses, including alkaloids and hydroxycinnamic acid amides (Fuell et al. 2012). Until now, little has been known about the effect of UVR and salinity on the content of PAs in brown algae. In marine algae, PAs have been studied in relation to their occurrence within different algal groups (Hamana and Matsuzaki 1982), in particular, their involvement in cell division (Cohen et al. 1984). Endogenous levels, uptake, and transport of PAs within the thallus have been reported for *Ulva rigida* C. Agardh (Baldini et al. 1994). Lee (1998) reported the accumulation of PUT and SPD in relation to lethal hyposaline stress in several species of intertidal marine macroalgae. In addition, PAs have been used to study the in vitro regulatory events of sporeling morphogenesis for *Grateloupia doryphora* (Montagne) M.A. Howe (García-Jiménez et al. 1998; Marián et al. 2000). Schweikert et al. (2014) found that changes in the PA synthesis pathway in *Pyropia cinnamomea* (W.A. Nelson) W.A. Nelson in response to UVR were related to arginine decarboxylase (ADC) activity, an enzyme responsible for increased PA levels during stress exposure.

In past years, metabolomics has emerged as the newest area in functional genomic studies to survey both quantitatively and qualitatively the whole metabolites of an organism, reflecting the genome and proteome of a given sample as analyzed. Among the spectroscopic techniques, attenuated total reflection Fourier transform infrared spectroscopy (ATR-FTIR) has been a high-throughput technique commonly used in the chemical investigation of complex biological matrices, allowing the detection of metabolic profiles in a nondestructive, rapid, and reagentless way and representing a snapshot of the sample's biochemistry at any given time. In this sense, unsupervised classification methods, such as principal component analysis (PCA), may be employed to explain the model by establishing a subset of class-discriminating features. It compresses the attribute space by identifying the strongest patterns in the data. In this way, the attribute space is reduced by the smallest possible amount of information about the original data (Kuhnen et al. 2010).

The present study is a complementary investigation to a previous study by Polo et al. (2014). When *Sargassum cymosum* was treated with UVR and different salinities, this study used light and transmission electron microscopy to assess its (1) photoacclimation performance and photoprotection response relative to cellular organization and (2) physiological responses, including growth rate,

pigment contents, production of phenolic compounds, DPPH radical scavenging capacity, and photosynthetic performance.

Sargassum C. Agardh is a genus of brown macroalgae widely distributed along the Brazilian coast. Its growth in amid rocky shores provides habitat and refuge for a large number of marine invertebrate juveniles, highlighting its importance to the coastal ecosystem. Some species are considered economically important because they produce chemical compounds with potential biotechnological applications. *Sargassum* is mostly found along rocky shores and could be partially or completely exposed during low tides when the entire thallus is exposed to high UVR. Some studies have reported the effects of UVR on macroalgal photosynthetic performance, but only a few reports have examined the effects of UVR on other biochemical processes. For this study, it was hypothesized that exposure to UVR and different salinities would alter the biochemical, physiological, and morphological processes in *S. cymosum*. Therefore, this study aimed to examine the biological effect of UVR (PAR+UVA, PAR+UVB, and PAR+UVA+UVB) and salinity (30, 35, and 40 psu) on the biochemical profile of the brown macroalga *S. cymosum* by analyzing CN levels, soluble protein contents, free PAs, carbohydrates, total phenolics, and enzymatic activities of NADH dehydrogenase and complex II. As a complement to the work of Polo et al., a better understanding of *S. cymosum*'s physiological behavior under different UVR and salinity regimens is thought to be achieved. Since this report has employed a metabolomics approach, the metabolic profiles of the studied samples were determined by using a nonselective detection analytical technique, i.e., ATR-FTIR spectroscopy, followed by multivariate analysis of the spectral dataset.

Materials and methods

Several individuals of *Sargassum cymosum* were collected at Armação Beach, Ponta das Campanhas (27° 44′ 42″ S and 48° 30′ 27″ W), Florianopolis, SC, Brazil, from November 2012 to February 2013, during the Southern Hemisphere summer season. The algal samples were collected from the rocky shore and transported at ambient temperature in dark containers to LABCEV-Federal University of Santa Catarina (Plant Cell Laboratory, UFSC, Florianopolis, SC, Brazil). Macroepiphytes were meticulously eliminated by cleaning with a brush and washing with filtered seawater. Apical portions of approximately 6 cm were acclimated for 7 days in culture medium with filtered natural seawater (35 psu) plus von Stosch enrichment solution at half strength (VSES/2) and laboratory-controlled conditions of 24±2 °C, continuous aeration, 70±10 μmol photons m^{-2} s^{-1} PAR (fluorescent lamps, Phillips C-5 Super 84 16 W/840, Brazil; LI-COR light meter 250, USA) and 12-h photocycle (starting at 8 a.m.).

After acclimation, apical portions (±2.0 g) were cultivated for 7 days in beakers containing 500 mL of natural sterilized seawater and VSES/2 at 30, 35 (control), and 40 psu under four different conditions of radiation: PAR-only (control), PAR+UVA, PAR+UVB, and PAR+UVA+UVB for 3 h per day. Total doses of PAR, UVA, and UVB irradiances were 657.40 (70±10 μmol photons m^{-2} s^{-1}), 7.56 (0.70 W m^{-2}), and 3.78 kJ m^{-2} (0.35 W m^{-2}), respectively. The different light treatments were achieved based on daily measurements in the natural condition. Twelve treatments were then performed, and four replicates were made for each experimental group. Culture conditions were the same as those described for the acclimation period. VSES was not changed during the 7-day experimental period. Low salinities were obtained with the addition of distilled water, while high salinities were attained through gradual freezing and thawing of seawater until the final concentration was reached. UVR was provided through a Vilber Lourmat lamp (VL-6LM, France) with peak output at 312 nm for UVB radiation (UVBR) and peak output at 365 nm for UVAR, as measured with a radiometer Model IL 1400A (International Light, USA).

Carbon and nitrogen analysis

The quantification of cellular carbon (C) and nitrogen (N) was carried out in the Analytic Center of the Chemistry Institute, University of Sao Paulo, Brazil, by using a Perkin-Elmer 2400 (USA) elemental composition analyzer. Dry samples (60 °C) of 500 mg were ground to a fine powder, and aliquots of 1 mg were ashed at 925 °C under pure oxygen, triggering complete oxidation of the material. All C was converted to CO_2. N was changed into several oxides (NxOx) and then to N_2. Individual components from the resultant mixture were separated by reduction chromatographic column (640 °C) and detected through thermal conductivity changes of the products. The total amount of C and N in samples was calculated as a percentage, standardized per dry weight (DW), and expressed as μg g^{-1} DW.

Respiratory chain complex activities

To measure respiratory chain complex activities, samples (n= 4) were homogenized in five volumes of 50 mM phosphate buffer, pH 7.4, containing 0.3 M sucrose, 5.0 mM MOPS, 1.0 mM EGTA, and 0.1 % bovine serum albumin. The homogenates were centrifuged at 2,000×g for 10 min at 4 °C. The pellet was then discarded, and the supernatants were used to measure NADH dehydrogenase activity, succinate-2,6-dichloroindophenol (DCIP)-oxidoreductase (complex II) activity, and soluble protein content. NADH dehydrogenase activity was assessed in supernatants by the rate of NADH-dependent ferricyanide reduction at 420 nm (1.0 mm^{-1} cm^{-1}), as previously described by Martins et al. (2013). The method

©Fungyi Chow / 2021

described to determine this activity was slightly modified, as detailed in a previous report by Latini et al. (2005). The activity of complex II was determined according to the method of Fischer et al. (1985). The method described to determine this activity was slightly modified, as detailed in a previous report by Glaser et al. (2013). Enzyme activity was calculated as nmol min^{-1} mg $protein^{-1}$.

Proteins

Approximately 200 mg fresh weight (FW; $n=4$) of samples were macerated and homogenized in 600 μL of 50 mM potassium phosphate buffer, pH 7.4, and sonicated for 5 min. The amount of soluble protein was determined spectrophotometrically, as described in Lowry et al. (1951), by using bovine serum albumin (BSA, 0–60 mg mL^{-1}; $y=5.9705x+0.0199$; $r^2=0.994$) as standard.

Polyamines

Putrescine (PUT), spermidine (SPD), spermine (SPM), and cadaverine (CAD) were determined according to the procedures described by Silveira et al. (2004) in the Plant Cell Biology Laboratory of the Institute of Bioscience, University of Sao Paulo, Brazil, in association with Dr. Eny I. S. Floh. All procedures were carried out at 4 °C, and the analyses were performed in triplicate. Samples (200 mg FW; $n=3$) were ground in 3 mL of 5 % (*v*/*v*) perchloric acid. After 1 h, the extracted samples were centrifuged for 20 min at 15,000×*g* at 4 °C. The supernatants containing the free PAs were removed and the pellets re-extracted. Supernatants were then combined and the pellets eliminated. Free PAs were determined directly from the supernatant. Aliquots of 40 μL of each sample were derived by adding 100 μL of dansyl chloride, 20 μL of 0.05 mM diaminoheptane, and 50 μL of saturated sodium carbonate. The samples were then incubated in the dark for 50 min at 70 °C for 30 min. The excess of dansyl chloride was eliminated by adding 25 μL of proline solution (100 mg mL^{-1}); the extracts were mixed with 200 μL of toluene and dried under N flux. The dansylated PAs were solubilized in 200 μL of acetonitrile, and aliquots of 20 μL of the dansylated PAs were separated by reverse phase HPLC in a C-18 reverse phase column (Shimadzu Shin-pack CLC ODS, 5-μm particle size, L×I.D. 25 cm×4.6 mm). The gradient was developed by mixing increasing proportions of absolute acetonitrile to 10 % acetonitrile in water (pH 3.5). The gradient of absolute acetonitrile was programmed to 65 % over the first 10 min, from 65 to 100 % between 10 and 13 min, and 100 % between 13 and 21 min. The flow was 1 mL min^{-1} at 40 °C. The fluorescence detector was set at 340 nm (excitation) and 510 nm (emission). A mixture of PUT, SPD, and SPM was used as standard and then calculated as mg g^{-1}. All the analytical HPLC-grade reagents were from Sigma-Aldrich or Merck and were used or prepared as recommended by the manufacturer.

Metabolic profiling by attenuated total reflectance Fourier transform infrared spectroscopy

Algal samples (1 g FW) were dried at 45 °C for 24 h and powdered; KBr was then added for further infrared (IR) spectroscopy analysis. Using a Bomem spectrometer (MB-100) with a DTGS detector, ATR-FTIR spectra were recorded between 4,000 and 400 cm^{-1}, with 64 scans having a resolution of 4 cm^{-1}. A background spectrum was previously acquired, and the samples (100 mg) were spread and measured directly after pressing them on the crystal. Three replicate spectra (128 co-added scans before Fourier transform) were collected for each sample for a total of 130 spectra. Spectra were normalized, and the baseline was corrected in the region of interest (3,000 to 600 cm^{-1}) by drawing a straight line before resolution enhancement (K-factor of 1.5) using Fourier self-deconvolution (Opus v. 5.0, Bruker BioSpin).

Data analysis

Data were analyzed by bifactorial analysis of variance (ANOVA) and the Tukey's a posteriori test. All statistical analyses were performed using the Statistica software package (Release 10.0), considering $p\leq0.05$. For chemometric analysis, principal component analysis (PCA) was applied to the preprocessed FTIR dataset with the help of The Unscrambler software (Release 10.2, Camo AS, Norway). PCA is a form of multivariate analysis frequently used as a preprocessing and linear dimensionality reduction technique to capture linear dependencies among attributes of a dataset. Therefore, it is commonly used for metabolomics profile studies.

Results

Table 1 shows the two-way ANOVA for the analyzed factors, including contents of C and N; NADH dehydrogenase and complex II activities and protein content; content of free polyamines (PAs), including PUT, CAD, and SPD; and total free PAs and ratio of PUT/SPD.

Carbon and nitrogen analysis

After 7 days of exposure to UVR and different salinity treatments, samples of *S. cymosum* presented statistical differences between the levels of CN (Fig. 1a, b). C levels showed very significant variation in *S. cymosum* (Fig. 1a) under UVR, with a decreasing trend under PAR+UVA and almost all salinities.

Table 1 Two-way ANOVA analysis for carbon (C) and nitrogen (N), NADH dehydrogenase, complex II and proteins, and content of free polyamines (PAs)

	Sum of squares (SS)	Degrees of Freedom	Mean square (MS)	Statistical index (F)	Probability (p)
Carbon					
Intercept	3,249,817	1	3,249,817	980,521.9	**0.000000**
Radiation	1,251	3	417	125.8	**0.000000**
Salinity	189	2	95	28.6	**0.000000**
Radiation x salinity	1,094	6	182	55.0	**0.000000**
Nitrogen					
Intercept	7,365.931	1	7,365.931	195,339.6	**0.000000**
Radiation	2.177	3	0.726	19.2	**0.000001**
Salinity	1.985	2	0.993	26.3	**0.000001**
Radiation x salinity	18.225	6	3.038	80.6	**0.000000**
Putrescine					
Intercept	514.1264	1	514.1264	1,843.257	**0.000000**
Radiation	1.0937	2	0.5468	1.961	0.162688
Salinity	38.7296	3	12.9099	46.285	**0.000000**
Radiation x salinity	2.5268	6	0.4211	1.510	0.217429
Spermidine					
Intercept	0.042641	1	0.042641	795.2644	**0.000000**
Radiation	0.001107	2	0.000554	10.3233	**0.000582**
Salinity	0.004175	3	0.001392	25.9522	**0.000000**
Radiation x salinity	0.001653	6	0.000275	5.1381	**0.001604**
Cadaverine					
Intercept	0.071863	1	0.071863	474.7538	**0.000000**
Radiation	0.000045	2	0.000022	0.1479	0.863323
Salinity	0.001835	3	0.000612	4.0401	**0.018522**
Radiation x salinity	0.002857	6	0.000022	0.1479	0.863323
Free polyamines					
Intercept	536.6422	1	536.6422	1,886.210	**0.000000**
Radiation	1.1360	2	0.5680	1.996	0.157742
Salinity	39.5625	3	13.1875	46.352	**0.000000**
Radiation x salinity	2.5608	6	0.4268	1.500	0.220551
Putrescine/Spermidine					
Intercept	533,870.6	1	533,870.6	636.4587	**0.000000**
Radiation	10,103.2	2	5,051.6	6.0223	**0.007593**
Salinity	16,065.5	3	5,355.2	6.3842	**0.002460**
Radiation x salinity	18,682.6	6	3,113.8	3.7121	**0.009417**
NADH					
Intercept	92,221.83	1	92,221.83	1,778.534	**0.000000**
Radiation	283.92	2	141.96	2.738	0.078195
Salinity	1,923.40	3	641.13	12.364	**0.000010**
Radiation x salinity	421.90	6	70.32	1.356	0.258621
Complex II					
Intercept	481.9669	1	481.9669	1,856.694	**0.000000**
Radiation	3.2045	2	1.6022	6.172	**0.004956**
Salinity	9.8298	3	3.2766	12.623	**0.000009**
Radiation x salinity	18.4918	6	3.0820	11.873	**0.000000**
Proteins					
Intercept	91.19053	1	91.19053	2,030.907	**0.000000**
Radiation	0.45180	2	0.22590	5.031	**0.011837**
Salinity	0.19178	3	0.06393	1.424	0.251789
Radiation x salinity	0.59543	6	0.09924	2.210	0.064473

The bold entries significe (p <0.05)

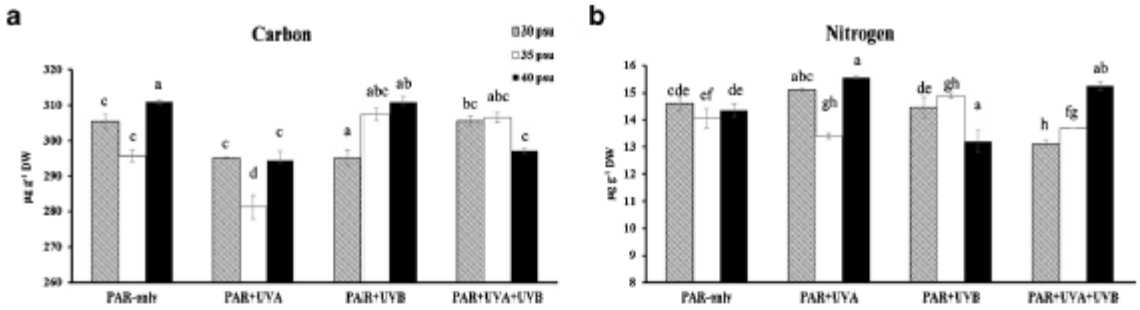

Fig. 1 Content of carbon (C) and nitrogen (N) in *S. cymosum* plants after 7 days of exposure to different laboratory radiation and salinity treatments (n=4, mean±SD). *Letters* indicate significant differences according to bifactorial ANOVA and Tukey's test ($p \leq 0.05$). **a** Carbon. **b** Nitrogen

N levels (Fig. 1b) showed variable fluctuation with no major clear trend for any UVR or salinity.

Respiratory chain complex activities and proteins

After 7 days of cultivation of *S. cymosum* with different radiation and salinity treatments, bifactorial ANOVA showed few statistical differences in the biochemical analyses (Fig. 2a–c). NADH dehydrogenase activity (Fig. 2a) and soluble protein content (Fig. 2c) showed no statistical differences when treated with UVR and salinity. Complex II activity (succinate-2,6-DCIP-oxidoreductase activity) (Fig. 2b) was the only biochemical profile with significant differences between the treatments.

Polyamines

The content of PAs in *S. cymosum* plants under UVR and salinity treatments showed statistical differences (Fig. 3a–e) when compared to control PAR-only. SPM was not detected in any treatment. Putrescine content (Fig. 3a) was negatively influenced by UVR and salinity treatments, especially when treated with PAR+UVA and PAR+UVB. Even though CAD content showed no significant differences under UVR and salinity treatments (Fig. 3b), a diminishing trend was observed in all UVR treatments when compared to control. SPD content presented a significant decrease in almost all UVR and salinity treatments when compared to control at 30 and 35 psu (Fig. 3c).

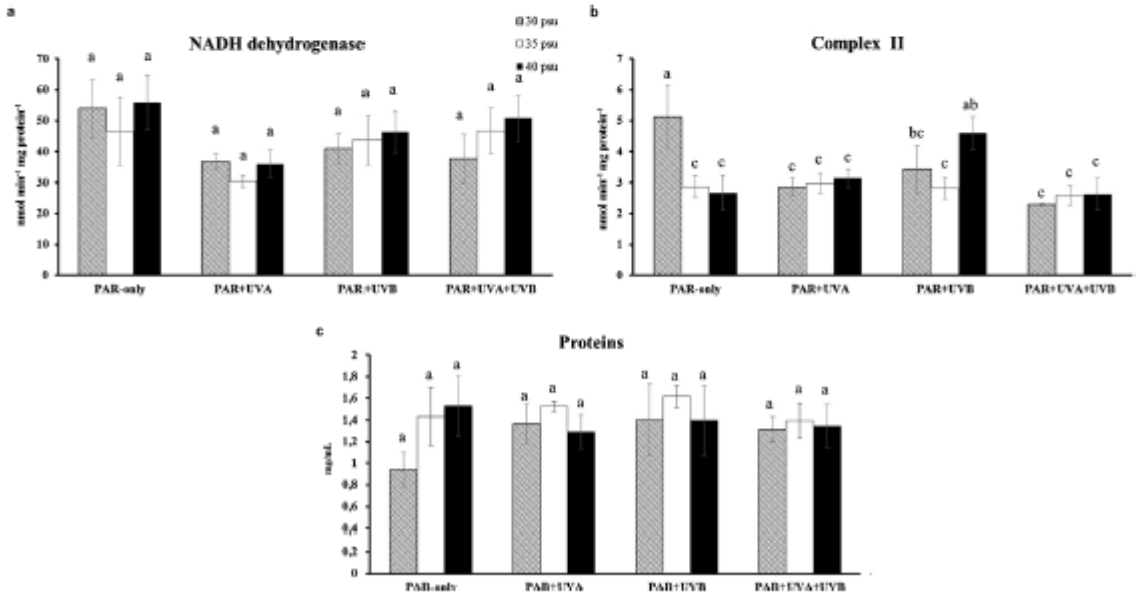

Fig. 2 NADH dehydrogenase and complex II activities and soluble protein content of *S. cymosum* plants after 7 days of exposure to different laboratory radiation and salinity treatments (n=4, mean±SD). *Letters* indicate significant differences according to bifactorial ANOVA and Tukey's test ($p \leq 0.05$). **a** NADH dehydrogenase activity. **b** Complex II activity. **c** Protein content

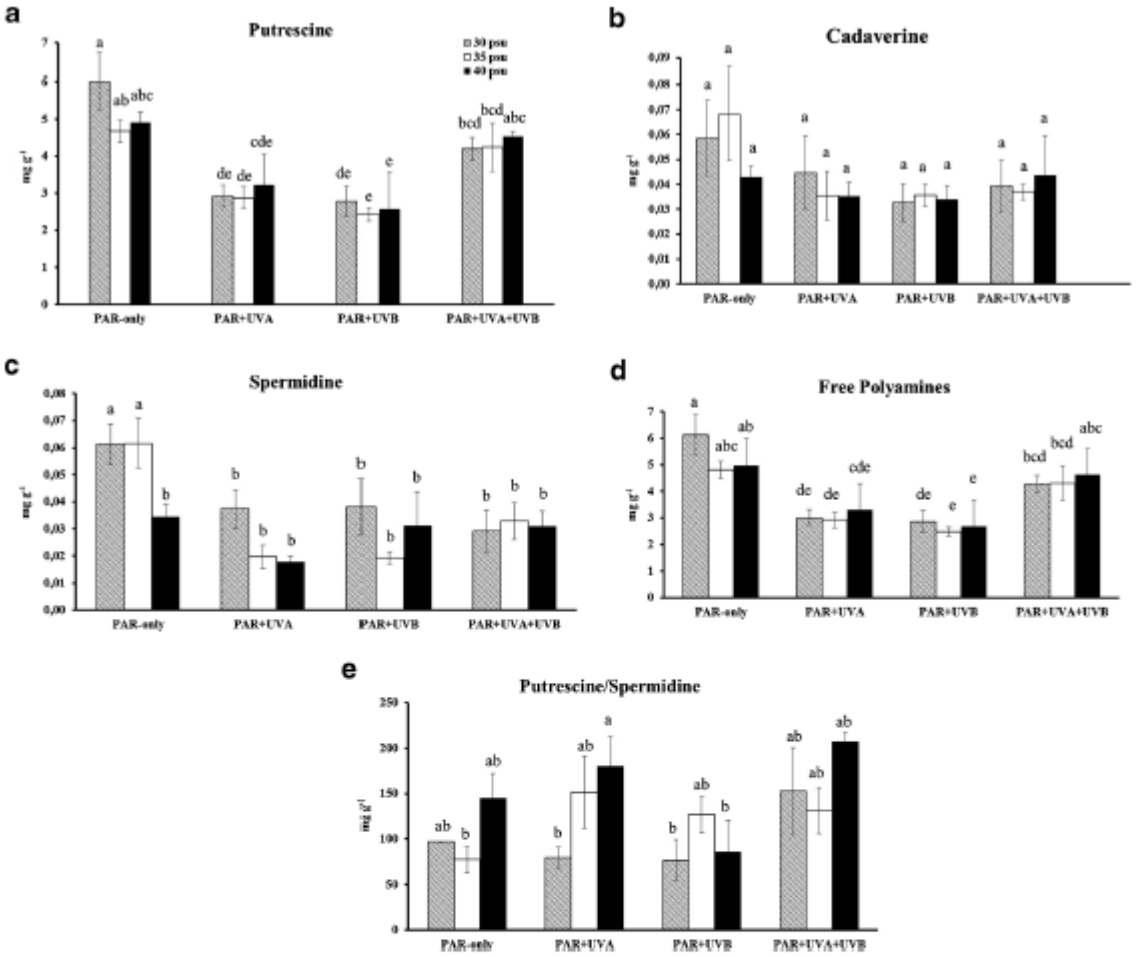

Fig. 3 Content of free polyamines (PAs) of *S. cymosum* plants after 7 days of exposure to different laboratory radiation and salinity treatments ($n=4$, mean±SD). *Letters* indicate significant differences according to bifactorial ANOVA and Tukey's test ($p \leq 0.05$). **a** Putrescine. **b** Cadaverine. **c** Spermidine. **d** Total free polyamines. **e** Ratio of putrescine/spermidine (spermine was determined, and the values for all samples were 0).

Total free PAs (PUT+CAD+SPD) showed statistical differences (Fig. 3d), with a major reduction in their content when plants were treated with PAR+UVA and PAR+UVB. The ratio of PAs (PUT/SPD) also showed statistical differences when treated with UVR and salinity (Fig. 3e). This ratio was lower in control plants and treatment with PAR+UVB in all salinities. The highest values were observed in plants treated with PAR+UVA and PAR+UVB in 40 psu. Salinity itself showed no differences in the ratio of PAs between treatments.

Metabolic profiling by attenuated total reflection Fourier transform infrared spectroscopy and chemometrics

One- and two-dimensional ATR-FTIR spectroscopy has increasingly been used for complex matrix analysis, such as biofluids and plant extracts in metabolomics studies (Kuhnen et al. 2010). FTIR is a physicochemical method that measures the vibrations of bonds within functional groups and generates a spectrum that can be regarded as a metabolic "fingerprint" of the sample. It is a flexible analytical technique that can supply qualitative and, in some cases, quantitative information with minimal, or no, sample preparation of complex biological matrices (Coimbra et al. 1998; Ferreira et al. 2001).

In this study, a descriptive model was built based on the calculation of the principal components (PCAs) for the FTIR dataset. PCA of the FTIR spectral dataset (3,000–600 cm^{-1}) allowed classification of the samples into three groups (data not shown) which, according to the factorial contribution values (loadings), resulted mostly from the carbohydrate constituents (1,057 and 1,012 cm^{-1}) of the algal biomass. Thus, in

a further series of experiments, the principal component calculation took into account the dataset from the spectral windows typical of carbohydrates (1,200–950 cm^{-1}), proteins (1,650–1,550 cm^{-1}), lipids (2,950–2,850 and 1,743 cm^{-1}), and phenolics (920–800 cm^{-1}), as previously reported (Schulz and Baranska 2007; Kuhnen et al. 2010).

The spectral dataset from the fingerprint region of lipids did not allow a clear discrimination of the samples, in contrast to that of carbohydrates, proteins, and phenolic compounds. Similarity was detected in the carbohydrate composition of algal biomasses from the 35 psu plus PAR+UVA treatment and the 30 and 40 psu plus PAR+UVA+UVB treatments which were grouped into PC1+/PC2− (Fig. 4, samples surrounded by ellipsis), mostly by their starchy fraction (1,012 and 1,055 cm^{-1}). However, it was possible to show a distinct metabolic profile resulting from the exposure of the algae to the 40 psu plus PAR+UVA+UVB treatment by using the fingerprint regions of proteins and phenolics. In both cases, the samples were found to co-occur in PC2+/PC1−.

Discussion

In photosynthetic organisms, the stress caused by UVR can lead to diverse morphological-like tissue necrosis and deformation, loss of parts of the thalli, blistering, curling, and thickening of the meristematic region ((Michler et al. 2002; Roleda et al. 2004), as well as anatomical, physiological, biochemical, and molecular alterations. In this sense, high doses of UVR trigger acclimation mechanisms in exposed benthic macroalgae, enabling them to tolerate the stressful condition and generating, in turn, a series of responses to maintain control over biological homeostasis (Viñegla and Figueroa 2009). Fluctuations in salinity represent another stress factor that can have a deleterious effect on marine aquatic organisms by, for example, affecting reproductive patterns in *S. muticum* (Hales and Fletcher 1990; Norton et al. 1996; Steen 2004) and growth rates in *L. digitata*, *F. vesiculosus*, and *F. serratus* (Gordillo et al. 2002). The present study shows that *S. cymosum* presented a series of metabolic responses when exposed to UVR and salinity treatments. Carbon (C) content of *S. cymosum* exhibited a fluctuation between treatments but generally decreased under the influence of UVA, UVB, and UVA+UVB. This reduction of cellular content can represent a defense mechanism by using C storage sources to activate the antioxidant system in order to protect cells against UVR damage. This response can be supported by the carbon-nutrient balance hypothesis (CNBH) which holds that plants acquiring resources in excess of growth demands shunt these resources into the production of secondary metabolites (Lerdau and Coley 2002). Thus, under stressful conditions, such as excess light, temperature, UVR, and fluctuating salinity, but with limited availability of

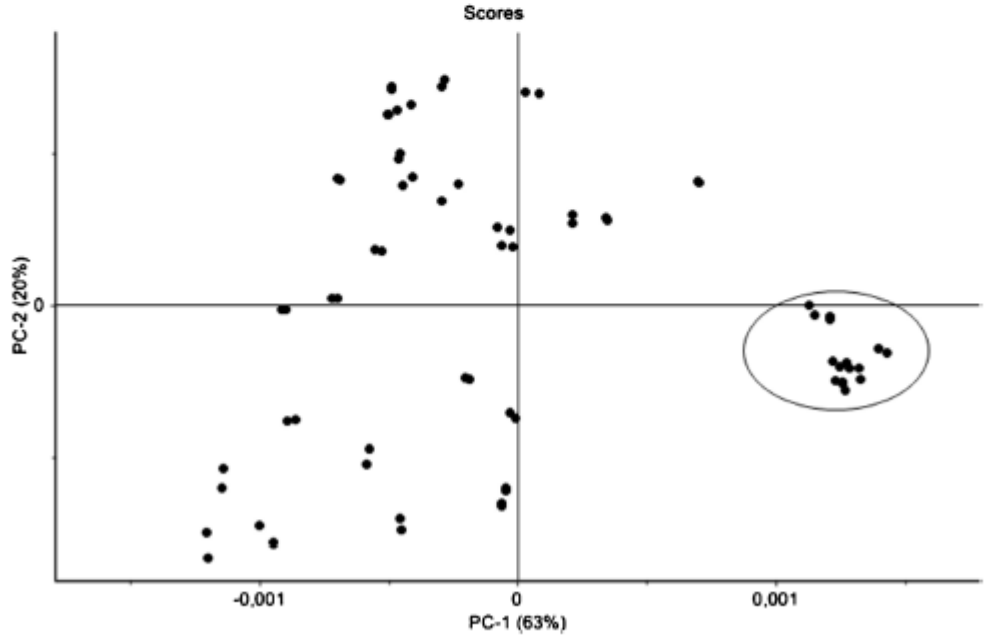

Fig. 4 Principal component analysis (PCA) scores scatterplot for FTIR spectra of *S. cymosum* plants after 7 days of exposure to different laboratory radiation and salinity treatments in the fingerprint region of carbohydrates (950–1,250 cm^{-1} wave number). The grouping of the treated samples with 35 psu plus PAR+UVA and the 30 and 40 psu plus PAR+UVA+UVB into PC1+/PC2− is highlighted by *ellipsis*

©Fungyi Chow / 2021

nutrients, plants are predicted to allocate the "excess" of C to produce phenolic compounds or increase cell wall thickness, as C-based defenses. Polo et al. (2014) reported both phenomena by ultrastructural studies. When *S. cymosum* was treated with UVR, the plant showed an increase in cell wall thickness by the accumulation of multiple cell layers that could act as a protection against the negative effects of high irradiation (Gómez and Huovinen 2011). In the same study (Polo et al. 2014), the authors reported an increase in physodes containing phenolic compounds nearly to the cell wall and extruding through it, probably acting as a photoprotective mechanism against UVR. On the other hand, although nitrogen (N) content did not show a clear trend, it was still significantly affected. Again, the dynamic fluctuation of tissue N can be related to the allocation of energy (C) and nutrient (N) to activate defense mechanisms that preserve physiological homeostasis and cellular integrity. However, according to Hamilton et al. (2001), C and N are allocated to the production of secondary metabolites only after the requirements for growth are met.

Tissue C and N contents, which are closely related to the nutritional state of macroalgae for normal growth (Lapointe 1981; Lapointe and Duke 1984; Hwang et al. 1987; Andria et al. 1999), act as a dynamic source of storage for allocation of C and N balance. C allocation under stress conditions has been reported for other algae (Shuter 1979; Arnold and Manley 1985; Macler 1988; Smith et al. 1989; Legendre et al. 1992; Mock and Gradinger 2000; Plante and Arts 2000; Lee et al. 2008), and C flux through glycolytic and respiratory pathways can boost protective mechanisms, thus avoiding unnecessary accumulation as reserve (Turpin et al. 1988; García-Sánchez et al. 1993; Vergara et al. 1995). The fluctuating response of C content in *S. cymosum* exposed to UVR condition could explain the increasing trend of growth rate observed for the same species by Polo et al. (2014). In this case, C storage was found to be allocated for both growth and defense, most likely by producing secondary metabolites as phenolic compounds.

In conditions of high availability of N, it has been reported that tissue C content decreases in response to N assimilation (García-Sánchez et al. 1993; Vergara et al. 1995). In the present study, this situation was observed in all UVR-treated *S. cymosum* plants, with C levels trending toward reduction when exposed to UVR and salinity. The influence of N on the metabolism of macroalgae is important since this element is essential for the maintenance of several metabolic routes. In addition, algae are more sensitive to environmental variations when their intracellular N reserves are exhausted. No consensus has been reached on the ultimate limiting nutrient in the marine environment, but several studies suggest N as the immediately limiting nutrient (Lobban and Harrison 1994), and as reported by some authors, an increase in availability of N, such as nitrate and ammonium, will result in higher growth rates in various algae (Ryther and Dustan 1971; DeBoer et al. 1978; Bird et al. 1982; Lapointe and Duke 1984; Hanisak 1990; García-Sánchez et al. 1993; Chow and Oliveira 2008; Chow 2012).

In the present study, NADH dehydrogenase activity of *S. cymosum* showed no differences in any of the treatments. These results differ from those observed by Schmidt et al. (2012b) for the macroalga *Hypnea musciformis* (Wulfen) J.V. Lamouroux in which an increase in NADH dehydrogenase activity was evidenced when exposed to PAR+UVBR. Complex II activity decreased in all *S. cymosum* plants cultivated in 30 psu after exposure to UVR. These results agree with impaired mitochondrial function, probably resulting from a blockage in the electron transport system induced by the stress-inducing treatments. Under these conditions, complexes I and II of the respiratory chain favor the generation of mitochondrial reactive oxygen species (ROS) (Turrens 1997; Turrens and Boveris 1980). Furthermore, ROS formed at the NADH dehydrogenase site of complex I are released into the mitochondrial matrix (Chen et al. 2003), thereby eliciting oxidative damage to mitochondrial enzymes, including the complexes of the respiratory chain, enzymes of the Kreb's cycle, and several other sensitive proteins, as well as mtDNA (Bandy and Davison 1990; Zhang et al. 1990; Hausladen and Fridovich 1994). However, *S. cymosum* plants treated with 35 and 40 psu showed no differences in NADH dehydrogenase and complex II activity.

Soluble protein content of *S. cymosum* showed no significant differences. However, for other macroalgae species, the combination of PAR+UVR has been reported to inhibit protein metabolism, probably by altering biosynthesis pathways or protein mobilization for repair processes, including the activation of antioxidant defense (Poppe et al. 2002; Schmidt et al. 2012a).

Few reports have examined the metabolism of polyamines (PAs) in macroalgae, and many studies have focused on the roles that PAs play in cellular development or in response to salinity (Schweikert et al. 2011). Recent studies have correlated the function of PAs with abiotic stress defense mechanisms, and in the present study, PA levels showed significant changes when treated with UVR and salinity. PAs are a group of aliphatic amines important for both plant and algal development and stress resistance (Martin-Tanguy 2001; Li and Burritt 2003; Hunter and Burritt 2005; Baron and Stasolla 2008; Burritt 2008), and their importance in the membranes of photosynthetic complexes has also been demonstrated in unicellular algae (Beigbeder et al. 1995; Doernemann et al. 1996; Sfichi et al. 2004; Sfichi-Duke et al. 2008). They are found as free amines bound to small molecules, such as hydroxycinnamic acid, or to larger molecules, such as proteins or nucleic acids, with the most common PAs being putrescine (PUT), spermidine (SPD), and spermine (SPM) (Tiburcio et al. 1993; Lee 1998). While SPM was not detected in this

©Fungyi Chow / 2021

study, the more uncommon cadaverine (CAD) was detected. Other authors have also reported CAD in a large number of biological systems, including land plants, animals, and other groups of algae and bacteria (Smith et al. 2001).

UVR and salinity trigger biochemical and metabolic protective responses in plants and algae, including changes in antioxidant molecules and enzymatic activities, as well as the content of PAs. PUT usually increases in response to stress (Flores 1991), but in this study, a decrease in PUT and SPD contents was observed in plants treated with UVR. These results also differ from those of Schweikert et al. (2011) who reported that exposure of *P. cinnamomea* to UVA showed nonsignificant fluctuations in the levels of PAs, but when treated with UVB, an increase in PAs was observed. Smith et al. (2001) also found that UVA had no statistically significant effect on the level of PAs in higher plants.

Several environmental stresses, like temperature, gaseous pollutants, and contrary to the findings of the present study, UVB, are related to an increase in free PUT (Flores 1991; Kramer et al. 1991, 1992). Although levels can increase in response to stress, the efficacy of PUT in plant defense is uncertain, and its high levels are often associated with high levels of cell division and DNA replication (Galston and Kaur-Sawhney 1995). Since (1) SPD is synthesized from PUT and (2) the levels of PUT decreased in response to UVR, a reduction in SPD is also expected. SPD is not usually associated with responses to environmental stress (Flores 1991), but its exogenous application has been reported to be effective in preventing stress-induced injury via unknown mechanisms (Bors et al. 1989).

Several factors could play an important role in the reduction of PAs, as observed in this study. First, the amount of PAR delivered during exposure to UVR in the present study was 70 μmol photons m^{-2} s^{-1}, which is a low irradiance treatment when compared to other studies. Studies on higher plants have shown that changes of PAs under UVB are dependent on the amount of PAR delivered during the application of UVB such that PAR levels below 300 μmol photons $m^{-2}s^{-1}$cause a general decline in total PAs (Cen and Bornman 1990; Kramer et al. 1992; Smith et al. 2001). It has been observed that the background level of PAR determines whether PAs will increase or decrease in response to stress, suggesting light as a regulatory factor. Second, levels of PAs can increase in response to UVB by binding to phenolic molecules. Moreover, PAs are involved in establishing the primary cell wall by helping to cross-link cellular components, such as polysaccharide-bound phenols (Miret et al. 1992; Berta et al. 1997). Therefore, levels of major PAs could be a reflection of PAs bound to phenolic compounds and polysaccharides as conjugates, the most defensive form of PAs. Additionally, Polo et al. (2014), using microscopy analyses, detected phenolic compounds migrating through the cell wall, but degrading. This could also explain the low levels of free PAs found in *S. cymosum*. In addition, the same authors found that the absorbance screening of the extruded substance to the seawater from UVR treatments showed an increase of compounds absorbing between 300 and 400 nm, probably related to the outflow of phenolic compounds and other UV-absorbing compounds. This could explain why it was not possible to detect conjugated PAs. Third, chlorophyll levels are also dependent on light, and they are closely associated with PAs. All photosynthetic pigment-protein complexes contain PAs in the conjugated form, including the reaction center of PSII (Kotzabasis et al. 1993). These complexes also regulate chlorophyll biosynthesis (Beigbeder and Kotzabasis 1994), stabilize thylakoid membrane, retard protein degradation, and inhibit chlorophyll decomposition (Besford et al. 1993). Given these collective functions, the decrease of free PAs in *S. cymosum* plants treated with UVR could be associated with the chlorophyll loss reported by Polo et al. (2014) for this species. In this way, PAs degraded in response to UVB may contribute to the oxidative burst that initiates the signal transduction pathway leading to the induction of stress defense mechanisms (Smith et al. 2001). Finally, it has been reported that PAs play a key role in regulating the structure and function of the photosynthetic apparatus (Kotzabasis et al. 1993; Sfichi et al. 2004). For example, when endogenous plant balances have been restored by secondary responses (e.g., biosynthesis of carotenoids, in the case of UVB treatment) and the plant is acclimating to the altered environmental conditions, thylakoid-associated PAs are reduced (Lütz et al. 2005). Under these conditions, an increase in bound PAs, whether by conjugation to phenolics or by establishing the primary cell wall, could cause the content of free PAs to decrease as a hypersensitive response (Torrigiani et al. 1997), which bears a resemblance to common UVB responses, i.e., an oxidative burst and subsequent cell death (Allen and Fluhr 1997).

Similarities in metabolic profiles of carbohydrates, proteins, and phenolics of *S. cymosum* exposed to UVR were also detected through ATR-FTIR coupled to PCA, a multivariate statistical technique, thus adding extra information not detected by the biochemical analyses. The starch metabolism of the algae seemed to be sensitive to the variations of UVR and salinity according to the findings herein shown. Moreover, the exposure to 40 psu plus PAR+UVA+UVB treatment imposed a perturbation to the plants' phenolic and protein metabolism. While it is not a selective technique, ATR-FTIR spectroscopy has been able to discriminate among biological samples according to their chemical components when coupled to multivariate statistical techniques as employed in the present study. Taken together, the results from this preliminary metabolomics approach suggest the need for further studies on the phenolic compounds and protein metabolism of *S. cymosum* in response to exposure to high salinity and PAR+UVA+UVB radiation.

Meanwhile, based on the results of the present study, we can conclude that *S. cymosum* is more sensitive to UVR than salinity. The fluctuation of CN could be explained by the carbon-nitrogen balance hypothesis, in which the allocation of these resources is used to maintain such basic biological pathways as growth and promote defense mechanisms against UV radiation, such as polysaccharide thickening of the cell wall, phenolics compounds as physodes, and PAs. Decrease in the content of PAs could be related to (1) the low amount of PAR delivered during exposure to UVR, (2) PAs bound to phenolic compounds migrating through the cell wall and subsequently being degraded, or (3) chlorophyll degradation and concurrent reduction of PAs associated with chlorophylls. This is one of the few studies relating abiotic stress conditions to the content of PAs; however, further studies are required to elucidate variations in the levels of free and conjugated PAs upon exposure of algae to UVR. The fact that PUT was found at levels similar to those of the seaweed concentrate made from *Ecklonia maxima* (Osbeck) Papenfuss (Papenfus et al. 2012), which is used to improve the health and growth of higher plants as a natural biostimulus, suggests that *S. cymosum* could be exploited as a complementary compound added to commercial fertilizers. Finally, the fact that *S. cymosum* possesses effective defense mechanisms against UVR and salinity makes it a potential species for studies related to its use as a natural product, in addition to its potential use in nutraceutical products, human food, and animal feed.

Acknowledgments The authors would like to acknowledge CAPES. Éder C. Schmidt holds a postdoctoral fellowship from CAPES. Zenilda L. Bouzon is a CNPq fellow. Fungyi Chow is a FAPESP and CAPES fellow. This study is part of the MSc dissertation of the first author.

References

Allen AC, Fluhr R (1997) Two distinct sources of elicited reactive oxygen species in tobacco epidermal cells. Plant Cell 9:1559–1572

Andria JR, Vergara JJ, Llorens LP (1999) Biochemical responses and photosynthetic performance of *Gracilaria* sp. (Rhodophyta) from Cádiz, Spain, cultured under different inorganic carbon and nitrogen levels. Eur J Phycol 34:497–504

Arnold KE, Manley SL (1985) Carbon allocation in *Macrocystis pyrifera* (Phaeophyta): intrinsic variability in photosynthesis and respiration. J Phycol 21:154–167

Baldini L, Pitocchi R, Bagni N (1994) Polyamine transport in the seaweed *Ulva rigida* (Chlorophyta). J Phycol 30:599–605

Bandy B, Davison AJ (1990) Mitochondrial mutations may increase oxidative stress: implications for carcinogenesis and aging? Free Rad Biol Med 8:523–539

Baron K, Stasolla C (2008) The role of polyamines during in vivo and in vitro development. In Vitro Cell Dev Biol Plant 44:384–395

Beigbeder A, Kotzabasis K (1994) The influence of exogenously supplied spermine on protochlorophyllide and chlorophyll biosynthesis. J Photochem Photobiol B 23:201–206

Beigbeder A, Vavadakis M, Navakoudis E, Kotzabasis K (1995) Influence of polyamine inhibitors on light-independent and light-dependent chlorophyll biosynthesis and on the photosynthetic rate. J Photochem Photobiol B 28:235–242

Berta G, Altamura MM, Fusconi A, Cerruti F, Capitani F, Bagni N (1997) The plant cell wall is altered by inhibition of polyamine biosynthesis. New Phytol 137:569–577

Besford R, Richardson C, Campos J, Tiburcio AF (1993) Effect of polyamines on stabilisation complexes in thylakoid membranes of osmotically stressed oat leaves. Planta 189:201–206

Bird K, Hablg T, DeBusk T (1982) Nitrogen allocation and storage patterns in *Gracilaria tikvahiae* (Rhodophyta). J Phycol 18:344–348

Bors W, Langebartels C, Michel C, Sandermann HJ (1989) Polyamines as radical scavengers and protectants against ozone damage. Phytochemistry 28:1589–1595

Burritt DJ (2008) The polycyclic aromatic hydrocarbon phenanthrene causes oxidative stress and alters polyamine metabolism in the aquatic liverwort *Riccia fluitans* L. Plant Cell Environ 31:1416–1431

Cen YP, Bornman JF (1990) The response of bean plants to UV-B radiation under different irradiances of background visible light. J Exp Bot 41:1489–1495

Chen Q, Vazquez EJ, Moghaddas S, Hoppel CL, Lesnefsky EJ (2003) Production of reactive oxygen species by mitochondria: central role of complex III. J Biol Chem 278:36027–36031

Chow F (2012) Nitrate assimilation: the role of in vitro nitrate reductase assay as nutritional predictor. In: Najafpour MM (ed) Agricultural and Biological Sciences, Applied photosynthesis, In Tech, pp. 105–120.

Chow F, Oliveira MC (2008) Rapid and slow modulation of nitrate reductase activity in the red macroalga *Gracilaria chilensis* (Gracilariales, Rhodophyta): influence of different nitrogen sources. J Appl Phycol 20:325–332

Cohen E, Shoshana A, Heimer YH, Mizrahi Y (1984) Polyamine biosynthetic enzymes in the cell cycle of *Chlorella*. Plant Physiol 74:385–388

Coimbra MA, Barros A, Barros M, Rutledge DN, Delgadillo I (1998) Multivariate analysis of uronic acid and neutral sugars in whole pectic samples by FT-IR spectroscopy. Carbohydr Polym 37:41–248

de Paula MR, Glaser V, da Luz Scheffer D, de Paula Ferreira PM, Wannmacher CM, Farina M, de Oliveira PA, Prediger RD, Latini A (2013) Platelet oxygen consumption as a peripheral blood marker of brain energetics in a mouse model of severe neurotoxicity. J Bioenerg Biomembr 45:449–57

DeBoer JA, Guigli HJ, Israel TL, D'Elia CF (1978) Nutritional studies of two red algae. I. Growth rate as a function of nitrogen source and concentration. J Phycol 14:261–266

Diffey BL (2002) Sources and measurement of ultraviolet radiation. Methods 28:4–13

Doernemann D, Navakoudis E, Kotzabasis K (1996) Changes in the polyamine content of plastidal membranes in light- and dark-grown wildtype and pigment mutants of the unicellular green alga *Scenedesmus obliquus* and their possible role in chloroplast photodevelopment. J Photochem Photobiol B 36:293–299

Ferreira G, Fontes RF, Fontes M, Alvares V (2001) Comparing calcium chloride, barium chloride, and hot water extractions and testing activated charcoal plus azomethine-H dosage for boron determination in Brazilian soils. Commun Soil Sci Plant Anal 32:3153–3167

Fischer JC, Ruitenbeek W, Berden JA, Trijbels JM, Veerkamp JH et al (1985) Differential investigation of the capacity of succinate oxidation in human skeletal muscle. Clin Chim Acta 153:23–36

Flores HE (1991) Changes in polyamine metabolism in response to abiotic stress. In: Slocum RD, Flores HE (eds) Biochemistry and physiology of polyamines in plants. CRC Press Ltd., Boca Raton, pp 41–56

Fredersdorf J, Müller R, Becker S, Wiencke C, Bischof K (2009) Interactive effects of radiation, temperature and salinity on different

life history stages of the Arctic kelp *Alaria esculenta* (Phaeophyceae). Oecologia 160:483–492
Fuell C, Elliott KA, Hanfrey CC, Franceschetti M, Michael AJ (2012) Polyamine biosynthetic diversity in plants and algae. Plant Physiol Biochem 48:513–520
Galston AW, Kaur-Sawhney R (1995) Polyamines as endogenous growth regulators. In: Davies PJ (ed) Plant hormones: physiology, biochemistry, and molecular biology. Kluwer, Dordrecht, pp 158–178
Gao K, Xu J (2008) Effects of solar UV radiation on diurnal photosynthetic performance and growth of *Gracilaria lemaneiformis* (Rhodophyta). Eur J Phycol 43:297–307
García-Jiménez P, Rodrigo M, Robaina R (1998) Influence of plant growth regulators, polyamines and glycerol interaction on growth and morphogenesis of carposporelings of *Grateloupia* cultured in vitro. J Appl Phycol 10:95–100
García-Sánchez MJ, Fernández JA, Niel FX (1993) Biochemical and physiological responses of *Gracilaria tenuistipitata* under two different nitrogen treatments. Physiol Plant 88:631–637
Glaser V, Moritz B, Schmitz A, Dafré AL, Nazari EM, Rauh Müller YM, Felsa L, Straliotto MR, de Bem AF, Farina M, da Rocha JB, Latini A (2013) Protective effects of diphenyl diselenide in a mouse model of brain toxicity. Chem Biol Interact 206:18–26
Gómez I, Huovinen P (2011) Morpho-functional patterns and zonation of 13 South Chilean seaweeds: the importance of photosynthetic and bio-optical traits. Mar Ecol Prog Ser 422:77–91
Gordillo F, Dring M, Savidge G (2002) Nitrate and phosphate uptake characteristics of three species of brown algae cultured at low salinity. Mar Ecol Prog Ser 234:111–118
Häder DP, Figueroa FL (1997) Photoecophysiology of marine macroalgae. Photochem Photobiol 66:1–14
Häder DP, Kumar HD, Smith RC, Worrest RC (2007) Effects of solar UV radiation on aquatic ecosystems and interactions with climate change. J Photochem Photobiol 46:53–68
Hales J, Fletcher R (1990) Studies on the recently introduced brown alga *Sargassum muticum* (Yendo) Fensholt. V. Receptacle initiation and growth, and gamete release in laboratory culture. Bot Mar 33:241–249
Hamana K, Matsuzaki S (1982) Widespread occurrence of norspermidine and norspermine in eukaryotic algae. J Biochem 91:1321–1328
Hamilton J, Thomas R, DeLucia E (2001) Direct and indirect effects of elevated CO_2 on leaf respiration in a forest ecosystem. Plant Cell Environ 24:975–982
Hanelt D, Roleda MY (2009) UVB radiation may ameliorate photoinhibition in specific shallow-water tropical marine macrophytes. Aquat Bot 91:6–12
Hanisak MD (1990) The use of *Gracilaria tikvahiae* (Gracilariales, Rhodophyta) as a model system to understand the nitrogen nutrition of culture seaweeds. Hydrobiologia 204(205):79–87
Hausladen A, Fridovich I (1994) Superoxide and peroxynitrite inactivate aconitases, but nitric oxide does not. J Biol Chem 269:29405–29408
Hunter DC, Burritt DJ (2005) Light quality influences the polyamine content of lettuce (*Lactuca sativa* L.) cotyledon explants during shoot production in vitro. Plant Growth Regul 45:53–61
Hwang SP, Williams SL, Brinkhuis BH (1987) Changes in internal dissolved nitrogen pools as related to nitrate uptake and assimilation in *Gracilaria tikvahiae* McLachlan (Rhodophyta). Bot Mar 30:11–19
Karsten U (2007) Salinity tolerance of Arctic kelps from Spitsbergen. Phycol Res 55:257–262
Kotzabasis K, Fontinou C, Roubelakis-Angelakis KA, Ghanotakis D (1993) Polyamines in the photosynthetic apparatus. Photosystem II highly resolved subcomplexes are enriched in spermine. Photosynth Res 38:83–88
Kramer GF, Norman HA, Krizek DT, Mirecki RM (1991) Influence of UV-B radiation on polyamines, lipid peroxidation and membrane lipids in cucumber. Phytochemistry 30:2101–2108
Kramer GF, Krizek DT, Mirecki RM (1992) Influence of photosynthetically active radiation and spectral quality on UV-B induced polyamine accumulation in soybean. Phytochemistry 31:1119–1125
Kuhnen S, Bernard-Ogliari J, Dias PF, Boffo EF, Correia I, Ferreira AG, Delgadillo I, Maraschin M (2010) ATR-FTIR spectroscopy and chemometric analysis applied to discrimination of landrace maize flours produced in southern Brazil. Int J Food Sci Technol 45:1673–1681
Lapointe BE (1981) The effects of light and nitrogen on growth, pigment content, and biochemical composition of *Gracilaria foliifera* v. *angustissima* (Gigartinales, Rhodophyta). J Phycol 17:90–95
Lapointe BE, Duke CS (1984) Biochemical strategies for growth of *Gracilaria tikvahiae* (Rhodophyta) in relation to light intensity and nitrogen availability. J Phycol 20:488–495
Latini A, Rodriguez M, Borba Rosa R, Scussiato K, Leipnitz G, Reir de Assis D, da Costa FG, Funchal C, Jacques-Silva MC, Buzin L, Giugliani R, Cassiana A, Radi R, Wajner M (2005) 3-Hydroxyglutaric acid moderately impairs energy metabolism in brain of young rats. Neuroscience 135:111–120
Lee TM (1998) Investigations of some intertidal green macroalgae to hyposaline stress: detrimental role of putrescine under extreme hyposaline conditions. Plant Sci 138:1–8
Lee SH, Whitledge TE, Kang SH (2008) Carbon uptake rates of sea ice algae and phytoplankton under different light intensities in a landfast Sea Ice zone, Barrow, Alaska. Artic 61:281–291
Legendre L, Ackley SF, Dieckmann GS, Gulliksen B, Horner R, Hoshiai T, Melnikov IA, Reeburgh WS, Spindler M, Sullivan CW (1992) Ecology of sea ice biota. Polar Biol 12:429–444
Lerdau M, Coley PD (2002) Benefits of the carbon-nutrient balance hypothesis. Oikos 98:534–536
Li ZL, Burritt DJ (2003) Changes in endogenous polyamines during the formation of somatic embryos from isogenic lines of *Dactylis glomerata* L. with different regenerative capacities. Plant Growth Regul 40:65–74
Lobban CS, Harrison PJ (1994) Seaweed ecology and physiology. Cambridge University Press, Cambridge
Lowry OH, Rosebough N, Farr AL (1951) Protein measurement with the folin phenol reagent. J Biol Chem 193:265–275
Lütz C, Navakoudis E, Seidlitz HK, Kotzabasis K (2005) Simulated solar irradiation with enhanced UV-B adjust plastid- and thylakoid-associated polyamine changes for UV-B protection. Biochim Biophys Acta 1710:24–33
Macler BA (1988) Salinity effects on photosynthesis, carbon allocation and nitrogen assimilation in the red alga, *Gelidium coulteri*. Plant Physiol 88:690–694
Marián FD, García-Jiménez P, Robaina R (2000) Polyamines in marine macroalgae: levels of putrescine, spermidine and spermine in the thalli and changes in their concentration during glycerol-induced cell growth in vitro. Physiol Plant 110:530–534
Martins I, Oliveira J, Flindt M, Marques J (1999) The effect of salinity on the growth rate of the macroalgae *Enteromorpha intestinalis* (Chlorophyta) in the Mondego estuary (west Portugal). Acta Oecol 20:259–265
Martin-Tanguy J (2001) Metabolism and function of polyamines in plants: recent development (new approaches). Plant Growth Regul 34:135–148
Michler T, Aguilera J, Hanelt D, Bischof K, Wiencke C (2002) Long-term effects of ultraviolet radiation on growth and photosynthetic performance of polar and cold-temperate macroalgae. Mar Biol 140:1117–1127
Miret JJ, Solari AJ, Barderi PA, Goldemberg SH (1992) Polyamines and cell wall organization in *Saccharomyces cerevisiae*. Yeast 8:1033–1041

Mock T, Gradinger R (2000) Changes in photosynthetic carbon allocation in algal assemblages of Arctic sea ice with decreasing nutrient concentrations and irradiance. Mar Ecol Prog Ser 202:1–11
Norton TA (1977) The growth and development of *Sargassum muticum* (Yendo) Fensholt. J Exp Mar Biol Ecol 26:41–53
Norton T, Melkonian M, Andersen R (1996) Algal biodiversity. J Appl Phycol 35:308–326
Pakker H, Martins R, Boelen P, Buma A, Nikaido O, Breeman A (2000a) Effects of temperature on the photoreactivation of ultraviolet-B-induced DNA damage in *Palmaria palmata* (Rhodophyta). J Phycol 36:334–341
Pakker H, Beekman C, Breeman A (2000b) Efficient photoreactivation of UVBR-induced DNA damage in the sublittoral macroalga *Rhodymenia pseudopalmata* (Rhodophyta). Eur J Phycol 35:109–114
Papenfus HB, Stirk WA, Finnie JF, Van SJ (2012) Seasonal variation in the polyamines of *Ecklonia maxima*. Bot Mar 55:539–546
Parry ML, Canziani OF, Palutikof JP, van der Linden PJ, Hanson CE (2007) Contribution of Working Group II to the Fourth Assessment Report of the Intergovernmental Panel on Climate Change. Cambridge University Press, Cambridge, pp 581–615
Pescheck F, Lohbeck K, Roleda M, Bilger W (2014) UVB-induced DNA and photosystem II damage in two intertidal green macroalgae: distinct survival strategies in UV-screening and non-screening Chlorophyta. J Photochem Photobiol B 132:85–93
Plante AJ, Arts MT (2000) Effects of chronic, low levels of UV radiation on carbon allocation in *Cryptomona serosa* and competition between *C. erosa* and bacteria in continuous cultures. J Plankton Res 22:1277–1298
Polo LK, Felix MR, Kreush M, Pereira D, Costa G, Simioni C, Ouriques L, Chow F, Ramlov F, Maraschin M, Bouzon ZL, Schmidt EC (2014) Photoacclimation responses of the brown macroalga *Sargassum cymosum* to the combined influence of UV radiation and salinity: cytochemical and ultrastructural organization and photosynthetic performance. Photochem Photobiol 90:560–573
Poppe F, Hanelt D, Wiencke C (2002) Changes in ultrastructure, photosynthetic activity and pigments in the Antarctic red alga *Palmaria decipiens* during acclimation to UV radiation. Bot Mar 45:253–261
Roleda M, Hanelt D, Kräbs G, Wiencke C (2004) Morphology, growth, photosynthesis and pigments in *Laminaria ochroleuca* (Laminariales, Phaeophyta) under ultraviolet radiation. Phycologia 43:603–613
Ryther JG, Dustan W (1971) Nitrogen, phosphorus and eutrophication in the coastal environment. Science 171:1008–1013
Santa-Catarina C, Silveira V, Scherer GFE, Floh EIS (2007) Polyamine and nitric oxide levels correlate with morphogenetic evolution in somatic embryogenesis of *Ocotea catharinensis*. Plant Cell Tissue Org Cult 90:93–101
Scherner F, Ventura R, Barufi J, Horta P (2012) Salinity critical threshold values for photosynthesis of two cosmopolitan seaweed species: providing baselines for potential shifts on seaweed assemblages. Mar Environ Res 79:1–12
Schmidt ÉC, Pereira B, Pontes CLM, Santos R, Scherner F, Horta PA, Martins RP, Latini A, Maraschin M, Bouzon ZL (2012a) Alterations in architecture and metabolism induced by ultraviolet radiation-B in the carrageneophyte *Chondracanthus teedei* (Rhodophyta, Gigartinales). Protoplasma 249:353–367
Schmidt ÉC, Pereira B, Santos R, Gouveia C, Costa GB, Faria GSM, Scherner F, Horta PA, Martins RP, Latini A, Ramlov F, Maraschin M, Bouzon ZL (2012b) Responses of the macroalgae *Hypnea musciformis* after in vitro exposure to UV-B. Aquat Bot 100:8–17
Schulz H, Baranska M (2007) Identification and quantification of valuable plant substances by IR and Raman spectroscopy. Vib Spectrosc 43:13–25
Schweikert K, Sutherland JES, Hurd CL, Burritt DJ (2011) UV-B radiation induces changes in polyamine metabolism in the red seaweed *Porphyra cinnamomea*. Plant Growth Regul 65:389–399
Schweikert K, Hurd CL, Sutherland JE, Burritt DJ (2014) Regulation of polyamine metabolism in *Pyropia cinnamomea* (W.A. Nelson), an important mechanism for reducing UV-B-induced oxidative damage. J Phycol 50:267–279
Sfichi L, Ioannidis N, Kotzabasis K (2004) Thylakoid-associated polyamines adjust the UV-B sensitivity of the photosynthetic apparatus by means of light-harvesting complex II changes. Photochem Photobiol 80:499–506
Sfichi-Duke L, Ioannidis NE, Kotzabasis K (2008) Fast and reversible response of thylakoid-associated polyamines during and after UV-B stress: a comparative study of the wild type and a mutant lacking chlorophyll b of unicellular green alga *Scenedesmus obliquus*. Planta 228:341–353
Shuter B (1979) A model of physiological adaptation in unicellular algae. J Theor Biol 8:519–552
Silveira V, Floh EIS, Handro W, Guerra MP (2004) Effect of plant growth regulators on the cellular growth and levels of intracellular protein, starch and polyamines in embryogenic suspension cultures of *Pinustaeda*. Plant Cell Tissue Org Cult 76:53–60
Smith RE, Clement P, Cota GF, Li WK (1989) Intracellular photosynthate allocation and the control of arctic marine ice algal production. J Phycol 23:124–132
Smith J, Burrit D, Bannister P (2001) Ultraviolet-B radiation leads to a reduction in free polyamines in *Phaseolus vulgaris* L. Plant Growth Regul 35:289–294
Steen H (2004) Effects of reduced salinity on reproduction and germling development in *Sargassum muticum* (Phaeophyceae, Fucales). Eur J Phycol 39:293–299
Tiburcio AF, Kaur-Sawhney R, Galston AW (1993) Spermidine biosynthesis as affected by osmotic-stress in oat leaves. Plant Growth Regul 13:103–109
Torrigiani P, Rabiti AL, Bortolotti C, Betti L, Marsi F, Canova A (1997) Polyamine synthesis and accumulation in the hypersensitive response to TMV in *Nicotiana tabacum*. New Phytol 135:467–473
Turpin DH, Elrifi IR, Birch DG, Weger HG, Holmes JJ (1988) Interactions between photosynthesis, respiration and nitrogen assimilation in microalgae. Can J Bot 66:2083–2097
Turrens JF (1997) Superoxide production by the mitochondrial respiratory chain. Biosci Rep 17:3–8
Turrens JF, Boveris A (1980) Generation of superoxide anion by the NADH dehydrogenase of bovine heart mitochondria. Biochem J 191:421–427
Vergara JJ, Bird KT, Niell FX (1995) Nitrogen assimilation following NH_4^+ pulses in the red alga *Gracilariopsis lemaneiformis*: effect on C metabolism. Mar Ecol Prog Ser 122:253–263
Viñegla B, Figueroa LF (2009) Effect of solar and artificial UV radiation on photosynthetic performance and carbonic anhydrase activity in intertidal macroalgae from southern Spain. Cienc Mar 35:59–74
Wilkinson M (1981) Survival strategies of attached algae in estuaries. Mar Sci 15:29–38
Wilkinson M, Wood P, Wells E, Scanlan C (2007) Using attached macroalgae to assess ecological status of British estuaries for the European Water Framework Directive. Mar Pollut Bull 55:136–150
Xu Z, Gao K (2009) Impacts of UV radiation on growth and photosynthetic carbon acquisition in *Gracilaria lemaneiformis* (Rhodophyta) under phosphorus-limited and replete conditions. Funct Plant Biol 36:1057–1064
Zhang Y, Marcillat O, Giulivi C, Ernster L, Davies KJ (1990) The oxidative inactivation of mitochondrial electron transport chain components and ATPase. J Biol Chem 265:16330–16336

ANEXO 6

SCIENTIA MARINA 84(1)
March 2020, 59-70, Barcelona (Spain)
ISSN-L: 0214-8358
https://doi.org/10.3989/scimar.04982.22A

Physiological performance by growth rate, pigment and protein content of the brown seaweed *Sargassum filipendula* (Ochrophyta: Fucales) induced by moderate UV radiation exposure in the laboratory

Luz K. Polo, Fungyi Chow

Laboratory of Marine Algae "Édison José de Paula", Department of Botany, Institute of Biosciences, University of São Paulo, CEP 05508-090, São Paulo, Brazil.
(LP) (Corresponding author) E-mail: luzkapolo@gmail.com. ORCID iD: https://orcid.org/0000-0002-9318-4042
(FC) E-mail: fchow@ib.usp.br. ORCID iD: https://orcid.org/0000-0003-2462-3117

Summary: UV radiation is a factor affecting the distribution and physiology of photosynthetic organisms in an aquatic ecosystem. Studies with macroalgae indicate diverse biological disturbances in response to UV radiation. This work aimed to study sensitivity of the brown macroalga *Sargassum filipendula* exposed to UV radiation: PAR (control), PAR+UVA+UVB(++) and PAR+UVA(++)+UVB. Changes in the physiological parameters growth rate, total soluble proteins, photosynthetic pigments and the UV-vis absorbing compounds were analysed after T0, T4, T7 and T10 (days) of UV exposure. Physiological parameters showed little variation between treatments and over time, suggesting that moderate UV radiation doses could regulate resistance responses to re-establish the cellular homoeostasis condition through activation of an antioxidant defence system, such as an overproduction of phenolic compounds. Responses recorded in *S. filipendula* would be related to acclimation mechanisms against acute UV radiation stress, triggering resistance responses to avoid serious damage to the metabolic machinery, activating control systems to maintain hormesis, and homoeostasis of deleterious actions of reactive species, similar to the phenomenon known as preparation for oxidative stress. Finally, UV-visible absorption spectra showed absorption bands evidencing the presence of mainly UV-absorbing compounds with photoprotective function, such as phlorotannins, flavonoids and carotenoids, which could provide adaptive advantages for organisms exposed to UV radiation.

Keywords: algae; growth rate; photosynthetic pigments; proteins; ultraviolet radiation; UV-absorbing compounds.

Rendimiento fisiológico de acuerdo a la tasa de crecimiento, contenido de pigmentos y proteínas de la macroalga parda *Sargassum filipendula* (Ochrophyta: Fucales) inducida a radiación UV en el laboratorio

Resumen: La radiación UV es un factor que afecta la distribución y la fisiología de los organismos fotosintéticos en el ecosistema acuático. Los estudios con macroalgas indican diversas alteraciones biológicas en respuesta a la radiación UV. Este trabajo tuvo como objetivo estudiar la sensibilidad de la macroalga parda *Sargassum filipendula* expuesta a radiación UV: PAR (control), PAR + UVA + UVB (++) y PAR + UVA (++) + UVB. Los cambios en la tasa de crecimiento, proteínas solubles totales, pigmentos fotosintéticos y compuestos absorbentes de UV-vis se analizaron después de T0, T4, T7 y T10 (días) de exposición a UV. Los parámetros fisiológicos mostraron poca variación entre los tratamientos y con el tiempo, lo que sugiere que dosis moderadas de radiación UV podrían regular las respuestas de resistencia para restablecer la condición de homeostasis celular a través de la activación del sistema de defensa antioxidante, como la sobreproducción de compuestos fenólicos. Las respuestas registradas en *S. filipendula* estarían relacionadas con mecanismos de aclimatación contra el estrés agudo por radiación UV, desencadenando respuestas de resistencia para evitar daños severos en la maquinaria metabólica, activando sistemas de control para mantener la hormesis y homeostasis de acciones deletéreas de especies reactivas, similar al fenómeno llamado preparación para el estrés oxidativo (POS). Finalmente, los espectros de absorción UV-visible mostraron bandas de absorción que evidencian la presencia de compuestos absorbentes de UV principalmente con función fotoprotectora, como los florotaninos, flavonoides y carotenoides que podrían proporcionar ventajas adaptativas para los organismos expuestos a la radiación UV.

Palabras clave: algas; tasa de crecimiento; pigmentos fotosintéticos, proteínas, radiación ultravioleta; compuestos absorbentes de rayos UV.

Citation/Como citar este artículo: Polo L.K., Chow F. 2020. Physiological performance by growth rate, pigment and protein content of the brown seaweed *Sargassum filipendula* (Ochrophyta: Fucales) induced by moderate UV radiation exposure in the laboratory. Sci. Mar. 84(1): 59-70. https://doi.org/10.3989/scimar.04982.22A

Editor: X. Turon.

Received: July 29, 2019. **Accepted:** December 20, 2019. **Published:** February 4, 2020.

Copyright: © 2020 CSIC. This is an open-access article distributed under the terms of the Creative Commons Attribution 4.0 International (CC BY 4.0) License.

INTRODUCTION

Solar radiation is the most important prerequisite for life on Earth, since it provides the light, heat and energy demanded for photosynthesis processes. This radiation mainly consists of UV radiation, visible light (photosynthetically active radiation, PAR), and infrared radiation (Diffey 2002). The UV radiation corresponds to a small part of the electromagnetic spectrum and is divided into three spectral regions: 1) UVA (400-315 nm), which is the closest radiation to the visible spectrum and is not absorbed by the ozone (O_3) layer; 2) UVB (315-280 nm), which is not completely absorbed by O_3 and is harmful to living organisms; and 3) UVC (280-100 nm), which is extremely harmful but is quantitatively absorbed by oxygen and ozone in the Earth's atmosphere (Madronich et al. 1998).

Since man-made changes in the stratospheric O_3 layer began to be reported, the effect of UV radiation on the aquatic ecosystem has become an important subject. Interactions between global climate change, O_3 and UV radiation are having important consequences for UV exposure in this ecosystem (Bais et al. 2015). However, the attenuation of UV radiation that penetrates the water column varies according to the location (e.g. oceanic versus coastal environments), latitude, and concentrations of particulate and dissolved matters (Villafañe et al. 2003). UV radiation has been considered one of the main factors affecting the distribution of photosynthetic organisms in the aquatic ecosystem. It has diverse biological effects, most of them with unfavourable consequences (Björn 2007).

Macroalgae are major biomass producers on rocky shores and the continental shelf, which provide microhabitats for many larval stages of fishes, crustaceans, epibionts and epiphytes, and other marine organisms (Lippert et al. 2001). Due to tidal exposure, intertidal macroalgae are constantly exposed to fluctuating environmental stresses such as high temperature, desiccation and high radiation levels (PAR and UV radiation) (Sampath-Wiley et al. 2008) that could easily lead to the formation and accumulation of free radicals and reactive species, triggering oxidative stress. Photobiological studies in macroalgae indicate diverse physiological disturbances in response to UV radiation, including alterations in growth and development (Altamirano et al. 2003, Gao and Xu 2008, Navarro et al. 2016), pigment degradation (Heo and Jeon 2009), dynamic or chronic photoinhibition of photosynthesis (Barufi et al. 2011, Ayres-Ostrock and Plastino 2014, Figueroa et al. 2014), protein and DNA damage (Buma et al. 2001, Kumar et al. 2004), decrease in lipid/fatty acid content (Khotimchenko and Yakovleva 2005, Liang et al. 2006), inhibition of enzyme activity (Lee and Shiu 2009), alterations in polyamines content (Polo et al. 2014b), and modifications in cellular organization and ultrastructure (Holzinger and Lütz 2006, Polo et al. 2014a, Schmidt et al. 2015). As a photoprotective mechanism against UV radiation, especially UVB, macroalgae can increase the production of UV-absorbing compounds such as mycosporine-like amino acids, phenolic compounds and carotenoids, which play protective roles by mitigating the damage caused by the increase in reactive species (Ruhland et al. 2007), therefore giving advantages that enable macroalgae to survive in the presence of UV radiation.

The genus *Sargassum* C. Agardh is dominant in the coverage of coastal consolidate substrate areas in both tropical and subtropical regions, often forming the so-called *Sargassum* beds. It plays an important ecological role as shelter, protection and a food resource for several marine species (Széchy et al. 2001) and is considered a host because it provides microhabitats for several other algae and marine fauna. The genus is highly sensitive to variations in salinity, temperature, and pollutants (Paula and Eston 1987, Gorostiaga and Díez 1996, Amado Filho et al. 1999), an interesting requisite of bioindicator species. In addition, the position that *Sargassum* occupy in the littoral zone, between the lower intertidal and the infralittoral, means that they are subjected to higher levels of UV radiation with possible consequences on their general performance, which may cause shifts within the whole ecosystem due to their role as community engineers providing a habitat and energy source (Häder et al. 2007).

Given the many changes that UV radiation may have on seaweeds, it is important to study the sensitivity and tolerance of these organisms in order to understand possible biological consequences under an extremely dynamic environment and predicted global climate changes scenarios. Therefore, the aim of this study was to evaluate the biological effect of a moderate dose of UV radiation (UVA and UVB) on the physiological performance and sensitivity of the brown macroalga *Sargassum filipendula* C. Agardh by analysing growth rate, photosynthetic pigments (chlorophyll (Chl) *a*, Chl *c*, and carotenoids), total soluble proteins and UV-absorbing compounds under laboratorial conditions.

MATERIALS AND METHODS

Collection site and algal material

Specimens of *S. filipendula* were collected at Cigarras Beach (24°43'55.74"S and 45°23'54.48"W) located in São Sebastião on the north coast of São Paulo State, Brazil, during the summer season (February-March 2016). Material was transported in cooler boxes to the laboratory, cleaned of macroepiphytes and washed with abundant filtered seawater. Five individuals were fixed in 4% v/v formaldehyde (diluted in seawater), herborized and then deposited in the SPF Herbarium of the University of São Paulo (voucher SPF 58087). The remaining biomass was used for subsequent experiments.

Cleaned apical portions (±8 cm) were acclimated for one week under laboratory conditions in sterilized seawater at 32 psu enriched with von Stosch solution diluted to 50% (Ursi and Plastino 2001) based on Edwards (1970), with a PAR of 60±5 µmol photons m^{-2} s^{-1}, 25±1°C, a photoperiod of 14 h and intermittent aeration every 30 min. The culture ratio was 3 g of alga per 1 L of culture medium.

Table 1. – Values of total radiation doses and intensities for PAR, PAR+UVA+UVB (++) and PAR+UVA (++) +UVB treatments. The total dose was calculated from the absolute intensity values for 1, 4, 7 and 10 days (d). UVA and UVB irradiance were 2.01 W m^{-2} and 7.04 W m^{-2}, respectively.

Treatment	Total irradiance		Total dose (KJ m^{-2})			
	Time UV/d (h)	Absolute intensity (W m^{-2})	1 d	4 d	7 d	10 d
PAR	-	13.04	563.32	2253.31	3943	5633.33
PAR+UVA+UVB(++)	3	15.05	1950.5	7801.9	13653.4	19505
PAR+UVA(++)+UVB	3	20.08	2602.4	10409.5	18216.6	26023.7

Laboratory conditions and experimental setup

After the acclimation period, the material was exposed to three different radiation treatments: a) PAR (control treatment), b) PAR+UVA+UVB(++) and, c) PAR+UVA(++)+UVB under the laboratory culture conditions described above, using five biological replicates for each treatment. The experiments were performed under 3 h exposure to UVR per day in the middle of the light phase for ten days. During this exposure, aeration was increased in all treatments to encourage greater movement of the algal fragments in order to promote a homogeneous exposure for all branches, and culture medium was added at the seventh day of exposure to avoid nutrient limitation.

UVB (312 nm; 2.04 W m^{-2}; 21.71 kJ m^{-2} day^{-1}) and UVA (365 nm; 7.04 W m^{-2}; 76.32 kJ m^{-2} day^{-1}) radiations were provided by Philips lamps models TL 20W/12 and Actinic BL TL-K 40 W/10-R, respectively. Table 1 presents the values of total radiation doses and intensities for the different treatments for 1, 4, 7 and ten days of UV exposure.

The measurements of total radiation spectrum emitted by radiation sources (PAR and UV) were obtained using the SphereOptics SMS-500 (Spectral Measurements System) spectroradiometer and are summarized in Figure 1. It must be taken into account that the Philips TL12 UVB lamp also has emission in the UVA region of the spectra in a ratio of 0.51 (UVB/UVA), and the same occurs for BL TL-k40, which also has emission in the UVB region in a ratio of 0.04 (UVA/UVB).

The UVR intensities were chosen based on previous studies with brown macroalgae (Bischof et al. 1998, Holzinger et al. 2011, Cruces et al. 2013), in which the selected intensities did not cause an acute stress in response to UVR and are therefore considered to have a moderate impact.

The PAR irradiance intensity measurements were obtained in µmol photons m^{-2} s^{-1} using a LI-COR

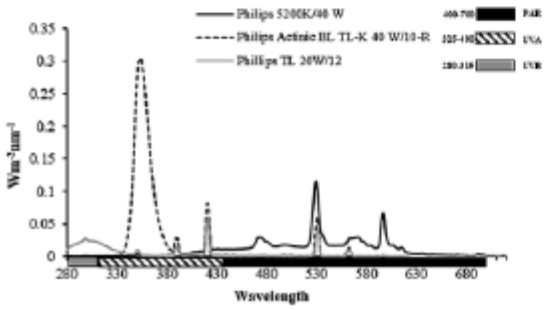

Fig. 1. – Total radiation spectrum emitted by radiation sources: PAR (400-700 nm), UVA (315-400 nm) and UVB (280-315 nm).

Biosciences Model Li-250A quantameter (Lincoln-Nebraska, USA) connected to the underwater spherical LI-COR sensor SPQSA1346 (USA). The UVR intensity was obtained in W m^{-2}, with a MACAM Ultraviolet Radiometer (Scotland) connected to the UVB or UVA specific sensors. The measurements of total radiation spectrum emitted by radiation sources (PAR and UV) were obtained using the SphereOptics SMS-500 (Spectral Measurements System) spectroradiometer (USA).

Growth rate (GR), total soluble proteins, and photosynthetic pigments were evaluated before the start of the experiment (T0) and after 4, 7, and 10 days (T4, T7 and T10, respectively).

Growth rate

The growth rate was evaluated through measurements of fresh biomass weight over the experimental period (t), following Penniman et al. (1986) as follows, where Wi is the initial wet mass, Wf is the final wet mass, and t is the time in days:

$$GR\ [\%\ day^{-1}] = [(Wf / Wi)^{1/t} - 1] \times 100$$

Total soluble proteins and photosynthetic pigments, and UV/visible-absorbing spectrum

The soluble proteins and photosynthetic pigments were extracted from frozen fresh samples of approximately 70 mg fresh weight (FW) at T0, T4, T7 and T10. The material was ground in liquid nitrogen until a fine powder was obtained, extracted in 1 mL of cold sodium phosphate buffer 0.05 mM (pH 5.5), protecting the extract from photo- and thermooxidation, and then centrifuged for 15 min at 4°C and 12000 rpm. The obtained supernatant was called buffered extract.

From an aliquot of the buffered extract, the total soluble protein content was analysed according to the Bradford spectrophotometric method (Bradford 1976) using the Bio-Rad solution for the protein assay (Bio-Rad, USA), and the absorbance at 595 nm was recorded in a UV-visible 96-well microplate spectrophotometer. Bovine serum albumin was used for the standard curve with concentrations ranging from 2 to 16 µg mL^{-1} ($y=0.0434x+0.049$; $R^2=0.97$).

From the pelleted material obtained after the extraction of soluble proteins, photosynthetic pigments were analysed by resuspending the pellet in 1.5 mL of methanol and extracted for 3 h at 4°C, protecting the extract from photo- and thermaloxidation. Subsequently, centrifugation was carried out for 15 min at 12000 rpm and 4°C. The obtained supernatant was called methanolic extract. From an aliquot of 300 µL of the methanolic extract, UV-absorbing and visible-absorbing com-

pounds were analysed by determining the absorption spectrum in a UV-visible microplate spectrophotometer by reading the absorbance in the range of 200 to 750 nm. Chl *a* and Chl *c* content was calculated using the absorbance coefficients (Eλ) from Ritchie (2008) for methanol, where $E\lambda_{632}$=16.4351 and $E\lambda_{665}$=3.2416 for Chl *a* and $E\lambda_{632}$=34.2247 and $E\lambda_{665}$=1.5492 for Chl *c*, following the formulas:

$$\text{Chl a } (\mu g\ g\ FW^{-1}) = 16.4351\ A_{665} - 3.2416\ A_{632}$$
$$\text{Chl c } (\mu g\ g\ FW^{-1}) = 34.2247\ A_{632} - 1.5492\ A_{665}$$

From the same methanolic extract, the absorbance at 470 nm was used to calculate the total carotenoid concentration using the model proposed by Lichtenthaler (1987), in which absorbance coefficients for Chl *a* (Eλ=1.63) and Chl *c* (Eλ=119.5) were based on Lichtenthaler and Buschmann (2001) and Jeffrey (1963), respectively, following the formula modified by Urrea-Victoria and Chow (pers. comm):

$$\text{Carotenoids } (\mu g\ g\ FW^{-1}) = (1000\ A_{470} - 1.63\ \text{Chl } a - 119.5\ \text{Chl } c) / 221$$

where A is the absorbance at the respective wavelength.

UV-visible absorption spectra of buffer and methanolic extracts

From aliquots of 300 µL of the buffered and methanolic extracts, UV-absorbing and visible-absorbing compounds were assessed by determining the absorption spectra in a UV-visible microplate spectrophotometer by reading the absorbance in the range of 200 to 750 nm. From the UV- and visible-absorbing spectra of the both extracts, maximal absorption bands were identified and analysed by calculating the area under the curve (AUC) based on the Riemann sum. Data were standardized by the sample biomass in grams (absorbance/biomass).

Seawater UV-visible absorption spectrum

The absorption spectrum (200-750 nm) of the seawater, in which samples were cultivated during the experiment, was also recorded using a 300 µL aliquot of seawater read in a UV-visible microplate spectrophotometer. Maximal absorption bands were identified and analysed by calculating the AUC of each band based on the Riemann sum.

Data analysis

Statistical analysis of the data set was performed with the STATISTICA software (version 10.0). Five replicates were used for all studied parameters. Data were checked for normality (Kolmogorov-Smirnov test) and homoscedasticity (Bartlett test) and then submitted to unifactorial, multifactorial or repeated measures analysis of variance (ANOVA), followed by the Newman-Keuls post hoc test to verify the significance of the differences ($p<0.05$).

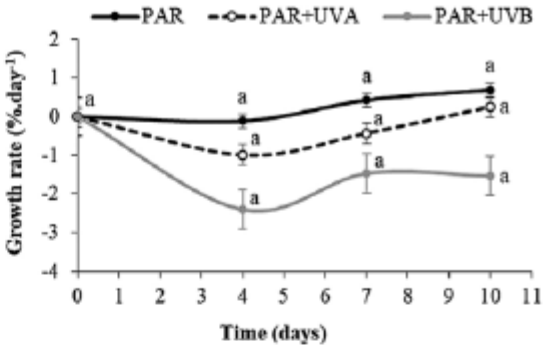

Fig. 2. – Growth rate of Sargassum filipendula over 10 days of exposure to PAR, PAR+UVA, and PAR+UVB radiation treatments (n=5; mean±SD). Letters indicate differences according to repeated measures ANOVA.

RESULTS

Growth rate

After 10 days of experiment with different radiation treatments (PAR, PAR+UVA, and PAR+UVB), the growth rate of *S. filipendula* analysed by radiation and time (two-way evaluation) showed no differences within the treatments over time (Fig. 2). Despite these results, higher growth rate values were observed for the PAR treatment over time followed by PAR+UVA and then by PAR+UVB (Fig. 1). Also, samples treated with PAR+UVA showed an increase in the growth rate at the tenth day (T10), which was close to the value shown in PAR at the same time. At T10, *S. filipendula* exposed to UVB treatment showed the most negative growth rate (–1.53 % day^{-1}) in comparison with PAR and PAR+UVA (0.68 % day^{-1} and 0.25 % day^{-1}, respectively) (Fig. 1).

Proteins and photosynthetic pigments

Figure 3A shows the content of total soluble proteins of *S. filipendula* over 10 days of exposure to PAR, PAR+UVA, and PAR+UVB radiation. With few exceptions, no differences were observed within the days for each radiation treatment, within the radiation for the same time and between the interaction time and radiation. The PAR treatment at T10 showed a noteworthy increase in proteins when compared over time with the same treatment and between the other radiation treatments. Differences were also observed at T7 in PAR+UVA and T10 in PAR+UVB in comparison with PAR. No clear response pattern was observed.

The content of photosynthetic pigments (Chl *a* and *b* and carotenoids) in *S. filipendula* showed little variation when compared over time and after treatment with UV (Fig. 3B-D). No differences were observed in the concentration of Chl *a* (Fig. 3B) when compared within times and UV treatments, except for PAR+UVB at T10 (606.46±2.88 µg g^{-1}), in which a significant reduction was evidenced in comparison with the other radiation treatments at the same time (846.90±3.82 µg g^{-1} for

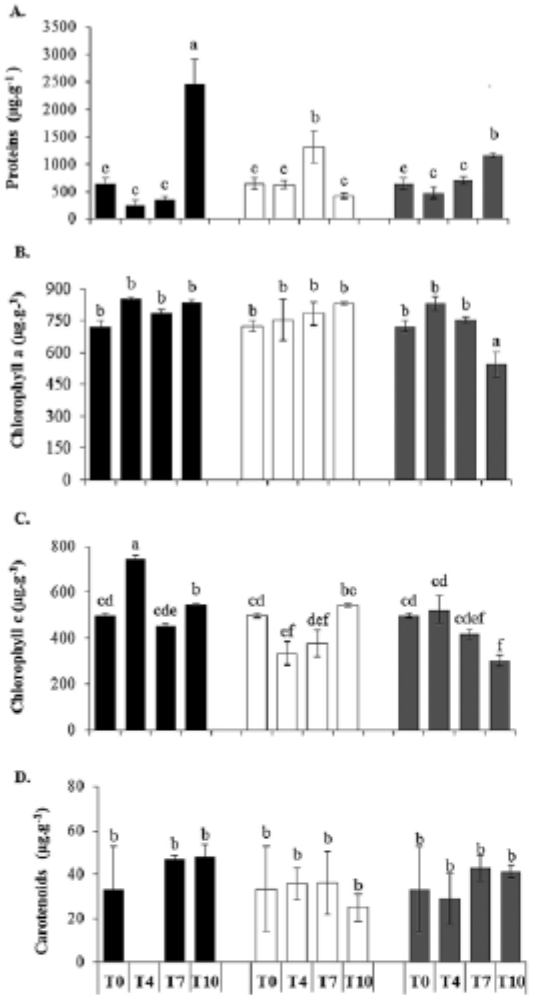

Fig. 3. – A, total soluble proteins; B, chlorophyll *a*; C, chlorophyll *c*; and D, carotenoids of *Sargassum filipendula* over 10 days of exposure to PAR, PAR+UVA and PAR+UVB radiation treatments (n=5; mean±SD). T0 represents samples before the start of the experiment and T4, T7 and T10 correspond to the respective exposition time. Letters indicate differences according to bifactorial ANOVA and the Newman-Keuls post hoc test ($p<0.05$).

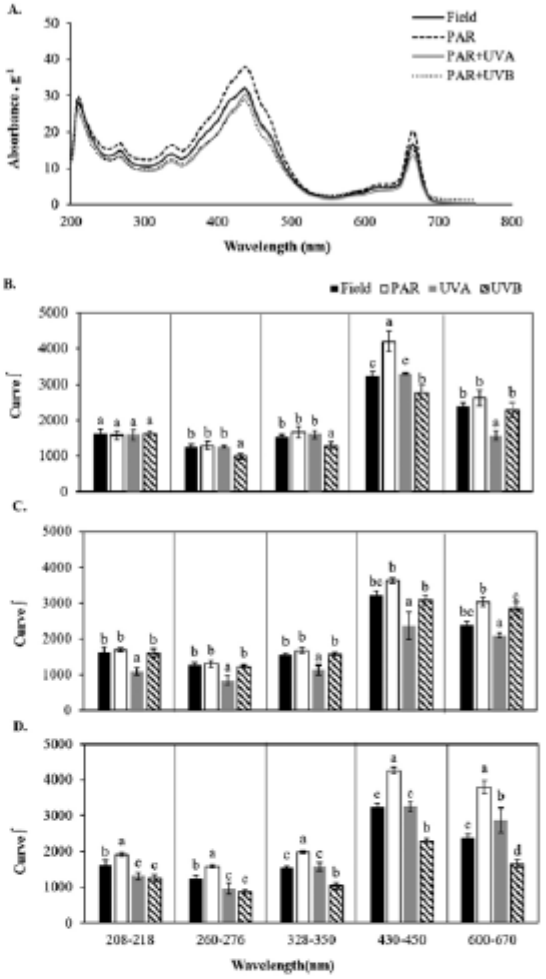

Fig. 4. – Absorption spectrum of buffer extract and area under the curve (AUC) of maximal absorption bands at 220-240 and 260-280 nm. **A**, general UV spectrum at T4; **B**, **C** and D, the AUC (n=5; mean±SD) at T4, T7 and T10 of radiation exposure, respectively, at two specific absorption bands, 220-240 and 260-280 nm. Letters indicate differences according to unifactorial ANOVA and the Newman-Keuls post hoc test ($p<0.05$). The analyses were performed for each absorption band separately.

PAR and 833.46±2.88 µg g^{-1} for PAR+UVA). The content of Chl *c* showed no clear response trend (Fig. 3C), but it varied significantly over time and among the treatments, showing a reduction at T4 in PAR+UVA and at T10 in PAR+UVB when compared with the other times and between treatments. Finally, carotenoid concentrations showed no differences over time or between the treatments (Fig. 3D). The samples of PAR at T4 were lost, so the mean±SD does not appear in the figure.

UV-visible absorption spectra of buffer and methanolic extracts and seawater

Considering independently the buffer and methanolic extracts and the seawater samples, a similar pattern of the spectrum profile was observed for all treatments and over time (T4, T,7, and T10), so only one spectrum (T4) for each one is presented. The absorption spectra of buffer and methanolic extracts and seawater are shown in the Figures 4A, 5A and 6A, respectively. Additionally, the AUC for the maximal absorption bands for buffer and methanolic extracts and seawater are represented in Figures 4B-D, 5B-D and 6B-D for T4, T7 and T10.

Figure 3A presents the general UV absorption spectrum for buffer extract. Since no maximal absorption bands were observed in the visible region for this extract, the spectrum between 400 and 750 nm is not shown. Maximal absorption bands were identified between 220-240 and 260-280 nm for T4 (Fig. 4B), T7 (Fig. 4C) and T10 (Fig. 4D). For the times T4 and T7, similar trends were observed, with differences for both wavelength ranges (220-240 and 260-280 nm) and a

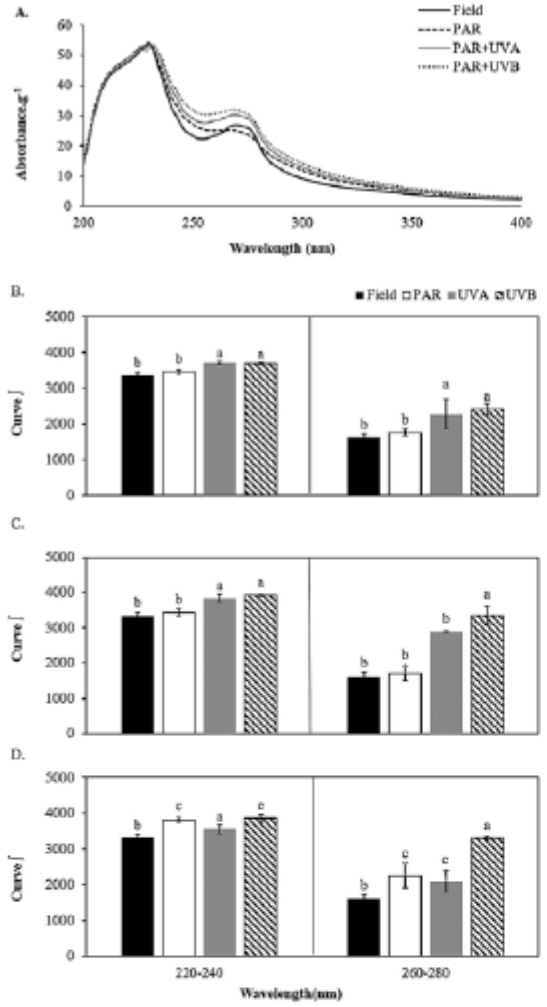

Fig. 5. – Absorption spectrum of methanolic extract and area under the curve (AUC) of maximal UV-visible absorption bands. A, general UV spectrum at T4; B, C and D, the AUC (n=5; mean±SD) at T4, T7, and T10 of radiation exposure, respectively, at three specific UV-absorption bands, 208-218, 260-276 and 328-350 nm, and two specific visible-absorption bands, 430-450 and 600-670 nm. Letters indicate differences according to unifactorial ANOVA and the Newman-Keuls post hoc test ($p<0.05$). The analyses were performed for each absorption band separately.

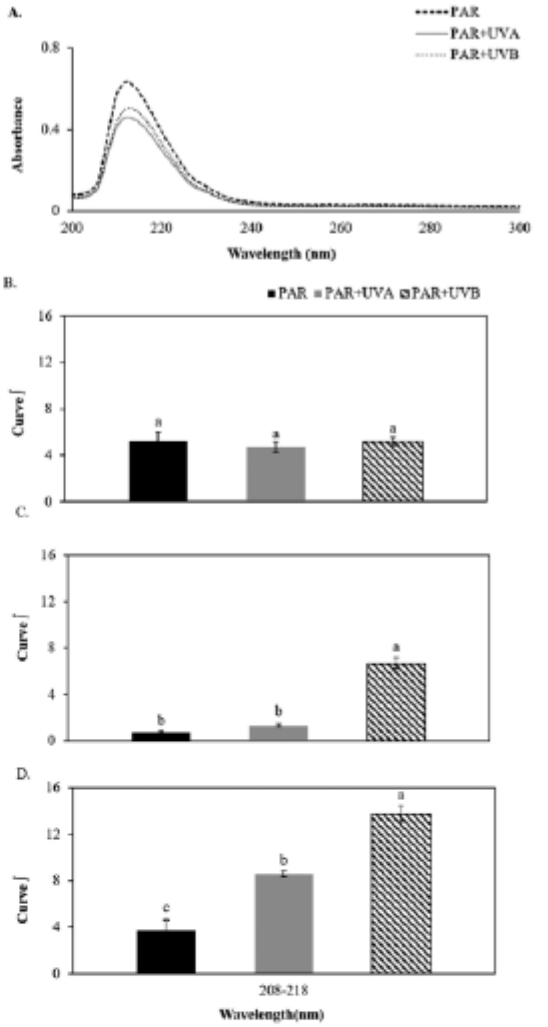

Fig. 6. – Absorption spectrum of seawater and area under the curve (AUC) of maximal UV-visible absorption bands. A, general UV spectrum at T4; B, C and D, the AUC (n=5; mean±SD) at T4, T7, and T10 of radiation exposure, respectively, at 208-218 nm. Letters indicate differences according to unifactorial ANOVA and the Newman-Keuls post hoc test ($p<0.05$).

higher AUC for UV radiation treatments than for the PAR treatment. For T10, the amplitude of variances between the PAR and UV radiation treatments was higher for 260-280 nm (Fig. 4D).

For the absorption spectrum of methanolic extract, we identified five maximum bands in the UV-visible spectrum: 208-218, 260-276 and 328-350 nm for the UV spectrum, and 430-450 and 600-670 nm for the visible spectrum (Fig. 5). More visible-absorbing compounds than UV-absorbing compounds were registered (Fig. 5A). For T4 (Fig. 5B), T7 (Fig. 5C) and T10 (Fig. 5D), similar lower AUC values at UV maximum bands of 260-276, 328-350 and 430-450 nm than visible maximum bands of 430-450 and 600-670 nm were observed. When comparing the treatments over time, higher absorbance values were recorded in PAR exposure at both UV and visible regions for T10 (Fig. 5D).

The seawater samples in which the algae were cultivated during the experiment show maximal absorption bands in the UV region, specifically in the range 208-218 nm (Fig. 6A), and no absorption was observed at visible wavelengths. No differences for AUC among the treatments were observed at T4 (Fig. 6B), whereas at T7 and T10 greater AUC levels were observed for PAR+UVB > PAR+UVA > PAR (Fig. 6C-D, respectively); additionally, the magnitude of UV-absorbing compounds was greater at T10. This last result agrees with the yellowish colour of the seawater after 10 days of UV radiation exposure, compared with a more brownish coloration over the experimental time for the PAR+UVB treatment (Fig. 7).

©Fungyi Chow / 2021

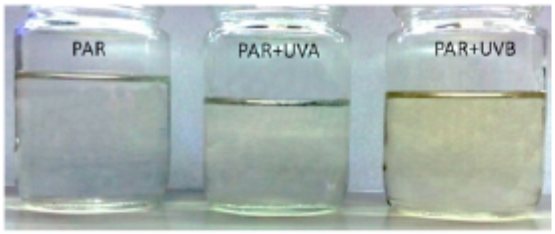

Fig. 7. – Appearance of seawater in which *Sargassum filipendula* was cultivated after 10 days of experimentation at three different radiation treatments.

DISCUSSION

Ultraviolet radiation can lead to manifold effects on biological systems, resulting in anatomical, physiological, biochemical and molecular alterations. Therefore, elevated doses of UV radiation trigger acclimation mechanisms in exposed benthic macroalgae, enabling them to tolerate the stressful condition and generating, in turn, a series of responses to maintain control over biological homoeostasis (Viñegla and Figueroa 2009). Furthermore, UV-induced oxidative stress seems to elicit diverse and complex defence mechanisms as a response to avoid cellular damage and assure the hormesis.

The present study shows that the growth rate of *S. filipendula* showed no differences when treated with the specified doses of PAR+UVA and PAR+UVB over 10 days of experiment. Usually, UVA radiation causes indirect DNA damage through the formation of chemical intermediates, such as oxygen and hydroxyl radicals that interact with DNA to form cross-links and breaks in the DNA-protein chain (Dahms et al. 2011). However, moderate doses of UVA such as the one used for this experiment have been shown to stimulate photosynthesis and macroalgal growth, as reported by Döhler et al. (1995) and Xu and Gao (2010). Additionally, as stated by Xu and Gao (2010), UVA radiation can activate photoprotective mechanisms to counteract the negative effect of UVB radiation, resulting in a decreasing impact of UV radiation on growth rates.

In a previous study using *Sargassum cymosum* C. Agardh as a biological model to evaluate the combined effects of UV radiation and salinity, Polo et al. (2014a) found that UVA and UVB together in low doses such as the ones used herein stimulated the growth rate, leading to an increase in the amount of mitochondria, which could support the metabolic energy demand required for this process. Indeed, studies with different algal species at low doses of UV radiation show that the UV level modulates diverse physiological responses besides growth through up- or downregulation, such as induction of Chl *a*, phenolic compounds and antioxidant activity (Polo et al. 2014a), alteration in putrescine/spermidine ratio (Polo et al. 2014b), variation of photosynthetic performance and accessory pigments (Simioni et al. 2014, Schmidt et al. 2015), and ultrastructural organization (Bouzon et al. 2012, Pereira et al. 2017).

At elevated doses of UV radiation (98 kJ m^{-2} and 27 kJ m^{-2} per day for UVA and UVB, respectively), negative effects on algal growth and development are usually related to the damage caused to photosynthetic machinery, photosynthetic pigments, antioxidant enzymes and lipid peroxidation (Xu and Gao 2010). Makarov (1999) reported a decrease in growth rate of the brown algae *Laminaria saccharina* (Linnaeus) J.V. Lamouroux, *Alaria esculenta* (Linnaeus) Greville, *Saccorhiza dermatodea* (Bachelot de la Pylaie) J. Agardh, *Fucus distichus* Linnaeus, *F. serratus* Linnaeus, and *F. vesiculosus* Linnaeus when exposed to UVB radiation. Likewise, Michler et al. (2002) reported a pronounced thallus necrosis and loss of parts of the thalli in the arctic *L. solidungula* J. Agardh after one week of daily exposure (18 h) to UV radiation, a process that ultimately led to weight loss. However, it must be taken into account that their study was carried out in the field, with higher doses of UV radiation (324 kJ m^{-2} and 12.96 kJ m^{-2} per day for UVA and UVB, respectively) and a longer exposure time than the experimented with *S. filipendula* in this study (75.6 kJ m^{-2} and 16.2 kJ m^{-2} for UVA and UVB per day, respectively). Tissue deformation observed as partial necrosis of the apical segments has also been reported for red macroalgae such as *Gracilaria domingensis* (Kützing) Sonder ex Dickie (Schmidt et al. 2010a), *Kappaphycus alvarezii* (Doty) Doty ex P.C. Silva (Schmidt et al. 2010b) and *Gelidium floridanum* W.R. Taylor (Schmidt et al. 2012) after UV radiation exposure. In the present study, thallus necrosis was not observed. However, it could be expected that long-term and higher dose exposures to UV radiation may result in tissue deformation and serious damage in *S. filipendula*, and long-term growth measurements and observations on morphological integrity of the algal tissue may represent a more holistic indication of the negative impact of this stress factor (Roleda et al. 2004).

Protein content of *S. filipendula* showed an increase in certain radiation treatments, indicating the possibility of stimulating its accumulation. At control radiation (PAR treatment), an increase in protein level at T10 could represent a response to the nutrient reload caused by the addition of von Stosch enrichment solution to the culture medium after seven days of cultivation. However, this response is unclear. Proteins are known to be strong absorbers of UVB radiation (Karentz 1994), and an increased protein degradation followed by resynthesis in order to replace UVB sensitive proteins could thus be expected during UVB exposure (Cullen and Neale 1994). Repair mechanisms for UVB harm induce damage to membranes and electron transport components, which demand increasing enzymatic activity with higher nitrogen requirements. For example, photosynthetically important proteins such as ribulose-1,5-biphosphate carboxylase/oxygenase (RubisCO) and D1 protein show an increased turnover under UV exposure, leading to a decrease in photosynthetic activity (Aro et al. 1993, Bornman and Teramura 1993, Strid et al. 1994). Moreover, it has been shown that UVB can directly affect the nitrogen uptake system in phytoplankton and leads to decreased uptake rates of ammonium and nitrate (Behrenfeld et al. 1995, Döhler 1997). In addition, algae are more sensitive to environ-

mental variations when their intracellular nitrogen reserves are exhausted. As reported by some authors, an increase in nitrogen availability, in the form of nitrate and ammonium, will result in higher growth rates in various algae (Chow and Oliveira 2008). In addition, Bischof et al. (2000b) suggest a possible mechanistic linkage between susceptibility to UV radiation and N metabolism, because the limitation of this element could inhibit D1 protein turnover and the synthesis of RubisCO in the brown macroalga *A. esculenta*. When analysing the UV spectrum

The increase in overall UV-PAR absorption and in absorption at specific ranges are consequences of protein-phenolic interactions. Bonding with phenolics results in the increased absorption of complexes due to the ability of these compounds to absorb UV-PAR radiation. Additionally, the interactions of phenolic compounds with proteins may lead to changes in physico-chemical properties of proteins such as solubility, thermal stability, and digestibility (Labuckas et al. 2008).

Photosynthetic pigments showed little variation during UV exposure within and between treatments. Some authors have reported that UVB radiation is responsible for the loss of photosynthetic pigments (Bischof et al. 2000a, Holzinger and Lütz 2006) and can also reduce the expression of genes involved in photosynthesis (Holzinger and Lütz 2006). When analysing the visible spectrum from methanolic extract, maximal absorption bands were recorded in the region between 430-450 and 600-670 nm, indicating the presence of Chl *a* (with maximal absorption bands at 432, 617 and 666 nm). However, no differences were observed for *S. filipendula*. Chl *a* is the main pigment constituent of the reaction centre, in which the D1 protein is closely associated with the occurrence of the electron transport chain of the photosystems. Moreover, the alteration of the size of the harvesting antenna complex and the carotenoid antioxidant composition indicate that photosynthesis is a dynamic process that attempts to safeguard the integrity of the reaction centre and Chl *a*. Therefore, specifically Chl *a* must be tolerant to different stressing impacts, and, as demonstrated in our study, this stability is also observed at moderate UV exposure, showing the ability to acclimate to variations in light intensity and spectral quality (Senger and Bauer 1987, Falkowski and LaRoche 1990).

Additionally, accessory pigments such as Chl *c* (with maximal absorption bands at 445, 584, and 633 nm) and carotenoids were also observed. These pigments serve as an antenna to increase the energy absorption capacity to be directed to the reaction centre. However, under stress conditions, the accessory pigments may be degraded in order to reduce the excess energy being directed to the reaction centre and thus not overburden the Chl *a* and hence prevent oxidation. These facts could explain the reduction in Chl *c* observed herein. Similar results were observed by Polo et al. (2014b), in which Chl *c* was diminished, thus preventing oxidative damage of the photosynthetic apparatus under exposure to UV radiation.

Carotenoids have a recognized antioxidant activity, in which an increase will act as an antioxidant mechanism for protecting the photosynthetic apparatus against oxidative stress. For the present study, total carotenoid content showed no significant variations. According to Teramura (1983), carotenoids are generally less affected than chlorophylls in cropland plants exposed to UVB radiation. Additionally, accumulation of carotenoids specifically in response to UV radiation in both phytoplankton (Goes et al. 1994) and macroalgae (Polo et al. 2014b) suggests that this condition could induce antioxidant defences triggering by these pigments. Within these pigments, fucoxanthin (maximal absorption bands at 428, 448 and 468 nm), one of the most abundant carotenoids in brown algae, has attracted considerable interest due to its biological properties, such as antioxidant, anti-inflammatory, anticancer, anti-obese, antidiabetic, antiangiogenic, and antimalarial activities (D'Orazio et al. 2012). The fact that the protection mechanism by pigment degradation and/or increase in carotenoids was apparently not very evident for *S. filipendula* under the UV radiation effect could indicate the participation of other mechanisms in response to UV radiation. As has been recorded for other macroalgae, the establishment of physical barriers such as the increase in the cell wall polysaccharide layer can shield the photosynthetic apparatus against damaging radiation or the induction and synthesis of UV-absorbing compounds, such as phenolic compounds, which are additional mechanisms that might be involved in UV radiation acclimation of radiation protecting processes (Schoenwaelder 2002).

For a large group of organisms, a biological phenomenon referred to as preparation for oxidative stress (POS) has been reported (Hermes-Lima and Storey 1998), in which an antioxidant upregulation linked exclusively to low oxygen stress is established. Several laboratory studies have shown increases in activity of the enzymes catalase, superoxide dismutases, and glutathione peroxidases and reduced levels of glutathione under hypoxia conditions (Moreira et al. 2017). Although POS has not been reported for conditions other than low oxygen, changes in enzymatic and non-enzymatic antioxidant systems have been widely reported for other stress conditions than hypoxia. We therefore suggest the expansion of this term to other situations in which there is activation of the antioxidant systems, as occurs in response to other types of stressors such as UV radiation.

Macroalgae produce a large diversity of UV-absorbing compounds that are known to protect against UV radiation stress (Korbee et al. 2005, Abdala-Diaz et al. 2006). The measurement of the UV-visible absorption spectrum is an easy and valuable tool for comparing the presence and biosynthesis of UV-absorbing compounds and elucidating hypothetic chemical classes with a photoprotective function. For *S. filipendula*, maximal absorption bands in the UV region were widely observed, suggesting the presence of secondary metabolites such as phenolic compounds, which are largely distributed among brown algae, acting as a defence mechanism (Li et al. 2011) and a potent antioxidant (Al-Azzawie and Alhamdani 2006).

From the maximal UV absorption bands identified in *S. filipendula* some compounds can be suggested,

such as tannins with λmax near 278 nm, phlorotannins with λmax close to 220-240 and 260-280 nm, flavonoids such as flavone/flavonols with λmax about 210, 240/260 and 370 nm (like apigenins) and morin with λmax close to 240-280 and 350-385 nm, and phenolic acids with λmax of 220 nm and 320 nm (Chakraborty and Joseph 2016, Abirami and Kowsalya 2017).

Polyphenols are the most prominent phenolic compounds in brown seaweeds, particularly phlorotannins, which are exclusive to this taxon. They are found free or forming complexes with components of the cell walls (Wang et al. 2012), such as polysaccharides, and are essential to the physiological integrity of algae, with important roles involved in chemical defences and protection against oxidative damage in response to changes in nutrient availability and UV radiation (Li et al. 2017).

In addition, the λmax at 210 nm was previously reported by Salgado et al. (2007) in *Padina gymnospora* (Kützing) Sonder, and the authors attribute this absorption band to a linkage between phenolic compounds and alginates. Other studies in which this linkage has been observed (Schoenwaelder 2002, Berglin et al. 2004, Salgado et al. 2005) reveal that this coupling preserves the UV absorption capability of phenolic compounds over time. Moreover, there is an extensive literature reporting their properties, especially their capacity to act as an antioxidant, with positive effects on human and animal health improving the current interest in disease therapy and chemoprevention (Panche et al. 2016).

The phlorotannins fucophloroethol, phloroethol, eckol, and dieckol have been identified in several species of brown algae, including species of the genus *Sargassum* (Li et al. 2011). No identification of these compounds was performed in our study, but our results suggest the presence of phlorotannins because they have maximal absorption bands within the ranges observed herein. Additionally, by analysing the ultrastructure of *S. cymosum*, Polo et al. (2014a) reported the degradation and high migration of phlorotannins contained in physoids through the cell wall as a response caused by UV radiation. This phenomena leads to the liberation of phenolic compounds into the surrounding medium, creating a UV-absorbing microenvironment (UV refuge) (Roleda et al. 2010, Celis-Plá et al. 2014, 2018). This acclimation strategy against UV radiation was also observed in the present study: the seawater that *S. filipendula* was cultivated in during radiation exposure showed a yellowish colour as an indicator of this exudation, with greater intensity in the PAR+UVB treatment.

Our results for *S. filipendula* show the capacity of the species to synthesize and accumulate UV- and visible-absorbing compounds, probably phlorotannins and carotenoids, respectively, that could provide adaptive advantages for organisms exposed to different ambient stressors such as UV radiation, since brown algae could be more sensitive to UV exposure. This feature is of great importance for macroalgae inhabiting the coasts of Brazil because of the high radiation levels to which they are subjected, especially during low tides and in summer. In addition, the isolation, identification, and comprehension of the biosynthesis action of these compounds will undoubtedly be of great benefit for the development of functional bioproducts with potential application in the medical, pharmaceutical, food and agricultural fields.

In this paper we present the results of a basic research study that contributes to knowledge of the sensitivity and tolerance to UV radiation of *S. filipendula*, a species that is valuable for community structuring in tropical and subtropical marine habitats and is widely distributed on the Brazilian coast in the lower intertidal zone. The integrative data on physiological performance presented herein give insights into the biological implications of this stressor factor for the species. Additionally, the results suggest environmental consequences such as a decrease in primary production due to the possible inhibition of photosynthesis at population level, affecting growth rate and reproduction and leading to the devastation of the trophic base for associated species and the elimination of the ecological niche diversity in this ecosystem. The sensitivity of *S. filipendula* to changes in abiotic factors can therefore be used for environmental monitoring to support decision-making of monitoring and mitigation programmes

ACKNOWLEDGEMENTS

The authors thank CAPES (Coordination for the Improvement of Higher Education Personnel, Brazil; 2014/2326859) and FAPESP (São Paulo Research Foundation, Brazil; 2016/03095-0) for the PhD fellowships. F. Chow acknowledges a FAPESP research grant (Biota/FAPESP 2013/50731-1) a CNPq research productivity grant (National Council for Scientific and Technological Development, Brazil; 303937/2015-7).

The authors declare that they have no conflict of interest.

REFERENCES

Abdala-Díaz R.T., Cabello-Pasini A., Pérez-Rodríguez E., et al. 2006. Daily and seasonal variations of optimum quantum yield and phenolic compounds in *Cystoseira tamariscifolia* (Phaeophyta). Mar. Biol. 148: 459-465. https://doi.org/10.1007/s00227-005-0102-6

Abirami R.G., Kowsalya S. 2017. Quantification and correlation study on derived phenols and antioxidant activity of seaweeds from Gulf of Mannar. J. Herbs, Spices Med. Plants 23: 9-17. https://doi.org/10.1080/10496475.2016.1240132

Al-Azzawie H.F., Alhamdani M.S.S. 2006. Hypoglycemic and antioxidant effect of oleuropein in alloxan-diabetic rabbits. Life Sci. 78: 1371-1377. https://doi.org/10.1016/j.lfs.2005.07.029

Altamirano M., Flores-Moya A., Figueroa F.L. 2003. Effects of UV radiation and temperature on growth of germlings of three species of *Fucus* (Phaeophyceae). Aquat. Bot. 75: 9-20. https://doi.org/10.1016/S0304-3770(02)00149-3

Amado Filho G.M., Andrade L.R., Karez C.S., et al. 1999. Brown algae species as biomonitors of Zn and Cd at Sepetiba Bay, Rio de Janeiro, Brazil. Mar. Environ. Res. 48: 213-224. https://doi.org/10.1016/S0141-1136(99)00042-2

Aro E.M., Virgin I., Andersson B. 1993. Photoinhibition of Photosystem II. Inactivation, protein damage and turnover. BBA - Bioenerg. 1143: 113-134. https://doi.org/10.1016/0005-2728(93)90134-2

Ayres-Ostrock L.M., Plastino E.M. 2014. Effects of short-term exposure to ultraviolet-B radiation on photosynthesis and pigment content of red (wild types), greenish-brown, and green strains of *Gracilaria birdiae* (Gracilariales, Rhodophyta). J. Appl. Phycol. 26: 867-879.

https://doi.org/10.1007/s10811-013-0131-3
Bais A.F., McKenzie R.L., Bernhard G., et al. 2015. Ozone depletion and climate change: impacts on UV radiation. Photochem. Photobiol. Sci. 14: 19-52. https://doi.org/10.1039/C4PP90032D
Baruti J., Korbee N., Oliveira M., et al. 2011. Effects of N supply on the accumulation of photosynthetic pigments and photoprotectors in *Gracilaria tenuistipitata* (Rhodophyta) cultured under UV radiation. J. Appl. Phycol. 23: 457-466. https://doi.org/10.1007/s10811-010-9603-x
Behrenfeld M.J., Lean D.R.S., Lee H. 1995. Ultraviolet-B radiation effects on inorganic nitrogen uptake by natural assemblages of oceanic plankton. J. Phycol. 31: 25-36. https://doi.org/10.1111/j.0022-3646.1995.00025.x
Berglin M., Delage L., Potin P., et al. 2004. Enzymatic cross-linking of a phenolic polymer extracted from the marine alga *Fucus serratus*. Biomacromolecules 5: 2376-2383. https://doi.org/10.1021/bm0496864
Bischof K., Hanelt D., Tüg H., et al. 1998. Acclimation of brown algal photosynthesis to ultraviolet radiation in Arctic coastal waters (Spitsbergen, Norway). Polar Biol. 20: 388-395. https://doi.org/10.1007/s003000050319
Bischof K., Hanelt D., Wiencke C. 2000a. Effects of ultraviolet radiation on photosynthesis and related enzyme reactions of marine macroalgae. Planta 211: 555-562. https://doi.org/10.1007/s004250000313
Bischof K., Kräbs G., Hanelt D., et al. 2000b. Photosynthetic characteristics and mycosporine-like amino acids under UV radiation: A competitive advantage of *Mastocarpus stellatus* over *Chondrus crispus* at the Helgoland shoreline? Helgol. Mar. Res. 54: 47-52. https://doi.org/10.1007/s101520050035
Björn L.O. 2007. Stratospheric ozone, ultraviolet radiation, and cryptogams. Biol. Conserv. 135: 326-333. https://doi.org/10.1016/j.biocon.2006.10.006
Bornman J.F., Teramura A.H. 1993. Effects of enhanced UV-B radiation on terrestrial plants. In: Young A.R., Bjorn L.O., et al. (eds) Environmental UV Photobiology. Plenum Press, New York, pp, 427-471. https://doi.org/10.1007/978-1-4899-2406-3_14
Bouzon Z.L., Chow F., Zitta C.S., et al. 2012. Effects of natural radiation, photosynthetically active radiation and artificial ultraviolet radiation-b on the chloroplast organization and metabolism of *Porphyra acanthophora* var. *brasiliensis* (Rhodophyta, Bangiales). Microsc. Microanal. 18: 1467-1479. https://doi.org/10.1017/S1431927612013359
Bradford M.M. 1976. A rapid and sensitive method for the quantitation of microgram quantities of protein utilizing the principle of protein-dye binding. Anal. Biochem. 72: 248-254. https://doi.org/10.1016/0003-2697(76)90527-3
Buma A.G.J., Walter Helbling E., Karin De Boer M., et al. 2001. Patterns of DNA damage and photoinhibition in temperate South-Atlantic picophytoplankton exposed to solar ultraviolet radiation. J. Photochem. Photobiol. B Biol. 62: 9-18. https://doi.org/10.1016/S1011-1344(01)00156-7
Celis-Plá P.S.M., Korbee N., Gómez-Garreta A., et al. 2014. Patrones estacionales de fotoaclimatación en el alga intermareal, *Cystoseira tamariscifolia* (Ochrophyta). Sci. Mar. 78: 377-388. https://doi.org/10.3989/scimar.04053.05A
Celis-Plá P.S.M., Brown M.T., Santillán-Sarmiento A., et al. 2018. Ecophysiological and metabolic responses to interactive exposure to nutrients and copper excess in the brown macroalga *Cystoseira tamariscifolia*. Mar. Pollut. Bull. 128: 214-222. https://doi.org/10.1016/j.marpolbul.2018.01.005
Chakraborty K., Joseph D. 2016. Antioxidant potential and phenolic compounds of brown seaweeds *Turbinaria conoides* and *Turbinaria ornata* (Class: Phaeophyceae). J. Aquat. Food. Prod. Technol. 25: 1249-1265. https://doi.org/10.1080/10498850.2015.1054540
Chow F., De Oliveira M.C. 2008. Rapid and slow modulation of nitrate reductase activity in the red macroalga *Gracilaria chilensis* (Gracilariales, Rhodophyta): Influence of different nitrogen sources. J. Appl. Phycol. 20: 775-782. https://doi.org/10.1007/s10811-008-9310-z
Cruces E., Huovinen P., Gómez I. 2013. Interactive effects of UV radiation and enhanced temperature on photosynthesis, phlorotannin induction and antioxidant activities of two sub-Antarctic brown algae. Mar. Biol. 160: 1-13. https://doi.org/10.1007/s00227-012-2049-8
Cullen J., Neale P. 1994. Ultraviolet radiation, ozone depletion, and marine photosynthesis. Photosynth. Res. 39: 303-320. https://doi.org/10.1007/BF00014589
D'Orazio N., Gemello E., Gammone M.A., et al. 2012. Fucoxantin: A treasure from the sea. Mar. Drugs 10: 604-616. https://doi.org/10.3390/md10030604
Dahms H.U., Dobretsov S., Lee J.S. 2011. Effects of UV radiation on marine ectotherms in polar regions. Comp. Biochem. Physiol. - C Toxicol. Pharmacol. 153: 363-371. https://doi.org/10.1016/j.cbpc.2011.01.004
Diffey B.L. 2002. Sources and measurement of ultraviolet radiation. Methods 28: 4-13. https://doi.org/10.1016/S1046-2023(02)00204-9
Döhler G. 1997. Impact of UV radiation of different wavebands on pigments and assimilation of 15N-ammonium and 15N-nitrate by natural phytoplankton and ice algae in Antarctica. J. Plant. Physiol. 151: 550-555. https://doi.org/10.1016/S0176-1617(97)80229-5
Döhler G., Hagmeier E., David C. 1995. Effects of solar and artificial UV irradiation on pigments and assimilation of 15N ammonium and 15N nitrate by macroalgae. J. Photochem. Photobiol. B Biol. 30: 179-187. https://doi.org/10.1016/1011-1344(95)07189-9
Edwards P. 1970. Illustre ated guide of seaweeds and sea grasses in vicinity of Porto Arkansas, Texas. Contrib. Mar. Sci. 15: 1-228.
Falkowski P., LaRoche J. 1990. Acclimation to spectral irradiance in algae. J. Phycol. 27: 8-14. https://doi.org/10.1111/j.0022-3646.1991.00008.x
Figueroa F.L., Domínguez-González B., Korbee N. 2014. Vulnerability and acclimation to increased UVB radiation in three intertidal macroalgae of different morpho-functional groups. Mar. Environ. Res. 97: 30-38. https://doi.org/10.1016/j.marenvres.2014.01.009
Gao K., Xu J. 2008. Effects of solar UV radiation on diurnal photosynthetic performance and growth of *Gracilaria lemaneiformis* (Rhodophyta). Eur. J. Phycol. 43: 297-307. https://doi.org/10.1080/09670260801986837
Goes J.I., Handa N., Taguchi S., et al. 1994. Effect of UV-B radiation on the fatty-acid composition of the marine-phytoplankton *Tetraselmis* sp.: relationship to cellular pigments. Mar. Ecol. Prog. Ser. 114: 259-274. https://doi.org/10.3354/meps114259
Gorostiaga J.M., Díez I. 1996. Changes in the sublittoral benthic marine macroalgae in the polluted area of Abra de Bilbao and proximal coast (Northern Spain). Mar. Ecol. Prog. Ser. 130: 157-167. https://doi.org/10.3354/meps130157
Häder D.-P., Kumar H.D., Smith R.C., et al. 2007. Effects of solar UV radiation on aquatic ecosystems and interactions with climate change. Photochem. Photobiol. Sci. 6: 267-285. https://doi.org/10.1039/B700020K
Heo S.J., Jeon Y.J. 2009. Protective effect of fucoxanthin isolated from *Sargassum siliquastrum* on UV-B induced cell damage. J. Photochem. Photobiol. B Biol. 95: 101-107. https://doi.org/10.1016/j.jphotobiol.2008.11.011
Hermes-Lima M., Storey K. 1998. Role of antioxidant defenses in the tolerance of severe dehydration by anurans. The case of the leopard frog *Rana pipiens*. Mol. Cell. Biochem. 189: 79-89. https://doi.org/10.1023/A: 1006868208476
Holzinger A., Lütz C. 2006. Algae and UV irradiation: Effects on ultrastructure and related metabolic functions. Micron 37: 190-207. https://doi.org/10.1016/j.micron.2005.10.015
Holzinger A., di Piazza L., Lütz C., et al. 2011. Sporogenic and vegetative tissues of *Saccharina latissima* (Laminariales, Phaeophyceae) exhibit distinctive sensitivity to experimentally enhanced ultraviolet radiation: Photosynthetically active radiation ratio. Phycol. Res. 59: 221-235. https://doi.org/10.1111/j.1440-1835.2011.00620.x
Jeffrey S.W. 1963. Purification and Properties of Chlorophyll c from *Sargassum flavicans*. Biochem. J. 86: 313-318. https://doi.org/10.1042/bj0860313
Karentz D. 1994. Ultraviolet tolerance mechanisms in Antarctic marine organisms. Antarct. Res. Ser. 62: 93-110.
Khotimchenko S.V., Yakovleva I.M. 2005. Lipid composition of the red alga *Tichocarpus crinitus* exposed to different levels of photon irradiance. Phytochemistry 66: 73-79. https://doi.org/10.1016/j.phytochem.2004.10.024
Korbee N., Huovinen P., Figueroa F.L., et al. 2005. Availability of ammonium influences photosynthesis and the accumulation of mycosporine-like amino acids in two *Porphyra* species (Bangi-

ales, Rhodophyta). Mar. Biol. 146: 645-654. https://doi.org/10.1007/s00227-004-1484-6
Kumar A., Tyagi M.B., Jha P.N. 2004. Evidences showing ultraviolet-B radiation-induced damage of DNA in cyanobacteria and its detection by PCR assay. Biochem. Biophys. Res. Commun. 318: 1025-1030. https://doi.org/10.1016/j.bbrc.2004.04.129
Labuckas D.O., Maestri D.M., Perelló M., et al. 2008. Phenolics from walnut (*Juglans regia* L.) kernels: Antioxidant activity and interactions with proteins. Food. Chem. 107: 607-612. https://doi.org/10.1016/j.foodchem.2007.08.051
Lee T.M., Shiu C.T. 2009. Implications of mycosporine-like amino acid and antioxidant defenses in UV-B radiation tolerance for the algae species *Pterocladiella capillacea* and *Gelidium amansii*. Mar. Environ. Res. 67: 8-16. https://doi.org/10.1016/j.marenvres.2008.09.006
Li Y.X., Wijesekara I., Li Y., et al. 2011. Phlorotannins as bioactive agents from brown algae. Process. Biochem. 46: 2219-2224. https://doi.org/10.1016/j.procbio.2011.09.015
Li Y., Fu X., Duan D. et al. 2017. Extraction and identification of phlorotannins from the brown alga, *Sargassum fusiforme* (Harvey) Setchell. Mar. Drugs. 15: 1-15. https://doi.org/10.3390/md15020049
Liang Y., Beardall J., Heraud P. 2006. Effects of nitrogen source and UV radiation on the growth, chlorophyll fluorescence and fatty acid composition of Phaeodactylum tricornutum and *Chaetoceros muelleri* (Bacillariophyceae). J. Photochem. Photobiol. B Biol. 82: 161-172. https://doi.org/10.1016/j.jphotobiol.2005.11.002
Lichtenthaler H.K. 1987. Chlorophylls and carotenoids: Pigments of photosynthetic biomembranes. In: Packer L., Douce R. (eds), Plant Cell Membranes. Methods Enzymol. 148: 350-382. https://doi.org/10.1016/0076-6879(87)48036-1
Lichtenthaler H.K., Buschmann C. 2001. Chlorophylls and carotenoids: measurement and characterization by UV-VIS spectroscopy. Curr. Protoc. Food. Anal. Chem. 1: F4.3.1-F4.3.8. https://doi.org/10.1002/0471142913.faf0403s01
Lippert H., Iken K., Rachor E., et al. 2001. Macrofauna associated with macroalgae in the Kongsfjord (Spitsbergen). Polar Biol. 24: 512-522. https://doi.org/10.1007/s003000100250
Madronich S., McKenzie R.L., Björn L.O., et al. 1998. Changes in biologically active ultraviolet radiation reaching the Earth's surface. J. Photochem. Photobiol. B Biol. 46: 5-19. https://doi.org/10.1016/S1011-1344(98)00182-1
Makarov M. 1999. Influence of ultraviolet radiation on the growth of the dominant macroalgae of the Barents Sea. Chemosph - Glob. Chang. Sci. 1: 461-467. https://doi.org/10.1016/S1465-9972(99)00034-3
Michler T., Aguilera J., Hanelt D., et al. 2002. Long-term effects of ultraviolet radiation on growth and photosynthetic performance of polar and cold-temperate macroalgae. Mar. Biol. 140: 1117-1127. https://doi.org/10.1007/s00227-002-0791-z
Moreira D.C., Oliveira M.F., Liz-Guimarães L., et al. 2017. Current trends and research challenges regarding "preparation for oxidative stress". Front. Physiol. 8: 1-8. https://doi.org/10.3389/fphys.2017.00702
Navarro N.P., Figueroa F.L., Korbee N., et al. 2016. Differential responses of tetrasporophytes and gametophytes of *Mazzaella laminarioides* (Gigartinales, Rhodophyta) under solar UV radiation. J. Phycol. 52: 451-462. https://doi.org/10.1111/jpy.12407
Panche A.N., Diwan A.D., Chandra S.R. 2016. Flavonoids: An overview. J. Nutr. Sci. 5: 1-15. https://doi.org/10.1017/jns.2016.41
Paula E.J., Eston V.R. 1987. Are there other Sargassum species potentially as invasive as *S. muticum*? Bot. Mar. 30: 405-410. https://doi.org/10.1515/botm.1987.30.5.405
Penniman C., Mathieson C., Penniman C.E. 1986. Reproductive phenology and growth of *Gracilaria tikvahiae* McLachlan (Gigartinales, Rhodophyta) in the Great Bay Estuary, New Hampshire. Bot. Mar. 29: 147-154. https://doi.org/10.1515/botm.1986.29.2.147
Pereira D.T., Simioni C., Ouriques L.C., et al. 2017. Comparative study of the effects of salinity and UV radiation on metabolism and morphology of the red macroalga *Acanthophora spicifera* (Rhodophyta, Ceramiales). Photosynthetica 56: 799-810. https://doi-org/10.1007/s11099-017-0731-2
Polo L.K., Felix M., Kreusch M. et al. 2014a. Photoacclimation responses of the brown macroalga *Sargassum cymosum* to the combined influence of UV radiation and salinity: Cytochemical and ultrastructural organization and photosynthetic performance. Photochem. Photobiol. 90: 560-573. https://doi.org/10.1111/php.12224
Polo L.K., Felix M., Kreusch M., et al. 2014b. Metabolic profile of the brown macroalga *Sargassum cymosum* (Phaeophyceae, Fucales) under laboratory UV radiation and salinity conditions. J. Appl. Phycol. 27: 887-899. https://doi.org/10.1007/s10811-014-0381-8
Ritchie R.J. 2008. Universal chlorophyll equations for estimating chlorophylls *a, b, c*, and d and total chlorophylls in natural assemblages of photosynthetic organisms using acetone, methanol, or ethanol solvents. Photosynthetica 46: 115-126. https://doi.org/10.1007/s11099-008-0019-7
Roleda M.Y., Hanelt D., Kräbs G., et al. 2004. Morphology, growth, photosynthesis and pigments in *Laminaria ochroleuca* (Laminariales, Phaeophyta) under ultraviolet radiation. Phycologia 43: 603-613. https://doi.org/10.2216/i0031-8884-43-5-603.1
Roleda M.Y., Lüder U.H., Wiencke C. 2010. UV-susceptibility of zoospores of the brown macroalga *Laminaria digitata* from Spitsbergen. Polar Biol. 33: 577-588. https://doi.org/10.1007/s00300-009-0733-z
Ruhland C.T., Fogal M.J., Buyarski C.R., et al. 2007. Solar ultraviolet-B radiation increases phenolic content and ferric reducing antioxidant power in Avena sativa. Molecules 12: 1220-1232. https://doi.org/10.3390/12061220
Salgado LT., Andrade L.R., Amado G.M. 2005. Localization of specific monosaccharides in cells of the brown alga *Padina gymnospora* and the relation to heavy-metal accumulation. Protoplasma 225: 123-128. https://doi.org/10.1007/s00709-004-0066-2
Salgado L.T., Tomazetto R., Cinelli L.P., et al. 2007. The influence of brown algae alginates on phenolic compounds capability of ultraviolet radiation absorption in vitro. Brazilian J. Oceanogr. 55: 145-154. https://doi.org/10.1590/S1679-87592007000200007
Sampath-Wiley P., Neefus C.D., Jahnke L.S. 2008. Seasonal effects of sun exposure and emersion on intertidal seaweed physiology: fluctuations in antioxidant contents, photosynthetic pigments and photosynthetic efficiency in the red alga *Porphyra umbilicalis*. J. Exp. Mar. Bio. Ecol. 361: 83-91 https://doi.org/10.1016/j.jembe.2008.05.001
Schmidt É.C., dos Santos R., Horta P.A., et al. 2010a. Effects of UVB radiation on the agarophyte *Gracilaria domingensis* (Rhodophyta, Gracilariales): Changes in cell organization, growth and photosynthetic performance. Micron 41: 919-930. https://doi.org/10.1016/j.micron.2010.07.010
Schmidt É.C., Maraschin M., Bouzon Z.L. 2010b. Effects of UVB radiation on the carragenophyte *Kappaphycus alvarezii* (Rhodophyta, Gigartinales): Changes in ultrastructure, growth, and photosynthetic pigments. Hydrobiologia 649: 171-182. https://doi.org/10.1007/s10750-010-0243-6
Schmidt É.C., dos Santos R.W., de Faveri C., et al. 2012. Response of the agarophyte *Gelidium floridanum* after in vitro exposure to ultraviolet radiation B: Changes in ultrastructure, pigments, and antioxidant systems. J. Appl. Phycol. 24: 1341-1352. https://doi.org/10.1007/s10811-012-9786-4
Schmidt É.C., Kreusch M., Felix M., et al. 2015. Effects of ultraviolet radiation (UVA+UVB) and copper on the morphology, ultrastructural organization and physiological responses of the red alga *Pterocladiella capillacea*. Photochem. Photobiol. 91: 359-370. https://doi.org/10.1111/php.12396
Schoenwaelder M.E. 2002. The occurrence and cellular significance of physodes in brown algae. Phycologia 41: 125-139. https://doi.org/10.2216/i0031-8884-41-2-125.1
Senger H., Bauer B. 1987. The influence of light quality on adaptation and function of the photosynthetic apparatus. Photochem. Photobiol. 45: 939-946. https://doi.org/10.1111/j.1751-1097.1987.tb07905.x
Simioni C., Schmidt É.C., Felix M., et al. 2014. Effects of ultraviolet radiation (UVA+UVB) on young gametophytes of *Gelidium floridanum*: Growth rate, photosynthetic pigments, carotenoids, photosynthetic performance, and ultrastructure. Photochem. Photobiol. 90: 1050-1060. https://doi.org/10.1111/php.12296
Strid Å., Chow W.S., Anderson J.M. 1994. UV-B damage and protection at the molecular level in plants. Photosynth. Res. 39:

475-489.
https://doi.org/10.1007/BF00014600
Széchy M.T.M., Veloso V.G., De Paula É.J. 2001. Brachyura (Decapoda, Crustacea) of phytobenthic communities of the sublittoral region of rocky shores of Rio de Janeiro and São Paulo, Brazil. Trop. Ecol. 42: 231-242.
Teramura A.H. 1983. Effects of ultraviolet B radiation on the growth and yield of crop plants. Physiol. Plant. 58: 415-427.
https://doi.org/10.1111/j.1399-3054.1983.tb04203.x
Ursi S., Plastino E.M. 2001. Crescimento in vitro de linhagens de coloração vermelha e verde clara de *Gracilaria birdiae* (Gracilariales, Rhodophyta) em dois meios de cultura: análise de diferentes estádios reprodutivos. Rev. bras. Bot. 24: 587-594.
https://doi.org/10.1590/S0100-84042001000500014
Villafañe V.E., Sundback K., Figueroa F.L., et al. 2003. Environment, Photosynthesis in the aquatic UVR, as affected by UVR. In: Helbling E., Zagarese H. (eds), UV Effects in Aquatic Organisms and Ecosystems. Comprehensive Series in Photochemical and Photobiological Sciences, pp 359-383.
Viñegla B., Figueroa F. 2009. Effect of solar and artificial UV radiation on photosynthetic performance and carbonic anhydrase activity in intertidal macroalgae from southern Spain. Ciencias Mar. 35: 59-74.
https://doi.org/10.7773/cm.v35i1.1512
Wang W., Wang S.X., Guan H.S. 2012. The antiviral activities and mechanisms of marine polysaccharides: An overview. Mar. Drugs 10: 2795-2816.
https://doi.org/10.3390/md10122795
Xu J., Gao K. 2010. UV-A enhanced growth and UV-B induced positive effects in the recovery of photochemical yield in *Gracilaria lemaneiformis* (Rhodophyta). J. Photochem Photobiol. B Biol. 100: 117-122.
https://doi.org/10.1016/j.jphotobiol.2010.05.010

ANEXO 7

Comparative proteomic profile of the brown seaweed *Sargassum filipendula*: UV-mediated response

Luz K. Polo[1*], André Luis Wendt dos Santos[2], Eny Iochevet Segal Floh[2], Fungyi Chow[1*]

[1]Laboratory of Marine Algae "Édison José de Paula", Department of Botany, Institute of Biosciences, University of São Paulo, CEP 05508-090, São Paulo, Brazil.

[2]Laboratory of Plant Cell Biology, Department of Botany, Institute of Bioscience, University of São Paulo, CEP 05508-090, São Paulo, Brazil.

*Corresponding author e-mail: luzkapolo@gmail.com, fchow@ib.usp.br

ABSTRACT

Increasing exposure to UV radiation is a factor that can have a negative impact on the health of aquatic organisms as seaweeds, which are of particular significance within the coastal ecosystems. Then, changes in the metabolic control mechanisms hidden behind this physiological trait still need to be further investigated; however, information on the physiological and molecular regulation in algae associated with rising exposure to UV radiation is still scarce. Therefore, our objective was to evaluate the proteome changes of the sub-tropical seaweed *Sargassum filipendula* exposed to PAR (control), PAR+UVA, and PAR+UVB treatments by the analysis of differential abundance of proteins based on the shotgun proteomic approach. Proteins were extracted using the phenol method with the addition of a protease inhibitor cocktail. Differential abundance of proteins were assessed by label-free shotgun proteomic analysis. The obtained peptide data from *S. filipendula* under the UV radiation treatments were blasted against Sargassum-, Fucales-, and Ectocarpus-Uniprot databases, and larger matches were gained with Ectocarpus-Uniprot database. From the data against Ectocarpus-Uniprot database, 467 proteins were identified. These proteins were classified according to its metabolism/function and were mainly related with translation (6.4%), carbohydrate (5.8%), photosynthesis (4.3%), energy (3.4%), oxidoreduction (3.4%), and ROS scavenging defense and stress (2.4%). Additionally, 11% corresponds to uncharacterized peptides. In relation to the treatments, PAR presented 188 proteins with low molecular weight and 84 with high molecular weight and 22 proteins were exclusive for this treatment; 153 and 74 proteins had low and high molecular weight, respectively, for PAR+UVA, and nine proteins

were exclusive for this treatment. Finally, PAR+UVB had 198 proteins with low molecular weight and 97 with high molecular weight, with 60 exclusive proteins for this treatment. From the total identified proteins, 41 were differentially abundant within treatments, being most of them part of the photosynthesis metabolism (26.8%), followed by carbohydrate and energy metabolisms (14.6%), and ROS scavenging defense and stress (12.2%), while 9.8% were categorized as uncharacterized proteins. Our results have giving so far insights into UV stress responses in *S. filipendula* from a proteomic view, which suggests that this stressor may have a severe effect on proteins and, consequently, in all metabolism. Additionally, this analysis could provide target proteins that could improve the ability of *S. filipendula* to adapt to UV exposure. Therefore, proteome studies may lead to identify the proteins involved in stress responses and contribute significantly in our understanding of the molecular mechanisms underlying stress tolerance.

Key words: macroalgae, metabolism, proteome, UV exposure.

INTRODUCTION

Discover the function of genes whose expression responds to the stress caused by the effects of UV radiation is essential for understanding the molecular base that determine the main characteristics of the dynamic responses of stress-responsive genes (de Nadal et al. 2011). From this perspective, insight about differential proteome abundance under stress-related abiotic factors can help in understanding the dynamics of stress responses including stress acclimation and recovery.

Proteomic is a large-scale study of the total protein content of an organism or part of them including their structure and physiological role or function that helps protein identification, metabolic functionality and regulatory alterations, usually as a comparative approach of different stages of the life cycle or under stress conditions. As direct metabolism effector and stress responsive, proteome studies may lead to identify proteins involved in stress responses and contribute significantly in our understanding of the molecular mechanisms underlying stress tolerance. With the development and enhancement of protein separation and identification techniques, comparative proteomic in land plants has evolved into a powerful tool for the identification of proteins previously unrecognized in response to abiotic stress (*i.e.* heavy

metal, UV radiation, light, temperature, nutrient availability) (Kosová et al. 2011). Although, there are few studies with marine macroalgae and the proteomic large-scale studies are scarce. Additionally, secondary metabolites as polysaccharides and polyphenols present in large amounts in brown macroalgae interfere with protein separation and cause protein precipitation or degradation or generate artifact results, especially in approaches that include two-dimensional electrophoresis gels (2-DE) (Yotsukura et al. 2010). Therefore, the extraction procedure is a key point for proteomic approaches, in which the achievement of high protein yields with better purity and integrity are desirable.

Proteomic studies with brown macroalgae describe extraction methods and protein identification by 2-DE gels from *Scytosiphon gracilis* Kogame, *Ectocarpus siliculosus* (Dillwyn) Lyngb (Contreras et al. 2008), *Saccharina japonica* (Areschoug) C.E. Lane, C. Mayes, Druehl & G.W. Saunders (Kim et al. 2011), and *Ecklonia kurome* Okamura (Yotsukura et al. 2010). These works include Tris buffer (lysis buffer), trichloroacetic acid (TCA)/acetone precipitation, urea, and phenol extraction methods. Even after the identification of an improved extraction method, the best results were able to identify no more than 30 polypeptides, therefore, the proteomic approach was quite limited.

Other proteomic studies including comparative proteome changes to abiotic factors identified new proteins that may reveal the relationship of other metabolic pathways involved in stress tolerance. In *E. cava*, protein profile was markedly affected at increasing temperature, leading to a rise in the amounts of photosynthesis-related proteins that catalyzes the elimination of active oxygen species (Yotsukura et al. 2012). In *E. siliculosus*, crucial metabolic pathway proteins were altered during the response to Cu stress as the accumulation of proteins related to energy production such as the pentose phosphate pathway. From *Sargassum fusiforme* (Harvey) Setchell, Zhang et al. (2015) and Zou et al. (2015) investigated patterns of differentially enriched proteins when exposed to different concentration of Cd and Cu. Their results identified several pathways that are activated in response to both metals and distinct patterns of protein regulation were observed. In the case of Cd exposure, a down-regulation of primary carbon metabolism was observed; nevertheless, the high abundance of proteins associated with mRNA translation and protein folding indicates that *S. fusiforme* attempts to correct the errors in gene information processing to maintain cell survival. Exposure to Cu lead to an induction to proteins related to carbohydrate metabolism, protein destination, RNA degradation, and signaling regulation; moreover, novel target proteins involved to other metabolic pathways in Cu tolerance, such as riboflavin metabolism, were identified.

The cited researches, and almost all studies with macroalgal proteomic approaches, have employed the proteomic analysis by the 2-DE in polyacrylamide gel. As a disadvantage of this approach is the underestimated data, limiting a mid- or large-scale proteomic approach. Furthermore, the spots from the 2-DE analysis often represent more than one protein, making the quantification and identification susceptible to mistakes. Any 2-DE gel has restrictions imposed by the gel method, as limited dynamic range at molecular weights and pI values, low reproducibility, bench time-consuming, complexity of sample preparation, and requirement of high amount of sample (Zhu et al. 2010).

Due to the limitations that arise from 2-DE, the non-gel-based "shotgun" proteomic technique together label-free quantification (LFQ) method has been developed, which provides powerful tools for studying large-scale protein expression and characterization in complex biological systems. In this approach, each sample is separately prepared, then subjected to individual Liquid Chromatography coupled with tandem Mass Spectrometry (LC-MS/MS) or two-dimensional Liquid Chromatography (LC/LC). The spectral count-based LFQ allows both relative and absolute quantification of protein abundance and provide rigorous and powerful tools for analyzing protein changes in large-scale proteomic studies (Monteoliva and Albar 2004; Zhu et al. 2010).

Despite the advantages of shotgun proteomic techniques, there are not available researches that include this approach in brown seaweeds, and all studies are with microalgae; even more, the number of proteomic studies based on 2-DE gels, which evaluates stress responses in macroalgae, are scarce. Therefore, more studies are needed to expand our understanding of protein metabolic regulation under abiotic stress as UV radiation exposure and the mechanisms that underlie physiological acclimation and adaptation to this factor, especially with a more extensive and comprehensive mid- and large-scale analysis. Additionally, within the brown seaweeds, *Sargassum* species are valuable ecosystemic organisms as community structuring in tropical and subtropical marine habitats (Széchy et al. 2006) and include potentially prospecting species due the high content of bioactive compounds (Iwashima et al. 2005; Hwang et al. 2010; Sinha et al. 2010; Yende et al. 2014). Thereafter, it constitutes a biological model extremely relevant for future outlines of ecophysiological studies and technological applications. Thereat, proteomic studies could contribute to a better understanding of its biology, as well as of responses to stress conditions and global climate changes, besides providing subsidies for decision-making of monitoring and mitigation programs. In this context, the aim of the chapter was to identify the major revealed proteins and

evaluate the differential proteome profile of the sub-tropical seaweed *Sargassum filipendula* C. Agardh under PAR, PAR+UVA, and PAR+UVB treatments.

MATERIAL AND METHODS

Collection site and algal material. Specimens of *S. filipendula* were collected at Cigarras Beach (24°43'55.74"S and 45°23'54.48"W), localized in São Sebastião, north coast of São Paulo State, Brazil, during the spring season (October 2016). Material was transported in cooler boxes to the laboratory, cleaned of macroepiphytes, and washed with abundant filtered seawater. Cleaned apical portions (± 8 cm) were acclimated for one week under laboratory conditions, in sterilized seawater 32 psu enriched with von Stosch (VS) solution diluted at 50% (Ursi and Plastino (2001) based on Edwards (1970)), photosynthetically active radiation (PAR) of 60 ± 5 µmol photons.m^{-2}.s^{-1}, 25 ± 1 °C, photoperiod of 14 h and intermittent aeration every 30 min. The culture ratio was 3 g of alga per 1 L of culture medium.

Laboratory conditions and experimental setup. After the acclimation period, the material was exposed to three different radiation treatments: a) PAR (control), b) PAR+UVB, and c) PAR+UVA under the same laboratory culture conditions described above, using three biological replicates for each treatment. The experiments were performed under 3 h exposure to UV radiation per day in the middle of the light phase during four days, in which at final experimental period all biomass was weighted and frozen in liquid nitrogen and kept at -80 °C until analysis. During the exposure, aeration was increased in all treatments to promote greater movement of the algal fragments and homogeneous exposure for all branches. UVB (312 nm; 1.5 W.m^{-2}; 16.2 kJ.m^{-2} /day) and UVA (365 nm; 7 W.m^{-2}; 75.6 kJ.m^{-2} /day) radiations were provided by Philips lamps models TL 20W/12 and Actinic BL TL-K 40 W/10-R, respectively.

The measurements of PAR intensity were obtained in µmol photons.m^{-2}.s^{-1} using a quantameter LI-COR Biosciences Model Li-250A (Lincoln-Nebraska, USA) connected to the underwater spherical LI-COR sensor SPQSA1346 (USA). The UV radiation intensity was obtained in W.m^{-2}, with a MACAM Ultraviolet Radiometer (Scotland) connected to the UVB or UVA specific sensors. The measurements of total radiation spectrum emitted by radiation sources (PAR and UV) were obtained using the SphereOptics SMS-500 spectroradiometer (Spectral Measurements System, USA).

Protein extraction. Proteins were extracted following the phenol extraction method reported for brown algae and according to Zou et al. (2015) with modifications from the

biological replicates individually. Samples of approximately 10 g of fresh frozen biomass were grounded into a fine powder using the TissueLysser II (Qiagen, Germany) and suspended in 30 mL of extraction buffer (0.9 M sucrose; 0.1 M Tris–HCl; 0.01 M EDTA; 0.1 M KCl). Just before the extraction, 2% β-mercaptoethanol and 1 mM phenylmethylsulfonyl fluoride (PMSF) were added. The biological material was extracted by shaking for 1 h at 4 °C and then mixed with an equal volume of saturated phenol (pH 8.0) and incubated on a shaker for 10 min at room temperature. The homogenate was centrifuge at 6,500 rpm and 4 °C for 10 min. Phenolic phase, which was on top of the homogenate was carefully recovered to avoid contact with the interphase homogenate, poured into a new tube and back-extracted with 30 mL of extraction buffer. Samples were shaken for 3 min and vortexed, and the centrifugation was repeated at 6,500 rpm and 4 °C for 10 min. The final collection of phenolic phase was mixed with five volumes of precipitation buffer (0.1 M ammonium acetate in cold methanol) and then incubated overnight at −20 °C. Proteins were pelleted by centrifugation at 6,500 rpm and 4 °C for 10 min and the pellet was washed three times with cooled precipitation solution and finally with cooled acetone. The pellets were air-dried and recovered by shaking for 1 h at room temperature with freshly isoelectric focusing buffer containing 9 M urea; 2 M thiourea; 4% CHAPS; 20 mM DTT; 1.2% Pharmalytes pH 4 to 7 non-linear, 10% PMSF, and protease inhibitor cocktail (Sigma-Aldrich, USA) for avoiding protein degradation. Finally, the homogenates were centrifuged for 15 min at 13,500 rpm at room temperature and .

Protein quantification. Part of the precipitated proteins were resuspended in a copper-containing solution and an unbound copper, and quantified with a colorimetric agent (working color reagent) by the 2-D-Quant kit (GE Healthcare Life Sciences, USA) according to manufacturer's specifications. The assay has a linear response to protein in the range of 0–33 $\mu g.mL^{-1}$, and uses BSA (bovine serum albumin) as standard. Absorbances of each sample and standard were read at 480 nm using UV-visible microplate spectrophotometer (Epoch Biotek, USA).

Shotgun label-free quantitative proteomic analysis. Another part of the precipitated peptides was resuspended in 0.1% formic acid (FA) and analyzed using an LTQ-Orbitrap Velos ETD (Thermo, USA) coupled with Easy nanoLC II (Thermo, USA). The peptides were loaded onto a C18RP column (75 µm id × 10 cm, 3.5 µm particle size, 100 Å pore size; New Objective, Ringoes, USA) and separated on a 115 min gradient. The LTQ-Orbitrap Velos was operated in positive ion mode with data-dependent acquisition. The full scan was obtained in the Orbitrap with an automatic gain control (AGC) target value of $10e^6$ ions and a maximum fill time of 500

ms. Each precursor ion scan was acquired at a resolution of 60,000 FWHM in the 400–1500 m/z mass range. Peptide ions were fragmented by CID MS/MS using a normalized collision energy of 35. The 20 most abundant peptide were selected for MS/MS and dynamically excluded for a duration of 30 s. The instrumental conditions were checked using 50 fmol of a tryptic digest of BSA as standard. The sample carryover was completely removed between run. The quantitation analyses was performed using MaxQuant (v 1.6.1.0) and Perseus (v 1.6.1.1) software's.

Protein identification and classification. Identity of the protein dataset was directly searched against three UniProt databases (http://www.ebi.uniprot.org) on April 2018 to obtain the corresponding blast information from the same genus Sargassum_Uniprot, same order Fucales_Uniprot, and a biological brown alga model Ectocarpus_UniProt that has its genome sequenced and manually searched by using the accession numbers against the UniProt database. Based on the obtained information, proteins were categorized according to its molecular weight and functional classification. Additionally, total identified proteins from the three Uniprot databases were registered, as well as the amount of differentially abundant proteins against the Ectocarpus_UniProt database, since this database lead the highest protein identity.

Data analysis of differential abundant proteins. A Venn diagram was performed with the total set of proteins to identify which of them were exclusive between the treatments using the web tool available on http://bioinformatics.psb.ugent.be/webtools/Venn/. Statistical analysis of proteins differentially abundant data set from the treatments was performed against the Ectocarpus_Uniprot database with the software Perseus (v 1.6.1.1) by using three replicates for each radiation treatment, as this database allowed major protein identity. Significant differences in the radiation treatments were tested by Student *t* tests ($p < 0.05$) based on the protein abundance were performed by comparing between PAR versus PAR+UVA, PAR versus PAR+UVB, and PAR+UVA versus PAR+UVB. Additionally, a multiple comparison for evaluating the integration of the composition and abundance of differentially abundant proteins in each sample, a bi-dimensional hierarchical clusterization, followed by Euclidean distance and Paired group analyses combined with the Pearson correlation index was performed. The cluster results were associated to a heatmap graphic.

RESULTS

Shotgun label-free quantitative proteomic analysis. Results from proteomic analysis by shotgun LC-MS/MS were searched against three databases: (a) Sargassum_Uniprot database contains 2,471 proteins within 42 matches categorized as uncharacterized proteins, corresponding to 1.70%. When searching our proteins from *S. filipendula* under UV radiation exposure against this set, 188 had a match and only one was uncharacterized (Fig. 1). (b) Fucales_Uniprot database registers 3,996 proteins and 61 of them are still to be characterized (1.8%). In the same way, proteins from *S. filipendula* under UV radiation exposure were searched against this data set and 248 proteins were matches with only one uncharacterized protein (Fig. 1).

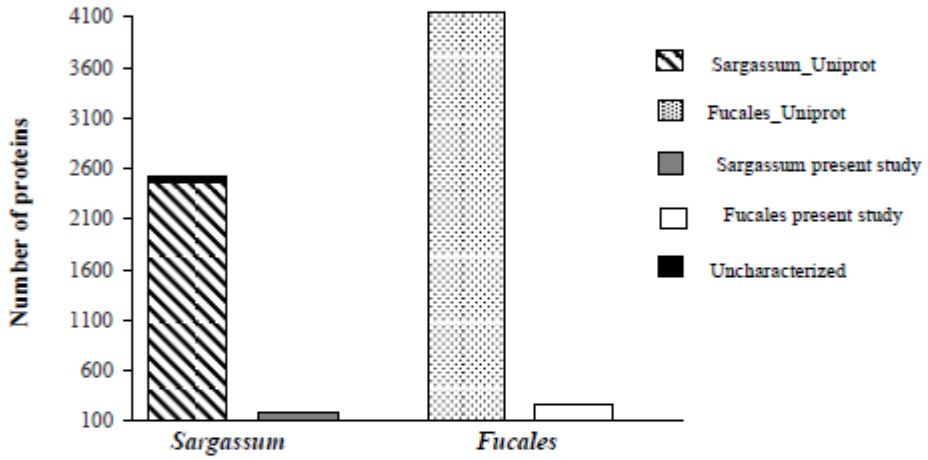

Figure 1. Total number of proteins from Sargassum_Uniprot and Fucales_Uniprot databases with the respective uncharacterized proteins, and the number of proteins from our study with *Sargassum filipendula* matched with the respective Uniprot database (Sargassum_Uniprot or Fucales_Uniprot) and the amount of uncharacterized proteins.

Finally, the last database used corresponds to Ectocarpus_Uniprot. This base was chosen since *Ectocarpus siliculosus* is one the few brown seaweeds with the complete genome sequenced, enabling a greater correspondence in protein identity. This database contains a list with 17,225 proteins, nevertheless, a great number of proteins (7,099, *ca.* 46%) are not yet characterized. When comparing against this set, 467 proteins from *S. filipendula* under UV radiation exposure found a match and 53 from this identification were in the category of uncharacterized (*ca.* 11 %). As the major amount of protein matches were obtained with Ectocarpus_Uniprot, this was the proteomic *S. filipendula* data set used for further analysis.

The main identified metabolism for proteomic *S. filipendula* data set were translation (6.4%), carbohydrate (5.8%), photosynthesis (4.3%), energy (3.4%), oxidoreduction (3.4%), and ROS scavenging, defense stress related (2.4%) (Fig. 2). The remaining 74.3% of matches proteins were distributed in several metabolisms, listed in detail in the Table S1.

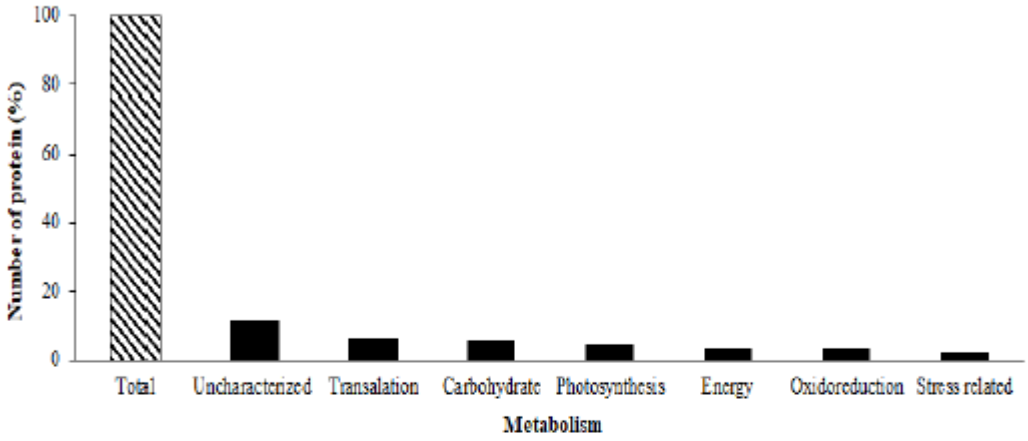

Figure 2. Percentage of matched proteins of *Sargassum filipendula* under the radiation treatments with the *Ectocarpus*_Uniprot database, including uncharacterized proteins and metabolic/function classification.

When comparing against this set, 467 proteins from *S. filipendula* under UV radiation exposure found a match and 53 from this identification were in the category of uncharacterized (*ca.* 11 %).

From the 467 proteins of *S. filipendula* matches with Ectocarpus_Uniprot data set and excluding the 53 proteins with uncharacterized category, the total of 414 identified proteins were plotted by the multiple overlapping Venn diagram (Fig. 3). When comparing within the treatments, 199 proteins were overlapping by the three treatments (PAR, PAR+UVA, and PAR+UVB), including in basic metabolic pathways such as 40S ribosomal protein S27, elongation factor G-mitochondrial and alanine transaminase involved in translation; RUBisCo, ribose-5-phosphate isomerase, glucose-6-phosphate 1-epimerase and fructose-bisphosphatase involved in carbohydrate metabolism; PSII 11 kDa protein, PSI reaction center subunit II and cytochrome c-550 with photosynthetic functions, among others. PAR and PAR+UVA treatments, shared 16 proteins (Fig. 3), most of them being part of the photosynthesis metabolism (PSII oxygen evolution complex protein PsbP, PSI subunit III, thylakoid lumen 15.0 kD protein). In the case of PAR and PAR+UVB treatments, they had 34 proteins in

common which are involved in diverse metabolism and function such as transport, carbohydrate, protein catabolic process, DNA binding, carbon metabolism, metallopeptidase activity, among others. The last comparison between PAR+UVA and PAR+UVB (Fig. 3) showed four common proteins, each one belonging to a different metabolism. Exclusive protein identities were also detected, 22 proteins were exclusive for PAR, such as V-type proton ATPase subunit F, peptidyl-prolyl cis-trans isomerase, SASA domain-containing protein, filamentous temperature sensitive Z; PAR+UVA presented nine exclusive proteins, including molecular chaperones HSP70/HSC70 and HSP70 superfamily PH which are related with ROS scavenging, defense and stress. Finally, PAR+UVB was the treatment with highest number of exclusively proteins (60), with a large group having oxidoreduction, ROS scavenging, defense and stress activities such as superoxide dismutase, PEROXIDASE_4 domain-containing protein, short-chain dehydrogenase/reductase SDR, SGT1 homologue, HSP70-putative and 2-cys peroxiredoxin, among others (Fig. 3).

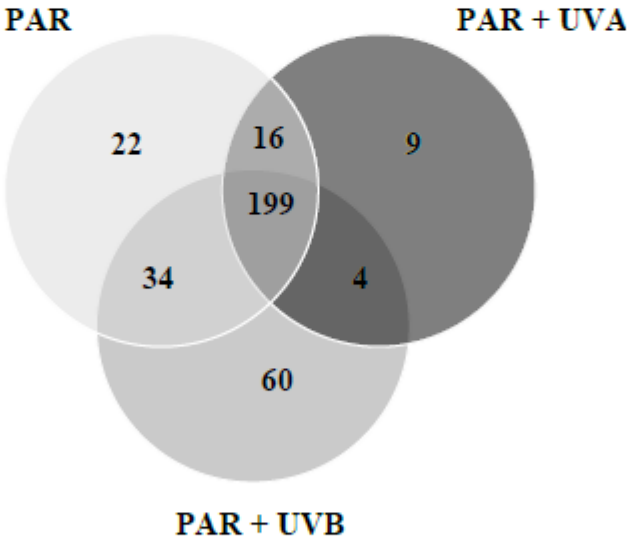

Figure 3. Multiple overlapping quantitative proteomic by the Venn diagram depicting exclusive and common detected proteins from PAR, PAR+UVA, and PAR+UVB treatments.

The list of 467 proteins matched for *S. filipendula* with the information obtained from the Ectocarpus_Uniprot database was also classified according to its molecular weight (low and high). Proteins with molecular weight up to 50 kDa are considered as low molecular weight (LMW) proteins, and above this value corresponds to high molecular weight (HMW) proteins.

From this classification, all treatments presented proteins with molecular weights close to both categories, LMW (ranging from 153 to 198) and HMW (ranging from 74 to 97) proteins.

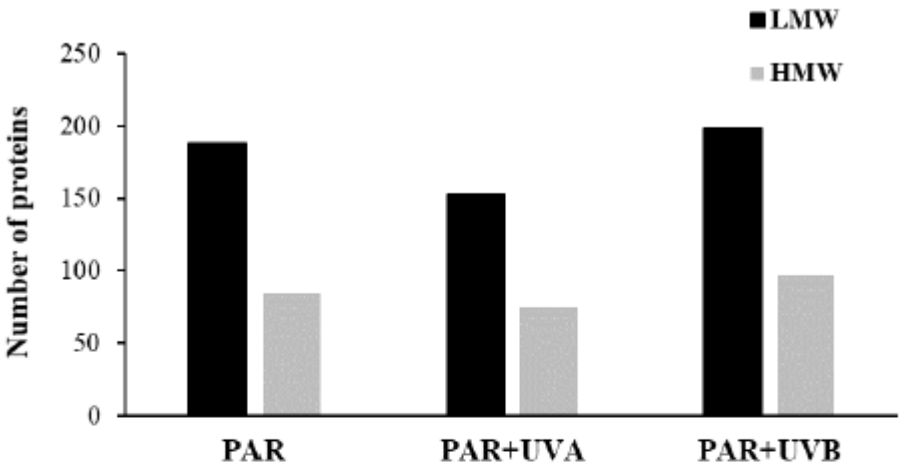

Figure 4. Classification of proteins of *Sargassum filipendula* matched with Ectocarpus_uniprot database (467 proteins) according to its molecular weight. Low ≥50 kD (LMW); High <50 kD (HMW).

In the same way, from the 467 matched proteins of *S. filipendula*, 41 of them presented differences in their abundances in relation to radiation treatments (Table 1) and were classified in four specific metabolic pathways (Fig. 5), most of them belonging to photosynthesis (26.8%), energy (14.6%), carbohydrate (14.6%), and ROS scavenging defense (12.6%) metabolisms. Additionally, 22% corresponded to other metabolisms and 9.8% to uncharacterized proteins.

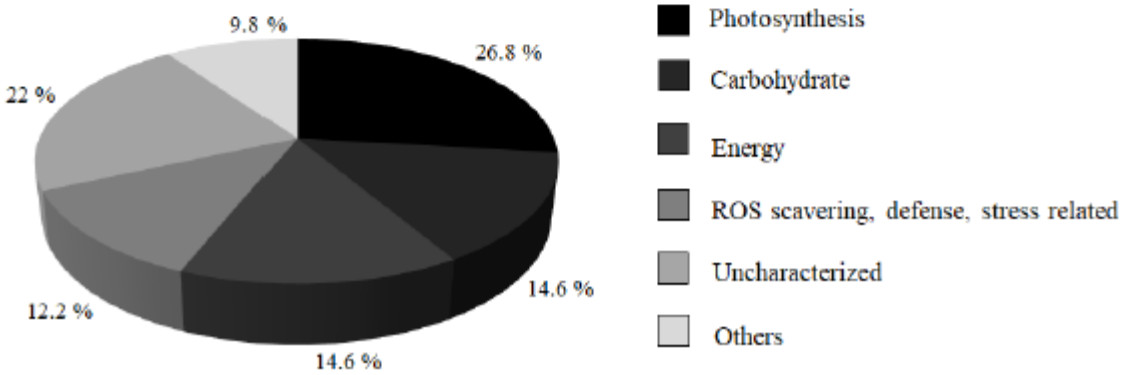

Figure 5. Metabolic classification of differential abundant proteins identified in *Sargassum*

filipendula after exposure to UV radiation treatments (41 proteins) against the Ectocarpus_Uniprot database match.

The Student *t* test comparing the differential abundance proteins in *S. filipendula* under the radiation treatments is showed in Table 1. Comparison between PAR and PAR+UVA treatments, only two proteins showed significant changes in their abundance: cytochrome c 6 and importin subunit alpha, which were down and up-regulated, respectively for PAR+UVA treatment. By comparing PAR versus PAR+UVB, 21 proteins presented differences in their abundances. Proteins involve in photosynthesis (PSI P700 chlorophyll *a* apoprotein A2, PSII CP43 and PSII CP47 reaction center proteins) and carbohydrate metabolisms (aldo/keto reductase family protein and RUBisCo small subunit). which were up-regulated for PAR+UVB; while other proteins related with energy metabolism (inorganic pyrophosphatase and ATP synthase O subunit, mitochondrial) and ROS scavenging activity (peroxidase) were down regulated. Finally, comparison between PAR+UVA and PAR+UVB treatments showed a large group of proteins being up-regulated for PAR+UVA; and most of the up-regulated proteins for PAR+UVB, such as cytochrome c-550, light harvesting complex, and hydroxymethylbilane synthase, belong to the photosynthesis metabolism.

Table 1. Proteins identified in *Sargassum filipendula* for which the level of abundance changed significantly (41; $p < 0.05$) after UV exposure. Database accession numbers according to Uniprot.

Accession number	Protein name	Molecular weight (kD)	Fold change	(*p*-value)
PAR vs PAR+UVA				
D1GJF8	Cytochrome c6	12.094	6.399823189	0.0005
D8LJF5	Importin subunit alpha	60.752	-1.3454360	0.0007
PAR vs PAR+UVB				
D8LL62	Dihydrolipoamide acetyltransferase	31.106	-3.4326505	0.0153
D7FU74	RanBD1 domain-containing protein	12.276	-1.9511833	0.0175
D1J7A4	PSI P700 chlorophyll *a* apoprotein A2	82.505	-2.0912923	0.0126

D8LGX8	Aldo/keto reductase family protein	37.532	-1.7289695	0.0140
D1J7D7	RUBisCo small subunit	15.899	-0.7304782	0.0028
D1J6Z5	PSII CP43 reaction center protein	52.429	-1.8115787	0.0007
D1J718	PSII CP47 reaction center protein	56.903	-2.0953855	0.0001
D1GJQ2	ATP-dependent zinc metalloprotease FtsH	69.652	-1.9281740	0.0002
D7FPA7	Glutamine synthetase	40.248	-0.8062353	0.0004
D7G6R8	AAA domain-containing protein	46.462	-1.0373792	0.0008
D8LJF5	Importin subunit alpha	60.752	-2.9638910	0.0015
D8LBH8	Ribulose-phosphate 3-epimerase	29.447	1.671618462	0.0004
D7FL45	Cytochrome b6-f complex iron-sulfur subunit	23.633	3.441204071	0.0003
D1J772	Cytochrome c6	12.094	6.439091682	0.0006
D7G5E4	Similar to arginine/serine-rich splicing factor 7	26.996	1.716190338	0.0137
D8LTK5	Peroxidase	38.276	0.586978912	0.0011
D7FKG7	Inorganic pyrophosphatase	31.884	2.299279213	0.0106
D8LJF7	PSII oxygen evolution complex protein PsbP	25.153	2.255345345	0.0039
D8LD75	Thylakoid lumen 15.0 kDa protein	28.564	3.701721191	0.0084
D7FN46	Uncharacterized protein	19.536	4.62314415	0.0049
D7FJT6	ATP synthase O subunit, mitochondrial	33.092	5.518550873	0.0060
PAR+UVA vs PAR+UVB				
D8LL62	Dihydrolipoamide acetyltransferase	31.107	-3.4322633	0.0153
D7FZ52	Leucyl aminopeptidase	51.49	-3.3237094	0.0190
D8LIQ8	PHB domain-containing protein	45.523	-2.7776193	0.0206
D8LKC6	Uncharacterized protein	21.435	-2.8832368	0.0057
D8LGX8	Aldo/keto reductase family protein	37.533	-1.8528175	0.0117
Q7GG88	RUBisCo large subunit	6.793	-2.26708889	0.0158
D7FVQ6	Alanine transaminase	55.47	-1.5995578	0.0034
D7FNT5	Methyltranfer_dom domain-containing protein	47.57	-1.5065784	0.0030
D8LCE0	Glutamate synthase (NADH/NADPH-dependent), C-terminal part	139.683	-1.9088058	0.0007

D7FLD4	Uncharacterized protein	65.752	-2.0871763	0.0004
D8LDT0	Flagellar associated protein	40.065	-1.0533475	0.0010
D7G0R3	Aldehyde dehydrogenase	58.754	-0.6694765	0.0010
D8LSE9	Obg-like ATPase 1	44.017	-0.7584762	0.0015
D8LBW0	Uncharacterized protein	90.87	-0.95298481	0.0017
D7FNQ3	Tubulin beta chain	52.835	-1.3745002	0.0097
D7G711	NAD(P)-bd_dom domain-containing protein	34.387	0.702216148	0.0026
D8LBI0	Phosphoribulokinase	47.739	0.960021019	0.0062
D1J771	Cytochrome c-550	17.583	2.144571304	0.0140
D7FIR0	Light harvesting complex protein	24.089	2.867315292	0.0229
D7FMY2	Hydroxymethylbilane synthase, putative chloroplast	39.654	2.987347603	0.0030

The biplot cluster analysis (Euclidean distance) associated to a heatmap graph (Fig. 6) formed two associations in relation to radiation treatments: PAR+UVA and PAR+UVB forming a closer cluster (Pearson's correlation of 0.70), and a second cluster with low correlation between PAR and PAR+UVA/PAR+UVB (Pearson's correlation of 0.45). Additionally, considering the clusterization between the protein abundance, it was observed five associated groups with a significance of 50% of distance, which correlate the protein abundance (minimum, mean or maximal value) regarding to the mean abundance value for each protein. A first group (Group I) was formed by proteins related to carbohydrate metabolism such as RUBisCo (small and large subunit) with higher abundance for PAR+UVB treatment. In the same way, proteins involved in photosynthesis metabolism (PSII CP43 and PSII CP47 reaction center proteins) were also more abundant for PAR+UVB. Proteins with ROS scavenging functions as peroxidase were higher for both PAR and PAR+UVA treatments, while glutamate synthase also involve in this activity was more abundant in PAR+UVB. In a second group (Group II), almost all the proteins presented a higher abundance for the UV treatments. Photosynthesis metabolism was the most representative within the group, with proteins such as cytochrome c6, cytochrome b6-f complex iron-sulfur subunit, thylakoid lumen 15.0 kD, and PSII oxygen evolution complex protein PsbP. Other proteins includes similar to arginine/serine-rich splicing factor 7 and hydroxymethylbilane synthase, putative chloroplast, which are related with genetic information processing and ammonia metabolism, respectively. Group III includes

proteins involved in photosynthesis (cytochrome c-550 and light harvesting complex), carbohydrate (ribulose-phosphate 3-epimerase), and phosphate (inorganic pyrophosphatase) metabolisms, which the level of abundance was lower for the PAR+UVB treatment. Group IV presented proteins belonging to diverse metabolisms such as aldehyde dehydrogenase and aldo/keto reductase family protein with ROS scavenging and oxireduction activities, and both presented higher abundance for PAR+UVB treatment. Other metabolisms and functions such as amino acid, transferase activity and catabolic process were represented by alanine transaminase, dihydrolipoamide acetyltransferase, and ATP-dependent zinc metalloprotease FtsH, respectively, and the abundance level were lower for both PAR and PAR+UVA treatments. Likewise, Group V includes proteins from different metabolisms, being most of them less abundant for PAR+UVA treatment. Proteins such as leucyl aminopeptidase, RanBD1 domain-containing protein and importin subunit alpha are related to transport. Additionally, aldehyde dehydrogenase, related to oxidoreduction activity was higher for PAR+UVB.

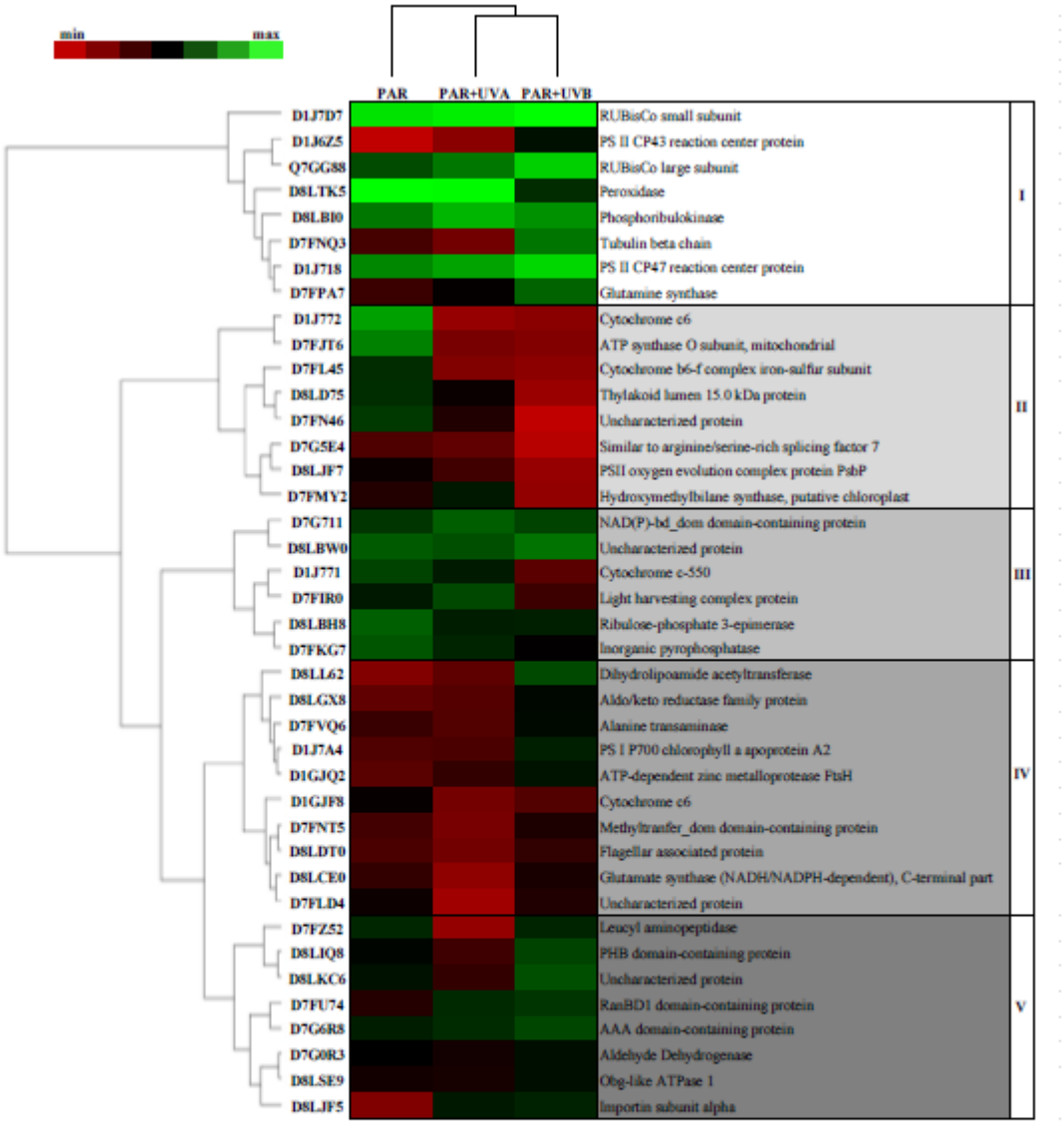

Figure 6. Biplot cluster analysis (Euclidean distance) of proteins differentially abundant of *Sargassum filipendula* after four days of exposure to UV radiation treatments, associated with a heatmap graph based on the mean value of abundance for each protein (n = 3). Dataset represent the ID code identity and protein name. The scale represents minimum ± mean ± maximum values reported for each protein.

DISCUSSION

Proteomic studies in algal research have been performed in both micro and macroalgae, however, the analysis of large amount of proteins is still quite limited, mainly due to the difficulty in the protein extraction, that compromises yield, integrity, and isolation, especially from brown seaweeds. This group of macroalgae is characterized by elevate concentrations of phenolic compounds and polysaccharides, which make difficult to extract any type of metabolite, can contaminate samples and degrade the metabolite of interest. On the other hand, cell disruption causes enzymes, such as proteases, to become free and active for the degradation of the target component in the lysate, in this case the proteins. In addition to the difficulty of establishing a suitable extraction protein that yields high amounts of proteins, facilitation of extracting solution contact by cellular disruption is also important. Thus, there are certain key aspects for proteomic assessment as cellular disruption, efficient extraction with high yield and preservation of protein integrity.

In the present study, the proteomic profile of *S. filipendula* was characterized and we evaluated the differential abundance after the exposure to UV radiation treatments under laboratorial conditions. As crucial performance of proteomic studies, protein yield and integrity are important concerns for obtaining suitable material for large-scale proteomic approaches. Therefore, we tested xx methods for extracting proteins. Protein extraction based on the phenol method increased with a protease inhibitor cocktail was the most successfully protocol for *S. filipendula* as was observed for other *Sargassum* species reported for Contreras et al., 2008; Nagai et al., 2008; Ritter et al., 2010; Zou et al., 2015), since compounds that may interfere in the protein quality, are mostly removed or inactivated. Moreover, the phenol method applied for *S. filipendula* was suitable for obtaining both low and high molecular weight proteins, identifying proteins ranging from 6 to 500 kD belonging to diverse metabolisms, similar to findings reported by Contreras et al. (2008) with proteins from 19 and 200 kD. After this preliminary methodological assessment to obtain high protein yield and quality, the protein characterization and comparison were performed allowing a greater proteomic coverage.

Sargassum_Uniprot and Fucales_Uniprot databases are the closest taxonomical categories to our experimental model, genera and order respectively. In turn, Ectocarpus_UniProt database provided more useful information with the recognition of hundreds of proteins of *S. filipendula* and a protein set that respond differentially to the UV radiation stimuli. Despite the xx% of uncharacterized proteins from Ectocarpus_UniProt database based on *Ectocarpus siliculosus*,

this species had its genome sequenced and annotated (Cock et al., 2012), which allowed a major number of protein identification.

The functional group with the largest number of proteins altered by UV radiation was photosynthesis. As a photosynthetic organism, in which this metabolism is crucial for growth and development and should be delicately regulated to minimize oxidative stress and damage to the photosynthetic apparatus, is expected to note protein alteration under UV radiation exposure. Several physiological studies have demonstrated that UV radiation affects photosynthesis rate and pigment concentration (Figueroa and Vinegla 2001; Sampath-Wiley et al. 2008; Heo et al. 2009; Figueroa et al. 2014; Polo et al. 2014a), reducing photosynthetic performance by impairing several target sites which absorb UV-B. Effects of UV radiation on seaweeds Dieter Hanelt1, C. Wiencke2, K. Bischof3.This fact could explain the down regulation of important proteins as photosystem II oxygen evolution complex, thylakoid lumen 15.0 kDa, and light harvesting complex in samples exposed UVB and cytochrome proteins for both types of UV radiation here studied.

In the same way, key enzymes involved in energy metabolism as ATP synthase, which have a central role in oxidative phosphorylation and photosynthesis, presented a lower abundance after *S. filipendula* was exposed to PAR+UVB treatment. In this way, higher abundance of proteins involves in carbohydrate metabolism in UV radiation treatments, as phosporibulokinase (PRK), an enzyme unique to the reductive pentose phosphate pathway of CO2 assimilation; and Ribulose bisphosphate carboxylase (RubisCo) large subunit, which catalyzes the first step in net photosynthetic CO2 assimilation and photorespiratory carbon oxidation (Spreitzer and Salvucci 2002), may compensate the energy loss from photosynthesis through the catabolism of photoassimilates (Zhang et al. 2015).

UV radiation can also cause changes in nitrogen metabolism by decreasing nitrogen assimilation. It has been reported that glutamine synthetase, an enzyme that catalyzes the assimilation of ammonium to glutamine using glutamic acid as substrate (Chen and Silflow 1996), can present a reduction under stress conditions. This response can be a defense signaling under derived-oxidative stress protective mechanism, as the synthesis of nitric oxide (NO) and NO-derived reactive species, intermediates of nitrogen assimilation, can suppress nitrogen reaction pathways for avoid the overproduction of reactive species and oxidative stress (Wang et al. 2004). Moreover, the reduction of enzymes (proteins) involved in primary nitrogen metabolism like nitrogen assimilation can be an evidence of nitrogen reallocation into other pathways, such as those involved in repair or protection processes.

However, glutamine synthase presented a higher abundance for both PAR+UVA and PAR+UVB treatments in relation to PAR. Additionally, several proteins involved in ROS scavenging and stress as superoxide dismutase (SOD), which constitute the first line of defense against oxidative damage caused by UV radiation (Alscher et al. 2002), were exclusive for the PAR+UVB treatment. It is known that the overproduction of ROS results in deleterious effects such as lipid peroxidation of polyunsaturated fatty acids (PUFA), DNA strand breaks and protein oxidation (Ruhland et al. 2007).

Previously studies have reported that depending on the degree of UVB exposure, the activity of SOD becomes stimulated, and two mechanisms might be involved in this response: either the enzyme becomes activated due to a light effect (due to exposure to short wavelength radiation) or it is the presence of previously generated oxygen radicals (ROS) which act as trigger for increasing SOD activity (Bischof et al. 2006). Moreover, NADH dehydrogenase was another enzyme activated in samples exposed to UVB, activation that could stimulates oxygen consumption and leading to more ROS formation. However, of NADH dehydrogenase activity can be attributed to extra energy production that is used for potential membrane loss and energy deficit (Gao et al. 2016).

Likewise, heat shock proteins as HSP70, HSP70 putative and SGT1 homologue (related to immune responses with HSP90) were exclusive for this treatment. HSPs have strong cytoprotective effects maintaining proteins in their functional conformations, preventing aggregation of non-native proteins. They also maintain a refolding of denatured proteins to regain their functional conformation and removal of non-functional but potentially harmful polypeptides, which often occurs in an ATP driven process, and is therefore frequently up-regulated under stress conditions in many organisms (Slabas et al. 2006; Suzuki et al. 2006; Timperio et al. 2008).

As mentioned earlier, few proteomics studies have focused on cortical parenchymatous macroalgae and compared with other group of organisms (*e.g.* vascular plant) protein extraction has been extraordinary difficult, which results in a limited knowledge at biochemical and molecular levels. Additionally, all the performed proteomic works have used 2-DE gels, an approach that has some limits. The method could fail in its reproducibility, inability to detect low abundant and hydrophobic proteins, low sensitivity in identifying proteins with pH values too low (pH < 3) or too high (pH < 10) and molecular masses too small (Mr < 10 kD) or too large (Mr > 150 kD); moreover, proteins could be poorly separated do to streaking of the gels (Godovac-Zimmermann and Brown 2001). In this context, shotgun proteomics arrives as a

powerful approach that allow identification and quantification of proteins presents in a mixture, that converted proteins to peptides by proteolytic digestion, and these peptides are used as surrogates for identification and quantitation of the proteins present in the original mixture (Liao et al. 2009). For the present research, the identification and quantification of a large number of proteins involved in several metabolic pathways in *S. filipendula*, demonstrated that this approach is reliable and feasible for the study of proteins that respond to abiotic stimuli as UV radiation. Moreover, mass spectrometry (MS)-based proteomic methods are a key technology for identification and quantification of complex protein mixtures with the potential to reveal unknown and novel changes in protein interactions and assemblies that regulate cellular and physiological processes.

Summarizing, the proteomic approach with *S. filipendula* as experimental model and the UV radiation effect constitutes a valuable scientific contribution, as proclaims the successful benefit of large-scale high-quality protein extraction in a parenchymatous phenolic- and polysaccharide-rich macroalgae with a mid-scale proteomic profile approach on metabolic responses under UV radiation stress condition. Additionally, our research opens major metabolic tools for understanding biological/physiological processes under stress abiotic conditions like UV radiation. In turn, this is the unique study, until the best of our knowledge of published literature, with a shotgun proteomic approach in macroalgae, in which the few available reports were performed with microalgae, making the contribution of this research even more valuable. Therefore, this investigation subscribes the scientific development by providing important insight for a better understanding of the biology of *S. filipendula*, as well as the responses to stress conditions and predicted global climate change.

REFERENCES

Alscher R, Erturk N, Heath L (2002) Role of superoxide dismutases (SODs) in controlling oxidative stress in plants. J Exp Bot 53:1331–1341

Andrés-Colás N, Van Der Straeten D Van Der (2017) Optimization of non-denaturing protein extraction conditions for plant PPR proteins. PLoS One 12:1–15. doi: 10.1371/journal.pone.0187753

Barbosa EB, Vidotto A, Polachini GM, et al (1992) Proteomics: methodologies and applications to the study of human diseases. Rev Assoc Med Bras 58:366–75

Carpentier SC, Witters E, Laukens K, et al (2005) Preparation of protein extracts from

recalcitrant plant tissues: An evaluation of different methods for two-dimensional gel electrophoresis analysis. Proteomics 5:2497–2507. doi: 10.1002/pmic.200401222

Chen Q, Silflow CD (1996) Isolation and characterization of glutamine synthetase genes in Chlamydomonas reinhardtii. Plant Physiol 112:987–96. doi: 10.1104/pp.112.3.987

Cock JM, Sterck L, Ahmed S, et al (2012) The Ectocarpus Genome and Brown Algal Genomics. The Ectocarpus Genome Consortium.

Contreras L, Ritter A, Dennett G, et al (2008) Two-dimensional gel electrophoresis analysis of brown algal protein extracts. J Phycol 44:1315–1321. doi: 10.1111/j.1529-8817.2008.00575.x

de Nadal E, Ammerer G, Posas F (2011) Controlling gene expression in response to stress. Nat Rev Genet 12:833–45. doi: 10.1038/nrg3055

De Széchy MTM, Galliez M, Marconi MI (2006) Quantitative variables applied to phenological studies of Sargassum vulgare C . Agardh (Phaeophyceae - Fucales) from Ilha Grande Bay , State of Rio de Janeiro. Rev Bras Bot 29:27–37. doi: 10.1590/S0100-84042006000100004

Figueroa F, Vinegla B (2001) Effects of solar UV radiation on photosynthesis and enzyme activities (carbonic anhydrase and nitrate) in marine macroalgae from southern Spain. Rev. Chil. Hist. Nat. 74:237–249

Figueroa FL, Domínguez-González B, Korbee N (2014) Vulnerability and acclimation to increased UVB radiation in three intertidal macroalgae of different morpho-functional groups. Mar Environ Res 97:30–38. doi: 10.1016/j.marenvres.2014.01.009

Ghazalpou A, Bennett B, Petyuk V, et al (2011) Comparative Analysis of Proteome and Transcriptome Variation in Mouse. PLOS Genet 7:1001393

Godovac-Zimmermann J, Brown LR (2001) Perspectives for mass spectrumetry and functional proteomics. Mass Spectrom Rev 20:1–57. doi: 10.1002/1098-2787(2001)20:1<1::AID-MAS1001>3.0.CO;2-J

Gómez I, Figueroa FL (1998) Effects of solar UV stress on chlorophyll fluorescence kinetics of intertidal macroalgae from southern Spain: a case study in Gelidium species. J Appl Phycol 10:285–297. doi: 10.1023/A

Häder DP, Kumar HD, Smith RC, Worrest RC (2007) Effects of solar UV radiation on aquatic

ecosystems and interactions with climate change. Photochem Photobiol Sci 6:267–285. doi: 10.1039/b700020k

Havanapan PO, Thongboonkerd V (2009) Are protease inhibitors required for gel-based proteomics of kidney and urine? J Proteome Res 8:3109–3117. doi: 10.1021/pr900015q

Hwang PA, Wu CH, Gau SY, et al (2010) Antioxidant and immune-stimulating activities of hot-water extract from seaweed sargassum hemiphyllum. J Mar Sci Technol 18:41–46

Iwashima M, Mori J, Ting X, et al (2005) Antioxidant and antiviral activities of plastoquinones from the brown alga Sargassum micracanthum, and a new chromene derivative converted from the plastoquinones. Biol Pharm Bull 28:374–377. doi: 10.1248/bpb.28.374

Kim EY, Kim DG, Kim YR, et al (2011) An improved method of protein isolation and proteome analysis with Saccharina japonica (Laminariales) incubated under different pH conditions. J Appl Phycol 23:123–130. doi: 10.1007/s10811-010-9550-6

Kosová K, Vítámvás P, Prášil IT, Renaut J (2011) Plant proteome changes under abiotic stress - Contribution of proteomics studies to understanding plant stress response. J Proteomics 74:1301–1322. doi: 10.1016/j.jprot.2011.02.006

Liao L, McClatchy DB, Yates JR (2009) Shotgun Proteomics in Neuroscience. Neuron 63:12–26. doi: 10.1016/j.neuron.2009.06.011

Lopez F, Mercado J, Jiménez C, et al (1998) Relation between the bio-optical characteristics of phytoplankton and photoinhibition by solar radiation. Aquat Bot 59:237–251

Madronich S, McKenzie RL, Björn LO, Caldwell MM (1998) Changes in biologically active ultraviolet radiation reaching the Earth's surface. J Photochem Photobiol B Biol 46:5–19. doi: 10.1016/S1011-1344(98)00182-1

Monteoliva L, Albar JP (2004) Differential proteomics: An overview of gel and non-gel based approaches. Briefings Funct Genomics Proteomics 3:220–239. doi: 10.1093/bfgp/3.3.220

Nagai K, Yotsukura N, Ikegami H, et al (2008) Protein extraction for 2-DE from the lamina of Ecklonia kurome (laminariales): Recalcitrant tissue containing high levels of viscous polysaccharides. Electrophoresis 29:672–681. doi: 10.1002/elps.200700461

Rabilloud T, Lelong C (2011) Two-dimensional gel electrophoresis in proteomics: A tutorial. J Proteomics 74:1829–1841. doi: 10.1016/j.jprot.2011.05.040

Ritter A, Ubertini M, Romac S, et al (2010) Copper stress proteomics highlights local

adaptation of two strains of the model brown alga Ectocarpus siliculosus. Proteomics 10:2074–2088. doi: 10.1002/pmic.200900004

Sampath-Wiley P, Neefus CD, Jahnke LS (2008) Seasonal effects of sun exposure and emersion on intertidal seaweed physiology: fluctuations in antioxidant contents, photosynthetic pigments and photosynthetic efficiency in the red alga Porphyra umbilicalis. J Exp Mar Bio Ecol 361:8391

Sinha S, Astani A, Ghosh T, et al (2010) Polysaccharides from Sargassum tenerrimum: Structural features, chemical modification and anti-viral activity. Phytochemistry 71:235–242. doi: 10.1016/j.phytochem.2009.10.014

Spreitzer RJ, Salvucci ME (2002) R UBISCO : Structure, Regulatory Interactions, and Possibilities for a Better Enzyme . Annu Rev Plant Biol 53:449–475. doi: 10.1146/annurev.arplant.53.100301.135233

Tan SC, Yiap BC (2009) DNA, RNA, and Protein Extraction: The Past and The Present. J Biomed Biotechnol 2009:1–10. doi: 10.1155/2009/574398

Wang SB, Chen F, Sommerfeld M, Hu Q (2004) Proteomic analysis of molecular response to oxidative stress by the green alga Haematococcus pluvialis (Chlorophyceae). Planta 220:17–29. doi: 10.1007/s00425-004-1323-5

Xu J, Li Y, Sun J, et al (2013) Comparative physiological and proteomic response to abrupt low temperature stress between two winter wheat cultivars differing in low temperature tolerance. Plant Biol (Stuttg) 15:292–303. doi: 10.1111/j.1438-8677.2012.00639.x

Xu Z, Gao K (2009) Impacts of UV radiation on growth and photosynthetic carbon acquisition in Gracilaria lemaneiformis (Rhodophyta) under phosphorus-limited and replete conditions. Funct Plant Biol 36:1057–1064. doi: 10.1071/FP09092

Yende SR, Harle UN, Chaugule BB (2014) Therapeutic potential and health benefits of Sargassum species. Pharmacogn Rev 8:1–7. doi: 10.4103/0973-7847.125514

Yotsukura N, Nagai K, Kimura H, Morimoto K (2010) Seasonal changes in proteomic profiles of Japanese kelp: Saccharina japonica (Laminariales, Phaeophyceae). J Appl Phycol 22:443–451. doi: 10.1007/s10811-009-9477-y

Yotsukura N, Nagai K, Tanaka T, et al (2012) Temperature stress-induced changes in the proteomic profiles of Ecklonia cava (Laminariales, Phaeophyceae). J Appl Phycol 24:163–171. doi: 10.1007/s10811-011-9664-5

Zhang A, Xu T, Zou H, Pang Q (2015) Comparative proteomic analysis provides insight into cadmium stress responses in brown algae Sargassum fusiforme. Aquat Toxicol 163:1–15. doi: http://dx.doi.org/10.1016/j.aquatox.2015.03.018

Zhang Y, Fonslow B, Shan B, et al (2013) Protein Analysis by Shotgun/Bottom-up Proteomics. Chem Rev 113:2343–2394. doi: 10.1021/cr3003533

Zhu W, Smith JW, Huang CM (2010) Mass spectrometry-based label-free quantitative proteomics. J Biomed Biotechnol 2010:. doi: 10.1155/2010/840518

Zou H-X, Pang Q-Y, Zhang A-Q, et al (2015) Excess copper induced proteomic changes in the marine brown algae Sargassum fusiforme. Ecotoxicol Environ Saf 111:271–280. doi: http://dx.doi.org/10.1016/j.ecoenv.2014.10.028

ANEXO 8

Brazilian Journal of Botany (2020) 43:733–745
https://doi.org/10.1007/s40415-020-00639-y

BIOCHEMISTRY & PHYSIOLOGY - ORIGINAL ARTICLE

Sargassum stenophyllum (Fucales, Ochrophyta) responses to temperature short-term exposure: photosynthesis and chemical composition

Vanessa Urrea-Victoria[1] · Allyson E. Nardelli[1] · Eny I. S. Floh[2] · Fungyi Chow[1]

Received: 25 September 2019 / Revised: 16 July 2020 / Accepted: 28 July 2020 / Published online: 31 August 2020
© Botanical Society of Sao Paulo 2020

Abstract
Sargassum species form extensive benthic beds in tropical and subtropical low intertidal and subtidal zones, acting as important drivers for marine community structure. Temperature, as one of the most important abiotic factor, affects seaweed performance and triggers changes in metabolic responses; therefore, laboratory experiments involving temperature ranges are tools for understanding seaweed engineering. The aim of this study was to assess the physiological vulnerability and sensitivity of *Sargassum stenophyllum* C. Martius exposed to five different temperatures by analyzing photosynthetic performance and chemical composition related to carbon and nitrogen metabolism. There were no significant differences in energy quenching between treatments, except at 35 °C, which showed decreased photochemical quenching and increased non-regulated non-photochemical quenching. Chlorophyll *a* and chlorophyll *c* at 15 °C and 35 °C exhibited lower amounts at the end of experiment. Protein content showed progressive diminution in the treatments. Total soluble carbohydrates content showed higher concentration as temperature increased. After 7 days, total amino acid content showed increase from 15 °C to 30 °C. No generalization between the amino acid patterns, although glutamine and glutamate content at 15 °C and 35 °C were reduced; and the highest values of isoleucine and leucine were detected at 35 °C. We postulated that accumulation of certain chemical compounds in *S. stenophyllum* results from a reallocation of carbon and nitrogen, osmoregulation responses and protection against oxidative stress. Results suggest this species' tolerance ranges between 15 °C and 30 °C and sensitivity at 35 °C.

Keywords Amino acids · Brown algae · Macroalgae · Pigments · Thermal stress

1 Introduction

In natural environment, seaweeds are constantly exposed to variations of both biotic (e.g., herbivory, competition) and abiotic (e.g., temperature, irradiance, UV radiation, nutrient, air exposure) factors in an air–water ecosystem interface imposed by tide-driven fluctuations. In the upper limit of intertidal zone, physical factors such as temperature, irradiance and UV radiation can determine algal distribution, while lower limits are usually set by biological interactions such as herbivory and competition (Druehl and Green 1982). Among the aforementioned abiotic factors, seawater temperature stands out as a main determinant of geographical distribution, development, reproduction and survival of macroalgae (Breeman 1988; Teoh et al. 2010).

Temperature oscillation affects macroalgae performance including growth, photosynthesis and respiration, inducing changes in metabolic reactions (Davison 1991). Macroalgae may display physiological plasticity to temperature fluctuations, observed as acclimation via metabolic pathway adjustments and changes in cellular biochemical composition. Generally, both growth and photosynthetic rates are positively correlated with temperature up to a threshold level,

Electronic supplementary material The online version of this article (https://doi.org/10.1007/s40415-020-00639-y) contains supplementary material, which is available to authorized users.

✉ Fungyi Chow
fchow@ib.usp.br

[1] Laboratory of Marine Algae "Édison José de Paula", Institute of Biosciences, University of São Paulo, Rua do Matão 277, São Paulo CEP 05508-090, Brazil

[2] Plant Cell Biology Laboratory, Institute of Biosciences, University of São Paulo, Rua do Matão 277, São Paulo CEP 05508-090, Brazil

©Fungyi Chow / 2021

and then, the relationship is reversed to a steep decline as these rates surpass the upper tolerance level (Muller et al. 2008; Ji et al. 2016).

Different macroalgal species have different range of temperature tolerance regarding their local environmental temperature. Temperate and cold species regularly attain higher photosynthetic rates at lower temperature compared to those subtropical and tropical species (Davison et al. 1991; Staehr and Wernberg 2009; Ji et al. 2016). And it is expected that warmer temperature species better tolerate warm conditions, normally with optimal physiological temperature between 25 °C and 30 °C for photosynthesis (Ji et al. 2016). Photosynthetic thermal acclimation is associated with responsive changes in cellular biochemical composition (Staehr and Wernberg 2009; Ji et al. 2016), with increasing concentrations of chlorophyll *a*, soluble proteins and soluble carbohydrates in colder-grown macroalgae compared with warmer-grown species. Photosynthesis of warm species may enhance under increasing temperature by extension of the activity of reaction centers at short-term and medium-term. As gradual long-term temperature rise becomes permanent beyond a certain tolerance threshold, photosynthesis begins to decline disclosing physiological and biochemical characteristics of exhaustion phase and chronic damage (Ji et al. 2016).

Changes in carbon (C), nitrogen (N) and protein contents and carbohydrate storage frequently have been used as indicator of physiological status for seaweeds (Lalegerie et al. 2020), as they are the basis of two of the main metabolic pathways, carbon (including photosynthesis) and nitrogen (amino acid, proteins and enzymes), both with essential implications for all development, growth and defense responses. Chemical composition variation is probably related to carbon-nutrient balance (Lerdau and Coley 2000), since seaweeds have been shown to differentially allocate C:N resources depending on metabolic demands and generally vary with season (Rosenberg and Ramus 1982; Marinho-Soriano et al. 2006; Polo et al. 2014). For *Sargassum* C. Agardh species (Fucales, Phaeophyceae), despite studies on amino acid profile (Ramos et al. 1999; Lourenço et al. 2002; Matanjun et al. 2009), there are few studies to date investigating the relationship between amino acid profile and thermal effects (Liu and Lin 2020), and the number of research related to the C: N balance is even scarcer.

Sargassum that is found in tropical and subtropical regions makes up dense natural forest beds (De Wreede 1976; Casas-Valdez et al. 2016), and in Brazil, they have representability in terms of abundance (Paula and Oliveira Filho 1980; Paula 1988; Széchy and Paula 2000). Although, in the last years, changes on *Sargassum*' coverage and biomass in Brazil have become to decline 2.6% per year by combined effects of urbanization and warming seas (Gorman et al. 2020). Experimental short-term approaches with *Sargassum* species at +3.5 °C treatment compared to ambient temperature resulted in 17–49% growth decline relative to controls and susceptibility to herbivory (Graba-Landry et al. 2020).

The current worldwide scenario is featured by environmental degradation of marine ecosystems, e.g., caused by heated effluents generate in nuclear power plant reactors that can raise water temperatures up to 8 °C (Teixeira et al. 2009). Furthermore, prediction models indicated an increase in temperature that continue over time. Marengo et al. (2007) predict for Brazil an increase in approximately 0.75 °C in the average atmospheric temperature until the end of the twentieth century. This thermal stress scenario may result in significant modification of marine benthic dynamics (Bernardino et al. 2015).

Therefore, considering the ecological importance, in articulation with the current scenario of increasing environmental degradation of marine ecosystems and global climate change projections, laboratory studies generating valuable understanding on the dynamic and vulnerability of *Sargassum* species are needed. Accordingly, the aim of our research was to assess the physiological vulnerability of *Sargassum stenophyllum* C. Martius exposed to different temperatures under laboratory conditions by analyzing photosynthetic performance and chemical composition responses to changes in carbon and nitrogen metabolism. Our hypothesis is that *S. stenophyllum*, which inhabits lower intertidal zones, has physiological plasticity under different temperatures, with changes in chemical composition; nevertheless, it would be sensitive to +5 °C above the maximum local environmental temperature.

2 Materials and methods

Material collection and experimental setup – *Sargassum stenophyllum* was collected in the low intertidal zone at Cibratel Beach (24° 13′ 31″ S and 46° 51′ 7″ W), situated at the Itanhaém District, southeast coast of the São Paulo State, Brazil, in November 2014 and transported to the laboratory in thermo-cooler containers. In the laboratory, the algae were cleaned of macroepiphytes and associated fauna and then washed with filtered seawater. Portions of five different adult individual's (fertile) were fixed in 4% formalin (v/v, diluted in seawater) and then herborized and deposited in the SPF Herbarium at the University of São Paulo (SPF 57850). The remained collected material, including several adult individuals and preferentially unfertile, was mixed as a complex sample and used for subsequent experiments.

The experimental setup was carried out with cleaned apex portions of 8 ± 2 cm length (presenting a bright brown color, apparently healthy), acclimated for 7 days in laboratory-controlled conditions with sterilized natural seawater (salinity

©Fungyi Chow / 2021

at 32) plus 50% von Stosch enrichment solution (Ursi and Plastino (2001) modified from Edwards (1970)), 25 ± 1 °C, 65 ± 5 µmol photons m^{-2} s^{-1}, 14 h photocycle and aeration every 30 min (on:off). After the acclimation, the material (5 ± 2 cm length) was cultivated under the experimental temperature conditions: 15, 20, 25, 30 and 35 °C for 7 days at the same laboratory-controlled conditions described above. Culture proportion of 3 g of biomass for 1 L of culture medium and five biological independent replicates ($n = 5$) composed as a complex sample for each temperature treatment. The experimental temperatures were selected based on data from National Institute for Space Research (INPE 2014) for the respective collection site and season, which ranged between 19 and 28 °C at spring 2014 and ranged at 2014–2015 from 14.5 °C to 31.5 °C.

After the acclimation period, photosynthetic performance and contents of photosynthetic pigments and soluble proteins were measured before start the experiment (Initial) and then after 1, 3, 5 and 7 days of experiment. Contents of soluble carbohydrates and amino acids profile were measured before the start of experiment (Initial) and after 7 days.

In vivo chlorophyll *a* fluorescence – Photosynthetic performance was estimated as in vivo fluorescence of the chlorophyll *a* of PSII by using a portable Pulse Amplitude Modulation fluorometer (PAM-2500, Walz, Germany) with red LED actinic light. The measurements were performed between 4 and 6 h after switching-on the photocycle. Effective quantum yield of PSII [Y(II)] or photochemical quenching [Y(PSII)] was measured from light-adapted samples and calculated following Schreiber and Neubaer (1990). Non-regulated non-photochemical quenching [Y(NO)] and regulated non-photochemical quenching [Y(NPQ)] were also estimated following Kramer et al. (2004).

Electron transport rate × light (ETR-PAR) curves were estimated on light-adapted samples at ten increasing PAR intensities (0, 23, 41, 60, 80, 107, 185, 300, 455 and 751 µmol photons m^{-2} s^{-1}). ETR was calculated as $ETR = Y(II) \times PAR \times A_p \times 0.8$, where PAR is the photosynthetically active radiation, A_p is the absorptance of the seaweeds (Ramus and Rosenberg 1980; Mercado et al. 1996) and 0.8 is the fraction of chlorophyll *a* associated to the PSII for brown algae (Figueroa et al. 2003). From the ETR-PAR curves, we determined the maximum ETR (ETR_{max}), photosynthetic efficiency (α) and light saturation (Ik) by fitting the curves to a hyperbolic tangent model following Jassby and Platt (1976).

Total soluble proteins, photosynthetic pigments and UV-absorbing spectrum – The extraction of soluble proteins was performed from 70 mg of fresh weight (FW) samples, following the method described by Harb et al. (2018). The material was ground in liquid nitrogen and extracted with 1 mL of cold sodium phosphate buffer (50 mM, pH 5.5) and then centrifuged at 12.000 rpm for 15 min at 4 °C (buffered extract). The precipitate of the buffered extract was used for extracting photosynthetic pigments (chlorophylls *a* and *c* and carotenoids) by its resuspension in 1.5 mL of methanol, extracted for 3 h at 4 °C, protected from light, and then centrifuged at 12.000 rpm for 15 min at 4 °C (methanolic extract).

From buffered extracts, the total soluble protein was quantified following the spectrophotometric Bradford method (Bradford 1976) by using the Bio-Rad® protein assay reagent (Bio-Rad, USA) and bovine serum albumin (BSA) as standard (2 to 16 µg mL^{-1}; $y = 0.0388x - 0.0711$; $R^2 = 0.9919$).

From methanolic extracts, the chlorophylls *a* and *c* were calculated by using the absorbance coefficients for spectrophotometric equations of Ritchie (2008) following the equations: Chlorophyll *a* (µg g^{-1} FW) = $(16.4351 \times A_{665}) - (3.2416 \times A_{632})$ and Chlorophyll *c* (µg g^{-1} FW) = $(34.2247 \times A_{632}) - (1.5492 \times A_{665})$, where *A* is the absorbance at the respective wavelength. Total carotenoids were estimated based on the Lichtenthaler (1987) model, using the absorption coefficients in methanol of chlorophyll *a* (1.63) from Lichtenthaler and Buschmann (2001) and chlorophyll *c* (119.5) from Jeffrey (1963). The total carotenoids were calculated as the equation described: total carotenoids (µg g^{-1} FW) = $\{1000 \times [A_{470} - (1.63 \times \text{chlorophyll } a) - (119.5 \times \text{chlorophyll } c)\}/221$; where *A* is the absorbance at the respective wavelength.

From aliquots of 200 µL of the buffered and methanolic extracts, the absorption spectra in the range of 200 to 400 nm (UV-absorbing compounds absorption spectrum) was assessed by using an UV–visible microplate spectrophotometer (Epoch Biotek, USA). From the UV-absorbing spectra of both extracts, maximal absorption bands were identified and analyzed by calculating the area under the curve based on Riemann's sum.

Soluble carbohydrates – Total soluble carbohydrates content was analyzed from frozen samples of 165 mg FW with the phenol–sulfuric acid method described in Matsuko et al. (2005). The material was ground in liquid nitrogen and extracted in 1 mL of ultrapure water at 70 °C for 3 h. Then, the homogenate was centrifuged at 12.000 rpm for 10 min at room temperature. The concentration of carbohydrates was calculated against fucose (60–240 µg mL^{-1}; $y = 0.0044x - 0.0318$; $R^2 = 0.9923$) and galactose (15–60 µg mL^{-1}; $y = 0.0193x - 0.0527$; $R^2 = 0.9906$) as standard curves and by using a microplate UV–visible spectrophotometer.

©Fungyi Chow / 2021

Amino acids – Amino acid profile was analyzed from frozen samples of 70 mg FW according to Santa-Catarina et al. (2006), with modifications (Schmidt et al. 2016). The samples were extracted with 6 mL of 80% ethanol for 2 h and centrifuged at 12.000 rpm for 10 min at room temperature and concentrated in speed vacuum. Then, the precipitate was re-suspended in 2 mL of ultrapure water, centrifuged at 12.000 rpm for 10 min at room temperature, and the supernatant was filtrated with a 0.2 µm Millipore membrane. Amino acids were derivatized with *o*-phthaldialdehyde (OPA) and identified by HPLC (Shimadzu Shin-pack CLC ODS) using a C18 reverse phase column (Supelcosil LC-18, 25 cm × 4.6 mm/L × i.d.). The gradient was developed by mixing increasing proportions of 65% methanol to a buffer solution (50 mM sodium acetate, 50 mM sodium phosphate, 20 mL L^{-1} methanol, 20 mL L^{-1} tetrahydrofuran and pH 8.1 adjusted with acetic acid). The gradient of 65% methanol was programmed according to Egydio et al. (2013). Fluorescence excitation and emission wavelengths of 250 nm and 480 nm, respectively, were used for amino acid detection. Peak areas and retention times were measured by comparison with known quantities of standard amino acids (Sigma-Aldrich, USA).

Statistical analysis – The experimental design follows a fixed effect factor, in which temperature was the factor and the different temperatures the levels. To evaluate the physiological plasticity we analyzed each parameter separately considering the temperatures and experimental time depending on the parameter to be analyzed. Photosynthetic performance, photosynthetic pigments and soluble proteins were analyzed by repeated measures analysis of variance (ANOVA). Total soluble carbohydrates and amino acids data were evaluated by one-way ANOVA. When differences were detected, we applied the Newman–Keuls post hoc test. Statistical analysis were performed with the Statistica software (version 10.0), including five biological replicates ($n = 5$) for all studied parameters at 95% confidence level ($p < 0.05$). Data were previously verified for normality (Kolmogorov–Smirnov test) and homoscedasticity (Bartlett's test).

Additionally, an integrative approach to assess variation and bring out strong patterns in the dataset after 7 days of experiment was carried out using principal component analysis (PCA) by Past software (version 2.17c), and the outcomes were plotted in two dimension components (Component 1, Component 2).

3 Results

Variation on photosynthetic performance and chemical composition of the brown seaweed *S. stenophyllum* was verified. At the end of the experiment was observed detached phylloids from the central axis at 30 °C and 35 °C (Supplementary Material S1), with thallus deterioration and necrosis at 35 °C. Additionally, in those temperatures, changes in the color of the seawater culture medium were noted (increasingly yellowish) (Supplementary Material S1).

Samples at 35 °C showed significant reduction of Y(PSII) from the first day of experimentation (Fig. 1), with lower levels at days 5 and 7 and concomitant variation on non-photochemical quenching [Y(NO) and Y(NPQ)]. Non-significant differences were noted in Y(PSII) of samples at 15, 20, 25 and 30 °C, which showed the same levels than Initial sample over time (Fig. 1).

The photosynthetic performance parameters ETR_{max}, Ik and α over time (Table 1) presented significant differences for the interaction between time–temperature ($p < 0.001$) and also for the factors individually (Supplementary Material S2). Photosynthetic parameters of samples at 35 °C were lower than the other temperatures from the third day, with significant reduction of ETR_{max}, Ik and α (Table 1). From the third day, samples at 25 °C showed the highest values of ETR_{max} and Ik when compared to the other temperature treatments (Table 1).

The concentration of photosynthetic pigments, chlorophyll *a* (Fig. 2a), chlorophyll *c* (Fig. 2c) and total carotenoids (Fig. 2c) showed no significant differences over time between the initial sample and experimental treatments; exception was noted at 15 °C and 35 °C from the 5 and 7 days with significant decrease at 35 °C. Differently from pigments, total soluble protein content of *S. stenophyllum* (Fig. 2d) showed no differences between the initial sample and 15, 20, 25 and 30 °C treatments after 1, 3 and 5 days of experiment, with significant reduction for samples at 35 °C from the third day and general decrease at 7 day. Soluble protein content exhibited differences for the interaction between time–temperature ($p < 0.001$).

Total soluble carbohydrate contents at 25 °C and 30 °C showed the highest concentrations, greater than the Initial sample (Fig. 3), with maximal concentration at 30 °C (82.89 ± 8.54 mg fucose g^{-1} FW, equivalent to 78.35 ± 7.85 mg galactose g^{-1} FW). At 35 °C, a reduction of approximately 43% was observed in relation to 25 °C ($F = 38.09$; $df = 5$; $p < 0.001$).

The UV absorption spectrum for buffered and methanolic extracts presented similar spectral trends among the treatments, with maximal absorption bands at 214 to 226 nm and 264 to 280 nm for buffered extracts and

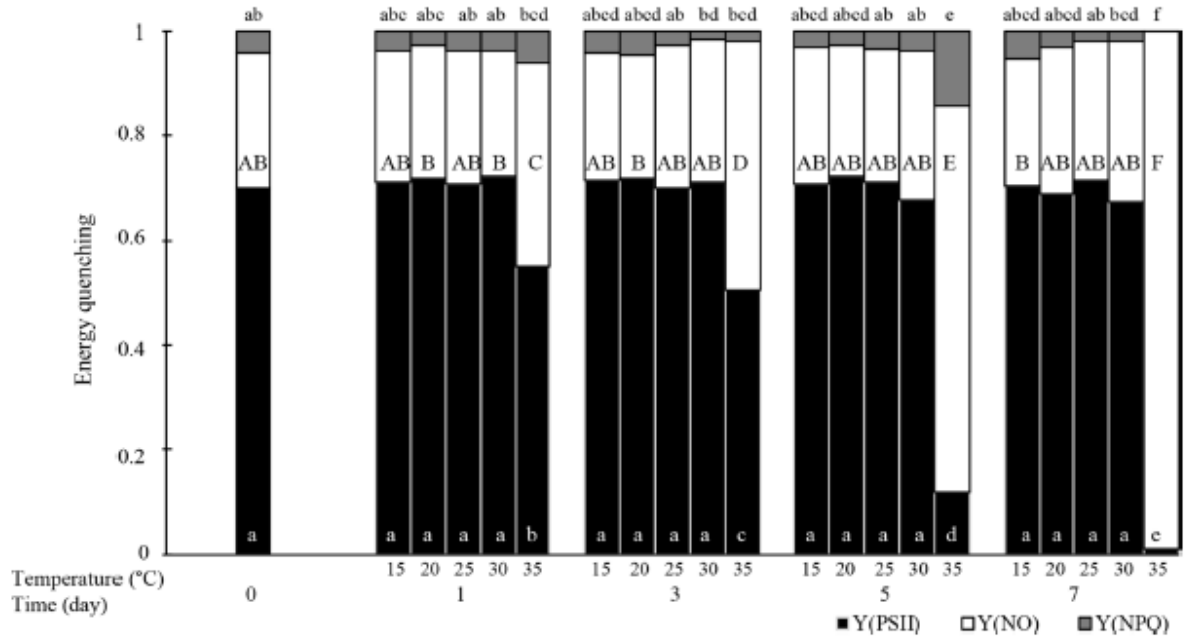

Fig. 1 Photosynthetic performance (mean ± SD, $n = 5$) of *S. stenophyllum* cultivated under different temperatures over time (initial and after 1, 3, 5 and 7 days), measured as Y(PSII)—effective quantum yield or photochemical quenching, Y(NO)—non-regulated non-photochemical quenching and Y(NPQ)—regulated non-photochemical quenching. Different letters (white lowercase, black uppercase and black lowercase) represent statistical differences for each variable ($p < 0.05$)

Table 1 Results of repeated measures analysis of variance (ANOVA) of the effect of temperature on the photosynthetic parameter (mean ± SD, $n = 5$) estimated from the ETR-PAR curve as maximum ETR (ETRmax), saturation light (Ik) and photosynthetic efficiency (α) of *S. stenophyllum* cultivated under different temperatures over time

Time (day)	Temperature (°C)	ETRmax (μmol electrons m^{-2} s^{-1})	Ik (μmol photons m^{-2} s^{-1})	α (electron photon^{-1})
Initial	25	39.61 ± 7.57^{bc}	105.61 ± 20.47^{bcde}	0.377 ± 0.042^{a}
1	15	31.15 ± 4.74^{cdef}	104.01 ± 3.67^{bcde}	0.300 ± 0.043^{bcd}
	20	22.95 ± 5.60^{f}	65.54 ± 22.09^{fg}	0.364 ± 0.067^{ab}
	25	31.83 ± 5.23^{cdef}	86.93 ± 16.96^{efg}	0.371 ± 0.046^{a}
	30	30.30 ± 5.71^{def}	80.19 ± 19.28^{cdefg}	0.382 ± 0.026^{ab}
	35	24.88 ± 3.12^{ef}	87.85 ± 11.60^{bcdef}	0.286 ± 0.045^{cd}
3	15	37.56 ± 3.64^{bcd}	111.07 ± 9.73^{bcd}	0.338 ± 0.008^{abc}
	20	29.43 ± 6.44^{def}	77.88 ± 11.59^{defg}	0.378 ± 0.058^{ab}
	25	36.19 ± 6.21^{bcde}	103.80 ± 24.43^{bcdef}	0.355 ± 0.042^{a}
	30	34.13 ± 8.06^{bcde}	86.42 ± 28.87^{cdef}	0.409 ± 0.064^{a}
	35	13.95 ± 4.14^{g}	54.27 ± 19.94^{g}	0.262 ± 0.043^{d}
5	15	38.69 ± 4.36^{bcd}	119.86 ± 11.30^{b}	0.323 ± 0.021^{abcd}
	20	24.88 ± 7.20^{ef}	64.73 ± 19.30^{fg}	0.386 ± 0.029^{a}
	25	42.62 ± 5.89^{bcd}	123.91 ± 16.26^{bc}	0.345 ± 0.040^{abc}
	30	22.74 ± 5.87^{f}	62.43 ± 25.48^{fg}	0.387 ± 0.076^{a}
	35	0.10 ± 0.00^{h}	0.10 ± 0.00^{h}	0.100 ± 0.000^{e}
7	15	43.96 ± 8.64^{b}	113.46 ± 22.71^{bc}	0.388 ± 0.017^{a}
	20	33.53 ± 5.86^{bcde}	97.26 ± 13.44^{bcde}	0.344 ± 0.031^{abc}
	25	51.41 ± 3.24^{a}	153.93 ± 8.91^{a}	0.330 ± 0.033^{abc}
	30	33.21 ± 2.11^{bcde}	87.60 ± 7.76^{bcdef}	0.380 ± 0.023^{ab}
	35	$0.10 \pm <0.00^{h}$	$0.10 \pm <0.00^{h}$	$0.100 \pm <0.001^{e}$

Letters represent correspond to $p < 0.05$

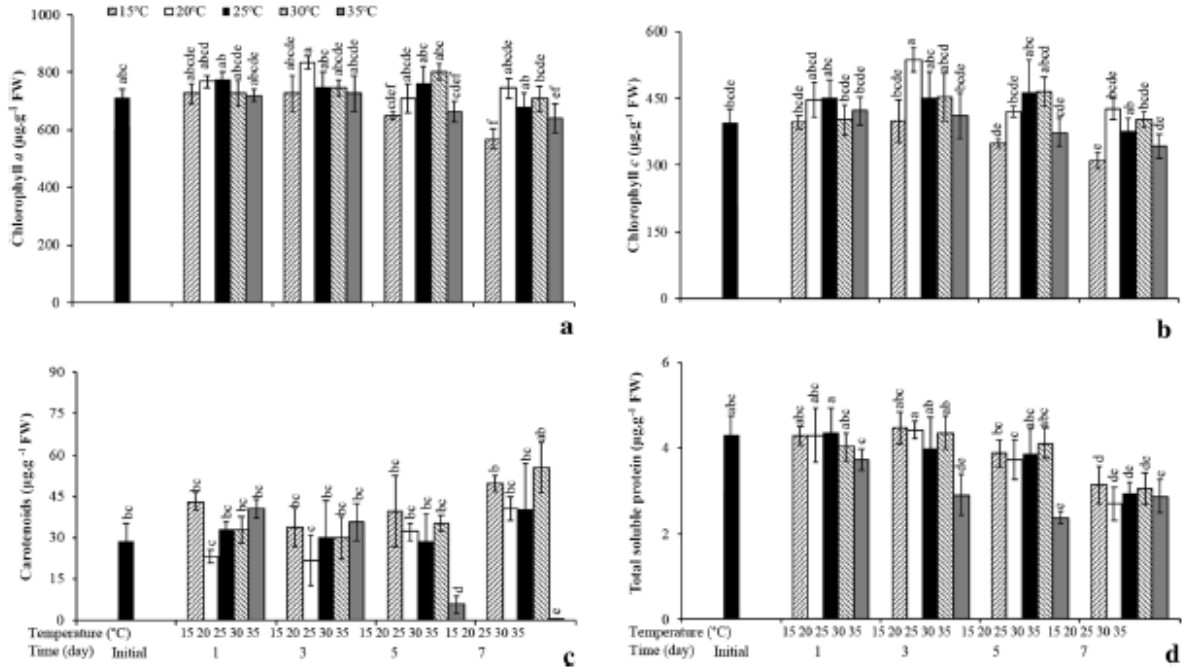

Fig. 2 Contents of **a** chlorophyll *a*, **b** chlorophyll *c*, **c** total carotenoids, and **d** total soluble proteins of *S. stenophyllum* (mean ± SD, $n = 5$) cultivated under different temperatures over time. Different letters represent statistical differences ($p < 0.05$)

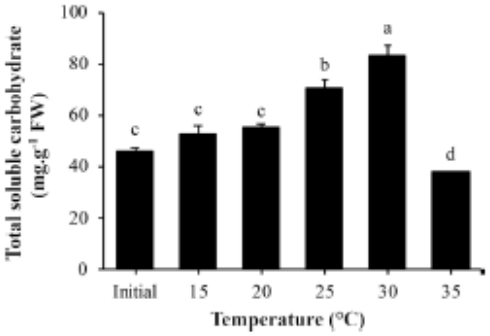

Fig. 3 Content of soluble carbohydrates (reported as fucose equivalents) of *S. stenophyllum* (mean ± SD, $n = 5$) cultivated under different temperatures at initial time and after 7 days of experimental period. Different letters represent statistical differences ($p < 0.05$)

maximal absorption bands at 206 to 214 nm, 266 to 276 nm and 320 to 340 nm for methanolic extracts. The area under the curve calculated from the maximal bands are shown in Table 2, in which differences were detected at 35 °C.

The amino acid profile of *S. stenophyllum* exhibited significant differences among the treatments (Fig. 4). The amino acids had different patterns by temperatures, except for cysteine, phenylalanine and tryptophan. After 7 days, the contents of arginine, glutamate and glutamine at 15 °C and 35 °C were reduced; the highest values of isoleucine and leucine were detected at 35 °C. Total amino acid content showed an increase at 30 °C (Fig. 4), similar to reported for total protein content with higher value at 30 °C (7.8 ± 0.4%). Total protein content at 20 °C and 25 °C was 6.3 ± 0.4% and 6.1 ± 0.5%, respectively; lower values were observed at 15 °C (3.8 ± 0.1%) and 35 °C (3.1 ± 0.4%).

PCA analysis (Fig. 5) explained 53.02% of the total variation with PC1 accounting for 32.99% and PC2 for 20.03% in data set. PC1 and PC2 differentiated three groups on the biplot graph related to temperature, a group between initial samples, 15 °C, 20 °C and 25 °C; another group at 30 °C and far from high extreme temperature at 35 °C. The PC1 and PC2 were positively and negatively correlated to all the measurements (Supplementary Material S3). The high components loadings of PC1 was positive correlation with Y(PSII) and negative correlation with Y(NO), and those correlated with PC2 was fucose with negative correlation. These measurements were mainly responsible for the variation between the three groups.

Table 2 Area under the curve (mean ± SD, $n = 5$) calculated of maximal UV absorption bands in buffered and methanolic extract of *S. stenophyllum* cultivated under different temperatures at initial time and after 7 days of experimental period

Extract	Treatment	Time (day)	
	Temperature (°C)	1	7
Area under the curve of UV absorption bands into 264 to 280 nm			
Buffered	Initial	1164.93 ± 293.78^{ab}	
	15	1194.16 ± 79.31^{a}	1002.51 ± 118.34^{ab}
	20	922.48 ± 181.66^{ab}	1108.42 ± 52.39^{ab}
	25	1264.92 ± 145.19^{a}	1167.17 ± 31.47^{ab}
	30	976.93 ± 191.87^{ab}	671.65 ± 180.75^{b}
	35	978.34 ± 146.11^{ab}	260.63 ± 40.54^{c}
Area under the curve of UV absorption bands into 266 to 276 nm			
Methanolic	Initial	486.8 ± 18.16^{a}	
	15	294.51 ± 36.38^{ce}	250.5 ± 16.91^{ce}
	20	343.75 ± 39.93^{bc}	318.86 ± 7.07^{bc}
	25	321.82 ± 22.35^{bce}	320.7 ± 39.46^{bc}
	30	356.87 ± 37.63^{bce}	239.51 ± 19.27^{e}
	35	271.25 ± 39.33^{cde}	183.75 ± 27.65^{df}

Letters represent correspond to $p < 0.05$

4 Discussion

The results of this study show variable short-term responses on the physiology and chemical composition of *S. stenophyllum* at different temperatures, with tolerance performance between 15 to 30 °C and sensitivity at 35 °C.

The characterization of physiological performance and biochemical variations are useful tools to assess the acclimation mechanisms, phenotypic plasticity and tolerance range level (Staehr and Wernberg 2009; Ji et al. 2016). As a warm species, it is expected that *S. stenophyllum* shows better tolerance to warm conditions, even above its tolerance limit. Notwithstanding, chronic response in photosynthesis and biochemical composition were observed in *S. stenophyllum* at 35 °C from the first day of experiment. On the other hand, tropical species can exhibit a narrow thermal tolerance and fast susceptibility responses with exhaustion and chronic damage as they evolved and actually inhabit a relative invariable thermal environment (Tewksbury et al. 2008; Sunday et al. 2012). Therefore, many of them live at or close to their maximal thermal limit.

In temperate regions, the optimum growth temperature for *Sargassum* spp. include low values as registered by Yuan et al. (2014) in *S. muticum* (Yendo) Fensholt at 15 °C and negative effects at 30 °C. In contrast, species from tropical regions had optimal temperature at 25 °C (Paula and Oliveira Filho 1980), and some of them show a range of thermotolerance between 25 °C and 35 °C as observed in *S. polycystum* C. Agardh (Widyartini et al. 2017) and between 20 °C and 28 °C for *S. fusiforme* (Harvey) Setchell (Kokubu et al. 2015). The upper limit of temperature tolerance, 30 °C, seems to remain similar for *S. stenophyllum* (present study) and *S. fusiforme* (Kokubu et al. 2015), in which negative effects were observed in photosynthesis and chemical composition, probably associated to a C:N misbalance affecting photosynthetic pigments, carbohydrates, amino acids and proteins.

At 15 °C and 35 °C, *S. stenophyllum* reported low values of glutamate. This amino acid is a precursor in chlorophyll synthesis (Forde and Lea 2007), which could be associated with the decrease in this photosynthetic pigment content. There are two reactions for chlorophylls associated with photoinhibition. The first one involves a structural adjustment of the molecule without destroying its macrocyclic conjugation (Louda et al. 1998), taking place in *S. stenophyllum* with samples at 15 °C at 7 day. The second one includes cleavage of the macrocyclic ring with pigment destruction (Louda et al. 1998), which might have happened in the samples at 35 °C with the lowest values of the photosynthetic pigments after fifth day and thalli deterioration. This reduction revealed a positive correlation between pigment content and photosynthetic rate (Louda et al. 1998). Therefore, as photosynthetic pigments and effective quantum yield of *S. stenophyllum* showed non-variation or slight fluctuations at 15, 20, 25 and 30 °C, the treatment + 5 °C seems to trigger a generalized dysfunction probably related to photosynthetic light-harvesting complex and cell integrity, since the phylloids showed unhealthy aspect.

The reduction of carotenoid content from the fifth day at 35 °C for *S. stenophyllum* can characterize a thalli-bleaching feature, which could be associated with a reduction of xanthophylls, such as fucoxanthin and violaxanthin (Lewey and Gorham 1984), the major carotenoids found in brown algae, analogous to studies for *S. muticum* at 30 °C by Yuan et al. (2014). At 15 °C to 30 °C, photosynthetic performance in *S. stenophyllum* can be related to photoprotective xanthophyll

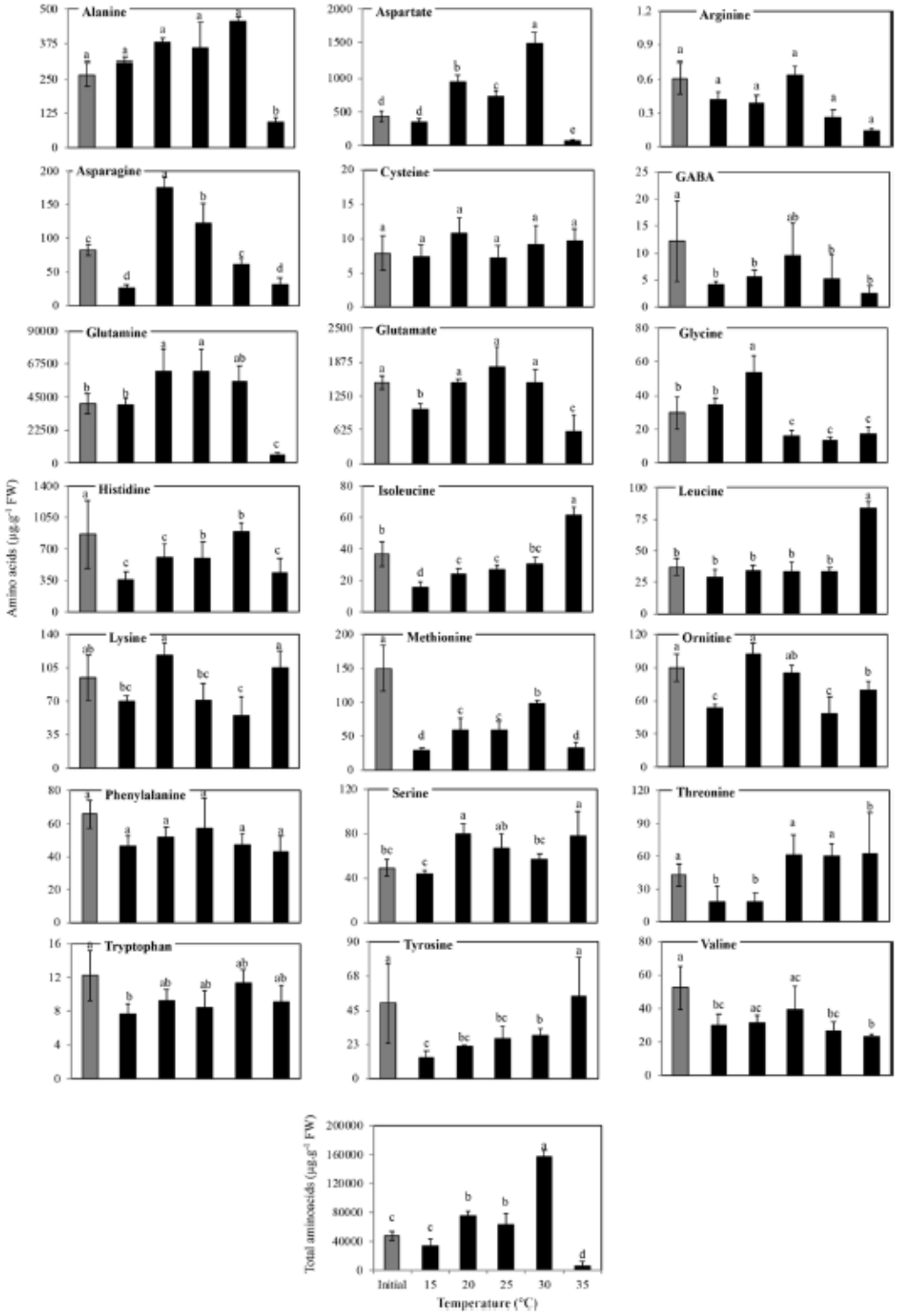

Fig. 4 Contents of amino acid profile (mean ± SD, $n = 5$) of *S. stenophyllum* cultivated under different temperatures after 7 days of experimental period. Different letters represent statistical differences ($p < 0.05$)

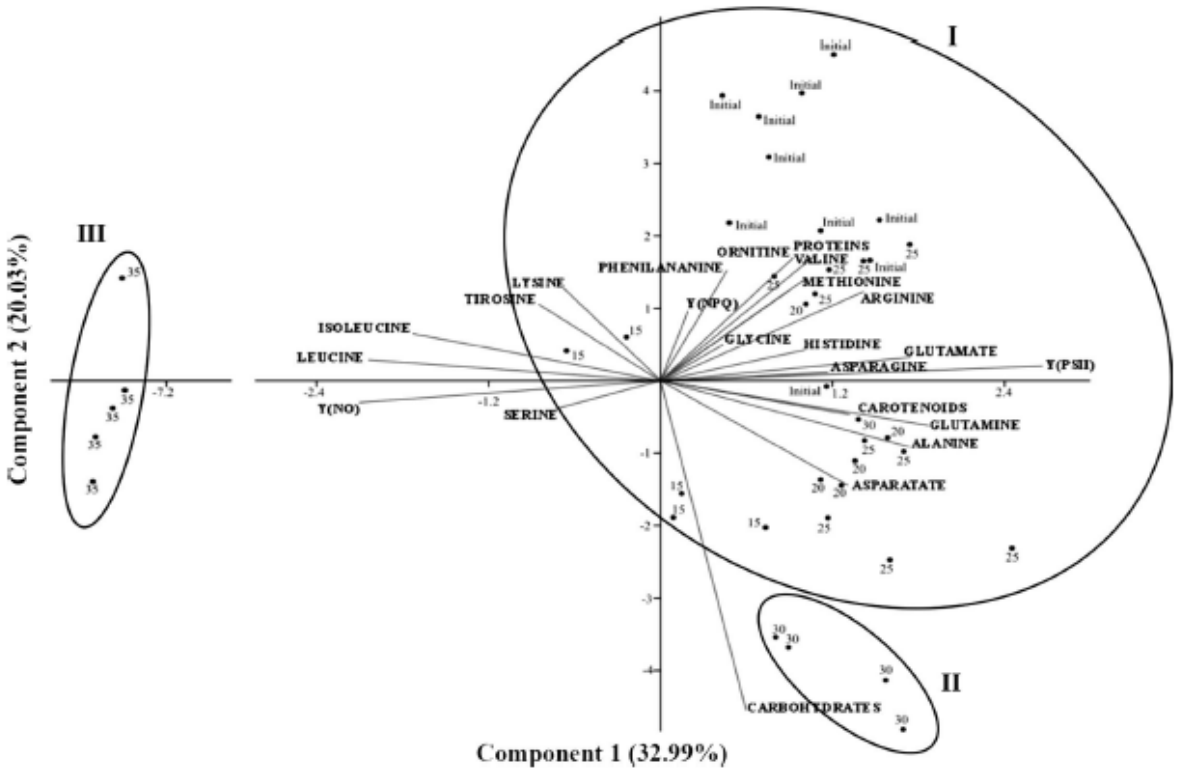

Fig. 5 PCA biplot of *S. stenophyllum* cultivated under different temperatures after 7 days of experimental period included the initial samples showing the loadings on PC1 and PC2, representing 32.99% and 20.03% of the total variance of the data, respectively. Treatments are represented by lowercase letters. Parameters are represented by uppercase letters

cycle, including fucoxanthin participation (Mikami and Hosokawa 2013). Fucoxanthin (maximal absorption bands at 428, 448 and 468 nm) is one of the most abundant carotenoid, almost 80% of the measured xanthophylls in brown seaweeds (Lewey and Gorham 1984), displaying functions as an essential component of the photosynthetic antenna complex, de-excitating chlorophyll *a* by quenching reactive singlet and triplet oxygen molecules (Schofield et al. 1998) and photoprotecting against oxidative stress (Latowski et al. 2011). Fucoxanthin is highly susceptible to degradation, leading to cis–trans isomerization, oxidative cleavage and epoxidation of the backbone as reported by Piovan et al. (2013). Accordingly, *S. stenophyllum* undergoes chronic damage in the metabolic responses, including a possibly fucoxanthin degradation at 35 °C after 5 days.

In addition, coloration change in the phylloids of *S. stenophyllum* was observed, showing dark-brown color, which can results by the presence of melanoidins (heterogeneous polymers of sugars and amino acids synthetized at high temperatures) and/or oxidation processes typical of thermal stress. Melanoidin substances are produced by a non-enzymatic browning reaction (known as Maillard reaction), which takes place between the carbonyl group of reduced sugar and the amino group of amino acids, peptides or proteins (Echavarría et al. 2016). This study emerges as a novelty for seaweed literature in the melanoidins synthesis that could be induced at 30 °C. For *S. stenophyllum*, melanoidins could have been presented by association between fucose, the major soluble carbohydrate recorded for the genus (reported by Duarte et al. 2001), linked with amino acids such as alanine, aspartate, isoleucine or leucine, although is needed further confirmation by other studies. Even though the melanoidins chemical structures is relatively unknown, it has been reported that some combinations contribute to the prevention of oxidative damage, acting as antioxidant with radical-scavenging activity and metal chelating capacity (Wang et al. 2011).

Among amino acid profiles that showed no statistically significant difference between treatments were cysteine, phenylalanine and tryptophan. Phenylalanine, tryptophan and tyrosine are precursors of many secondary metabolites, which are involved in the synthesis of phenolic compounds, important metabolites that act as defense system against abiotic stressors. In this study, *S. stenophyllum* extracts

indicated maximum absorbance bands from 260 to 280 nm, that represent the presence of phenolic acids and polyphenols as phlorotannins, typical in brown algae (Myung et al. 2005; Ferreres et al. 2012; Chakraborty and Joseph 2016). These phenolic compounds could accrue in intracellular space or be released in seawater. Gómez and Huovinen (2010) reported insoluble phlorotannins that remain inside the physodes for intrinsic morpho-functional processes and soluble phlorotannins, which are extruded to the surrounding water as a defense mechanism. During the experimental period with *S. stenophyllum*, a change in the appearance of the seawater color (to yellowish) at high temperatures was observed, which might indicate the release of these compounds. Similar results were reported for *S. cymosum* C. Agardh exposed to UV radiation, as evidenced by the absorbance screening of seawater, in which an increase at 300 nm was observed (Polo et al. 2014). Under abiotic stress, such as fluctuations of temperature and UV radiation, there is an increase of phlorotannins and rates of exudation of phenolic substances increase, which has been pointed out as a reflection of algal acclimatization to environmental changes (Endo et al. 2013; Abdala-Díaz and Cabello-Pasini 2014). Therefore, abiotic factors such as temperature could be inducing the liberation of phenolic compounds to seawater as a protection mechanism as well as for reducing the palatability or consumption rates to herbivores (Abdala-Díaz and Cabello-Pasini 2014). Additionally, Stern et al. (1996) reported the ability of tannins to precipitate proteins generating the formation of tannin-protein complexes. Then, the progressive reduction observed in the soluble protein content over time might also be related with a release of phlorotannins-protein complexes. In addition, total protein content in *S. stenophyllum*, quantified after 7 days, was within concentration ranges from 3% to 8% of dry weight, with higher value at 30 °C (7.8 ± 0.4%). Generally, the protein amount of brown seaweeds is lower than 15% (Fleurence 1999).

At 15 °C and 20 °C, *S. stenophyllum* showed rise of glycine content, which could be related with the production or accumulation of glycine betaine, an intracellular osmolyte whose levels increase under environmental stresses and which acts as antioxidant (Airs and Archer 2010). At 20 °C and 25 °C, the content of certain amino acids, such as glutamate and glutamine, was significantly higher, which could be associated with nitrogen availability to support growth (Azevedo et al. 2006). In these temperatures were accumulated ornithine, asparagine and γ-aminobutyrate (GABA), which are amino acids related with polyamines, phytohormone-like aliphatic amine compounds, involved in many processes of growth and development, thereby acting as anti-senescence and anti-stress agents (Gill and Tuteja 2010). At 30 °C, high values in methionine, histidine and tryptophan contents may be part of a defense response to thermal stress. For instance, methionine is a substrate for the synthesis of various polyamines with important roles in stress tolerance, the most prominent being putrescine, spermidine and spermine (Alcázar et al. 2010). Moreover, at 35 °C, *S. stenophyllum* reported the highest values of isoleucine and leucine, which are two branched-chain amino acids (BCAAs). It has been proposed that BCAAs serve for the synthesis of stress-induced proteins or as signaling molecules to regulate gene expression (Joshi et al. 2010). Additionally, Liu and Lin (2020) reported for *S. fusiforme* the contents of isoleucine increased significantly after the 27 °C that can enter the citric acid cycle and contribute to the redox potential. As a final point, threonine content increased gradually as the temperature increases, which could be related to antioxidant processes (Wu 2009).

Finally, as was confirmed by the PCA analysis, the set of physiological and chemical composition responses of *S. stenophyllum* under short-term thermal cultivation, three clusters were separated: (a) initial samples plus 15 °C, 20 °C and 25 °C, (b) 30 °C and (c) 35 °C. Photosynthesis performance and photosynthetic pigments were important drivers for this separation, in which the lower intertidal macroalgae *S. stenophyllum* showed physiological and chemical plasticity with thermal tolerance mechanisms between 15 to 30 °C. In turn, *S. stenophyllum* proved to be fully susceptible and sensitive to + 5 °C above the maximum local environmental temperature, evidencing a quickness exhaustion phase (1 day after exposure) and entire chronic damage in photosynthesis and chemical compounds degradation and necrosis over the experimental period.

Acknowledgements VUV acknowledges the PhD fellowships financed by the Coordenação de Aperfeiçoamento de Pessoal de Nível Superior—Brazil (CAPES; Finance Code 001) and Fundação de Amparo à Pesquisa do Estado de São Paulo (FAPESP; 2014/25073-3). FC acknowledges the financial support of FAPESP for the BIOTA-FAPESP Grant (2013/50731-1) and CNPq Research Productivity Grant (303937/2015-7). We also thanks Dra Eny I.S. Floh who kindly provided equipment and infrastructure for amino acids analysis.

Authors' contributions All authors significantly contributed by designing, collecting and analyzing the data, and preparing and revising the manuscript. FC conceived the idea and supervised critically the manuscript.

References

Abdala-Díaz RA, Cabello-Pasini E (2014) Marquez, Intra-thallus variation of phenolic compounds, antioxidant activity, and phenolsulphatase activity in *Cystoseira tamariscifolia* (Phaeophyceae) from southern Spain. Cienc Mar 40:1–10. https://doi.org/10.7773/cm.v40i1.2350

Airs R, Archer S (2010) Analysis of glycine betaine and choline in seawater particulates by liquid chromatography/electrospray ionization/mass spectrometry. Limnol Oceanogr 8:499–506. https://doi.org/10.4319/lom.2010.8.499

Alcázar R, Altabella T, Marco F, Bortolotti C, Reymond M, Koncz C, Carrasco P, Tiburcio A (2010) Polyamines: molecules with regulatory functions in plant abiotic stress tolerance. Planta 6:1237–1249. https://doi.org/10.1007/s00425-010-1130-0

Azevedo R, Lancien M, Lea M (2006) The aspartic acid metabolic pathway, an exciting and essential pathway in plants. Amino Acids 30:143–162. https://doi.org/10.1007/s00726-005-0245-2

Bernardino A, Netto S, Pagliosa P, Barros F, Christofoletti R, Rosa Filho J, Colling L, Lana P (2015) Predicting ecological changes on benthic estuarine assemblages through decadal climate trends along Brazilian Marine Ecoregions. Estuar Coast Shelf 166:74–82. https://doi.org/10.1016/j.ecss.2015.05.021

Bradford M (1976) A rapid sensitive method for the quantification of microgram quantities of protein utilizing the principle of protein-dye binding. Anal Biochem 72:248–254. https://doi.org/10.1016/0003-2697(76)90527-3

Breeman A (1988) Relative importance of temperature and other factors in determining geographic boundaries of seaweeds: experimental and phenological evidence. Helgol Meerestmters 42:199–241. https://doi.org/10.1007/BF02366043

Casas-Valdez M, Sánchez-Rodriguez I, Serviere-Zaragoza E, Aguila-Ramirez R (2016) Temporal changes in the biomass and distribution of *Sargassum* beds along the southeastern coast of the Baja California Peninsula. Cienc Mar 42:99–109. https://doi.org/10.7773/cm.v42i2.2592

Chakraborty K, Joseph D (2016) Antioxidant potential and phenolic compounds of brown seaweeds *Turbinaria conoides* and *Turbinaria ornata* (class: Phaeophyceae). J Aquat Food Prod Technol 1:29–49. https://doi.org/10.1080/10498850.2015.1054540

Davison I (1991) Environmental effects on algal photosynthesis: temperature. J Phycol 27:2–8. https://doi.org/10.1111/j.0022-3646.1991.00002.x

Davison I, Greene R, Podolak E (1991) Temperature acclimation of respiration and photosynthesis in the brown alga *Laminaria saccharina*. Mar Biol 110:449–454. https://doi.org/10.1007/BF01344363

De Wreede R (1976) The phenology of the three species of *Sargassum*. Phycologia 15:175–183. https://doi.org/10.2216/i0031-8884-15-2-175.1

Druehl L, Green J (1982) Vertical distribution of intertidal seaweeds as related to patterns of submersion and emersion. Mar Ecol Progr Ser 9:163–170. https://doi.org/10.3354/meps009163

Duarte M, Cardoso M, Noseda M, Cerezo A (2001) Structural studies on fucoidans from the brown seaweed *Sargassum stenophyllum*. Carbohydr Res 333:281–293. https://doi.org/10.1016/s0008-6215(01)00149-5

Echavarría A, Pagán J, Ibarz A (2016) Kinetics of color development in glucose/amino Acid model systems at different temperatures. Sci Agr 7:15–21. https://doi.org/10.17268/sci.agropecu.2016.01.02

Edwards P (1970) Illustrated guide to the seaweeds and sea grasses in the vicinity of Porto Aransas. University of Texas at Austin, Austin, Texas

Egydio A, Santa Catarina C, Floh E, Santos D (2013) Free amino acid composition of *Annona* (Annonaceae) fruit species of economic interest. Ind Crop Prod 45:373–376. https://doi.org/10.1016/j.indcrop.2012.12.033

Endo H, Suehiro K, Kinoshita J, Gao X, Agatsuma Y (2013) Combined effects of temperature and nutrient availability on growth and phlorotannins concentration of the brown alga *Sargassum patens* (Fucales; Phaeophyceae). Am J Plant Sci 4:1–7. https://doi.org/10.4236/ajps.2013.412A2002

Ferreres F, Lopes G, Gil A, Andrade P, Sousa C, Mouga T, Valentão P (2012) Phlorotannin extracts from Fucales characterized by HPLC-DAD-ESI-MSn: approaches to hyaluronidase inhibitory capacity and antioxidant properties. Mar Drugs 10:2766–2781. https://doi.org/10.3390/md10122766

Figueroa F, Nygard C, Ekelund N, Goméz I (2003) Photobiological characteristics and photosynthetic UV responses in two *Ulva* species (Chlorophyta) from Southern Spain. J Photochem Photobiol, B 72:35–44. https://doi.org/10.1016/j.jphotobiol.2003.09.002

Fleurence J (1999) Seaweed proteins: biochemical, nutritional aspects and potential uses. Trends Food Sci Tech 10:25–28. https://doi.org/10.1016/S0924-2244(99)00015-1

Forde B, Lea P (2007) Glutamate in plants: metabolism, regulation, and signaling. J Exp Bot 58:2339–2358. https://doi.org/10.1093/jxb/erm121

Gill S, Tuteja N (2010) Polyamines and abiotic stress tolerance in plants. Plant Signal Behav 5:26–33. https://doi.org/10.4161/psb.5.1.10291

Gómez I, Huovinen P (2010) Induction of phlorotannins during UV exposure mitigates inhibition of photosynthesis and DNA damage in the kelp *Lessonia nigrescens*. J Photochem Photobiol 86:1056–1063. https://doi.org/10.1111/j.1751-1097.2010.00786.x

Gorman D, Horta P, Flores A, Turra A, Berchez F, Batista MB, Lopes Filho ES, Melo MS, Ignacio BL, Carneiro IM, Villaça RC, Széchy M (2020) Decadal losses of canopy-forming algae along the warm temperate coastline of Brazil. Global Change Biol 26:1446–1457. https://doi.org/10.1111/gcb.14956

Graba-Landry A, Loffler Z, McClure E, Pratchett MS, Hoey AS (2020) Impaired growth and survival of tropical macroalgae (*Sargassum* spp.) at elevated temperatures. Coral Reefs 39:475–486. https://doi.org/10.1007/s00338-020-01909-7

Harb T, Nardelli A, Chow F (2018) Physiological responses of *Prerocladiella capillacea* (Rhodophyta, Gelidiales) under two light intensities. Photosynthetica 56:1093–1106. https://doi.org/10.1007/s11099-018-0805-9

INPE (2014) Instituto nacional de pesquisas espaciais. http://sinda.crn2.inpe.br/PCD/SITE/novo/site/historico/passo2.php Accessed 16 April 2015

Jassby A, Platt T (1976) Mathematical formulation of the relationship between photosynthesis and light for phytoplankton. Limnol Oceanogr 21:540–547. https://doi.org/10.4319/lo.1976.21.4.0540

Jeffrey S (1963) Purification and properties of chlorophyll *c* from *Sargassum flavicans*. Biochem J 86:313–318. https://doi.org/10.1042/bj0860313

Ji Y, Xu Z, Zou D, Gao K (2016) Ecophysiological responses of marine macroalgae to climate change factors. J Phycol 5:2953–2967. https://doi.org/10.1007/s10811-016-0840-5

Joshi V, Joung J-G, Fei Z, Jander G (2010) Interdependence of threonine, methionine and isoleucine metabolism in plants: accumulation and transcriptional regulation under abiotic stress. Amino Acids 39:933–947. https://doi.org/10.1007/s00726-010-0505-7

Kokubu S, Nishihara G, Watanabe Y, Tsuchiya Y, Amamo Y, Terada R (2015) The effect of irradiance and temperature on the photosynthesis of a native alga *Sargassum fusiforme* (Fucales) from Kagoshima, Japan. Phycologia 54:235–247. https://doi.org/10.2216/15-007.1

Kramer D, Johnson G, Kiirats O, Edwards G (2004) New fluorescence parameters for the determination of QA redox state and excitation energy fluxes. Photosynth Res 79:209–218. https://doi.org/10.1023/B:PRES.0000015391.99477.0d

Lalegerie F, Gager L, Stiger-Pouvreau V, Connan S (2020) The stressful life of red and brown seaweeds on the temperate intertidal zone: effect of abiotic and biotic parameters on the physiology of macroalgae and content variability of particular metabolites. Adv Bot Res 95:247–287. https://doi.org/10.1016/bs.abr.2019.11.007

Latowski D, Kuczynska P, Strzalka K (2011) Xanthophyll cycle: a mechanism protecting plants against oxidative stress. Redox Rep 16:78–90. https://doi.org/10.1179/174329211X13020951739938

Lerdau M, Coley P (2000) Benefits of the carbon-nutrient balance hypothesis. Oikos 98:534–536. https://doi.org/10.1034/j.1600-0706.2002.980318.x

Lewey S, Gorham J (1984) Pigment composition and photosynthesis in *Sargassum muticum*. Mar Biol 80:109–115. https://doi.org/10.1007/BF00393134

Lichtenthaler H (1987) Chlorophylls and carotenoids, the pigments of photosynthetic biomembranes. Method Enzymol. https://doi.org/10.1016/0076-6879(87)48036-1

Lichtenthaler H, Buschmann C (2001) Chlorophylls and carotenoids: measurement and characterization by UV–VIS spectroscopy. In: Current protocols in food analytical chemistry. Wiley, New York, pp F4.3.1–F4.3.8

Liu L, Lin L (2020) Effect of heat stress on *Sargassum fusiforme* leaf metabolome. J Plant Biol 63:229–241. https://doi.org/10.1007/s12374-020-09247-5

Louda J, Li L, Liu L, Winfree N, Baker E (1998) Chlorophyll-a degradation during cellular senescence and death. Org Geochem 29:1233–1251. https://doi.org/10.1016/S0146-6380(98)00186-7

Lourenço S, Barbarino E, De-Paula J, Otávio L, Lanfer U (2002) Amino acid composition, protein content and calculation of nitrogen-to-protein conversion factors for 19 tropical seaweeds. Phycol Res 50:233–241. https://doi.org/10.1046/j.1440-1835.2002.00278.x

Marengo J, Nobre C, Salati E, Ambrizzi T (2007) Caracterização do clima atual e definição das alterações climáticas para o território brasileiro ao longo do século XXI. Sumário Técnico, Brasília

Marinho-Soriano E, Fonseca P, Carneiro M, Moreira W (2006) Seasonal variation in the chemical composition of two tropical seaweeds. Biores Tech 97:2402–2406. https://doi.org/10.1016/j.biortech.2005.10.014

Matanjun P, Mohamed S, Mustapha N, Muhammad K (2009) Nutrient content of tropical edible seaweeds *Eucheuma cottonii*, *Caulerpa lentillifera* and *Sargassum polycystum*. J Appl Phycol 21:75–80. https://doi.org/10.1007/s10811-008-9326-4

Matsuko T, Minami A, Iwasaki N, Majima T, Nishimura S, Lee Y (2005) Carbohydrate analysis by a phenol-sulfuric acid method in microplate format. Anal Biochem 339:69–72. https://doi.org/10.1016/j.ab.2004.12.001

Mercado J, Jiménez C, Niell F, Figueroa F (1996) Comparison of methods for measuring light absorption by algae and their application to the estimation of package effect. Sci Mar 60:39–45

Mikami K, Hosokawa M (2013) Biosynthetic pathway and health benefits of fucoxanthin, an algae-specific xanthophyll in brown seaweeds. Int J Mol Sci 14:13763–13781. https://doi.org/10.3390/ijms140713763

Muller R, Wiencke C, Bischof K (2008) Interactive effects of UV radiation and temperature on microstages of Laminariales (Phaeophyceae) from the Arctic and North Sea. Clim Res 37:203–213. https://doi.org/10.3354/cr00762

Myung C, Shin H, Bao H, Yeo S, Lee B, Kang J (2005) Improvement of memory by dieckol and phlorofucofuroeckol in ethanol-treated mice: possible involvement of the inhibition of acetylcholinesterase. Arch Pharm Res 28:691–698. https://doi.org/10.1007/BF02969360

Paula E (1988) O gênero *Sargassum* C. Agarth (Phaeophyta, Fucales) no estado de São Paulo. Bol Bot 10:65–118

Paula E, Oliveira Filho E (1980) Phenology of two populations of *Sargassum cymosum* (Phaeophyta-Fucales) of São Paulo State coast, Brazil. Bol Bot 8:21–39

Piovan A, Seraglia R, Bresin B, Caniato R, Filippini R (2013) Fucoxanthin from *Undaria pinnatifida*: photostability and coextractive effects. Molecules 18:6298–6310. https://doi.org/10.3390/molecules18066298

Polo L, Felix M, Kreusch M, Pereira D, Costa G, Simioni C, Martins R, Latini A, Floh E, Chow F, Ramlov F, Maraschin M, Bouzon Z, Schmidt E (2014) Metabolic profile of the brown macroalga *Sargassum cymosum* (Phaeophyceae, Fucales) under laboratory UV radiation and salinity conditions. J Appl Phycol 27:887–899. https://doi.org/10.1007/s10811-014-0381-8

Ramos M, Oliveira A, Azevedo R, Carvalho A (1999) Amino acid composition of some Brazilian seaweed species. J Food Biochem 24:33–39. https://doi.org/10.1111/j.1745-4514.2000.tb00041.x

Ramus J, Rosenberg G (1980) Diurnal photosynthetic performance of seaweeds measured under natural conditions. Mar Biol 56:21–28. https://doi.org/10.1007/BF00390590

Ritchie R (2008) Universal chlorophyll equations for estimating chlorophylls *a*, *b*, *c*, and *d* and total chlorophylls in natural assemblages of photosynthetic organisms using acetone, methanol, or ethanol solvents. Photosynthetica 46:115–126. https://doi.org/10.1007/s11099-008-0019-7

Rosenberg G, Ramus J (1982) Ecological growth strategies in the seaweeds *Gracilaria foliifera* (Rhodophyceae) and *Ulva* sp. (Chlorophyceae): soluble nitrogen and reserve carbohydrates. Mar Biol 66:251–259. https://doi.org/10.1007/BF00397030

Santa-Catarina C, Silveira V, Balbuena T, Viana A, Estelita M, Handro W, Floh E (2006) IAA, ABA, polyamines and free amino acids associated with zygotic embryo development of *Ocotea catharinensis*. Plant Growth Regul 49:237–247. https://doi.org/10.1007/s10725-006-9129-z

Schmidt ÉC, Felix MRdL, Kreusch MG, Pereira D, Costa G, Simioni C, Ouriques Steiner N, Chow F, Floh E, Ramlov F, Maraschin M, Bouzon Z (2016) Profiles of carotenoids and amino acids and total phenolic compounds of the red alga *Prerocladiella capillacea* exposed to cadmium and different salinities. J Appl Phycol 28:1955–1963. https://doi.org/10.1007/s10811-015-0737-8

Schofield O, Evenes T, Millie D (1998) Photosystem II quantum yield and xanthophyll-cycle pigments to the macroalga *Sargassum natans* (Phaeophyceae): responses under natural sunlight. J Phycol 34:102–112. https://doi.org/10.1046/j.1529-8817.1998.340104.x

Schreiber U, Neubaer C (1990) O_2-dependent electron flow, membrane energization and the mechanism of non-photochemical quenching of chlorophyll fluorescence. Photosynth Res 25:279–293. https://doi.org/10.1007/BF00033169

Staehr P, Wernberg T (2009) Physiological responses of *Ecklonia radiata* (Laminariales) to a latitudinal gradient in ocean temperature. J Phycol 45:91–99. https://doi.org/10.1111/j.1529-8817.2008.00635.x

Stern J, Hagerman E, Steinberg P, Mason P (1996) Phlorotannin-protein interactions. J Chem Ecol 22:1877–1899. https://doi.org/10.1007/BF02028510

Sunday JM, Bates AE, Dulvy NK (2012) Thermal tolerance and the global redistribution of animals. Nat Clim Chang 2:686–690. https://doi.org/10.1038/nclimate1539

Széchy M, Paula E (2000) Padrões estruturais quantitativos de bancos de *Sargassum* (Phaeophyta - Fucales) do litoral dos estados do Rio de Janeiro e São Paulo, Brasil. Rev bras Bot 23:121–132. https://doi.org/10.1590/S0100-84042000000200002

Teixeira T, Neves L, Araújo F (2009) Effects of a nuclear power plant thermal discharge on habitat complexity and fish community structure in Ilha Grande Bay, Brazil. Mar Environ Res 68:188–195. https://doi.org/10.1016/j.marenvres.2009.06.004

Teoh M, Chu W, Phang S (2010) Effect of temperature change on physiology and biochemistry of algae: a review. Malays J Sci 29:82–97. https://doi.org/10.22452/mjs.vol29no2.1

Tewksbury JJ, Huey RB, Deutsch CA (2008) Putting the heat on tropical animals. Science 320:1296–1297. https://doi.org/10.1126/science.1159328

Ursi S, Plastino E (2001) Crescimento in vitro de linhagens de coloração vermelha e marrom-esverdeada clara de *Gracilaria* sp. (Gracilariales, Rhodophyta) em dois meios de cultura: análise de diferentes estádios reprodutivos. Rev Bras Bot 24:587–594. https://doi.org/10.1590/S0100-84042001000500014

Wang HY, Qian H, Yao WR (2011) Melanoidins produced by the Maillard reaction: structure and biological activity. Food Chem 128:573–584. https://doi.org/10.1016/j.foodchem.2011.03.075

Widyartini D, Widodo P, Susanto A (2017) Thallus variation of *Sargassum polycystum* from Central Java, Indonesia. Biodiversitas 18:1004–1011. https://doi.org/10.13057/biodiv/d180319

Wu G (2009) Amino acids: metabolism, functions and nutrition. Amino Acids 37:1–17. https://doi.org/10.1007/s00726-009-0269-0

Yuan C, Yang S, Wang Y, Cui K (2014) Effect of temperature on the growth and biochemical composition of *Sargassum muticum*. Adv Mater Res 989:747–750. https://doi.org/10.4028/www.scientific.net/AMR.989-994.747

Publisher's Note Springer Nature remains neutral with regard to jurisdictional claims in published maps and institutional affiliations.

ANEXO 9

J Appl Phycol (2013) 25:1847–1853
DOI 10.1007/s10811-013-0005-8

Modulation of nitrate reductase activity by photosynthetic electron transport chain and nitric oxide balance in the red macroalga *Gracilaria chilensis* (Gracilariales, Rhodophyta)

Fungyi Chow · Marianne Pedersén · Mariana C. Oliveira

Received: 12 September 2012 / Revised and accepted: 11 February 2013 / Published online: 1 March 2013
© Springer Science+Business Media Dordrecht 2013

Abstract Nitrate reductase (NR), a key enzyme in nitrogen metabolism, has been implicated in the production of nitric oxide (NO) in plants. The effect of photosynthetic electron transport chain inhibitors and NO scavengers or donors on NR activity of *Gracilaria chilensis* was studied under experimental laboratory conditions. Effective quantum yield (Φ_{PSII}) and NR activity were significantly diminished by 3-(3,4-dichlorophenyl)-1,1-dimethylurea and 2,5-dibromo-3-methyl-6-isopropyl-*p*-benzoquinone, two photosynthetic electron flux inhibitors of photosystem (PS) II and PSI, respectively, but not by diphenyleneiodonium, a NADPH oxidase inhibitor, indicating a direct dependence of NR activity on the PSII and PSI electron flux. Nitrate reductase activity was sensitive to a decrease or increase of NO levels when NO scavenger (2-(4-carboxyphenyl)-4,4,5,5-tetramethylimidazoline-1-oxyl-3-oxide) and NO donor (sodium nitroprusside) were added. Moreover, the addition of 8Br-cGMP, a secondary signal molecule, stimulated NR activity. These results evidence a modulation of the photosynthetic electron transport chain and NO balance on *G. chilensis* NR activity. This association could be linked to the crucial tight modulation of nitrogen assimilation and carbon metabolism to guarantee nitrite incorporation into organic compounds and to avoid toxicity by nitrite, reactive oxygen species, or nitric oxide in the cells. Nitric oxide showed to be an important signaling molecule regulating NR activity and cGMP could participate as secondary messenger on this regulation by phosphorylation and desphosphorylation processes.

Keywords *Gracilaria chilensis* · Nitrate reductase · Nitric oxide · Photosynthetic efficiency · Physiological stress

F. Chow · M. C. Oliveira
Department of Botany, Institute of Bioscience,
University of São Paulo, São Paulo, SP, Brazil

M. Pedersén
Department of Botany,
Stockholm University, Stockholm, Sweden

F. Chow (✉)
Departamento de Botânica, Instituto de Biociências,
Universidade de São Paulo, Rua do Matão 277,
05508-090, São Paulo, SP, Brazil
e-mail: fchow@ib.usp.br

Introduction

Gracilaria chilensis Bird, McLachlan et Oliveira (Gracilariales, Rhodophyta) is an economically important macroalga for the production of agar and agarose used in food and pharmaceutical and biotechnology industries. This species has been extensively harvested from natural beds and cultivated in Chile and New Zealand (Buschmann et al. 1995).

Nitrate reductase (NR, EC 1.6.6.1) is the first enzyme in the nitrogen assimilatory pathway, which reduces nitrate to nitrite. Nitrite can be further reduced to ammonium, and the accumulation of which has cytotoxic consequences for the cells. Nitrate reduction needs photosynthetic metabolites (e.g., reducing power and energy); therefore, a tight regulatory mechanism between these important processes must exist (Givan et al. 1988; Lea and Blackwell 1992; Huppe and Turpin 1994).

The use of electron transport chain inhibitors has been recommended to verify the identity and function of the

components of chain and to study the biochemical roles of the processes related to photosynthesis (Kleczkowski 1994). Commonly used inhibitors are the herbicides 3-(3,4-dichlorophenyl)-1,1-dimethylurea (DCMU) and atrazine. Both compounds inhibit the activity of photosystem II (PSII) by dislocating the plastoquinone (PQ) from the binding site of quinone B (QB), blocking effectively the electron flux, and inhibiting the photosynthesis (Moreland 1980; Sandmann and Böger 1986; Mazur and Falco 1989; Van Rensen 1989). The electron flux immediately after the QB can be inhibited by benzoquinone analog, for example 2,5-dibromo-3-methyl-6-isopropyl-p-benzoquinone (DBMIB), which interferes with PQ oxidation favoring cyclic photophosphorylation.

Recently, there has been a great interest to study the biological activity of nitric oxide (NO) in photosynthetic organisms after the discovery that NO, a free radical, is an important signaling molecule in plants and animals and rapidly produced by NR enzyme when the cellular level of nitrite increases. The role of NO in the metabolism of land plants and algae is not completely understood. In mammal cells, NO is mainly produced by the conversion of L-arginine to L-citrulline and NO, catalyzed by the enzyme nitric oxide synthase (NOS, EC 1.14.13.39). In plants, NOS activity has been identified, but the enzyme NOS has not been isolated. The proposed additional mechanisms for the production of NO in plants are: (a) nonenzymatically, as a result of chemical reactions between nitrogen oxides and metabolites of plants (Cooney et al. 1994), decomposition of nitrous oxide, or chemical reduction of nitrite at acid pH (Nishimura et al. 1986; Klepper 1991), and (b) enzymatically, produced from nitrite by the nitrate reductase NAD(P)H-dependent enzyme (Klepper 1991; Yamasaki and Sakihama 2000). Most recently, studies have proposed the mitochondria as a source of NO (Lacza et al. 2006) and the exactly involved processes are still unclear. Studies about the influence of NO on NR activity are scarce and the few existing have been done in land plants (Dean and Harper 1988; Desikan et al. 2002; Yamasaki and Sakihama 2000; Rockel et al. 2002; García-Mata and Lamattina 2003; Yamamoto-Katou et al. 2006) and microalgae (Mallick et al. 1999; Sakihama et al. 2002).

This work investigates the changes of in vitro NR activity in the macroalga *G. chilensis* under the addition of compounds interfering on the photosynthetic electron transport and NO balance (example NOS inhibitors, NO scavengers, and NO donors). The understanding of the regulation of NR is a key step for knowledge on the nitrogen metabolism. Besides, the study of the NO role as a fundamental signaling molecule opens leads to better understanding of the growth and stress mechanisms in this economically important red alga.

Material and methods

Algal culture

Tetrasporophytic thalli of *G. chilensis* were grown in sterile seawater enriched with 100 % von Stosch (VS) medium (Edwards 1970) at 10±2 °C, irradiance of 80±5 μmol photons m^{-2} s^{-1}, 32 psu, 12 h photoperiod (light/dark), and continuous air bubbling. The culture medium was replaced weekly. All experiments were performed with algae 24 h pre-enriched with 100 % VS to avoid nutrient deficiency.

Effect on NR activity

The experimental concentrations of DCMU, DBMIB, diphenyleneiodonium (DPI), L-NG-monomethyl arginine citrate (L-NMMA), 2-(4-carboxyphenyl)-4,4,5,5-tetramethylimidazoline-1-oxyl-3-oxide (CPTIO), sodium nitroprusside (SNP), and (Z)-1-{*N*-methyl-*N*-[6-(*N*-methylammoniohexyl)amino]}diazen-1-ium-1,2-diolate (NOC-9) (Table 1) were selected after previous determination of the inhibitory concentrations on NR activity and effective quantum yield of PSII (Φ_{PSII}). For methylene blue, 1*H*-[1,2,4]oxadiazole[4,3-a]quinoxalin-1-one (ODQ), and 8-bromo GMP (8-BrGMP), the concentrations were selected following the literature. Effective quantum yield of PSII was measured by using a pulse modulated chlorophyll fluorometer (model FMS1, Hansatech, England). After establishing the adequate concentration of the compounds above, unbranched tips (2 cm) of *G. chilensis* were treated for 2 h with each compound, added during the

Table 1 Summary of compounds used in this study on *G. chilensis* as metabolic inhibitors or enhancers

Compounds	Description	Selected concentration
DCMU[a]	PSII electron flux inhibitor	1 μM
DBMIB[a]	PSI electron flux inhibitor	8 μM
DPI[a]	NADPH oxidase and NOS inhibitor	16 μM
L-NMMA[b]	NOS inhibitor	1 mM
CPTIO[b]	NO scavenger	100 μM
SNP[b]	NO donor	1 mM
NOC-9[b]	NO donor	2 μM
Methylene blue[c]	Guanyl cyclase inhibitor	10 μM
ODQ[d]	Guanyl cyclase inhibitor	80 μM
8Br-cGMP[a]	Analogous compound of GMP	50 μM

[a] Sigma-Aldrich (Germany)
[b] Alexis Biochemicals (Swiss)
[c] Merck (Germany)
[d] Tocris (Sweden)

©Fungyi Chow / 2021

midday phase, once it is the period of maximal NR activity (Chow et al. 2004). Controls were performed under the same conditions, but without the addition of any of the compounds listed above. Cell extraction and in vitro assay of NR were performed following Chow et al. (2004).

Statistical analysis

All experiments were performed in triplicates and the data were analyzed statistically by one-way ANOVA and an a posteriori Newman–Keuls test with a probability of 95 % ($p<0.05$) (Zar 1999).

Results

For each chemical compound was evaluated the variation of Φ_{PSII} under increasing concentrations to select the adequate concentration that was used for nitrate reductase (NR) activity experiments. Figure 1 shows the decrease of Φ_{PSII} under increasing concentrations of DCMU (PSII electron flux inhibitor in the PQ pool; Fig. 1a), DBMIB (PQ oxidation inhibitor by the PSI; Fig. 1b), and DPI (NADPH oxidase and NOS inhibitor; Fig. 1c). In contrast, no effect on Φ_{PSII} was observed when L-NMMA, CPTIO, SNP, or NOC-9 was added (Fig. 2) and the experimental concentrations were based on literature and considering the inhibitory levels for NO-related processes. The experimental concentrations of methylene blue, ODQ, and 8-BrGMP were completely based on literature. The selected concentrations for further experiments are listed in Table 1.

The effect of PSII and PSI electron transport chains on NR activity was studied adding DCMU or DBMIB as an indirect estimative of the effect of photosynthesis on the nitrate assimilation metabolism. Nitrate reductase activity was significantly reduced when DCMU ($p=0.022$; ca. 51 % inhibition) or DBMIB ($p=0.010$; ca. 61 % inhibition; Fig. 3) was used. DPI, used to estimate the effect on NR activity of NADPH as reduction power, had no effect on the enzymatic activity (Fig. 3).

The addition of L-NMMA, a NOS inhibitor, did not display significant effect on NR activity (Fig. 3). However, the NO scavenger CPTIO and NO donor SNP reduced significantly the relative NR activity ($p=0.035$; ca. 33 % and $p=0.035$; ca. 99.98 %, respectively; Fig. 3). Another NO donor, NOC-9, did not evidence any difference.

Methylene blue, a guanyl cyclase inhibitor, and 8Br-cGMP, an analogous compound of the secondary messenger cGMP, increased significantly the enzymatic activity ($p=0.018$ and 52 % and $p<0.005$ and 141 %, respectively), whereas ODQ, a guanyl cyclase inhibitor, did not exhibit statistical variation (Fig. 3).

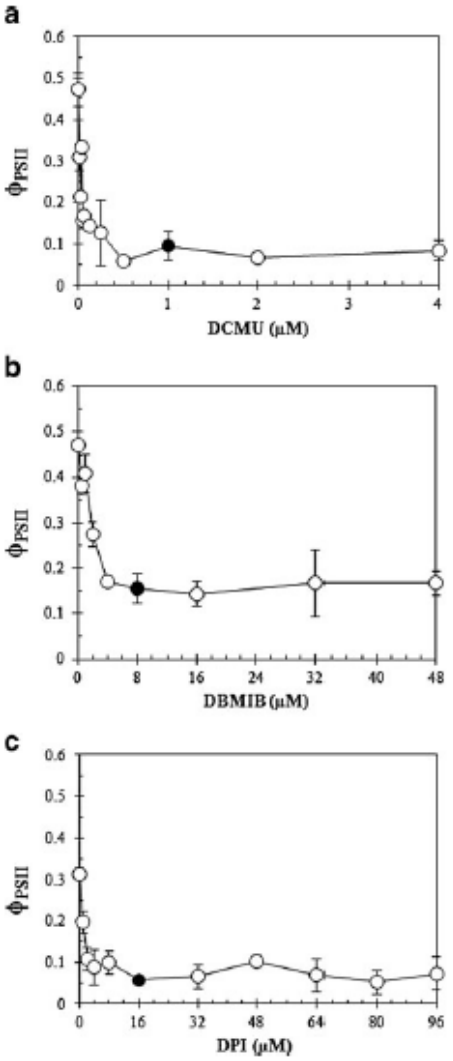

Fig. 1 Variation of effective quantum yield of PSII (Φ_{PSII}) of *G. chilensis* exposed 2 h to different concentrations of **a** DCMU, **b** DBMIB, and **c** DPI. *Black circle* represents the selected concentration for further experiments. Means±SD ($n=3$)

Discussion

Studies on the interaction of carbon and nitrogen metabolisms in plants and macroalgae are extensive; however, studies on NR activity related to NO balance are scarce in photosynthetic organisms and, until this date, absent in macroalgae. The nitrogen metabolism is dependent on photosynthesis, once the organic carbon skeleton (ketoacid), energy (ATP), and reducing agent (NADH) are required for the reduction of nitrate. In plant cells, an increase of nitrogen assimilation rate requests an increase of carbon flux through the respiratory pathways (Bassham et al. 1981;

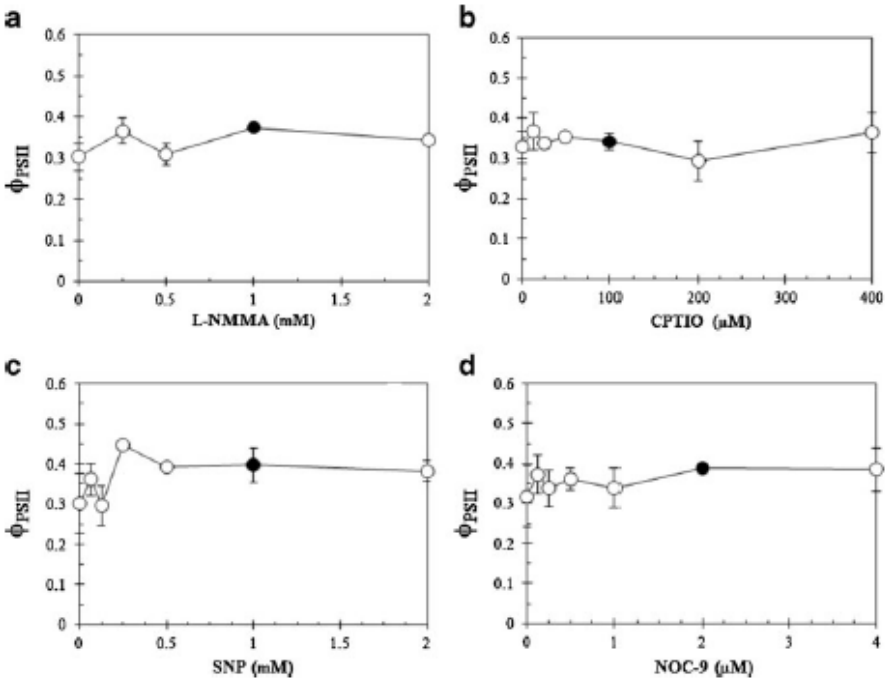

Fig. 2 Variation of effective quantum yield of PSII (Φ_{PSII}) of *G. chilensis* exposed 2 h to different concentrations of **a** L-NMMA, **b** CPTIO, **c** SNP, and **d** NOC-9. *Black circle* represents the selected concentration for further experiments. Means±SD (n=3)

Syrett 1981; Turpin 1991). Therefore, the integration of these important metabolic processes must have correlated regulatory mechanisms (Givan et al. 1988; Lea and Blackwell 1992; Huppe and Turpin 1994). This study is the first reporting the variation of NR activity under different compounds that affect electron transport chains of PSII and PSI and NO balance based on the use of NO scavenger, NO donors, NOS inhibitors, and secondary messengers.

The photosynthetic efficiency measured as Φ_{PSII} and NR activity of *G. chilensis* were inhibited when DCMU or DBMIB was added. Both inhibitors affect the electron transport chain of PSII and PSI, respectively. DCMU dislocates the PQ from the binding site of QB, blocking effectively the flux of electrons from PSII to PSI, inhibiting the photosynthesis (Moreland 1980; Sandmann and Böger1986; Mazur and Falco 1989; Van Rensen 1989). On the other hand, DBMIB inhibits the electron flux immediately after the QB, interfering with PQ oxidation and favoring cyclic photophosphorylation and affecting the photosynthesis. Treatments with DCMU or DBMIB create similar condition that darkness because photosynthetic reductant/ATP supplies are disturbed at different electron transport levels. Nitrate reduction occurs predominantly in photosynthetic tissues and indirectly depends on light for generating reducing power, ATP, and carbon supply via photosynthetic CO_2 fixation (Li and Oaks 1994; Provan and Lillo 1999; Basra et al. 2002). Thus, the production of photosynthetic reducing power and ATP is altered and also the carbon fixation and carbon skeleton availability to incorporating nitrogen molecules for nitrate assimilation. On the other hand, in *G. chilensis* and other macroalgae, in vitro NR activity is regulated by NADH concentration and the interruption of electron transport flux along the chain could indirectly affect the enzymatic activity. Theoretically, the amount of produced NADH in the cytoplasm (e.g., by pentose phosphate pathway) must be enough for in vivo enzymatic requirements and, therefore, the fluctuation of NADH production in the chloroplast would not affect NR activity. To verify this hypothesis, the effect of DPI, an inhibitor of NADPH

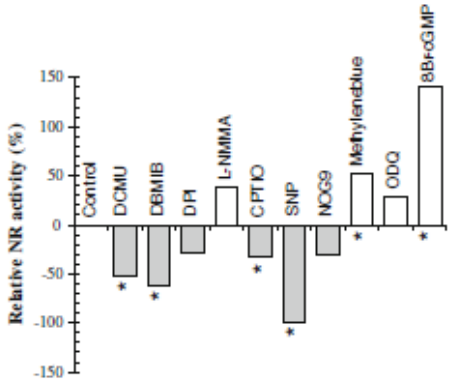

Fig. 3 Effect in percentage of 1 μM DCMU, 8 μM DBMIB, 16 μM DPI, 1 mM L-NMMA, 100 μM CPTIO, 1 mM SNP, 2 μM NOC-9, 10 μM methylene blue, 80 μM ODQ, and 50 μM 8Br-cGMP on NR activity of *G. chilensis*. The values were calculated as average percentage of increasing or decreasing effect considering the control as zero (n=3). *Asterisks* represent significant difference

©Fungyi Chow / 2021

oxidase, was evaluated. The addition of 16 μM DPI inhibited significantly Φ_{PSII} but it did not affect NR activity. These results indicate that regulation of NR activity is directly associated to the interruption of electron transport among the PSII and PSI, wherein the reduction of Φ_{PSII} is positively related to the decline of in vitro NR activity.

Moreover, the addition of DCMU and DBMIB as external drugs may induce production of free radical by the electron sequestration from the photosynthetic transport chain. Beligni and Lamattina (2001) suggested that NO in plants can act as a defense mechanism in cytotoxic processes related to the production of reactive oxygen species. This explains the participation of NO on hypersensibility responses (Van Camp et al. 1998), regulatory expression of defense genes (Delledonne et al. 1998), and increasing chlorophyll fluorescence (Leshesm 1996). Recent discoveries have related NR regulation to NO (Yamasaki et al. 1999; Yamasaki and Sakihama 2000; Desikan et al. 2002; Rockel et al. 2002; Meyer et al. 2005; Crawford 2006; Jansson et al. 2008). In addition, the production of NO by the enzyme NR has been demonstrated in leguminous plants (Dean and Harper 1988; Klepper 1990) and corn (Yamasaki et al. 1999). In both cases, the NO production was related with a high concentration of nitrite in the cell.

Increasing concentrations of L-NMMA, CPTIO, SNP, and NOC-9 did not show significant effect on Φ_{PSII}. Nevertheless, NR activity of *G. chilensis* was significantly decreased under the effect of NO scavenger CPTIO and NO donor SNP. In mammals and plants, a constant production of NO under normal environmental conditions has been demonstrated and it is necessary to sustain the endogenous metabolic homeostasis. The same seems to be true for *G. chilensis* once the unbalance of NO levels decrease or increase by the addition of NO scavenger or NO donor inhibited significant NR activity. The inhibition of NR from *G. chilensis* by adding CPTIO was also observed on Chinese cabbage pakchoi by Du et al. (2008) and on tomato roots fed with low concentration of nitrate (500 μM) by Jin et al. (2009), but opposite response was observed with 5,000 μM nitrate. This inhibition of NR activity can be explained by the requirement of basal endogenous NO level to stimulate NR activity. When NO scavenger is added, the decrease of this basal NO level affects the normal function of enzyme activity, resulting in reduction on NR activity. The regulatory mechanism and involved processes are still unknown for higher plants.

The inhibitory effect of NO on NR activity, under the supply of a NO donor, may be a response of *G. chilensis* to alleviate NO toxicity by reducing NO synthesis by NR. These results coincide with the observations by Jin et al. (2009) on tomato roots by supplying SNP and NONOate and Rosales et al. (2011) on wheat leaves using SNP or GSNO. Notwithstanding, SNP is commonly used as NO donor at the same concentration used in this study, and compounds other than NO, such as cyanide, can be generated from SNP addition, which might affect the biological activity. The higher inhibition of NR activity under the NO donor SNP compared to the NO donor NOC-9 could reflect the additional toxic effect of cyanide on NR activity.

The regulatory mechanisms exerted by supplying NO donors or scavengers on NR activity in higher plants and macroalgae and the physiological processes involved remain mostly unknown, and further studies are necessary to elucidate them.

In mammals, signals that involve NO are typically denominated as cGMP dependent or cGMP independent (McDonald and Murad 1995). cGMP is a secondary signaling molecule that regulates directly many metabolic processes by enzymatic cascade signals via phosphorylation and desphosphorylation. The regulatory relationship between NO, cGMP, and the enzyme that catalyzes cGMP has been observed in plants of tobacco by Durner et al. (1998). For *G. chilensis*, the addition of 8Br-cGMP, an analogous of cGMP, increased significantly the NR activity, possibly through processes related to phosphorylation and desphosphorylation mechanisms of dephosphorylated active NR. Our data point out that the NR activity of *G. chilensis* is posttranslational regulated by activation or inactivation of the synthetized NR protein probably mediated by cGMP.

This study is the first to describe the relationship of NR activity regulation and photosynthetic electron transport chain, NO balance, and cGMP for a macroalga. This complex regulation of NR activity is not surprising because nitrite and ammonium, the product of nitrate reduction, are toxic for the cells; therefore, nitrogen and carbon metabolism must be connected to guarantee nitrite and ammonium incorporation into carbon skeletons to avoid its toxicity. For *G. chilensis*, NO was shown to be an important signaling molecule controlling NR activity through cGMP that participates on NR regulation by phosphorylation and desphosphorylation as secondary messenger.

The role of NO as an important signaling molecule for many biological processes in mammals and plants has led to several hypotheses for future studies. These results corroborate the changes of NR activity in *G. chilensis* under the effect of drugs that alter the electron transport chain and NO balance. These data indicate the importance of these metabolic elements in the regulation of nitrogen assimilatory metabolism. Therefore, the data presented in this study help to elucidate the influence on some basic physiological processes in macroalgae, such as photosynthesis and nitrate assimilation, linked to NO production.

Acknowledgments This investigation was supported by the National Council for Research and Development (CNPq, Brazil), State of São Paulo Research Foundation (FAPESP, Brazil), and Swedish

Foundation for International Cooperation in Research and Higher Education (STINT). The authors thank Stanislaw Karpinski for laboratorial support with photosynthesis analysis.

References

Basra A, Dhawan AK, Goyal SS (2002) DCMU inhibits in vivo nitrate reduction in illuminated barley (C_3) leaves but not in maize (C_4): a new mechanism for the role of light? Planta 215:855–861

Bassham JA, Larsen PO, Cornwell AL (1981) Relationships between nitrogen metabolism and photosynthesis. In: Bewley JD (ed) Nitrogen and carbon metabolism. Development in plant and soil science. Dr. W. Junk, London, pp 135–163

Beligni MV, Lamattina L (2001) Nitric oxide in plants: the history is just beginning. Plant Cell Environ 24:267–278

Buschmann AH, Westermeier R, Retamales CA (1995) Cultivation of *Gracilaria* on the sea-bottom in southern Chile: a review. J Appl Phycol 7:291–301

Chow F, Oliveira MC, Pédersem M (2004) In vitro assay and light regulation of nitrate reductase in red alga *Gracilaria chilensis*. J Plant Physiol 161:769–776

Cooney RV, Harwood PJ, Custer LJ, Franke AA (1994) Light-mediated conversion of nitrogen-dioxide to nitric-oxide by carotenoids. Environ Health Persp 102:460–462

Crawford NM (2006) Mechanisms for nitric oxide synthesis in plants. J Exp Bot 57:471–478

Dean JV, Harper JE (1988) The conversion of nitrite to nitrogen oxide(s) by the constitutive NAD(P)H-nitrate reductase enzyme from soybean. Plant Physiol 88:389–395

Delledonne M, Xia YJ, Dixon RA, Lamb C (1998) Nitric oxide functions as a signal in plant disease resistance. Nature 394:585–588

Desikan R, Cheung M-K, Bright J, Henson D, Hancock JT, Neill SJ (2002) ABA, hydrogen peroxide and nitric oxide signalling in stomatal guard cells. J Exp Bot 55:205–212

Du S, Zhang Y, Lin X, Wang Y, Tang C (2008) Regulation of nitrate reductase by nitric oxide in Chinese cabbage pakchoi (*Brassica chinensis* L.). Plant Cell Environ 31:195–204

Durner J, Wendehenne D, Klessig DF (1998) Defense gene induction in tobacco by nitric oxide, cyclic GMP, and cyclic ADP-ribose. Proc Natl Acad Sci USA 95:10328–10333

Edwards P (1970) Illustrated guide to the seaweeds and sea grasses in the vicinity of Porto Aransas, Texas. Contr Mar Sci Austin 15:1–228

García-Mata C, Lamattina L (2003) Abscisic acid, nitric oxide and stomatal closure. Is nitrate reductase one of the missing links? Trends Plant Sci 8:20–26

Givan CV, Joy KW, Kleczkoski LA (1988) A decade of photorespiratory nitrogen cycling. Trends Biochem Sci 13:433–437

Huppe HC, Turpin DH (1994) Integration of carbon and nitrogen metabolism on plant and algal cells. Annu Rev Plant Physiol Mol Biol 45:577–607

Jansson EÅ, Huang L, Malkey R, Govoni M, Nihlén C, Olsson A, Stensdotter M, Petersson J, Holm L, Weitzberg E, Lundberg JO (2008) A mammalian functional nitrate reductase that regulates nitrite and nitric oxide homeostasis. Nat Chem Biol 4:411–417

Jin CW, Du ST, Zhang YS, Lin XY, Tang CX (2009) Differential regulatory role of nitric oxide in mediating nitrate reductase activity in roots of tomato (*Solanum lycocarpum*). Ann Bot 104:9–17

Kleczkowski LA (1994) Inhibitors of photosynthetic enzymes/carriers and metabolism. Annu Rev Plant Physiol Plant Mol Biol 45:339–367

Klepper L (1990) Comparison between NOx evolution mechanisms of wild-type and NR1 mutant soybean leaves. Plant Physiol 93:26–32

Klepper L (1991) NOx evolution by soybean leaves treated with salicylic-acid and selected derivates. Pestic Biochem Phys 39:43–48

Lacza Z, Pankotai E, Csordás A, Gero D, Kiss L, Horváth EM, Kollai M, Busija DW, Szabó C (2006) Mitochondrial NO and reactive nitrogen species production: does mtNOS exist? Nitric Oxide 14:162–168

Lea P, Blackwell RD (1992) The role of amino acid metabolism in photosynthesis. In: Singh BK, Shannon JC, Flores H (eds) Biosynthesis and molecular regulation of amino acids in plants. American Society of Plant Physiologists, Rockville, pp 98–110

Leshem YY (1996) Nitric oxide in biological systems. Plant Growth Regul 18:155–159

Li X, Oaks A (1994) Induction and turnover of nitrate reductase in *Zea mays*. Plant Physiol 106:1145–1149

Mallick N, Rai LC, Mohn FH, Soeder CJ (1999) Studies on nitric oxide (NO) formation by the green alga *Scenedesmus obliquus* and the diazotrophic cyanobacterium *Anabena doliolum*. Chemosphere 39:1601–1610

Mazur BJ, Falco SC (1989) The development of herbicide resistant crops. Annu Rev Plant Physiol Plant Mol Biol 40:441–470

McDonald LJ, Murad F (1995) Nitric oxide and cGMP signaling. Adv Pharmacol 34:263–276

Meyer C, Lea US, Provan F, Kaiser WM, Lillo C (2005) Is nitrate reductase a major player in the plant NO (nitric oxide) game? Photosynth Res 83:181–189

Moreland DE (1980) Mechanisms of action of herbicides. Annu Rev Plant Physiol 31:597–638

Nishimura H, Hayamizu T, Yanagisawa Y (1986) Reduction of NO_2 to NO by rush and other plants. Environ Sci Technol 20:413–416

Provan F, Lillo C (1999) Photosynthetic post-translational activation of nitrate reductase. J Plant Physiol 154:605–609

Rockel P, Strube F, Rockel A, Wildt J, Kaiser WM (2002) Regulation of nitric oxide (NO) production by plant nitrate reductase in vivo and in vitro. J Exp Bot 53:103–110

Rosales EP, Iannone MF, Groppa MD, Benavides MP (2011) Nitric oxide inhibits nitrate reductase activity in wheat leaves. Plant Physiol Biochem 49:124–130

Sakihama Y, Nakamura S, Yamasaki H (2002) Nitric oxide production mediated by nitrate reductase in the green alga *Chlamydomonas reinhardtii*: an alternative NO production pathway in photosynthetic organisms. Plant Cell Physiol 43:290–297

Sandmann G, Böger P (1986) Sites of herbicide inhibition at the photosynthetic apparatus. In: Stachelin LA, Arntzen CJ (eds) Encyclopedia of plant physiology, vol 19. Springer, Berlin, pp 596–602

Syrett PJ (1981) Nitrogen metabolism of microalgae. In: Platt T (ed) Physiological bases of phytoplankton ecology. Can Bull Fish Aquat Sci 210: 182–210

Turpin DH (1991) Effects of inorganic N availability on algal photosynthesis and carbon metabolism. J Phycol 27:14–20

Van Camp W, Van Montagu M, Inze D (1998) H_2O_2 and NO: redox signals in disease resistance. Trends Plant Sci 3:330–334

Van Rensen JJS (1989) Herbicides interacting with photosystem II. In: Dodge AD (ed) Herbicides and plant metabolism. Cambridge University Press, Cambridge, pp 21–36

Yamamoto-Katou A, Katou S, Yoshioka H, Doke N, Kawakita K (2006) Nitrate reductase is responsible for elicitin-induced nitric oxide production in *Nicotiana benthamiana*. Plant Cell Physiol 47:726–735

Yamasaki H, Sakihama Y (2000) Simultaneous production of nitric oxide and peroxynitrite by plant nitrate reductase: in vivo evidence for the NR-dependent formation of active nitrogen species. FEBS Lett 468:89–92

Yamasaki H, Sakihama Y, Takahashi S (1999) An alternative pathway for nitric oxide production in plants: new features of an old enzyme. Trends Plant Sci 4:128–129

Zar JH (1999) Biostatistical analysis, 4th edn. Prentice-Hall, Englewood Cliffs

ANEXO 10

5

Nitrate Assimilation: The Role of *In Vitro* Nitrate Reductase Assay as Nutritional Predictor

Fungyi Chow
University of Sao Paulo, Department of Botany, Institute of Bioscience
São Paulo, SP
Brazil

1. Introduction

Macroalgae or macrophytes are a heterogeneous assemblage of macroscopic eukaryotes belonging to various evolutionary lineages, which live predominantly in aquatic habitats. They have undifferentiated vegetative bodies organized in pseudoparanchymatous and parenchymatous bodies. As with higher plants, marine macroalgae or seaweeds are photosynthetic species that, by harvesting sunlight energy, convert carbon dioxide in oxygen to produce organic compounds, especially carbohydrates. In addition, they require mineral nutrients, essential for growth, development and reproduction, which are incorporated into carbon skeletons.

In natural aquatic ecosystems, 95% of the nitrogen which occurs as dissolved dinitrogen gas (N_2), is not directly accessible to most photosynthetic-oxygen organisms. Dissolved inorganic nitrogen (DIN) includes the ions, ammonium (NH_4^+), nitrite (NO_2^-), and nitrate (NO_3^-). In seawater, and under natural conditions, about 3,5% is NO_3^- (*ca.* 0.35 mg $NO_3^-.L^{-1}$), which, near to coastal zones, appears in abundance as a product of upwelling or pollution, whence, their importance as the predominant cause of local eutrophication.

Thus, nitrate constitutes the prevailing available nitrogen source for macroalgae in the marine environment. The available DIN may be supplemented by dissolved organic nitrogen (DON), this including urea and amino acids. For all eukaryotic photoautotrophs, NH_4^+, NO_2^-, and NO_3^- are the only directly assimilated sources.

Nitrogen, which is rapidly taken up, is a key element in several compounds present in the cells. It is used to build up amino acids, proteins, nucleoside phosphates, nucleic acids, and other organic N-containing macromolecules. The availability of nutrients, especially nitrogen, in marine habitats is one of the main regulating factors that limit growth, morphology, development, reproduction, distribution, and biochemical composition in seaweeds. The importance of nitrogen for biological life is evident, in that only oxygen, carbon, and hydrogen are more abundant in the cells of photosynthetic organisms.

Macroalgae and photoautotrophic organisms have considerable intracellular capacity for storing nitrogen as soluble nitrogen and organic molecules, whereby growth and development can be regulated and limited according to nitrogen uptake. This characteristic for storing and assimilating nutrients, when available and at high concentrations, besides

facilitating their use under external, restrictive conditions, provides certain species with ecological advantages for persistence and prolife during limiting stress periods.

Seasonal nutrient limitation in macroalgal growth is well known (Lobban & Harrison, 1994). The importance of nitrogen for the growth-cycle is related to life-strategy. In perennial species, nutrient availability is a determinant factor that plays an important role in the seasonal reproductive life-cycle (Kain, 1989). In annual species, nitrogen, when available, is uptake and stored inside the cells, whence its rapid conversion into new biomass.

During the past decades, substantial efforts have been made to understand the biochemistry, molecular biology and regulation of nitrate reductase (NR) in higher plants, to so further ecophysiological information and applied botany. The basic-action mechanisms and importance of NR in seaweeds are no different from higher plants. Notwithstanding, the amount of knowledge is still superficial and phycological studies scarce.

Based on higher plants and microalgae, the purpose is to briefly point out the role of NR in nitrogen metabolism, with a focus on macroalga research, and highlight the importance of *in vitro* NR assay optimization and its value as a physiological tool.

2. Overview of nitrate assimilation

Inorganic nitrogen availability plays a critical role in the physiology of marine macroalgae and the productivity of complete ecosystems (Lapointe & Duke, 1984). Nitrogen depletion has been shown to increase photoinhibitory responses in the photosynthesis of marine organisms, including macroalgae (Korbee-Peinado et al., 2004; Huovinen et al., 2006). On the other hand, photosynthetic pigments, through generally being positively correlated with nitrogen availability, rapidly respond to varying nitrogen levels (Davison et al., 2007). For example, phycobiliproteins, reported as nitrogen-storage compounds in N-rich conditions, act as nitrogen sources under N-limiting conditions (Lobban et al., 1985).

Much of what is known on nitrogen metabolism is based on studies with microalgae; the number with macroalgae is still few in comparison.

As nitrogen uptake by macroalgae are usually studied by monitoring the disappearance of the nutrient from the culture medium and is influenced by irradiance, temperature, water motion, desiccation, and age.

Macroalgae have either the plasticity or preference to uptake several forms of nitrogen. Hanisak (1983) noted that the uptake rate of ammonium generally exceeds that of nitrate. Chow et al. (2001) registered the same trend for *Gracilaria chilensis*, with total uptake of only ammonium, when present together with nitrate and nitrite. However, very high concentrations of ammonium (> 30 -50 μM) can saturate nitrate transport, thereby inducing toxification by ammonium. As ammonium can be used directly to synthesize amino acids, and nitrate stored inside vacuoles, the energetic cost of ammonium assimilation is lower than that of nitrate.

Nitrate uptake normally involves saturating kinetics (DeBoer, 1981). As greater concentrations of intracellular nitrate than that of the surrounding seawater constitute a negative gradient for transport, active transport can be considered as a primary process. Some authors have proposed that the NR plasma membrane acts as protein transporter to within the cell.

Considering the relative abundance of environmental nitrate in seawater, the nitrogen metabolism is usually commanded by nitrate assimilation fitness. Nitrate (NO_3^-) is taken up

by the cells and translocated across the plasmalemma by energy-dependent processes. Once inside the cells, any excess can be stored within vacuoles, while a fraction is being metabolized in the cytoplasm by reduction to nitrite, via the enzyme nitrate reductase (NR), and using NAD(P)H as electron donor. In turn nitrite (NO_2^-) is transported to chloroplasts and reduced to ammonium, prior to assimilation into organic compounds by enzyme nitrite reductase (NiR), by means of reduced ferredoxin (Fd_{red}) as electron source. Thus, the nitrogen assimilation pathway is a two-step process, first with NO_3^- reduction to NO_2^- (1) and then to ammonium (NH_4^+) (2) as described below:

Nitrate reductase (NR)

$$NO_3^- + NAD(P)H + 2e^- + H^+ \rightarrow NO_2^- + NAD(P)^+ + H_2O \quad (1)$$

Nitrite reductase (NiR)

$$NO_2^- + 6Fd_{red} + 6e^- + 8H^+ \rightarrow NH_4^+ + 6Fd_{ox} + 2\,H_2O \quad (2)$$

Nitrite and ammonium ions can not be accumulating inside cells, as they are cytotoxic through producing pH change and inducing reactive nitrogen species (RNS) and oxidative damage. Consequently, their incorporation into organic compounds must be relatively fast, in order to prevent accumulation and toxicity. In the case of photosynthetic organisms, fungi, and bacteria present a variety of mechanisms to regulate and control the expression of those enzymatic activities involved in nitrogen assimilatory pathways.

The assimilation of ammonia-N into carbon compounds (amino acids) primarily takes place through the sequential actions of glutamine synthetase (GS) and glutamine 2-oxoglutarate aminotransferase (GOGAT), inside chloroplasts, where both are localized, although isozymes of both may also be found in cytosol. Ammonium assimilation by GS requires glutamate (Glu) as substrate and ATP input to form glutamine (Gln) (3).

Glutamine synthetase (GS)

$$NH_4^+ + \text{glutamate (Glu)} + ATP \rightarrow \text{glutamine (Gln)} + ADP + Pi \quad (3)$$

The amino-N of glutamine, subsequently transferred to 2-oxoglutarate (2-OXG), is reduced by GOGAT to form two molecules of glutamate (4).

Glutamine 2-oxoglutarate aminotransferase (GOGAT)

$$\text{2-oxoglutarate} + \text{glutamine (Gln)} + NADPH \rightarrow 2\,[\text{glutamate}]\,(Glu) + NADP^+ \quad (4)$$

The production of glutamate can be through two pathways. The first involves the reductive amination of α-ketoglutarate catalyzed by the enzyme glutamate dehydrogenase (GDH), which is found in chloroplasts and mitochondria. In the latter, α-ketoglutarate is normally continually produced by the Krebs cycle.

Independent of the location of GS and GOGAT, glutamate is exported from chloroplasts to cytosols, where transamination reactions can proceed, thereby facilitating the synthesis of other amino acids.

The control of the nitrate assimilatory rate is attributed to NR action, as this is the first enzyme in the specific pathway. Consequently, it is of increasing interest to study its

molecular and catalytic properties, as well as the physiological responses to environmental stressing conditions and intracellular factors. Nitrate reductase activity has been proposed as an index of the rate of nitrate incorporation, with the additional inference that nitrate reduction is a rate limiting process for nitrogen assimilation, since any reduction in enzymatic activity results in a relative drop in nitrogen assimilation.

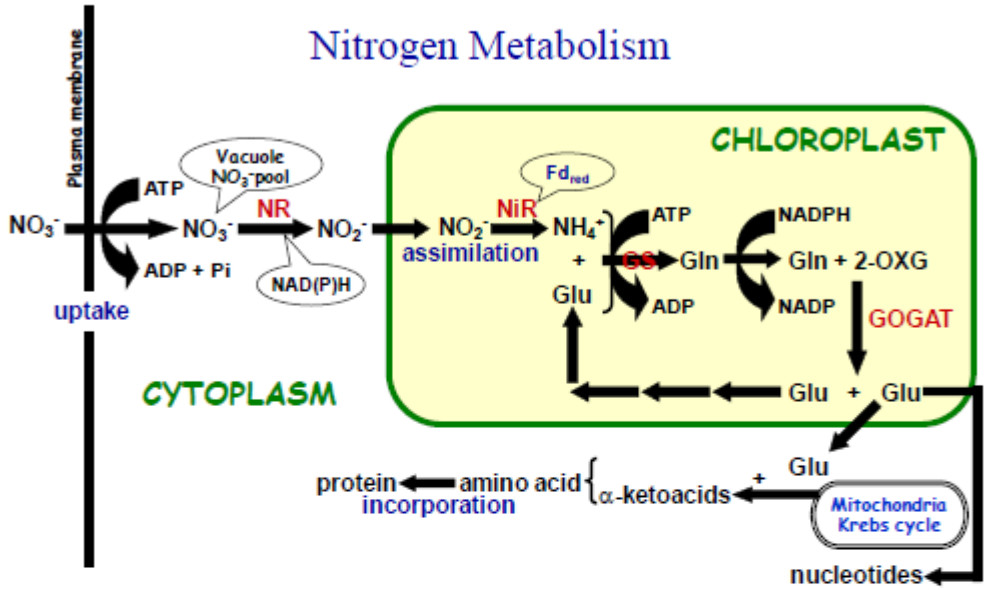

Fig. 1. General brief of nitrate assimilation pathway. Nitrate (NO_3^-) is actively transported from the external medium across the plasma membrane into the cytoplasm. It can be stored into vacuoles or reduced to incorporating in carbon skeletons. Nitrate is reduced to nitrite (NO_2^-) in the cytoplasm by nitrate reductase (NR) that uses NAD(P)H. Nitrite is transported inside the chloroplast and reduced to ammonium (NH_4^+) by nitrite reductase (NiR) that uses reduced ferredoxin (Fd_{red}). Ammonium is incorporated into glutamate (Glu) to form glutamine (Gln) via the action of glutamine synthetase (GS). The amino-N of Gln is then transferred to 2-oxoglutarate (2-OXG) via the action of glutamine 2-oxoglutarate aminotransferase (GOGAT). This reaction produces two molecules of Glu, one of them reenters to the assimilation pathway as substrate for GS and the second molecule of Glu is exported to the cytoplasm and will participate of transamination reactions with α-ketoacids to produces other amino acids and proteins (modified from Falkowski & Raven, 1997).

3. Interaction between nitrate assimilation and carbon metabolism

Nitrate assimilation is intrinsically dependent on the organic carbon substrates, reductants, and ATPs that are supplied for both processes photosynthesis and respiratory processes (Turpin, 1991). When nitrogen is limited, or photosynthesis and respiration are negatively affected, this dependency becomes multifactorial, whereupon compensatory mechanisms or regulation must be activated.

It is clearly evident that nitrogen metabolism in macroalgae is closely linked to photosynthetic carbon metabolism (Vergara et al., 1998). Nitrate reductase activity presents maximal enzymatic rates during the diurnal phase, and minimal during dark phase, with a narrow relationship of maximal and minimal photosynthetic rates. These responses indicate regulatory activation of both processes by light. The intracellular toxic conditions of nitrite and ammonium make the urgent incorporation of both into the carbon skeleton essential, to so avoid toxicity.

Carbon molecules and reductant sources proceeding from photosynthesis, is an indication of the existence of related regulatory mechanisms between both processes. Carbon and nitrogen metabolic pathways consume large amounts of photosynthetic carbon and energy sources. Both metabolic forms are connected, either by the organic carbon and energy that are directly supplied for photosynthetic electron transport and fixated CO_2, or by the respiration of fixed carbon, via glycolysis by the Krebs cycle, and the electron transport chain of mitochondria. Therefore, the integration of these important metabolic processes must have integrated regulatory mechanisms.

Nitrogen limitation affects photosynthetic processes. Under N-limiting conditions, there is a concomitant decrease in PSII photochemical efficiency, as a consequence of the dissipation of absorbed excitation energy in the center of pigments. Depleted photosynthetic efficiency appears to occur through a drop in the number of functional PSII reaction centers relative to the antennae system (Falkowski, 1992). On the other hand, the reduction in photosynthetic energy conversion under N-limiting conditions appears to affect amino acid biosynthetic processes. Nitrogen limitation also affects the respiration rate. The molecular basis of nitrogen limitation and respiratory rate alteration is unclear, but it appears to be related to the demand for carbon skeletons and ATP, two of the major products of respiratory pathways. Thus, the depletion of nitrogen creates a chain reaction that decompensates energy metabolism and amino acid biosynthesis, thereby affecting photosynthesis, respiration and growth.

4. Nitrate reductase in macroalgae

Nitrate reductase, a relatively large molecule, is usually composed of two or four subunits, each of which with approximately 100 kDa. Nakamura & Ikawa (1993) reported these subunits in *Porphyra yezoensis* at close to 100 kDa. The four in *Gracilaria tenuistipitata* var. *liui* (Lopes et al., 2002), were also of the same size, as were the possibly two in *Kappaphycus alvarezii* (Granbom et al., 2007).

Three assimilatory NR forms are recognized in eukaryotes: (a) EC 1.6.6.1 NADH-specific and (b) EC 1.6.6.2 NADP/NADPH, both occurring in eukaryotic algae and higher plants, and (c) EC 1.6.6.3 NADPH-specific.

The enzyme is preferentially present in the cytoplasm, although there is growing evidence of NR associated to chloroplast membranes (Solomonson & Barber, 1990) and plasmalemma (Tischner et al., 1989; Fernandez-Lopez et al., 1996).

Nitrate reductase becomes interesting through its usefulness as a model for prospecting multi-component interaction mechanisms related to redox enzymes. Nitrate reductase is one of the few inducible/repressible enzymatic systems reasonably well-characterized in photoautotrophs, especially in higher plants and microalgae, thus making it a fantastic biological model for physiological studies. On the other hand, it is of concern to use NR as an ecophysiological parameter for predicting nutritional rates of nitrate assimilation and

growth. Furthermore, as NR-protein characteristics differ among algal groups, this diversity may be of relevance in revealing evolutionary adaptation patterns (Zhou & Kleinhofs, 1996; Howartha & Baumb, 2002; Stolz & Basu, 2002).

Marine macrophytes inhabiting intertidal coastal regions are exposed to extreme fluctuations in physicochemical parameters, midday increased irradiance levels, UV radiation (UVR), nitrogen depletion, desiccation, high-temperature stress, etc. (Lobban et al., 1985). Individually or together these stressing conditions result in drastic physiological responses and acclimation. Thus, comprehension of macroalgal responses to daily and seasonal fluctuations in these abiotic factors is critical for a better understanding of the regulation of nitrogen metabolism.

Nitrate reductase-activity assaying has been used for indicating algal capacity in using nitrate and the internal nutritional index. A newer approach is to determine the protein at the molecular level by studies of gene NR-mRNA expression.

The use of NR in an ecological context is particularly relevant for marine environments where nitrogen is often limiting, thereby providing relevant information regarding the physiological nitrogen status of organisms (Hernández et al., 1993).

Nitrate reductase is considered as a key enzyme in nitrogen metabolism, through being, not only the rate-limiting enzyme in inorganic nitrogen assimilation, but also the major regulatory step in nitrogen metabolism (Crawford, 1995; Berges, 1997; Davison & Stewart, 1984; Lartigue & Sherman, 2005; Young et al., 2009). Changes in NR activity, both in the field or in laboratory, have been examined in very few macroalgae.

Nitrate reductase expression is a complex process regulated by various factors, such as levels of nitrate, CO2, light, carbon skeletons and nitrogen metabolites (Crawford, 1995, Lopes et al., 2002). Furthermore, it is highly regulated in multiple steps, transcriptionally, post-transcriptionally, translationally and post-translationally. These regulatory mechanisms can act individually or synergically, and are correlated to short and long-term NR response. Thus, NR activity can be modified rapidly in response to nitrate availability and other controlling factors.

This intricate control can be shown experimentally by adding nitrate to the medium. In *Gracilaria chilensis*, NR activity was thus rapidly stimulated within a few minutes (Chow et al., 2007; Chow & Oliveira, 2008), probably by post-translational NR-protein regulation. Lartigue & Sherman (2005) observed the same trend in *Enteromorpha* sp. A like inducing response, under the same conditions, has also been observed in other macroalgae (Gao, Smith & Alberte 1995; Lartigue & Sherman, 2005; Young et al., 2007; Martins et al., 2009; Cabello-Pasini et al., 2011).

Nitrate reductase activity in Arctic species appears to be directly enhanced by nitrate addition, with relatively little feedback from the N-status of the cell (Gordillo et al., 2006). Communities of Laminariales species apparently possess a high degree of resilience to disruption in natural nutrient-availability patterns.

Inactivation of NR activity and degradation of NR-protein have been observed in microalgae, macroalgae and higher plants undergoing nitrate deficiency or other forms of reduced nitrogen (*e.g.* ammonium and urea) (Weidner & Kiefer, 1981; Vergara et al., 1998; Solomonson & Barber, 1990; Balandin & Aparicio, 1992; Crawford &Arst, 1993; Berges et al., 1995; Vergara et al., 1998; Campbell, 1999; Gao et al., 2000; Chow & Oliveira, 2007; Nicodemus et al., 2008). The NR-inhibiting action mechanism is unknown, although it is thought to occur via feedback-regulation of ammonium assimilation by metabolites, *e.g.* glutamine (Flynn 1991, Vergara et al., 1998), or indirectly by inhibition of nitrate-uptake (Collos, 1989).

Synthesis of the NR protein is also regulated by its substrate with a half-life of a few hours. The induction of NR activity is preceded by an increase in NR mRNA, which is activated in a question of hours (Granbom et al., 2007).

Light is a regulatory factor of nitrogen metabolism. Light provides the energy to produce/reduce the power and ATP utilized in nitrate transport, nitrate and nitrite reduction and ammonium fixation into amino acids. Furthermore, light increases the production of carbon skeletons essential for nitrogen assimilation. Additionally, light may play a signaling role in controlling the activity-level and NR-protein synthesis.

As NR-protein degradation normally takes a few hours, near to the interphase light:dark cycle, NR is rapidly regulated by phosphorylation and dephosphorylation mechanisms. Transient induction of NR activity in *G. chilensis* by light pulse, during the dark phase, was inhibited by the addition of calyculin A (Chow et al., 2008), thereby inferring this rapid NR regulation, as already reported in higher plants (Kaiser & Spill, 1991; Huber et al., 1992a, b; Kaiser & Huber, 1994; Campbell, 1996).

Probably the quick-NR regulatory mechanisms by phosphorylation and dephosphorylation constitute an essential system for tolerating changes in environmental stress, especially for macroalgae, which undergo tidal variation that affects nutrient availability and irradiance intensity. Under permanent stressing-conditions on a scale of hours to weeks, the synthesis and degradation of NR proteins and mRNA would be the most functional mechanism in preventing unnecessary energy expenditure.

Nitrate reductase is also influenced by irradiance (Davison & Stewart, 1984; Gao et al., 1995; Lopes et al., 1997; Vergara et al., 1998; Lartigue & Sherman, 2002; Chow & Oliveira, 2008), the rapid suppression in darkness probably arising from the availability of carbon skeletons, ATP, and NAD(P)H from photosynthesis and respiration.

Ultraviolet radiation also affects NR activity in macroalgae (Figueroa & Viñegla, 2001). Nevertheless, studies are scarce, and the mechanisms of action unknown.

NR and NR-protein activities manifest a daily rhythm with circadian influence (Lillo, 1983; Deng et al., 1991; Lopes et al., 1997, 2002; Granbom et al., 2004, 2007; Chow et al., 2004, 2007; Granbom et al., 2007). Under the light:dark cycle, NR activity reaches a plateau around the middle of the photoperiod, as well as a nocturnal minimum (Weidner and Kiefer 1981, Gao et al. 1992, Ramalho et al. 1995, Lopes et al. 1997, Chow et al. 2004, 2007; Granbom et al. 2004), presumably the normal behavior in photosynthetic species.. The circadian diel cycle of NR seems to be primarily regulated transcriptionally and correlated to the rate of mRNA protein-synthesis (Smith et al., 1992; Ramalho et al., 1995; Granbom et al., 2007). The peaks of enzymatic activity appear to be in concert with maximal photosynthetic flow, when intracellular carbohydrates and end products of photosynthesis begin to accumulate. At this point, the importance of light in promoting NR activity and synthesis is indirectly linked to carbon metabolic requirements.

Low NR activities during darkness have been suppressed by the artificial apply of light-mimicry carbohydrate sources. Furthermore, a light-pulse of 15 minutes during the dark phase, also induced NR activity to levels similar to those of the light phase in *G. chilensis* (Chow & Oliveira, 2008), possibly indicating NR inducible behavior by post-translational mechanisms. When intracellular carbohydrates begin to accumulate in excess, NR mRNA transcription is suspended. Inversely, when carbohydrates become depleted, NR expression is enhanced.

Higher NR activities are also associated with parts with active metabolic rates, and probably, to high levels of photosynthetic activity. In macroalgae with apical growth, NR activity in the tips is higher than in the basal parts (Granbom et al., 2004, 2007; Chow, 2004), thereby implying post-translational regulation. Nevertheless, NR protein content in the basal parts is the highest (Granbom et al., 2007), possibly indicating that a large part of NR is in an active form, compared to the basal part of the thallus.

Post-translational regulatory mechanisms are common in NR enzymes, especially during short-term response. This mechanism includes phosphorylation (Huber et al., 1992) involving specific protein kinases, protein phosphatases and a protein inativator (MacKintosh et al., 1995; Glaab & Kaiser, 1996).

In most studies of macroalgae NR activity, it is possible to establish the same trend of physiological response, i.e., the pronounced dependence on the external and internal pool of available nitrate, light stimulation and low or constitutive dark activity, temperature range of action according to the natural habitat of the seaweed, and correlations with carbon and ATP availability from photosynthesis and respiration. The slight differences in NR behavior can be attributed to species-specific response depending on particular environmental conditions, and may reflect special turnover of NR activity, as a product of acclimation and adaptation response to the extremely changeable intertidal environment.

5. *In vitro* nitrate reductase assay (optimization)

For several years, we have been studying the physiology of the red macroalgae, gracilariods (Rhodophyta, Gracilariales), from different view-points. In most cases, these have been cultured in PES (Provasoli Enrichment Medium) and VSES (von Stosch Enrichment Solution), at different concentrations and biomass densities.

Nitrogen repletion and starvation causes, not only alterations in pigment content, nitrogen assimilation and photosynthesis, but also morphological changes in growth and ultrastructure. Consequently, certain studies in our laboratory were directed towards characterizing and understanding nitrogen assimilation regulation, especially as regards NR behavior. Undoubtedly, physiological changes in nitrate assimilation and NR activity are involved during alga growth and development. Knowledge of these responses would contribute towards a better optimization of laboratory efforts and in-field cultures for physiological studies and biomass yield, for possible economical usage.

Methods for estimating *in vitro* NR activity have been developed by Weidner & Kiefer (1981), Chapman & Harrison (1988), Thomas & Harrison (1988), Brinkhuis et al. (1989) and Chow et al. (2001). Assaying procedures of NR activity are based on quantifying the reduction rate of nitrate to nitrite during the reaction catalyzed by intracellular NR enzymes.

Enzymatic NR assays have been used without considering adequate optimization of the method. The low NR activity observed during assaying could be due to the loss of enzymatic cofactors during extraction, inhibition of activity by phenolic compounds or other inhibitors, and the presence of endogenous proteases. The key points in NR assaying depend on adequate enzyme extraction, preservation, and stability during the whole procedure. There are two important considerations in enzymatic assays: (a) the enzyme must to be completely or nearly completely extracted, and (b) assaying conditions, such as pH, temperature, substrate and electron donor concentrations, and protectant, must be optimal for maximal activity, in order to preserve enzymatic activity during the process. In

most cases, NR activity is measured by saturating the enzymatic system with substrate. Under saturation conditions, NR activity is used as a nutritional estimator of nitrogen metabolism capacity. Some researchers prefer to use *in vitro* NR data as "potential activity", this representing a theoretical maximum of real NR activity.

Furthermore, the amount of detectable NR activity depends on protocol optimization, since enzymatic activities can vary between and within species, according to environmental conditions, circadian fluctuation and endogenous nutritional status, as well as thallus portion, age and size. Thus, for reliable comparison and evaluation, it is important to optimize the enzymatic assay, and clearly establish the conditions of the biological material to be studied.

Nitrate redutase assay is based on defining, spectrophotometrically, nitrite concentrations of the product from nitrate substrate reduction by the NR enzyme at constant temperature and time (Eppley et al., 1969). Spectrophotometric *in vitro* NR assay, while relatively easy and fast, and conferring the advantage of kinetic dependence between activity and time, confirmable by quantification of nitrate reduction, is not sensitive to any enzymatically crude extract. Nevertheless, it is recommended for very active and induced extracts. The comparison between deficient N samples cannot be sensitive enough. Therefore, even for studies of limited N, it is recommended to supply nitrate before sampling, to thus guarantee NR induction during the assay.

Appropriate extraction of the complete NR enzyme for *in vitro* assaying was achieved by grinding the biological material in liquid nitrogen. Sample grinding under liquid nitrogen increases cell disruption, thus facilitating the extraction of larger amounts of NR enzymes. The addition of bovine serum albumin (BSA) is advisable for protection against proteolytic enzymes or phenolic compounds, although additional protectants must be used in the case of complex species, so as to avoid enzyme denaturation by proteases, or phenolic and other compounds (*e.g.* high phenolic-containing brown algae). Another precaution for preserving enzymatic activity is to maintain the crude extract at a low temperature (4°C or on ice), and protected from light, to so prevent activity-degradation until assaying.

In vitro assays require fixed conditions, as regards pH, temperature, and the concentration of substrate and reductant source, as well as strict testing of each parameter of all the biological material to be studied. Macroalgal pH assaying varies slightly between species, maximal activity having been observed close to pH 8.0 (Lopes et al., 1997; Chow et al., 2004, 2007; Granbom et al., 2004).

Nitrate reductase activity is temperature sensitive over a narrow range, with several optimum temperatures for the various species, depending on the habitat. For temperate macroalgae, this ranges from 10 to 25 °C (Gao et al., 2000; Berges et al., 2002; Chow et al., 2004). Activities at low temperatures may require a larger amount of NR protein or higher catalytic rates to so maintain the same catalytic activity, as during low winter temperatures enzymes function below the optimum. Species with high NR activity during the winter may present a cold acclimation component. This high activity has been reported in *Laminaria saccharina* (Davison & Davison 1987), *Fucus vesiculosus* (Collén & Davison 2001), and *L. digitata, Fucus serratus, Fucus vesiculosus* and *Fucus spiralis* (Young et al. (2007). Macroalgae in tropical and sub-tropical environments presented high temperature tolerance during assaying (Lopes et al., 1997; Chow et al., 2007; Granbom et al., 2004; Martins et al., 2009), the optimum usually being higher than normal.

Nitrate reductase activity can also vary considerably among and within species, depending on natural or laboratory growing conditions. Therefore, optimal concentrations of electron

donor (NAD(P)H) and substrate must be verified for each of the species studied, to so guarantee saturating conditions for assaying.

As nitrate reductase activity is daily cyclical, this requires care with the period of collecting samples, since differences among treatments can arise from natural circadian behavior, and not from treatment effects. Furthermore, NR is more active in areas with highly active metabolic rates, usually the meristematic region. For example, Granbom et al. (2004, 2007) and Chow (2004) detected higher NR activity in apical than basal parts in *Kappaphycus alvarezii* and *G. chilensis*, respectively. Thus, the appropriate choice of biological material for enzymatic assaying is also extremely important, as the amount of extractable enzyme varies drastically among and within species, with thallus part and age, internal nutritional stock, environmental nitrogen availability, culture conditions, etc.

Optimized *in vitro* NR activity in some macroalgae was studied and important highlights described (Lopes et al., 1997; Lartigue & Sherman, 2002; Chow et al., 2004, 2007; Granbom et al., 2004).

There is a growing interest in applying macroalga NR activity to evaluating nutritional physiology in the laboratory and field, as a useful ecophysiological index. On the other hand, NR is regarded as a focal point in regulating the nitrogen assimilation pathway and for integrating the control of carbon and nitrogen metabolism. However, the potential applicability of *in vitro* NR assaying, as an important parameter of N and C metabolism, must to be carefully considered, in which case optimal assaying procedures are required.

6. Important remarks

In general, the importance of nitrogen metabolism in the marine environment, particularly nitrate assimilation, is based on the frequent identification of nitrogen as limiting nutrients for macroalgal growth. Various species under the same environmental conditions have developed special strategies for remaining in the habitat and benefit from the adversity of nitrogen limitation, either by taking advantage of nitrogen pulses or learning to live with low nutrient levels.

On the other hand, the increasing eutrophication of coastal aquatic environments, associated with anthropogenic nitrogen inputs, is a global reality. Opportunistic green macroalgae, other bloom species and species susceptible to growing nitrogen concentration, can be rapidly affected by ammonium and nitrate availability altering ecological dynamics of both populations and communities.

Nitrate reductase, through being the first enzyme in the nitrogen assimilatory pathway, assumes the responsibility for controlling the nitrate assimilatory rate in all algal cells. Thus, due to its importance in the general metabolism connected to N and C pathways, there is a constantly growing interest in studying the molecular and catalytic properties of NR enzymes and physiological responses to environmental stressing conditions and intracellular factors.

Previous studies on NR activity in micro and macroalgae, encountered the contradiction of using assay protocols without optimization, thus making comparison difficult, with little emphasis being placed on appropriate NR extraction and assaying. Nitrate reductase, through being a sensitive enzyme, rapidly inducible and repressive at various molecular levels and with diverse internal and external factors, is important for establishing minimum optimal conditions, both for comparison and acquiring an understanding of nitrogen metabolism.

The constant accumulation of knowledge on NR activities, together with studies of nutrient uptake, will facilitate the collection of tools for: (1) identifying limiting, defective and saturating levels of growth-nutrients; (2) regulating pathways of nitrogen assimilation and incorporation; (3) providing environmental indicators for monitoring; (4) identifying macroalgae with high nitrate-reduction potential for biofilter application in eutrophized environments and increasing the standing crop in polycultures; (5) optimizing culture systems by regulating the reduction rate of nitrate with optimal nitrogen uptake and reduction; (6) developing management strategies for the culture of economically important algae; and (7) understanding evolutive patterns that support the adaptation of macroalgae to their environment.

Further studies of NR activity, both in the field and laboratory, are necessary as a contribution, both to understanding seaweed physiology, as well as to clarify the importance and role of these algae in near-shore biogeochemical cycling. Moreover, the constant changes in the coastal environment, brought about by anthropic action (artificial eutrophication), and variations arising from global climate change, will undoubtedly influence the ranges of tolerance and acclimation of algae, whereby the necessity for monitoring changes in coastal environments and communities.

7. Acknowledgment

The author would thank the research financial support of São Paulo Research Foundation (FAPESP).

8. References

Balandin, T. & Aparicio, P. J. (1992). Regulation of nitrate reductase in *Acetabularia mediterranea*. J. Exp. Bot. 43:625–631.

Berges, J.A. (1997). Algal nitrate reductases. Eur. J. Phycol. 32: 3-8.

Berges, J. A. & Harrison, P. J. (1995). Nitrate reductase activity quantitatively predicts the rate of nitrate incorporation under steady state light limitation: a revised assay and characterization of the enzyme in three species of marine phytoplankton. Limnol. Oceanogr. 40: 82-93.

Berges, J. A., Cochlan, W. P. & Harrison, P. J. (1995). Laboratory and field responses of algal nitrate reductase to diel periodicity in irradiance, nitrate exhaustion, and the presence of ammonium. Mar. Ecol. Prog. Ser. 124: 259-269.

Berges J.A.,Varela D.E. & Harrison P.J. (2002) Effects of temperature on growth rate, cell composition and nitrogen metabolism in the marine diatom *Thalassiosira pseudonana* (Bacillariophyceae). Marine Ecology Progress Series 225, 139–146.

Brinkhuis, B. H.; Renzhi, L.; Chaoyuan, W. & Xun-sen, J. (1989). Nitrite reductase transients and consequences for *in vivo* algal nitrate reductase assays. J. Phycol. 25: 539–45.

Cabello-Pasini, A.; Macías-Carranza, V.; Abdala, R.; Korbee, N. & Figueroa, F. L. (2011). Effect of nitrate concentration and UVR on photosynthesis, respiration, nitrate reductase activity, and phenolic compounds in *Ulva rigida* (Chlorophyta). J. Appl. Phycol. 23: 363–369.

Campbell, W. H. (1996). Nitrate reductase biochemistry comes of age. Plant Physiol. 111: 355–361.

Campbell, W. H. (1999). Nitrate reductase structure, function, and regulation: bridging the gap between biochemistry and physiology. Annu. Rev. Plant Physiol. Plant Mol. Biol. 50: 277–303.

Chapman, D.J. & P.J. Harrison. 1988. Experiment 22. Nitrogen metabolism and measurement of nitrate reductase. In: Experimental Phycology. A Laboratory Manual. Lobban, C.S., D.J. Chapman & B.P. Kremer (eds). Cambridge University Press, Cambridge, USA. Pp. 196-202.

Chow, F. & Oliveira, M. (2008). Rapid and slow modulation of nitrate reductase activity in the red macroalga *Gracilaria chilensis* (Gracilariales, Rhodophyta): influence of different nitrogen sources. J. Appl. Phycol. 20: 775–782.

Chow, F.; Oliveira, M. C. & Pedersén, M. (2004). *In vitro* assay and light regulation of nitrate reductase in the red alga *Gracilaria chilensis*. J. Plant Physiol. 161: 769–776.

Chow, F.; Capociama, F. V.; Faria, R. & Oliveira, M. C. (2007). Characterization of nitrate reductase activity in vitro in *Gracilaria caudata* J. Agardh (Rhodophyta, Gracilariales). Rev. Brasil. Bot. 30: 123-129.

Chow, F.; Macchiavello, J.; Santa-Cruz, S.; Fonck, E. & Olivares, J. (2001). Utilization of *Gracilaria chilensis* (Rhodophyta, Gracilariaceae) as a biofilter in the depuration of effluents from tank cultures of fish, oysters, and sea urchins. J. World Aquacul. Soc. 32: 215–20.

Collén, J. & Davison, I. R. (2001). Seasonality and thermal acclimation of reactive oxygen metabolism in *Fucus vesiculosus* (Phaeophyceae). J. Phycol. 37: 474–481.

Collos, Y. (1989). A linear model of external interactions during uptake of different forms of inorganic nitrogen by microalgae. J. Plankton. Res. 11: 521–523.

Corzo, A. & Niell, F. X. (1991). Determination of nitrate reductase activity in *Ulva rigida* C. Agardh by the in situ method. J. Exp. Mar. Biol. Ecol. 146: 181-191.

Crawford, N. M. (1995). Nitrate—nutrient and signal for plant growth. Plant Cell 7: 859–868.

Crawford, N. M. & Arst, H. N., Jr. (1993). The molecular genetics of nitrate assimilation in fungi and plants. Ann. Rev. Genet. 27: 115-46.

Davison I.R. & Davison J.O. (1987) The effect of growth temperature on enzyme activities in the brown alga *Laminaria saccharina*. British Phycol. J. 22: 77–87.

Davison I.R. & Stewart W.D.P. (1984) Studies on nitrate reductase activity in *Laminaria digitata* (Huds.) Lamour. II. The role of nitrate availability in the regulation of enzyme activity. J. Exp. Mar. Biol. Ecol. 79: 65–78.

Davison I.R., Andrews M. & Stewart W.D.P. (1984) Regulation of growth in *Laminaria digitata*: use of in vivo nitrate reductase activities as an indicator of nitrogen limitation in field populations of *Laminaria* spp. Mar. Biol. 84: 207–217.

Davison, I.; Jordan, T.; Fegley, J. & Grobe, C. (2007). Response of *Laminaria saccharina* (Phaeophyta) growth and photosynthesis to simultaneous ultraviolet radiation and nitrogen limitation. J. Phycol. 43: 636–646.

DeBoer, J.A. (1981). Nutrients. In: Lobban, C. S. & Wynne, M. J. (eds.). The Biology of Seaweeds, Bot. Monogr., pp. 356–392.

Deng, M.-D.; Moureaux, T.; Cherel, I.; Boutin, J.-P. & Caboche, M. (1991). Effects of nitrogen metabolites on the regulation and circadian expression of tobacco nitrate reductase. Plant Physiol. Biochem. 29: 239–247.

Eppley, J.; Coastworth, L. & Solorzado, L. (1969). Studies of nitrate reductase in marine phytoplankton. Limnol. Oceanogr. 14: 194-205.

Falkowski, P. G. (1992). Molecular ecology of phytoplankton photosynthesis. In: Falkowski, P. G. & Woodhead, A. (eds.). Primary Productivity and Biogeochemical Cycles in the Sea, pp. 47-67. Plenum Press, New York.

Falkowski, P. G. & Raven, J. A. (1997). Aquatic Photosynthesis. Blackwell Science, UK. 375 pp.

Fernández-López, M.; Olivares, J. & Bedmar, E. J. (1996). Purification and characterization of the membrane-bound nitrate reductase isoenzymes of *Bradyrhizobium japonicum*. FEBS Lett. 392: 1-5.

Figueroa, F.L. & Viñegla, B. (2001). Effects of solar radiation on photosynthesis and enzyme activities (carbonic anhydrase and nitrate reductase) in marine macroalgae from southern Spain. Rev. Chil. Hist. Nat. 74: 237–249.

Flynn, K. J. 1991. Algal carbon-nitrogen metabolism: a biochemical basis for modeling the interactions between nitrate and ammonium uptake. J. Plankton Res. 13: 373-387.

Gao, Y.; Smith, G. J. & Alberte, R. S. (1993). Nitrate reductase from the marine diatom *Skeletonema costatum* biochemical and immunological characterization. Plant Physiol. 103: 1437-1445.

Gao Y., Smith G.J. & Alberte R.S. (1995) Induction of nitrate reductase activity by light and NO_3^- in the marine diatom *Skeletonema costatum*. Plant Physiol. 108: 71.

Gao Y., Smith G.J. & Alberte R.S. (2000) Temperature dependence of nitrate reductase activity in marine phytoplankton: biochemical analysis and ecological, implications. J. Phycol. 36: 304–313.

Gao, Y.; Smith, G. J. & Alberte, R. S. (1992). Light regulation of nitrate reductase in *Ulva fenestrata* (Chlorophyceae). I. Influence of light regimes on nitrate reductase activity. Mar. Biol. 112: 691–696.

Glaab, J. & Kaiser, W. M. (1996). The protein kinase, protein phosphatase and inhibitor protein of nitrate redutase are ubiquitous in higher plants and independent of nitrate reductase turnover. Planta 199: 57-63.

Gordillo, F. J. L.; Aguilera, J. & Jiménez, C (2006). The response of nutrient assimilation and biochemical composition of Arctic seaweeds to a nutrient input in summer. J. Exp. Bot. 57: 2661–2671.

Granbom, M.; Pedersén, M.; Kadel, P. & Lüning, K. (2001). Circadian rhythm of photosynthesis in the red macroalga *Kappaphycus alvarezii*: dependence on light quantity and quality. J. Phycol. 37: 1020–1025.

Granbom, M.; Chow, F.; Lopes, P. F.; Oliveira, M. C.; Colepicolo, P.; Paula, J. P. & Pedersén, M. (2004). Characterisation of nitrate reductase in the marine macroalga *Kappaphycus alvarezii* (Rhodophyta). Aquat. Bot. 78: 295–305.

Granbom, M.; Lopes, P. F.; Pedersén, M. & Colepicolo, P. (2007). Nitrate reductase in the marine macroalga *Kappaphycus alvarezii* (Rhodophyta): oscillation due to the protein level. Bot. Mar. 50: 106-112.

Hanisak, M. D. (1983). The nitrogen relationships of marine macroalgae. In: Carpenter, E. J. & Capone, D. G. (eds.). Nitrogen in the Marine Environment. Academic Press, New York, pp. 699–730.

Hernández I., Corzo A., Gordillo F.J., Robles M.D., Saez E., Fernández J.A. & Niell F.X. (1993). Seasonal cycle of the gametophytic form of *Porphyra umbilicalis* – nitrogen and carbon. Mar. Ecol. Progress Ser. 99: 301–311.

Howartha, D. G. & Baumb, D. A. (2002). Phylogenetic utility of a nuclear intron from nitrate reductase for the study of closely related plant species. Molec. Phylog. Evol. 23: 525–528.

Huber, J. L.; Huber, S. C.; Campbell, W. H. & Redinbaugh, M. G. (1992a). Reversible light/dark modulation of spinach leaf nitrate reductase activity involves protein phosphorylation. Arch. Biochem. Biophys. 296: 58–65.

Huber, J. L.; Huber, S. C.; Campbell, W. H. & Redinbaugh, M. G. (1992b). Reversible light dark modulation of spinach leaf nitrate reductase-activity involves protein-phosphorylation. Arch. Biochem. Biophys. 296: 58–65.

Huovinen, P.; Matos, J.; Sousa-Pinto, I. & Figueroa, F. (2006). The role of nitrogen in photoprotection against high irradiance in the Mediterranean red alga *Grateloupia lanceola*. Aquat. Bot. 84: 208–316.

Hurd, C. L.; Berges, J. A.; Osborne, J. & Harrison, P. J. (1995). An in vitro nitrate reductase assay for marine macroalgae: optimization and characterization of the enzyme for *Fucus gardneri* (Phaeophyta). J. Phycol. 31: 835–43.

Kain, J. M. (1989). The seasons in the subtidal. Br. Phycol. J. 24: 203-215.

Kaiser, W. & Huber, S. C. (1994). Posttranslational regulation of nitrate reductase in higher plants. Plant Physiol. 106: 817-821.

Kaiser, W. M. & Spill, D. (1991). Rapid modulation of spinach leaf nitrate reductase by photosynthesis. II. *In vitro* modulation by ATP and AMP. Plant Physiol. 96: 368-375.

Korbee-Peinado, N.; Abdala-Díaz, R.; Figueroa, F. & Helbling, W. (2004). Ammonium and UV radiation stimulate the accumulation of mycosporine-like amino acids in Porphyra columbina (Rhodophyta) from Patagonia, Argentina. J. Phycol. 40: 248–259.

Lapointe, B. E. & Duke, C. S. (1984). Biochemical strategies for growth of *Gracilaria tikvahiae* (Rhodophyta) in relation to light intensity and nitrogen availability. J. Phycol. 20: 488–495.

Lartigue J. & Sherman T.D. (2002) Field assays for measuring nitrate reductase activity in *Enteromorpha* sp. (Chlorophyceae), *Ulva* sp. (Chlorophyceae) and *Gelidium* sp. (Rhodophyceae). J. Phycol. 38: 971–982.

Lartigue J. & Sherman T.D. (2005) Response of *Enteromorpha* sp. (Chlorophyceae) to a nitrate pulse: nitrate uptake, inorganic nitrogen storage, and nitrate reductase activity. Mar. Ecol. Progress Ser. 292: 147–157.

Lillo, C. (1983). Studies of diurnal variations of nitrate reductase activity in barley leaves using various assay methods. Physiol. Plant. 57: 357-362.

Lillo, C. (1994). Light regulation of nitrate reductase in green leaves of higher plants. Physiol. Plant. 90: 616-620.

Lobban, C. S. & Harrison, P. J. (1994). Seaweed Ecology and Physiology. Cambridge University Press, Cambridge. 366 pp.

Lobban, C. S.; Harrison, P. J. & Duncan, M. J. (1985). The physiological ecology of seaweeds. Cambridge University Press, Cambridge.

Lopes P.F., Oliveira M.C. & Colepicolo P. (1997). Diurnal fluctuation of nitrate reductase activity in the marine red alga. J. Phycol. 33: 225–231.

Lopes, P. F.; Oliveira, M. C. & Colepicolo P. (2002). Characterization and daily variation of nitrate reductase in *Gracilaria tenuistipitata* (Rhodophyta). Biochem. Biophys. Res. Commun. 295: 50–54

MacKintosh, C.; Douglas, P. & Lillo, C. (1995). Identification of a protein that inhibits the phosphorylated form of nitrate reductase from spinach (*Spinacia oleracea*) leaves. Plant Physiol. 107: 451–457.

Martins, A. P., Chow, F. & Yokoya, N. S. (2009). Ensaio *in vitro* da enzima nitrato redutase e efeito da disponibilidade de nitrato e fosfato em variantes pigmentares de *Hypnea musciformis* (Wulfen) J.V. Lamour. (Gigartinales, Rhodophyta). Rev. Brasil. Bot. 32: 635-645.

Nakamura, Y. & Ikawa, T. (1993). Purification and properties of NADH: nitrate reductase from red alga Pophyra yezoensis. Plant Cell Physiol. 34: 1239-49.

Nakamura, Y., Saji, H., Kondo, N. & Ikawa, T. (1994). Preparation of monoclonal antibodies against NADH-nitrate reductase from the red alga *Porphyra yezoensis*. Plant Cell Physiol. 35: 1185-1198.

Nicodemus, M. A.; Salifu, K. F. & Jacobs, D. F. (2008). Nitrate reductase activity and nitrogen compounds in xylem exudate of *Juglans nigra* seedlings: relation to nitrogen source and supply. Trees Struct. Funct. 22: 685–695.

Ramalho, C. B., Hastings, J. W. & Colepicolo. P. (1995). Circadian oscillation of nitrate reductase activity in *Gonyaulax polyedra*. Plant Physiol. 107: 225-231.

Smith, G. J.; Zimmerman, R. C. & Alberte, R. S. (1992). Molecular and physiological responses of diatoms to variable levels of irradiance and nitrogen availability: growth of *Skeletonema costatum* in simulated upwelling conditions. Limnol. Oceanogr. 37: 989-1007.

Solomonson, L. P. & Barber, M. J. (1990). Assimilatory nitrate reductase: functional properties and regulation. Annu. Rev. Plant Physiol. Plant Mol. Biol. 41: 225–253.

Stolz, J. F. & Basu, P. (2002). Evolution of nitrate reductase: molecular and structural variations on a common function. Chem. BioChem. 3: 198–206.

Thomas, T. E. & Harrison, P. J. (1988). A comparison of in vitro and in vivo nitrate reductase assays in three intertidal seaweeds. Bot. Mar. 31: 101-107.

Tischner, R.; Ward, M. R. & Huffaker, R. C. (1989). Evidence for a plasma-membrane-bound nitrate reductase involved in nitrate uptake of *Chlorella sorokiniana*. Planta 178: 19-24.

Vergara, J. J.; Berges, J .A. & Falkowski, P. G. (1998). Diel periodicity of nitrate reductase activity and protein levels in the marine diatom *Thalassiosira weissflogii* (Bacillariophyceae). J. Phycol. 34: 952–961.

Weidner, M.; & Kiefer, H. (1981). Nitrate reduction in the marine brown algae *Giffordia mitchellae* (Harv.) Ham. Z. Pflazenphysiol. Bd. 104: 341–351.

Young, E. B., Dring, M. J., Savidge, G., Birkett, D. A & Berges, J. A. (2007). Seasonal variations in nitrate reductase activity and internal N pools in intertidal brown algae are correlated with ambient nitrate concentrations. Plant, Cell and Environ. 30: 764–774.

Young, E. B., Berges, J. A. & Dring, M. J. (2009). Physiological responses of intertidal marine brown algae to nitrogen deprivation and resupply of nitrate and ammonium. Physiol. Plant. 135: 400–411.

Zhou, J. & Kleinhofs, A. (1996). Molecular evolution of nitrate reductase genes. J. Mol. Evol. 42: 432-442.

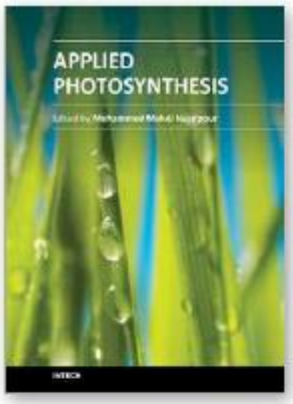

Applied Photosynthesis

Edited by Dr Mohammad Najafpour

ISBN 978-953-51-0061-4
Hard cover, 422 pages
Publisher InTech
Published online 02, March, 2012
Published in print edition March, 2012

Photosynthesis is one of the most important reactions on Earth, and it is a scientific field that is intrinsically interdisciplinary, with many research groups examining it. This book is aimed at providing applied aspects of photosynthesis. Different research groups have collected their valuable results from the study of this interesting process. In this book, there are two sections: Fundamental and Applied aspects. All sections have been written by experts in their fields. The book chapters present different and new subjects, from photosynthetic inhibitors, to interaction between flowering initiation and photosynthesis.

How to reference

In order to correctly reference this scholarly work, feel free to copy and paste the following:

Fungyi Chow (2012). Nitrate Assimilation: The Role of In Vitro Nitrate Reductase Assay as Nutritional Predictor, Applied Photosynthesis, Dr Mohammad Najafpour (Ed.), ISBN: 978-953-51-0061-4, InTech, Available from: http://www.intechopen.com/books/applied-photosynthesis/nitrate-assimilation-the-role-of-in-vitro-nitrate-reductase-assay-as-nutritional-predictor

INTECH
open science | open minds

InTech Europe
University Campus STeP Ri
Slavka Krautzeka 83/A
51000 Rijeka, Croatia
Phone: +385 (51) 770 447
Fax: +385 (51) 686 166
www.intechopen.com

InTech China
Unit 405, Office Block, Hotel Equatorial Shanghai
No.65, Yan An Road (West), Shanghai, 200040, China
中国上海市延安西路65号上海国际贵都大饭店办公楼405单元
Phone: +86-21-62489820
Fax: +86-21-62489821

ANEXO 11

Journal of Applied Phycology (2019) 31:847–856
https://doi.org/10.1007/s10811-018-1581-4

VI REDEALGAS WORKSHOP (RIO DE JANEIRO, BRAZIL)

Integrated multi-trophic farming system between the green seaweed *Ulva lactuca*, mussel, and fish: a production and bioremediation solution

Allyson E. Nardelli[1] · Vitor G. Chiozzini[2] · Elisabete S. Braga[2] · Fungyi Chow[1]

Received: 20 March 2018 / Revised and accepted: 11 July 2018 / Published online: 23 July 2018
© Springer Nature B.V. 2018

Abstract
Practices of aquaculture production may generate potential pollutants that cause environmental pressure. In this context, a recommendation to mitigate the environmental impacts caused by aquaculture waste would be using and recycling such nutrients, considered as "pollutants," in an eco-efficient way, with approaches such as the integrated multi-trophic aquaculture (IMTA). This system integrates the culturing of organisms with different and complementary ecosystem functions. This study aimed to investigate the ecosystem capacity of *Ulva lactuca* in wastewater bioremediation in an IMTA system with mussel and fish effluents. For such, three systems were set up: (1) algae cultivated with seawater, (2) algae with effluent from fish, and (3) algae with effluent from fish and mussels. *Ulva lactuca* proved to be a suitable species for the IMTA system with high growth and easy handling in cultivation. Algal growth rate, nutrient uptake (N and P) and O_2 production increased significantly as the succession of trophic levels increased, demonstrating the high ecosystem capacity of *U. lactuca* for wastewater bioremediation as well as the use and recycling of eutrophication agents for biomass production. The highest absorption/removal of dissolved nitrogen occurred in the form of NH_4^+, a N form with the greatest metabolic advantage for photosynthetic assimilation, but toxic in high concentrations. The present IMTA system showed a balance between inputs and outputs, denoting sustainable and efficient characteristics of several ecosystem goods and services.

Keywords Algae · Biomitigation · Bioremediation · Eutrophication · Integrated aquaculture · Sustainable aquaculture

Introduction

According to the United Nations Food and Agriculture Organization, aquaculture has expanded in the last decades (FAO 2016) and, with this increase, the concern for the sustainable use of aquatic ecosystems has grown (Tiller et al. 2012; Ertör and Ortega-Cerdà 2015). This concern is because aquaculture operations may have negative impacts in the waters surrounding of the farming sites, such as eutrophication caused by the increase of nutrient concentration, which in turn affects the dissolved oxygen levels. In this context, it is important to use production methods that aim not only at economic growth but also at sustainable practices that include ecological and social approaches (Ertör and Ortega-Cerdà 2015) such as the Integrated Multi-Trophic Aquaculture (IMTA) systems (Alexander and Hughes 2017).

IMTA is a production system that can be adopted to mitigate the possible negative effects of the monoculture of fed species (Chopin and Robinson 2006) and re-use the waste as resources. This aquaculture strategy is based on multiple aquatic production under the concept of reuse and recycling inorganic and organic wastes (Chopin and Robinson 2004). Instead of using a single species in cultivation and focusing efforts on its needs, IMTA tries to imitate a natural ecosystem by combining the cultivation of several species with complementary ecosystem functions and trophic levels, so that one type of food not consumed, e.g., waste, nutrients, and by-products, can be reused and converted into nutrients, food, and energy for other farmed species (Edwards et al. 1988; Chopin and Robinson 2006).

✉ Allyson E. Nardelli
allyson.nardelli@usp.br

[1] Laboratory of Marine Algae, Institute of Biosciences, University of São Paulo, São Paulo, SP 05508-090, Brazil

[2] Laboratory of Biogeochemistry of Nutrients, Micronutrients and Trace Elements in the Oceans, Institute of Oceanography, University of São Paulo, São Paulo, SP 05508-120, Brazil

©Fungyi Chow / 2021

Generally, IMTA studies combine, in the right proportions, the culture of fed species (fish or shrimp) with particulate organic matter (POM) filtering species (oysters, scallops, and mussels) and dissolved inorganic material (DIM) extractive species (seaweeds). Fish introduce POM into the water column due to unconsumed food and feces production, in addition to releasing DIM as NH_4^+, PO_4^{3-}, and CO_2 due to metabolic action (Wang et al. 2012). POM-filtering organisms may have a boost in their diet due to the provision of particulate food and feces from fed organisms by assimilating some of this material. Consequently, the POM load is reduced in the surroundings of the farming site (Irisarri et al. 2015). The DIM from the fed organisms, the suspension-feeders, and the biodegradation of organic material by the microbial community are used by primary producers, e.g., macroalgae, that use DIM for their growth and development. The macroalgae take up dissolved compounds such as NH_4^+, NO_2^-, and PO_4^{3-} which are toxic at certain concentrations to many organisms and incorporate them into their biomass (Chopin et al. 2001; Neori et al. 2004; Buschmann et al. 2008). In addition, seaweeds contribute to the increase of O_2 concentration and stabilization of water pH (Troell et al. 2003; Chopin et al. 2011). By the utilization of the residue of one farming subsystem (trophic level) as a nutrient for another within the same cultivation site, IMTA could even help to increase the production capacity of a low productivity site (Edwards et al. 1988).

Seaweeds are a fundamental part of IMTA systems since they contribute to the incorporation of dissolved nutrients (C, N, and P) derived from higher trophic levels, such as fish and shellfish, converting these compounds potentially harmful to the environment in biomass. Therefore, they convert nutrient-rich waters into usable resources, mitigating the effects of eutrophication and stabilizing water quality (Schuenhoff et al. 2003; Neori et al. 2004). Studies have shown that macroalgae grown in IMTA systems have a high content of proteins, polysaccharides, pigments, and functional compounds, thus contributing to the production of high quality nutritional biomass (Chopin et al. 1999; Martínez-Espiñeira et al. 2015) which find applications in various industries, from the production of food supplements, fertilizers, cosmetics, and food.

The aim of this study was to investigate the response of the green seaweed *Ulva lactuca* as regards growth rate and nutrient retention when exposed to IMTA systems with different trophic levels.

Material and methods

Experimental set-up

Ulva lactuca L. were collected at the beaches of Perequê-Mirim (23° 29′ 25.7640″ S and 45° 6′ 11.0268″ W) and Santa Rita (23° 29′ 31.7976″ S and 45° 6′ 12.1248″ W), in Ubatuba, SP, Brazil, and transported to the Research Station, Institute of Oceanography, University of São Paulo (Ubatuba, SP). The seaweed was cleaned to remove epiphytes and encrusting material and acclimated for 1 week in 200-L plastic tanks (0.5 m^2) with flowing seawater, constant aeration, and natural environment conditions (irradiance, temperature). *Ulva lactuca* were cultivated in clear seawater (A, control), with effluents of fish (*Rachycentron canadum* L) (AF) and with fish + mussel (*Perna perna* L) effluents (AMF). The effluent from the fish tank was passed through the tank with mussels and then to the macroalgae tank. Each system was run in triplicate (Fig. 1).

Additionally, two experimental conditions in the algal culture tanks were tested one with low algal density per area (280 g m^{-2}) and low water flow (20 L h^{-1}), and another with high density of seaweed per area (660 g m^{-2}) and high flow (40 L h^{-1}). They were denoted as the ratio between the density per area (g m^{-2}) and the inlet flow rate in the algae tanks (L h^{-1}), corresponding to 14 g of seaweed m^{-2} L^{-1} h (E14) and 16.5 g of seaweed m^{-2} L^{-1} h (E16.5).

Ten fish of 63.96 ± 18.04 g and 152.35 ± 19.63 g (mean ± SD) were stocked in 500-L tanks for E14 and E16.5 treatments. Fish were fed daily a commercial feed at 2% body mass. Mussels were placed in 30-cm diameter baskets and suspended in 200-L tanks. For treatments E14 and E16.5, 45 individuals with mean weight of 13.92 ± 1.25 g and 77 individuals of 15.5 ± 1.42 g were used, respectively. Mussels fed on leftover feed and feces from the fish tank.

Environmental parameters

Environmental parameters, i.e., illuminance and temperature, were measured daily with a datalogger (Illuminance UV Recorder TR-74Ui, Japan). In addition, water temperature and dissolved O_2 were measured daily with an electrode (Yellow Spring Instruments model YSI-85) in each algal tank.

Algal growth rate

The algal biomass was measured weekly and the growth rates (*GR*) in percent day^{-1} were calculated according to Lignell and Pedersén (1989): $GR = [(M_f/M_i)^{1/t} - 1] \times 100$, where M_f = final mass (g), M_i = initial mass (g), and t = time between measurements (days). The *GR* was calculated weekly for the 3-week experimental period.

Biomass production versus feed expenditure

To calculate the yield of the farming systems, the final weight was subtracted from the initial weight of the fish, mussels, and seaweed. In addition, fish were weighed weekly to adjust the amount of feed to be fed.

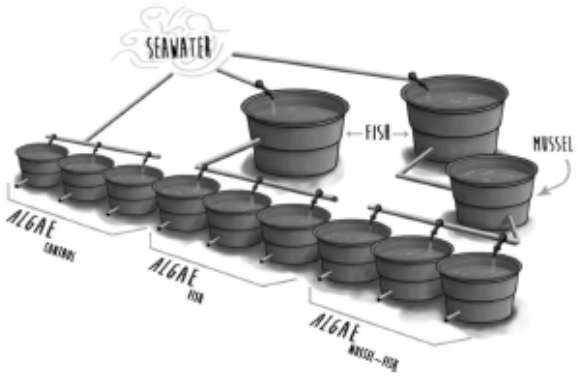

Fig. 1 General scheme of the integrated multi-trophic culture system, showing the treatments: control Algae (A), Algae + Fish (AF), and Algae + Mussels + Fish (AMF)

Nutrient concentration

Seawater samples were collected weekly at the inlet and outlet of the macroalgae tanks to determine the concentrations of dissolved inorganic nutrients (PO_4^{3-}, NH_4^+, NO_2^-, and NO_3^-) and the dissolved organic matter (N and P). PO_4^{3-} concentrations were determined by colorimetric method, as described by Grasshoff et al. (1999) and spectrophotometrically read at 880 nm (± 0.01 μM, Evolution 200 Thermo). NH_4^+ was analyzed by the method described by Tréguer and Le Corre (1975) and spectrophotometrically read at 630 nm (± 0.05 μM, Evolution 200 Thermo). NO_3^- and NO_2^- were measured automatically (AutoAnalyzerII Bran-Luebbe) using a colorimetric method described by Tréguer and Le Corre (1975) and Braga (1997a, 1997b). The reduction of NO_3^- to NO_2^- was using a cadmium column (Wood et al. 1967). The precision of the method for NO_2^- was ± 0.01 μM and for NO_3^- was ± 0.02 μM. The retention of inorganic nutrient was calculated as the difference between the concentrations in the water outlet and inlet of the macroalgae tanks.

Dissolved organic P and N were determined by photooxidation with UV light, according to Armstrong et al. (1966), Armstrong and Tibbits (1968), and Saraiva (2003), producing nitrate and phosphate that were analyzed as described previously. The total N and P obtained were reduced from the initial nitrate + nitrite fractions, obtaining the dissolved organic nitrogen, and in the case of total phosphorus, the reduction of the initial phosphate gave the dissolved organic phosphorus value.

Statistical analyses

Data are presented as mean ± standard deviation ($n = 3$). All data were checked for normality (Jarque-Bera JB test) and homogeneity of variances with the Levene test (Zar 1996). One-way ANOVA was used to compare the treatments and significant difference between means were detected by the Tukey test ($P < 0.05$). Principal components analysis (PCA) was used to show the relationship between treatments and growth rate, nutrient retention and dissolved O_2. All statistical tests were performed using the software Past v. 2.17c.

Results

Environmental parameters

For the E14 experiment, daily mean values of irradiance varied from 99.6 to 394.9 μmol photons m^{-2} s^{-1} during the experimental period and temperature ranged from 24.8 to 29.2 °C (Fig. 2a). For E16.5, the irradiance fluctuated from 88.2 to 241.2 μmol photons m^{-2} s^{-1} and temperature from 22.4 to 28.6 °C (Fig. 2b).

The temperature of the seaweed cultivation tanks did not show significant differences within Algae (A), Algae + Fish (AF), and Algae + Mussels + Fish (AMF) treatments (Fig. 3a) within the same experiment (E14 or E16.5), but differences between E14 and E16.5 experiments were observed ($P < 0.001$, $F = 46.07$, $df = 2$ [F-critical = 9.963]).

Dissolved O_2 concentration in the macroalgae tanks increased in E14 (Fig. 3b) as the number of trophic levels increased ($P = 0.0001$, $F = 28.99$, and $df = 2$ [F-critical = 45.76]). For E16.5, there was no significant difference between A and AF treatments, but they were significantly different from AMF ($P = 0.0013$, $F = 7.627$, and $df = 2$ [F-critical = 45.39]).

Algal growth rate

In E14 experiment, all treatments had their algal biomass increased over the weeks (Fig. 4a), except A treatment ($P = 0.0001$, $F = 1998$, and $df = 2$ [F-critical = 3.97]). E16.5 showed the same trend of biomass response as E14 (Fig. 4b; $P = 0.0002$, $F = 215.1$, and $df = 2$ [F-critical = 3.433]). The AF and AMF treatments reached the final biomass of 321.82 ± 5.58 g and 379.95 ± 6.45 g, respectively for E14 and for E16.5 AF and AMF had 504.95 ± 68.99 and 652.95 ± 14.86 g, respectively.

Algal growth rates for the two experiments (Fig. 4c, d) followed the same trends of increased growth rates over time and inclusion of trophic levels; however, the mean values from the E16.5 treatments were lower than those from the E14. For E14; the best growth rate was observed in the third week of culture, with the values of 4.75 ± 0.36 and 6.32 ± 0.41% day^{-1} for the AF and AMF treatments, respectively ($P = 0.0001$, $F = 492.3$, and $df = 2$ [F-critical = 3.91]). For E16.5, the highest growth rates also occurred in the third week, with the values of 3.83 ± 0.50 and 4.86 ± 0.54% day^{-1} for AF and AMF treatments, respectively ($P = 0.0008$, $F = 296.5$, and $df = 2$ [F-critical = 2.678]).

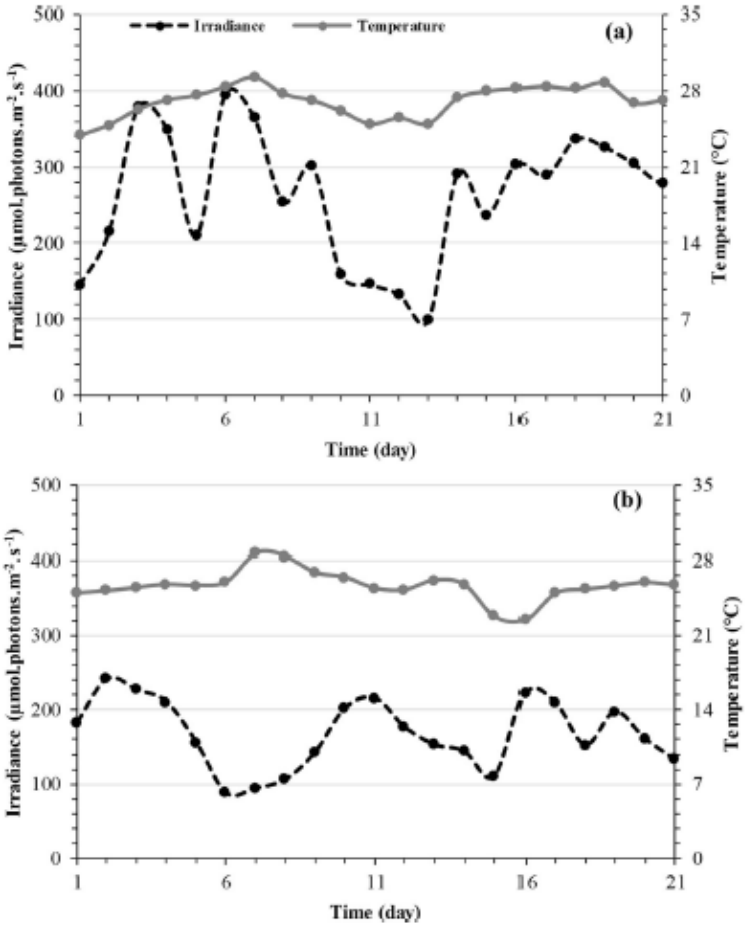

Fig. 2 Environmental climatic data during the experimental period including the average of **a** daily solar irradiance and daily temperature for E14 and **b** daily solar irradiance and daily temperature for E16.5

Figure 4e, f presents the general aspects of the macroalgae at the end of the experiments E14 and E16.5. A clear difference could be noted between algae grown in clear water and in consortium with fish or fish + mussels effluents.

In E14, both AMF and AF treatments yielded higher biomass than feed expenditure, as AMF produced 1.86 times what was spent with feed (Table 1). In E16.5, the AMF treatment also had higher biomass production than feed expenditure producing 1.14 times what was spent with feed, whereas the AF treatment yielded nearly half of the value observed in the same treatment in E14.

Nutrient concentration

With the accretion of trophic levels, the phosphate concentration in the algal tanks and the retention by the algae were also elevated in both E14 and E16.5 (Fig. 5). In E14 (Fig. 5a), phosphate input in the AF treatment was 2.08 ± 0.18 µmol L^{-1} and a retention of 0.60 ± 0.18 µmol L^{-1}, nearly 29% of PO_4^{3-} retention. In the AMF treatment, input was 3.24 ± 0.11 µmol L^{-1} and a retention of 1.41 ± 0.11 µmol L^{-1}, equivalent to 39.72% of PO_4^{3-} ($P = 0.0007$, $F = 542.6$, and $df = 2$ [F-critical = 3.567]). In E16.5 (Fig. 5b), a similar trend of the PO_4^{3-} values was observed. Treatment AF retained 0.35 ± 0.05 µmol L^{-1}, approximately 11.98% of the PO_4^{3-} and AMF retained 1.16 ± 0.05 µmol L^{-1}, 27.49% of PO_4^{3-}, with significant differences between treatments ($P < 0.0001$, $F = 106.9$, and $df = 2$ [F-critical = 5.907]).

The variation of the NH_4^+ concentrations in each treatment showed the same trend as PO_4^{3-}. Figure 5c shows that the AF treatment input 9.05 ± 1.17 µmol L^{-1}, with mean retention of 62.4% of NH_4^+ and AMF retained 18.61 ± 0.4 µmol L^{-1}, equivalent to 70.88% of NH_4^+ for E14, with significant difference between treatments ($P < 0.0001$, $F = 2418$, and $df = 2$ [F-critical = 2.686]). Figure 5d shows a similar trend of NH_4^+ values in E16.5 for retention values as the AF treatment had an input of 11.64 ± 0.92 µmol L^{-1} with a retention of 33.40% NH_4^+ and the AMF treatment input of 19.31 ± 0.34 µmol L^{-1} with a mean retention of 50.6% of NH_4^+ ($P < 0.0001$, $F = 3011.1$, and $df = 2$ [F-critical = 2.995]).

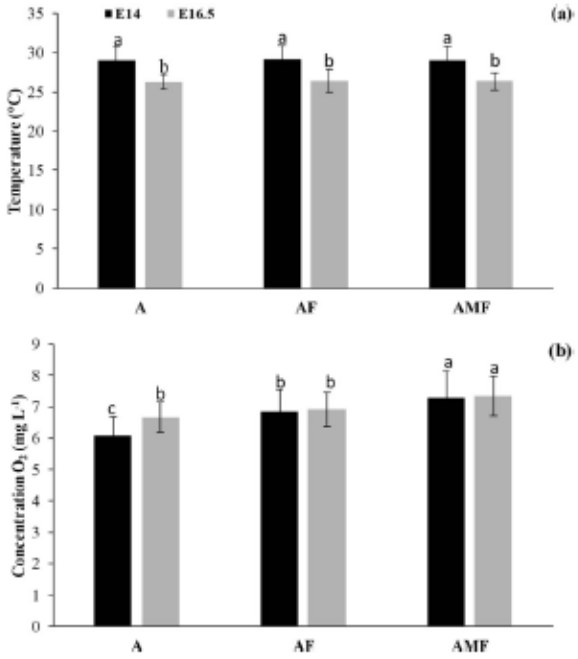

Fig. 3 Average values in the algae tanks of (mean ± SD, $n = 3$) **a** water temperature and **b** dissolved oxygen concentration for the E14 and E16.5 experiments. Treatments: A algae, AF algae + fish, and AMF algae + mussel + fish. Statistical differences are represented as lowercase letters

They also followed the same trend in the input concentration in the three treatments, whereas the retention rates did not (Fig. 5e, f). In E14, retention rates did not differ significantly between treatments (Fig. 5e), whereas in E16.5, treatment A retained more NO_2^- than the other treatments (Fig. 5f). Figure 5e shows the NO_2^- retention in E14, A retained 0.21 ± 0.07 μmol L^{-1}, a mean retention percentage of 63.44%; AF retained 0.36 ± 0.10 μmol L^{-1}, a mean retention percentage of 48.69%; and AMF retained 0.52 ± 0.33 μmol L^{-1}, a mean retention percentage of 44.34% ($P = 0.015$, $F = 2.3$, and $df = 2$ [F-critical = 3.532]). Figure 5f shows that NO_2^- retention in E16.5 for AMF was of 0.26 ± 0.16 μmol L^{-1} with a retention percentage of 14.21%, AF was of 0.41 ± 0.04 μmol L^{-1} with retention of 27.69% and A was of 0.73 ± 0.07 μmol L^{-1} with a mean retention percentage of 81.02% ($P = 0.015$, $F = 9.069$, and $df = 2$ [F-critical = 5.906]).

Nitrate input was not significantly different in both experiments and retention in treatment A was higher than the other treatments (Fig. 5g, h). Figure 5g shows that the NO_3^- retention in E14 for A was 0.53 ± 0.07 μmol L^{-1} with a mean retention percentage of 95.28%, AF was 0.39 ± 0.01 μmol L^{-1} with a retention of 60.49%, and AMF was 0.40 ± 0.03 μmol L^{-1} with a retention of 45.12% ($P = 0.001$, $F = 87.95$, and $df = 2$ [F-critical = 3.487]). Figure 5h shows that the NO_3^- retention in E16.5 for A was 2.14 ± 0.07 μmol L^{-1} with a mean retention percentage of 89.07%, AF was 0.90 ± 0.01 μmol L^{-1} with a retention percentage of 34.90%, and AMF was 0.96 ± 0.10 μmol L^{-1} with a retention of 33.44% ($P < 0.00001$, $F = 1299$, and $df = 2$ [F-critical = 3.127]).

Mean dissolved organic nitrogen in the inlet water of the algae tanks in E14 (Fig. 6a) was of 32.4 ± 0.80 μmol L^{-1} for AF treatment, whereas AMF and A were not significantly different. In E16.5 (Fig. 6a), AMF had the lowest values of organic nitrogen, 17.91 ± 0.62 μmol L^{-1}, differing from the other treatments, 19.80 ± 0.15 μmol L^{-1} for A and 20.83 ± 0.76 μmol L^{-1} for AF ($P = 0.034$, $F = 13.34$, and $df = 2$ [F-critical = 2.896]). Figure 6b shows that the mean dissolved organic phosphorus in E14 showed the same trend observed for the organic nitrogen; the treatment AF had 1.16 ± 0.07 μmol L^{-1}, and AMF and A had values of 1.26 ± 0.22 μmol L^{-1} and 1.15 ± 0.05 μmol L^{-1}, respectively ($P = 0.031$, $F = 44.21$, and $df = 2$ [F-critical = 3.547]). In E16.5 (Fig. 6b), AMF had 0.91 ± 0.02 μmol L^{-1}, AF had 1.06 ± 0.06 μmol L^{-1}, and A 0.52 ± 0.018 μmol L^{-1}, with all treatments differing from each other ($P < 0.0001$, $F = 340.1$, and $df = 2$ [F-critical = 3.544]).

A principal component analysis (PCA) was performed with the percentages of dissolved nutrient retention, growth rate, and O_2 concentration in macroalgae tanks (Fig. 7). The first main component (PC1) accounted for 66.26% of the data variation and the second main component (PC2) accounted for 25.72%. Control A treatments were grouped into two groups, one for E14 and one for E16.5. For A treatment and E16.5, it had greater influence of NO_2^- and NO_3^- retention. The AMF treatments grouped in both E14 and E16.5 experiments had greater influence of retention of NH_4^+, PO_4^{-3}, growth rate (GR), and O_2 concentration. AF also grouped in both tests.

Discussion

For the development of an efficient integrated system of biomass production, it is essential that resources that have not been harvested by a trophic level arrive in the most efficient way for the use of another trophic level. Accordingly, cultivating macroalgae under conditions that favor the availability of dissolved inorganic nitrogen (DIN) is advantageous. The growth of macroalgae is closely linked to the availability of DIN in the seawater. *Ulva lactuca* is considered a nitrophilic species as it requires high nitrogen amounts mainly in the form NH_4^+ (Cohen and Neori 1991) and thus is a suitable candidate for bioremediation purposes (Neori et al. 2000). In this study, higher growth rates were demonstrated for *U. lactuca* at increasing trophic level from AF to AMF treatments in which a concomitant rise of DIN and PO_4^{3-} was also observed. The higher amount of DIN in the AMF treatment results from the organic residues from fish metabolism. This, in turn, was taken advantage of by the mussels incorporating part of this

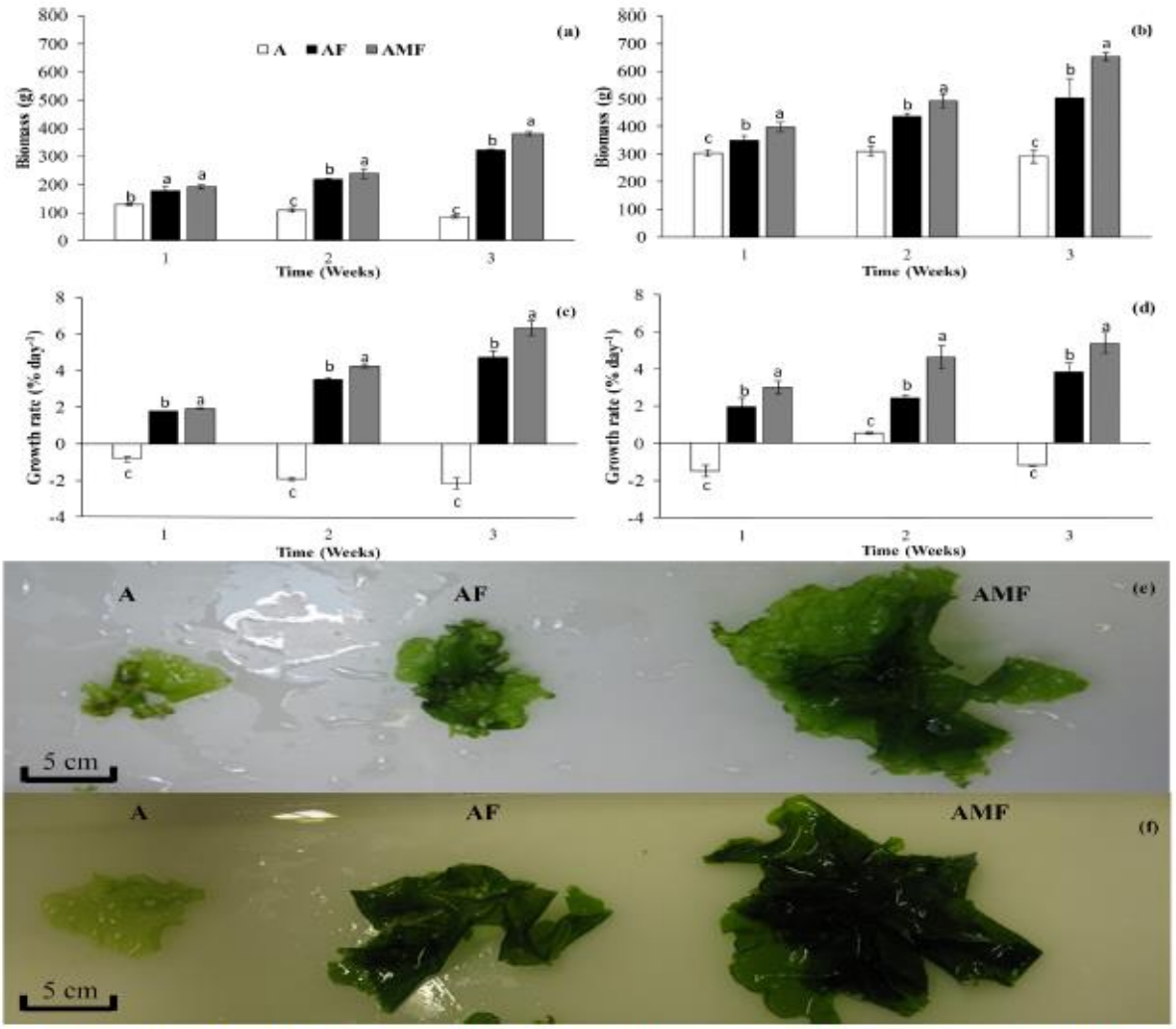

Fig. 4 **a**, **b** Growth of biomass (mean ± SD, $n = 3$), E14 and E16.5 respectively. **c**, **d** Growth rate, E14 and E16.5 respectively over time. **e**, **f** General aspect of *U. lactuca* at the end of each experiment, E14 and E16.5 respectively. Treatments: A algae, AF algae + fish, and AMF algae + mussel + fish. Statistical analyses were performed separately for each week and different lowercase letters represent significant differences

material and excreting additional DIN. As reported in the literature, the integration of different trophic levels tends to increase the productivity of photosynthetic organisms (Shpigel and Neori 1996; Neori et al. 1998) due to the mineralization of organic compounds in DIN. Additionally, Chow et al. (2001) reported increasing levels of NH_4^+ from fish culture and NO_3^- from oyster culture, demonstrating the different contribution of DIN residues by these two cultures, a secondary consumer

Table 1 Biomass produced in relation to feed expenditure for the experiments E14 and E16.5. Δ seaweeds, Δ fishes, and Δ mussels are the biomass variations in the test. Yield is the rate between the total mass and the feed spent on the 100-fold test

	Δ Seaweeds (g)	Δ Fishes (g)	Δ Mussels (g)	Total (g)	Feed (g)	Yield (%)
E14						
AF	581.58	171.89	–	753.47	491.21	153.39
AMF	694.24	187.38	83	964.62	518.49	186.06
E16.5						
AF	899.77	508.57	–	1408.34	1615.99	87.12
AMF	1200.54	409.98	180	1790.52	1560.20	114.80

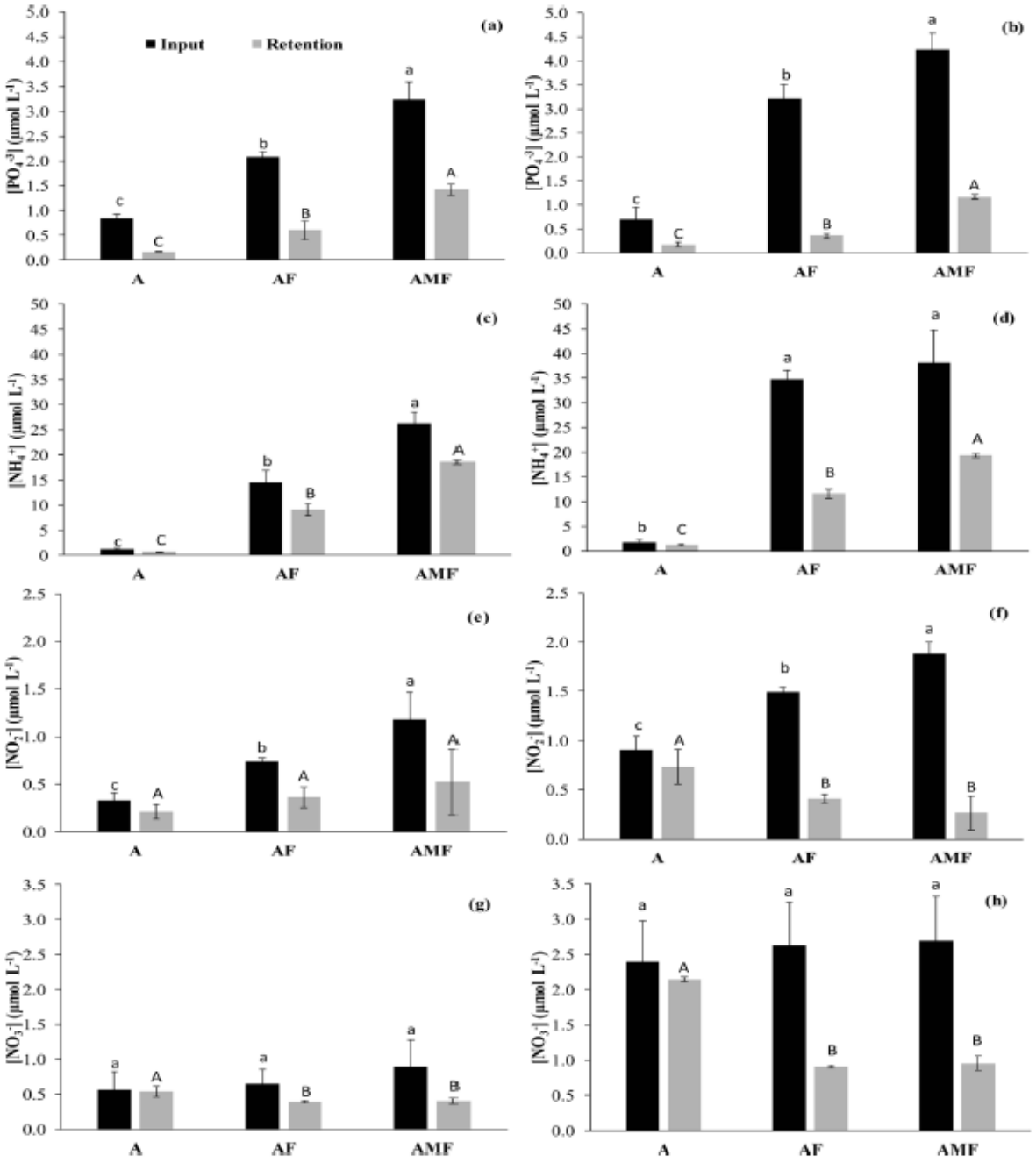

Fig. 5 Input and retention of dissolved inorganic nutrients in the macroalgae tanks (mean ± SD, $n = 3$), E14 (right; **a**, **c**, **e**, **g**) and E16.5 (left; **b**, **d**, **f**, **h**). Treatments: A algae, AF algae + fish, and AMF algae + mussel + fish. Statistical analyses were performed separately for input (lowercase letters) and retention (uppercase letters)

and a filter feeder. Thus, high availability of DIN, mainly in the NH_4^+ form, is beneficial for *U. lactuca* as observed in the present study, with 34–40% higher growth rate in the culture with fish and mussel effluents in relation to cultivation with fish only.

The conditions of the IMTA culture system verified in this study were efficient in the production of algal biomass as growth rates remained positive for treatments with aquaculture effluents in all periods of the experiments. The AMF treatment showed a growth rate similar to that observed by

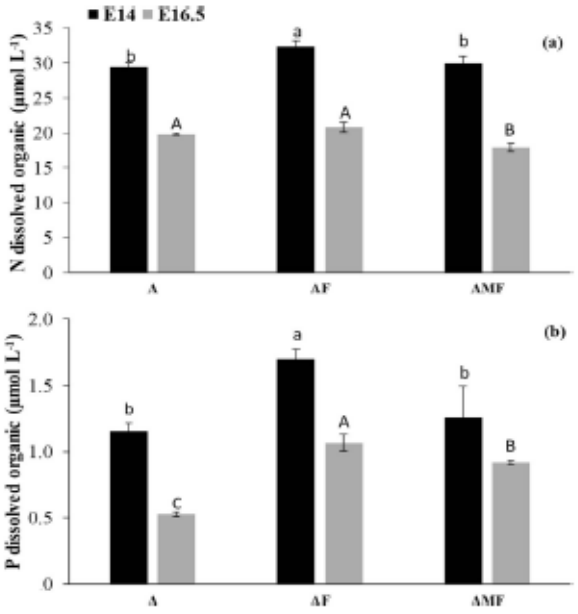

Fig. 6 Input of dissolved organic nutrients in the macroalgae tanks (mean ± SD, $n = 3$), for E14 and F16.5 of **a** organic nitrogen and **b** organic phosphorus. Statistical analyses were performed separately for input (lowercase letters) and retention (uppercase letters)

Robertson-Andersson et al. (2008) (4.7% day^{-1}, algal density of 2 kg m^{-2}, with abalone effluents). Nevertheless, it was lower than that obtained by Neori (1991) (16% day^{-1}, algal density of 2 kg m^{-2}, with fish effluents), most probably because of comparatively much higher availability of DIN, higher NH_4^+ concentration and higher irradiation.

The suitability of *U. lactuca* for ammonium retention was verified in the weekly nutrient retention analyses. In AF and AMF treatments, where NH_4^+ input was high, the mean percentage of retention was of 62.4% in the AF treatment and of 70.3% in the AMP treatment, which are consistent with previously reported values (Cohen and Neori 1991; Neori et al. 1996; Neori and Shpigel 1999; Schuenhoff et al. 2003). For NO_2^- and NO_3^-, the uptake was lower in the AMF and AF treatments, probably because nitrogenous NO_2^- and NO_3^- sources are kinetically less interesting within the nitrogen assimilation pathway since NH_4^+ uptake would allow faster incorporation into organic compounds with lower energy expenditure. Studies have shown that the presence of significant concentrations of NH_4^+ inhibit the uptake of NO_2^- and NO_3^- (Haines and Wheeler 1978; Topinka 1978; Ryther et al. 1981; Chow et al. 2013. PO_4^{3-} presented mean retention values of 28.9% in the AF treatment and 39.7% in the AMF treatment, whereas Neori et al. (1998) reported 25% retention. PO_4^{3-} is well assimilated by seaweeds due to its importance in the constitution of algal cells and its main function is associated with energy transportation in the form of ATP, both in photosynthesis and respiration (Lee et al. 2005).

The integrated aquaculture system assessed in this study using *U. lactuca* as a biological model demonstrated the tendency of increased NH_4^+ and PO_4^{3-} retention, higher growth rate and an increase in water oxygen concentration. Such results in production models are extremely advantageous as they enhance yield and improve water quality, helping maintaining a healthy farming environment. Thus, the incorporation of *U.*

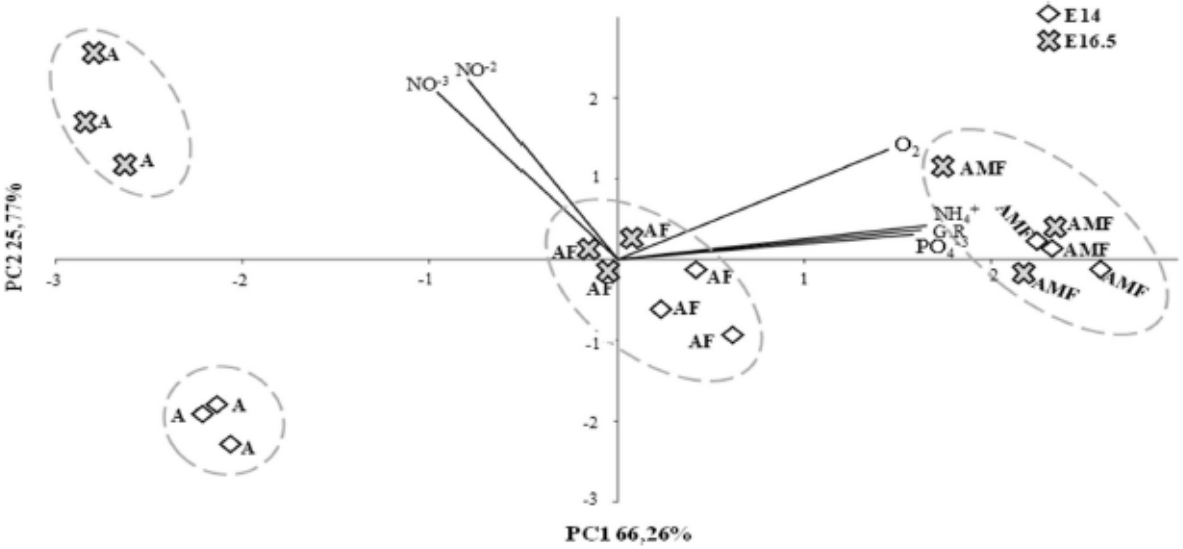

Fig. 7 Principal component analysis biplot of algae cultivation treatments (A algae, AF algae + fish, AMF algae + mussels + fish) and growth rate (GR), retention of dissolved inorganic nutrients (PO_4^{-3}, NH_4^+, NO_2^-, and NO_3^-), and O_2 concentration for E14 and E16.5 experiments. Vectors represent the descriptors

lactuca into an IMTA system, especially when it includes fish and filter-feeders, showed to be sustainable, efficient, and productive.

Conclusion

The cultivation of *U. lactuca* integrated with fish and mussels proved to be efficient in both increasing system yield and bioremediation of its own effluents. Having the ability to assimilate much of NH_4^+ and PO_4^{-3} in addition to having a lower release of organic compounds into the environment, they also increase production with a diverse and productive portfolio, requiring less resource for high yield. This shows the high ecosystem capacity of *U. lactuca*. However, further studies are needed on the complex interactions between species to obtain better results on improving the products yielded by the integrated crop and in preserving the surrounding environment.

Acknowledgments The first author thanks Daniel Eduardo Lavanholi de Lemos for the infrastructure facilities, Luis Felipe de Freitas Fabrizio and Ricardo Otta for help in the construction and maintenance of cultivation systems, FC thanks CNPq for the productivity fellowship (Proc. 303937/2015-7).

References

Alexander KA, Hughes ADA (2017) A problem shared: technology transfer and development in European integrated multi-trophic aquaculture (IMTA). Aquaculture 473:13–19

Armstrong FAJ, Williams PM, Strickland JDH (1966) Photo-oxidation of organic matter in sea water by ultraviolet radiation, analytical and application. Nature 5048:481–463

Armstrong FAJ, Tibbits S (1968) Photochemical combustion of organic matter in sea water for nitrogen, phosphorus and carbon determination. J Mar Biol Assoc UK 48:143–152

Braga ES (1997a) Determinação automática de nitrato. In: Wagener ARL, Carreira R (eds) Métodos analíticos de referência em Oceanografia Química. Rio de Janeiro, MMA/SMA, 6:27–29

Braga ES (1997b) Determinação automática de nitrito. In: Wagener ARL, Carreira R (eds) Métodos analíticos de referência em Oceanografia Química. Rio de Janeiro, MMA/SMA, 7:31–35

Buschmann AH, Varela DA, Hernández-González MC, Huovinen P (2008) Opportunities and challenges for the development of an integrated seaweed-based aquaculture activity in Chile: determining the physiological capabilities of *Macrocystis* and *Gracilaria* as biofilters. J Appl Phycol 20:571–577

Chopin T, Kerin BF, Mazerolle R (1999) Phycocolloid chemistry as a taxonomic indicator of phylogeny in the Gigartinales, Rhodophyceae: a review and current developments using Fourier transform infrared diffuse reflectance spectroscopy. Phycol Res 47:167–188

Chopin T, Buschmann AH, Halling C, Troell M, Kautsky N, Neori A, Kraemer GP, Zertuche-González JA, Yarish C, Neefus C (2001) Integrating seaweeds into aquaculture systems: a key towards sustainability. J Appl Phycol 37:975–986

Chopin T, Robinson S (2004) Defining the appropriate regulatory and policy framework for the development of integrated multi-trophic aquaculture practices: introduction to the workshop and positioning of the issues. Bull Aquacult Assoc Canada 104:4–10

Chopin T, Robinson S (2006) Ration for developing integrated multi-trophic aquaculture (IMTA): an example from Canada. Fish Farmer Mag 65:20–21

Chopin T, Neori A, Buschmann A, Pang S, Sawhney M (2011) Diversification of the aquaculture sector. Seaweed cultivation, integrated multi-trophic aquaculture, integrated sequential biorefineries. Global Aquaculture Advocate 14:58–60

Chow F, Macchiavello J, Santa Cruz S, Fonck E, Olivares J (2001) Utilization of *Gracilaria chilensis* (Rhodophyta: Gracilariaceae) as a biofilter in the depuration of effluents from tank cultures of fish, oysters, and sea urchins. J World Aquacult Soc 32:215–220

Chow F, Pedersén M, Oliveira MC (2013) Modulation of nitrate reductase activity by photosynthetic electron transport chain and nitric oxide balance in the red macroalga *Gracilaria chilensis* (Gracilariales, Rhodophyta). J Appl Phycol 25:1847–1853

Cohen I, Neori A (1991) *Ulva lactuca* biofilters for marine fishpond effluents. I. Ammonia uptake kinetics and nitrogen content. Bot Mar 34:475–482

Edwards P, Pullin RSV, Gartner JA (1988) Research and education for the development of integrated crop-livestock-fish farming systems in the tropics. ICLARM Stud Rev 16:1–53

Ertör I, Ortega-Cerdà M (2015) Political lessons from early warnings: marine finfish aquaculture conflicts in Europe. Mar Policy 51:202–210

FAO (2016) The state of world fisheries and aquaculture 2016. Contributing to food security and nutrition for all. FAO, Rome

Grasshoff K, Kremling K, Ehrhardt M (1999) Methods of seawater analysis, 3rd edn. Wiley-VCH, Weinheim

Haines KC, Wheeler PA (1978) Ammonium and nitrate uptake by the marine macrophytes *Hypnea musciformis* (Rhodophyta) and *Macrocystis pyrifera* (Phaeophyta). J Phycol 14:319–324

Irisarri J, Fernández-Reiriz MJ, Cranford P, Shawn MC (2015) Availability and utilization of waste fish feed by mussels *Mytilus edulis* in a commercial integrated multi-trophic aquaculture (IMTA) system: a multi-indicator assessment approach. Ecol Indic 48:673–686

Lee TM, Tsai PF, Shyu YT, Sheu F (2005) The effects of phosphite on phosphate starvation responses of *Ulva lactuca* (Ulvales, Chlorophyta). J Phycol 41:975–982

Lignell A, Pedersén NM (1989) Agar composition as a function of morphology and growth rate. Studies on some morphological strains of *Gracilaria secundata* and *Gracilaria verrucosa* (Rhodophyta). Bot Mar 32:219–227

Martínez-Espiñeira R, Chpoin T, Robinson S, Noce A, Knowler D, Yip W (2015) Estimating the biomitigation benefits of integrated multi-trophic aquaculture: a contingent behavior analysis. Aquaculture 437:182–194

Neori A (1991) Use of seaweed biofilters to increase mariculture intensification and upgrade its effluents. Rev Fish Israel 24:171–179 (in Hebrew)

Neori A, Krom SP, Ellner CE, Boyd D, Popper R, Rabinovitch PJ, Davison O, Dvir D, Zuber M, Ucko D, Gordin H (1996) Seaweed biofilters as regulators of water quality in integrated fish-seaweed culture units. Aquaculture 141:183–199

Neori A, Ragg NLC, Shpigel M (1998) The integrated culture of seaweed, abalone, fish and clams in modular intensive land-based systems: II. Performance and nitrogen partitioning within an abalone (*Haliotis tuberculata*) and macroalgae culture system. Aquac Eng 17:215–239

Neori A, Shpigel M (1999) Algae treat effluents and feed invertebrates in sustainable integrated mariculture. World Aquac 30:46–51

Neori A, Shpigel M, Ben-Ezra D (2000) A sustainable integrated system for culture of fish, seaweed and abalone. Aquaculture 186:279–291

Neori A, Chopin T, Troell M, Buschmann AH, Kraemer GP, Halling C, Shpigel M, Yarish C (2004) Integrated aquaculture: rationale, evolution and state of the art emphasizing seaweed biofiltration in modern mariculture. Aquaculture 231:361–391

Robertson-Andersson DV, Potgieter M, Hansen J, Bolton JJ, Troell M, Anderson RJ, Halling C, Probyn T (2008) Integrated seaweed cultivation on an abalone farm in South Africa. J Appl Phycol 20:579–595

Ryther JH, Corwin N, Debusk TA, Williams LD (1981) Nitrogen uptake and storage by the red algae *Gracilaria tikvahiae* McLachlan 1979. Aquaculture 26:107–115

Saraiva ESBG (2003) Nitrogênio e fósforo totais dissolvidos e suas frações inorgânicas e orgânicas: Considerações sobre a metodologia aplicada e estudo de caso em dois sistemas estuarinos do estado de São Paulo. Thesis, Institute of Oceanography, University of Sao Paulo

Schuenhoff A, Shpigel M, Lupatsch I, Ashkenazi A, Msuya FE, Neori A (2003) A semirecirculating, integrated system for the culture of fish and seaweed. Aquaculture 221:167–181

Shpigel M, Neori A (1996) The integrated cultures of seaweed, abalone, fish and clams in modular intensive land-based systems: I. Proportions of size and projected revenues. Aquac Eng 15:313–326

Tiller R, Brekken T, Bailey J (2012) Norwegian aquaculture expansion and integrated coastal zone management (ICZM): simmering conflicts and competing claims. Mar Policy 36:1086–1095

Topinka JA (1978) Nitrogen uptake by *Fucus spiralis* (Phaeophyceae). J Phycol 14:241–247

Tréguer P, Le Corre P (1975) Manuel d'analysis des sels nutritifs dans l'eau de mer. 2ème éd. Brest, Université de Bretagne Occidentale

Troell M, Halling C, Neori A, Buschmann AH, Chopin T, Yarish C, Kautsky N (2003) Integrated mariculture: asking the right questions. Aquaculture 226:69–90

Wang X, Olsen LM, Reitan KI, Olsen Y (2012) Discharge of nutrient wastes from salmon farms: environmental effects, and potential for integrated multi-trophic aquaculture. Aquacult Environ Interact 2:267–283

Wood ED, Armstrong FA, Richards FA (1967) Determination of nitrate in seawater by cadmium-cooper reduction nitrite. J Mar Biol Ass UK 47:23–31

Zar JH (1996) Biostatistical analysis, 3rd edn. Prentice-Hall International Editions, New Jersey

ANEXO 12

Aquatic Botany 113 (2014) 107–116

Contents lists available at ScienceDirect

Aquatic Botany

journal homepage: www.elsevier.com/locate/aquabot

Phenology and photosynthetic performance of *Porphyra* spp. (Bangiophyceae, Rhodophyta): Seasonal and latitudinal variation in Chile

F. Tala [a,b,c,*], F. Chow [a]

[a] Instituto de Biociências, Departamento de Botânica, Universidade de São Paulo, Rua do Matão 321, Trav. 14, São Paulo, Brazil
[b] Facultad de Ciencias del Mar, Universidad Católica del Norte, Larrondo 1281, Coquimbo, Chile
[c] Centro de Investigación y Desarrollo Tecnológico en Algas (CIDTA-UCN), Universidad Católica del Norte, Larrondo 1281, Coquimbo, Chile

ARTICLE INFO

Article history:
Received 30 August 2013
Received in revised form 31 October 2013
Accepted 17 November 2013
Available online 7 December 2013

Keywords:
ETR-curve
Phenology
Photosynthesis
Porphyra
Reproduction
Seaweed

ABSTRACT

Phenological studies attempt to understand the seasonal development of organisms in response to environmental variations. Seaweeds can respond (1) as a "seasonal anticipator" with growth occurring due to specific triggers and (2) as a "seasonal responder", with growth and photosynthesis occurring during more favorable conditions. *Porphyra* C. Agardh is an ecophysiologically successful genus that occurs in the uppermost rocky intertidal zone due to its biochemical and physiological traits. In Chile, *Porphyra* is distributed throughout all rocky shores (20–56° S), with at least five types of morphological strains and a still unclear taxonomic status. The phenology (cover, biomass, reproductive porcentage) and photosynthetic performance (ETR–light curves) were studied along a seasonal (winter 2010–winter 2011) and latitudinal gradient (25–34° S) in order to characterize the populations and promote their utilization for human food. Four different morphotypes were detected within the studied populations. Seasonal and latitudinal variations of the environment determined the phenological and ecophysiological responses of *Porphyra* spp. A decline in algal abundance, reproductive potential and photosynthetic performance during warm periods and from southern toward northern latitudes was observed. In a seasonal context, variation in temperature and irradiance can be crucial for the phenological and ecophysiological responses of *Porphyra*, whereas in a latitudinal context, temperature appeared to be more relevant. Most of the patterns observed, probably occurred due to biochemical and physiological traits. Studies on a seasonal and latitudinal scale might enhance the management and use of *Porphyra* as human food.

© 2013 Elsevier B.V. All rights reserved.

FEEDBA

1. Introduction

Phenological studies attempt to understand the seasonal development of organisms (biological events) in response to environmental variations that occur annually (seasonal changes), and how certain abiotic factors induce internal cues at molecular, biochemical, and physiological levels that end up manifesting changes in abundance and reproduction (Espinoza-Avalos, 2005; Forrest and Miller-Rushing, 2010). In a general context, phenology is the temporal dimension of life history, but this temporal dimension is critical because it determines the stage of development reached by an organism or population and its interaction with particular components of the environment (Forrest and Miller-Rushing, 2010). Seaweeds can respond to environmental variability in two ways (*sensu* Kain, 1989): (1) anticipating seasonal changes as an annual strategy rhythm for the species ("seasonal anticipator"), then the growth occurs as a response to a specific trigger and not necessarily when the environmental conditions are suitable for photosynthesis (e.g. day length, level of nutrients) and (2) as a "seasonal responder" when growth and photosynthesis occur when environmental conditions are favorable (e.g. high light).

Phenological-dependence of reproductive strategies plays an important role for dispersal, recruitment, and population maintenance (Santelices, 1990) and are crucial for the dynamic and stability of ecological functioning of marine populations. The life cycle phases can be morphologically and/or physiologically different, showing variations in environmental tolerance with more susceptibility of microscopic stages, impacting directly in the

Abbreviations: A, absorptance; Chl a, chlorophyll a; ETR_{max}, maximum electron transport rate; α_{ETR}, initial slope that define the electron transport efficiency; Fm, maximal fluorescence of dark-adapted sample; Fm′, maximal fluorescence in light pulse; Fv/Fm, maximal quantum yield of PSII; I_k, saturation irradiance; MAAs, mycosporine like-amino acids; NPQ, non-photochemical quenching; PAR, photosynthetically active radiation; *P–I* curve, photosynthetic vs. irradiance curve; P_{max}, maximum photosynthesis; PSI, photosystem I; PSII, photosystem II; ROS, reactive oxygen species; UVR, ultraviolet radiation; Φ_{PSII}, effective quantum yield.

* Corresponding author at: Facultad de Ciencias del Mar, Universidad Católica del Norte, Larrondo 1281, Coquimbo, Chile. Tel.: +56 51 209 797; fax: +56 51 209 812.
E-mail address: ftala@ucn.cl (F. Tala).

0304-3770/$ – see front matter © 2013 Elsevier B.V. All rights reserved.
http://dx.doi.org/10.1016/j.aquabot.2013.11.005

©Fungyi Chow / 2021

phenological patterns (Destombe et al., 1993; Lobban and Harrison, 1994; Vieira and Santos, 2012). The capacity of adjustment and tolerance also depends on the seasonal fluctuation of environmental conditions. Seasonal changes in radiation and temperature are the major drivers for growth, reproduction, and photosynthesis of seaweeds in temperate and polar regions (Kain, 1989; Lüning, 1991; Lobban and Harrison, 1994; Wiencke et al., 2007). However, seaweeds can cope with these adverse conditions by self-shading and overall physiological adjustments, thereby increasing their abundance during winter. The seasonal photosynthetic performance is mainly related to changes in pigment concentrations and photosynthetic parameters (P_{max}, ETR_{max}, α_{ETR} and I_k), which rise during reduced light conditions (Falkowski and LaRoche, 1991; Figueroa et al., 1997; Sampath-Wiley et al., 2008). In general, adaptations to temperature are directly associated with light responses. A decrease in maximal quantum yield of PSII (Fv/Fm) caused by low temperature is also observed during exposure to high-light conditions (Huner et al., 1995). Photoacclimation responses of algae to seasonal changes should enable them to maintain an optimal photosynthetic rate even in extremely variable environments with the time in short- (daily) and long- (annual or interannual) scales.

A large variety of seaweeds inhabits the intertidal zone, which is characterized by fluctuating and extreme abiotic conditions such as e.g. tidal emersions and air exposure. Under these conditions, sessile benthic organisms become constantly exposed to increasing irradiance (PAR and UVR), changes in temperature, salinity, desiccation, and nutrient unavailability (Lüning, 1991; Lobban and Harrison, 1994; Davison and Pearson, 1996). Seaweed survival under extreme environmental conditions is possible due to several morphological changes (i.e. thallus shape, size, and thickness) and biochemical/physiological advantages such as cellular ability to tolerate desiccation during tidal regimen (Davison and Pearson, 1996; Sampath-Wiley et al., 2008), variation in organic osmolytes compensating hyperosmotic conditions (Karsten et al., 1996; Karsten, 1999), high photosynthetic recovery capacity following air exposure (Figueroa et al., 1997; Gómez et al., 2004; Sampath-Wiley et al., 2008), high content of photoprotective compounds (Gröniger et al., 1999; Huovinen et al., 2004; Bouzon et al., 2012) and efficient enzymatic and non-enzymatic mechanisms to attenuate the oxidative damage (Mittler, 2002; Sampath-Wiley et al., 2008; Contreras-Porcia et al., 2011; Bouzon et al., 2012). Given these characteristics, seaweeds are able to recover quickly during rehydration (Davison and Pearson, 1996; Kim et al., 2008). Their tolerance mechanisms have been related to patterns of vertical zonation, where individuals with an enhanced capacity of responses are able to inhabit the uppermost areas in the intertidal zone (Collén and Davidson, 1999; Gómez et al., 2004; Hays, 2007; Kim et al., 2008).

Porphyra C. Agardh is one of the ecophysiologically most successful red alga, and grows abundantly along rocky intertidal or shallow subtidal zones of cold-temperate, polar and boreal shores of the Northern and Southern hemispheres. Some species from genus *Porphyra*, *Bangia*, *Blidingia*, *Prasiola*, and *Pelvetia* are well adapted to occur in the uppermost intertidal zone, where the occurrence of other algae is unusual or hard (Lüning, 1991). *Porphyra* is characterized by a heteromorphic biphasic life cycle with a particular long fertile season. Foliose blades (gametophytic stage) alternate with a small filamentous sporophyte (called the shell-boring "conchocelis" phase), having the ability to become fertile for several seasons (Israel, 2010). Most species of *Porphyra* show a seasonal recruitment pattern, with distinct seasonal gametophyte development (Dickson and Waaland, 1985; Griffin et al., 1999; Holmes and Brodie, 2004; Varela-Alvarez et al., 2007). Temperature and photoperiod are shown to have strong effects on the phenological and morphological patterns in *Porphyra* species (Brown et al., 1990; Israel, 2010). *Porphyra* (commonly known as *nori* in Japan and *zicai* in China) is the major source of red algae as food for humans and actually it is the most valuable seaweed grown in mariculture (Israel, 2010).

In Chile, *Porphyra* spp. (*luche*, common name) is distributed along the coast (20–56° S), with at least five different morphological strains (Ramírez and Santelices, 1991). The genus has a simple morphology but the differentiation between species due to morphological characteristics is a difficult task (Israel, 2010) and the taxonomic elucidation for *Porphyra* species in Chile still needs to be clarified (Brodie et al., 2008). Since early times, the exploitation of *Porphyra* in Chile is mainly restricted to southern regions by artisanal fishermen communities with a great annual variation in biomass landing (Buschmann et al., 2008). In the last decades, it has been considered as a candidate for the development of small-scale aquaculture for fishermen in the frame of an intergovernmental program that expands aquaculture in the country. Commercially more interesting species such as *P. linearis* Greville, *P. pseudolinearis* Ueda, *P. miniata* (C. Agardh) C. Agardh, *P. capensis* Kützing, *P. woolhousiae* Harvey, *P. lanceolata* Smith et Hollenberg, *P. torta* Krishnamurthy, and *P. thuretii* Dawson also occur in Chile (González and Santelices, 2003), are attracting new possibilities for *Porphyra* cultivation and exploitation. Some of these species are referred now as *Pyropia* J. Agardh and *Wildemania* De Toni genus (Sutherland et al., 2011).

The phenological development of the *Porphyra* complex is poorly known in Chile and its management as well as exploitation proposals need to be supported by biological and ecophysiological knowledge. The phenology (cover, biomass, reproductive frequency) and photosynthesis performance (ETR–light curves as productivity indicators) of *Porphyra* spp. were studied along a seasonal and latitudinal gradient in three locations between 25° S and 34° S in Chile in order to characterize the populations and promote their economic usage, depending on latitudinal conditions.

2. Materials and methods

2.1. Location, sampling and environmental characterization

Since the taxonomic situation of the genus *Porphyra* is not yet fully resolved in Chile, and specimens along the coast can be represented by different species and morphotypes within the same or between different locations, in the present study each population was treated as a separate identity, maintaining *Porphyra* as a genus. Three coastal sites along the north-center of Chile were selected for sampling *Porphyra* spp. populations. The sites are characterized by exposed rocky shores, with a typical zonal distribution of *Porphyra* in the higher intertidal. Within the macrozone considered in the study, the northern area corresponds to Taltal (Region of Antofagasta at 25°27′23″ S–70°31′17″ W) the central area to Tongoy (Region of Coquimbo at 30°15′ S–71°2′ W) and the southern area to Pichilemu (Region of O'Higgins at 34°22′ S–72°00′ W) (Fig. 1). Between the northern and the southern sampling area there is a distance of 1400 km, with Tongoy being situated in the middle.

Algae were sampled from austral winter 2010 to 2011. This sampling time was chosen in order to characterize the seasonal phenological cycle of *Porphyra* spp. populations. Due to logistic problems there was no sampling for Taltal during springtime. The abiotic characteristics of the geographic zones were registered from www.shoa.cl (Hydrographic and Oceanographic Service of the Chilean Navy) for seawater temperature, and from the Project CHI/00/G32 (Sarmiento, 2008) for global radiation. Data for UV index were obtained by www.meteochile.cl. The Humboldt Current System acts along the coast of Chile with an equatorward flow, and different climatic areas are mainly present with respect to temperature and rainfalls (Fernandez et al., 2000).

©Fungyi Chow / 2021

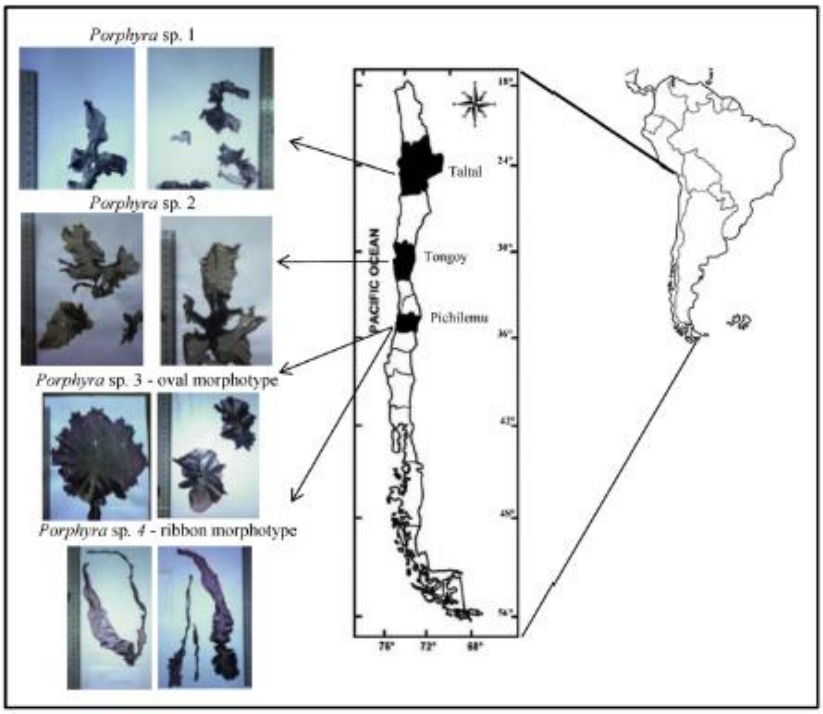

Fig. 1. Map of Chile with the locations of the studied populations of *Porphyra* spp. and the respective morphotypes for each locality. *Porphyra* sp.1 from Taltal (north) with small blades and ovate to lanceolate morphology, *Porphyra* sp.2 from Tongoy (central) with ovate blade morphology that is simple or divided, *Porphyra* sp.3 from Pichilemu (south) with oval morphology and wavy margins, *Porphyra* sp.4 from Pichilemu with ribbon blade morphology between linear to lanceolate shape.

Within the studied populations four different morphoytpes of *Porphyra* were detected (Fig. 1). Therefore, each morphotype was treated separately. The *Porphyra* sp.1 morphotype was found within the Taltal population and is characterized by mainly small blades with an obovate to lanceolate morphology, while *Porphyra* sp.2 was found in Tongoy, having an ovate blade morphology that can be single or divided into 2 or more linear to lanceolate blades. The *Porphyra* sp.3 morphotype is from Pichilemu, characterized by oval blade morphology with wavy margins. Additionally, the *Porphyra* sp.4 morphotype was found in Pichilemu, showing a ribbon blade morphology that can vary between linear and lanceolate shapes (Fig. 1).

2.2. Phenology: percentage of cover, biomass and reproductive porcentage

Seasonal and latitudinal changes of blade abundance of *Porphyra* spp. were evaluated as cover (%) by using three frames of 10 m^2 (10 m length and 1 m width) that were positioned parallel to the coastline in the distribution area. In each frame, three sampling units of 1 m^2 (1 m × 1 m) were placed randomly in order to determine the total cover ($n = 9$ replicates). In addition, total biomass (g wet weight m^{-2}) and reproductive biomass (%) were evaluated by placing inside each 1 m^2 quadrat a smaller quadrat of 20 cm × 20 cm from wherever all blades were carefully detached and transported in coolers to the Marine Botany Laboratory, Universidad Católica del Norte, Coquimbo, Chile. From the sampled blades, total and reproductive biomass was determined as wet weight (ww) from the smaller quadrat and extrapolated to 1 m^2. The annual mean algal dry weight (%) was 16.3 ± 0.2 for Taltal; 18.5 ± 2.9 for Tongoy; 19.4 ± 3.3 for Pichilemu-oval, and 19.5 ± 2.8 for Pichilemu-ribbon morphotypes.

Reproductive monoecious blades were recognized by the presence of a reddish color in the center as well as at the distal part of the blade, where carposporangial and spermatangial cells are formed. Due to the fact that two morphotypes occur together in Pichilemu, abundance and reproductive frequency were not possible to register separately. Entire blades of *Porphyra* spp. from each morphotype were acclimated for 24 h in a flow-through seawater tank (60 L) to measure photosynthetic performance. The indoor tank was maintained with natural solar light across an acrylic roof and without control of seawater temperature.

2.3. Photosynthetic performance

Electron transport rate (ETR) from curves of photosynthetic vs. light curves (P–I) were used to evaluate the seasonal and latitudinal performance of *Porphyra* spp. as an indirect estimate of primary production (Figueroa et al., 2003). Each blade ($n = 9$ by season and locality) was dark-adapted for 5 min and then irradiated with increasing intensities of PAR (0–1300 μmol photons m^{-2} s^{-1}) provided by a light-emitting-diode lamp of the portable fluorometer (PAM-2500, Walz, Effeltrich, Germany). The ETRs were estimated from $ETR = \Phi_{PSII} \times PAR \times A \times 0.15$ (Maxwell and Johnson, 2000) where Φ_{PSII} is the effective quantum yield, A is the absorptance of the blade, and 0.15 is the fraction of absorbed quanta directed to PSII for red algae (Grzymski et al., 1997). The blade absorptance of each sample (ratio of absorbed irradiance to incident upon the sample) was measured by placing the blade on a cosine-corrected PAR sensor (LI-190SA, Lincoln, USA) and according to Mercado et al. (1996) calculated from $A = 1 - I_t/I_o$, where I_t is

©Fungyi Chow / 2021

the transmitted light across the blade sample and I_o is the incident light from a fixed light source.

To estimate ETR parameters, a modified nonlinear function of Jassby and Platt (1976) was fitted to each data set from $ETR = ETR_{max} \times \tanh(\alpha_{ETR} \times PAR/ETR_{max})$. ETR_{max} is a maximum electron transport rate (μmol eletrons m^{-2} s^{-1}) at saturating irradiance; tanh is the hyperbolic tangent function; α_{ETR} [μmol eletrons m^{-2} s^{-1}] [μmol photons m^{-2} s^{-1}] is the initial slope of *P–I* curve that indicates the electron transport efficiency at low irradiance; and *I* is the irradiance. The saturation irradiance for electron transport (I_k) was calculated as the intercept between α_{ETR} and ETR_{max} values (ETR_{max}/α_{ETR}). Non-photochemical quenching (NPQ) was calculated from the *P–I* curve as (Fm – Fm′)/Fm′ (Maxwell and Johnson, 2000), where Fm is the maximal fluorescence of dark-adapted samples and Fm′ is the maximal fluorescence of the last saturating light pulse.

2.4. Statistical analyses

One-way ANOVA was used to evaluate the seasonal variations of the studied variables for each population in a separate way. A two-way ANOVA, with season and latitude as main factors was applied for latitudinal comparisons. Considering the unbalanced design, due to missing spring data for Taltal, the latitudinal differences were evaluated only including the contrast season (summer and winter 2011) for variables such as abundance (cover), reproductive frequency, *P–I* curve parameters (ETR_{max}, α_{ETR}, and I_k), and NPQ. Prior to analyses, percentage cover data as well as reproductive frequencies were arcsine transformed. Normality (Kolmorov–Smirnov test) and homogeneity of variances (Levene test) were used. Since data transformation in some cases did not remove heteroscedasticity, all data were analyzed using a more conservative $\alpha = 0.01$ (Underwood, 1997). When ANOVA revealed significant differences, a post hoc Tukey HSD was applied.

3. Results

3.1. Environmental characteristics in geographic zones

Seasonal changes in seawater surface temperature, global radiation, and UV index were detected for all geographic zones. In general, higher values were observed toward spring and summer, whereas lower values were observed during winter (Fig. 2). For seawater temperature significant latitudinal differences were shown ($F_{(2,42)} = 16.362$; $P < 0.01$), with lowest values toward the southern sampling area (Fig. 2A). The monthly global radiation and UV index showed a slight latitudinal difference during autumn–winter months (Fig. 2B and C), but without significant differences ($F_{(2,33)} = 0.737$, $P = 0.486$; $F_{(2,33)} = 0.216$, $P = 0.807$ respectively).

3.2. Abundance variation

The three populations studied showed different phenological patterns among seasons, with significant differences ($P < 0.001$) in algal cover and biomass (for all populations). In Taltal, the northernmost population, *Porphyra* sp.1 blades disappeared completely from the intertidal rocky shore during summer and recruits were observed in autumn (Fig. 3A; Cover $F_{(2,33)} = 117.94$, $P < 0.001$; Biomass $F_{(2,33)} = 54.35$, $P < 0.001$). The population of Tongoy situated in the center of the sampling area, with *Porphyra* sp.2 morphotype, showed low abundances of macroscopic blades during spring and summer (Fig. 3A; Cover $F_{(4,40)} = 109.61$, $P < 0.001$; Biomass

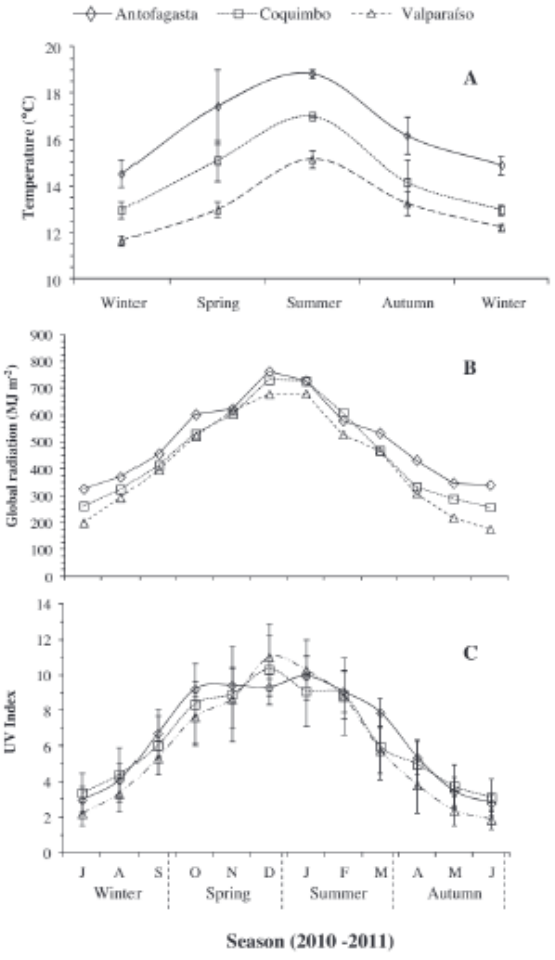

Fig. 2. Seasonal and latitudinal variation of (A) seawater temperature from winter 2010 to winter 2011 (source: www.shoa.cl); (B) global radiation within 10 years (source: Project CHI/00/G32 – PNUD), and (C) annual UV index between 2010 and 2011 (source: www.meteochile.cl) in the geographic zones studied. Antofagasta represents Taltal (north), Coquimbo represents Tongoy (central), and Valparaíso represents Pichilemu (south).

$F_{(4,40)} = 42.13$, $P < 0.001$). Overall algae were characterized by small sized and discolored yellowish thalli. Contrarily, in the southernmost sampling area (Pichilemu), blades of *Porphyra* maintained their high coverage (Fig. 3A) and biomass during the year (Fig. 3B), with a slight decrease in summer (Cover $F_{(4,40)} = 32.77$, $P < 0.001$; Biomass $F_{(4,40)} = 2.71$, $P = 0.043$). Both morphotypes (*Porphyra* sp.3 and sp.4) were always observed mixed without any apparent difference in their frequency of occurrence throughout the sampling period.

A decrease in the abundance of *Porphyra* was observed from southern to northern populations. A significant difference in algal cover with latitude ($F_{(2,53)} = 147.921$; $P < 0.01$) and an interaction effect ($F_{(2,53)} = 20.306$; $P < 0.01$) between latitude × season was detected (Table 1). Similarly, for algal biomass, differences were detected between season ($F_{(1,53)} = 48.914$; $P < 0.01$), latitude ($F_{(2,53)} = 32.579$; $P < 0.01$) and for the interaction between latitude × season ($F_{(2,53)} = 5.009$; $P < 0.01$) (Table 1).

©Fungyi Chow / 2021

Table 1
Two-way ANOVA for latitude (Taltal, Tongoy and Pichilemu) and season (summer 2011 and winter 2011) for the variables of cover, biomass, and reproductive biomass of *Porphyra* spp. in the populations studied. Taltal represents the northern area (*Porphyra* sp.1), Tongoy the central area (*Porphyra* sp.2) and Pichilemu the southern area (*Porphyra* sp.3 and sp.4). For post hoc results S = summer; W = winter; Ta = Taltal; To = Tongoy; P = Pichilemu.

Source of variation	df	*F*-ratio	Post hoc results (Tukey HSD)
Cover			
Latitude (L)	2	147.921*	Ta < To < P
Season (S)	1	383.646*	S 2011 < W 2011
L × S	2	20.306*	S-Ta < S-To < W-Ta < S-P < W-To < W-P
Residual	48		
Biomass			
Latitude	2	32.579*	Ta < To < P
Season	1	48.914*	S 2011 < W 2011
L × S	2	5.009*	S-Ta < S-To < W-Ta < W-To = S-P = W-P
Residual	48		
Reproductive biomass			
Latitude	2	89.868*	Ta < To < P
Season	1	90.441*	S 2011 < W 2011
L × S	2	39. 006*	S-Ta = S-To < W-Ta < S-P = W-P (=W-To)
Residual	48		

* $P < 0.001$.

3.3. Reproductive biomass

The seasonal variation in reproductive biomass was dependent on the latitude and different patterns were observed in each locality (Fig. 3). The population from Taltal (north) was reproductive only in winter, while the Tongoy population (center) was reproductive almost all year, with highest abundance of reproductive blades during winter that decreased in autumn and spring (Fig. 3C). In Pichilemu (south), *Porphyra* maintained more than 50% of its reproductive porcentage during the year without a clear seasonal pattern (Fig. 3C). Overall, seasonal differences in the reproductive biomass ($P < 0.01$) were only detected for the population from Taltal ($F_{(3,32)} = 36.83$, $P < 0.001$) and Tongoy ($F_{(4,40)} = 146.23$, $P < 0.001$). Pichilemu population did not show significant variation in reproductive porcentage ($F_{(3,32)} = 36.83$, $P = 0.473$).

Differences in the reproductive biomass were detected between the localities ($F_{(2,53)} = 89.868$; $P < 0.01$) and for the interaction ($F_{(2,53)} = 39.006$; $P < 0.01$) between latitude × season (Table 1). A decrease in reproductive biomass was observed for the northern population of Taltal whereas Pichilemu maintained the higher values.

3.4. Photosynthetic performance

Seasonal and latitudinal variation of maximal electron transport rates (ETR_{max}), saturation irradiance (I_k), photosynthetic efficiency (α_{ETR}) (Fig. 4), and blade absorptance (Fig. 5) were shown for all populations as well as differences in photosynthesis vs. irradiance (*P–I*) curves.

The Taltal population (*Porphyra* sp.1) showed a seasonal adjustment in ETR_{max} ($F_{(2,24)} = 6.158$; $P < 0.01$) with higher values in autumn than in winter (Fig. 4A and Table 2). No differences in the seasonal change of I_k ($F_{(2,24)} = 2.424$, $P = 0.11$) and α_{ETR} ($F_{(2,24)} = 1.273$, $P = 0.298$) in the Taltal (north) population were detected (Table 2). For the Tongoy (center) population (*Porphyra* sp. 2), seasonal variations were observed for ETR_{max} ($F_{(4,44)} = 23.676$; $P < 0.01$), I_k ($F_{(4,44)} = 25.528$; $P < 0.01$), and α_{ETR} ($F_{(4,44)} = 14.499$; $P < 0.01$), with higher ETR_{max} and α_{ETR} in autumn and winter 2011, and maximal I_k in summer (Fig. 4B and Table 2). Both morphotypes from the Pichilemu (south) population (*Porphyra* sp.3 and 4) showed similar photosynthetic responses within all seasons (Fig. 4C and D and Table 2). For *Porphyra* sp.3, seasonal variations were observed only for ETR_{max} ($F_{(4,32)} = 4.222$; $P < 0.01$) and I_k ($F_{(4,32)} = 11.903$; $P < 0.01$). Whereas *Porphyra* sp.4 showed significant seasonal changes for the three parameters: ETR_{max} ($F_{(4,32)} = 3.187$, $P = 0.026$); I_k ($F_{(4,32)} = 6.886$, $P < 0.01$); α_{ETR} ($F_{(4,32)} = 6.466$, $P < 0.01$), maximal values were estimated for ETR_{max} in spring, for I_k in autumn, and for α_{ETR} in winter and spring (Table 2). Only minor differences in the *P–I* curves were detected between winter 2010 and winter 2011 for all studied populations (Fig. 4 and Table 2).

Comparative analyses of photosynthetic parameters among populations showed that the two morphotypes from Pichilemu had a higher ETR_{max}, α_{ETR} and I_k than the morphotype from Taltal, whereas the morphotype from Tongoy showed an intermediate response (Fig. 4). For ETR_{max}, significant differences between latitude, season (summer 2011 vs. winter 2011) as well as an interaction between latitude × season were detected ($P < 0.01$) (Table 3). Similarly, for I_k significant differences were shown between latitude and for the interaction latitude × season (Table 3). For the photosynthetic efficiency (α_{ETR}) a significant interaction between latitude × season was observed ($P < 0.01$).

Non-photochemical quenching (NPQ) indexes showed no clear seasonal variations but were dependent on latitude (Table 2). Seasonal changes in NPQ were significantly different only for populations from Tongoy (central) ($F_{(2,44)} = 8.948$; $P < 0.01$), and for the Pichilemu (south) ribbon morphotype ($F_{(2,36)} = 9.704$; $P < 0.01$), showing higher values in autumn and winter 2011 (Table 2). Latitude differences ($F_{(3,69)} = 51.026$; $P < 0.01$) in NPQ were also detected when compared summer 2011 and winter 2011 (Table 3), and among seasons ($F_{(1,69)} = 23.246$; $P < 0.01$). Additionally, a latitude–season interaction in NPQ values ($F_{(3,69)} = 7.153$; $P < 0.01$) was valid (Table 3). Latitudinal differences were observed for all populations except between the Tongoy (center) and the Pichilemu (south) oval morphotype. All *Porphyra* morphotypes tested herein showed high NPQ values in winter 2011 with the exception of the Pichilemu oval morphotype. No significant difference in NPQ between summer and winter was detected for this morphotype (Table 2).

Porphyra spp. thallus absorptance varied between 0.4 and 0.9, depending on season and latitude (Fig. 5). Significant seasonal changes in thallus absorptance ($P < 0.01$) were detected for morphotypes from Taltal ($F_{(2,24)} = 26.86$, $P < 0.01$), Tongoy ($F_{(4,40)} = 50.603$, $P < 0.01$), and for the Pichilemu ribbon morphotype ($F_{(4,32)} = 6.648$, $P < 0.01$). The Pichilemu oval morphotype maintained similar values ($P > 0.01$) throughout the seasons. A decrease during spring–summer and an increase toward autumn was shown (Fig. 5). Latitudinal differences ($F_{(3,69)} = 91.783$; $P < 0.01$) in the absorptance were also detected when compared between summer 2011 and winter 2011 (Table 3). Significant variations in thallus

©Fungyi Chow / 2021

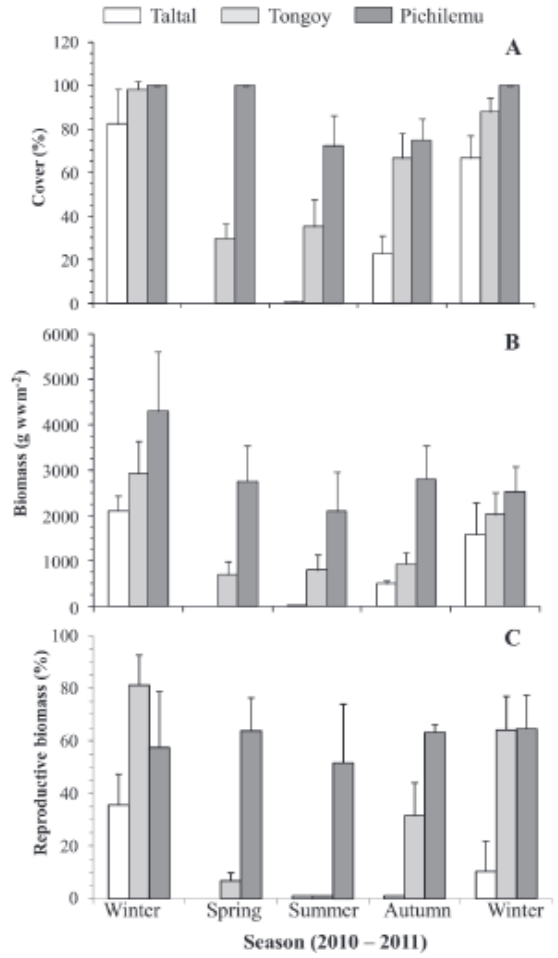

Fig. 3. Seasonal and latitudinal variation of (A) abundance (cover – %); (B) biomass (g ww 0.04 m^{-2}) and (C) reproductive biomass (%) of *Porphyra* spp. in the geographic zones studied in Chile. No data were obtained for Taltal in spring, and no reproductive blades were detected for Taltal and for Tongoy in summer, as well as for Taltal in autumn. Taltal represents the northern area (*Porphyra* sp.1), Tongoy the central area (*Porphyra* sp.2) and Pichilemu the southern area (*Porphyra* sp.3 and *Porphyra* sp.4). Data shown are means ± SD.

absorptance were dependent on season, since only during summer the populations showed differences ($P < 0.01$), with higher values for both Pichilemu (south) morphotypes compared to the morphotype from Tongoy (center) (Fig. 5).

4. Discussion

Seasonal and latitudinal variations of environmental conditions determine the phenological and ecophysiological responses of *Porphyra* spp. from the different populations tested herein along the Chilean coast. The most notorious temporal adjustment comprises an annual vs. perennial development with an increase in abundance with latitude. Whereas different phenological and photosynthetic patterns were observed between morphotypes, the taxonomic clarity is crucial in order to explain species-specific patterns or ecotypic differentiation within temporal and latitudinal responses. Molecular and culture studies under controlled environmental conditions can be helpful to resolve the species or ecotype differentiation observed in the morphotypes.

As was mention by Brodie et al. (2008), the *Porphyra* flora in Chile is rich, with many unidentified species that request more studies. However, some species refereed early as *Porphyra*, now are in the genus *Pyropia* and *Wildenmania* (Sutherland et al., 2011), so the real Bangiales richness in Chile is undetermined. Considering some general characteristics observed in the morphotypes, the genus *Wildenmenia* could be discarded because it is manly bistromatic and inhabits in the low intertidal and subtidal (González and Santelices, 2003; Sutherland et al., 2011). All morphotypes studied occur in the upper intertidal, with a monostromatic and monoecious blade. The knowledge contribution of some aspects of Bangiales flora in the south-east Pacific coast is important in ecological and biogeographic level in one of the oldest group of eukaryote; also in an economic context by the potential of new resources for food and other industries. In general, the phenological pattern follow the same trend than another *Porphyra* species (Brown et al., 1990; Griffin et al., 1999; González and Santelices, 2003; Holmes and Brodie, 2004; Varela-Alvarez et al., 2007; Kim et al., 2008; Sampath-Wiley et al., 2008; Israel, 2010) from temperate-cold coast that also showed photosynthetic adjust with season and latitude changes.

4.1. Seasonal pattern in abundance, reproduction and photosynthetic traits

Phenological differences within or between species can result from gradients of physical factors and their variation over time (e.g. Brown et al., 1990; Griffin et al., 1999; González and Santelices, 2003; Holmes and Brodie, 2004). Differences in seasonal phenological patterns have been described for species of *Porphyra* with annual gametophyte recruitment that occurred either in spring–summer or autumn–winter, leading to distinct annual summer or winter gametophyte populations (Dickson and Waaland, 1985; Waaland et al., 1990; Griffin et al., 1999; Holmes and Brodie, 2004).

A clear seasonal reproduction was only observed for Taltal (north) and Tongoy (center), both having their reproductive peak in winter, whereas the Pichilemu population (south) maintained more than 50% of their reproductive blades during all seasons. The Taltal population (*Porphyra* sp.1) can be defined as an annual species that the macroscopic blades disappeared completely in summer. In contrast, the populations from Tongoy (*Porphyra* sp.2) and Pichilemu (*Porphyra* sp.3 and sp.4) persisted throughout the year. Abundance patterns have been described for *Porphyra* species in central Chile, showing interannual and seasonal variation (González and Santelices, 2003). Short and seasonal peaks in abundance during late winter and early spring are described (*P. linearis* and *P. pseudolinearis*) in contrast to relative persistent densities (*P. columbina*) (González and Santelices, 2003). In the north, the macroscopic thallus of *Porphyra* sp.1 might be susceptible to high summer environmental conditions (radiation and temperature), and tissue deterioration can occur after the release of reproductive gametes during winter. Possibly, during spring–summer conditions the microscopic stage (conchocelis phase) develops, which might then grow protected in bivalve shells or in soft substrate within the intertidal zone. Subsequently, in late autumn to early winter, the conchocelis stages mature and release spores (i.e. conchospores), resulting in a foliose phase (Brown et al., 1990; Waaland et al., 1990; Israel, 2010). The persistent cover and higher reproductive frequency observed for both morphotypes from the southern *Porphyra* suggests a non-seasonal population. The blades can develop from either vegetative archeospores or by conchospores from conchocelis stage that are maintained in the microhabitat. Both mechanisms have been described frequently for *Porphyra* species (Holmes and Brodie, 2004; Israel, 2010).

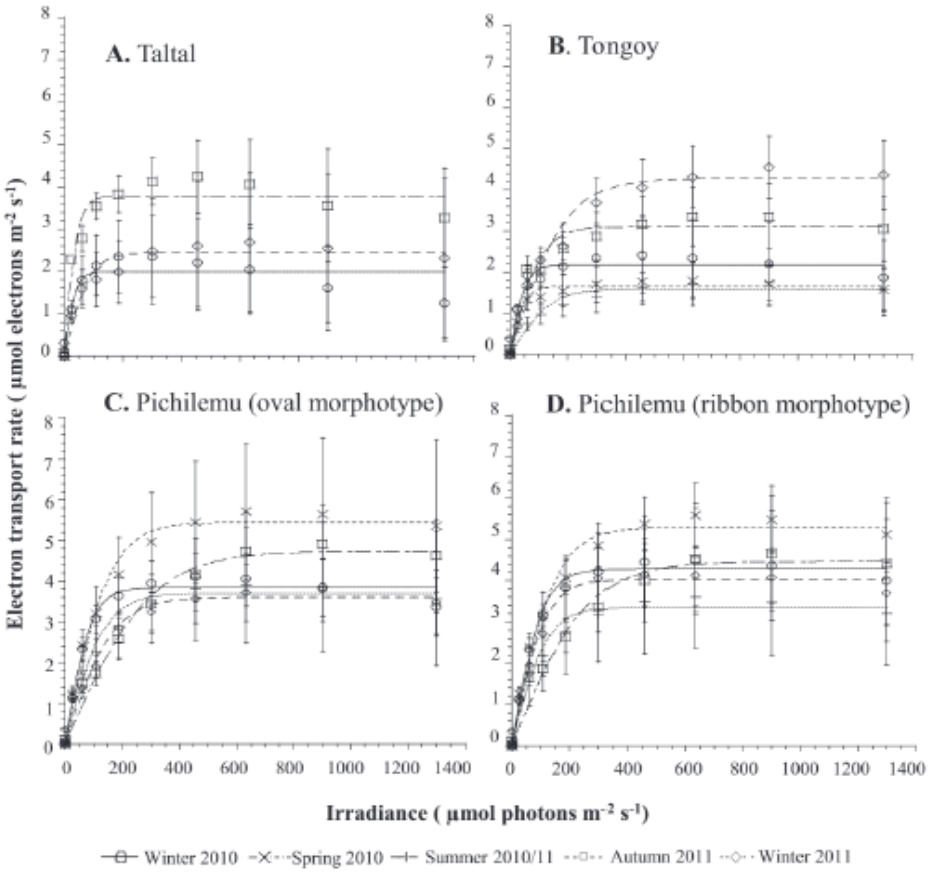

Fig. 4. Seasonal and latitudinal variation in ETR-irradiance curves of (A) Taltal represents the northern area (*Porphyra* sp.1), (B) Tongoy the central area (*Porphyra* sp.2) and Pichilemu the southern area for (C) *Porphyra* sp.3 and (D) *Porphyra* sp.4. No data were present for Taltal in spring, and no blades were detected for Taltal in summer. Data shown are means ± SD.

Table 2
Photosynthetic parameters (mean ± SD) ETR_{max} (µmol electrons $m^{-2} s^{-1}$); I_k (saturation irradiance, µmol photons $m^{-2} s^{-1}$); α (photosynthetic efficiency [µmol electrons $m^{-2} s^{-1}$] [µmol photons $m^{-2} s^{-1}]^{-1}$); NPQ (non-photochemical quenching) in *Porphyra* spp. from the populations studied in Chile. For each parameter and locality letters represent the post hoc results of seasonal comparison.

	ETR_{max}	I_k	α	NPQ
Taltal				
Winter 2010	2.0 ± 0.9^{a}	38.8 ± 19.3^{a}	0.06 ± 0.02^{a}	0.430 ± 0.118^{a}
Autumn 2011	3.9 ± 0.9^{b}	77.4 ± 32.7^{a}	0.06 ± 0.03^{a}	0.650 ± 0.099^{b}
Winter 2011	2.6 ± 1.5^{ab}	85.9 ± 54.8^{a}	0.04 ± 0.02^{a}	0.490 ± 0.281^{ab}
Tongoy				
Winter 2010	2.2 ± 0.9^{abc}	55.5 ± 32.2^{a}	0.05 ± 0.020^{a}	0.499 ± 0.164^{a}
Spring 2010	1.7 ± 0.4^{b}	54.2 ± 18.1^{a}	0.03 ± 0.010^{ab}	0.604 ± 0.133^{a}
Summer 2011	1.6 ± 0.4^{ab}	209.7 ± 51.7^{bc}	0.01 ± 0.002^{c}	0.650 ± 0.118^{ac}
Autumn 2011	3.1 ± 0.7^{c}	85.4 ± 61.2^{a}	0.05 ± 0.020^{a}	0.895 ± 0.198^{b}
Winter 2011	4.2 ± 0.8^{d}	158.8 ± 24.0^{c}	0.03 ± 0.003^{b}	0.828 ± 0.191^{c}
Pichilemu (oval morphotype)				
Winter 2010	3.9 ± 0.6^{a}	90.1 ± 19.4^{a}	0.04 ± 0.010^{a}	0.482 ± 0.153^{a}
Spring 2010	5.6 ± 1.7^{b}	151.9 ± 54.5^{ac}	0.04 ± 0.010^{a}	0.588 ± 0.214^{a}
Summer 2011	3.7 ± 1.4^{a}	118.0 ± 62.3^{ac}	0.05 ± 0.050^{a}	0.689 ± 0.120^{a}
Autumn 2011	4.7 ± 0.9^{ab}	257.5 ± 41.5^{b}	0.02 ± 0.004^{a}	0.750 ± 0.178^{a}
Winter 2011	3.6 ± 0.7^{a}	166.4 ± 42.4^{c}	0.02 ± 0.004^{a}	0.634 ± 0.237^{a}
Pichilemu (ribbon morphotype)				
Winter 2010	4.3 ± 1.2^{ab}	105.1 ± 28.6^{a}	0.04 ± 0.005^{a}	0.540 ± 0.163^{a}
Spring 2010	5.3 ± 0.8^{a}	151.0 ± 22.0^{ab}	0.04 ± 0.003^{ab}	0.664 ± 0.221^{ab}
Summer 2011	3.4 ± 1.2^{b}	134.6 ± 49.3^{a}	0.03 ± 0.010^{bc}	0.858 ± 0.154^{b}
Autumn 2011	4.4 ± 1.4^{ab}	212.0 ± 70.8^{b}	0.02 ± 0.003^{c}	0.788 ± 0.215^{abc}
Winter 2011	4.0 ± 0.7^{ab}	116.7 ± 19.4^{a}	0.03 ± 0.01^{ab}	1.051 ± 0.130^{bc}

©Fungyi Chow / 2021

Table 3
Two-way ANOVA for latitude (Taltal, Tongoy and Pichilemu) and season (summer 2011 and winter 2011) for the photosynthetic characteristics of *Porphyra* spp. in the populations studied in Chile. ETR_{max} (μmol electrons m^{-2} s^{-1}); I_k (saturation irradiance, μmol photons m^{-2} s^{-1}); α (photosynthetic efficiency [μmol electrons m^{-2} s^{-1}] [μmol photons m^{-2} s^{-1}]$^{-1}$); *A* (absorptance); NPQ (non-photochemical quenching).

Source of variation	ETR_{max}		α_{ETR}		I_k		*A*		NPQ	
	df	*F*-ratio	df	*F*-ratio	df	*F*-ratio	df	*F*-ratio	df	*F*-ratio
Latitude (L)	3	23.993*	3	2.786*	3	29.415*	3	119.232*	3	51.026*
Season (S)	1	36.836*	1	4.711*	1	2.155n.s.	1	89.349*	1	23.246*
L × S	3	9.212*	3	7.940*	3	7.983*	3	91.783*	3	7.153*
Residual	62		62		62		62		62	

* $P<0.001$.

Seasonal variation in temperature and radiation have been inferred to be the most important abiotic factors controlling the growth, reproduction, and morphology of seaweeds in temperate regions, by influencing the rates of biochemical/physiological processes (Kain, 1989; Brown et al., 1990; Lüning, 1991; Santelices, 1990; Israel, 2010). Environmental data show a seasonal pattern in temperature and radiation with maximum values in summer and minimum values during winter, and non-notorious differences between spring and autumn. Seasonal changes in biomass and chemical components in *P. columbina* from New Zealand were correlated with seawater nitrate concentrations and temperature. Highest blade growth was observed with decreasing temperature and day length and increasing nitrate availability. The opposite pattern was true for the reproductive features (Brown et al., 1990). Despite of the differences among the populations, the seasonal dynamic of *Porphyra* tested herein, showed an active growth during colder months.

Growth and reproduction require high energy input that can be regulated by photosynthetic adjustments (physiological changes), depending on season and latitude. Different abiotic factors influence photosynthetic rates and pigment levels, and consequently the primary production and reproduction of seaweeds. The capacity of algae to acclimate to environmental changes that in some seasons can cause serious cell damages, can determine their successful development (Abdala-Díaz et al., 2006; Sampath-Wiley et al., 2008). Photosynthetic characteristics from ETR curves showed a seasonal pattern in all tested *Porphyra* spp. morphotypes but the parameters were population dependent. Maximum ETR was detected mainly in autumn–winter for Taltal (north) and Tongoy (center), while for Pichilemu (south) morphotypes highest values were detected during spring. Seasonal changes in tissue absorptance were detected for the ribbon morphotype from Pichilemu and for morphotypes from central (Tongoy) and northern (Taltal) Chile. In a mid-term experiment (one week) where *P. leucosticta* was exposed to different irradiances, a reduction in the absorbed quanta has been explained as a consequence of pigment content variations (photoacclimation) (Figueroa et al., 2003). High solar radiation can reduce the photosynthetic activity of marine algae during short- (daily) and large-periods (seasons) as an adjustment to allow dynamic photoacclimation, which is shown by a depression of the effective quantum yield and other parameters (Φ_{PSII}, ETR_{max} and O_2 production) (Figueroa et al., 1997, 2003). Photoprotective responses such as pigment variation and antioxidant activity are expected to occur in *Porphyra* spp. populations as a response to seasonal changes.

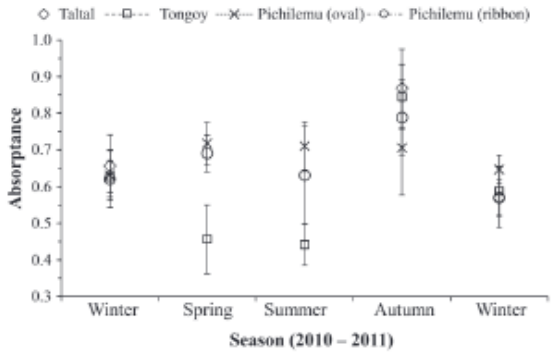

Fig. 5. Seasonal and latitudinal variation in absorptance of *Porphyra* spp. blades in the geographic zones studied in Chile. No data were present for Taltal in spring, and no blades were detected for Taltal in summer. Taltal represents the northern area (*Porphyra* sp.1), Tongoy the central area (*Porphyra* sp.2), and Pichilemu the southern area for *Porphyra* sp.3 (oval morphotype) and *Porphyra* sp.4 (ribbon morphotype). Data shown are means ± SD.

No clear seasonal pattern or relationship was observed for non-photochemical quenching (NPQ) as well as for the other photosynthetic parameters tested. The NPQ processes occurs in almost all photosynthetic eukaryotes by different mechanisms such as i.e. energy dissipation by carotenoids, state-transition between PSII and PSI, and spillover of excitation energy, and photoinhibition-associated quenching (Müller et al., 2001). Thus photosynthesis is regulated and protected in a changing environment when the time of light energy absorption exceeds the capacity for light harvesting. Higher ETR_{max} can be maintained by a series of adjustment mechanisms, including mainly the modification of I_k and NPQ performances. The oval morphotype (*Porphyra* sp.3) from the southernmost population did not show seasonal changes in quantum efficiencies, absorptance, and NPQ compared to the other populations tested. Thus, it can be suggested that different mechanisms for seasonal acclimation of photosynthetic processes, associated to species-specific regulatory systems might be effective. Anticipating predictable environmental changes ("seasonal anticipator" species *sensu* Kain, 1989) on both diurnal and seasonal time scales, *Porphyra* spp. might be able to adjust its physiological and phenological responses to a gradual changing environment. Considering the geographic distribution of the taxa, these changes can also have a latitudinal component of variation.

4.2. Latitudinal pattern in abundance, reproduction and photosynthetic traits

Latitudinal changes in the seasonal environmental variation (e.g. irradiance, temperature, nutrient, wave exposure) have been associated to phenological and ecophysiological responses in macroalgae (Brown et al., 1990; Holmes and Brodie, 2004; Varela-Alvarez et al., 2007; Wiencke et al., 2007). A clear seasonal pattern in phenology with a decrease in abundance and reproductive potential was observed for the central and northern population. Even though similar phenological patterns have been described for *P. linearis*, morphological and growth dissimilarities were produced by microhabitats and local climatic characteristics that were related to wave exposure, nutrient availability, and temperature (Varela-Alvarez et al., 2007).

©Fungyi Chow / 2021

A strong latitudinal temperature gradient (from <14 °C in the south to >20 °C in the north) can be registered along the surface waters of Chile (Fernandez et al., 2000). Temperature fluctuations are dependent on local upwelling and the existing irradiance. Even though strongest daily episodes of maximum radiation occur within northern latitudes during summer, the day length (photoperiod) can counteract the sun altitude effect in higher latitudes during summer. Thus the mean radiation can be similar along a latitudinal gradient (Kain, 1989). In this context, daily radiation (intensities and light hours) can be more important than seasonal changes for the phenological and photosynthetic patterns of populations from different latitudes (Figueroa et al., 1997; Gómez et al., 2004; Abdala-Díaz et al., 2006). The three localities studied herein, showed main differences in temperature and they are characterized in different climatic areas. The north (Taltal) corresponds to the arid zone, Tongoy (central) to the semiarid zone, and Pichilemu (south) to the central zone (Fernandez et al., 2000). A latitudinal asynchrony observed in reproduction can be related to different climatic regimes that affects the life-history traits (Mediterranean vs. desert climate in southern-central and northern Chile, respectively). Results showed that in a seasonal context, local variation in temperature and irradiance (intensities and light hours) might be crucial for the phenological and ecophysiological responses of *Porphyra* spp., whereas in a latitudinal context, temperature appeared to be more relevant. Also, the taxonomic status of the Chilean *Porphyra* species is unknown, possibly provoking differences in the patterns observed.

4.3. Potential of Porphyra as local resources

In Chile *Porphyra* is poorly exploited (Buschmann et al., 2008) but its economic usage can be stimulated, considering that different species have been described as high valuable food because of its high level of proteins (25–50%), vitamins (B12, C), trace minerals, and dietary fiber that helps to improve human health (Noda, 1993; MacArtain et al., 2007). Considering the phenological and photosynthetic patterns observed for the *Porphyra* spp. populations tested, chemical diversity can be studied in seasonal and latitudinal context in order to elucidate the potential and quality of the exploitable biomass. Most of these patterns depend on biochemical and physiological features, stimulating or inhibiting specific antioxidant and functional nutraceutic compounds. High irradiances, together with desiccation and/or nutrient limitation can cause severe damage in diverse cellular constituents and the photosynthetic apparatus. This damage results largely from the accumulation of reactive oxygen species (ROS). Thus, *Porphyra* spp. should present high accumulation of antioxidants during unfavorable conditions, which allows them to persist in the highest part of the intertidal zone, characterized by high irradiance and low nutrient availability (Sampath-Wiley et al., 2008; Contreras-Porcia et al., 2011). Morphological and organoleptic properties required for human consumption can be considered to define the potential usage of the studied populations as food source, similar as realized before for *Porphyra* species from central Chile (González and Santelices, 2003). Other marine compounds such as pigments, antioxidants, and mycosporine like-amino acids (MAAs), which are all important photoprotectors, can be considered for future studies.

Acknowledgments

We thank Danilo Peralta, Felipe Saez and Hernán Venturino for assistance with field support and Catalina Herrera, Fatme Tala and Vieia Villalobos for laboratory work. Research was supported by DGIT-UCN to F.T. and by FAPESP to F.C. We are also grateful to E. Rothäusler for the comments and review of the manuscript. This work was part of fulfillment for the doctor of science degree of F.T. in the University of Sao Paulo, Brazil.

References

Abdala-Díaz, R.T., Cabello-Pisini, A., Pérez-Rodríguez, E., Conde Alvarez, R.M., Figueroa, F.L., 2006. Daily and seasonal variations of optimum quantum yield and phenolic compounds in *Cystoseira tamariscifolia* (Phaeophyta). Mar. Biol. 148, 459–465.

Bouzon, Z.L., Chow, F., Zitta, C.S., dos Santos, R.W., Ouriques, L.C., Felix, M.R.L., Polo, L.K., Gouveia, C., Martins, R.P., Latini, A., Ramlov, F., Maraschin, M., Schmidt, E.C., 2012. Effects of natural radiation, photosynthetically active radiation and artificial ultraviolet radiation-B on the chloroplast organization and metabolism of *Porphyra acanthophora* var. *brasiliensis* (Rhodophyta, Bangiales). Microsc. Microanal. 18, 1467–1479.

Brodie, J., Mortensen, A.M., Ramirez, M.E., Russell, S., Rinkel, B., 2008. Making the links: towards a global taxonomy for the red algal genus *Porphyra* (Bangiales, Rhodophyta). J. Appl. Phycol. 20, 939–949.

Brown, M.T., Frazer, A.W.J., Brasch, D.J., Melton, L.D., 1990. Growth and reproduction of *Porphyra columbina* Mont. (Bangiales, Rhodophyceae) from southern New Zealand. J. Appl. Phycol. 2, 35–44.

Buschmann, A.H., Hernández-González, M.C., Varela, D., 2008. Seaweed future cultivation in Chile: perspectives and challenges. Int. J. Environ. Pollut. 33, 432–456.

Collén, J., Davidson, I.R., 1999. Stress tolerance and reactive oxygen metabolism in the intertidal red seaweeds *Mastocarpus stellatus* and *Chondrus crispus*. Plant Cell Environ. 22, 1143–1151.

Contreras-Porcia, L., Thomas, D., Flores, V., Correa, J.A., 2011. Tolerance to oxidative stress induced by desiccation in *Porphyra columbina* (Bangiales, Rhodophyta). J. Exp. Bot. 62, 1815–1829.

Davison, I.R., Pearson, G.A., 1996. Environmental stress in intertidal seaweeds. J. Phycol. 32, 197–211.

Destombe, C., Godin, J., Nocher, M., Richerd, S., Valero, M., 1993. Differences in responses between haploid and diploid isomorphic phases of *Gracilaria verrucosa* (Rhodophyta: Gigartinales) exposed to artificial environmental conditions. Hidrobiologia 260–261, 131–137.

Dickson, L.G., Waaland, J.R., 1985. *Porphyra nereocystis*: a dual daylength seaweed. Planta 165, 548–553.

Espinoza-Avalos, J., 2005. Phenology of marine macroalgae (Fenología de macroalgas marinas). Hidrobiológica 15, 109–122.

Falkowski, P.G., LaRoche, J., 1991. Acclimation to spectral irradiance in algae. J. Phycol. 27, 8–14.

Fernandez, M., Jaramillo, E., Marquet, P.A., Moreno, C.A., Navarrete, S.A., Ojeda, F.P., Valdovinos, C.R., Vasquez, J.A., 2000. Diversity, dynamics and biogeography of Chilean benthic nearshore ecosystems: an overview and guidelines for conservation. Rev. Chil. Hist. Nat. 73, 797–830.

Figueroa, F., Conde-Alvarez, R., Gómez, I., 2003. Relations between electron transport rates determined by pulse amplitude modulated chlorophyll fluorescence and oxygen evolution in macroalgae under different light conditions. Photosynth. Res. 75, 259–275.

Figueroa, F.L., Salles, S., Aguilera, J., Jiménez, C., Mercado, J., Viñegla, B., Flores-Moya, A., Altamirano, M., 1997. Effects of solar radiation on photoinhibition and pigmentation in the red alga *Porphyra leucosticta*. Mar. Ecol. Progr. Ser. 151, 81–90.

Forrest, J., Miller-Rushing, A.J., 2010. Toward a synthetic understanding of the role of phenology in ecology and evolution. Phil. Trans. R. Soc. B 365, 3101–3112.

Gómez, I., López-Figueroa, F.L., Ulloa, N., Morales, V., Lovengreen, C., Huovinen, P., Hess, S., 2004. Patterns of photosynthesis in 18 species of intertidal macroalgae from southern Chile. Mar. Ecol. Prog. Ser. 270, 103–116.

González, A., Santelices, B., 2003. A re-examination of the potential use of central Chilean *Porphyra* (Bangiales, Rhodophyta) for human consumption. In: Chapman, A.R.O., Anderson, R.J., Vreeland, V.J., Davidson, I. (Eds.), Proc. 17th Intern. Seaweed Symp. Oxford University Press Inc., NY, pp. 249–255.

Griffin, N.J., Bolton, J., Anderson, R.J., 1999. Distribution and population dynamics of *Porphyra* (Bangiales, Rhodophyta) in the southern Western Cape, South Africa. J. Appl. Phycol. 11, 429–436.

Gröniger, A., Hallier, C., Häder, D.P., 1999. Influence of UV radiation and visible light on *Porphyra umbilicalis*: photoinhibition and MAA concentration. J. Appl. Phycol. 11, 437–445.

Grzymski, J., Johnsen, G., Sakshaug, E., 1997. The significance of intracellular self-shading on the biooptical properties of brown, red, and green macroalgae. J. Phycol. 33, 408–414.

Hays, C.G., 2007. Adaptive phenotypic differentiation across the intertidal gradient in the alga *Silvetia compressa*. Ecology 88, 149–157.

Holmes, M.J., Brodie, J., 2004. Morphology, seasonal phenology and observations on some aspects of the life history in culture of *Porphyra dioica* (Bangiales, Rhodophyta) from Devon, UK. Phycologia 43, 176–188.

Huner, N.P.A., Maxwell, D.P., Gray, G.R., Savitch, L.V., Laudenbach, D.E., Falk, S., 1995. Photosynthetic response to light and temperature: PSII excitation pressure and redox signalling. Acta Physiol. Plant. 17, 167–176.

Huovinen, P., Gómez, I., Figueroa, F.L., Ulloa, N., Morales, V., Lovengreen, C., 2004. Ultraviolet-absorbing mycosporine-like amino acids in red macroalgae from Chile. Bot. Mar. 47, 21–29.

Israel, A., 2010. The extreme environments of *Porphyra*, a fast growing and edible red marine macroalga. In: Seckbach, J., Chapman, D.J. (Eds.), Red Algae in the

©Fungyi Chow / 2021

Genomic Age, Cellular Origin, Life in Extreme Habitats and Astrobiology, vol.13. Springer Science + Business Media B.V., pp. 61–75.
Jassby, A.D., Platt, T., 1976. Mathematical formulation of the relationship between photosynthesis and light for phytoplankton. Limnol. Oceanogr. 21, 540–547.
Kain, J., 1989. The seasons in the subtidal. Br. Phycol. J. 24, 203–215.
Karsten, U., 1999. Seasonal variation in heteroside concentrations of field-collected *Porphyra* species (Rhodophyta) from different biogeographic regions. New Phytol. 143, 561–571.
Karsten, U., Barrow, K.D., Nixdorf, O., King, R.J., 1996. The compatibility with enzyme activity of unusual organic osmolytes from mangrove red algae. Aust. J. Plant Physiol. 23, 577–582.
Kim, J.G., Kraemer, G.P., Yarish, C., 2008. Physiological activity of *Porphyra* in relation to eulittoral zonation. J. Exp. Mar. Biol. Ecol. 365, 75–85.
Lobban, C., Harrison, P., 1994. Seaweed Ecology and Physiology. Cambridge University Press, Cambridge, UK.
Lüning, K., 1991. Seaweeds. Their Environment, Biogeography and Ecophysiology. Wiley-Interscience Publication, John Wiley and Sons, New York, 527 pp.
MacArtain, P., Gill, C.I.R., Brooks, M., Campbell, R., Rowland, I.R., 2007. Nutritional value of edible seaweeds. Nutr. Rev. 65, 535–543.
Maxwell, K., Johnson, G.N., 2000. Chlorophyll fluorescence a practical guide. J. Exp. Bot. 51, 659–668.
Mercado, J.M., Jiménez, C., Niell, F.X., Figueroa, F.L., 1996. Comparison of methods for measuring light absorption by algae and their application to the estimation of the package effect. Sci. Mar. 60 (Suppl. 1), 39–45.
Mittler, R., 2002. Oxidative stress, antioxidants and stress tolerance. Trends Plant Sci. 7, 405–410.
Müller, P., Li, X.-P., Niyogi, K.K., 2001. Non-photochemical quenching. A response to excess light energy. Plant Physiol. 125, 1558–1566.
Noda, H., 1993. Health benefits and nutritional properties of nori. J. Appl. Phycol. 5, 255–258.
Ramírez, M.E., Santelices, B., 1991. Catalogue of the benthic marine algae from temperate Pacific coast of South America (Catálogo de las algas marinas bentónicas de la costa temperada del Pacífico de Sudamérica). Monogr. Biol. 5, 1–437.
Sampath-Wiley, P., Neefus, C.D., Jahnke, J.S., 2008. Seasonal effects of sun exposure and emersion on intertidal seaweed physiology: fluctuations in antioxidant contents, photosynthetic pigments and photosynthetic efficiency in the red alga *Porphyra umbilicalis* Kützing (Rhodophyta, Bangiales). J. Exp. Mar. Biol. Ecol. 361, 83–91.
Santelices, B., 1990. Patterns of reproduction, dispersal and recruitment in seaweeds. Oceanogr. Mar. Biol. Ann. Rev. 28, 177–276.
Sarmiento, P., 2008. Solar irradiance in territories of the Republic of Chile. In: National Energy Commission of Chile, United Nations Program for Development (Eds.), Chile: Removing Barriers for Rural Electrification with Renewable Energy (Chile: Remoción de Barreras para la Electrificación Rural con Energías Renovables). Universidad Técnica Federico Santa María de Chile, Chile (Proyect CHI/00/G32).
Sutherland, E., Lindstrom, S., Nelson, W., Brodie, J., Lynch, M., Sook, N., Choi, H.-G., Miyata, M., Kikuchi, N., Oliveira, M., Neefus, C., Mols-Mortensen, A., Milstein, D., Müller, K., 2011. A new look at an ancient order: generic revision of the Bangiales (Rhodophyta). J. Phycol. 47, 1131–1151.
Underwood, A.J., 1997. Experiments in Ecology. Their Logical Design and Interpretation Using Analysis of Variance. Cambridge University Press, Cambridge.
Varela-Alvarez, E., Stengel, D.B., Guiry, M.D., 2007. Seasonal growth and phenotypic variation in *Porphyra linearis* (Rhodophyta) populations on the west coast of Ireland. J. Phycol. 43, 90–100.
Vieira, V., Santos, R., 2012. Regulation of geographic variability in haploid:diploid ratios of biphasic seaweed life cycles. J. Phycol. 48, 1012–1019.
Waaland, J.R., Dickson, L.G., Duffiedl, E.C.S., 1990. Conchospore production and seasonal occurrence of some *Porphyra* species (Bangiales, Rhodophyta) in Washington state. Hydrobiologia 204–205, 453–459.
Wiencke, C., Clayton, M.N., Gómez, I., Iken, K., Lüder, U.H., Amsler, C.D., Karsten, U., Hanelt, D., Bischof, K., Dunton, K., 2007. Life strategy, ecophysiology and ecology of seaweeds in polar waters. Rev. Environ. Sci. Biotechnol. 6, 95–126.

ANEXO 13

J Appl Phycol (2014) 26:2159–2171
DOI 10.1007/s10811-014-0249-y

Ecophysiological characteristics of *Porphyra* spp. (Bangiophyceae, Rhodophyta): seasonal and latitudinal variations in northern-central Chile

Fadia Tala · Fungyi Chow

Received: 12 October 2013 / Revised and accepted: 22 January 2014 / Published online: 12 February 2014
© Springer Science+Business Media Dordrecht 2014

Abstract The red macroalga *Porphyra* C. Agardh is one of the most ecologically successful genera that lives in the upper intertidal zone. Biochemical, physiological, and morphological acclimation strategies allow their growth and distribution as well as a quick recuperation between tidal regimens. Studies of *Porphyra* are poorly developed in Chile, and management and exploitation proposals need to be supported by biological and ecophysiological approaches. This study evaluated seasonal and latitudinal physiological performances of *Porphyra* spp. via maximum quantum yield (F_v/F_m), pigments, proteins, phenolic compounds, and antioxidant activity in order to describe how algae can acclimate to their environment and to provide insights to their management and use. Sampling was done at three costal sites in Chile between 25°S and 34°S between winters 2010 and 2011. A total of four different morphotypes were identified (one in the north, one in the center, and two in the south locations) and evaluated separately. Results showed seasonal and latitudinal patterns for all ecophysiological variables studied, with a general tendency of decrease in F_v/F_m, pigments, and soluble proteins during spring–summer seasons accompanied by an increase in the antioxidant capacity. Latitudinal differences were observed with a tendency of higher values for ecophysiological traits in central and southern morphotypes. Phenology patterns were different between an annual population in the north location and a perennial one for central-south populations. The taxonomic clarity should be evaluated in order to better understand if there exists intraspecific (dependent on morphology) or interspecific variation.

Keywords Antioxidants · Pigments · Phenolic compounds · Photosynthesis · *Porphyra* · Seaweed

F. Tala · F. Chow
Instituto de Biociências, Departamento de Botânica, Universidade de São Paulo, Rua do Matão 321, Trav. 14, São Paulo, Brazil

F. Tala (✉)
Centro de Investigación y Desarrollo Tecnológico en Algas (CIDTA), Facultad de Ciencias del Mar, Universidad Católica del Norte (UCN), Larrondo 1281, Coquimbo, Chile
e-mail: ftala@ucn.cl

Introduction

Land plants and macroalgae are sessile organisms; therefore, acclimation strategies to variable stressors are key mechanisms to maintain their growth, development, and reproduction for survival. The responses to these abiotic and biotic environmental changes are organized via a network of signals at molecular levels, which trigger a cascade reaction driven by adjustments in biochemical and physiological metabolic pathways, consequently expressing variations in growth rates, reproduction, and phenology (Lüning and tom Dieck 1989; Schwachtje and Baldwin 2008).

The intertidal zone is considered as a harsh habitat for living organisms, especially for sessile organisms, because it comprises the transition zone between terrestrial and marine characteristics with continuous exposure to a wide range of environmental stressors, such as solar radiation, temperature, desiccation, nutrient depletion, and salinity (Lüning 1991; Davison and Pearson 1996; Helmuth et al. 2006; Eggert 2012; Karsten 2012). These changes can occur at small (tide and daily cycles) and large (seasonal and interannual cycles) temporal scales. Additionally, at a small spatial scale, the disruptions by chemical and physical stressors must be more frequent than those present in subtidal habitats (Kain 1989; Davison and Pearson 1996; Collen and Davison 1999; Sampath-Wiley et al. 2008). Abiotic changes at large spatial

©Fungyi Chow / 2021

scales (latitudinal variations) are important for species with wide distributions, being an important trigger for biogeographical distribution patterns that occur through temperature-dependent effects on physiological performances (e.g., photosynthesis) and temperature tolerance (i.e., survival) (Eggert 2012). Morphological and physiological plasticity responses across a wide range of environmental gradients can represent either phenotypic variability (e.g., *Ecklonia radiata*, Wernberg et al. 2003; Fowler-Walker et al. 2006) or genotypic divergence (e.g., *Lessonia berteroana* vs *Lessonia spicata*, González et al. 2012; *Hormosira banksii*, Clark et al. 2013).

Efficient physiological acclimation is crucial to cope with extreme solar radiation, high temperature, and desiccation. One of the first changes occurring during stressful conditions is at the oxidative reaction level, resulting in oxidative stress and accumulation of free radicals and non-radical oxidants (i.e., reactive oxygen species (ROS)). Processes of primary metabolism, such as photosynthesis and respiration, are natural sources of ROS (Mittler 2002; Bischof and Rautenberger 2012). However, abiotic stress can cause an unbalance in the production of oxidative species that disrupts cellular homeostasis, and active antioxidant systems are important to prevent oxidative damage of important molecules and cellular structures (Mittler 2002; Collen and Davison 1999; Collen et al. 2003; Bischof and Rautenberger 2012; Bouzon et al. 2012; Gouveia et al. 2013). Different responses of seaweeds to solar radiation and temperature changes have been described. Seaweeds can respond with the alteration in pigment content and ratio of photosynthetic pigments/photoprotective pigments (Falkowski and Laroche 1991; Staehr and Wernberg 2009), dynamic photoinhibition (Figueroa et al. 1997; Franklin and Forster 1997; Gómez et al. 2004; Abdala-Díaz et al. 2006), efficient activity of antioxidant systems (Bischof and Rautenberger 2012), cellular carboxylation activity (Davison 1991), and variation in lipid composition and fluidity in membranes (Raison et al. 1980; Steinhoff et al. 2012). Seaweeds are also capable of producing chemical compounds in response to various environmental stresses such as mycosporine-like amino acids (MAAs), phenolic compounds, polyamines, and stress proteins (Van Alstyne 1988; Hoyer et al. 2001; Huovinen et al. 2004; Abdala-Díaz et al. 2006; Cruces et al. 2012). The efficiency of absorbing–dissipating energy and the acclimation responses to fluctuating environmental factors reflect a wide range of adaptive abilities and tolerances in macroalgae species across their range of distribution. Thus, within the tolerance range of the alga (e.g., during autumn or spring conditions in many temperate regions), it is expected that physiological acclimation may operate efficiently (Eggert 2012).

Some species of the red macroalga *Porphyra* C. Agardh, particularly abundant in cold temperate and boreal shores of the Northern and Southern Hemispheres, are most successful in inhabiting the upper intertidal zone where other species cannot. A series of strategies (biochemical, physiological, and morphological) allow the distribution of *Porphyra* spp. in the intertidal and contribute to their quick recuperation between tidal regimens (Davison and Pearson 1996; Gómez et al. 2004; Huovinen et al. 2004; Sampath-Wiley et al. 2008; Contreras-Porcia et al. 2011; Bouzon et al. 2012). In Chile, different species of *Porphyra* spp. (*luche*, local name) are distributed throughout the coast (20–52°S) with at least five morphological strains (Ramírez and Santelices 1991; Candia et al. 1999). Molecular analysis of Bangiales has questioned the presence and number of species of *Porphyra* in Chile (Brodie et al. 2008, 2011), proposing *Pyropia columbina* (Montagne) W. A. Nelson to replace *Porphyra columbina* Montagne, which is the species commonly referred to in Chile (Nelson and Broom 2010; Sutherland et al. 2011). However, the taxonomy of *Porphyra* in Chile is as yet poorly known. *Porphyra columbina* (now *Pyropia columbina*) has been referred as the intertidal Chilean species with high content of MAAs (Huovinen et al. 2004), a compound with photoprotective function against high solar radiation. Morphological and photosynthetic changes have been described in *P. columbina* during desiccation as tolerance mechanisms, principally to prevent biomolecular alterations and cellular collapse (Contreras-Porcia et al. 2011), similar as shown for *Porphyra acanthophora* under PAR and UVR-B radiation (Bouzon et al. 2012).

Porphyra species represent one of the largest food sources in the world market, originating from cultivation systems of Japan and South Korea since the seventeenth century and from local markets of the Philippines, China, and Chile (Israel 2010). Since ancient times, the management of *Porphyra* in Chile is mainly restricted to the southern region by coastal fishermen communities but shows great annual variations in biomass landing (Buschmann et al. 2001, 2008). In the last decades, it has been considered as a good candidate for the development of small-scale aquaculture for fishermen as an intergovernmental program for aquaculture diversification in the country. At least one study has demonstrated that the cultivation of *P. columbina* is biologically feasible (Seguel and Santelices 1988). However, due to its morphological and organoleptic characteristics, it is not considered as a good candidate for human consumption (González and Santelices 2003). In contrast, other species such as *Porphyra linearis* Greville, *Porphyra pseudolinearis* Ueda (*Pyropia pseudolinearis* (Ueda) N.Kikuchi, M.Miyata, M.S.Hwang & H.G.Choi), and *Porphyra woolhousiae* Harvey recorded for central Chile appear to be important candidates for future aquaculture. Considering the fact that organoleptic characteristics have been accepted for these species by international markets (González and Santelices 2003), this may result overall in new possibilities for *Porphyra* cultivation. Nevertheless, when algal raw material is not

appropriate as an edible product but has nutritional value (e.g., better content in vitamins, proteins, lipids, antioxidants), the biomass could be used as a natural source of antioxidants and pigment production for food supply, nutraceutical, and cosmetology industries. New uses of marine biomass have achieved attention in the last years due to the benefit for human health (Plaza et al. 2008; Sekar and Chandramohan 2008; Shahidi 2009; Vilchez et al. 2011; Jiménez-Escrig et al. 2012).

Phenological studies of *Porphyra* are poorly developed in Chile, and management and exploitation proposals need to be supported by biological and ecophysiological approaches. Previous work with northern-central *Porphyra* populations showed morphological variations and different seasonal and latitudinal patterns in phenology and photosynthetic light curves, with an annual population in the north opposed to perennial characteristics of central-south populations (Tala and Chow 2014). In the present study, the photosynthetic efficiencies (maximum quantum yield of photosystem II (PSII)) and the physiological adjustments (photosynthetic pigments, total soluble proteins, phenolic compounds, and total antioxidant activity) of *Porphyra* spp. were studied along seasonal and latitudinal gradients in northern-central Chile in order to describe the population adjustment and to provide information that support their potential management and uses.

Material and methods

Localities, environmental characteristics, and sampling

Three costal sites along northern and central Chile were selected to characterize the seasonal and latitudinal patterns in the physiological fitness of *Porphyra* spp. populations. All sampling sites are semi-exposed rocky shores with a typical zonation occurrence of *Porphyra*, which dominates the cover and biomass in the uppermost level of the intertidal zone. The northern sampling area corresponds to Taltal (region of Antofagasta at 25°27′23″S–70°31′17″W), the central sampling area corresponds to Tongoy (region of Coquimbo at 30°15′S–71°2′W), and the southern sampling area corresponds to Pichilemu (region of O'Higgins at 34°22′S–72°00′W). Between the northern and the southernmost sampling areas, there is a distance of 1,400 km, with Tongoy being situated in the middle (Fig. 1). Environmental seasonal patterns along the Chilean coast showed with higher values of temperature and solar radiation toward spring–summer seasons and lower in winter (Thiel et al. 2007; Sarmiento 2008). In a latitudinal context, seawater temperature differed ($F_{(2,42)}$=16.362; P<0.01) between the geographically studied zones (annual averages in °C±SD; Antofagasta 16.4±1.8; Coquimbo 14.4±1.7; Valparaíso 13.1±1.3, the last one is equivalent to the region of O'Higgins; www.shoa.cl). Despite of the fact that the Chilean coast is defined as the province of warm temperate Southeastern Pacific (Spalding et al. 2007), different climatic areas occur in the studied zones (Taltal, arid zone; Coquimbo, semiarid zone; Pichilemu, Mediterranean zone), which are mainly related to temperature and rainfall (Fernandez et al. 2000).

Since the taxonomic elucidation of *Porphyra* in Chile is still unresolved, each population was treated as a separate identity and denominated as *Porphyra* genus with their respective morphology. Four morphotypes based on the blade form were considered: *Porphyra* sp.1 from Taltal (small obovate to lanceolate blade) and *Porphyra* sp.2 from Tongoy (ovate form that can be single or divided in two or more linear to lanceolate blades). Two morphotypes were detected in the Pichilemu sampling area with *Porphyra* sp.3 (oval blade and wavy margins) and *Porphyra* sp.4 (ribbon morphology that varied between linear and lanceolate) (Fig. 1).

Entire blades of *Porphyra* spp. (gametophytic phases) were randomly sampled between winters 2010 and 2011. The sampling protocol is described in detail by Tala and Chow (2014). Briefly, random smaller quadrat of 20×20 cm was positioned parallel to the coastline in the distribution area of *Porphyra*, from where all blades were carefully detached and transported in coolers to the Marine Botany Laboratory, Universidad Católica del Norte, Coquimbo, Chile, in order to determine the seasonal and latitudinal physiological characteristics of *Porphyra* spp. Considering that seasonal and daily environmental changes could affect the physiological and chemical responses, all samplings was during the middle of the season and in the morning tide. Due to logistic problems, no sampling was performed for Taltal during spring. Entire blades of *Porphyra* spp. from each population were acclimated for 24 h in a flow-through seawater tank (60 L) after sampling. The indoor tank was maintained with natural solar light across an acrylic roof and without control of seawater temperature.

Photosynthetic performance

Photosynthetic performance was estimated by in vivo chlorophyll *a* (chl *a*) fluorescence of PSII using a portable pulse amplitude fluorometer (PAM-2500, Walz, Germany). Each blade (n=9 replicates for each locality and season) was dark adapted for 20 min, and the maximal quantum yield (F_v/F_m) was measured (Schreiber et al. 1994). The photosynthetic measurements were made in the vegetative portion of each blade.

Pigments

The determination of chl *a* and total carotenoids (TCs) was based on samples that were frozen at −80 °C (~300 mg; n=9 replicates for each locality and season). Pigments were extracted with *N*,*N*-dimethylformamide (DMF) for 24 h at 4 °C

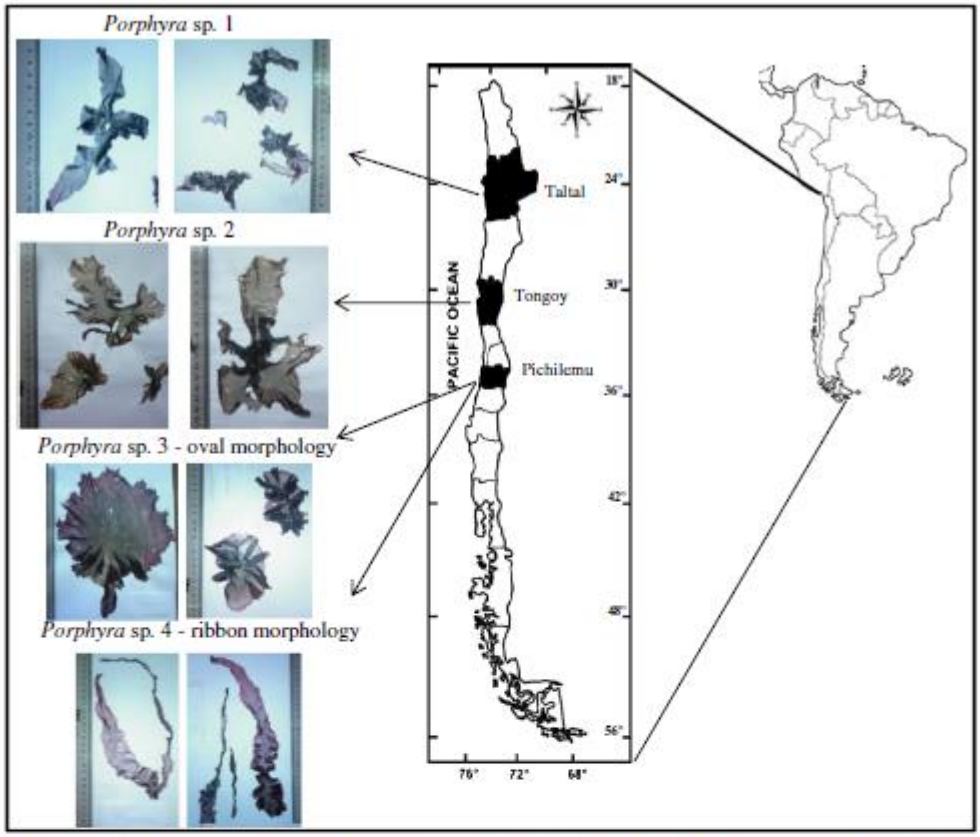

Fig. 1 Chilean map showing the locations of the studied populations of *Porphyra* spp. and the respective morphotype. *Porphyra* sp.1 from *Taltal* (northern area) with small blades and obovate to lanceolate morphology; *Porphyra* sp.2 from *Tongoy* (center area) with ovate morphology, simple or divides; *Porphyra* sp.3 from *Pichilemu* (south area) with oval morphology and wavy margins; *Porphyra* sp.4 from *Pichilemu* with ribbon morphology between linear and lanceolate shapes

in darkness. The chl *a* and TC contents (mg pigment g^{-1} ww) were calculated using the dichromatic equations described by Inskeep and Bloom (1985) and Henley and Dunton (1995). Phycobiliproteins [phycoerythrin (PE) and phycocyanin (PC)] were quantified from lyophilized ground samples (~50 mg; $n=8$ replicates for each locality and season) as suggested by Denis et al. (2008). The extracts were obtained with 0.1 M phosphate buffer (pH 6.8) for 24 h at 4 °C in darkness. The content of phycobiliproteins (mg pigment g^{-1} dry weight (dw)) was calculated according to the specific equations for *Porphyra* (Sampath-Wiley and Neefus 2007) and was adjusted for the absorption peaks of our extracts (556 and 624 nm). The absorbance of all pigment supernatants was measured in a UV–visible spectrophotometer (Rayleigh, model UV-1601, China). The annual mean algal dry weight (%) was 16.3±0.2 for Taltal, 18.5±2.9 for Tongoy, 19.4±3.3 for Pichilemu oval, and 19.5±2.8 for Pichilemu ribbon morphotype.

Other compounds

Soluble total proteins were determined from the aqueous extracts done for phycobiliproteins ($n=9$ replicates for each locality and season). The Bradford assay was performed by using the microassay procedure of the Bio-Rad Protein Assay Kit (Bio-Rad Laboratories, 500-0001). Absorbance was measured at 595 nm and expressed as mg protein g^{-1} dw based on a standard curve of bovine serum albumin (BSA). Soluble phenolic compounds were determined by the Folin–Ciocalteu assay (Gómez and Huovinen 2010). Algal samples (~10 mg dw; $n=5$ replicates for each locality and season) were extracted overnight at 4 °C in 5 mL acetone (70 %). Supernatant aliquot (250 μL) was mixed to 1,250 μL of dH_2O, 500 μL of 1 N Folin–Ciocalteu reagent, and 1 mL of 20 % $NaCO_3$, incubated for 45 min at room temperature in darkness and centrifuged at 5,000 rpm for 3 min. Then, the absorbance was read at 760 nm, and the total content of soluble phenolic

©Fungyi Chow / 2021

compounds was expressed as mg phenolics g^{-1} dw, which was based on a standard curve of *p*-coumaric acid (Sigma-Aldrich).

Total antioxidant activity

The antioxidant activity was tested by the 2,2-diphenyl-1-picrylhydrazyl (DPPH) radical scavenging capacity (Brand-Williams et al. 1995). The powdered algal sample (~50 mg dw; $n=9$ replicates for each locality and season) was extracted with 1 mL 70 % ethanol at 50 °C for 60 min. Then, 800 μL DPPH (50 mg L^{-1} 70 % methanol) was mixed with 200 μL of algal extract, and the decay of absorbance was measured at 0 and 15 min at 520 nm. Consumption of DPPH was calculated as a percentage of radical scavenging activity (%RSA)=$[1-(A_m/A_o)]\times 100$ and standardized by algal biomass (% mg^{-1} dw), where A_m represents the absorbance of algal extract in solution after reaction with DPPH (at final time), and A_o is the initial absorbance at time 0 (Molyneux 2004).

Statistical analyses

One-way ANOVA was used to evaluate the seasonal variations for each population separately. A two-way ANOVA, with locality and season as main factors, was applied for latitudinal comparison. Considering that unbalance designs are presented without data for Taltal spring (see above), the latitudinal differences were evaluated which only included two contrast seasons (summer and winter 2011) for all variables. As the abundance for *Porphyra* sp.1 from Taltal during summer was zero and in order to have a balanced design to allow the interactions, a minor factor (0.005) was included for each variable. Normality (Kolmogorov–Smirnov test) and homogeneity of variances (Levene's test) were used. The percentage data were arcsine transformed. When ANOVA revealed significant differences, a post hoc Tukey's honestly significant difference (HSD) test was applied. Since some data showed heteroscedasticity, all data were analyzed using a more conservative $\alpha=0.01$ (Underwood 1997).

Results

Seasonal and latitudinal patterns were observed for all ecophysiological variables studied, with a general tendency of lower photosynthetic efficiencies and pigments during warm seasons accompanied with higher antioxidant activity. The patterns showed also an important population (latitudinal) component in the level of variation. For some cases, both studied winter seasons (2010 vs 2011) showed different responses in the *Porphyra* populations.

Photosynthetic performance

Seasonal changes in maximum photosynthetic quantum yield (F_v/F_m) efficiencies depended of the population (Fig. 2). *Porphyra* sp.1 from Taltal showed higher F_v/F_m in autumn with only significant differences ($F_{(2,23)}=3.582$, $P=0.044$) between both winter seasons (2010 and 2011). *Porphyra* sp.2 (Tongoy) and *Porphyra* sp.4 (Pichilemu ribbon) showed a significant decrease of F_v/F_m in summer compared to the other seasons ($F_{(4,44)}=15.281$, $P<0.001$; $F_{(4,44)}=5.695$, $P<0.001$, respectively). *Porphyra* sp.3 (Pichilemu oval) was the only species that maintained similar values of F_v/F_m ($F_{(4,44)}=2.389$, $P=0.067$) during all the studied periods, showing no significant differences.

The two-way ANOVA showed significant differences ($P<0.01$) between seasons (summer and winter 2011), localities, and for the interaction (Table 1). The global pattern showed decreasing F_v/F_m for *Porphyra* in summer and higher values toward southern population (both Pichilemu morphotypes). The population differences disappeared during winter 2011 (Table 1).

Pigments

Photosynthetic pigments presented changes during the different seasons for all populations; however, no clear latitudinal tendency was observed (Fig. 3). Seasonal changes in chl *a* showed a significant decrease toward summer for Tongoy ($F_{(4,44)}=15.690$, $P<0.001$) and Pichilemu (oval $F_{(4,44)}=26.313$, $P<0.001$; ribbon $F_{(4,44)}=10.235$, $P<0.001$) and winter 2011 for Taltal ($F_{(2,26)}=5.796$, $P=0.009$). Higher values of chl *a* were observed in winter and autumn depending on the population (Fig. 3(a)). The differences between the studied populations were mainly detected during summer. In autumn 2011, *Porphyra* sp.1 from Taltal, the most northern

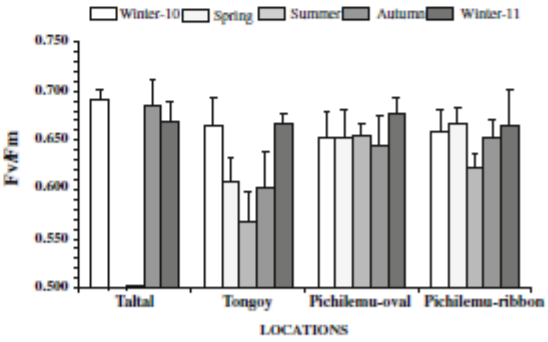

Fig. 2 Seasonal and latitudinal variation in the maximum quantum yield (F_v/F_m) of *Porphyra* spp. from *Taltal* (*Porphyra* sp.1), *Tongoy* (*Porphyra* sp.2), and *Pichilemu* (*Porphyra* sp.3 oval morphology and *Porphyra* sp.4 ribbon morphology). No data were registered for Taltal spring. Data are shown as means±SD

©Fungyi Chow / 2021

Table 1 Two-way ANOVA for seasonal (summer 2011 and winter 2011) and local (Taltal, Tongoy, and Pichilemu) variation in F_v/F_m, chlorophyll *a*, total carotenoids, phycoerythrin, and phycocyanin of *Porphyra* spp. and post hoc Tukey's HSD results for each factor and interaction

Source of variation	*DF*	SS	MS	*F*	*P*
F_v/F_m					
Seasons	1	0.753	0.753	1,586.677	*<0.001*
Localities	3	1.266	0.422	889.415	*<0.001*
Seasons × localities	3	1.246	0.415	875.265	*<0.001*
Error	64	0.0304	4.74E-4		
Post hoc (Tukey's test)					
Seasons	Summer 2011 < Winter 2011				
Localities	Taltal < Tongoy < Pichilemu ribbon < Pichilemu oval				
Interaction	S-Ta < S-To < S-Pr < S-Po < W-Pr = W-To = W-Ta = W-Po				
Chlorophyll *a*					
Seasons	1	0.128	0.128	75.400	*<0.001*
Localities	3	0.0517	0.0172	10.140	*<0.001*
Seasons × localities	3	0.172	0.0573	33.656	*<0.001*
Error	64	0.109	1.70E-3		
Post hoc (Tukey's test)					
Seasons	Summer 2011 < winter 2011				
Localities	Taltal = Pichilemu oval < Pichilemu ribbon = Tongoy				
Interaction	S-Ta < S-Po < S-Pr = W-Po = S-To = W-To = W-Pr < W-Ta				
Total carotenoids					
Seasons	1	0.128	0.128	66.006	*<0.001*
Localities	3	0.0517	0.0357	18.393	*<0.001*
Seasons × localities	3	0.172	0.0279	14.383	*<0.001*
Error	64	0.109	1.94E-3		
Post hoc (Tukey's test)					
Seasons	Summer 2011 < winter 2011				
Localities	Taltal = Pichilemu oval < Pichilemu ribbon = Tongoy				
Interaction	S-Ta < S-Po = S-Pr = S-To < W-Po = W-To = W-Pr = W-Ta				
Phycoerythrin					
Seasons	1	33.726	33.726	895.507	*<0.001*
Localities	3	6.438	2.146	56.985	*<0.001*
Seasons × localities	3	10.234	3.411	90.583	*<0.001*
Error	56	2.109	0.038		
Post hoc (Tukey's test)					
Seasons	Summer 2011 < winter 2011				
Localities	Tongoy = Taltal < Pichilemu oval = Pichilemu ribbon				
Interaction	S-Ta < S-Pr < S-To = S-Po < W-To < W-Ta = W-Po < W-Pr				
Phycocyanin					
Seasons	1	18.05	18.05	890.089	*<0.001*
Localities	3	2.836	0.945	46.621	*<0.001*
Seasons × localities	3	4.115	1.372	67.635	*<0.001*
Error	56	1.136	0.0203		
Post hoc (Tukey's test)					
Seasons	Summer 2011 < winter 2011				
Localities	Taltal = Tongoy < Pichilemu ribbon < Pichilemu oval				
Interaction	S-Ta < S-Pr < S-To = S-Po < W-To < W-Ta < W-Pr = W-Po				

P values in italic highlight represent significant differences at $p<0.01$

DF degree of freedom, *SS* square sum, *MS* medium square, *F* statistic index, *P* probability, *S* summer, *W* winter, *Ta* Taltal, *To* Tongoy, *Po* Pichilemu oval, *Pr* Pichilemu ribbon

population, presented the highest level of chl *a* compared to the other populations and seasons (Fig. 3(a)). Significant differences ($P<0.01$) between seasons (summer and winter 2011), localities, and the interaction were also detected for chl *a* (Table 1).

Seasonal changes in TCs were also dependent of the population (Fig. 3(b)). *Porphyra* sp.1 did not show seasonal changes in TC concentrations (Taltal $F_{(2,26)}=2.598$; $P=0.095$). The other populations showed similar patterns than chl *a* with decreasing TC levels during summer (Tongoy $F_{(4,44)}=7.690$, $P<0.001$; Pichilemu oval $F_{(4,44)}=29.936$, $P<0.001$; Pichilemu ribbon $F_{(4,44)}=10.523$, $P<0.001$). Significant differences ($P<0.01$) between seasons (summer and winter 2011), localities, and the interaction were observed (Table 1). Changes between populations were detected only during summer (Table 1, Fig. 3(b)).

The phycobiliproteins PE and PC showed seasonal changes in the studied populations (Fig. 3(c, d), respectively). Likely, chl *a* and TC, which significantly diminish toward summer, were observed in both PE (Taltal $F_{(2,21)}=20.651$, $P<0.001$; Tongoy $F_{(4,35)}=25.512$, $P<0.001$; Pichilemu oval $F_{(4,35)}=50.005$, $P<0.001$; Pichilemu ribbon $F_{(4,35)}=179.636$, $P<0.001$) and PC (Taltal $F_{(2,21)}=61.61$, $P<0.001$; Tongoy $F_{(4,35)}=54.154$, $P<0.001$; Pichilemu oval ($F_{(4,35)}=50.138$, $P<0.001$; Pichilemu ribbon $F_{(4,35)}=113.793$, $P<0.001$) (Fig. 3(c, d)). *Porphyra* from Taltal (sp.1) and Tongoy (sp.2) showed higher values of PE and PC during autumn, whereas in both morphotypes (sp.3 oval and sp.4 ribbon) from Pichilemu, higher values were found during winter (Fig. 3(c, d), respectively).

The two-way ANOVA showed significant differences between seasons (summer and winter 2011), localities, and the interaction for both PE and PC (Table 1). Higher PE was detected for winter 2011 compared to summer. Phycoerythrin of Pichilemu ribbon morphotype and phycocyanin of both morphotypes from Pichilemu showed higher values during winter 2011 compared to the other populations (Table 1, Fig. 3(c, d)).

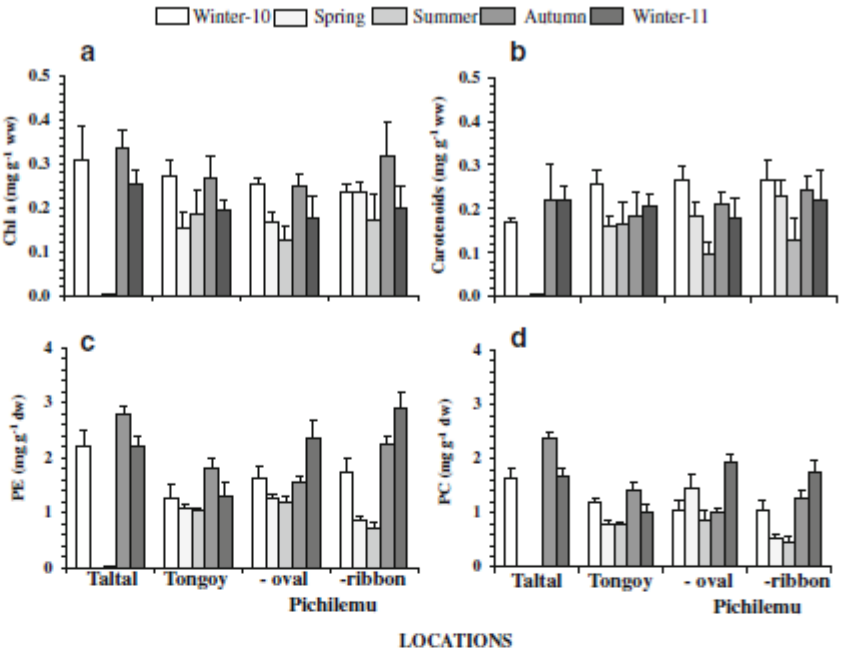

Fig. 3 Seasonal and latitudinal variation in *a* chlorophyll *a* (*chl a*), *b* total carotenoids, *c* phycoerythrin (*PE*), and *d* phycocyanin (*PC*) of *Porphyra* spp. from *Taltal* (*Porphyra* sp.1), *Tongoy* (*Porphyra* sp.2), and *Pichilemu* (*Porphyra* sp.3 oval morphology and *Porphyra* sp.4 ribbon morphology). No data were registered for Taltal spring. Data are shown as means±SD

Other compounds

Seasonal variations in protein content showed a tendency of low values during summer for *Porphyra* populations (Fig. 4(a)). Significant high soluble protein was detected in autumn for Taltal population ($F_{(2,26)}$=4.466, P=0.022) and in winter for Tongoy ($F_{(4,44)}$=4.363, P=0.005), Pichilemu oval ($F_{(4,44)}$=17.286, P<0.001), and Pichilemu ribbon ($F_{(4,44)}$=20.341, P<0.001) (Fig. 4(a)). Significant differences (P<0.01) between seasons (summer and winter 2011), localities, and the interaction were obtain in the two-way analyses that confirmed low protein levels for Taltal during summer (Table 2).

Although seasonal variation was detected for phenolic contents, there was no similar seasonal pattern for the populations (Fig. 4(b)). For *Porphyra* sp.1 (Taltal $F_{(2,26)}$=160.972, P=0.022) and *Porphyra* sp.2 (Tongoy $F_{(4,44)}$=6.211, P<0.001), high mean values were found for winter 2011 compared to the other seasons, while for *Porphyra* (sp.3 and sp.4) from Pichilemu, high values occurred during autumn (oval $F_{(4,44)}$=4.435, P=0.005; ribbon $F_{(4,44)}$=8.449, P<0.001). Similar to the other physiological variables, significant differences were detected between seasons (summer and winter 2011), localities, and the interaction (Table 2). The high mean value was found for Taltal winter 2011, and there was no difference between both seasons for Pichilemu oval morphotypes (Table 2, Fig. 4(b)).

Total antioxidant activity

The RSA showed seasonal variation with opposite tendency to the other physiological variables, with high values toward spring–summer time (Fig. 4(c)). Considering no samples for Taltal during spring and zero thallus developed during summer, significant differences ($F_{(2,26)}$=4.584, P=0.021) were detected only between both winter periods (Fig. 4(c)). Tongoy population showed a clear seasonal variation ($F_{(4,44)}$=28.876, P<0.001) with high RSA in summer, while for Pichilemu populations (oval $F_{(4,44)}$=5.636, P<0.001; ribbon $F_{(4,44)}$=8.556, P<0.001), it was showed during spring (Fig. 4(c)). Significant differences between seasons (summer and winter 2011), localities, and the interaction were found for RSA (Table 2). The lowest RSA was observed in Taltal and the highest in Tongoy. In Pichilemu, only during winter 2011, ribbon morphotype reached higher values and differed from oval morphotype (Table 2, Fig. 4(c)).

Discussion

The main results show seasonal and latitudinal variations for all the ecophysiological characteristics evaluated in the *Porphyra* spp. populations. A general pattern of decrease in photosynthetic efficiencies, pigments, and soluble proteins occurs in warm time accompanied by an increase in the

©Fungyi Chow / 2021

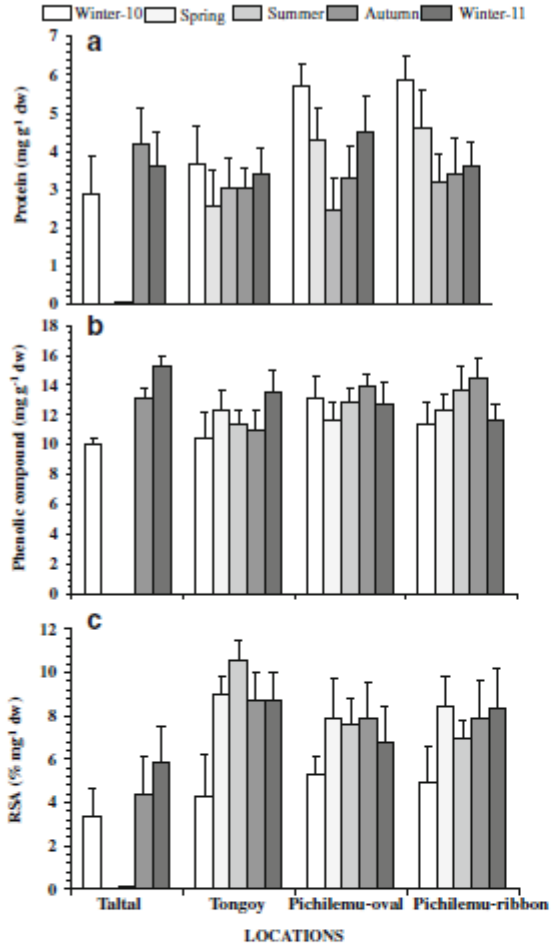

Fig. 4 Seasonal and latitudinal variation in *a* total soluble protein, *b* phenolic compounds, and *c* radical scavenging activity (*RSA*, antioxidant activity) of *Porphyra* spp. from *Taltal* (*Porphyra* sp.1), *Tongoy* (*Porphyra* sp.2), and *Pichilemu* (*Porphyra* sp.3 oval morphology and *Porphyra* sp.4 ribbon morphology). No data were recorded for Taltal spring. Data are shown as means±SD

antioxidant capacity. However, the magnitude of these changes depended on each population and local environmental conditions. Latitudinal differences were observed for the populations, and depending on the ecophysiological trait, higher values for Tongoy (center population) and Pichilemu (southern) morphotypes were reported. Taltal (northern) population contrasted with the others by showing a short annual development with disappearance fully during summer, while *Porphyra* from Tongoy (sp.2) and Pichilemu (sp.3 and sp.4) displays perennial characteristics. Considering the ecophysiological responses besides the morphology and phenological patterns, it is supposed that there are different species, and taxonomic validation by molecular approaches is recommended.

Table 2 Two-way ANOVA for seasonal (summer 2011 and winter 2011) and local (Taltal, Tongoy, and Pichilemu) variation in total soluble protein, phenolic compounds, and antioxidant activity of *Porphyra* spp. and post hoc Tukey's HSD results for each factor and interaction

Source of variation	*DF*	SS	MS	*F*	*P*
Protein					
Seasons	1	39.459	39.459	70.849	*<0.001*
Localities	3	23.958	7.986	14.339	*<0.001*
Seasons × localities	3	23.434	7.811	14.025	*<0.001*
Error	64	35.644	0.557		
Post hoc (Tukey's test)					
Seasons	Summer 2011 < winter 2011				
Localities	Taltal < Tongoy = Pichilemu oval = Pichilemu ribbon				
Interaction	S-Ta < S-Pr = S-To = S-Po < W-To = W-Ta = W-Po < W-Pr				
Phenolics					
Seasons	1	244.709	244.709	179.110	*<0.001*
Localities	3	303.909	101.303	74.147	*<0.001*
Seasons × localities	3	775.910	258.637	189.304	*<0.001*
Error	64	87.440	1.366		
Post hoc (Tukey's test)					
Seasons	Summer 2011 < winter 2011				
Localities	Taltal < Tongoy = Pichilemu ribbon = Pichilemu oval				
Interaction	S-Ta < S-To = W-Pr < W-Po = S-Po < W-To = S-Pr < W-Ta				
Antioxidant activity					
Seasons	1	21.252	21.252	12.270	*<0.001*
Localities	3	440.284	146.761	84.736	*<0.001*
Seasons × localities	3	145.652	48.551	28.032	*<0.001*
Error	64	110.847	1.732		
Post hoc (Tukey's test)					
Seasons	Winter 2011 < summer 2011				
Localities	Taltal < Pichilemu oval = Pichilemu ribbon < Tongoy				
Interaction	S-Ta < W-Ta < W-Po = S-Pr = S-Po < W-Pr = W-To < S-To				

P values in italic highlight represent significant differences at $p<0.01$

DF degree of freedom, *SS* square sum, *MS* medium square, *F* statistic index, *P* probability, *S* summer, *W* winter, *Ta* Taltal, *To* Tongoy, *Po* Pichilemu oval, *Pr* Pichilemu ribbon

Seasonal pattern in ecophysiological characteristics

Daily and seasonal variation in temperature and solar radiation (photoperiod and intensity) have been referred as the most important abiotic factor controlling growth, reproduction, and morphology of seaweed including *Porphyra*, mainly in temperate regions (Kain 1989; Falkowski and Laroche 1991; Lobban and Harrison 1994; Franklin and Forster 1997; Eggert 2012). Changes in the biochemical/physiological processes as photosynthetic rates, pigment levels, and other

©Fungyi Chow / 2021

metabolites occur in order to protect the cell integrity from damage and loss of homeostasis (Demmig-Adams and Adams 1992; Franklin and Forster 1997; Häder and Figueroa 1997; Cruces et al. 2012). The seasonal variations observed in the maximal quantum yield of PSII (F_v/F_m) and pigments support the idea that *Porphyra* from Tongoy and Pichilemu can temporarily cope with the changes in the solar radiation and temperature in moderate conditions that occur in these zones. In contrast, *Porphyra* sp.1 (Taltal) would be susceptible to summer conditions from the northern of Chile (higher radiation and temperature), and tissue deterioration occurs also after the release of reproductive gametes mainly in winter, without the capacity to maintain the macroscopic thallus during summer. These changes were in accordance with the variation of cover and biomass in each population (Tala and Chow 2014) that diminishes during spring and summer, and *Porphyra* sp.1 (Taltal) disappears completely in summer.

Excess of radiation can reduce the photosynthetic activity of marine algae during short (daily) and large periods (seasons) by a direct damage of the pigment protein complexes and by metabolic adjustments as dynamic photoacclimation which is shown by depression of the effective quantum yield (Y(II)), maximum electron transport rate $(ETR)_{max}$, and O_2 production (Figueroa et al. 1997, 2003; Bischof et al. 2006). Changes in the pigment content and absorbed quanta have been described for *Porphyra leucosticta* Thuret in long-term experiments (1 week) exposed to different irradiances as a photoacclimation response (Figueroa et al. 2003). Reduction in the levels of phycobiliprotein pigments observed during summer can be related with their importance as photoacclimation compounds or as nitrogen reserves that can be used during nitrogen depletion conditions. This decrease could be a photoprotective mechanism to avoid the excess of exciting energy to the chlorophyll *a* of the reaction center and, consequently, the oxidative photodamage. In the red algae, the phycobiliproteins are located outside of the thylakoids in the phycobilisomes, and phycoerythrin is located more externally and used during the photoacclimation process (Gantt et al. 2010; Bouzon et al. 2012). Phycobiliproteins should be recovered during periods with high environmental nutrient availability, usually in autumn and winter (Brown et al. 1990; Lobban and Harrison 1994; Rico and Fernández 1996; Lin and Stekoll 2011). Moreover, changes in the tissue absorptance and ETR curves also have been detected for Taltal, Tongoy, and Pichilemu ribbon morphotype with highest values during autumn and lowest in spring–summer (Tala and Chow 2014). Alterations in the cellular organization and ultrastructure have been also related to radiation responses that can accompany the physiological modifications of macroalgae (Contreras-Porcia et al. 2011; Bouzon et al. 2012). The success of these adjustments would depend on a combination of factors that are related to the magnitude of environmental changes, genetic performances, cope with stress levels, and availability of reserves and/or nutrients to redistribute the energy costs involved in these changes (Häder and Figueroa 1997; Bischof et al. 2006; Gantt et al. 2010).

Photoprotective responses as variation in the photosynthetic efficiency and pigment concentrations during warm conditions were accompanied with high antioxidant activity mainly in Tongoy population. Variations in other metabolites can also reflect the temporal physiological adjustments that are occurring by changes in the environmental and energy availability. Although the responses are locality dependent, soluble proteins showed a clear seasonal pattern with decreasing values during summer. Seasonal changes in protein levels have been describe for red (*Palmaria palmata* (L.) Weber & Mohr), brown (*Laminaria digitata* (Hudson) J.V. Lamouroux), and green (*Ulva lactuca* L.) seaweeds associated to nutrient depletion and changes in radiation that can cause destruction of proteins during summer (Fleurence 1999; Galland-Irmouli et al. 1999).

Phenolic compounds in plant and algae have also been associated with environmental protection against herbivory, fouling, and solar radiation acting as an induced or constitutive metabolite (Van Alstyne 1988; Gómez et al. 1998; Abdala-Díaz et al. 2006; Pansch et al. 2009). Some phenols can act as scavenging compounds preventing oxidative damage (Huovinen et al. 2010; Schmidt et al. 2012). Although the statistical analysis showed a seasonal variation in phenolic levels for each locality, they did not show a clear seasonal tendency. Abdala-Díaz et al. (2006) described in the brown algae *Cystoseira tamariscifolia* (Hudson) Papenfuss opposite pattern between phenolic compounds and incident irradiance in an annual versus daily cycle. Exudation of phenolic compounds at high irradiances regulated their concentration, and rapid synthesis and turnover time in the tissue serve as a photoprotective mechanism. In this context, rapid daily change may be masking seasonal patterns in *Porphyra*, and the results suggest that the seasonal variation can be population (species) specific. On the other hand, it is possible that soluble phenolic compounds did not represent an important defense mechanism against solar conditions in *Porphyra* and red seaweeds as been described for brown macroalgae (Leal Martins et al. 2013). Probably, other specific compounds such as pigments (carotenoids, phycoerythrin), MAAs, and antioxidant enzymes (CAT, APX) (Figueroa et al. 1997; Huovinen et al. 2004; Sampath-Wiley et al. 2008; Contreras-Porcia et al. 2011) could be more active in this red alga. Flavonoids, such as catechin, rutin, and hesperidin, and phenolic acids (salicylic acid, coumaric acid, caffeic acid) have been detected in some *Porphyra* species and related with their bioactivity as antioxidant (Yoshie et al. 2003; Kazłowska et al. 2010; Onofrejová et al. 2010).

Several enzymes and compounds can act as efficient antioxidant mechanisms, thus the total antioxidant activity should

©Fungyi Chow / 2021

reflect the sum of these acting systems. The results showed a seasonal tendency of increasing antioxidant activity toward summer and the most notoriously way for *Porphyra* sp.2 (Tongoy). Damage caused by the increase of radiation and temperature during summer is ameliorated by high antioxidant activities of glutathione reductase, catalase, and carotenoids in *Porphyra umbilicalis* Kützing during emersion (Sampath-Wiley et al. 2008). In contrast, emersion during winter did not have the same physiological effect (Sampath-Wiley et al. 2008). The results showed that for the Tongoy and Pichilemu populations, the antioxidant capacity increased during spring–summer and, for Taltal, during winter 2011. These characteristic together with the photosynthetic adjustment would allow the development of *Porphyra* in the upper intertidal zone. Morphological and physiological responses observed in *P. columbina* during desiccation confirm this capacity (Contreras-Porcia et al. 2011). Although desiccation causes overproduction and accumulation of reactive oxygen species (ROS) during low tides, it is efficiently attenuated for antioxidant enzymes that return it to basal levels during rehydration during high tides (Sampath-Wiley et al. 2008; Contreras-Porcia et al. 2011).

The temporal physiological adjustments would be in accordance with abundance changes observed in the field (Tala and Chow 2014). Brief and seasonal peaks in abundance during autumn–winter (*Porphyra* sp.1 Taltal) contrast with the relative persistent abundances in the time toward more central populations (Tongoy and Pichilemu). Similar abundance patterns have been described for *Porphyra* species in central Chile with interannual and seasonal variations (González and Santelices 2003). Differences observed for some variables between both winters (2010 and 2011) may be due to alternant cycles El Niño–La Niña impacting occasionally in the Chilean coast with climatic and oceanographic effects over the marine populations (Fernandez et al. 2000; Thiel et al. 2007). Sampling during winter 2010 occurred after El Niño (winter 2009–autumn 2010), and winter 2011 preceded a period La Niña finished at the middle of 2012 (http://www.esrl.noaa.gov/psd/people/klaus.wolter/MEI/). During these period changes in thermocline, tide levels and upwelling frequencies should impact the development and survival of coastal communities. In this sense, adjustments for changing environmental conditions would be occurring associated to local conditions with different metabolic, physiologic, and demographic patterns. Considering the geographic distribution of the taxa, these changes also can have a latitudinal component of variation.

Latitudinal pattern in ecophysiological characteristics

Latitudinal changes in the environmental conditions (irradiance, temperature, nutrient, wave exposure) have been associated with the phenology and ecophysiological responses in macroalgae and tolerance levels that define the geographic limits of distributions of species (Lüning 1991; Davison and Pearson 1996; Helmuth et al. 2006; Wiencke et al. 2007; Eggert 2012). Differences in the latitudinal temperatures more than radiation can be detected from Chilean database (www.shoa.cl; Sarmiento 2008) for the zones considered in the present study. Irradiation along a geographic gradient in South America shows that, at least during summer at any given location, all organisms are exposed to general high effective damage of UV radiation (Sarmiento 2008; Vernet et al. 2009). A strong latitudinal temperature gradient (from <14 °C in south to >20 °C in north) can be observed along the surface coastal waters in Chile (Fernandez et al. 2000; Thiel et al. 2007).

The latitudinal variation in the most of physiological traits could be associated with local seasonal patterns. For example, during winter 2011, high levels of phenols in Taltal are observed to be decreasing toward south populations. However, an opposite pattern was observed during winter 2010 and the other seasons. *Porphyra* sp.1 from Taltal showed a short annual cycle without development of macroscopic phases (gametophytic foliose blades) during summer when the environmental condition of radiation and temperature can injure them. Higher photosynthetic efficiencies, pigment, and protein were detected during autumn after the macroscopic thallus phase recovery. On the other hand, Tongoy (*Porphyra* sp.2) and both morphotypes from Pichilemu (*Porphyra* sp.3 and sp.4) were present at all times, but with more seasonal pattern for Tongoy populations than for Pichilemu in some physiological characteristics and in cover and biomass (Tala and Chow 2014). Considering latitudinal and seasonal responses between the studied populations, taxonomic clarity should be evaluated in order to understand better if there is intraspecific variation (dependent morphology) or interspecific variation.

Porphyra potential as local economic resources

The Chilean *Porphyra* spp. are actually poorly exploited and used in small local coast villages (Buschmann et al. 2001, 2008). Species of *Porphyra* have attractive characteristics as human food or supplements because they exhibit a high level of proteins (25–50 %), vitamins (B_{12}, C), trace minerals, dietary fibers, and different functional ingredients that can contribute to improve the human health (Noda 1993; MacArtain et al. 2007; Plaza et al. 2008; Blouin et al. 2011). Important metabolites from the primary and secondary metabolism in land plants, macroalgae, and microalgae are used as commodities for diverse industries that are looking for health promotion and disease risk reduction (Fleurence 1999; MacArtain et al. 2007; Shahidi 2009; Vilchez et al. 2011; Jiménez-Escrig et al. 2012). This situation is based on the valuable characteristic of sessile organism that should cope

©Fungyi Chow / 2021

with the environmental changes to preserve cell integrity, metabolic defenses, growth, and reproduction. Therefore, seasonal and latitudinal studies of ecophysiological adjustments and nutritional characteristics are also complementary and important in evaluating the potential use of *Porphyra* spp. and other algae as resources. Moreover, important photoprotectors against UV radiation as mycosporine-like amino acids (MAAs) and polyamines have been described for different *Porphyra* species (Figueroa et al. 2003; Huovinen et al. 2004; Cruces et al. 2012). Considering the seasonal and latitudinal patterns of some metabolites and the abundance of *Porphyra*, different exploitation strategies and new purpose of the raw material could be applied. Morphological and organoleptic properties required for human consumption could be considerate to define its potential use as food for these local *Porphyra* as have done for central species (González and Santelices 2003). Other commodities like pigment and antioxidant could be considered. Aspect related with extraction and stability of compounds, as well as yield and identification of potential market uses, would be considered. These concerns should be based on the knowledge of phenological development patterns (annual vs perennial) that may influence the strategies of exploitation and management of populations at local scale.

Acknowledgments We thank Danilo Peralta, Felipe Saez, and Hernán Venturino for their assistance with field support and Catalina Herrera, Fatme Tala, and Vieia Villalobos for their laboratory work. Research was supported by DGIT-UCN to F.T. and by FAPESP to F.C. We are also grateful to E. Rothäusler for the comments and review of the manuscript. This work was a part of fulfillment for the doctor of science degree of F.T. in the University of Sao Paulo, Brazil.

References

Abdala-Díaz RT, Cabello-Pisini A, Pérez-Rodríguez E, Conde Alvarez RM, Figueroa FL (2006) Daily and seasonal variations of optimum quantum yield and phenolic compounds in *Cystoseira tamariscifolia* (Phaeophyta). Mar Biol 148:459–465

Bischof K, Rautenberger R (2012) Seaweed responses to environmental stress: reactive oxygen and antioxidative strategies. In: Wiencke C, Bischof K (eds) Seaweed biology novel insights into ecophysiology, ecology and utilization. Springer, Berlin, pp 109–132

Bischof K, Gómez I, Molis M, Hanelt D, Karsten U, Lüder U, Roleda MY, Zacher K, Wiencke C (2006) Ultraviolet radiation shapes seaweed communities. Rev Environ Sci Biotechnol 5:141–166

Blouin NA, Brodie JA, Grossman AC, Xu P, Brawley SH (2011) *Porphyra*: a marine crop shaped by stress. Trends Plant Sci 16:29–37

Bouzon ZL, Chow F, Zitta CS, Santos RW, Ouriques LC, Felix MRL, Polo LK, Gouveia C, Martins RP, Latini A, Ramlov F, Maraschin M, Schmidt ÉC (2012) Effects of natural radiation, photosynthetically active radiation and artificial ultraviolet radiation-B on the chloroplast organization and metabolism of *Porphyra acanthophora* var. *brasiliensis* (Rhodophyta, Bangiales). Microsc Microanal 18:1467–1479

Brand-Williams W, Cuvelier M, Berset C (1995) Use of a free radical method to evaluate antioxidant activity. Food Sci Biotechnol 28:25–30

Brodie J, Mortensen AM, Ramirez ME, Russell S, Rinkel B (2008) Making the links: towards a global taxonomy for the red algal genus *Porphyra* (Bangiales, Rhodophyta). J Appl Phycol 20:939–949

Brodie J, Ramirez ME, Shaw R, Wyatt C, Mansilla A, Broom J (2011) Sorting out the locals: biodiversity of *Porphyra* sensu lato (Bangiales, Rhodophyta) in Magallanes region, Chile. Eur J Phycol 46:93

Brown MT, Frazer AWJ, Brasch DJ, Melton LD (1990) Growth and reproduction of *Porphyra columbina* Mont. (Bangiales, Rhodophyceae) from southern New Zealand. J Appl Phycol 2:35–44

Buschmann AH, Correa JA, Westermeier R, Hernández-González M, Norambuena R (2001) Red algal farming in Chile: a review. Aquaculture 194:203–220

Buschmann AH, Hernández-González MC, Varela D (2008) Seaweed future cultivation in Chile: perspectives and challenges. Int J Environ Pollut 33:432–456

Candia A, Lindstrom S, Reyes E (1999) *Porphyra* sp. (Bangiales, Rhodophyta): reproduction and life form. Hydrobiologia 398/399:115–119

Clark J, Poore A, Ralph PJ, Doblin MA (2013) Potential for adaptation in response to thermal stress in an intertidal macroalga. J Phycol 49:630–639

Collen J, Davison I (1999) Stress tolerance and reactive oxygen metabolism in the intertidal red seaweeds *Mastocarpus stellatus* and *Chondrus crispus*. Plant Cell Environ 22:1143–1151

Collen J, Pinto E, Pedersen M, Colepicolo P (2003) Induction of oxidative stress in the red macroalga *Gracilaria tenuistipitata* by pollutant metals. Arch Environ Con Tox 45:337–342

Contreras-Porcia L, Thomas D, Flores V, Correa JA (2011) Tolerance to oxidative stress induced by desiccation in *Porphyra columbina* (Bangiales, Rhodophyta). J Exp Bot 62:1815–1829

Cruces E, Huovinen P, Gómez I (2012) Stress proteins and auxiliary antistress compounds in intertidal macroalgae. Lat Am J Aquat Res 40:822–834

Davison IR (1991) Environmental effects on algal photosynthesis, temperature. J Phycol 27:2–8

Davison IR, Pearson GA (1996) Stress tolerance in intertidal seaweeds. J Phycol 32:197–211

Demmig-Adams B, Adams WW (1992) Photoprotection and other responses of plants to high light stress. Annu Rev Plant Phys 3:599–626

Denis C, Ledorze C, Jaoven P, Fleurence J (2008) Comparison of different procedures for the extraction and partial purification of R-phycoerythrin from the red macroalga *Grateloupia turuturu*. Bot Mar 52:278–281

Eggert A (2012) Seaweed responses to temperature. In: Wiencke C, Bischof K (eds) Seaweed biology novel insights into ecophysiology, ecology and utilization. Springer, Berlin 3:47–66

Falkowski PG, Laroche J (1991) Acclimation to spectral irradiance in algae. J Phycol 27:8–14

Fernandez M, Jaramillo E, Marquet PA, Moreno CA, Navarrete SA, Ojeda FP, Valdovinos CR, Vasquez JA (2000) Diversity, dynamics and biogeography of Chilean benthic nearshore ecosystems: an overview and guidelines for conservation. Rev Chil Hist Nat 73:797–830

Figueroa FL, Salles S, Aguilera J, Jiménez C, Mercado J, Viñegla B, Flores-Moya A, Altamirano M (1997) Effects of solar radiation on photoinhibition and pigmentation in the red alga *Porphyra leucosticta*. Mar Ecol Progr Ser 151:81–90

Figueroa F, Conde-Alvarez R, Gómez I (2003) Relations between electron transport rates determined by pulse amplitude modulated chlorophyll fluorescence and oxygen evolution in macroalgae under different light conditions. Photosynth Res 75:259–275

Fleurence J (1999) Seaweed proteins: biochemical, nutritional aspects and potential uses. Trends Food Sci Technol 10:25–28
Fowler-Walker MJ, Wernberg T, Connell SD (2006) Differences in kelp morphology between wave sheltered and exposed localities: morphologically plastic or fixed traits? Mar Biol 148:755–767
Franklin LA, Forster RM (1997) The changing irradiance environment: consequences for marine macrophyte physiology, productivity and ecology. Eur J Phycol 32:207–232
Galland-Irmouli AV, Fleurence J, Lamghari R, Luçon M, Rouxel C, Barbaroux O, Bronowicki JP (1999) Nutritional value of proteins from edible seaweed *Palmaria palmata* (dulse). J Nutr Biochem 10: 353–359
Gantt E, Berg G-M, Bhattacharya D, Blouin NA, Brodie JA, Chan CX, Collén J, Cunningham Jr FX, Gross J, Grossman AR, Karpowicz S, Kitade Y, Klein AS, Levine IA, Lin S, Lu S, Lynch M, Minocha SC, Müller K, Neefus CD, Cabral de Oliveira M, Rymarquis L, Smith A, Stiller JW, Wu WK, Yarish C, Zhuang Y, Brawley SH (2010) *Porphyra*: complex life histories in a harsh environment: *P. umbilicalis*, an intertidal red alga for genomic analysis. In: Seckbach J and Chapman DJ (eds) Red algae in the genomic age. Springer, Dordrecht 13:129–148
Gómez I, Huovinen P (2010) Induction of phlorotannins during UV exposure mitigates inhibition of photosynthesis and DNA damage in the kelp *Lessonia nigrescens*. Photochem Photobiol 86:1056–1063
Gómez I, Pérez-Rodríguez E, Viñegla B, Figueroa FL, Karsten U (1998) Effects of solar radiation on photosynthesis and UV-absorbing compounds of the Mediterranean green alga *Dasycladus vermicularis* from southern Spain. J Photochem Photobiol B 47:46–57
Gómez I, López-Figueroa FL, Ulloa N, Morales V, Lovengreen C, Huovinen P, Hess S (2004) Patterns of photosynthesis in 18 species of intertidal macroalgae from southern Chile. Mar Ecol Progr Ser 270:103–116
González A, Santelices B (2003) A re-examination of the potential use of central Chilean *Porphyra* (Bangiales, Rhodophyta) for human consumption. In: Chapman ARO, Anaderson RJ, Vreeland VJ, Davisen IR (eds) Proceedings of the 17th international seaweed symposium. Oxford University Press, New York, pp 249–255
González A, Beltrán J, Hiriart-Bertrand L, Flores V, De Reviers B, Correa JA, Santelices B (2012) Identification of cryptic species in the *Lessonia nigrescens* complex (Phaeophyceae, Laminariales). J Phycol 48:1153–1165
Gouveia C, Kreusch M, Schmidt ÉC, Felix MRL, Polo LK, Pereira DT, Santos R, Ouriques LC, Martins RP, Latini A, Ramlov F, Carvalho TJG, Chow F, Maraschin M, Bouzon ZL (2013) The effects of lead and copper on the cellular architecture and metabolism of the red alga *Gracilaria domingensis*. Microsc Microanal 19:513–524
Häder DP, Figueroa FL (1997) Photoecophysiology of marine macroalgae. Photochem Photobiol 66:1–14
Helmuth B, Mieszkowska N, Moore P, Hawkins SJ (2006) Living on the edge of two changing worlds: forecasting the responses of rocky intertidal ecosystems to climate change. Annu Rev Ecol Evol Syst 37:373–404
Henley WJ, Dunton KH (1995) A seasonal comparison of carbon, nitrogen, and pigment content in *Laminaria solidungula* and *L. saccharina* (Phaeophyta) in the Alaskan Arctic. J Phycol 31:325–31
Hoyer K, Karsten U, Sawall T, Wiencke C (2001) Photoprotective substances in Antarctic macroalgae and their variation with respect to depth distribution, different tissues and developmental stages. Mar Ecol Prog Ser 211:117–129
Huovinen P, Gómez I, Figueroa FL, Ulloa N, Morales V, Lovengreen C (2004) Ultraviolet absorbing mycosporine-like amino acids in red macroalgae from Chile. Bot Mar 47:21–29
Huovinen P, Leal P, Gómez I (2010) Interacting effects of copper, nitrogen and ultraviolet radiation on the physiology of three south Pacific kelps. Mar Freshwater Res 61:330–341
Inskeep WP, Bloom PR (1985) Extinction coefficients of chlorophyll *a* and q in *N,N*-dimethyl-formamide and 80 % acetone. Plant Physiol 77:483–485
Israel A (2010) The extreme environments of *Porphyra*, a fast growing and edible red marine macroalga. In: Seckbach J, Chapman DJ (eds) Red algae in the genomic age. Springer, Dordrecht 13:61–75
Jiménez-Escrig A, Gómez-Ordóñez E, Rupérez P (2012) Brown and red seaweeds as potential sources of antioxidant nutraceuticals. J Appl Phycol 24:1123–1132
Kain J (1989) The seasons in the subtidal. Brit Phycol J 24:203–215
Karsten U (2012) Seaweed acclimation to salinity and desiccation stress. In: Wiencke C, Bischof K (eds) Seaweed biology novel insights into ecophysiology, ecology and utilization. Springer, Berlin 5:87–108
Kazlowska K, Hsuc T, Houb C-C, Yang W-C, Tsai G-J (2010) Anti-inflammatory properties of phenolic compounds and crude extract from *Porphyra dentate*. J Ethnopharmacol 128:123–130
Leal Martins CD, Ramlov F, Peixoto NNC, Gestinari LM, dos Santos BF, Bento LM, Lhullier C, Gouvea L, Bastos E, Horta PA, Soares AR (2013) Antioxidant properties and total phenolic contents of some tropical seaweeds of the Brazilian coast. J Appl Phycol 25:1179–1187
Lin R, Stekoll MS (2011) Phycobilin content of the conchocelis phase of Alaskan *Porphyra* (Bangiales, Rhodophyta) species: responses to environmental variables. J Phycol 47:208–214
Lobban C, Harrison P (1994) Seaweed ecology and physiology. Cambridge University Press, Cambridge, p 366
Lüning K (1991) Seaweeds: their environment, biogeography and ecophysiology. Wiley, New York, p 527
Lüning K, Tom Dieck I (1989) Environmental triggers in algal seasonality. Bot Mar 32:389–397
MacArtain P, Gill CIR, Brooks M, Campbell R, Rowland IR (2007) Nutritional value of edible seaweeds. Nutr Rev 65:535–543
Mittler R (2002) Oxidative stress, antioxidants and stress tolerance. Trends Plant Sci 7:405–410
Molyneux P (2004) The use of the stable free radical diphenylpicrylhydrazyl (DPPH) for estimating antioxidant activity. J Sci Technol 26:211–219
Nelson W, Broom JE (2010) The identity of *Porphyra columbina* (Bangiales, Rhodophyta) originally described from the New Zealand subantarctic islands. Aust Syst Bot 23:16–26
Noda H (1993) Health benefits and nutritional properties of nori. J Appl Phycol 5:255–258
Onofrejová L, Vasicková J, Klejdus B, Stratil P, Misurcová L, Krácmar S, Kopecky J, Vacek J (2010) Bioactive phenols in algae: the application of pressurized-liquid and solid-phase extraction techniques. J Pharm Biomed 51:464–470
Pansch C, Cerda O, Lenz M, Wahl M, Thiel M (2009) Consequences of light reduction for anti-herbivore defense and bioactivity against mussels in four seaweed species from northern-central Chile. Mar Ecol Prog Ser 381:83–97
Plaza M, Cifuentes A, Ibáñez E (2008) In the search of new functional food ingredients from algae. Trends Food Sci Tech 19:31–39
Raison JK, Berry JA, Armond PA, Pike CS (1980) Membrane properties in relation to the adaptation of plants to temperature stress. In: Turner NC, Kramer PJ (eds) Adaptation of plants to water and temperature stress. Wiley, New York, pp 261–273
Ramírez ME, Santelices B (1991) Catálogo de las algas marinas bentónicas de la costa temperada del Pacífico de Sudamérica. Monografía Biol 5:1–437
Rico JM, Fernández C (1996) Seasonal nitrogen metabolism in an intertidal population of *Gelidium latifolium* (Gelidiaceae, Rhodophyta). Eur J Phycol 31:149–155
Sampath-Wiley P, Neefus C (2007) An improved method for estimating R-phycoerythrin and R-phycocyanin contents from crude aqueous extracts of *Porphyra* (Bangiales, Rhodophyta). J Appl Phycol 19: 123–129

Sampath-Wiley P, Neefus CD, Jahnke JS (2008) Seasonal effects of sun exposure and emersion on intertidal seaweed physiology: fluctuations in antioxidant contents, photosynthetic pigments and photosynthetic efficiency in the red alga *Porphyra umbilicalis* Kützing (Rhodophyta, Bangiales). J Exp Mar Biol Ecol 361:83–91

Sarmiento P (2008) Irradiancia solar en territorios de la república de Chile. In: Comisión Nacional de Energía de Chile (eds) Chile: remoción de barreras para la electrificación rural con energías renovables. Project CHI/00/G32, United Nations Development Programme, Universidad Técnica Federico Santa María de Chile

Schmidt EC, Santos RW, De Faveri C, Horta PA, De Paula MR, Latini A, Ramlov F, Maraschin M, Bouzon ZL (2012) Response of the agarophyte *Gelidium floridanum* after in vitro exposure to ultraviolet radiation B: changes in ultrastructure, pigments, and antioxidant systems. J Appl Phycol 24:1341–1352

Schreiber U, Bilger W, Neubauer C (1994) Chlorophyll fluorescence as a non-intrusive indicator for rapid assessment of in vivo photosynthesis. Ecol Stud 100:49–70

Schwachtje J, Baldwin IT (2008) Why does herbivore attack reconfigure primary metabolism? Plant Physiol 146:845–851

Seguel M, Santelices B (1988) Cultivo masivo de la fase conchocelis de luche, *Porphyra columbina* Montagne (Rhodophyta, Bangiaceae). Gayana 45:317–327

Sekar S, Chandramohan M (2008) Phycobiliproteins as a commodity: trends in applied research, patents and commercialization. J Appl Phycol 20:113–136

Shahidi F (2009) Nutraceuticals and functional foods: whole versus processed foods. Trends Food Sci Tech 20:376–387

Spalding MD, Fox HE, Al AG (2007) Marine ecoregions of the world: a bioregionalization of coastal and shelf areas. Bioscience 57:573–583

Staehr PA, Wernberg T (2009) Physiological responses of *Ecklonia radiata* (Laminariales) to a latitudinal gradient in ocean temperature. J Phycol 45:91–99

Steinhoff FS, Graeve M, Bischof K, Wiencke C (2012) Phlorotannin production and lipid oxidation as a potential protective function against high photosynthetically active and UV radiation in gametophytes of *Alaria esculenta* (Alariales, Phaeophyceae). Photochem Photobiol 88:46–57

Sutherland E, Lindstrom S, Nelson W, Brodie J, Lynch MDL, Sook Hwang M, Choi H-G, Miyata M, Kikuchi N, Oliveira MC, Farr T, Neefus C, Mols-Mortensen A, Milstein D, Müller KM (2011) A new look at an ancient order: generic revision of the Bangiales (Rhodophyta). J Phycol 47:1131–1151

Tala F, Chow F (2014) Phenology and photosynthetic performance of *Porphyra* spp. (Bangiophyceae, Rhodophyta): seasonal and latitudinal variation in Chile. Aquat Bot 113:107–116

Thiel M, Macaya EC, Acuña E, Arntz WE, Bastias H, Brokordt K, Camus PA, Castilla JC, Castro LR, Cortés M, Dumont CP, Escribano R, Fernandez M, Gajardo JA, Gaymer CF, Gomez I, González AE, González HE, Haye PA, Illanes J-E, Iriarte JL, Lancellotti DA, Luna-Jorquera G, Luxoro C, Manriquez PH, Marí V, Muñoz P, Navarrete SA, Perez E, Poulin E, Sellanes J, Sepúlveda HH, Stotz W, Tala F, Thomas A, Vargas CA, Vasquez JA, Vega JM (2007) The Humboldt Current System of northern and central Chile: oceanographic processes, ecological interactions and socioeconomic feedback. Oceanogr Mar Biol Ann Rev 45:195–344

Underwood AJ (1997) Experiments in ecology. Their logical design and interpretation using analysis of variance. Cambridge University Press, Cambridge

Van Alstyne KL (1988) Herbivore grazing increases polyphenolic defenses in the brown alga *Fucus distichus*. Ecology 69:655–663

Vernet M, Diaz S, Fuenzalida H, Camilion C, Booth CR, Cabrera S, Casiccia C, Deferrari G, Lovengreen C, Paladini A, Pedroni J, Rosales A, Zagarese HE (2009) Quality of UVR exposure for different biological systems along a latitudinal gradient. Photochem Photobiol 8:1329–1345

Vilchez C, Forján E, Cuaresma M, Bédmar F, Garbayo I, Vega JM (2011) Marine carotenoids: biological functions and commercial applications. Mar Drugs 9:319–333

Wernberg T, Coleman M, Fairhead A, Miller S, Thomsen M (2003) Morphology of *Ecklonia radiata* (Phaeophyta: Laminariales) along its geographic distribution in south-western Australia and Australasia. Mar Biol 143:47–55

Wiencke C, Clayton MN, Gómez I, Iken K, Lüder UH, Amsler CD, Karsten U, Hanelt D, Bischof K, Dunton K (2007) Life strategy, ecophysiology and ecology of seaweeds in polar waters. Rev Environ Sci Biotechnol 6:95–126

Yoshie Y, Hsieh YP, Suzuki T (2003) Distribution of flavonoids and related compounds from seaweed in Japan. J Tokyo Univ Fish 88:1–6

ANEXO 14

Journal of Applied Phycology (2019) 31:1333–1341
https://doi.org/10.1007/s10811-018-1615-y

Seasonal effects on antioxidant and anti-HIV activities of Brazilian seaweeds

Janaína Pires Santos[1] · Priscila Bezerra Torres[1] · Déborah Y. A. C. dos Santos[1] · Lucimar B. Motta[1] · Fungyi Chow[1]

Received: 8 May 2018 / Revised and accepted: 27 August 2018 / Published online: 4 September 2018
© Springer Nature B.V. 2018

Abstract
In recent years phytotherapy has been encouraged by Brazilian government agencies and has gained more and more credibility as a way of alternative therapy to complement allopathy. Although little explored in Brazil, seaweeds are promising marine bioresources as herbal medicine. In this context, the aim of the present study was to evaluate the antioxidant activities and reverse transcriptase inhibition (RT-HIV) of crude extracts (methanolic, aqueous, and hot aqueous) from three abundant species in Brazilian rocky shores, *Sargassum vulgare* (Ochrophyta), *Palisada flagellifera* (Rhodophyta), and *Ulva fasciata* (Chlorophyta), under two seasons (dry and rainy). Methanolic extracts from *S. vulgare* ($EC_{50} = 18.22 \pm 2.91$ μg mg^{-1}, dry), *P. flagellifera* ($EC_{50} = 24.85 \pm 3.13$ μg mg^{-1}, rainy), and *U. fasciata* ($EC_{50} = 33.41 \pm 1.53$ μg mg^{-1}, dry) showed the highest β-carotene bleaching activities, while hot aqueous extracts from *S. vulgare* showed the highest RT-HIV inhibition and antioxidant activities in ABTS, FRAP, and Folin-Ciocalteu assays. In general, the three macroalgae showed considerable antioxidant effects; however, only *S. vulgare* showed an anti-HIV potential (IC_{50} 10.15 ± 1.77 mg mL^{-1} for the dry season and $IC_{50} = 22.41 \pm 5.74$ μg mL^{-1} for rainy season). Regarding both extract yields and bioactivities, *S. vulgare* in the rainy season was the most promising alga. In conclusion, the studied seaweeds may be an effective alternative for Brazilian herbal medicine; additionally, seasonal studies are essential, since there were significant differences mainly for extract yields.

Keywords Anti-HIV · Antioxidants · Biotechnology · Seasonality · Seaweeds

Introduction

One third of the world's population does not have regular access to essential medicines, comprising more than 50% of the population of lowest-income countries in Africa and Asia (World Health Organization 2007). Because of the high price of medicines and the low purchasing power of the population of these countries, the use of traditional medicine has been the first line for the treatment of diseases or disorders (World Health Organization 2005; Nwobike 2006). Traditional medicine still remains almost restricted to the developing countries; however, the use of complementary and alternative medicine has grown in countries, such as Canada, France, and Australia (World Health Organization 2005). Within this world scene, the Brazilian government has encouraged the use of herbal medicines, which are low cost and an efficient way of treatment. The popular and institutional interests have been growing in the sense of strengthening phytotherapy in the Brazilian Unified Health System (Rosa et al. 2011), a public health organization of which over 75% of the Brazilian population depend on exclusively for health coverage (Cerri 2016).

In Asian countries, such as Japan, China, and Korea, many species of seaweeds have been used as food or with a medicinal intent since ancient times (Jeong et al. 2015; Yermak et al. 2016). For example, the crude extract of the brown seaweed *Sargassum naozhouense* C.K. Tseng & Lu Baoren, abundant on the Chinese coast, has been used to treat fever, infections, laryngitis, and other ailments by the local population (Wang et al. 2010). In traditional Vietnamese medicine, species of *Kappaphycus* and *Eucheuma* are used to reduce the occurrence of tumors, ulcers, and headaches, while *Sargassum* is used for treating iodine deficiency disorders such as goiter (Huynh and Nguyen 1998).

The herbal medicine value and the benefits of including seaweeds in the diet are well documented (Fleurence and Levine 2016). Seaweeds are rich in carotenoids, phycobilins (e.g., phycocyanins), fatty acids, polysaccharides, vitamins,

✉ Janaína Pires Santos
janainaps@usp.br

[1] University of São Paulo, Institute of Biosciences, Rua do Matão, 277, São Paulo, SP 05508-090, Brazil

©Fungyi Chow / 2021

sterols, and tocopherol, among others (Lordan et al. 2011). In recent years, the number of studies about biotechnological properties of macroalgae has grown exponentially and these organisms have became the focus of commercial interest as a source of valuable products for healthcare and potentially attractive as functional foods (Sekmokienė et al. 2007; Almeida et al. 2011; Hamed et al. 2015). However, the chemical composition and bioactivity attributed to seaweed extracts vary widely among species, and even intraspecific variants, depending on factors like geographical location, seasonality, and processing methods (Holdt and Kraan 2011; Lordan et al. 2011; Mols-Mortensen et al. 2017; Wells et al. 2017). Therefore, seasonal studies may suggest the best harvesting season and, consequently, increase the commercial value by improving the quality of final products (Suresh Kumar et al. 2015).

Among the biological potentials of seaweeds, antioxidant properties have an important role in the medicinal field (Kohen and Nyska 2002). Although the benefit to antioxidant consumption is mostly associated with land plants (vegetables and fruits), an increase in the number of scientific research with seaweeds has shown the same antioxidant benefits to human health (Cornish and Garbary 2010). In addition, algal extracts have several other bioactivities, such as antitumor, cytostatic activities, and antimicrobial (antibacterial, antifungal, antiprotozoal, and antiviral) (Almeida et al. 2011; Jeong et al. 2015; Vieira et al. 2017).

Antiviral power is an important point for deepening the research due to the fact that viruses are responsible for several serious illnesses. Distinctive structure and complicated life cycle of viruses have hampered the discovery of safe and effective drugs against viral infections. Despite comprehensive studies for suitable vaccines and treatments, several infections, such as Acquired Immunodeficiency Syndrome (AIDS), continue to afflict a substantial share of the world population in all generations (Ruzagira et al. 2011; Loutfy et al. 2013). In this scenario, reports show that herbal medicines have improved the immunostimulatory effects for the user, giving hope to patients infected by the HIV virus in poor countries, mainly in Africa, where only 37% of the population has access to the conventional treatment of this disease (World Health Organization 2005; Unaids 2013) and marine organisms, including seaweeds, could be attractive candidates. Teas et al. (2004), based on epidemiological studies, proposed a correlation between the low incidence of AIDS and regular eating of algae, including the infection process of HIV and simultaneous stimulation of the immune response.

Despite all this potential of seaweeds, seasonal studies that investigate the biological potential and applications in tropical macroalgae extracts, including Brazilian algae, are still scarce. Studies involving seasonality are also important for applied researches because it is crucial to know the best period to harvest algae for both the chemical composition of the extracts (qualitative), as well as for biomass (quantitatively). Therefore, the present work aimed to investigate the antioxidant and anti-HIV potentials and the seasonal variation of methanolic, aqueous, and hot aqueous extracts from three abundant algae on the northeast coast of Brazil, *Sargassum vulgare* C. Agardh (Fucales, Ochrophyta), *Palisada flagellifera* (J. Agardh) K.W. Nam (Ceramiales, Rhodophyta), and *Ulva fasciata* Delile (Ulvales, Chlorophyta).

Materials and methods

Chemicals

All chemicals were of analytical grade from Sigma-Aldrich: β-carotene (Cat. No. 22040), butylated hydroxytoluene (BHT; purity ≥99%, Cat. No. w218405), Folin-Ciocalteu reagent (Cat. No. 47641), sodium phosphonoformate tribasic hexahydrate (Foscamet; Cat. No. P6801), dimethyl sulfoxide (DMSO; Cat. No. D8418), gallic acid (purity ≥97.5%, Cat. No. g7384), linoleic acid (Cat. No. l1012), polyoxyethylenesorbitan monopalmitate (Tween 40; Cat. No. 9005-66-7), 2,2′-azino-bis(3-ethylbenzothiazoline-6-sulfonic acid) diammonium salt (ABTS; Cat. No. a1888), Trolox (purity of 97%, Cat. No. 238813), 2,2-diphenyl-1-picrylhydrazyl (DPPH; Cat. No. d9132), 3-(2-pyridyl)-5,6-diphenyl-1,2,4-triazine-4′,4″-disulfonic acid sodium salt (Ferrozine; Cat. No. 82950), and 2,4,6-tris(2-pyridyl)-s-triazine (TPTZ; Cat. No. 93285).

Collection of seaweed samples and extract preparation

The seaweeds were collected from the Northeast Brazilian coast at Morro de Pernambuco beach, municipality of Ilheus, Bahia State (14°48′21.6″S, 39°01′25.6″W) in the dry (November 2013) and rainy season (May 2014). Sampling was carried out manually from the rocky shore midlittoral zone during the low tide period. The brown macroalga *S. vulgare* usually inhabits tidal pools, which are protected from the waves. The red macroalga *P. flagellifera* lives in fissures protected from the direct impact of the waves, while the green macroalga *U. fasciata* inhabits regions of the rocky shore that is exposed to waves and desiccation. These three seaweed species are representative of region rocky shore. Only thalli with healthy appearance were collected, and the complete thalli were used for analyses of this study. Dr. Beatriz Nogueira Torrano da Silva and Dr. Valeria Cassano from the Institute of Bioscience of the University of São Paulo, Brazil, using barcoding techniques (Saunders 2005) performed the molecular taxonomical identification. The DNA sequences of each species were compared with public reference GenBank database. Voucher specimens have been deposited

©Fungyi Chow / 2021

in the Herbarium of the University of São Paulo (SPF) for future reference (*S. vulgare* SPF 57907, SPF 57908, and SPF 57909; *P. flagellifera* SPF 57902, SPF 57904, and SPF 57905; *U. fasciata* SPF 57903, SPF 57905, and SPF 57906).

Once harvested, the algal material was pooled per species, rinsed in tap water, and oven dried at 40 °C for 2 days. The three species were milled into powder with a knife mill with a 30 mesh sieve (Fortinox STAR FT 80). The powdered material per species and season was separated in five subsamples ($n = 5$). Each subsample was extracted by maceration (1:10 *w*/*v*) successively in methanol and then water for 24 h at room temperature and lastly hot water for 1 h at 70 °C. The macerations were performed three times with each solvent. The extracts were filtered, pooled per solvent, concentrated in a rotary evaporator at 40 °C, and finally freeze-dried. In the end, three crude extracts for each subsample per species and season were obtained, as follows: methanolic extract (MeOH), aqueous extract (Aq), and hot aqueous extract (H-Aq), which were tested for antioxidant and antiviral potential in five different concentrations. The extract yield was calculated based on the initial dry mass of each subsample.

Antioxidant activities

The antioxidant assays were performed in a 96-well microplate reader (Epoch, BioTek Instruments, USA). Methanol or 10% DMSO (dimethyl sulfoxide in ultrapure water) was used to dilute the crude extracts, reference standards (gallic acid, BHT, and Trolox), and negative controls. The three crude extracts of each subsample ($n = 5$) were tested at final concentrations of 0, 25, 50, 100, 150 to 200 μg mL^{-1}. The EC_{50} values (the half maximal effective concentration which induces a response halfway of the maximum after a specified exposure time) were calculated by a dose-response sigmoid model using the GraphPad Prism 7 software. Additionally, standard equivalents were calculated from the calibration curves of gallic acid or Trolox and expressed based on the dry mass of the extract. For evaluating the antioxidant activity, six antioxidant assays were applied: DPPH radical scavenging, β-carotene/linoleic acid system, ABTS radical scavenging, ferric reducing antioxidant power (FRAP), metal chelating, and reducing substances by the Folin-Ciocalteu reagent, as described below.

β-Carotene/linoleic acid system The assay was prepared as the methodology of Marco (1968) and Miller (1971) with modifications to microplate format. The reactive solution was prepared by combining 16 μL of linoleic acid, 160 μL of Tween 40, and 160 μL of β-carotene (2 mg mL^{-1} in dichloromethane). This solution was heated in a water bath at 45 °C until complete evaporation of the dichloromethane and then 20 mL of ultrapure water saturated in oxygen was added and the solution homogenized. The reactive solution was checked for its translucent appearance and absorbance between 0.8 and 1 at 450 nm. Aliquots of 20 μL of samples (extracts, standards, or negative controls) and 280 μL of reactive solution were added in each well of the 96-well microplate. The absorbance was measured at 450 nm in time = 0 min (initial) and every 20 min for 2 h under constant stirring at 45 °C. Trolox ($n = 3$) was used as reference compound (0.5–2 μg mL^{-1}; $Y = 1.0412X + 0.9684$; $R^2 = 0.99$).

$ABTS^{+\cdot}$ radical scavenging activity The assay was performed as described by Torres et al. (2017) modified from Rufino et al. (2007). The solution of the $ABTS^{+\cdot}$ was prepared by mixing 1 mL of ABTS (7 mM) with 17.6 μL of potassium persulfate (140 mM). The solution reacted for 16 h at room temperature. The absorbance of this solution was adjusted to 0.8 at 734 nm by diluting in methanol (1:60 *v*/*v*). In each well of the microplate, 20 μL of samples was added (extracts, standards, or negative controls) and 280 μL of $ABTS^{+\cdot}$ solution (pH 6.7). Absorbance was measured at 734 nm after 20 min at room temperature. Trolox ($n = 3$) was used as reference compound for the calibration curve (1–10 μg mL^{-1}; $Y = -0.3942X + 0.8178$; $R^2 = 0.99$).

Ferric reducing antioxidant power The FRAP assay was performed as Urrea-Victoria et al. (2016) modified from Benzie and Strain (1996). The FRAP reagent solution was prepared by mixing 25 mL of acetate buffer (0.3 M; pH 3.6), 2.5 mL of TPTZ (10 mM in 40 mM hydrochloric acid), and 2.5 mL of 20 mM ferric chloride. Aliquots of 20 μL of samples (extracts, standards, or negative controls), 15 μL de ultrapure water, and 265 μL of FRAP reagent solution were added to each well. The microplate was incubated at 37 °C for 30 min and the absorbance readings were measured at 595 nm. Trolox ($n = 3$) was used for preparing the reference curve (1.5–7.5 μg mL^{-1}; $Y = 0.6522X + 0.0024$; $R^2 = 0.99$).

Reducing compounds by the Folin-Ciocalteu method The reducing capacity assay of Folin-Ciocalteu was performed as Pires et al. (2017a) modified from Waterman and Mole (1994). Aliquots of 20 μL of samples (extracts, standards, or negative controls), 200 μL ultrapure water, 20 μL of Folin-Ciocalteu reagent, and 60 μL of a saturated solution of sodium carbonate were added to each well. Absorbance was measured at 760 nm after 30 min at 25 °C. Gallic acid ($n = 3$) was used for the reference curve (1.5–8.5 μg mL^{-1}; $Y = 0.3201X + 0.009$; $R^2 = 0.99$).

DPPH radical scavenging activity The assay was prepared following Pires et al. (2017b) modified from Brand-Williams et al. (1995). Aliquots of 20 μL of samples (extracts, standards, or negative controls) and 280 μL of a methanolic solution of DPPH (0.080 mM; absorbance ca. of 0.8 at 517 nm) were added to each well. The microplate was incubated at 25 °C

©Fungyi Chow / 2021

for 20 min at room temperature and then the absorbance was measured at 517 nm. Gallic acid ($n = 3$) was used as reference compound for the calibration curve (0.5–2.0 μg mL^{-1}; $Y = -1.0684X + 0.7303$; $R^2 = 0.99$).

Metal chelating activity The assay was performed as Harb et al. (2016) modified from Min et al. (2011). Aliquots of 20 μL of samples (extracts, standards, or negative controls), 250 μL of 10% ammonium acetate, and 15 μL of 1 mM ammonium sulfate solution were added into each well. After 5 min, 15 μL of 6.1 mM ferrozine was added and the reactive mixture was incubated for 10 min at room temperature under stirring and then the absorbance readings were taken at 562 nm. Gallic acid ($n = 3$) was used as reference compound for the standard curve (1.5–3.5 μg mL^{-1}; $Y = -0.3842X + 0.7542$; $R^2 = 0.99$).

Anti-HIV activity

The potential for antiviral activity of the extracts was assessed by testing the inhibition of the reverse transcriptase enzyme (RT) of the human immunodeficiency virus type 1 (HIV-1) using a colorimetric kit RT assay (Roche Diagnostics, Switzerland) with modification according to manufacturer's instructions. The three crude extracts of each subsample ($n = 5$) were dissolved in 10% DMSO prepared with ultrapure DEPEC-treated water and tested at final concentrations range of 100 to 1400 μg mL^{-1}. In microtubes, 20 μL of each concentration of crude extracts, 1 μL of HIV-1 RT enzyme (1 μg $well^{-1}$), 19 μL of incubation buffer, and 20 μL of polyA+ oligo solution were added. This combination, called reaction mixture, was incubated for 1 h at 37 °C. Afterwards, 60 μL of the reaction mixture was transferred to a microplate with streptavidin provided by the manufacturer, sealed, and incubated for 1 h at 37 °C. Then, the microplate was washed five times with wash buffer and 198 μL of incubation buffer. Aliquots of 200 μL of anti-DIG-POD (peroxidase-anti-digoxigenin antibody), working dilution, were added in each well and the microplate was sealed and incubated for 1 h at 37 °C and then washed again five times with wash buffer. In the last step, after the complete drying of the microplate, 200 μL of ABTS was added and the microplate was incubated for 30 min at 25 °C. The absorbances of the samples were measured in a microplate reader at 405 and 490 nm. Two controls were used: (a) 10% DMSO without sample (negative control) and (b) Foscarnet with the addition of the RT enzyme (positive control). A calibration curve was made with Foscarnet, a positive control, at final concentrations of 0.0625, 0.125, 0.25, 0.5, 1, 2, and 4 μg mL^{-1}. The results of the positive control and extracts were expressed as the percentage of inhibition of the RT enzyme and calculated using the formula of Woradulayapinij et al. (2005): % Inhibition = $[[(Abs_{405blank} - Abs_{490blank}) - (Abs_{405sample} - Abs_{490sample})] \times 100] / (Abs_{405blank} - Abs_{490blank})$. In addition, the IC_{50} value was estimated at μg mL^{-1}, which corresponds to the concentration required for the extract or sample to inhibit 50% of maximal enzyme activity of RT, using the GraphPad Prism 7 software.

Statistical analysis

All of the statistical analyses were performed with STATISTICA 12 software. Datasets for antioxidant activity and anti-HIV were tested for normality using the test of Kolmogorov-Smirnov and homoscedasticity by Bartlett's test ($p < 0.05$). The antioxidant activity was analyzed for EC_{50} values and standard equivalent, while the RT-HIV samples were analyzed only for IC_{50} values, both were tested by two-way ANOVA, which were defined as first factor seasonal period (dry or rainy) and the three types of extracts (MeOH, aqueous, and hot aqueous) as the second factor separately for each species. When significant differences were verified, multiple comparisons among treatments were determined by the Newman-Keuls post hoc test ($p < 0.05$). Principal Components Analysis (PCA) method was performed using a Pearson correlation matrix.

Results and discussion

Antioxidant activities

Antioxidant methods measure the potential of the extracts for inhibit oxidation processes, but each assay has a principle and a specific chemical affinity with the components of each extract. Therefore, it is recommended that the extracts are tested by at least two different colorimetric methods to fully evaluate their antioxidant potential (Matanjun et al. 2008). The results for methanolic (MeOH), aqueous (Aq), and hot aqueous (H-Aq) extracts of the macroalgae *S. vulgare*, *P. flagellifera*, and *U. fasciata* are presented in Table 1.

In the DPPH assay, the EC_{50} values for all extracts and species were > 200 μg mL^{-1} (data not shown), showing lower activities in this assay as compared to EC_{50} values for the standard compounds, gallic acid (1.87 μg mL^{-1}), and Trolox (7.51 μg mL^{-1}). In contrast, Zubia et al. (2007) studying several brown, green, and red algae found some results in the DPPH assay more promising than those found in the present study. Similar results to DPPH were obtained for metal chelating assay, with EC_{50} > 200 μg mL^{-1} (data not shown) for all crude extracts. These values were much higher than the EC_{50} value found for gallic acid (8.33 μg mL^{-1}).

The three species of this study showed promising antioxidant power in β-carotene/linoleic acid assay. The results for MeOH extracts from *S. vulgare* (both seasons), *P. flagellifera* (both seasons), and *U. fasciata* (dry season) were similar or more active than the EC_{50} value of gallic acid (Table 1). These

Table 1 Antioxidant activities for *Sargassum vulgare*, *Palisada flagellifera*, and *Ulva fasciata*. The values are expressed in mean ± SD ($n = 5$) based on the EC_{50} value (half effective concentration) or dry mass of extracts calculated on base of gallic acid equivalent (GAE) or Trolox equivalent (TE). Different letters within the same species and antioxidant assay indicate differences between the means (two-way ANOVA and post hoc Newman-Keuls test; $p < 0.05$). MeOH = methanolic extract, Aq = aqueous extract, H-Aq = hot aqueous extract

Samples	β-Carotene bleaching EC_{50} (μg mL^{-1})		ABTS EC_{50} (μg mL^{-1})		FRAP (μmol TE g^{-1})		Folin-Ciocalteu (mg GAE g^{-1})	
	Dry	Rainy	Dry	Rainy	Dry	Rainy	Dry	Rainy
S. vulgare								
MeOH	18.22 ± 2.91^{a}	28.58 ± 2.24^{a}	165.82 ± 16.93^{a}	128.71 ± 20.13^{d}	216.40 ± 24.56^{a}	166.02 ± 62.83^{a}	10.84 ± 1.24^{a}	6.70 ± 0.44^{d}
Aq	142.70 ± 15.62^{b}	78.92 ± 5.99^{d}	73.29 ± 5.66^{b}	55.69 ± 4.12^{c}	102.14 ± 11.57^{b}	169.08 ± 6.54^{a}	13.31 ± 0.88^{b}	18.07 ± 1.39^{c}
H-Aq	66.47 ± 5.73^{c}	118.06 ± 4.36^{c}	46.46 ± 5.06^{c}	21.58 ± 2.64^{e}	198.28 ± 10.05^{a}	414.80 ± 26.03^{c}	18.94 ± 1.16^{c}	38.93 ± 1.88^{e}
P. flagellifera								
MeOH	39.75 ± 4.18^{a}	24.85 ± 3.13^{a}	> 200	128.58 ± 7.05^{a}	152.85 ± 32.75^{a}	126.36 ± 38.94^{d}	5.69 ± 1.25^{a}	8.30 ± 1.11^{b}
Aq	167.37 ± 5.25^{b}	121.63 ± 7.70^{c}	136.97 ± 30.30^{a}	145.86 ± 20.27^{a}	99.51 ± 5.83^{b}	080.12 ± 7.71^{bc}	8.23 ± 0.42^{b}	4.67 ± 0.72^{a}
H-Aq	> 200	139.45 ± 34.59^{c}	> 200	> 200	70.04 ± 2.97^{bc}	054.47 ± 8.13^{c}	4.91 ± 1.11^{a}	4.67 ± 0.63^{a}
U. fasciata								
MeOH	33.41 ± 1.53^{a}	101.87 ± 10.11^{b}	> 200	> 200	86.20 ± 1.38^{a}	117.62 ± 31.66^{c}	5.58 ± 0.86^{a}	6.42 ± 0.91^{a}
Aq	> 200	>200	> 200	> 200	65.36 ± 6.66^{b}	024.03 ± 7.83^{d}	4.42 ± 0.29^{b}	3.01 ± 0.80^{c}
H-Aq	> 200	>200	> 200	> 200	50.91 ± 5.33^{b}	057.79 ± 7.72^{b}	2.74 ± 0.33^{c}	3.30 ± 1.06^{c}
Standards								
Gallic acid	34.36		0.79		–		–	
BHT	0.11		31.92		–		–	
Trolox	0.02		3.42		–		–	

extracts were as active as the aromatic plants used in traditional medicine, such as common sage (*Salvia officinalis* L.; $EC_{50} = 14.49$ μg mL^{-1}) and apple mint (*Mentha suaveolens* Ehrh.; $EC_{50} = 27.37$ μg mL^{-1}) (Kasrati et al. 2017). Chew et al. (2008) evaluated MeOH extracts of three macroalgae (*Padina antillarum*, *Caulerpa racemosa*, and *Kappaphycus alvarezii*) and also found high antioxidant power, similar to quercetin. The β-carotene bleaching assay evaluates the antioxidants of lipophilic nature (Lage et al. 2013). The high activities observed in this work suggest that the studied macroalgae can also be used as a food preservative, preventing lipid peroxidation, which can cause deterioration in food (Gupta and Abu-Ghannam 2011).

The H-Aq extracts followed by Aq extracts of *S. vulgare* had the highest reduction potential (Folin-Ciocalteu, ABTS radical, and FRAP assays), being the extracts from the rainy season the most active (Table 1). The results for these extracts showed higher or similar antioxidant power than some medicinal plants or food rich in antioxidants reported in the literature. For example, black raspberry (*Rubus occidentalis* L.; $EC_{50} = 609$ μg mL^{-1}) (Jeong et al. 2010) and pomegranate fruit (*Punica granatum* L.; $EC_{50} = 34.78$ μg mL^{-1}) (Rajan et al. 2011) in the ABTS radical assay; lemongrass (*Cymbopogon citratus* (DC) Stapf.; 478.33 mM TE g^{-1}) in the FRAP assay; and lavender (*Lavandula angustifolia* Mill; 5.4 mg GAE g^{-1}) and chamomile (*Matricaria recutita* L.; 9.1 mg GAE g^{-1}) (Miliauskas et al. 2004) in the Folin-Ciocalteu assay. Pirian et al. (2017) observed similar results for organic extracts from *Sargassum* spp., which presented high antioxidant activity in the ABTS and FRAP assays.

In general, the highest antioxidant potentials were found in the MeOH and Aq extracts for *P. flagellifera* and in the MeOH extracts for *U. fasciata* (Table 1). In *S. vulgare*, different behaviors between crude extracts were observed: while the Aq and H-Aq extracts showed higher activities when the reaction mechanism of the assay is based on electron transfer ($ABTS^{+\cdot}$, FRAP, and Folin-Ciocalteu assays), the MeOH extracts had higher activities in the lipid peroxidation assay (Table 1). Thus, complementary and different antioxidant mechanisms were observed for the studied species and extracts.

Epidemiological studies have shown that diets rich in antioxidants reduce the incidence of degenerative diseases, such as cardiovascular, diabetes, and cancer, which kill thousands of people worldwide (Devasagayam et al. 2004). Thus, there is a great demand for antioxidants from natural sources, such as seed oil, grains, beans, vegetables, fruits, bark, roots, seaweeds, spices, and hulls (Guiry and Blunden 1991; Gülçin 2012; Anwar et al. 2018). Studies, which evaluate the clinical uses for the treatment or prevention of degenerative diseases from seaweeds, are close to be approved for use in human. Myers et al. (2010) made a clinical study (phases 1 and 2) with three brown algae: *Fucus vesiculosus*, *Macrocystis pyrifera*,

©Fungyi Chow / 2021

and *Saccharina* (*Laminaria*) *japonica*. The authors administered gel pills for 12 weeks with a mix of these extracts in patients suffering from osteoarthritis, and they could perceive that the extracts significantly reduced the symptoms of the disease and suggested to start Phase 3 clinical trial for this promising herbal medicine coming from marine algae.

Antiviral activity

Since inhibitors of HIV-1 reverse transcriptase (RT) are effective compounds in limiting HIV virus propagation (Holec et al. 2018), the anti-HIV potential of the extracts from the three species of algae of this study was addressed based on the in vitro inhibition of RT.

In general, the highest potentials of inhibition were in the H-Aq extracts in both seasons of *S. vulgare*, with IC_{50} values of 10.15 ± 1.77 and 22.41 ± 5.74 μg mL^{-1} for the dry and rainy seasons, respectively (Table 2). Meanwhile, the best antiviral responses for *P. flagellifera* were for Aq extracts with IC_{50} values of 277.60 ± 44.46 and 200.07 ± 57.14 μg mL^{-1} for dry and rainy seasons, respectively (Table 2). *Ulva fasciata* presented the smallest value of inhibition of RT enzyme (IC_{50} < 1400 μg mL^{-1}). Thus, the most active algae, *S. vulgare* and *P. flagellifera*, presented the aqueous extracts (H-Aq and Aq, respectively) as the most active extracts against the RT enzyme.

Table 2 Values of IC_{50} (half inhibitory concentration) (μg mL^{-1}) for crude extracts of *Sargassum vulgare*, *Palisada flagellifera*, and *Ulva fasciata* (mean ± SD; $n = 5$) against the activity of HIV-1 reverse transcriptase (HIV-1 RT) enzyme. Different letters within the same species indicate differences between the means (two-way ANOVA and post hoc Newman-Keuls test ($p < 0.05$). MeOH = methanolic extract, Aq = aqueous extract, H-Aq = hot aqueous extract

Samples	IC_{50} for the HIV-1 RT activity	
	Dry	Rainy
S. vulgare		
MeOH	>1400	186.04 ± 38.52^{c}
Aq	305.35 ± 26.28^{a}	183.77 ± 40.69^{c}
H-Aq.	10.15 ± 1.77^{b}	22.41 ± 5.74^{b}
P. flagellifera		
MeOH	>1400	>1400
Aq	277.60 ± 44.46^{a}	200.07 ± 57.17^{a}
H-Aq	>1400	>1400
U. fasciata		
MeOH	>1400	>1400
Aq	>1400	>1400
H-Aq	>1400	>1400
Standard		
Foscarnet	0.10	

Aqueous extracts and fractions of seaweed have been reported to be active through various phases of HIV replication. Some examples include the Carraguard® microbicide gel obtained from red algae (Cutler and Justman 2008) and aqueous fractions rich in fucoidan from *Sargassum swartzii* (Dinesh et al. 2016). The sulfated polysaccharides are generally considered the bioactives of these aqueous extracts and fractions. The IC_{50} observed for the extracts of the present study were higher than that obtained for the positive control (Foscarnet). However, studies using other standard compounds have pointed out the high sensitivity of Foscarnet to this assay. For example, Mahapatra et al. (2012) using Doxorubicin, a known HIV-1 RT enzyme inhibitor, found $IC_{50} = 47$ μg mL^{-1}, a higher value than those found for H-Aq extracts of *S. vulgare* (Table 2).

People who suffer from serious viral infections have to cope with aggressive treatments. Algae may play an important role in alternative antiviral therapies, with the advantage of the different forms of preparation of the algae have shown low toxicity to patients (Brown et al. 2014). In many countries, herbal treatments are very popular among HIV-infected individuals being used as complementary or primary treatments (Orisatoki and Oguntibeju 2010). For example, Teas and Irhimeh (2012) conducted a proof of concept clinical study which demonstrated that algae supplementation did no harm, and helped some of the patients participating in this study without access to retroviral therapy. However, regarding positive results obtained in vitro and in vivo assays with algae, only animal studies provide the majority of data in which current understanding is based, but these data cannot be extrapolated into the human scenario, therefore, clinical studies with algae are very important to complete these research cycles but they are still scarce (Brown et al. 2014).

Principal component analysis

Multivariate statistical analysis by Principal Component Analysis to identify the promising potential of the extracts of *S. vulgare*, *P. flagellifera*, and *U. fasciata* at the two studied seasons was developed for the data set (Fig. 1).

The first component, PC1, was able to explain 66.45% of the entire data variation, while PC2 explained 22.33% of the data variation (Fig. 1). The variables Folin-Ciocalteu (28.5%), ABTS (28.2%), FRAP (26.3%), and RT-HIV (16.6%) had a greater weight on PC1, and they influenced the separation of MeOH, Aq, and H-Aq extracts of *S. vulgare* (group 1) from extracts from the other algae (negative axis of PC1). Three groups were evident in the PCA, the group 1 consisted in the Aq and H-Aq extracts of *S. vulgare* (dry and rainy season) influenced by the variables RT-HIV and reduction power (Folin-Ciocalteu, FRAP and ABTS); the group 2 associated to Bcar variable (85.9%) (β-carotene/linoleic acid assay) with great deal of weight on PC2 and formed by

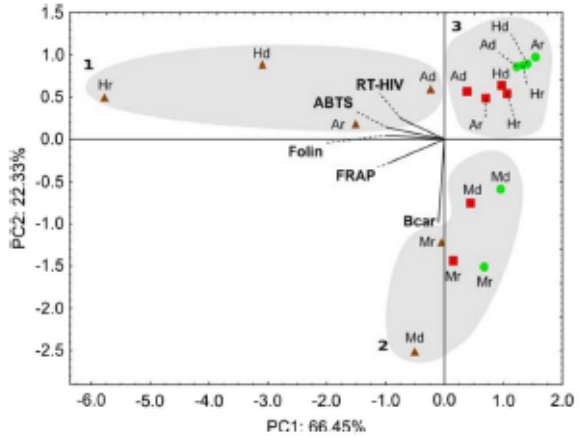

Fig. 1 Principal Components Analysis (PCA) biplot of antioxidant and antiviral activities of *S. vulgare* (brown triangles), *P. flagellifera* (red squares), and *U. fasciata* (green circles) for all data set of crude extracts. The extracts are represented by uppercase letters "M" for methanolic, "A" for aqueous, and "H" hot aqueous extracts. Dry and rainy seasons are represented by lowercase letters "d" and "r," respectively. Different numbers (1–3) represent the clusters

Table 3 Yields of crude extracts of *Sargassum vulgare*, *Palisada flagellifera*, and *Ulva fasciata* (mean ± SD; $n = 5$) expressed as percentage of dry weight of seaweed. Different letters within the same species indicate differences between the means (two-way ANOVA and post hoc Newman-Keuls test; $p < 0.05$). MeOH = methanolic extract, Aq = aqueous extract, H-Aq = hot aqueous extract

Samples	Yield (%)	
	Dry	Rainy
S. vulgare		
MeOH	2.38 ± 0.08^{a}	11.05 ± 0.58^{c}
Aq	7.88 ± 0.96^{b}	48.63 ± 1.04^{d}
H-Aq	2.81 ± 0.79^{a}	38.23 ± 0.34^{e}
P. flagellifera		
MeOH	5.89 ± 2.36^{a}	16.27 ± 1.36^{b}
Aq	19.63 ± 0.91^{b}	9.16 ± 0.80^{a}
H-Aq	16.72 ± 8.11^{b}	43.35 ± 3.50^{c}
U. fasciata		
MeOH	13.01 ± 1.25^{a}	12.32 ± 1.36^{a}
Aq	12.51 ± 2.82^{a}	16.28 ± 7.90^{a}
H-Aq	12.18 ± 1.78^{a}	58.28 ± 4.25^{b}

MeOH extracts from the two seasons for all three species of this study (Fig. 1); and the group 3, which grouped the aqueous extracts (Aq and H-Aq) from the algae *P. flagellifera* and *U. fasciata* (Fig. 1).

In general, the data set of PCA suggests that the aqueous extracts of *S. vulgare* have a distinct behavior than the other extracts and studied species with high correlation between antioxidant potential and anti-HIV power, MeOH extracts of all species showed similar relationship action as one cluster was formed, aqueous extracts of *P. flagellifera* and *U. fasciata* showed low correlations with the measured parameters, and finally *S. vulgare* showed the best correlation scores for antioxidant and antiviral assays highlighting the potential application of this species as a phycotherapic natural complement.

Yields and bioactivities of extracts

The highest yields were in the extracts of the rainy season for Aq and H-Aq extracts from *S. vulgare* (48.63 ± 1.04 and 38.23 ± 0.34%, respectively) and H-Aq extracts from *P. flagellifera* (43.35 ± 3.50%) and from *U. fasciata* (58.28 ± 4.25%) (Table 3). Although the H-Aq extracts from *P. flagellifera* and *U. fasciata* present high yields, they did not show significant bioactivities (Tables 1 and 2). In contrast, the H-Aq and Aq extracts from *S. vulgare* were the most promising in reducing antioxidants and HIV-RT inhibitors (Tables 1 and 2). It is possible to conclude that the H-Aq and Aq extracts from *S. vulgare* are the most promising for biotechnological applications, due to the high bioactivities and the high yield of these extracts during the rainy season.

The MeOH extracts showed high activities in the inhibition of lipid peroxidation (Table 1). For these extracts, the rainy season showed the highest yields for *P. flagellifera* (16.27 ± 1.36%) and *S. vulgare* (11.05 ± 0.58%), while *U. fasciata* did not show difference between rainy and dry seasons (13.01 ± 1.25 and 12.32 ± 1.36%, respectively) (Table 3). The Aq extracts of *P. flagellifera* had a significant inhibition of RT enzyme and lipid peroxidation (Tables 1 and 2); the yield was twice as high in the dry season (19.63 ± 0.91%) as it was in rainy season (9.16 ± 0.80%) (Table 3). Thus, as shown in Table 3, it was possible to verify a seasonal variation (dry and rainy seasons) for the extract yields, suggesting a strategy for screening of the species according to the seasonality of extract yields and bioactivities.

In general, the rainy season presented the greatest potential for use as nutraceutical or herbal medicine of *S. vulgare* and *P. flagellifera*. On the other hand, the active results for *U. fasciata* were independent of seasons. However, records on which seaweed species are most suited for the production of highly bioactive and sustainable extracts, including recommendation as harvesting period, most appropriate algal portions, and life cycle stage, are scarce (Verkleij 1992; Stengel et al. 2011). Craigie et al. (2008) is one of the very few studies that currently provide evidence for the impact of seasonal harvesting and processing on commercial product properties. More rigorous chemical analyses are likely to reveal further significant changes in the composition and the resulting quality of many commercial algal products. Likewise, although widely recognized as a source of variability, the impact of natural environmental changes on the composition and

content of bioactives has not been a primary feature of algal bioactive discovery and requires attention mainly about commercial seaweed species (Stengel et al. 2011).

Conclusion

In general, the extracts of these three macroalgal species showed interesting antioxidant and antiviral activities. Regarding the yields and bioactivities, it is possible to list the main results for each alga: (i) for *U. fasciata*, only MeOH extracts were promising with significant inhibition of lipid peroxidation; (ii) for *P. flagellifera*, the more promising extract was Aq extract (dry season) with significant inhibition of RT enzyme and lipid peroxidation; and (iii) *S. vulgare* was the most promising species mainly in rainy season. For this brown alga, the Aq and H-Aq extracts showed highest activities in the reduction potential and inhibition of RT enzyme, besides the MeOH extracts with the highest inhibition of lipid peroxidation. In general, the most promising algal extracts were those obtained from *S. vulgare*, followed for *P. flagellifera*, while the less promising algal extract was that from *U. fasciata*. Brazilian seaweed extracts have been shown in this study to be a potential bioresource in the use of nutraceuticals and/or phytotherapeutic agents and can also be an efficient and innovative alternative source for Brazilian herbal medicine.

Acknowledgements The authors thank Dr. Beatriz Torrano da Silva, Marizete Pereira dos Santos, and CEPLAC (Comissão Executiva de Planejamento da Lavoura Cacaueira) for research cooperation.

Funding information The authors would like to thank CAPES (Coordenação de Aperfeiçoamento de Pessoal de Nível Superior) and FAPESP (Fundação de Amparo à Pesquisa do Estado de São Paulo (Biota/Fapesp 2013/50731-1) for financial support. FC thanks CNPq (Conselho Nacional de Desenvolvimento Científico e Tecnológico) for the productivity fellowship (Proc. 303937/2015-7).

References

Almeida CL, Falcão HS, Lima GR, Montenegro CA, Lira NS, de Athayde-Filho PF, Rodrigues LC, De Souza MFV, Barbosa-Filho JM, Batista LM (2011) Bioactivities from marine algae of the genus *Gracilaria*. Int J Mol Sci 12:4550–4573

Anwar H, Hussain G, Mustafa I (2018) Antioxidants from natural sources. In: Shalaby E, Azzam GM (eds) Antioxidants in foods and its applications. IntechOpen. https://www.intechopen.com/books/antioxidants-in-foods-and-itsapplications/antioxidants-from-natural-sources. Accessed 2 Sept 2018

Benzie IFF, Strain JJ (1996) The ferric reducing ability of plasma (FRAP) as a measure of "antioxidant power": the FRAP assay. Anal Biochem 239:70–76

Brand-Williams W, Cuvelier ME, Berset C (1995) Use of a free radical method to evaluate antioxidant activity. LWT- Food Sci Technol 28:25–30

Brown EM, Allsopp PJ, Magee PJ, Gill CIR, Nitecki S, Strain CR, McSorley EM (2014) Seaweed and human health. Nutr Rev 72:205–216

Cerri GG (2016) The challenges of health care in Brazil. Rev Med 95(60):60

Chew YL, Lim YY, Omar M, Khoo KS (2008) Antioxidant activity of three edible seaweeds from two areas in South East Asia. LWT - Food Sci Technol 41:1067–1072

Comish ML, Garbary DJ (2010) Antioxidants from macroalgae: potential applications in human health and nutrition. Algae 25:155–171

Craigie JS, MacKinnon SL, Walter JA (2008) Liquid seaweed extracts identified using ^{1}H NMR profiles. J Appl Phycol 20:665–671

Cutler B, Justman J (2008) Vaginal microbicides and the prevention of HIV transmission. Lancet Infect Dis 8:685–697

Devasagayam TPA, Tilak JC, Boloor KK, Sane KS, Ghaskadbi SS, Lele RD (2004) Free radicals and antioxidants in human health: current status and future prospects. J Assoc Physicians India 52:794–804

Dinesh S, Menon T, Hanna LE, Suresh V, Sathuvan M, Manikannan M (2016) In vitro anti-HIV-1 activity of fucoidan from *Sargassum swartzii*. Int J Biol Macromol 82:83–88

Fleurence J, Levine I (eds) (2016) Seaweed in health and disease prevention. Elsevier, Amsterdam, p 476

Guiry MD, Blunden G (1991) Seaweed resources in Europe: uses and potential. Wiley, Chichester

Gülçin I (2012) Antioxidant activity of food constituents: an overview. Arch Toxicol 86:345–391

Gupta S, Abu-Ghannam N (2011) Recent developments in the application of seaweeds or seaweed extracts as a means for enhancing the safety and quality attributes of foods. Innov Food Sci Emerg Technol 12:600–609

Hamed I, Özogul F, Özogul Y, Regenstein JM (2015) Marine bioactive compounds and their health benefits: a review. Compr Rev Food Sci Food Saf 14:446–465

Harb TB, Torres PB, Pires JP, Santos DYAC, Chow F (2016) Ensaio em microplaca do potencial antioxidante através do sistema quelante de metais para extratos de algas. Instituto de Biociências, Universidade de São Paulo, São Paulo. Retrieved from http://www2.ib.usp.br/index.php?option=com_docman&task=doc_view&gid=67&tmpl=component&format=raw&Itemid=98 on 06 May 2018

Holdt SL, Kraan S (2011) Bioactive compounds in seaweed: functional food applications and legislation. J Appl Phycol 23:543–597

Holec AD, Mandal S, Prathipati PK, Destache CJ (2018) Nucleotide reverse transcriptase inhibitors: a thorough review, present status and future perspective as HIV therapeutics. Curr HIV Res 15:411–421

Huynh QN, Nguyen HD (1998) The seaweed resources of Vietnam. In: Critchley AT, Ohno M (eds) Seaweed resources of the world. JICA: 62–69

Jeong JH, Jung H, Lee SR, Lee HJ, Hwang KT, Kim TY (2010) Antioxidant, anti-proliferative and anti-inflammatory activities of the extracts from black raspberry fruits and wine. Food Chem 123:338–344

Jeong SC, Jeong YT, Lee SM, Kim JH (2015) Immune-modulating activities of polysaccharides extracted from brown algae *Hizikia fusiforme*. Biosci Biotechnol Biochem 79:1362–1365

Kasrati A, Jamali CA, Abbad A (2017) Antioxidant properties of various extracts from selected wild Moroccan aromatic and medicinal species. Trends Phytochem Res 1:175–182

Kohen R, Nyska A (2002) Oxidation of biological systems: oxidative stress phenomena, antioxidants, redox reactions, and methods for their quantification. Toxicol Pathol 30:620–650

Lage MÁP, García MAM, Álvarez JAV, Anders Y, Curran TP (2013) A new microplate procedure for simultaneous assessment of lipophilic and hydrophilic antioxidants and pro-oxidants, using crocin and β-carotene bleaching methods in a single combined assay: tea extracts as a case study. Food Res Int 53:836–846

Lordan S, Ross RP, Stanton C (2011) Marine bioactives as functional food ingredients: potential to reduce the incidence of chronic diseases. Mar Drugs 9:1056–1100

Loutfy MR, Wu W, Letchumanan M, Bondy L, Antoniou T, Margolese S, Zhang Y, Rueda S, McGee F, Peck R, Binder L, Allard P, Rourke SB, Ronchon PA (2013) Systematic review of HIV transmission between heterosexual serodiscordant couples where the HIV-positive partner is fully suppressed on antiretroviral therapy. PLoS One 8:e55747

Mahapatra A, Tshikalange TE, Meyer JJM, Lall N (2012) Synthesis and HIV-1 reverse transcriptase inhibition activity of 1,4-naphoquinone derivatives. Chem Nat Compd 47:776–779

Marco G (1968) A rapid method for evaluation of antioxidants. J Am Oil Chem Soc 45:594–598

Matanjun P, Mohamed S, Mustapha NM, Muhammad K, Ming CH (2008) Antioxidant activities and phenolics content of eight species of seaweeds from north Borneo. J Appl Phycol 20:367–373

Miliauskas G, Venskutonis PR, Van Beek TA (2004) Screening of radical scavenging activity of some medicinal and aromatic plant extracts. Food Chem 85:231–237

Miller HE (1971) A simplified method for the evaluation of antioxidants. J Am Oil Chem Soc 48:91–91

Min B, McClung AM, Chen MH (2011) Phytochemicals and antioxidant capacities in rice brans of different color. J Food Sci 76:C117–C126

Mols-Mortensen A, Ortind EG, Jacobsen C, Holdt SL (2017) Variation in growth, yield and protein concentration in *Saccharina latissima* (Laminariales, Phaeophyceae) cultivated with different wave and current exposures in the Faroe Islands. J Appl Phycol 29:2277–2286

Myers SP, O'Connor J, Fitton JH, Brooks L, Rolfe M, Connellan P, Wohlmuth H, Cheras P, Morris C (2010) A combined phase I and II open label study on the effects of a seaweed extract nutrient complex on osteoarthritis. Biol Targets Ther 4:33–44

Nwobike JC (2006) Pharmaceutical corporations and access to drugs in developing countries: the way forward. Int J Hum Rights 4:126–143

Orisatoki RO, Oguntibeju OO (2010) The role of herbal medicine use in HIV/AIDS treatment. Arch Clin Microbiol 1(3)

Pires JS, Torres PB, Santos DYAC, Chow F (2017a) Ensaio em microplaca de substâncias redutoras pelo método do Folin-Ciocalteu para extratos de algas. Instituto de Biociências, Universidade de São Paulo, São Paulo. Retrieved from http://www2.ib.usp.br/index.php?option=com_docman&task=doc_view&gid=73&tmpl=component&format=raw&Itemid=98 on 06 May 2018

Pires J, Torres PB, Santos DYAC dos Chow F (2017b) Ensaio em microplaca do potencial antioxidante através do método de sequestro do radical livre DPPH para extratos de algas. Instituto de Biociências, Universidade de São Paulo, São Paulo. Retrieved from http://www2.ib.usp.br/index.php?option=com_docman&task=doc_view&gid=72&tmpl=component&format=raw&Itemid=98 on 06 May 2018

Pirian K, Moein S, Sohrabipour J, Rabiei R, Blomster J (2017) Antidiabetic and antioxidant activities of brown and red macroalgae from the Persian Gulf. J Appl Phycol 29:3151–3159

Rajan S, Mahalakshmi S, Deepa VM, Sathya K, Shajitha S, Thirunalasundari T (2011) Antioxidant potentials of *Punica granatum* fruit rind extracts. Int J Pharm Pharm Sci 3:82–88

Rosa C, Câmara SG, Béria JU (2011) Representações e intenção de uso da fitoterapia na atenção básica à saúde. Cien Saude Colet 16:311–318

Rufino MSM, Alves RE, Brito ES, Morais SM, Sampaio CG, Pérez-Jimenez J, Saura-Calixto FD (2007) Metodologia científica: determinação da atividade antioxidante total em frutas pela captura do radical livre ABTS•+ Embrapa, Fortaleza

Ruzagira E, Wandiembe S, Abaasa A, Bwanika AN, Bahemuka U, Amornkul P, Price MA, Grosskurth H, Kamali A (2011) HIV incidence and risk factors for acquisition in HIV discordant couples in Masaka, Uganda: an HIV vaccine preparedness study. PLoS One 6(8):e0024037

Saunders GW (2005) Applying DNA barcoding to red macroalgae: a preliminary appraisal holds promise for future applications. Phil Trans Roy Soc B 360:1879–1888

Sekmokienė D, Liutkevičius A, Malakauskas M (2007) Functional food and its ingredients. Vet Zoot 37:72–78

Stengel DB, Connan S, Popper ZA (2011) Algal chemodiversity and bioactivity: sources of natural variability and implications for commercial application. Biotechnol Adv 29:483–501

Suresh Kumar K, Ganesan K, Subba Rao PV (2015) Seasonal variation in nutritional composition of *Kappaphycus alvarezii* (Doty) Doty—an edible seaweed. J Food Sci Technol 52:2751–2760

Teas J, Irhimeh MR (2012) Dietary algae and HIV/AIDS: proof of concept clinical data. J Appl Phycol 24:575–582

Teas J, Hebert JR, Fitton JH, Zimba PV (2004) Algae—a poor man's HAART? Med Hypotheses 62:507–510

Torres PB, Pires JS, Santos DYAC, Chow F (2017) Ensaio do potencial antioxidante de extratos de algas através do sequestro do $ABTS^{\bullet+}$ em microplaca. Instituto de Biociências, Universidade de São Paulo, São Paulo. Retrieved from http://www2.ib.usp.br/index.php?option=com_docman&task=doc_view&gid=74&tmpl=component&format=raw&Itemid=98 on 06 May 2018

Unaids (2013) Global report: UNAIDS report on the global AIDS epidemic 2013. Retrieved from http://www.unaids.org/sites/default/files/media_asset/UNAIDS_Global_Report_2013_en_1.pdf on 08 May 2018

Urrea-Victoria V, Pires J, Torres PB, Santos DYAC, Chow F (2016) Ensaio antioxidante em microplaca do poder de redução do ferro (FRAP) para extratos de algas. Instituto de Biociências, Universidade de São Paulo, São Paulo. Retrieved from http://www2.ib.usp.br/index.php?option=com_docman&task=doc_view&gid=66&tmpl=component&format=raw&Itemid=98 on 06 May 2018

Verkleij FN (1992) Seaweed extracts in agriculture and horticulture: a review. Biol Agric Hortic 8:309–324

Vieira C, Gaubert J, De Clerck O, Payri C, Culioli G, Thomas OP (2017) Biological activities associated to the chemodiversity of the brown algae belonging to genus *Lobophora* (Dictyotales, Phaeophyceae). Phytochem Rev 16:1–17

Wang B, Huang H, Xiong HP, Xie EY, Li ZM (2010) Analysis on nutrition constituents of *Sargassum naozhouense* sp.nov Food Res Dev 31:195–197

Waterman PG, Mole S (1994) Extraction and chemical quantification. In: Analysis of phenolic plant metabolites. Wiley Blackwell, pp 333–360

Wells ML, Potin P, Craigie JS, Raven JA, Merchant SS, Helliwell KE, Smith AG, Camire ME, Brawley SH (2017) Algae as nutritional and functional food sources: revisiting our understanding. J Appl Phycol 29:949–982

Woradulayapinij W, Soonthornchareonnon N, Wiwat C (2005) In vitro HIV type 1 reverse transcriptase inhibitory activities of Thai medicinal plants and *Canna indica* L. rhizomes. J Ethnopharmacol 101:84–89

World Health Organization (2005) WHO Traditional Medicine Strategy 2002–2005. World Health Organization, Geneva. Retrieved from http://www.wpro.who.int/health_technology/book_who_traditional_medicine_strategy_2002_2005.pdf on 06 May 2018

World Health Organization (2007) Countries at the core. WHO Medicines Strategy 2004–2007 1–12. World Health Organization, Geneva. Retrieved from http://www.who.int/management/background_4a.pdf on 07 August 2018

Yermak IM, Sokolova EV, Davydova VN, Solov'eva TF, Aminin DL, Reunov AV, Lapshina LA (2016) Influence of red algal polysaccharides on biological activities and supramolecular structure of bacterial lipopolysaccharide. J Appl Phycol 28:619–627

Zubia M, Robledo D, Freile-Pelegrin Y (2007) Antioxidant activities in tropical marine macroalgae from the Yucatan Peninsula, Mexico. J Appl Phycol 19:449–458

ANEXO 15

Algal Research 41 (2019) 101572

Contents lists available at ScienceDirect

Algal Research

journal homepage: www.elsevier.com/locate/algal

Temporal stability in lipid classes and fatty acid profiles of three seaweed species from the north-eastern coast of Brazil

J.P. Santos[a,*], F. Guihéneuf[b,1], G. Fleming[c], F. Chow[a,*], D.B. Stengel[b]

[a] Laboratory of Marine Algae "Édison José de Paula", Institute of Biosciences, University of São Paulo, São Paulo, Brazil
[b] Botany and Plant Science, School of Natural Sciences, Ryan Institute for Environmental, Marine and Energy Research, National University of Ireland Galway, Galway, Ireland
[c] Microbiology, Schools of Natural Sciences, Ryan Institute for Environmental, Marine and Energy Research, National University of Ireland Galway, Galway, Ireland

ARTICLE INFO

Keywords:
Biotechnology
Lipids
LC-PUFA
Nutraceuticals
Seaweeds

ABSTRACT

Lipid and fatty acid profiles provide nutritional information of marine algae, but the analysis of algal fatty acid composition has also been proposed as a chemotaxonomic tool. Although the total lipid (TL) content of macroalgae is usually only 1–6% dry weight (DW), much lower than in microalgae, some species can accumulate interesting long-chain polyunsaturated fatty acids (LC-PUFA) which are essential fatty acids, not produced by humans or animals, that show beneficial health effects. This study aimed to evaluate the lipid and fatty acid profiles of three Brazilian seaweeds, *Sargassum vulgare* (Ochrophyta), *Palisada flagellifera* (Rhodophyta), and *Ulva fasciata* (Chlorophyta) collected from the north-east of Brazil at two seasons (dry and rainy). Lipid and fatty acid profiles in the three macroalgae were stable across seasons. The total fatty acid (TFA) contents of *S. vulgare* and *U. fasciata* ranged from 1.3 to 1.5% DW, with the main fatty acids represented by palmitic and oleic acids; however, there was no large accumulation of LC-PUFA. By contrast, *P. flagellifera* exhibited a lower TFA content (0.8–0.9% DW), but eicosapentaenoic and arachidonic acids accounted for 15–16% and 16–20% of TFA, up to 1.5 and 1.9 mg g-1 DW, respectively. In all species, glycolipids were the most abundant lipid class (60–70%), followed by phospholipids (10–25%), and neutral lipids (10–15%). The composition of each lipid fractions demonstrated that fatty acid profiles of each lipid class were highly species-specific, and lipid profiles were indicative of tropical species. Based on these algae lipid profiles, *P. flagellifera* could be considered a good source of omega-3 (LC-PUFA). The seasonal stability in the lipid content and fatty acid profiles confers a strong advantage for potential exploitation of those species in the north-eastern regions of Brazil, representing a source of algal biomass with constant biochemical composition all year-round.

FEEDBA

1. Introduction

Lipids found in seaweeds (0.12–6.73% dry weight, DW) may contain a large proportion of essential fatty acids. The two main functions of lipids in algae are polar lipids as structural components of cellular membranes and neutral lipids that function as storage compounds [1]. The ability of algae to survive or proliferate over a wide range of environmental conditions is, to a largely extent, reflected in the wide diversity and patterns of cellular lipids as well as their ability to modify lipid metabolism efficiently in response to changes in environmental factors [2–4].

Under environmental conditions unfavorable or stressful for growth, many algal species alter their lipid biosynthetic pathways towards the formation and accumulation of neutral lipids, mainly in triacylglycerol (TAG) forms [5–8]. Unlike the glycerolipids, which are found in membranes, TAG does not perform a structural role but instead serve primarily as a storage base of carbon and energy. There is some evidence suggesting that environmental stressors, including nutrient-starvation, can trigger TAG accumulation in algae [9–11]. However, the interactions between growth and lipid contents under stress conditions are still poorly understood, particularly in macroalgae [10,11].

Recently, algae have attracted significant interest from the food industry to underpin the need for the development of healthier eating habits. In particular, algal pigments including chlorophylls, carotenoids and phycobilins, and fatty acids (mainly long-chain polyunsaturated fatty acids, LC-PUFA), are of potential value as food ingredients due to their various and proven human health benefits [12,13]. Specifically, an incorporation of LC-PUFA into the daily diet is thought to reduce the

* Corresponding authors at: Department of Botany, Institute of Bioscience, University of São Paulo, Rua do Matão, 277, São Paulo 05508-090, SP, Brazil.
E-mail addresses: janainaps@usp.br (J.P. Santos), fchow@ib.usp.br (F. Chow).
[1] Current address: Sorbonne Université, CNRS, Laboratoire d'Océanographie de Villefranche, LOV, F-06230 Villefranche-sur-Mer, France.

https://doi.org/10.1016/j.algal.2019.101572
Received 2 November 2018; Received in revised form 2 June 2019; Accepted 4 June 2019
Available online 15 June 2019
2211-9264/ © 2019 Published by Elsevier B.V.

©Fungyi Chow / 2021

risk of heart disease, cancer, mental disorders, and depression, as well as supporting a healthy nervous system [14–16].

The omega-6 family produces eicosanoids that cause inflammation and are carcinogenic, increasing the risk of situations such as cancers, sudden death, heart diseases, vasoconstriction, increased blood pressure, elevated triglyceride rate, depression, among other inflammatory diseases [15]. On the other hand, omega-3 fatty acids have known anti-inflammatory [17], improve brain and visual functioning [18], cardiovascular disease prevention [19], and anticancer properties [20]. These beneficial effects are reported to be efficient in the attenuation of heart diseases, hypertension, type 2 diabetes, rheumatoid arthritis, among others [21]. Degenerative diseases such as diabetes, arthritis, and cancers are related, in part, to the current disproportion of the concentration of omega-6 and omega-3 fatty acids in our diet; for example, a high concentration of omega-6 and a shortage of omega-3 [21].

The fatty acid profiles of the lipids in macroalgae appear to be strongly linked to their taxonomic classification and can represent differentiation up to family level [22–26]. For example, members of the Rhodophyta and Phaeophyceae (Ochrophyta) are able to synthesize LC-PUFA with high percentages of C20 PUFA such as EPA (eicosapentaenoic acid) and ARA (arachidonic acid) [27,28]. Fatty acids in Chlorophyta are more similar to those in vegetative tissues of land plants, with mainly C18 unsaturated fatty acids [e.g. linoleic acid (LA) and alpha-linolenic acid (ALA)] within their PUFA [29]. Green algae usually contain only very small quantities of fatty acids with chains longer than 18 carbons, and are richer in PUFA such as ALA. For example, levels of ALA in the genera *Ulva*, *Caulerpa* and *Udotea* range from 14 to 48% of TFA [30].

The future potential application of macroalgae as a rich source of LC-PUFA requires a better understanding of their spatial and temporal variations of their fatty acid profiles and composition [31,32]. Of 16 species studied, Schmid et al. [28] observed the highest total fatty acid (TFA) contents in the brown alga *Pelvetia canaliculata* (6.4 ± 0.3% DW) and the lowest in the red alga *Porphyra dioica* (0.8 ± 0.2% DW). Strong seasonal and spatial variation in EPA levels has also been reported in the red alga *Palmaria palmata* which is considered a promising source of omega-3 LC-PUFA [32].

Some previous studies suggest that tropical algae have a lower ratio of omega-3 to omega-6 fatty acids, and a lower degree of unsaturation, than temperate macroalgae which are commonly richer in PUFA [33–37]. However, generally, tropical seaweeds remained poorly explored and their nutritional potential has only rarely been compared to that of cold-water seaweeds [37,38].

Although the north-eastern coast of Brazil is known for its high macroalgal diversity, this study represents the first characterization of the lipid and fatty acid profiles of three abundant seaweed species, *Sargassum vulgare* (Ochrophyta, Fucales), *Palisada flagellifera* (Rhodophyta, Ceramiales) and *Ulva fasciata* (Chlorophyta, Ulvales), from this area. Our aim was to evaluate potential variations on fatty acid and lipid composition of three Brazilian macroalgae associated with dry and rainy seasons.

2. Material and methods

2.1. Collection and sample preparation

Seaweed samples were collected during low tide at Morro de Pernambuco Beach (14°47′00″S, 39°02′00 ″W), Municipality of Ilheus, Bahia State (Brazil), in November 2013 (dry-spring) and May 2014 (rainy-autumn). The species investigated were *S. vulgare*, *P. flagellifera* and *U. fasciata*. Algal samples were thoroughly cleaned of epiphytes, rinsed in tap water to remove salt, dried with absorbent paper and transported to the laboratory. Sub-samples of approximately 500 g of fresh weight (FW) of each species were separated as replicates (n = 5), frozen at −80 °C and freeze-dried (Liobras model L202, Brazil) and stored until further analysis.

2.2. Collection of climatological data

The climatological data, which includes precipitation and ultraviolet radiation index (UVI), were obtained from the meteorological station of Free University of the Sea and the Wood, and the Institute of Environment and Hydric Resources in the State of Bahia, Brazil (Inema; www.inema.ba.gov.br), respectively. Data collection was performed during 2013 and 2014 relating to the sampling period, following a previous climatic study of this region by Molion and Bernardo [39] providing supporting data to assess potential climatological impacts on results.

2.3. Lipid analyses

2.3.1. Total lipid extraction

Total lipids were extracted from lyophilized ground samples (4.5 to 6.5 g) with chloroform/methanol (1:2 v/v). To avoid oxidation, the samples were closed under nitrogen gas and the algal material was extracted three times for 12 h each. All three extracts were pooled before adding chloroform and water, aiming to reach chloroform/methanol/water (1:1:0.9 v/v/v). After separation, the chloroform layer, containing total lipids, was collected and the solvents were removed by evaporating under high vacuum using a rotary evaporator (Büchi, Switzerland). Samples were then dissolved in a known volume of chloroform.

2.3.2. Separation and characterization of main lipid classes

Separation of polar and neutral lipids was performed by silica cartridge separation. Before separation, the silica cartridge (Bond Elut Si, 5000 mg, 20 mL, Agilent Technologies, USA) was equilibrated with 10 mL of methanol followed by 10 mL of chloroform. A known amount of crude lipid extract was slowly loaded onto the cartridge. Then neutral lipid fractions were eluted with 40 mL of chloroform and collected in a round bottom flask. The glycolipid fractions were eluted with 40 mL of chloroform/methanol (5:1 v/v) and collected in a round-bottom flask. The phospholipids were eluted with 40 mL of methanol and collected in a round-bottom flask. All fractions were evaporated in a rotary evaporator (40 °C), re-dissolved in 10 mL of chloroform and transferred to tubes closed under nitrogen and stocked at −20 °C prior further analysis of fatty acids.

2.3.3. Fatty acids analysis

Finely ground freeze-dried seaweed biomass (50 mg) or aliquots of total lipids or each lipid fraction (i.e. 200 μL evaporated under nitrogen gas) were used and processed identically for fatty acid analysis. Fatty acid methyl esters (FAME) were obtained by *trans*-methylation using 2 mL of dry methanol (2% [v/v] H_2SO_4). To avoid oxidation, the samples were closed under nitrogen and heated for 1.5 h at 80–90 °C with continuous stirring. Samples were left to cool before adding 1 mL of ultrapure-water. Hexane (2 mL) was then added to extract FAME. All chemicals were of analytical grade (Fischer Scientific, UK).

FAME were identified and quantified from biomass, total lipid extract, and each lipid fraction using an Agilent 7890A GC/5975C MSD Series (Agilent Technologies, Santa Clara, CA, USA), outfitted with a flame ionization detector (detector temperature 300 °C) and a fused silica capillary column (DB-WAXetr, 0.25 mm × 30 m × 0.25 mm, Agilent Technologies). Sample volumes of 2 μL were injected in split mode (split ratio 20:1) using an Agilent auto-injector 7683B series. The temperature was programmed at 140 °C for 1 min, raised from 140 to 200 °C by rate of 15 °C min^{-1} and then from 200 to 250 °C at a rate of 2 °C min^{-1}. Identification of FAME was obtained by co-chromatography with commercially available FAME standards (Supelco™ 37 Component FAME Mix, Supelco, Bellefonte, PA, USA) and FAME of fish oil (Menhaden Oil, Supelco). Fatty acid contents were quantified by

comparison with a known amount (20 μL) of internal standard (15:0, 5 mg mL^{-1}, pentadecanoic acid, 98%, Alfa Aesar, Heysham, UK), added before *trans*-methylation to the seaweed powder, aliquots of lipid extracts or lipid fractions. Results are expressed as the mean values of five replicates (n = 5). Agilent MSD Productivity ChemStation Software was used for instrument control, data acquisition, and data analysis (integration, retention times, and peak areas).

2.4. Statistical analysis

Fatty acid data were analyzed with Prisma Graph Pad * 6 software. The seasonal (dry and rainy) effect on individual fatty acid composition were determined using Student's *t*-test for independent samples and total fatty acid content and lipid class composition were determined using the Mann-Whitney-U test for unpaired samples with * $P \leq 0.05$ and ** $P \leq 0.01$. The multiple comparison for evaluating the integration of all data profiles, as a general lipidomic analysis, was performed by a bi-dimensional hierarchical clusterization of log-transformed data, and then by Euclidean distance and Paired group analyses, combined with the Pearson correlation index. The cluster results were associated to a heatmap graphic using the software R version 3.5.0.

3. Results

3.1. Climatological data

The Northeastern region of Brazil, where the seaweed materials were collected, is characterized by the occurrence of well-defined rainy and dry seasons (November to April and May to October, respectively), distinguished by the volume of precipitation. During the first six months of both 2013 and 2014, a reduction of the UV radiation index was registered, with the lowest values recorded in June, which coincided with the highest volumes of rainfall (Fig. 1), conditions that clearly demarcate the difference between the two seasons.

3.2. Total fatty acid content and composition

Total fatty acid (TFA) content in the three groups of algae ranged from 0.85 to 1.56% DW (Fig. 2). The smallest quantities were detected in *P. flagellifera* (Rhodophyta) and the largest in *U. fasciata* (Chlorophyta). While statistical significance in *P. flagellifera* ($P = 0.002$) variations in TFA contents were limited, with 0.92% DW during the dry season and 0.85% DW during the rainy season. No significant changes in TFA contents were observed for *S. vulgare* (Ochrophyta; 1.29–1.49% DW, $P = 0.103$) and *U. fasciata* (1.47–1.56% DW, $P = 0.665$).

3.2.1. Sargassum vulgare

The content of individual fatty acids (mg g^{-1} DW) and the total fatty acid composition (% TFA) in *S. vulgare* are displayed in Fig. 3 and Table 1, respectively. The species contained high levels of saturated fatty acids (SFA) with 48.77 ± 0.18% for the dry season and 43.70 ± 4.59% for the rainy season (Table 1). Polyunsaturated fatty acids (PUFA) accounted for 24.79 ± 0.27% (dry) and 27.49 ± 2.28% (rainy) of TFA, while monounsaturated fatty acids (MUFA) represented the smallest proportion within this species, with values ranging from 22.57 ± 0.27% (dry) to 25.60 ± 1.33% (rainy). Among the SFA, palmitic acid (16:0) and myristic acid (14:0) were the most abundant fatty acids and did not vary between collection times. The fatty acid 16:0 represented 41.15 ± 0.49% during the dry season and 35.47 ± 11.54% during the rainy season, whereas 14:0 only accounted for 5.54 ± 0.13% during the dry season and 5.87 ± 1.14% for rainy season (Table 1). Within the MUFA, oleic acid (18:1 n-9) was the major fatty acid for this species, with percentages of 11.51 ± 0.81% (dry) and 14.98 ± 3.69% (rainy) of TFA.

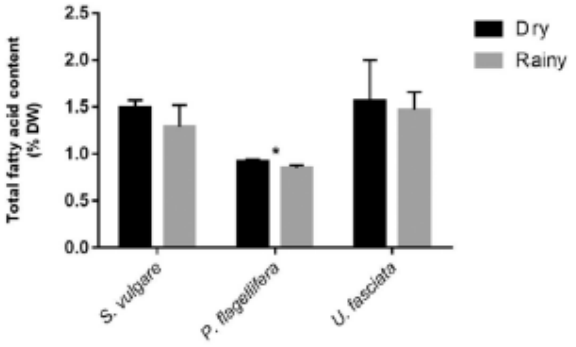

Fig. 2. Total fatty acid content (% DW) of three species of macroalgae, *Sargassum vulgare*, *Palisada flagellifera* and *Ulva fasciata*, collected during dry and rainy seasons (mean ± SD; n = 5). Significant differences (*) between dry and rainy seasons for the respective species were determined by Mann-Whitney-U test, $P < 0.05$.

In *S. vulgare*, the content in omega-3 LC-PUFA such as EPA remained low, with values of 0.31 ± 0.04 mg g^{-1} DW (dry) and 0.23 ± 0.04 mg g^{-1} DW (rainy) (Fig. 3). On the other hand, the content in omega-6 LC-PUFA, such as ARA, which is biologically important, was one of the main PUFA with values of 1.45 ± 0.05 mg g^{-1} DW (dry) and 1.25 ± 0.71 mg g^{-1} DW (rainy). In addition to ARA and EPA, other essential PUFA were detected for this species, such as linoleic acid (LA, 18:2 n-6) and alpha-linolenic acid (ALA, 18:3 n-3), with values of 4.52 ± 0.21% (dry) versus 5.73 ± 1.57% (rainy) and 5.30 ± 0.55% (dry) versus 4.21 ± 1.06% (rainy) of TFA, respectively.

Considering the nutritional indices, the ratio of n-6/n-3 fatty acids of *S. vulgare* ranged from 1.57 (dry) to 2.79 (rainy) with lower values for the dry season (Table 1).

3.2.2. Palisada flagellifera

The content of individual fatty acids and TFA composition in *P. flagellifera* are presented in Fig. 4 and Table 1, respectively. *Palisada*

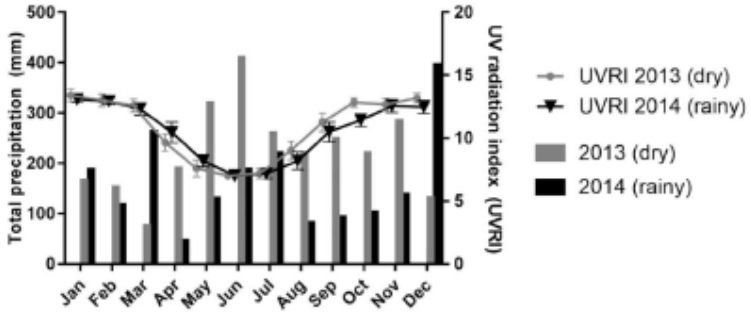

Fig. 1. Climatological data for rainfall dynamic (average precipitation in mm of monthly rainfall), represented by grey (2013, dry season) and black (2014, rainy season) bars, and UV radiation index (UVRI), represented by the grey and black lines, referring to the years 2013 and 2014 for the Municipality of Ilheus, Bahia, Brazil.

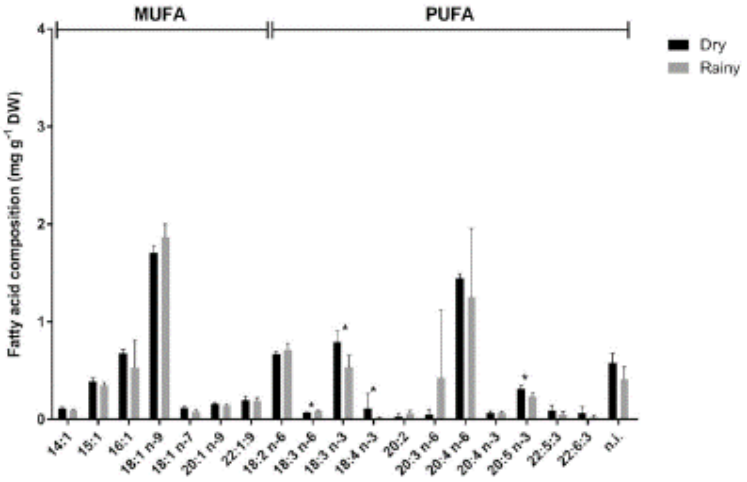

Fig. 3. Fatty acid composition (mg g^{-1} DW) of *Sargassum vulgare* from direct biomass (mean ± SD; n = 5), comparing dry and rainy seasons. Significant differences (*) between dry and rainy seasons were determined by Student's t-test, $P < 0.05$.

Table 1
Fatty acid composition (% TFA) of total lipids in *Sargassum vulgare*, *Palisada flagellifera* and *Ulva fasciata* collected during dry and rainy seasons (mean ± SD; n = 5). Bold values represent fatty acids with at least 1% of the total fatty acid composition of the species studied.

Fatty acids (% TFA)	*Sargassum vulgare*		*Palisada flagellifera*		*Ulva fasciata*	
	Dry	Rainy	Dry	Rainy	Dry	Rainy
14:0	5.5 ± 0.1	5.9 ± 1.1	6.4 ± 0.0	6.4 ± 0.2	0.7 ± 0.0	0.7 ± 0.1
16:0	41.1 ± 0.5	35.5 ± 11.5	37.6 ± 0.4	38.7 ± 0.7	45.0 ± 3.4	49.0 ± 3.8
17:0	n.d.	n.d.	0.3 ± 0.0	0.3 ± 0.0	0.4 ± 0.0	0.5 ± 0.0
18:0	1.1 ± 0.1	1.3 ± 0.3	1.1 ± 0.1	0.8 ± 0.0	0.7 ± 0.1	0.8 ± 0.1
20:0	0.3 ± 0.1	0.4 ± 0.1	0.2 ± 0.1	0.1 ± 0.0	0.2 ± 0.1	0.4 ± 0.1
22:0	0.6 ± 0.0	0.6 ± 0.1	n.d.	n.d.	2.0 ± 0.3	2.0 ± 0.3
24:0	n.d.	n.d.	n.d.	n.d.	0.3 ± 0.0	0.2 ± 0.1
Sum SFA (%)	48.8 ± 0.2	43.7 ± 4.5	45.7 ± 0.1	46.3 ± 0.2	49.3 ± 1.1	53.5 ± 1.3
14:1.	0.8 ± 0.1	0.8 ± 0.2	0.7 ± 0.1	0.6 ± 0.1	0.6 ± 0.1	0.8 ± 0.3
15:1	2.6 ± 0.1	2.8 ± 0.6	0.1 ± 0.0	0.1 ± 0.0	2.5 ± 0.2	3.1 ± 0.4
16:1 n-7	4.6 ± 0.1	3.9 ± 2.0	1.4 ± 0.1	1.1 ± 0.1	2.4 ± 0.1	3.1 ± 0.2
17:1	n.d.	n.d.	0.4 ± 0.0	0.3 ± 0.0	0.8 ± 0.2	1.0 ± 0.3
18:1 n-9	11.5 ± 0.8	15.0 ± 3.7	7.7 ± 0.2	8.0 ± 0.3	2.4 ± 0.1	2.0 ± 0.1
18:1 n-7	0.8 ± 0.1	0.6 ± 0.2	1.2 ± 0.0	1.2 ± 0.1	8.2 ± 0.2	8.9 ± 0.4
20:1 n-9	1.1 ± 0.1	1.1 ± 0.3	n.d.	n.d.	0.2 ± 0.1	0.2 ± 0.1
22:1 n-9	1.3 ± 0.2	1.5 ± 0.4	n.d.	n.d.	0.2 ± 0.0	0.1 ± 0.1
Sum MUFA (%)	22.6 ± 0.3	25.6 ± 1.4	11.5 ± 0.0	11.3 ± 0.1	17.2 ± 0.1	19.0 ± 0.1
16:2	n.d.	n.d.	n.d.	n.d.	0.1 ± 0.1	0.1 ± 0.1
16:3	n.d.	n.d.	n.d.	n.d.	0.4 ± 0.0	0.4 ± 0.1
16:4	n.d.	n.d.	n.d.	n.d.	3.1 ± 0.8	2.4 ± 1.0
18:2 n-6 (LA)	4.5 ± 0.2	5.7 ± 1.6	1.7 ± 0.1	1.3 ± 0.1	5.9 ± 0.7	4.6 ± 0.6
18:3 n-6	0.5 ± 0.0	0.7 ± 0.1	0.5 ± 0.0	0.4 ± 0.0	0.8 ± 0.1	0.5 ± 0.2
18:3 n-3 (ALA)	5.3 ± 0.6	4.2 ± 1.1	2.6 ± 0.1	0.8 ± 0.1	7.8 ± 1.5	6.0 ± 1.6
18:4 n-3 (SDA)	0.8 ± 1.0	0.1 ± 0.1	1.5 ± 0.2	0.6 ± 0.1	5.4 ± 1.4	3.8 ± 1.5
20:2	0.2 ± 0.2	0.5 ± 0.2	0.3 ± 0.3	0.3 ± 0.2	n.d.	n.d.
20:3 n-6 (DGLA)	0.3 ± 0.4	3.3 ± 5.3	0.6 ± 0.0	0.6 ± 0.0	0.2 ± 0.0	0.1 ± 0.1
20:4 n-6 (ARA)	9.7 ± 0.5	10.2 ± 6.5	16.2 ± 0.3	20.6 ± 0.5	0.5 ± 0.2	0.5 ± 0.1
20:4 n-3	0.4 ± 0.1	0.5 ± 0.1	n.d.	n.d.	0.3 ± 0.1	0.2 ± 0.1
20:5 n-3 (EPA)	2.1 ± 0.2	1.8 ± 0.3	16.1 ± 0.3	14.8 ± 0.4	0.6 ± 0.1	0.5 ± 0.1
22:5 n-3	0.6 ± 0.3	0.3 ± 0.2	0.6 ± 0.7	0.7 ± 0.5	2.1 ± 0.2	1.2 ± 0.4
22:6 n-3 (DHA)	0.4 ± 0.4	0.1 ± 0.1	0.6 ± 0.2	0.5 ± 0.4	0.4 ± 0.4	0.2 ± 0.0
Sum PUFA (%)	24.8 ± 0.1	27.5 ± 2.2	40.6 ± 0.2	40.6 ± 0.2	27.7 ± 0.5	20.6 ± 0.5
FA unidentified	3.9 ± 0.5	3.3 ± 0.9	2.3 ± 0.1	1.8 ± 0.1	5.8 ± 0.7	6.9 ± 0.8
Nutritional index						
Σ n-3	9.6 ± 2.0	7.1 ± 1.6	21.4 ± 6.7	17.4 ± 6.3	16.6 ± 3.1	12.0 ± 2.4
Σ n-6	15.0 ± 0.2	19.9 ± 3.0	18.9 ± 0.1	22.9 ± 0.2	7.5 ± 0.3	5.8 ± 0.3
ratio n-6/n-3	1.6	2.8	0.9	1.3	0.5	0.5

n.d. = not detected.

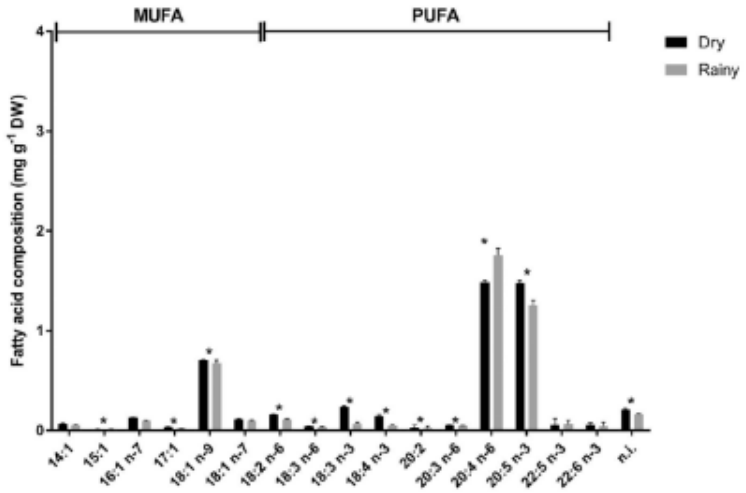

Fig. 4. Fatty acid composition (mg g^{-1} DW) of *Palisada flagellifera* from direct biomass (mean ± SD; n = 5), comparing dry and rainy seasons. Significant differences (*) between dry and rainy seasons were determined by Student's *t*-test, $P < 0.05$.

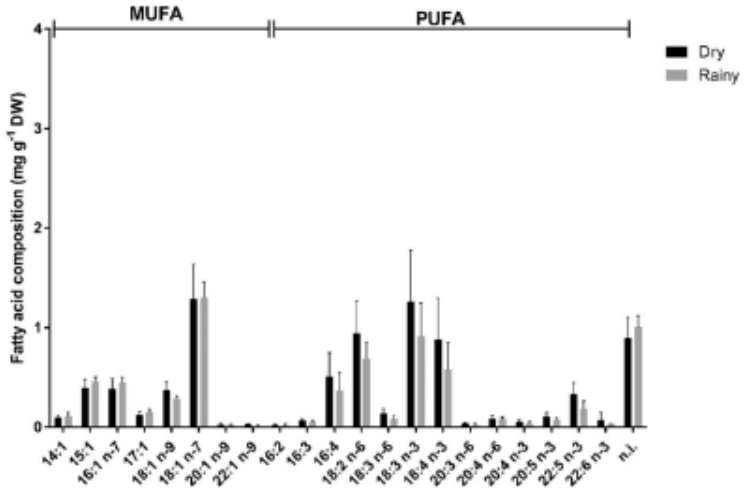

Fig. 5. Fatty acid composition (mg g^{-1} DW) of *Ulva fasciata* from direct biomass (mean ± SD; n = 5) comparing dry and rainy seasons. Significant differences (*) between dry and rainy seasons were determined by Student's *t*-test, $P < 0.05$.

flagellifera contained higher percentages of SFA and PUFA than the other two species, with percentages of 45.71 ± 0.15% (SFA) and 40.59 ± 0.19% (PUFA) of TFA for the dry season, and 46.27 ± 0.26% (SFA) and 40.62 ± 0.19% (PUFA) for the rainy season (Table 1). MUFA only accounted for 11.45 ± 0.05% (dry) and 11.27 ± 0.10% (rainy). Among the SFA, palmitic acid (16:0) was also the main fatty acid for this red algal species, and proportions varied slightly between dry (37.63 ± 0.40%) and rainy (38.72 ± 0.67%) seasons. Myristic acid (14:0) represented 6.41 ± 0.03% (dry) and 6.40 ± 0.19% (rainy), without changes over seasons. Oleic acid (18:1 n-9) was the most abundant MUFA for this species with 7.68 ± 0.16% (dry) and 7.96 ± 0.29% (rainy), thus not displaying variation between seasons. Similarly, only little variation was observed for palmitoleic acid (16:1 n-7), the second major MUFA for this species, with 1.37 ± 0.08% (dry) and 1.11 ± 0.08% (rainy). Major LC-PUFA in *P. flagellifera* were ARA and EPA, both of which varied over time. ARA content for the dry season was 1.48 ± 0.03 mg g^{-1} DW, and during the rainy season, it was 1.75 ± 0.07 mg g^{-1} DW. The EPA content presented values of 1.47 ± 0.03 mg g^{-1} DW during the dry, and 1.25 ± 0.05 mg g^{-1} DW during the rainy, season. Other PUFA, such as 18:2 n-6, 18:3 n-3 and 18:4 n-3 (Fig. 4) also were present but in smaller quantities, and also varied over time.

The ratio of n-6/n-3 fatty acids for *P. flagellifera* ranged between 0.88 (dry) and 1.31 (rainy) with lower values for dry season.

3.2.3. *Ulva fasciata*

The content of individual fatty acids and TFA in *U. fasciata* are presented in Fig. 5 and Table 1, respectively. SFA were the most dominant group of fatty acids in *U. fasciata*, with values of 49.28 ± 1.16% for the dry, and 53.52 ± 1.33% for rainy season, respectively. Percentage of PUFA varied over time, with 27.68 ± 0.13% reported for the dry season and 20.60 ± 0.57% for the rainy season; finally, MUFA represented 17.22 ± 0.06% (dry) and 18.99 ± 0.13% (rainy) of TFA. Palmitic acid (16:0) was the most frequent fatty acid

©Fungyi Chow / 2021

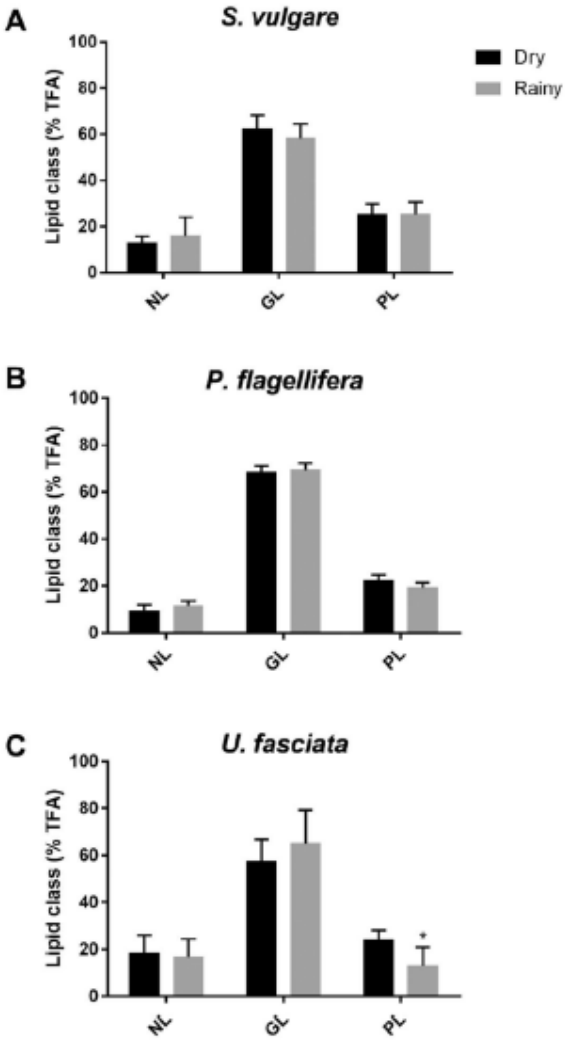

Fig. 6. Lipid class composition (% TFA) of *Sargassum vulgare* (A), *Palisada flagellifera* (B) and *Ulva fasciata* (C), collected during dry and rainy seasons (mean ± SD; n = 5). Significant differences (*) between dry and rainy seasons for the respective species were determined by Mann-Whitney-U test, $P < 0.05$. NL = Neutral lipids, GL = Glycolipids and PL = Phospholipids.

among SFA and did vary over time. Palmitic acid displayed percentages of 44.97 ± 3.37% (dry) and 48.99 ± 3.84% (rainy). Vaccenic acid (18:1 n-7) was the major fatty acid within MUFA, representing 8.24 ± 0.19% (dry) and 8.88 ± 0.35% (rainy), respectively. In addition to 18:1 n-7, seasonal variations were also observed for palmitoleic (16:1 n-7) and oleic (18:1 n-9) acids, with slight increase and decrease in percentage during the rainy season, respectively. Linoleic (18:2 n-6), alpha-linolenic (18:3 n-3), and stearidonic (18:4 n-3) acids were the main PUFA within *U. fasciata*. 18:3 n-3, 7.79 ± 1.45% (dry) and 6.05 ± 1.62% (rainy) represented the highest proportions within the PUFA, followed by 18: 2 n-6 with values of 5.94 ± 0.66% (dry) and 4.62 ± 0.62% (rainy), and finally 18:4 n-3, which presented values of 5.36 ± 1.39% (dry) and 3.79 ± 1.50% (rainy). Only traces of EPA and ARA (< 0.01 mg g^{-1} DW) were observed for this species.

The ratio of n-6/n-3 fatty acids in *U. fasciata* ranged from 0.45 (dry) to 0.48 (rainy) (Table 1).

3.3. Lipid class composition

Lipid class composition of the three macroalgal species investigated is presented in Fig. 6. Lipid classes showed no variations between dry and rainy seasons for any of the species. Glycolipids (GL) and phospholipids (PL) represented the main lipid constituents for those species, except for *U. fasciata*. In *S. vulgare*, fatty acids partitioned to GL accounted for 62.1% (dry) and 58.4% (rainy) of the overall TFA and PL for 25.3% (dry) and 25.5% (rainy) (Fig. 6A). Within neutral lipids (NL), percentages of TFA varied between 12.7% (dry) and 16.1% (rainy). In *P. flagellifera*, GL also represented the majority, with 68.3% (dry) and 69.3% (rainy) of the overall TFA, followed by PL with 22.2% (dry) and 19.2% (rainy) (Fig. 6B). TFA partitioned to NL accounted for 9.4% (dry) and 11.5% (rainy) (Fig. 6B). In *U. fasciata*, fatty acids partitioned to GL represented 57.6% (dry) and 65.2% (rainy). GL was the main lipid group of this species, followed by PL, containing 23.9% (dry) and 12.9% (rainy), and NL containing 18.4% (dry) and 16.7% (rainy) of TFA (Fig. 6C).

3.4. Fatty acid composition of the main lipid classes

The detailed fatty acid composition of each lipid fraction for the three seaweed species is displayed Table 2 (NL – neutral lipids), Table 3 (GL – glycolipids) and Table 4 (PL – phospholipids). Fatty acids partitioned to NL of *S. vulgare* were mainly composed of SFA with 35.19% (dry) and 37.48% (rainy) of TFA; 16:0 was the major fatty acid (15.44–21.17%) (Table 2). PUFA within NL presented higher levels during the dry season (29.65%) when DGLA (20:3 n-6, 9.08%) and DPA (22:5 n-3, 8.96%) were the main LC-PUFA; significant seasonal variation was observed for DPA within this lipid fraction. The fatty acid composition of the GL fraction in *S. vulgare* (Table 3) displayed high levels of SFA (45.36–45.91% of TFA), with 36.54–35.53% of 16:0 as the major SFA and these proportions were stable over time. PUFA accounted for 31.93 and 32.94% of TFA partitioned to GL during the dry and rainy seasons, respectively; ARA was the main LC-PUFA with 10.42% (dry) and 13.24% (rainy), and no seasonal variation was observed. PL were richer in SFA (61.91–66.28% of TFA) (Table 4), with 16:0 accounting for 52.08–55.87%, and, again, there was no significant change over time. PUFA within PL contained low levels of EPA (1.28–1.47% of TFA), and DGLA was the major LC-PUFA within this lipid class (5.81–6.47% of TFA).

In *P. flagellifera*, the fatty acid profiles of NL presented high levels of SFA (37.62–38.08%; Table 2), and 16:0 was the major fatty acid with 28.47% (dry) and 26.92% (rainy). PUFA within NL accounted for 35.31% (dry) and 39.58% (rainy), with DGLA (13.87%) and ARA (6.61%) representing the main LC-PUFA, but no significant seasonal variation was observed for either fatty acid. The fatty acid composition of the GL fraction contained high levels of SFA (44.27–48.67% of TFA) with 37.46–38.63% of 16:0 as the major SFA, and no observed seasonal variation (Table 3). PUFA accounted for 42.12% and 37.75% of TFA partitioned to GL during dry and rainy seasons, respectively; EPA represented the main LC-PUFA with 21.18% (dry) and 17.90% (rainy), thus exhibiting some seasonal variation. PL (Table 4) were richer in SFA (70.26–78.30% TFA), with 16:0 accounting for 51.26–57.63% of TFA and displaying a significant increase from the dry to the rainy season. PUFA within PL consisted of high levels of EPA (7.86–4.47% of TFA), with some seasonal variations, and ARA (7.14–8.96% of TFA) was the major LC-PUFA within this lipid class.

The fatty acid profiles of NL (Table 2) in *U. fasciata* presented high levels of SFA (36.28–44.72%), and 16:0 was the major fatty acid representing 34.50% (dry) and 29.06% (rainy). PUFA within NL accounted for 17.64% (dry) and 20.44% (rainy). Linoleic acid (16.0%) and ALA (5.67%) were the main LC-PUFA. The fatty acid composition of the GL fraction in *U. fasciata* (Table 3) showed high levels of SFA (47.05–55.16% of TFA) with 42.54–46.72% of 16:0 as the major SFA. PUFA accounted for 27.22% and 18.30% of TFA partitioned to GL

©Fungyi Chow / 2021

Table 2
Neutral lipid composition (% TFA) of *Sargassum vulgare*, *Palisada flagellifera* and *Ulva fasciata* collected during dry and rainy seasons (mean ± SD; n = 5). Bold values represent fatty acids with at least 1% of the total fatty acid composition of the species studied. Significant differences (*) between dry and rainy seasons for the respective species were determined by Mann-Whitney-U test, $P < 0.05$.

Fatty acids (% TFA)	*Sargassum vulgare*		*Palisada flagellifera*		*Ulva fasciata*	
	Dry	Rainy	Dry	Rainy	Dry	Rainy
SFA						
14:0	**3.9 ± 0.8**	**1.4 ± 1.3**	**2.8 ± 1.3**	**3.8 ± 0.8**	**2.2 ± 0.7**	**1.8 ± 0.3**
16:0	**21.2 ± 11.6**	**15.4 ± 9.2**	**28.5 ± 12.0**	**26.9 ± 2.9**	**34.5 ± 4.2**	**29.1 ± 3.0**
17:0	*n.d.*	*n.d.*	**1.0 ± 1.0**	0.4 ± 0.8	**3.3 ± 1.8**	**1.5 ± 1.0**
18:0	**9.2 ± 9.2**	**18.8 ± 7.3**	**5.2 ± 1.5**	**6.1 ± 2.1**	**3.0 ± 1.2**	**2.1 ± 0.2**
20:0	0.1 ± 0.3	0.5 ± 0.7	0.6 ± 0.9	0.5 ± 0.9	0.0 ± 0.1	0.0 ± 0.0
22:0	0.7 ± 0.9	**1.3 ± 1.4**	*n.d.*	*n.d.*	0.6 ± 0.8	0.7 ± 0.5
24:0	*n.d.*	*n.d.*	*n.d.*	*n.d.*	**1.1 ± 1.6**	**1.2 ± 0.4**
Sum SFA (%)	**35.2 ± 4.8**	**37.5 ± 3.5**	**38.1 ± 4.3**	**37.6 ± 0.8**	**44.7 ± 1.2**	**36.3 ± 1.0**
MUFA						
14:1	**9.9 ± 4.3**	**5.5 ± 1.7***	**5.0 ± 1.4**	**3.1 ± 1.6**	**2.0 ± 0.5**	**3.1 ± 1.0***
15:1	**1.6 ± 1.3**	**1.8 ± 1.4**	0.6 ± 0.5	0.8 ± 0.8	**6.6 ± 1.2**	**5.1 ± 0.6**
16:1 n-7	**3.5 ± 1.1**	**2.1 ± 1.5**	**1.8 ± 1.4**	0.9 ± 0.8	**1.1 ± 0.6**	**2.9 ± 0.9***
17:1	*n.d.*	*n.d.*	**3.5 ± 2.1**	**2.3 ± 1.5**	**1.8 ± 0.6**	**3.5 ± 1.1***
18:1 n-9	**7.7 ± 1.5**	**9.3 ± 1.9**	**6.9 ± 0.9**	**7.8 ± 1.6**	**5.4 ± 2.4**	**3.5 ± 0.4**
18:1 n-7	**3.0 ± 2.7**	**2.8 ± 1.5**	0.9 ± 0.7	0.7 ± 0.5	**5.7 ± 3.3**	**9.4 ± 0.5**
20:1 n-9	0.7 ± 0.8	**5.0 ± 5.2**	*n.d.*	*n.d.*	0.1 ± 0.1	0.0 ± 0.0
22:1 n-9	0.3 ± 0.5	0.5 ± 0.7	*n.d.*	*n.d.*	0.4 ± 0.6	0.0 ± 0.0
Sum MUFA (%)	**26.8 ± 1.2**	**27.1 ± 1.4**	**18.8 ± 0.5**	**15.7 ± 0.5**	**23.0 ± 1.0**	**27.6 ± 0.4**
PUFA						
16:2	*n.d.*	*n.d.*	*n.d.*	*n.d.*	0.2 ± 0.4	0.4 ± 0.2
16:4	*n.d.*	*n.d.*	*n.d.*	*n.d.*	0.4 ± 0.9	0.8 ± 0.7
18:2 n-6 (LA)	**3.2 ± 1.2**	**2.3 ± 2.3**	**1.7 ± 0.9**	**1.0 ± 1.0**	**5.2 ± 3.0**	**6.0 ± 0.5**
18:3 n-6	**1.2 ± 1.8**	0.4 ± 0.5	**7.8 ± 6.4**	**2.9 ± 5.8**	0.4 ± 0.4	0.6 ± 0.1
18:3 n-3 (ALA)	**2.7 ± 1.7**	**2.6 ± 1.5**	**1.8 ± 1.8**	0.0 ± 0.0^	**5.8 ± 1.9**	**5.7 ± 2.1**
18:4 n-3 (SDA)	0.1 ± 0.1	0.5 ± 0.5	**1.4 ± 2.7**	**2.8 ± 3.5**	**2.7 ± 3.0**	**3.2 ± 1.6**
20:2	0.3 ± 0.4	**3.6 ± 3.5**	**3.4 ± 6.2**	**3.5 ± 7.0**	*n.d.*	*n.d.*
20:3 n-6 (DGLA)	**9.1 ± 2.4**	**5.9 ± 4.4**	**3.2 ± 6.3**	**13.9 ± 11.5**	0.1 ± 0.1	0.5 ± 0.4*
20:4 n-6 (ARA)	**1.7 ± 2.8**	**3.6 ± 4.4**	**10.4 ± 5.2**	**6.6 ± 7.8**	0.9 ± 0.7	**1.1 ± 0.5**
20:4 n-3	0.7 ± 0.9	**1.4 ± 0.6**	*n.d.*	*n.d.*	0.4 ± 0.3	0.2 ± 0.3
20:5 n-3 (EPA)	**1.7 ± 0.8**	**3.1 ± 1.0**	**5.7 ± 3.5**	**5.7 ± 2.8**	**1.2 ± 1.1**	0.6 ± 0.8
22:5 n-3	**9.0 ± 9.3**	0.2 ± 0.4*	*n.d.*	**1.8 ± 3.6**	0.3 ± 0.7	**1.4 ± 0.8**
22:6 n-3 (DHA)	*n.d.*	*n.d.*	*n.d.*	**1.5 ± 3.0**	0.0 ± 0.1	0.0 ± 0.0
Sum PUFA (%)	**29.6 ± 2.5**	**23.6 ± 1.6**	**35.3 ± 2.5**	**39.6 ± 3.3**	**17.6 ± 1.0**	**20.4 ± 0.6**
FA unidentified	**8.4 ± 3.5**	**11.8 ± 4.9**	**7.9 ± 1.8**	**7.1 ± 1.4**	**14.7 ± 2.2**	**15.7 ± 5.0**
Nutritional index						
Σ n-3	14.2 ± 3.4	7.8 ± 1.3	8.9 ± 2.3	11.7 ± 2.1	10.4 ± 2.2	11.0 ± 2.2
Σ n-6	15.2 ± 3.6	12.3 ± 2.3	23.1 ± 4.0	24.4 ± 5.7	6.6 ± 2.4	8.2 ± 2.6
ratio n-6/n-3	1.1	1.6	2.6	2.1	0.6	0.7

n.d. = not detected.

during dry and rainy seasons, respectively, and ALA was the main LC-PUFA with 9.40% (dry) and 5.60% (rainy). PL were richer in SFA with 55.96 and 52.46% of TFA during the dry and rainy season, respectively (Table 4), with 16:0 accounting for 53.15–46.81% of TFA, displaying a significant seasonal decrease. PUFA within PL presented low levels of EPA (1.04–1.72% of TFA). ALA (9.03–7.30% of TFA) was the major LC-PUFA and no seasonal variation was observed within this lipid class.

Finally, lipidomic cluster analysis for all fatty acids and lipids for the three species studied, as well as the seasonal variations, is presented in Fig. 7. The correlations between dry and rainy season profiles were significantly high for each species, and formed three clusters: *U. fasciata* (Pearson's correlation of 0.7819), *S. vulgare* (Pearson's correlation of 0.9324) and *P. flagellifera* (Pearsons correlation of 0.9184), with these last two species more closely correlated than *U. fasciata*. The composition and abundance were relatively homogeneous across species and season, but with important peculiarities such as an elevated amount of SFA in *U. fasciata*; specifically, palmitic acid (16:0) formed a separate branch from other fatty acids; a large amount of LC-PUFA for *P. flagellifera*; and glycolipids were the most abundant lipid class for the species studied.

4. Discussion

4.1. Fatty acid and lipid class composition and taxonomic variability

The analysis of fatty acid composition revealed significant differences between the representatives of brown, red and green algae from the tropical coast in Brazil. As fatty acid profiles are considered characteristic of different taxonomic algal groups, their specificity has previously been used in chemotaxonomic studies [e.g. Kumari et al. [25], Kumari et al. [30], Cardoso et al. [40]]. Additionally, particular suitable profiles can be selected for nutritional and biochemical studies [24,28,41,42]. Chemotaxonomic studies, which use the fatty acid profile as a molecular signature, have gained recent interest as they potentially provide valuable information on the role of macrophytes as a source of essential fatty acids (n-3 and n-6) to higher trophic levels. Such knowledge also underpins the potential development of further commercial applications [22]. Fatty acid composition can also provide algal taxonomic resolution at order and family levels, allowing an insight into evolutionary processes [22,43].

The results for the main lipid classes of the species studied was corroborated by data presented in the literature; glycolipids (GL) are known as dominant lipids of the chloroplast, particularly of the

©Fungyi Chow / 2021

Table 3
Glycolipid composition (% TFA) of *Sargassum vulgare*, *Palisada flagellifera* and *Ulva fasciata* collected during dry and rainy seasons (mean ± SD; n = 5). Bold values represent fatty acids with at least 1% of the total fatty acid composition of the species studied. Significant differences between dry and rainy seasons for the respective species were determined by Mann-Whitney-U test, $^{*}P < 0.05$ and $^{**}P < 0.01$.

Fatty acids (% TFA)	*Sargassum vulgare*		*Palisada flagellifera*		*Ulva fasciata*	
	Dry	Rainy	Dry	Rainy	Dry	Rainy
SFA						
12:0	*n.d.*	*n.d.*	0.2 ± 0.1	0.6 ± 0.8	0.9 ± 0.2	1.0 ± 0.4
14:0	**5.8 ± 0.1**	**5.8 ± 0.5**	**4.1 ± 0.3**	**3.5 ± 0.3**	**42.5 ± 5.5**	**46.7 ± 1.0**
16:0	**36.5 ± 2.4**	**35.5 ± 1.2**	**37.5 ± 0.5**	**38.6 ± 1.8**	0.6 ± 0.4	0.4 ± 0.3
17:0	*n.d.*	*n.d.*	0.1 ± 0.1	0.3 ± 0.1*	**2.1 ± 0.3**	**4.7 ± 1.4**
18:0	**2.3 ± 0.1**	**3.9 ± 1.6****	**2.2 ± 0.2**	**5.3 ± 2.4****	*n.d.*	0.2 ± 0.1*
20:0	0.8 ± 0.3	0.7 ± 0.3	0.1 ± 0.1	0.2 ± 0.3	0.7 ± 0.6	**2.0 ± 1.0***
22:0	*n.d.*	*n.d.*	*n.d.*	*n.d.*	0.2 ± 0.3	0.2 ± 0.1*
Sum SFA (%)	**45.4 ± 1.0**	**45.9 ± 0.5**	**44.2 ± 0.2**	**48.7 ± 0.9**	**47.0 ± 1.8**	**55.2 ± 0.5**
MUFA						
14:1	0.2 ± 0.1	0.2 ± 0.1	0.2 ± 0.1	0.3 ± 0.2	0.7 ± 0.1	1.2 ± 0.3*
15:1	0.9 ± 0.3	1.0 ± 0.3	0.1 ± 0.1	0.4 ± 0.3*	1.7 ± 0.4	1.8 ± 0.4
16:1 n-7	**4.9 ± 0.1**	**2.8 ± 1.9****	**1.5 ± 0.1**	**1.5 ± 0.9**	**1.9 ± 0.6**	**3.0 ± 0.3***
17:1	*n.d.*	*n.d.*	0.7 ± 0.3	0.8 ± 1.1	**4.9 ± 1.5**	**2.7 ± 1.7***
18:1 n-9	**11.9 ± 0.7**	**13.9 ± 0.7****	**8.9 ± 0.1**	**7.6 ± 3.3**	**2.9 ± 0.3**	**2.5 ± 0.2**
18:1 n-7	0.8 ± 0.3	0.6 ± 0.2	0.9 ± 0.0	**1.0 ± 0.5**	**10.0 ± 0.4**	**11.4 ± 1.1***
20:1 n-9	0.4 ± 0.3	0.7 ± 0.1	*n.d.*	*n.d.*	*n.d.*	0.1 ± 0.1*
22:1 n-9	*n.d.*	*n.d*	*n.d.*	*n.d.*	0.1 ± 0.1	0.3 ± 0.3
Sum MUFA (%)	**19.1 ± 0.2**	**19.2 ± 0.6**	**12.3 ± 0.1**	**11.5 ± 1.1**	**22.2 ± 0.5**	**23.0 ± 0.5**
PUFA						
16:2	*n.d.*	*n.d.*	*n.d.*	*n.d.*	0.4 ± 0.2	**1.2 ± 0.4***
16:4	*n.d.*	*n.d.*	*n.d.*	*n.d.*	*n.d.*	**1.5 ± 1.3***
18:2 n-6 (LA)	**5.4 ± 0.0**	**6.2 ± 0.6**	**1.8 ± 0.1**	**1.5 ± 0.2***	**7.0 ± 1.0**	**4.4 ± 0.5***
18:3 n-6	0.6 ± 0.1	**1.1 ± 0.5****	0.4 ± 0.1	0.3 ± 0.2	0.5 ± 0.2	0.3 ± 0.2
18:3 n-3 (ALA)	**7.8 ± 0.1**	**4.4 ± 0.6****	**2.3 ± 1.1**	0.5 ± 0.4	**9.4 ± 2.0**	**5.6 ± 1.7***
18:4 n-3 (SDA)	**2.8 ± 0.3**	**2.5 ± 0.5**	**1.9 ± 0.3**	0.5 ± 0.5**	**6.8 ± 1.9**	**3.4 ± 1.7***
20:2	0.2 ± 0.1	0.8 ± 0.9*	0.1 ± 0.1	0.2 ± 0.2	*n.d.*	*n.d.*
20:3 n-6 (DGLA)	0.4 ± 0.4	0.6 ± 0.5	0.6 ± 0.3	0.3 ± 0.4	0.0 ± 0.1	0.1 ± 0.1
20:4 n-6 (ARA)	**10.4 ± 1.1**	**13.2 ± 0.9****	**13.3 ± 0.1**	**16.2 ± 1.1****	0.5 ± 0.5	0.3 ± 0.1
20:4 n-3	0.2 ± 0.2	0.6 ± 0.1**	*n.d.*	*n.d.*	0.4 ± 0.5	*n.d.*
20:5 n-3 (EPA)	**3.0 ± 0.3**	**2.1 ± 0.3****	**21.2 ± 0.5**	**17.9 ± 0.7****	**1.4 ± 0.9**	0.6 ± 0.6
22:5 n-3	0.6 ± 0.4	1.3 ± 1.7	0.5 ± 0.7	0.3 ± 0.3	0.4 ± 0.3	0.9 ± 0.6
22:6 n-3 (DHA)	0.5 ± 0.6	0.1 ± 0.1	0.1 ± 0.2	*n.d.*	0.4 ± 0.5	*n.d.*
Sum PUFA	**31.9 ± 1.0**	**32.9 ± 0.4**	**42.1 ± 0.3**	**37.8 ± 0.3**	**27.2 ± 0.6**	**18.3 ± 0.5**
FA unidentified	**3.6 ± 1.0**	**2.0 ± 0.5**	**1.4 ± 0.4**	**2.1 ± 1.1**	**3.6 ± 0.9**	**3.5 ± 0.5**
Nutritional index						
Σ n-3	14.96 ± 2.9	11.0 ± 1.6	25.9 ± 9.0	19.2 ± 7.9	18.8 ± 3.9	10.6 ± 2.3
Σ n-6	16.7 ± 4.7	21.1 ± 5.9	16.1 ± 6.2	18.3 ± 7.8	8.1 ± 3.3	1.3 ± 0.4
ratio n-6/n-3	1.1	1.9	0.6	0.9	0.4	0.1

n.d. = not detected.

thylakoid membranes, while phospholipids (PL) are the components of other cellular membranes [61]. Although classically GL are the major lipid class in all marine algae, followed by neutral lipids (NL) and PL. Despite this, NL and GL do not seem to be specific to particular taxa but are present in all species, contrary to PL [62].

The clustering of fatty acids and lipid profiles showed non-distinction between dry or rainy seasons for each species, with similar composition and abundance. However, differences were observed among the species, with closer grouping proximity between the red alga ***P. flagellifera (Rhodophyta)*** and the brown alga ***S. vulgare (Ochrophyta)***, and ***P. flagellifera*** the most basal species of the dendrogram. The stark divergence of ***P. flagellifera*** from the other species could represent adaptation of higher taxonomic levels; for example, Lang et al. [63] previously observed a similar fatty acid composition for cyanobacteria and red algae, but characteristics of these two groups were distinct from organisms which had acquired adaptations in addition to those inherited from the ancestral cyanobacteria (i.e. as could be the case of the green and brown species in our study).

The Brazilian samples of the brown alga *S. vulgare* contained a large proportion of SFA such as myristic and palmitic acids, MUFA such as oleic acid, as well as C18 and C20 PUFAs. Our results agree with Kumari et al. [25] who studied the profile of five tropical brown macroalgae and concluded that such profiles were typical of representatives of the order Dictyotales and Fucales; irrespective of substantial morphological differences within these groups, a distinct pattern in fatty acids has been demonstrated in several studies [44–47]. According to Chen et al. [48], fatty acid composition can thus be considered as a potential chemotaxonomic signature for *Sargassum* spp., but there is poor evidence for species-specific fatty acid signatures within this genus.

Myristic, palmitic and oleic acids, as well as ARA and EPA, were the main fatty acids in *P. flagellifera*. Profiles within this rhodophyte were thus similar to Kumari et al. [25] who observed a great diversity in the lipid composition of red algae; but as in the present work, they observed that C20 LC-PUFA (ARA and EPA) were typically the main PUFAs in red algae.

Similarly, the profile of the green algal representative in this study, *U. fasciata*, which was characterized by high amount of SFA (especially palmitic acid (16: 0)) and MUFA rich in vaccenic acid (18: 1 n-7), was similar to that found for other green seaweeds (*Ulva lactuca*) from other global regions (Japan) by Khotimchenko [49]. This suggests that such composition is characteristic of Chlorophyta and even more specifically of *Blidingia minima, Ulva fenestrata, Ulva linza* and *Ulva flexuosa*.

©Fungyi Chow / 2021

Table 4
Phospholipid composition (% TFA) of *Sargassum vulgare*, *Palisada flagellifera* and *Ulva fasciata* collected during dry and rainy seasons (mean ± SD; n = 5). Bold values represent fatty acids with at least 1% of the total fatty acid composition of the species studied. Significant differences between dry and rainy seasons for the respective species were determined by Mann-Whitney-U test, * $P < 0.05$ and ** $P < 0.01$.

Fatty acids (% TFA)	*Sargassum vulgare*		*Palisada flagellifera*		*Ulva fasciata*	
	Dry	Rainy	Dry	Rainy	Dry	Rainy
SFA						
14:0	**7.8 ± 0.2**	**6.2 ± 0.4****	**16.5 ± 0.4**	**19.2 ± 2.7***	0.9 ± 0.1	0.7 ± 0.5
16:0	**52.1 ± 3.3**	**55.9 ± 1.2***	**51.3 ± 0.5**	**57.6 ± 5.1***	**53.1 ± 2.9**	**46.8 ± 5.6***
17:0	*n.d.*	*n.d*	0.1 ± 0.2	*n.d.*	0.0 ± 0.1	*n.d.*
18:0	**1.7 ± 0.4**	**3.7 ± 1.3****	**2.3 ± 0.9**	**1.5 ± 0.9**	**1.3 ± 0.6**	**2.4 ± 1.5**
20:0	0.3 ± 0.0	0.5 ± 0.3	0.1 ± 0.2	*n.d.*	0.2 ± 0.2	*n.d.*
22:0	*n.d.*	*n.d.*	*n.d.*	*n.d.*	0.3 ± 0.5	1.7 ± 1.2*
24:0	*n.d.*	*n.d.*	*n.d.*	*n.d.*	0.1 ± 0.2	0.7 ± 0.4*
Sum SFA (%)	**61.9 ± 1.3**	**66.3 ± 0.4**	**70.3 ± 0.3**	**78.3 ± 2.0**	**56.0 ± 0.9**	**52.5 ± 1.8**
MUFA						
14:1	0.1 ± 0.1	*n.d.*	0.1 ± 0.1	*n.d.*	0.2 ± 0.2	0.3 ± 0.3
15:1	0.2 ± 0.1	0.3 ± 0.2	0.3 ± 0.1	0.5 ± 0.3	0.3 ± 0.2	0.8 ± 0.1*
16:1 n-7	**4.3 ± 0.1**	**1.9 ± 1.5****	**1.5 ± 0.5**	0.8 ± 0.5	**4.3 ± 0.7**	**5.9 ± 1.5**
17:1	*n.d.*	*n.d.*	0.1 ± 0.1	*n.d.*	**1.3 ± 0.6**	0.8 ± 0.2
18:1 n-9	**12.2 ± 0.3**	**14.4 ± 0.7****	**5.0 ± 0.7**	**3.8 ± 2.3**	**4.0 ± 2.4**	**4.6 ± 1.5**
18:1 n-7	**1.0 ± 0.2**	0.6 ± 0.3	**1.3 ± 0.6**	**1.3 ± 0.7**	**4.0 ± 3.7**	**2.8 ± 1.9**
20:1 n-9	0.1 ± 0.1	0.1 ± 0.2	*n.d.*	*n.d.*	0.1 ± 0.2	**1.0 ± 1.0***
22:1 n-9	*n.d.*	*n.d.*	*n.d.*	*n.d.*	0.3 ± 0.4	**1.2 ± 0.6***
Sum MUFA (%)	**17.9 ± 0.1**	**17.3 ± 0.5**	**8.2 ± 0.3**	**6.3 ± 0.8**	**14.4 ± 1.2**	**17.2 ± 0.7**
PUFA						
16:2	*n.d.*	*n.d.*	*n.d.*	*n.d.*	*n.d.*	**3.9 ± 2.6***
16:4	*n.d.*	*n.d.*	*n.d.*	*n.d.*	*n.d.*	*n.d.*
18:2 n-6 (LA)	**3.6 ± 0.8**	**3.3 ± 0.1**	**1.4 ± 0.7**	0.6 ± 0.4	**5.3 ± 0.3**	**4.4 ± 0.7***
18:3 n-6	0.4 ± 0.1	0.2 ± 0.2	0.2 ± 0.2	*n.d.*	**2.5 ± 0.3**	**1.7 ± 0.5***
18:3 n-3 (ALA)	**3.6 ± 0.6**	**2.6 ± 0.3***	**2.1 ± 1.7**	0.7 ± 0.6	**9.0 ± 0.9**	**7.3 ± 1.7***
18:4 n-3 (SDA)	**1.0 ± 0.2**	0.7 ± 0.4	**1.0 ± 0.5**	0.3 ± 0.3	**6.2 ± 0.7**	**3.5 ± 1.3***
20:2	0.3 ± 0.2	*n.d.*	0.2 ± 0.2	*n.d.*	*n.d.*	*n.d.*
20:3 n-6 (DGLA)	**6.5 ± 2.8**	**5.8 ± 1.1**	0.5 ± 0.4	*n.d.*	*n.d.*	*n.d.*
20:4 n-6 (ARA)	*n.d.*	*n.d.*	**7.1 ± 0.7**	**8.9 ± 1.4**	0.7 ± 0.1	0.7 ± 0.2
20:4 n-3	0.3 ± 0.1	0.3 ± 0.5	*n.d.*	*n.d.*	*n.d.*	*n.d.*
20:5 n-3 (EPA)	**1.3 ± 0.1**	**1.5 ± 0.7**	**7.9 ± 0.7**	**4.5 ± 2.6***	**1.0 ± 0.2**	**1.7 ± 1.6**
22:5 n-3 (DPA)	0.8 ± 0.8	0.2 ± 0.3	0.1 ± 0.3	*n.d.*	**1.5 ± 1.4**	**1.8 ± 0.6**
22:6 n-3 (DHA)	0.7 ± 0.4	*n.d.*	0.4 ± 0.3	*n.d.*	*n.d.*	0.1 ± 0.24
Sum PUFA (%)	**18.4 ± 0.4**	**14.6 ± 1.9**	**20.9 ± 0.4**	**15.0 ± 0.8**	**26.4 ± 0.4**	**25.1 ± 0.8**
FA unidentified	**1.8 ± 0.4**	**1.8 ± 0.3**	0.6 ± 0.3	0.4 ± 0.4	**3.2 ± 0.4**	**5.2 ± 1.0***
Nutritional index						
Σ n-3	7.6 ± 1.2	5.3 ± 1.0	11.5 ± 3.2	5.5 ± 1.9	17.8 ± 3.8	14.4 ± 2.7
Σ n-6	10.5 ± 3.0	9.3 ± 2.8	9.2 ± 3.3	9.5 ± 4.4	8.6 ± 2.4	6.8 ± 1.9
ratio n-6/n-3	1.4	1.7	0.8	1.7	0.5	0.5

n.d. = not detected.

Furthermore, Sato [50] reported large amounts of C16 PUFA, such as 16:3 and 16:4 in green algae, and this was replicated in the *Ulva* samples from Brazil in our study. Johns et al. [51] proposed that 16:4 could be taxonomically characteristic of green macrophytic algae because only traces of these fatty acids were found in other algal groups. Important PUFAs such as linoleic acid and linolenic acid were also contained in *U. fasciata*, and some seasonal changes were observed. It has previously been suggested that green algae are characterized by mostly containing these two C18 PUFAs, which is a feature in common with vascular plants [46,52]. Arachidonic acid, an important LC-PUFA, was the major fatty acid among PUFAs for *S. vulgare* and *P. flagellifera*. On the other hand, eicosapentaenoic acid was present at low levels in *S. vulgare* but higher levels in *P. flagellifera*. These results are consistent with those found in the literature [28,41,53], again highlighting that the fatty acid constitution can be related to the taxonomic group.

4.2. Temporal stability in lipid and fatty acid profiles on the Brazilian north-eastern coast

The three tropical species studied showed high, but relatively stable, levels of the SFA: *S. vulgare* (43–48%), *P. flagellifera* (45–46%) and *U. fasciata* (49–53%). Such results are consistent with the literature [37,38,54,55] for tropical seaweeds; and samples analyzed in this study were collected from a tropical zone characterized by warm water throughout the year. Narayan et al. [38] suggested that a high amount of SFA was directly related to water temperatures as a high SFA content appeared to be a physiological adaptation of tropical seaweed species. An opposite trend has been observed in cold-water species where high PUFA levels provide a mechanism for thermo-adaptive regulation of membrane lipid fluidity [56].

Rainfall patterns can directly influence the production and composition of fatty acids in seeds of terrestrial plants, which is well documented in the literature [57,58]. Supported by our meteorological data, rainfall and UV patterns for 2013 and 2014 appeared to cause only small changes in the distribution and composition of the fatty acids of the algae studied here. With some exceptions, the lipid content and composition, as well as the fatty acid composition of each lipid class within the three species was relatively stable over both seasons, most likely because of the low influence of tide at this latitude and therefore rare exposure to freshwater from rainfall or UV radiation.

The reported stability in fatty acid levels and composition across the two main seasons is in contrast to recent observations on temperate

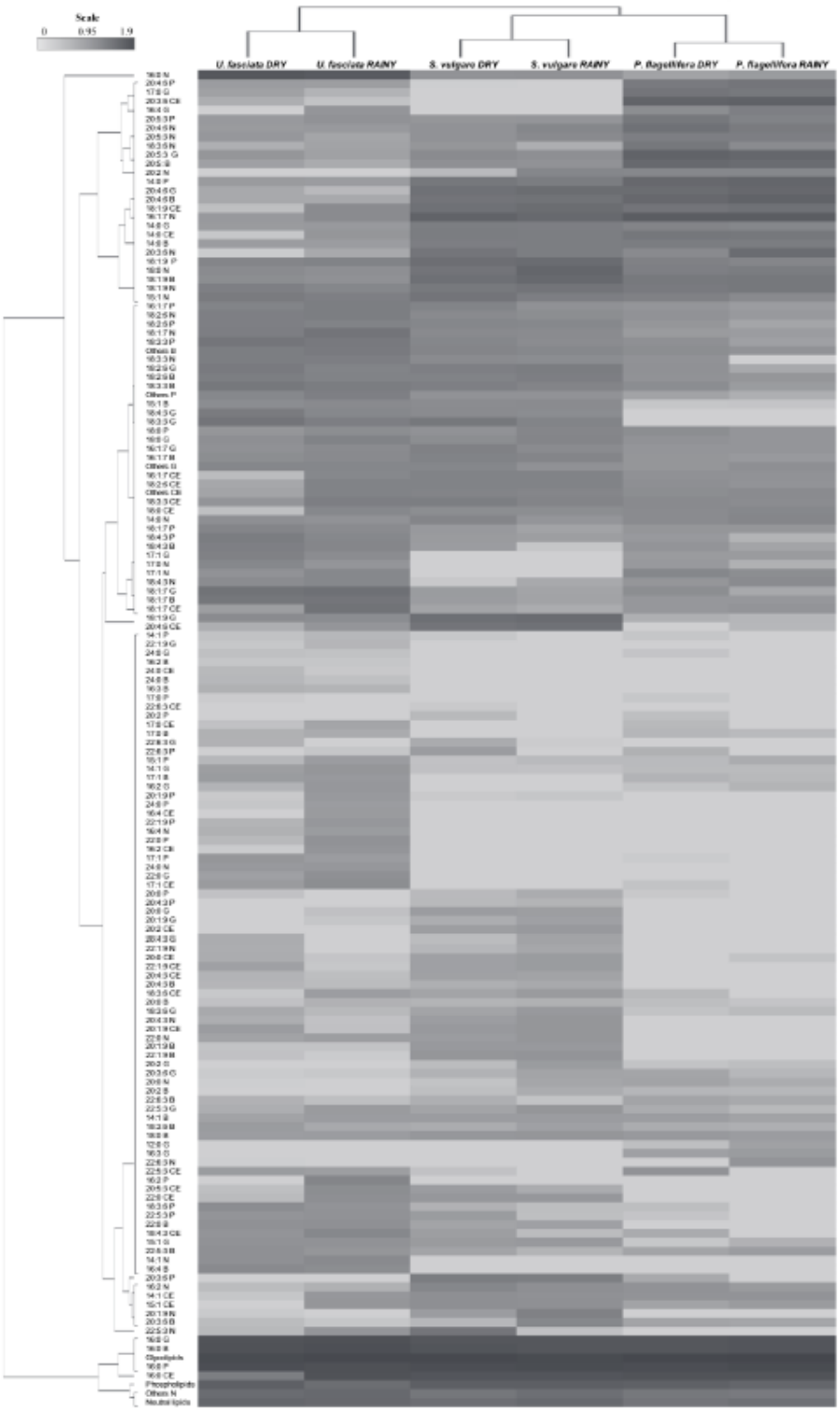

(caption on next page)

©Fungyi Chow / 2021

Fig. 7. Bidimensional heatmap dendrogram showing hierarchical clustering (Complete linkage - Pearson correlation) of lipid and fatty acids profiles of three species of macroalgae, *Sargassum vulgare*, *Palisada flagellifera* and *Ulva fasciata*, collected during dry and rainy seasons. B = fatty acid from direct biomass; CE = fatty acids from crude extracts; G = glycolipids; N = neutral lipids; P = phospholipids. Five replicates of all samples were analyzed.

species exhibiting seasonal and spatial variation in fatty acid profiles (e.g. Schmid et al. [32]). It is of particular interest from an economic point of view as it facilitates potential all year-round utilization of macroalgae. Seaweed biomass with a consistent biochemical profile, and thus quality, is commercially preferable [59,60] and represents a strong advantage for exploitation as a source of fatty acids, especially PUFAs, from the north-eastern coast of Brazil. The combined ecological (growth, abundance) and chemical (biochemical composition) knowledge of local seaweeds may underpin the future development of seaweed cultivation or harvesting strategies.

5. Conclusions

Although the total fatty acid content of macroalgae is generally lower than that of microalgae, they are still considered a valuable potential source of PUFAs. This study has demonstrated that *P. flagellifera* represents an interesting source of LC-PUFA, mainly of ARA and EPA. The three seaweed species examined here had low ratios of omega-6 to omega-3 fatty acids, which suggest that they might represent useful functional component as food or food supplement with the potential to improve the omega-3 deficiency in western diets. Increasing the amounts of omega-3 in the diet reduces the chance of developing inflammatory, cardiovascular and autoimmune disorders and on this aspect, the World Health Organization recommends that this ratio is < 10/1 in western countries [15,47]. Therefore, *P. flagellifera* could be an alternative resource for human and animal nutrition such as the production of functional foods or animal feeds.

This study also confirmed highly specific fatty acid and lipid class profiles for different macroalgal species, supporting the use of these components in chemotaxonomy and the study of evolutionary processes.

The tropical seaweeds studied here contained high SFA levels compared to related algae from temperate waters, which may represent a physiological adaptation of tropical species to warm water temperatures. There was little evidence of temporal changes in environmental parameters influencing the distribution and composition of fatty acids, resulting in a relatively stable lipid content and composition across seasons. This would imply that seaweeds from north-eastern Brazil can be exploited all year-round based on their similar biochemical profiles, and thus quality, for applications in food or feed industries.

Statement of informed consent, human/animal rights

No informed consent, human or animal rights applicable.

Declaration of authors' contributions to the work

JPS, FC, FG and DBS conceived and designed the experiments, analyzed and interpreted the results. All authors helped to draft the manuscript, read, contributed with a critical revision of the article for important intellectual content and approved the final article.

Declaration of Competing Interest

The authors declare that there is no conflict of interest for this paper.

Acknowledgments

JPS and FC thank CAPES (Coordenação de Aperfeiçoamento de Pessoal de Nível Superior) and FAPESP (Fundação de Amparo à Pesquisa do Estado de São Paulo (Biota/Fapesp 2013/50731-1) for financial support. FC thanks CNPq (Conselho Nacional de Desenvolvimento Científico e Tecnológico) for Productivity Research Fellowship (Proc. 303937/2015-7). JSP and FC also thank CEPLAC (Comissão Executiva de Planejamento da Lavoura Cacaueira) for technical support. DBS and FG were supported by Marine Biotechnology ERA-NET (ERA-MarineBiotech) ('NEPTUNA', PBA/MB/15/01).

References

[1] M.J. Pérez, E. Falqué, H. Domínguez, Antimicrobial action of compounds from marine seaweed, Mar. Drugs 14 (2016) 1–38, https://doi.org/10.3390/md14030052.
[2] G.A. Thompson, Lipids and membrane function in green algae, Biochim. Biophys. Acta 1302 (1996) 17–45, https://doi.org/10.1016/0005-2760(96)00045-8.
[3] H. Wada, N. Murata, Membrane lipids in cyanobacteria, in: P.-A. Siegenthaler, N. Murata (Eds.), Lipids in Photosynthesis, Kluwer Academic Publishers, Dordrecht, The Netherlands, 1998, pp. 65–81, , https://doi.org/10.1007/0-306-48087-5_4.
[4] L.A. Guschina, J.L. Harwood, Lipids and lipid metabolism in eukaryotic algae., Prog. Lipid Res. 45 (2006) 160–186, https://doi.org/10.1016/j.plipres.2006.01.001.
[5] M.J. Griffiths, S.T.L. Harrison, Lipid productivity as a key characteristic for choosing algal species for biodiesel production, J. Appl. Phycol. 21 (2009) 493–507, https://doi.org/10.1007/s10811-008-9392-7.
[6] M.J. Griffiths, R.P. van Hille, S.T.L. Harrison, Lipid productivity, settling potential and fatty acid profile of 11 microalgal species grown under nitrogen replete and limited conditions, J. Appl. Phycol. 24 (2012) 989–1001, https://doi.org/10.1007/s10811-011-9723-y.
[7] S.S. Merchant, J. Kropat, B. Liu, J. Shaw, J. Warakanont, TAG, you're it! *Chlamydomonas* as a reference organism for understanding algal triacylglycerol accumulation, Curr. Opin. Biotechnol. 23 (2012) 352–363, https://doi.org/10.1016/j.copbio.2011.12.001.
[8] G. Markou, E. Nerantzis, Microalgae for high-value compounds and biofuels production: a review with focus on cultivation under stress conditions, Biotechnol. Adv. 31 (2013) 1532–1542, https://doi.org/10.1016/j.biotechadv.2013.07.011.
[9] Q. Hu, M. Sommerfeld, E. Jarvis, M. Ghirardi, M. Posewitz, M. Seibert, A. Darzins, Microalgal triacylglycerols as feedstocks for biofuel production: perspectives and advances, Plant J. 54 (2008) 621–639, https://doi.org/10.1111/j.1365-313X.2008.03492.x.
[10] C. Adams, V. Godfrey, B. Wahlen, L. Seefeldt, B. Bugbee, Understanding precision nitrogen stress to optimize the growth and lipid content trade-off in oleaginous green microalgae, Bioresour. Technol. 131 (2013) 188–194, https://doi.org/10.1016/j.biortech.2012.12.143.
[11] S. Schmollinger, T. Mühlhaus, N.R. Boyle, I.K. Blaby, D. Casero, T. Mettler, J.L. Moseley, J. Kropat, F. Sommer, D. Strenkert, D. Hemme, M. Pellegrini, A.R. Grossman, M. Stitt, M. Schroda, S.S. Merchanta, Nitrogen-sparing mechanisms in *Chlamydomonas* affect the transcriptome, the proteome, and photosynthetic metabolism, Plant Cell 26 (2014) 1410–1435, https://doi.org/10.1105/tpc.113.122523.
[12] C.S. Kumar, P. Ganesan, P.V. Suresh, N. Bhaskar, Seaweeds as a source of nutritionally beneficial compounds - a review, J. Food Sci. Technol. 45 (2008) 1–13.
[13] M. Kumar, P. Kumari, N. Trivedi, M.K. Shukla, V. Gupta, G.R.K. Reddy, B. Jha, Minerals, PUFAs and antioxidant properties of some tropical seaweeds from Saurashtra coast of India, J. Appl. Phycol. 23 (2011) 797–810, https://doi.org/10.1007/s10811-010-9578-7.
[14] A.P. Simopoulos, The importance of the ratio of omega-6/omega-3 essential fatty acids, Biomed. Pharmacother. 56 (2002) 365–379, https://doi.org/10.1016/S0753-3322(02)00253-6.
[15] A.P. Simopoulos, The importance of the omega-6/omega-3 fatty acid ratio in cardiovascular disease and other chronic diseases, Exp. Biol. Med. 233 (2008) 674–688, https://doi.org/10.3181/0711-MR-311.
[16] S. Gite, R.P. Ross, D. Kirke, F. Guihéneuf, J. Aussant, D.B. Stengel, T.G. Dinan, J.F. Cryan, C. Stanton, Nutraceuticals to promote neuronal plasticity in response to corticosterone-induced stress in human neuroblastoma cells, Nutr. Neurosci. 29 (2018) 1–18, https://doi.org/10.1080/1028415X.2017.1418728.
[17] R. Wall, R.P. Ross, G.F. Fitzgerald, C. Stanton, Fatty acids from fish: the anti-inflammatory potential of long-chain omega-3 fatty acids, Nutr. Rev. 68 (2010) 280–289, https://doi.org/10.1111/j.1753-4887.2010.00287.x.
[18] J.P. SanGiovanni, E.Y. Chew, The role of omega-3 long-chain polyunsaturated fatty acids in health and disease of the retina, Prog. Retin. Eye Res. 24 (2005) 87–138, https://doi.org/10.1016/j.preteyeres.2004.06.002.
[19] A.P. DeFilippis, M.J. Blaha, T.A. Jacobson, Omega-3 fatty acids for cardiovascular disease prevention, Curr. Treat. Options Cardiovasc. Med. 12 (2010) 365–380, https://doi.org/10.1007/s11936-010-0079-4.
[20] M. Dimri, P.V. Bommi, A.A. Sahasrabuddhe, J.D. Khandekar, G.P.H. Dimri, Dietary omega-3 polyunsaturated fatty acids suppress expression of EZH2 in breast cancer cells, Carcinogen 31 (2010) 489–495, https://doi.org/10.1093/carcin/bgp305.
[21] L.A. Fagundes, Ômega-3 & ômega-6: o equilíbrio dos ácidos gordurosos essenciais

na prevenção de doenças, Fundação de Radioterapia do Rio Grande do Sul, Porto Alegre, 2002, p. 111.
[22] A.W.E. Galloway, K.H. Britton-Simmons, D.O. Duggins, P.W. Gabrielson, M.T. Brett, Fatty acid signatures differentiate marine macrophytes at ordinal and family ranks, J. Phycol. 48 (2012) 956–965, https://doi.org/10.1111/j.1529-8817.2012.01173.x.
[23] B.J. Gosch, M. Magnusson, N.A. Paul, R. De Nys, Total lipid and fatty acid composition of seaweeds for the selection of species for oil-based biofuel and bioproducts, G.C.B. Bioener. 4 (2012) 919–930, https://doi.org/10.1111/j.1757-1707.2012.01175.x.
[24] C.E. Hanson, G.A. Hyndes, S.F. Wang, Differentiation of benthic marine primary producers using stable isotopes and fatty acids: implications to food web studies, Aquat. Bot. 93 (2010) 114–122, https://doi.org/10.1016/j.aquabot.2010.04.004.
[25] P. Kumari, M. Kumar, V. Gupta, C.R.K. Reddy, B. Jha, Tropical marine macroalgae as potential sources of nutritionally important PUFAs, Food Chem. 120 (2010) 749–757, https://doi.org/10.1016/j.foodchem.2009.11.006.
[26] N.M. Sanina, S.N. Goncharova, E.Y. Kostetsky, Fatty acid composition of individual polar lipid classes from marine macrophytes, Phytochem 65 (2004) 721–730, https://doi.org/10.1016/j.phytochem.2004.01.013.
[27] V.M. Dembitsky, E.E. Pechenkina-Shubina, O.A. Rozentsvet, Glycolipids and fatty acids of some seaweeds and marine grasses from the Black Sea, Phytochem 30 (1991) 2279–2283, https://doi.org/10.1016/0031-9422(91)83630-4.
[28] M. Schmid, F. Guihéneuf, D.B. Stengel, Fatty acid contents and profiles of 16 macroalgae collected from the Irish coast at two seasons, J. Appl. Phycol. 26 (2014) 451–463, https://doi.org/10.1007/s10811-013-0132-2.
[29] M. Graeve, G. Kattner, C. Wiencke, U. Karsten, Fatty acid composition of Arctic and Antarctic macroalgae: indicator of phylogenetic and trophic relationships, Mar. Ecol. Prog. Ser. 231 (2002) 67–74, https://doi.org/10.3354/meps231067.
[30] P. Kumari, M. Kumar, C.R.K. Reddy, B. Jha, Nitrate and phosphate regimes induced lipidomic and biochemical changes in the intertidal macroalga *Ulva lactuca* (Ulvophyceae, Chlorophyta), Plant Cell Physiol. 55 (2014) 52–63, https://doi.org/10.1093/pcp/pct156.
[31] M.L. Colombo, P. Rise, F. Giavarini, L. De Angelis, C. Galli, C.L. Bolis, Marine macroalgae as sources of polyunsaturated fatty acids, Plant Foods Hum. Nutr. 61 (2006) 67–72, https://doi.org/10.1007/s11130-006-0015-7.
[32] M. Schmid, F. Guihéneuf, D.B. Stengel, Plasticity and remodelling of lipids support acclimation potential in two species of low-intertidal macroalgae, *Fucus serratus* (Phaeophyceae) and *Palmaria palmata* (Rhodophyta), Algal Res. 26 (2017) 104–114, https://doi.org/10.1016/j.algal.2017.07.004.
[33] M.K. Kim, J.P. Dubacq, J.C. Thomas, G. Giraud, Seasonal variations of triacylglycerols and fatty acids in *Fucus serratus*, Phytochem 43 (1996) 49–55, https://doi.org/10.1016/0031-9422(96)00243-9.
[34] M.M. Nelson, C.F. Phleger, P.D. Nichols, Seasonal lipid composition in macroalgae of the northeastern Pacific Ocean, Bot. Mar. 45 (2002) 58–65, https://doi.org/10.1515/BOT.2002.007.
[35] V. Venkatesalu, P. Sundaramoorthy, M. Anantharaj, M. Chandrasekaran, A. Senthilkumar, Seasonal variation on fatty acid composition of some marine macroalgae from gulf of Mannar Marine Biosphere Reserve, Southeast coast of India, Indian J. Geo-Mar. Sci. 41 (2012) 442–450.
[36] M. Kendel, A. Couzinet-Mossion, M. Viau, J. Fleurence, G. Barnathan, G. Wielgosz-Collin, Seasonal composition of lipids, fatty acids, and sterols in the edible red alga *Grateloupia turuturu*, J. Appl. Phycol. 25 (2013) 425–432, https://doi.org/10.1007/s10811-012-9876-3.
[37] E. Susanto, A. Suhaeli, M. Abe, Lipids, fatty acids, and fucoxanthin content from temperate and tropical brown seaweeds, Aquat. Proce. 7 (2016) 66–75, https://doi.org/10.1016/j.aqpro.2016.07.009.
[38] B. Narayan, K. Miyashita, M. Hosakawa, Comparative evaluation of fatty acid composition of different *Sargassum* (Fucales, Phaeophyta) species harvested from temperate and tropical waters, J. Aquat. Food Prod. Technol. 13 (2005) 53–70, https://doi.org/10.1300/J030v13n04_05.
[39] L.C.B. Molion, S.O. Bernardo, Uma revisão da dinâmica das chuvas no nordeste Brasileiro, Rev. Bras. Meteorol. 17 (2002) 1–10.
[40] C. Cardoso, A. Ripol, C. Afonso, M. Freire, J. Varela, H. Quental-Ferreira, P. Pousão-Ferreira, N. Bandarra, Fatty acid profiles of the main lipid classes of green seaweeds from fish pond aquaculture, Food Sci. Nutr. 5 1186–1194. doi:https://doi.org/10.1002/fsn3.511.
[41] H. Pereira, L. Barreira, F. Figueiredo, L. Custodio, C. Vizetto-Duarte, C. Polo, E. Resek, A. Engelen, J. Varela, Polyunsaturated fatty acids of marine macroalgae: potential for nutritional and pharmaceutical applications, Mar. Drugs 10 (2012) 1920–1935, https://doi.org/10.3390/md10091920.
[42] M. Kendel, G. Wielgosz-Collin, S. Bertrand, C. Roussakis, N. Bourgougnon, G. Bedoux, Lipid composition, fatty acids and sterols in the seaweeds *Ulva armoricana*, and *Solieria chordalis* from Brittany (France): an analysis from nutritional, chemotaxonomic, and antiproliferative activity perspectives, Mar. Drugs 13 (2015) 5606–5628, https://doi.org/10.3390/md13095606.
[43] G.A. Dunstan, M.R. Brown, J.K. Volkman, Cryptophyceae and Rhodophyceae; chemotaxonomy, phylogeny, and application, Phytochem 66 (2005) 2557–2570.
[44] C. Dawezynski, R. Schubert, G. Jahreis, Amino acids, fatty acids and dietary fiber in edible seaweed products, Food Chem. 103 (2007) 891–899, https://doi.org/10.1016/j.phytochem.2005.08.015.
[45] S.V. Khotimchenko, V.E. Vaskovsky, T.V. Titlyanova, Fatty acids of marine algae from the Pacific coast of North California, Bot. Mar. 45 (2002) 17–22, https://doi.org/10.1515/BOT.2002.003.
[46] X. Li, X. Fan, L. Han, Q. Lou, Fatty acids of some algae from the Bohai Sea, Phytochem 59 (2002) 157–161, https://doi.org/10.1016/S0031-9422(01)00437-X.
[47] D.I. Sánchez-Machado, J. López-Cervantes, J. López-Hernández, P. Paseiro-Losada, Fatty acids, total lipid, protein and ash contents of processed edible seaweeds, Food Chem. 85 (2004) 439–444, https://doi.org/10.1016/j.foodchem.2003.08.001.
[48] Z. Chen, Y. Xu, T. Liu, L. Zhang, H. Liu, H. Guan, Comparative studies on the characteristic fatty acid profiles of four different Chinese medicinal *Sargassum* seaweeds by GC-MS and chemometrics, Mar. Drugs 14 (2016) 1–11, https://doi.org/10.3390/md14040068.
[49] S.V. Khotimchenko, Fatty acids of green macrophytic algae from the sea of Japan, Phytochem 32 (1993) 1203–1207, https://doi.org/10.1016/S0031-9422(00)95092-1.
[50] S. Sato, Effects of environmental factors on the lipid components of *Porphyra* species, Bull. Jpn. Soc. Sci. Fish. 41 (1975) 326–339.
[51] R.B. Johns, P.D. Nichols, G.J. Perry, Fatty acid composition of ten marine algae from Australian waters, Phytochem 18 (1979) 799–802, https://doi.org/10.1016/0031-9422(79)80018-7.
[52] P. Kumari, C.R.K. Reddy, B. Jha, Comparative evaluation and selection of a method for lipid and fatty acid extraction from macroalgae, Anal. Biochem. 415 (2011) 134–144, https://doi.org/10.1016/j.ab.2011.04.010.
[53] M. Terasaki, A. Hirose, B. Narayan, Y. Baba, C. Kawagoe, H. Yasui, S. Naotsune, H. Masashi, K. Miyashita, Evaluation of recoverable functional lipid components of several brown seaweeds (Phaeophyta) from Japan with special reference to fucoxanthin and fucosterol contents, J. Phycol. 45 (2009) 974–980, https://doi.org/10.1111/j.1529-8817.2009.00706.x.
[54] A.E.A. Hamdy, C.J. Dawes, Proximate constituents and lipid chemistry in two species of Sargassum from the west coast of Florida, Bot. Mar. 31 (1998) 79–81, https://doi.org/10.1515/botm.1988.31.1.79.
[55] S.V. Khotimchenko, Fatty acids of species in the genus *Codium*, Bot. Mar. 46 (2003) 456–460, https://doi.org/10.1515/BOT.2003.046.
[56] Y. Nozawa, Adaptive regulation of membrane lipids and fluidity during thermal acclimation in *Tetrahymena*, Proc. Jpn. Acad. Ser. B Phys. Biol. Sci. 87 (2011) 450–462, https://doi.org/10.2183/pjab.87.450.
[57] F.M. Pritchard, H.A. Eagles, R.M. Norton, P.A. Salisbury, M. Nicolas, Environmental effects on seed composition of *Victorian canola*, Aust. J. Exp. Agric. 40 (2000) 679–685, https://doi.org/10.1071/EA99146.
[58] G. Beltrán, D.C. Rio, S. Sánchez, L. Martínez, Influence of harvest date and crop yield on the fatty acid composition of Viggin olive oils from cv. Picual, J. Agric. Food Chem. 52 (2004) 3434–3440, https://doi.org/10.1021/jf049894n.
[59] K.W. Gellenbeck, Utilization of algal materials for nutraceutical and cosmeceutical applications – what do manufacturers need to know? J. Appl. Phycol. 24 (2012) 309–313, https://doi.org/10.1007/s10811-011-9722-z.
[60] J.T. Hafting, A.T. Critchley, M.L. Cornish, S.A. Hubley, A.F. Archibald, On-land cultivation of functional seaweed products for human usage, J. Appl. Phycol. 24 (2012) 385–392, https://doi.org/10.1007/s10811-011-9720-1.
[61] S.V. Khotimchenko, Variations in lipid composition among different developmental stages of *Gracilaria verrucosa* (Rhodophyta), Bot. Mar. 49 (2006) 34–38, https://doi.org/10.1515/BOT.2006.004.
[62] S.V. Khotimchenko, V.E. Vaskovsky, Distribution of C20 polyenoic fatty acids in red macrophytic algae, Bot. Mar. 33 (1990) 525–528, https://doi.org/10.1515/botm.1990.33.6.525.
[63] I. Lang, L. Hodac, T. Friedl, I. Feussner, Fatty acid profiles and their distribution patterns in microalgae: a comprehensive analysis of more than 2000 strains from the SAG culture collection, BMC Plant Biol. 11 (2011) 1–16, https://doi.org/10.1186/1471-2229-11-124.